

The research results described in the following summaries were submitted by the investigators on May 10, 1984 and cover the 6-months period from October 1, 1983 through May 1, 1984. These reports include both work performed under contracts administered by the Geological Survey and work by members of the Geological Survey. The report summaries are grouped into the three major elements of the National Earthquake Hazards Reduction Program.

Open File Report No. 84-628

This report has not been reviewed for conformity with USGS editorial standards and stratigraphic nomenclature. Parts of it were prepared under contract to the U.S. Geological Survey and the opinions and conclusions expressed herein do not necessarily represent those of the USGS. Any use of trade names is for descriptive purposes only and does not imply endorsement by the USGS.

The data and interpretations in these progress reports may be reevaluated by the investigators upon completion of the research. Readers who wish to cite findings described herein should confirm their accuracy with the author.

UNITED STATES
DEPARTMENT OF THE INTERIOR
GEOLOGICAL SURVEY

SUMMARIES OF TECHNICAL REPORTS, VOLUME XVIII

Prepared by Participants in

NATIONAL EARTHQUAKE HAZARDS REDUCTION PROGRAM

Compiled by

Muriel L. Jacobson

Thelma R. Rodriguez

CONTENTS

Earthquake Hazards Reduction Program

| | Page |
|---|----------|
| I. <u>Recent Tectonics and Earthquake Potential (T)</u> | |
| Determine the tectonic framework and earthquake potential of U.S. seismogenic zones with significant hazard potential. | |
| <u>Objective T-1. Regional seismic monitoring.....</u> | 1 |
| <u>Objective T-2. Source zone characteristics</u> | |
| Identify and map active crustal faults, using geophysical and geological data to interpret the structure and geometry of seismogenic zones. | |
| Identify and map active faults in seismic regions. Combine geophysical and geologic data to interpret tectonic setting of seismogenic zones..... | 35 |
| <u>Objective T-3. Earthquake potential</u> | |
| Estimate fault slip rates, earthquake magnitudes, and recurrence intervals for seismogenic zones and faults disclosed by research under Objectives T-1 and T-2, using geological and geophysical data. | |
| Earthquake potential estimates for regions of the U.S. west of 100°W. | |
| Earthquake potential estimates for regions of the U.S. east of 100°W. | |
| Support studies in geochemistry, geology, and soils science that enable fault movements to be accurately dated..... | 86 |
| II. <u>Earthquake Prediction Research (P)</u> | |
| Collect observational data and develop the instrumentation, methodologies, and physical understanding needed to predict damaging earthquakes. | |
| <u>Objective P-1. Prediction Methodology and Evaluation</u> | |
| Develop methods to provide a rational basis for estimates of increased earthquake potential. Evaluate the relevance of various geophysical, geochemical, and hydrological data for earthquake prediction. | |

| | |
|--|-----|
| Develop, operate and evaluate instrumentation for monitoring potential earthquake precursors. | |
| Analyze and evaluate seismicity data collected prior to medium and large earthquakes. | |
| Obtain and analyze data from seismically active regions of foreign countries through <u>cooperative</u> projects with the host countries. | |
| Systematically evaluate data and develop statistics that relate observations of specific phenomena to earthquake occurrence. | |
| Develop, study and test prediction methods that can be used to proceed from estimates of long-range earthquake potential to specific short-term predictions..... | 157 |

Objective P-2. Earthquake Prediction Experiments

Conduct data collection and analysis experiments in areas of California capable of great earthquakes, where large populations are at risk. The experiments will emphasize improved coordination of data collection, data reporting, review and analysis according to set schedules and standards.

Collect and analyze data for an earthquake prediction experiment in southern California, concentrating on the southern San Andreas fault from Parkfield, California to the Salton Sea.

Collect and analyze data for an earthquake prediction experiment in central California, concentrating on the San Andreas fault north of Parkfield, California..... 283

Objective P-3. Theoretical, Laboratory and Fault Zone Studies

Improve our understanding of the physics of earthquake processes through theoretical and laboratory studies to guide and test earthquake prediction observations and data analysis. Measure physical properties of those zones selected for earthquake experiments, including stress, temperature, elastic and anelastic characteristics, pore pressure, and material properties.

Conduct theoretical investigations of failure and pre-failure processes and the nature of large-scale earthquake instability.

Conduct experimental studies of the dynamics of faulting and the constitutive properties of fault zone materials. Through the use of drilled holes and appropriate down hole instruments, determine the physical state of the fault zone in regions of earthquake prediction experiments..... 358

| | Page |
|--|------|
| <u>Objective P-4.</u> Induced Seismicity Studies | |
| Determine the physical mechanism responsible for reservoir-induced seismicity and develop techniques for predicting and mitigating this phenomena. | |
| Develop, test, and evaluate theories on the physics of induced seismicity. | |
| Develop techniques for predicting the character and severity of induced seismicity. | |
| Devise hazard assessment and mitigation strategies at sites of induced seismicity..... | 395 |
| | |
| <u>III. Evaluation of Regional and Urban Earthquake Hazards (U)</u> | |
| Delineate, evaluate, and document earthquake hazards and risk in urban regions at seismic risk. Regions of interest, in order of priority, are: | |
| 1) The Wasatch Front | |
| 2) Southern California | |
| 3) Northern California | |
| 4) Anchorage Region | |
| 5) Puget Sound | |
| 6) Mississippi Valley | |
| 7) Charleston Region | |
| | |
| <u>Objective U-1.</u> Establishment of information systems..... | 410 |
| | |
| <u>Objective U-2.</u> Mapping and synthesis of geologic hazards | |
| Prepare synthesis documents, maps and develop models on surface faulting, liquefaction potential, ground failure and tectonic deformation..... | 423 |
| | |
| <u>Objective U-3.</u> Ground motion modeling | |
| Develop and apply techniques for estimating strong ground shaking..... | 455 |

Objective U-4. Loss estimation modeling

Develop and apply techniques for estimating earthquake losses.

Objective U-5. Implementation

| | |
|--|-----|
| Index 1: Alphabetized by Principal Investigator..... | 528 |
| Index 2: Alphabetized by Institution..... | 533 |

Most of the technical summaries contained in this volume are for research contracts solicited by RFP-1284. The description in the previous table of contents corresponds to respective Elements and Objectives of that RFP. Additionally some of the summaries are for research objectives that were initiated in earlier years. These objectives are covered in the descriptions found in the following table of contents.

Initiated before FY83

| | Page |
|--|------|
| I. Earthquake Hazards and Risk Assessment (H) | |
| Objective 1. Establish an accurate and reliable national earthquake data base. | |
| Objective 2. Delineate and evaluate earthquake hazards and risk in the United States on a national scale. | |
| Objective 3. Delineate and evaluate earthquake hazards and risk in earthquake-prone urbanized regions in the western United States. | |
| Objective 4. Delineate and evaluate earthquake hazards and risk in earthquake-prone regions in the eastern United States.----- | 468 |
| Objective 5. Improve capability to evaluate earthquake potential and predict character of surface faulting.----- | 475 |
| Objective 6. Improve capability to predict character of damaging ground shaking.----- | 480 |
| Objective 7. Improve capability to predict incidence, nature and extent of earthquake-induced ground failures, particularly landsliding and liquefaction.----- | 494 |
| Objective 8. Improve capability to predict earthquake losses. | |
| II. Earthquake Prediction (P) | |
| Objective 1. Obtain pertinent geophysical observations and attempt to predict great or very damaging earthquakes. | |
| Operate seismic networks and analyze data to determine character of seismicity preceding major earthquakes. | |
| Measure and interpret geodetic strain and elevation changes in regions of high seismic potential, especially in seismic gaps.----- | 499 |

| | | |
|--------------|---|-----|
| Objective 2. | Obtain definitive data that may reflect precursory changes near the source of moderately large earthquakes. Short term variations in the strain field prior to moderate or large earthquakes require careful documentation in association with other phenomena. Measure strain and tilt near-continuously to search for short term variations preceding large earthquakes. Complete development of system for stable, continuous monitoring of strain. Monitor radon emanation water properties and level in wells, especially in close association with other monitoring systems. Monitor apparent resistivity, magnetic field to determine whether precursory variations in these field occur. Monitor seismic velocity and attenuation within the (San Andreas) fault zone.----- | 513 |
| Objective 3. | Provide a physical basis for short-term earthquake predictions through understanding the mechanics of faulting. Develop theoretical and experimental models to guide and be tested against observations of strain, seismicity, variations in properties of the seismic source, etc., prior to large earthquakes.----- | 516 |
| Objective 4. | Determine the geometry, boundary conditions, and constitutive relations of seismicity active regions to identify the physical conditions accompanying earthquakes. Measure physical properties including stress, temperature, elastic and anelastic properties, pore pressure, and material properties of the seismogenic zone and the surrounding region. | |

III. Global Seismicity (G)

- Objective 1. Operate, maintain, and improve standard networks of seismographic stations.
- Objective 2. Provide seismological data and information services to the public and to the research community.

| | Page |
|---|------------|
| Objective 3. Improve seismological data services through basic and applied research and through application of advances in earthquake source specification and data analysis and management. | |
| | |
| IV. Induced Seismicity Studies (IS) | |
| Objective 1. Establish a physical basis for understanding the tectonic response to induced changes in pore pressure or loading in specific geologic and tectonic environments.----- | 526 |
| | |
| Index 1: Alphabetized by Principal Investigator----- | 528 |
| Index 2: Alphabetized by Institution----- | 533 |

Southern California Seismic Arrays

Contract No. 14-08-0001-21854

Clarence R. Allen

Seismological Laboratory, California Institute of Technology
Pasadena, California 91125 (818-356-6904)**Investigations**

Despite the fact that promised USGS funds to support this work have not yet been received after 7 months of effort (funded in the interim by Caltech), this semi-annual report summary covers the six-month period from 1 October 1983 to 31 March 1984. The proposed contract's purpose is the partial support of the joint USGS-Caltech Southern California Seismographic Network, which is also supported by other groups as well as by direct USGS funding through its own employees at Caltech. According to the proposed contract the primary visible product will be a joint Caltech-USGS catalog of earthquakes in the southern California region; quarterly epicenter maps and preliminary catalogs are also required and have been submitted as would have been due during the proposed contract period. About 250 preliminary catalogs are routinely distributed to interested parties.

Results

Figure 1 shows the epicenters of all cataloged shocks that have been located during the 6-month period from 1 October 1983 to 31 March 1984. Some of the seismic highlights during the period are as follows:

Number of earthquakes entered into the catalog: 9029

Number of earthquakes of $M = 3.0$ and greater: 219

Number of earthquakes of $M = 4.0$ and greater: 9

Largest shock within network area: $M = 4.5$ (21 October, Walker Pass area)

Number of shocks reported felt: 40

Smallest felt earthquake: $M = 2.1$ (7 March, SW Long Beach)

Number of earthquakes for which systematic telephone notification to agencies was made: 5

This was not a period of unusual seismic activity, although the activity in the southern Sierra Nevada along the general alignment of the Kern Canyon fault became even more obvious than before (Fig. 1). This activity is clearly distinct from that of the Coso region to the east and represents somewhat of a quandary, because the Kern Canyon fault in this area is allegedly truncated by unbroken Pliocene volcanic rocks. Two significant advances in processing procedures occurred during the reporting period: This was the first period during which all of the timing was done with the new CUSP system, and most large events have been assigned final M_L magnitudes.

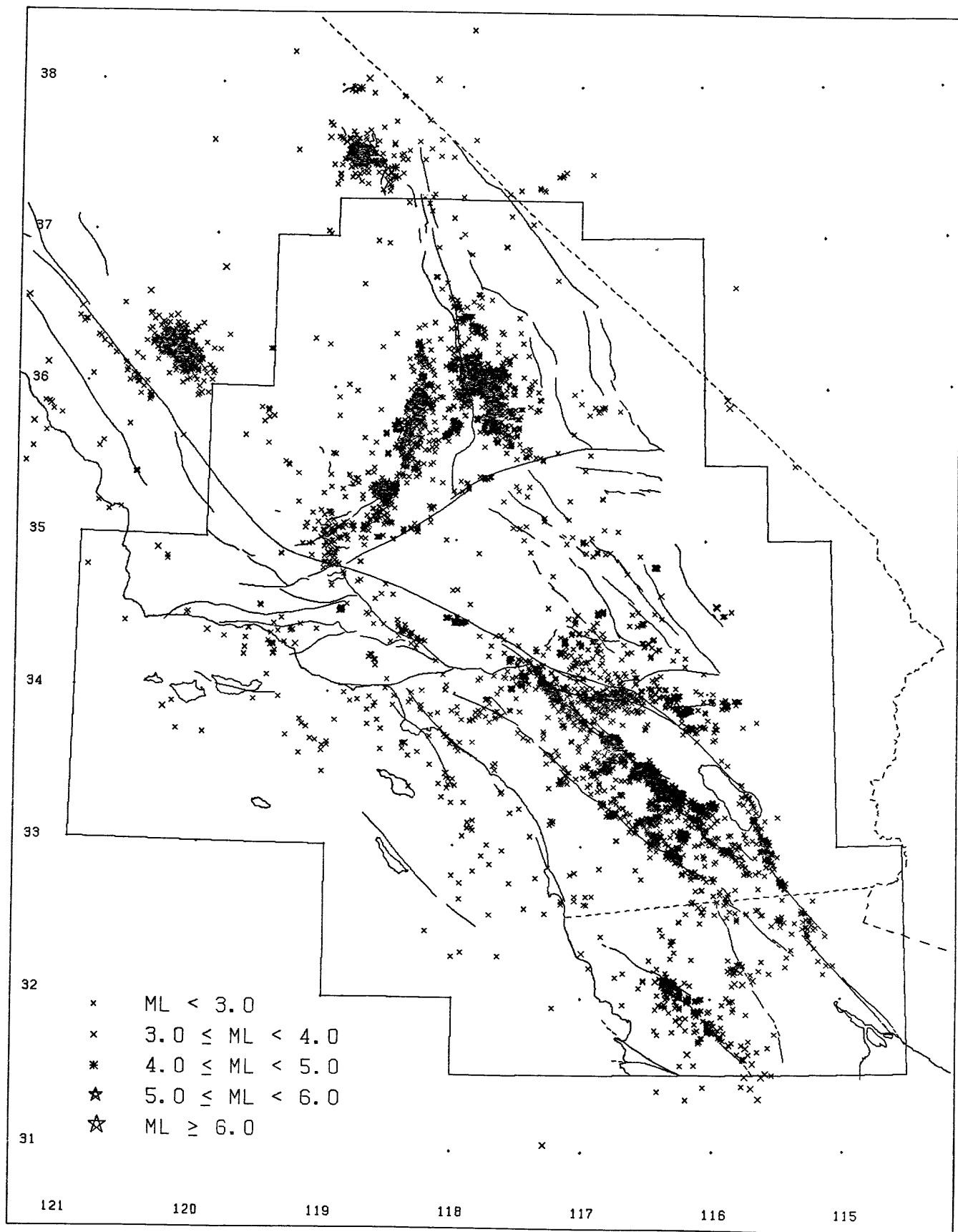


Fig. 1.--Epicenters of larger earthquakes in the southern California region, 1 October 1983 to 31 March 1984.

REGIONAL SEISMIC MONITORING ALONG THE WASATCH FRONT URBAN
CORRIDOR AND ADJACENT INTERMOUNTAIN SEISMIC BELT

14-08-0001-21857

W.J. ARABASZ, R.B. SMITH, J.C. PECHMANN, and W.D. RICHINS*

Department of Geology and Geophysics
University of Utah
Salt Lake City, Utah 84112
(801)581-6274

Investigations

This contract supports "network operations" (including a computerized central recording laboratory) associated with the University of Utah 80-station regional seismic telemetry network. USGS support focuses on the seismically hazardous Wasatch Front urban corridor of north-central Utah but also encompasses neighboring areas of the Intermountain seismic belt (ISB). The University of Utah maintains de facto responsibility for earthquake surveillance, including emergency response and direct public interface, for an 800-km-long segment of the ISB between Yellowstone Park and southernmost Utah. The State of Utah, the U.S. Bureau of Reclamation, and the U.S. Park Service also contributed support to operation of the University of Utah network during the report period. Primary products of this USGS contract are quarterly earthquake catalogs and a semi-annual data submission, in magnetic-tape form, to the USGS Data Archive. Following the October 1983 Borah Peak, Idaho, earthquake (M_s 7.3), supplemental funds were received from the USGS (1) to carry out aftershock recording with a 12-station temporary seismic network, and (2) to compile a summary listing of earthquakes for the central Idaho earthquake sequence.

Results

The University of Utah operated 12 portable seismic stations in the Borah Peak, Idaho region for a period of three weeks following the M_s 7.3 mainshock on October 28, 1983. Approximately 45 additional instruments were deployed by other institutions during this time including the U.S. Geological Survey, the Idaho National Engineering Laboratory (INEL), Boise State University, the University of Washington, Montana Bureau of Mines and Geology, and the University of Wisconsin at Madison (Figure 1). We have merged arrival time and first motion data contributed by other investigators with our own

*P. J. Oehmich and L. L. Sells also contributed significantly to this project during the report period.

data to create a master data set containing over 7,000 arrival times from more than 80 different instrument sites. These data have been used to locate 374 aftershocks. Station delays for permanent stations in Idaho, Montana, and Wyoming were calibrated using 6 of the larger, well-located aftershocks. These station delays were used to relocate the mainshock and 47 aftershocks larger than magnitude 2.7 that occurred before the portable instruments were installed. Details of the aftershock distribution are discussed in the report for Contract No. 14-08-0001-21856.

Local magnitudes have been determined using the Wood-Anderson instruments at Dugway and Salt Lake City for 21 events that occurred during the first three weeks of the aftershock sequence. Our minimum magnitude threshold on the Wood-Anderson instruments in Utah is about 3.7 for the Borah Peak area. Only three aftershocks over magnitude 5 occurred (5.8, 5.8, and 5.4). Preliminary size estimates for the smaller events have been determined from duration measurements on INEL helicorder records using the duration magnitude scale of Griscom and Arabasz (1979) pending systematic reevaluation of magnitudes for the Borah Peak sequence.

Final analysis of Utah earthquake activity for the six-month reporting period is not yet complete due to the large number of earthquakes associated with the Borah Peak sequence. Figure 2 shows Utah seismicity for the period October 1, 1983, to February 17, 1984. The largest event was an M_L 4.3 earthquake on October 8, 1983, located 3 km south of the Salt Lake International Airport. This event was widely felt throughout north-central Utah. Other felt earthquakes during this report period include an M_L 4.0 event on November 19, 1983 in Pocatello Valley near the Idaho-Utah border and an M_L 3.6 event on December 9, 1983, near Cove Fort in southwestern Utah.

Reports and Publications

Richins, W. D., Smith, R. B., King, J. J., Langer, C. J., Meissner, C. W., Pechmann, J. C. Arabasz, W. J., and Zollweg, J. E., 1984, The 1983 Borah Peak, Idaho, earthquake: A progress report on the relationship of aftershocks to the mainshock, surface faulting, and regional tectonics (abs.), Earthquake Notes 55 (1).

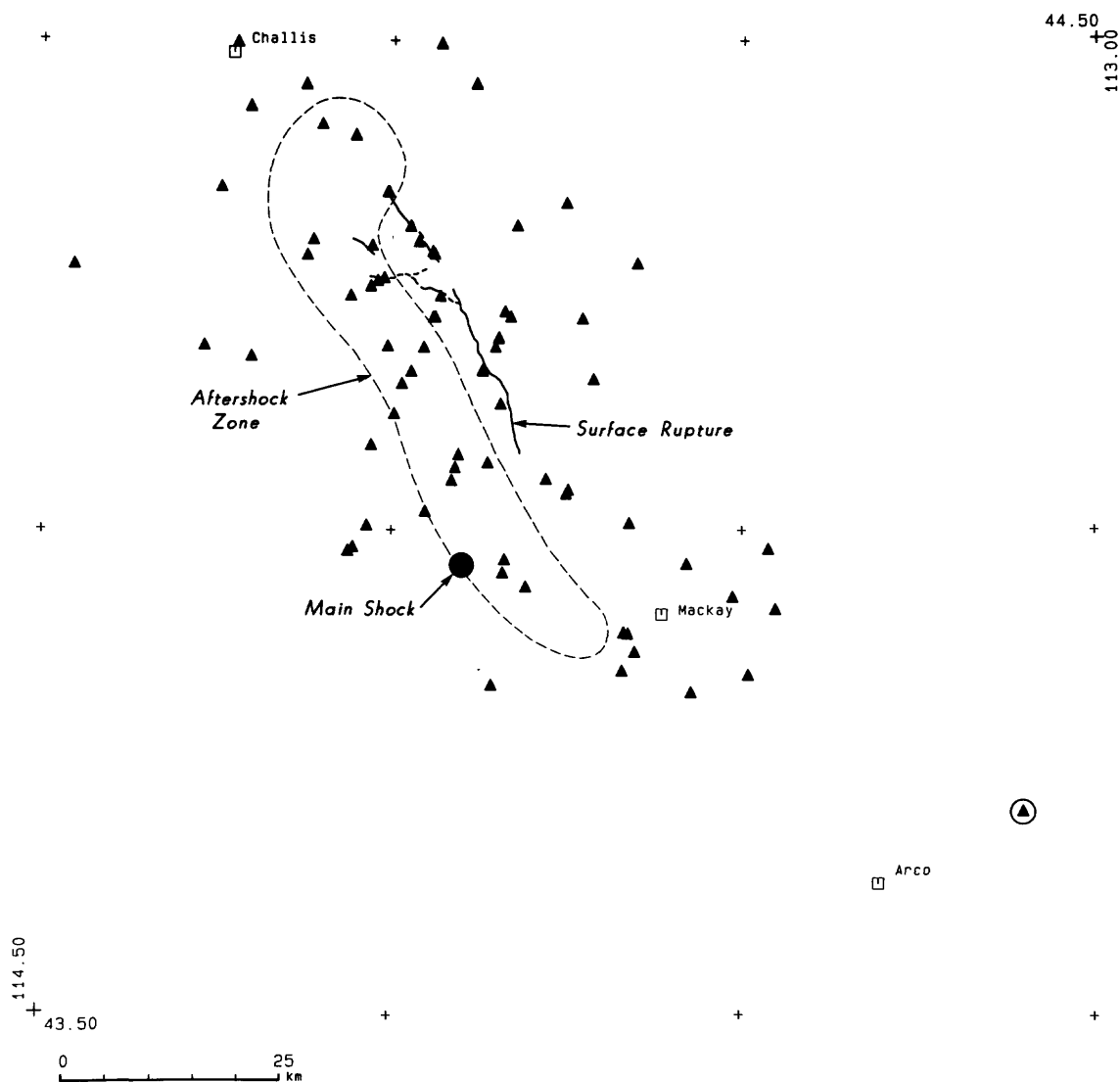


Figure 1. Locations of portable stations deployed in the vicinity of the M_s 7.3 Borah Peak earthquake of October 28, 1983 (triangles). The circled station is the closest permanent station that was operating at the time of the main shock.

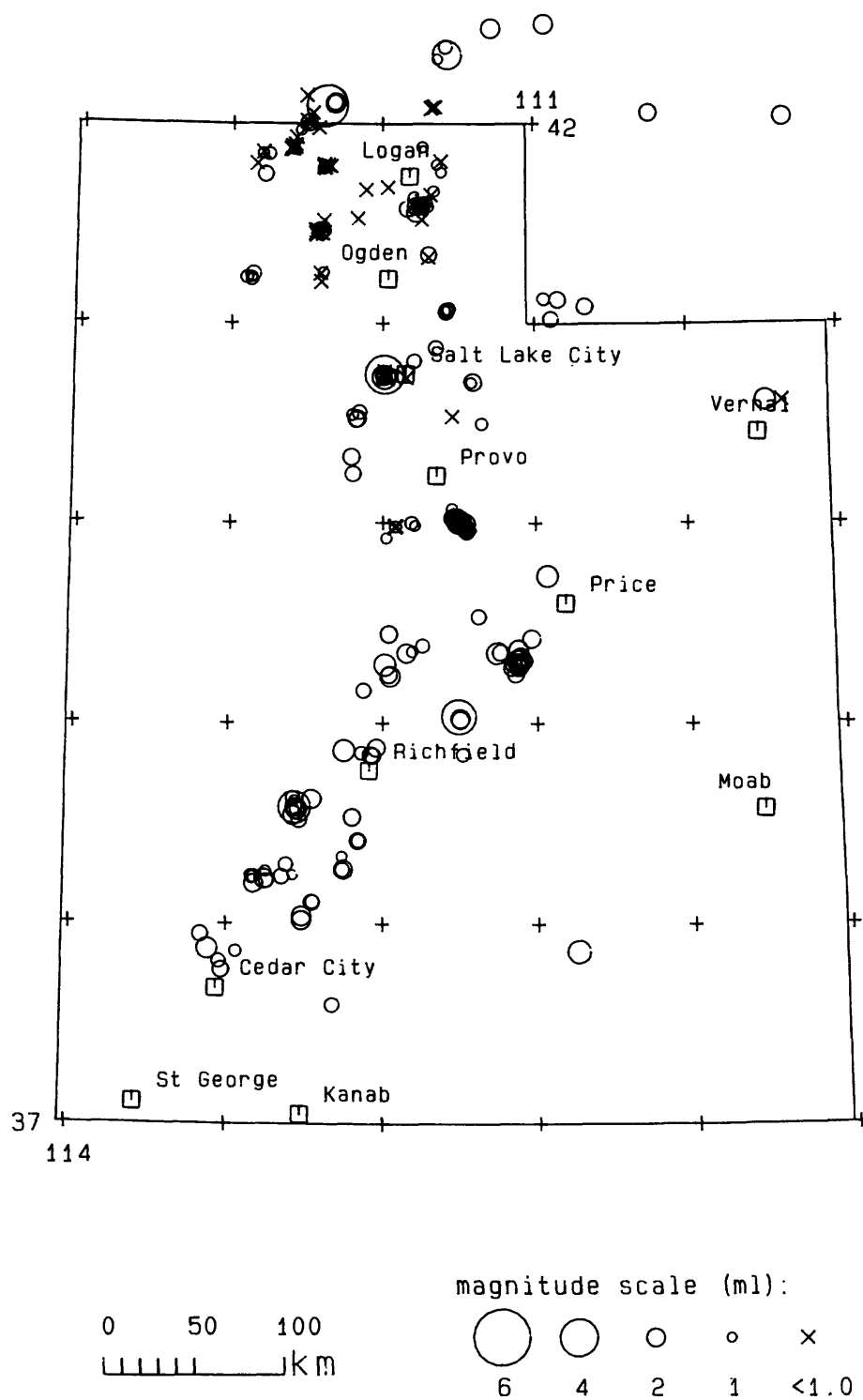


Figure 2. Utah region earthquakes, October 1, 1983 to February 17, 1984.

Seismic Source Mechanism Studies
In the Anza-Coyote Seismic Gap

14-08-0001-21271

Jonathan Berger and James N. Brune
Institute of Geophysics and Planetary Physics
Scripps Institution of Oceanography
University of California, San Diego
La Jolla, CA 92093

Investigations

This report covers the progress of the research investigating the Anza-Coyote Canyon seismic gap for the period of the second half of 1983. The objectives of this research are: 1) To study the mechanisms and seismic characteristics of small and moderate earthquakes; 2) To determine if there are premonitory changes in seismic observables preceding small and moderate earthquakes. This work is carried out in cooperation with Tom Hanks, Joe Fletcher and Linda Haar, of the U.S. Geological Survey, Menlo Park.

Network Status

During the period of this report, up to ten stations of the Anza Seismic Network were telemetering three component data. The network was set at a low gain to try to record earthquakes up to magnitude 4 occurring inside the array.

After the problems of the previous winter, we spent much of the summer and fall modifying various aspects of the data acquisition equipment. Modifications were made to the radio telemetry and to the digitizing components. We rebuilt the antenna array at our central receiving site, Toro Peak, to improve radio reception and make it structurally stronger. The radio transmitters and receivers were modified to extend their operational temperature range in the digitizers. Several boards were modified to reduce the instrument generated noise. By the end of 1983, there were apparently no more critical improvements necessary for the remote telemetry system. In the future, we need to improve the interface unit between the microwave equipment and the data logging computer to allow implementation of better array diagnostics.

Seismicity

In the six months of summer and fall, the Anza Network recorded 42 events which were large enough to locate and determine source parameters. These events had moments ranging from 6.8×10^{17} to 1.4×10^{21} dyne-cm and stress drops ranging from about 1 to 240 bars (Brune model). The seismicity pattern seems unchanged from what has been observed before. The seismicity does not appear to be associated with the main trace of the San Jacinto fault on the north-west end of the array. These events in this area tend to be between the Hot Springs fault at depths of 12 to 19 km. The events on the south-east end of the array near the trifurcation of the San Jacinto fault also do not have any obvious associations with the identified fault traces. These earthquakes are occurring at depths between 8 and 12 km. The shallowest events are still occurring in the Coahuilla area. Events have been located with depths of 3 km. One other trend is noticeable. The events with the larger moments ($>10^{20}$) and larger stress drops (>50 bars) all appear to be near major faults. The next problems which need to be addressed will be to improve the velocity structure and attempt to get an attenuation versus depth model.

Glen Canyon Dam

9920-01211

Marvin A Carlson
Branch of Global Seismology and Geomagnetism
U.S. Geological Survey
National Earthquake Information Service, MS 967
Box 25046, Denver Federal Center
Denver, Colorado 80225
(303) 234-3994

Investigation

Glen Canyon Dam - Recorded, compiled, interpreted and reported local earthquakes in the vicinity of the dam and reservoir to attempt to determine whether there are detectable influences on the seismicity by the dam and/or reservoir.

Results

Glen Canyon Dam - Memorandum type reports are being submitted to the Bureau of Reclamation periodically concerning status of local earthquakes recorded at seismograph station "GCA."

The goal of the Glen Canyon Project is to record, compile, interpret, and report local earthquakes in the vicinity of the dam and reservoir to accumulate data to aid in determining whether there are detectable influences on the seismicity by changes in water level in the reservoir.

U.S. Seismic Network

9920-01899

Marvin A. Carlson
Branch of Global Seismology and Geomagnetism
U.S. Geological Survey
National Earthquake Information Service, MS 967
Box 25046, Denver Federal Center
Denver, Colorado 80225
(303) 234-3994

Investigations

U.S. Seismicity. Data from the U.S. Seismic Network are used to obtain preliminary locations of significant earthquakes worldwide.

Results

As an operational program, the U.S. Seismic Network operated normally throughout the report period. Data were recorded continuously in real time at the NEIS main office in Golden, Colorado. At the present time, 100 channels of SPZ data are being recorded at Golden on developorder film. This includes data telemetered to Golden via satellite from both the Alaska Tsunami Warning Center, Palmer, Alaska and the Pacific Tsunami Warning Center, Ewa Beach, Hawaii. A representative number of SPZ channels are also recorded on Helicorders to give NEIS real time monitoring capability of the more active seismic areas of the United States. In addition, 15 channels of LPZ data are recorded in real time a multiple pen Helicorders.

Data from the U.S. Seismic Network are interpreted by record analysts and the seismic readings are entered into the NEIS data base. The data are also used by NEIS standby personnel to monitor seismic activity in the U.S. and worldwide on a real time basis. Additionally, the data are used to support the Alaska Tsunami Warning Center and the Pacific Tsunami Warning Service. At the present time, all earthquakes large enough to be recorded on several stations are worked up using the "Quick Quake" program to obtain a provisional solution as rapidly as possible. Finally, the data are used in such NEIS publications as the "Preliminary Determination of Epicenters" and the "Earthquake Data Report."

Objectives

The U.S. Seismic Network is an operational program as the data generated are routinely used to support the NEIS operational requirement of timely location and publication of earthquakes worldwide. Also, the network data directly support the NEIS standby personnel who are responsible for locating and reporting to the media, disaster agencies and other organizations all significant earthquakes worldwide. Thirdly, support is given to the Alaska Tsunami Warning Center and the Pacific Tsunami Warning Service as network data are exchanged with both organizations.

Reanalysis of Instrumentally-Recorded U.S. Earthquakes

9920-01901

J. W. Dewey

Branch of Global Seismology and Geomagnetism
U.S. Geological Survey
Denver Federal Center, MS 967
Denver, Colorado 80225
(303) 234-4041

Investigations

1. Relocate instrumentally recorded U.S. earthquakes using the method of joint hypocenter determination (JHD) or the master event method, using subsidiary phases (Pg, S, Lg) in addition to first arriving P-waves, using regional travel-time tables, and expressing the uncertainty of the computed hypocenter in terms of confidence ellipsoids on the hypocentral coordinates.
2. Evaluate the implications of the revised hypocenters on regional tectonics and seismic risk.

Results

Jim Dewey has used locally-recorded aftershocks of the $M_S = 7.3$ Borah Peak, Idaho, earthquake of October 28, 1983, to calibrate the determination of epicenters of early aftershocks in the Borah Peak sequence and to calibrate the determination of epicenters of regionally recorded earthquakes in central Idaho that occurred prior to the Borah Peak earthquake. The locally-recorded aftershock data had been collected by research groups from the U.S. Geological Survey and several universities; a number of the locally-recorded aftershocks were recorded at regional and teleseismic distances, enabling station delays to be computed for the stations at regional and teleseismic distances.

Dewey also computed m_{bLg} magnitudes for regionally recorded central Idaho earthquakes that occurred in the period from 1963 through mid-1983.

The following conclusions result from the reanalysis of the central Idaho earthquakes:

1. A plot of cumulative-frequency versus magnitude for the central Idaho earthquakes suggests that the catalog of regionally recorded central Idaho earthquakes is essentially complete above magnitude 3.5 for the period 1963-1983.

2. None of the regionally recorded earthquakes occurred within 20 km of the Borah Peak mainshock hypocenter prior to the mainshock. The Lost River fault (on which the Borah Peak earthquake occurred) is therefore a clear example of a major, previously quiescent, normal fault that produced a large earthquake without having first entered a period of increased moderate-magnitude earthquake activity.
3. The epicenter of the Borah Peak mainshock is at the southernmost end of the aftershock zone and its position is consistent with the mainshock rupture beginning at depth on the Lost River fault approximate 7 km southwest of the southernmost associated surface faulting.

Reports

- (O) Dewey, J. W., 1983, A global search of continental midplate seismic regions for specific characteristics bearing on the 1886 Charleston, South Carolina, earthquake, in Hayes, W. W., and Gori, P. L., eds., Proceedings of Conference XX, A workshop on "The Charleston earthquake and its implications for today": U.S. Geological Survey Open-File Report 83-843, p. 391-426.
- (A) Dewey, J. W., 1983, Analysis of the seismicity of central Idaho using data from the Borah Peak earthquake sequence of 1983, EOS, 65, p. 239.

WESTERN GREAT BASIN-EASTERN SIERRA NEVADA SEISMIC NETWORK

Contract 14-08-0001-21867

A.S. Ryall, W.F. Nicks, and E.J. Corbett
Seismological Laboratory
University of Nevada
Reno, NV 89557
(702) 784-4975

Investigations

This program supports continued operation of a seismic network in the western Great Basin of Nevada and eastern California, with research focused on: (1) recording and location of earthquakes occurring in the western Great Basin; (2) possible precursory seismicity patterns in the White Mountains gap; and (3) evaluation of the contribution that high-quality digital broad-band seismic stations can make to regional network-seismic studies.

Results**A. Seismic Network Operation**

During the last half of 1983 we deployed eight additional seismic stations north and east of Long Valley caldera. The US Geological Survey has concurrently installed 12 new stations in the caldera region. This brings to 33 the number of seismographic stations recording in and around the Long Valley caldera. All of the University of Nevada stations and many of the USGS stations are being recorded on analog magnetic tape at Reno. Station spacing in the southwest part of the caldera is less than 10 km; north of the caldera it is 15-20 km. This network is sufficient to provide at least 20 readings for the location of all earthquakes in the Mammoth Lakes area with magnitude $> 1.5 M_L$.

The University of Nevada has developed and tested a digital seismographic system for remote operation. The digital station is a data acquisition system that provides broad-band (0.05-30 Hz), wide dynamic-range (96 dB) digitization of signals from a three-component set of seismometers, and telemeters the data to a central facility where it is continuously recorded. This system has been tested in an experiment in Hot Creek Valley, central Nevada, and three stations are now operating in mine-tunnels at Mina, Bodie, and Washoe Lake. A fourth station is to be installed in the Las Vegas area in the near future. These stations will be used to determine spectral characteristics of seismic signals affected by attenuation in Long Valley caldera.

B. On-line System

A computer-based earthquake recording system has been installed that will provide on-line event detection and digitization of the analog seismic signals transmitted to the Reno data facility. This will facilitate analysis of large numbers of earthquakes and will allow waveform analysis of the network data. The on-line system is currently up and running and triggering successfully on local events, teleseisms, and nuclear tests at NTS. We are currently correcting some hardware-software interaction problems and are tuning the triggering algorithm to be more responsive to our network geometry. We anticipate that within a few weeks the on-line system will replace our current system of recording data on analog magnetic tape.

C. Data Analysis

Our routine analysis is complete through January 1984, and we are in the process of finalizing the 1983 catalog prior to publication. During 1983 the Seismological Laboratory registered 1,711 earthquakes (Fig. 1). Of these events:

573 were magnitude 2 or greater;
117 were magnitude 3 or greater;
20 were magnitude 4 or greater;
3 were magnitude 5 or greater.

The vast majority of the recorded earthquakes (73%) occurred within 30 km of the town of Mammoth Lakes (Fig. 2). Much of the Mammoth Lakes activity was part of an intense swarm that occurred January 7-11 along the south rim of the Long Valley caldera.

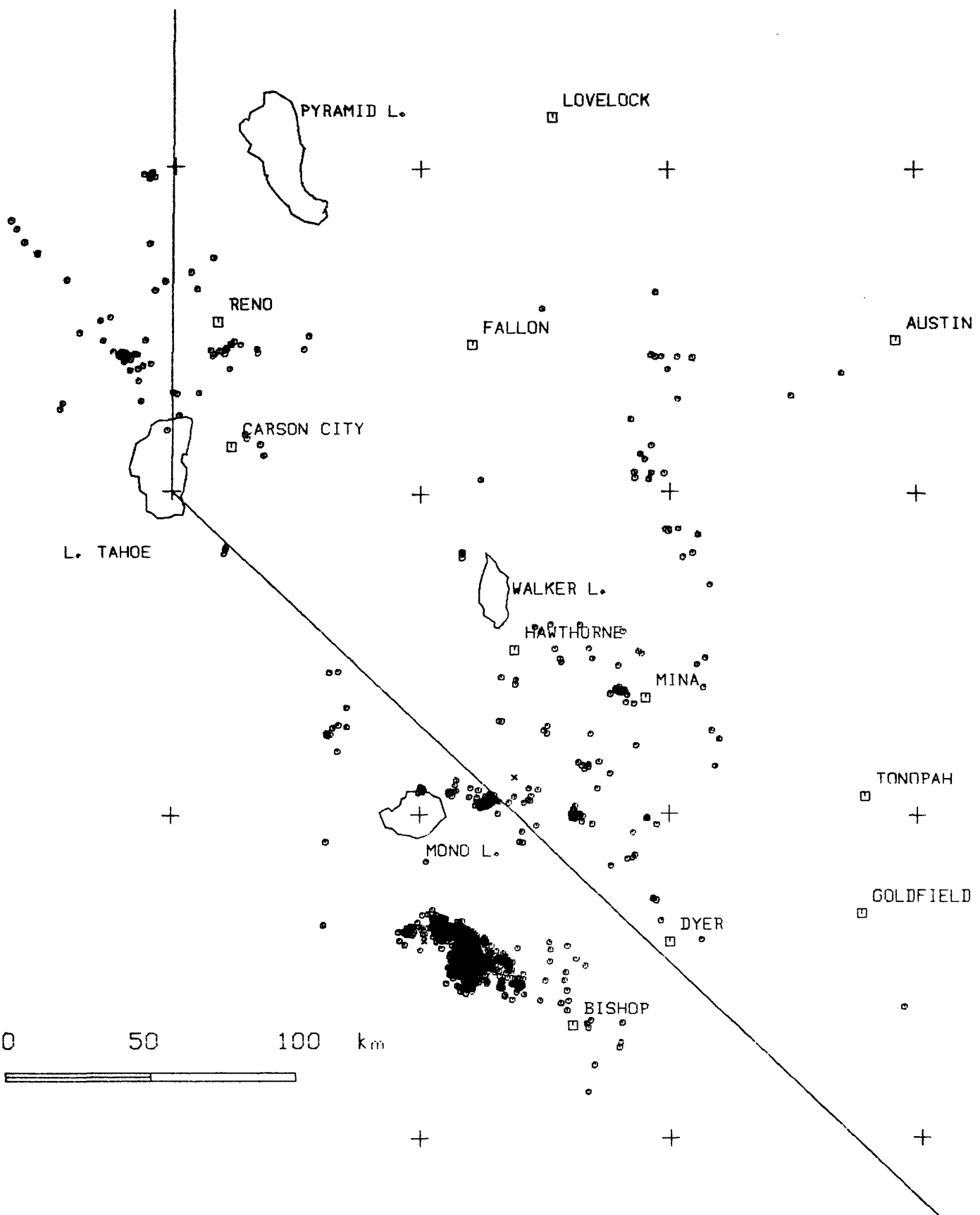


Figure 1. Map of eastern California and western Nevada showing all earthquakes located by the University of Nevada Seismological Lab in 1983.

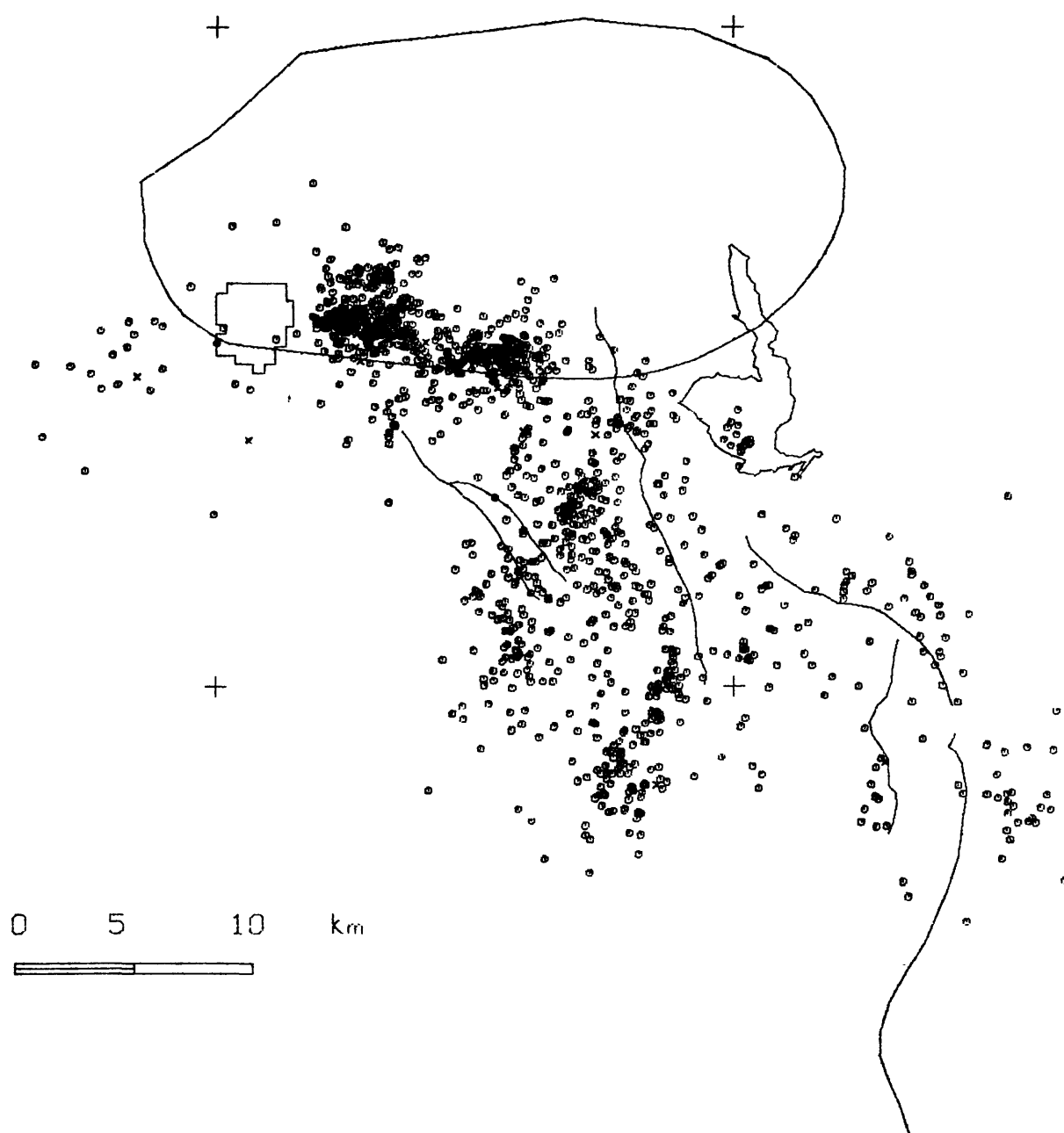


Figure 2. Map of the Long Valley region showing all earthquakes located by the University of Nevada Seismological Lab in 1983. Most of the activity occurred along the south rim of the Long Valley caldera during an intense swarm in mid-January.

EARTHQUAKE HAZARD STUDIES IN THE NORTHEASTERN UNITED STATES
 USGS 14-08-000-21876
 L. Seeber and L. Sykes
 Lamont-Doherty Geological Observatory
 Palisades, New York 10964
 (914) 359-2900

INVESTIGATIONS

The New York - New Jersey Seismic Network Project includes systematic earthquake data collection and analysis as well as basic investigations on the neotectonics and earthquake hazard of this area along the Atlantic seaboard. Studies include the comparison of hypocentral and first-motion data with geologic structure directed at testing models of Appalachian intraplate neotectonics, attenuation and source characteristics using digital data, velocity structure, intensity distribution and historic seismicity, to establish the long-term level of activity and/or establish whether secular changes in the pattern of seismicity have occurred.

RESULTS

1) Hypocenter distribution and fault-plane solutions suggest that two seismic zones can be distinguished. One of these zones is in the pre-Appalachian (Grenville) basement, primarily active where this basement is either exposed, such as in the Adirondacks, or where it is under a relatively thin cover, in the Appalachian Plateau and outer fold belt, such as in western New York. Fault-plane solutions for earthquakes in the pre-Appalachian basement are consistent with ENE axis of maximum horizontal compressive stress. Another seismic zone is spatially correlated with allochthonous crystalline slabs of the Appalachians, such as the Hudson Highlands/Redding Prong. Comparing hypocenters and subsurface structural data suggest that this seismicity is confined above the master detachment. Fault-plane solutions in this zone suggest a non-uniform pattern of stress.

2) Seismic zones can be recognized in the Adirondacks from \approx 10 years of epicentral data produced by a regional network. Two arcuate E-NE epicentral belts are correlated with structural trends of Grenville age. One is near the adjacent to the root zone of the Wakely Mt. nappe. Individual earthquakes in these belts are found, however, to rupture NNW striking faults with reverse slip consistent with ENE subhorizontal P-axes. These faults cannot be related to any known Grenville structural trend. Thus the control of the seismicity by the Grenville structure is not by simple reactivation of weaknesses directly associated with this structure, but must be indirect, possibly through the control that structure has on the spatial (depth) distribution of particular rock types.

3) The aftershock sequence of the Oct. 7, 1983 Goodnow earthquake in the central Adirondacks is well constrained by data from a temporary network and conforms with the pattern of earthquake faulting found in the Adirondacks (Figs. 1 and 2). The time-space distribution of 96 aftershocks delineate a circular zone dipping $\approx 60^\circ$ with a diameter of ≈ 1.5 km, extending from a depth of ≈ 7 to ≈ 8.5 km (Figs. 3 and 4). If this small aftershock zone is an upper-limit of the size of the main rupture, a relatively high stress-drop is obtained for the main rupture. The moment of the main shock, $M_0 = 2.5 \times 10^{23}$, is determined from surface waves and is somewhat low compared with $M_L = 5.1$ (PAL). From this value of the moment and the aftershock area we obtain

a lower bound for the stress drop of 140 bars. Both the fault-plane solution from the main shock and the composite solution for most of the aftershocks indicate reverse faulting on a N 10° - 20° W plane dipping 60° - 70° west. On the 10th day of the aftershock sequence an apparently conjugate fault became active and the activity migrated up and west from the main aftershock plane (Fig. 5). This shallow-dipping "conjugate" fault is subparallel to and displaced by only a few kilometers from a 20 km downdip extrapolation of the Blue mt. Lake fault active during swarms in 1971-1973 (Fig. 2). The Goodnow and Blue Mt. Lake faults, if extrapolated beyond the currently active segments, delimit a wedge-shaped block that is being uplifted by the fault movement. The high topography that characterizes this block may be related to this motion (Fig. 2). The 40 km long NNW Catlin Lake lineament is subparallel to the inferred Goodnow rupture zone and close to the surface intersection of the planar extrapolation of this fault (Fig. 9). The rapidly growing constraints on active faulting from seismicity and on Grenville structure from surface mapping are expected to improve our understanding of the complex interaction between Precambrian structure and the current state of stress to generate seismicity in the Adirondacks.

Selected Reports

- Kafka, A.L., E.A. Schlesinger-Miller, N.L. Barstow, D. Cramp, and L.R. Sykes, Earthquake magnitudes and seismicity in the New York City Metropolitan Area, submitted to Bull. Seismol. Soc. Am., 1983.
- Kafka, A.L., N.L. Barstow, and E.A. Schlesinger-Miller, Earthquake activity and state of stress in the Newark Basin and surrounding geologic provinces, N.E. Geol. Soc. Am. Abstr. with Programs, 1983.
- Seeber, L. and J.G. Armbruster, Time-varying distribution of seismicity and thin-skin model of intraplate Appalachian neotectonics, Abst., Seismol. Soc. Am., Eastern Section, p. 3, 1983.
- Seeber, L., A.L. Kafka, S.G. Ambruster and S. Nishenko, A comparison of the seismotectonics of the northern and southern Appalachians, GSA Abstract, North Eastern Section, 1983.

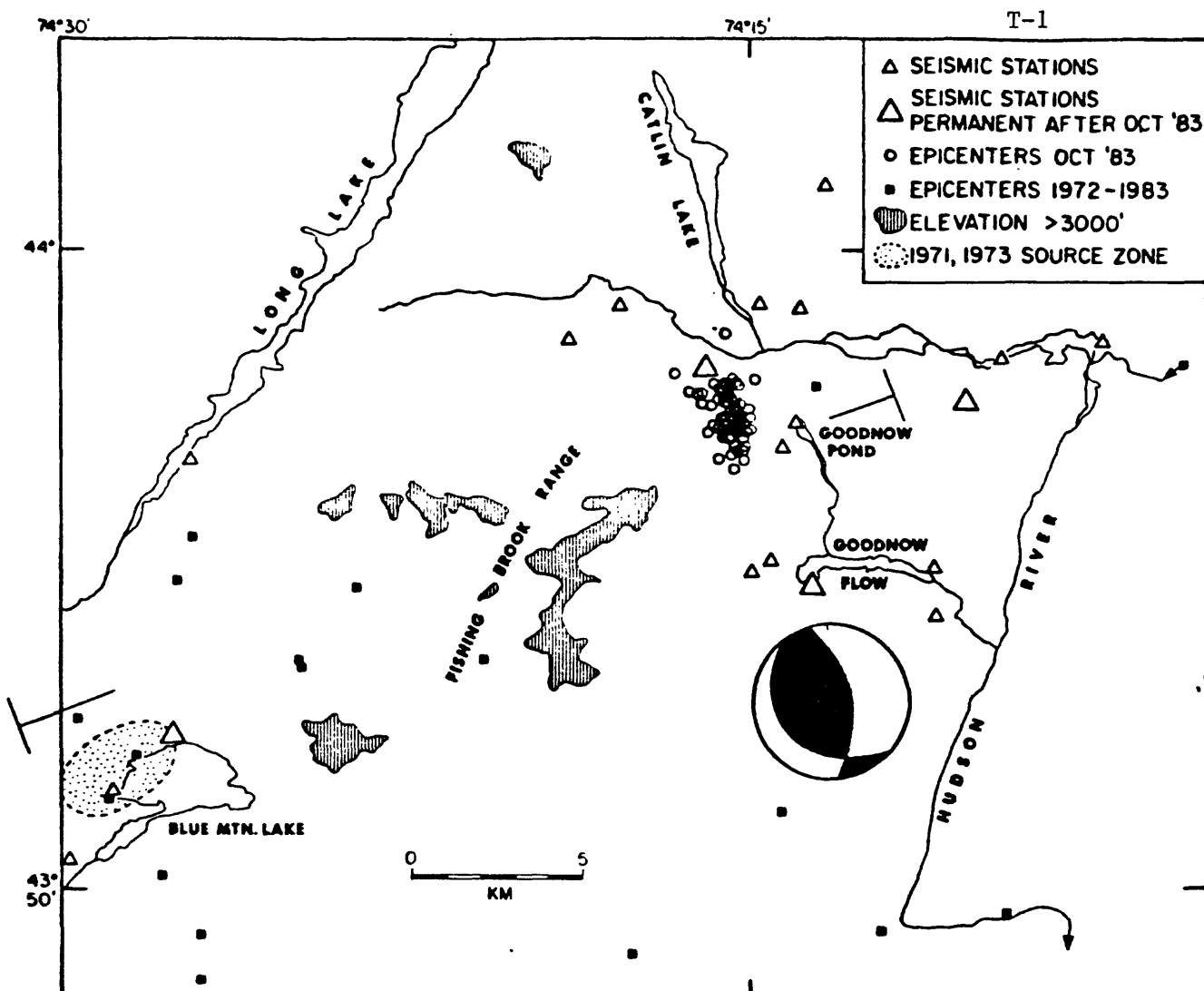


Fig. 1. Blue Mt. Lake - Goodnow area of the central Adirondacks. Seismicity 1972-83 (squares) as located by the regional seismic network and Oct. 7-29, 1983 (circles) as located by a network of temporary stations (triangles; L-DGO and USGS). The area of the 1971 and 1973 Blue Mt. Lake swarms is also indicated. Large triangles are stations of the permanent network after Nov. 1, 1983. Catlin Lake and Long Lake are part of linear topographic features possibly associated with brittle faults.

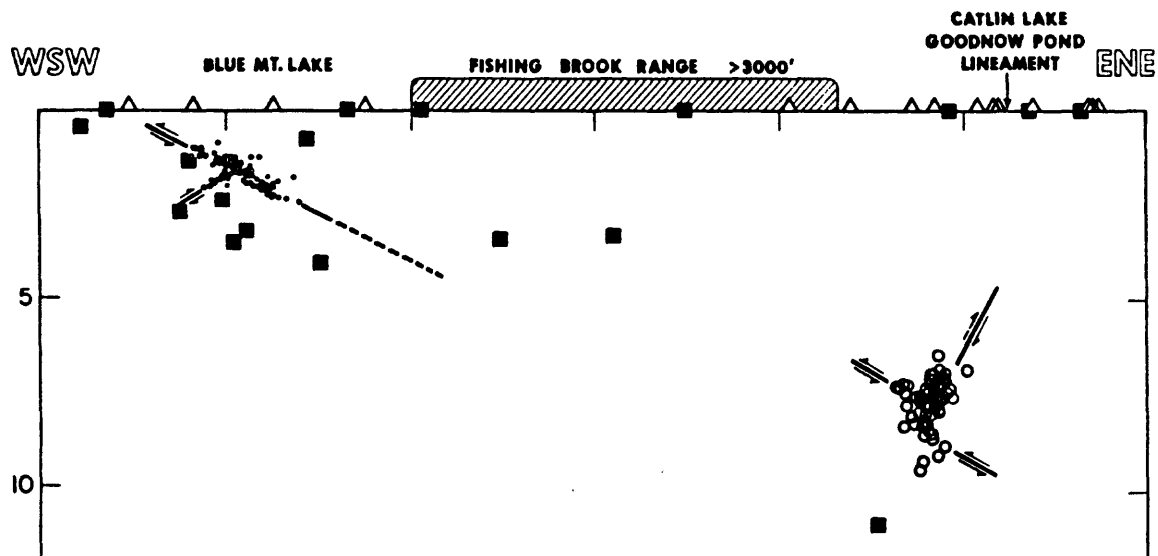


Fig. 2. Section through the Goodnow and Blue Mt. lake area (located in Fig. 2; no vertical exaggeration). Seismicity in Fig. 2 + 20 km from plane of section is included (same symbols). Hypocenters for the 1971-73 Blue Mt. Lake swarms are from Yang & Aggarwal, 1981. Active faults delineated by spacial and temporal distribution of hypocenters and by first-motion data are indicated. Depth control for events located only by the regional network is generally poor. It is possible that seismicity after the Blue Mt. Lake swarms and before the Goodnow event (squares) was on the same system of faults active during the intensely studied sequences in 1971, 1973 and 1983.

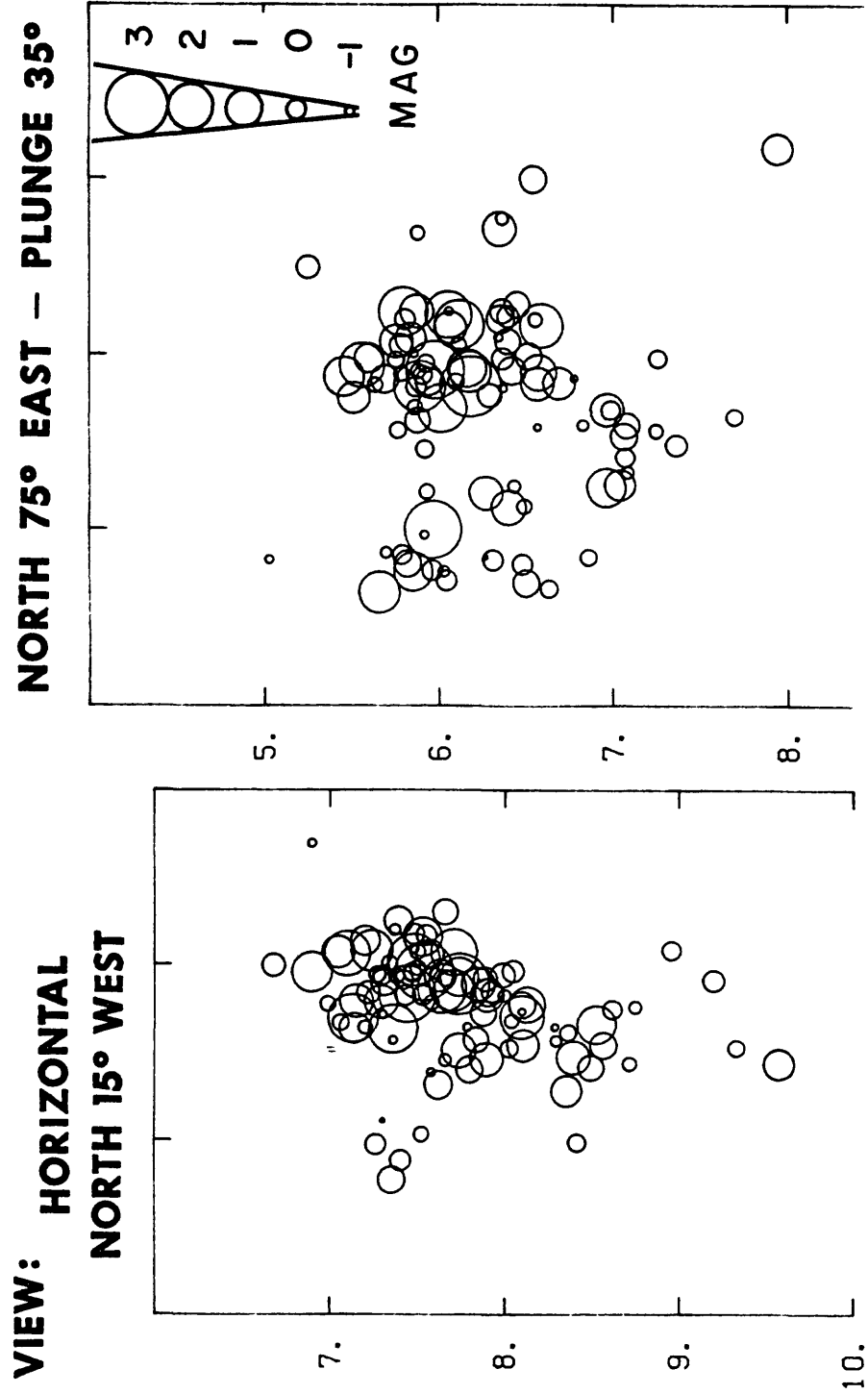


Fig. 3. 96 aftershocks of the Goodnow earthquake Oct. 7, 1983, in the Central Adirondacks recorded by a temporary local network (L-DG0/USGS) operated from 15 hrs to 22 days after the main shock. The view is along the strike of the inferred rupture which dips $\sim 60^\circ$ WSW.

Fig. 4. The same hypocenters of Goodnow aftershocks as in Fig. 3 seen perpendicularly to the inferred rupture plane. From these data we infer a rupture no more than 1.5 km in diameter, dipping 60° WSW and ranging from a depth 7 to 8.5 km. Note clustering of hypocenters around the rim of the inferred rupture.

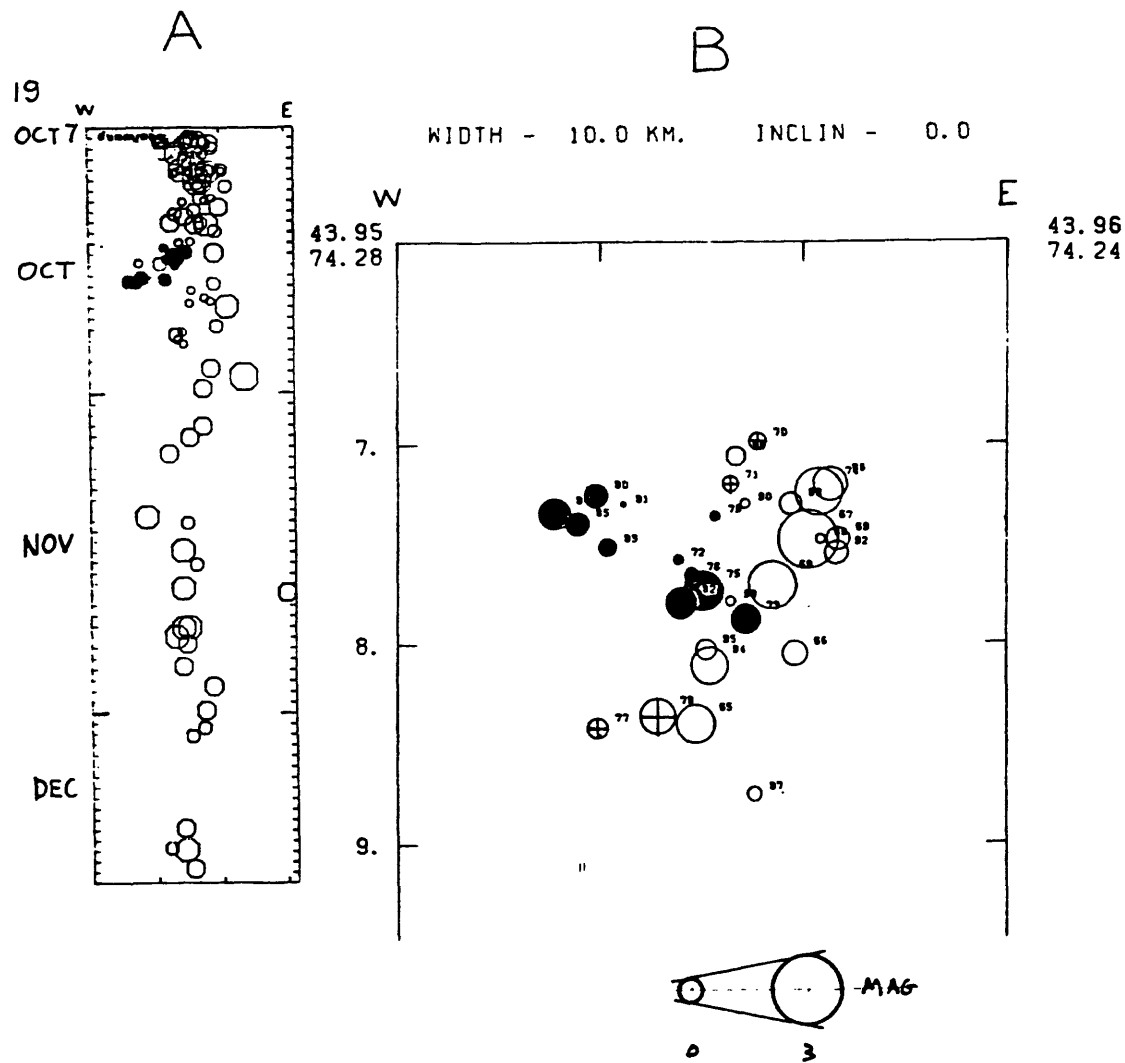


Fig. 5. Time-space data suggesting the propagation of slip along a conjugate fault away from the main rupture. A is a time-space plot of the Goodnow epicenters projected on the line of the section in B (view along main rupture as in Fig. 1). Most of the earthquakes in a tight westward migrating sequence occur on a plane dipping eastward and extending about 1 km from the main rupture (blackened symbols). This migration seems to take about 4 days.

Earthquake Hazard Studies in Southeast Missouri

14-08-0001-21262

William Stauder
Robert B. Herrmann
Department of Earth and Atmospheric Sciences
Saint Louis University
P.O. Box 8099 Laclede Station
St. Louis, MO 63156
(314) 658-3131

Goals

1. Monitor seismic activity in the New Madrid Seismic Zone, using data from a 60 station regional seismic array sponsored by the USGS and the USNRC.
2. Conduct research on eastern United States seismic sources using array and supplemental data.

Investigations

1. The project consists of monitoring data from a network of 32 USGS and 16 NRC seismograph stations located in the central Mississippi Valley. In addition telemetered data from eight Tennessee Earthquake Information Center stations in the southern part of the New Madrid Seismic Zone are recorded digitally. The seismic data are also recorded on 16mm film and on a PDP 11/34 digital computer. Operation, analysis and publication of quarterly bulletins are an ongoing task. Cooperative arrangements with other organizations, such as the Tennessee Earthquake Information Center and the University of Kentucky, have been made in order to make the quarterly published Central Mississippi Valley Seismic Bulletin as complete as possible.

The 192 earthquakes located by the USGS and other cooperating networks during the year 1983 are given in the attached figure. The size of the symbols is scaled to the magnitude of the events. Of particular interest is the tight grouping of events on the Ohio River, 25 km upstream of its confluence with the Mississippi River. An extensive swarm with several magnitude 3+ earthquakes occurred at the same place in February, 1984.

2. We are continuing to function as a 'beta' site for the new Berkeley 2.9BSD version of the UNIX (TM ATT Technologies) operating system. In addition we have upgraded the Version 7 license to a UNIX System V license to acquire advanced software. The 2.9BSD system is adequately supporting a 2 Mbyte memory system with load averages often above 20.

Results

1. A Master's Thesis by L. Himes has been submitted. This thesis consists of a JHD inversion for earthquake locations, station corrections

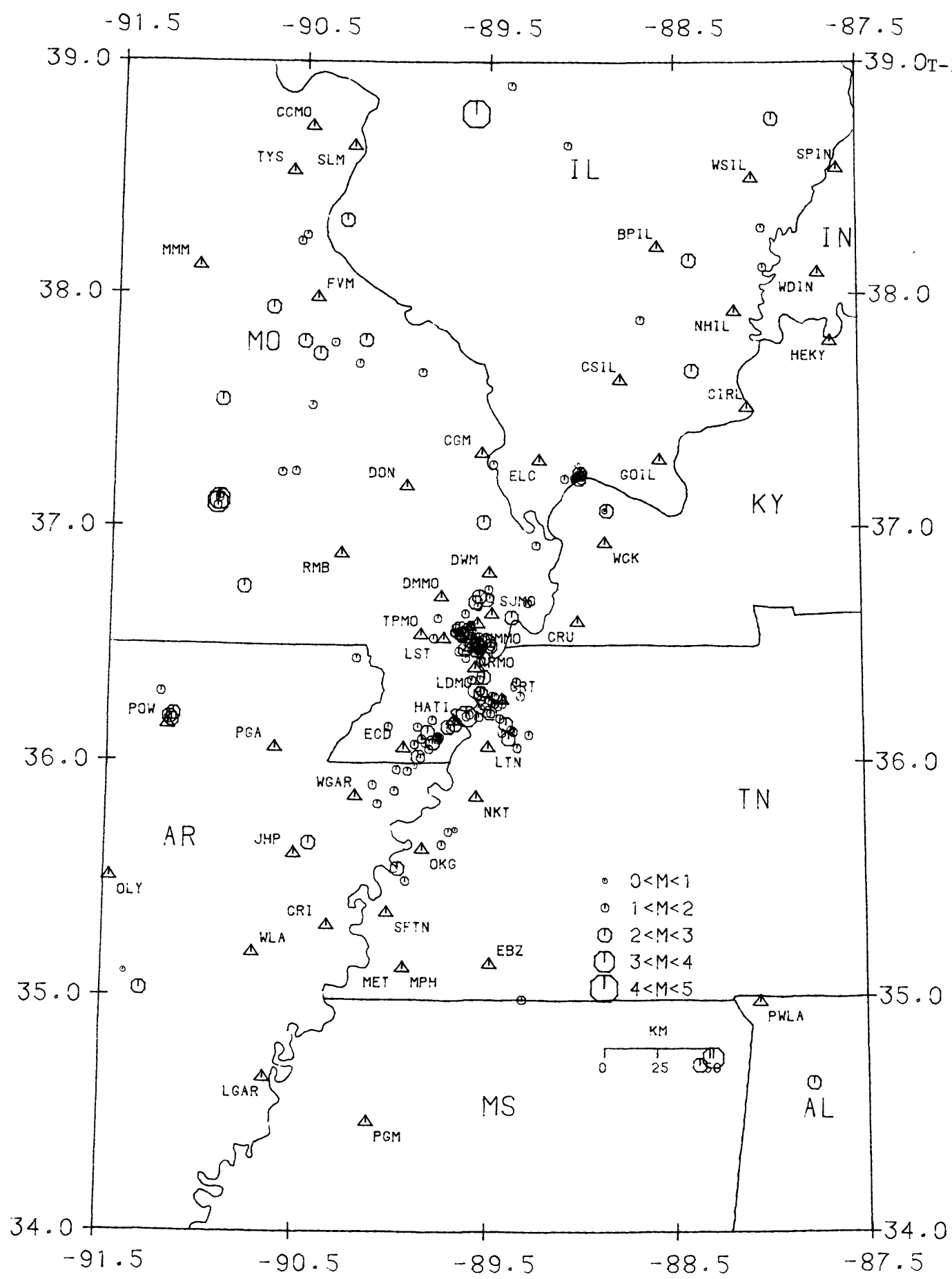
and velocity model for earthquakes on the main seismicity trends. Digital waveform data were used in a composite focal mechanism study of the relocated earthquakes. The effort of carefully sieving the earthquake data has provided good three-dimensional patterns of earthquake locations compatible with the composite focal mechanisms.

2. Spectral scaling studies of the Miramichi, New Brunswick, earthquake sequence continues using Canadian ECTN data. Lg attenuation in several frequency bands is defined. A comparison of near-field and far-field spectra is also a subject of investigation.

3. Major research results are listed in the paper below.

Publications

Herrmann, R. B. and A. Kijko (1983). Short period Lg magnitudes: Instrument, attenuation and source effects, Bull. Seism. Soc. Am. 1835-1850.



CUMULATIVE EVENTS 01 JAN 1983 TO 31 DEC 1983
 LEGEND □ STATION ○ EPICENTER

United States Earthquakes

9920-01222

Carl W Stover

Branch of Global Seismology and Geomagnetism
U.S. Geological Survey
Denver Federal Center, MS 967
Denver, Colorado 80225
(303) 234-3994

Investigations

1. Ninety-five earthquakes in 24 states and Puerto Rico were canvassed by a mail questionnaire for felt and damage data. Twenty-five of these occurred in California and 16 in Idaho. The most significant event was the Borah Peak, Idaho earthquake of October 28, 1983 which was located at 44.058°N., 113.857°W., fixed depth of 10 km., magnitude 6.2mb and 7.3MS. There were four events that caused damage in the United States; one each in Hawaii, Idaho, New York, and Utah. The most damaging were the Hawaii and Idaho earthquakes with a maximum intensity of VII.
2. The United States earthquakes for the period October 1, 1983 through March 31, 1984, have been located and the hypocenters, magnitudes, and maximum intensities have been published in the Preliminary Determination of Epicenters.
3. Preliminary reports and isoseismal maps for the May 3, 1983, Coalinga, California; the October 7, 1983, Blue Mountain Lake, New York; and the October 28, 1983, Borah Peak, Idaho have been published.

Results

A maximum Modified Mercalli intensity of VII was assigned to November 16, 1983 Hawaii and the Borah Peak, Idaho earthquakes. Two deaths and \$12.5 million damage was attributed to the Idaho earthquake and about \$6 million damage to the Hawaii event. Most of the damage in Idaho occurred in Challis and Mackay, in Hawaii the damage was mostly in the Hilo area.

United States earthquake data for April-September 1982 has been published in circular 896-B and 896-C. The data for October-December 1982 has the Director's approval and is being printed.

United States earthquake data for 1981 has been published in the first annual issue of "United States Earthquakes", a U.S. Geological Survey Special Publication.

Reports

Reagor, B.G., Stover, C.W., Minsch, J.H., and Brewer, L.R., 1983, Earthquakes in the United States, April-June 1982: U.S. Geological Survey Circular 896-B, 28 p.

Stover, C.W., 1983, Intensity distribution and isoseismal map, in the 1983 Coalinga, California Earthquakes: California Department of Conservation, Division of Mines and Geology, Special Publication 66, p. 1-4.

Minsch, J.H., Stover, C.W., Brewer, L.R., and Baldwin, F.W., 1984, Earthquakes in the United States, July-September 1982: U.S. Geological Survey Circular 896-C, 30 p.

Stover, C.W., Reagor, B.G., and Algermissen, S.T., 1984, United States earthquake data file: U.S. Geological Survey Open-File Report 84-225, 123 p.

Stover, C.W., 1984, Preliminary isoseismal map for the Blue Mountain Lake, New York, earthquake of October 7, 1983: U.S. Geological Survey Open-File Report 84-263, 6 p.

Stover, C.W., 1984, Preliminary isoseismal map and intensity distribution for the Borah Peak, Idaho, earthquake of October 28, 1983: U.S. Geological Survey Open-File Report 84-297, 6 p.

Reagor, B.G., and Baldwin, F.W., 1984, Intensity survey of the Borah Peak, Idaho, earthquake of October 28, 1983: U.S. Geological Survey Open-File Report 84-166, 79 p.

The Historical Seismicity of Central United States: 1811-1928

14-08-0001-21251

Ronald L. Street
Department of Geology
University of Kentucky
Lexington, KY 40506
(606) 257-4777

1. Objective

The objective of this project is to upgrade the record of seismicity for the central United States, consisting of earthquakes that occurred prior to 1928 when the U.S. Coastal and Geodetic Survey began to systematically collect such data.

2. Discussion

For the purposes of this study, a total of eighty-one earthquakes that occurred in the seven state area of Kentucky, Tennessee, Arkansas, Missouri, Illinois, Indiana and Ohio were selected for detailed documentation. Table 1 is a list of those earthquakes being studied: data sources for the indicated dates, origin times, epicentral locations, and felt areas are Nuttli (1979), Street (1980 and 1982), and personal notes that will be fully documented in the final report. The earthquakes studied were selected on the basis of their published felt areas.

The plan for the study consists of four phases: organization, documentation, interpretation and presentation of the results. The first two phases have been completed, while the third and final phases of the study are nearing completion. The results of the work completed to date indicates that sufficient evidence exists that many of the earthquakes parameters listed in Table 1 will need to be revised.

3. Conclusions and Recommendations

The original intent of this study was to investigate all of the earthquakes in the seven state area that supposedly occurred in that region prior to 1928. However, due to funding limitations, it was necessary to restrict the work effort to just the larger events. Based on the results of this study, it is probable that many of the smaller central United States earthquakes are not well documented. Therefore it is suggested that either the smaller central United States earthquakes not be incorporated into seismicity studies of the region, or else that an effort be made to more thoroughly document them.

4. References

- Nuttli, O. W. (1979). Seismicity of the central United States, Geo. Soc. Am., Reviews in Eng. Geology, IV, 67-93.
- Street, R. (1980). The southern Illinois earthquake of September 27, 1891, Bull. Seism. Soc. Am., 915-920.
- Street, R. (1982). A contribution to the documentation of the 1811-1812 Mississippi Valley earthquake sequence, Earthquake Notes, 53, 39-52.

TABLE 1

CENTRAL UNITED STATES EARTHQUAKES REVIEWED

| DATE mo-day-yr | TIME (GMT) hr - min | LAT/LONG N /W | FELT AREA sq. km. |
|-------------------|------------------------|------------------|----------------------|
| 12-16-1811 | 08-15 | 36.0/90.0 | 5000000. |
| 12-16-1811 | 14-15 | 36.0/90.0 | 5000000. |
| 01-23-1812 | 15-00 | 36.3/89.6 | 5000000. |
| 02-07-1812 | 09-45 | 36.5/89.6 | 5000000. |
| 07-05-1827 | 11-30 | 38.3/85.8 | 430000. |
| 02-04-1833 | | 42.3/85.6 | 20000. |
| 06-09-1838 | 14-45 | 38.5/89.0 | 500000. |
| 12-28-1841 | 05-50 | 36.5/89.5 | 100000. |
| 01-05-1843 | 02-45 | 35.5/90.5 | 1500000. |
| 02-17-1843 | 05 | 35.5/90.5 | 250000. |
| 08-09-1843 | | 35.5/88.2 | 40000. |
| 12-18-1853 | | 36.6/89.2 | 100000. |
| 02-28-1854 | 08-45 | 37.6/84.5 | 20000. |
| 11-09-1856 | 10 | 36.6/89.5 | 80000. |
| 10-08-1857 | 10 | 38.7/89.2 | 200000. |
| 08-07-1860 | 15-30 | 37.8/87.5 | 80000. |
| 08-17-1865 | 15 | 36.5/89.5 | 250000. |
| 05-03-1873 | 21 | 36.0/80.6 | 30000. |
| 06-18-1875 | 13-43 | 40.2/84.0 | 100000. |
| 09-25-1876 | 06-15 | 38.5/87.8 | 150000. |
| 07-15-1877 | 00-40 | 36.8/89.7 | 65000. |
| 03-12-1878 | 10 | 36.8/89.1 | 40000. |
| 11-19-1878 | 05-52 | 36.7/89.3 | 350000. |
| 07-14-1880 | 02-30 | 35.5/90.3 | 25000. |
| 07-28-1882 | | 37.6/90.6 | 25000. |
| 09-27-1882 | 10-20 | 39.0/89.5 | 100000. |
| 10-15-1882 | 05-50 | 39.0/89.5 | 20000. |
| 10-15-1882 | 10-35 | 39.0/89.5 | 20000. |
| 01-11-1883 | 07-12 | 37.0/89.2 | 200000. |
| 07-14-1883 | 07-30 | 37.0/89.1 | 25000. |
| 12-05-1883 | 15-20 | 36.3/91.2 | 250000. |
| 09-19-1884 | 20-14 | 40.7/84.1 | 320000. |
| 03-18-1886 | 05-59 | 37.0/89.2 | 45000. |
| 02-06-1887 | 22-15 | 38.7/87.5 | 170000. |
| 08-02-1887 | 18-36 | 37.0/89.2 | 170000. |
| 09-27-1891 | 04-55 | 37.0/89.2 | 500000. |
| 10-31-1895 | 11-08 | 37.0/89.4 | 2500000. |
| 04-26-1897 | 04 | 35.8/89.6 | 20000. |
| 06-14-1898 | 15-20 | 36.0/89.4 | 120000. |
| 04-30-1899 | 02-05 | 38.8/87.0 | 100000. |
| 02-15-1901 | 00-15 | 36.0/90.0 | 30000. |
| 01-24-1902 | 10-48 | 38.6/90.2 | 130000. |
| 02-09-1903 | 00-21 | 37.8/89.3 | 180000. |

| | | | |
|------------|-------|-----------|---------|
| 10-05-1903 | 02-56 | 37.0/90.0 | 120000. |
| 11-04-1903 | 18-18 | 36.9/89.3 | 340000. |
| 11-04-1903 | 19-14 | 36.9/89.3 | 340000. |
| 11-27-1903 | 09-20 | 36.5/89.5 | 180000. |
| 08-22-1905 | 05-08 | 36.8/89.6 | 325000. |
| 12-28-1908 | 21-15 | 37.0/89.0 | 80000. |
| 05-26-1909 | 14-42 | 42.5/89.0 | 800000. |
| 07-19-1909 | 04-34 | 40.2/90.0 | 100000. |
| 08-16-1909 | 22-45 | 38.3/90.1 | 45000. |
| 09-27-1909 | 09-45 | 39.5/87.4 | 250000. |
| 10-23-1909 | 07-10 | 37.0/89.5 | 125000. |
| 03-31-1911 | | | |
| 01-02-1912 | 16-21 | 41.5/88.5 | 150000. |
| 12-07-1915 | 18-40 | 36.7/89.1 | 120000. |
| 05-21-1916 | 18-34 | 36.6/89.5 | 20000. |
| 04-09-1917 | 20-52 | 38.1/90.2 | 550000. |
| 06-09-1917 | 13-14 | 36.8/90.4 | 45000. |
| 10-04-1918 | | | |
| 10-16-1918 | 02-15 | 36.0/89.2 | 100000. |
| 05-25-1919 | 09-45 | 38.4/87.5 | 65000. |
| 05-01-1920 | 15-15 | 38.5/89.5 | 60000. |
| 03-14-1921 | 12-15 | 39.5/87.5 | 65000. |
| 01-11-1922 | 03-42 | 37.9/87.8 | 25000. |
| 03-22-1922 | 22-30 | 37.3/88.9 | 150000. |
| 03-23-1922 | 21-45 | 37.0/88.9 | 50000. |
| 03-30-1922 | 16-53 | 36.1/89.6 | 40000. |
| 11-27-1922 | 03-31 | 37.8/88.5 | 130000. |
| 10-28-1923 | 17-10 | 35.5/90.4 | 120000. |
| 11-26-1923 | 23-25 | 35.5/90.4 | 23000. |
| 01-01-1924 | 03-05 | 35.4/90.3 | 150000. |
| 04-02-1924 | 11-18 | 37.0/89.1 | 80000. |
| 06-07-1924 | 05-42 | 36.4/89.5 | 25000. |
| 04-27-1925 | 04-05 | 38.3/87.6 | 250000. |
| 09-02-1925 | 11-55 | 38.8/87.5 | 200000. |
| 09-20-1925 | 09-09 | 37.8/87.5 | 25000. |
| 05-07-1927 | 08-28 | 35.7/90.6 | 300000. |
| 07-20-1927 | | 35.8/86.0 | 180000. |
| 08-13-1927 | 16-10 | 36.4/89.5 | 65000. |

EARTHQUAKE HAZARD RESEARCH IN THE GREATER LOS ANGELES BASIN
AND ITS OFFSHORE AREA
14-08-0001-21858

Ta-Liang Teng
Thomas L. Henyey
Center for Earth Sciences
University of Southern California
Los Angeles, California 90089-0741

INVESTIGATIONS

The Geophysics Laboratory at the University of Southern California is conducting a detailed investigation of earthquake activities and related phenomena in the greater Los Angeles basin and its offshore area. Particular attention has been given to the evaluation of parameters of importance in earthquake hazards along active faults in the Los Angeles basin, and the possible causal effect on seismicity due to waterflooding in oil fields along the Newport-Inglewood fault.

A modern 40-element seismic network has been operating in the Los Angeles basin area for the past ten years. In addition to conventional surface sensors, we have successfully developed and deployed downhole seismometers to improve the detection threshold in the central Los Angeles basin area where high urban noise prevents surface instruments from operating at high gain.

SUMMARY

The first of our seismic stations went into operation a week before the February 9, 1971 San Fernando earthquake. During the first three years of seismic monitoring, attention was centered on the Newport-Inglewood fault which passes through west-central Los Angeles from Beverly Hills to Newport Beach. As seismic data accumulated during the course of this investigation, it became clear that several other nearby faults -- the Malibu Coast-Santa Monica-Raymond fault, the Palos Verdes fault, and faults in the San Pedro Channel and the Santa Monica basin -- are all potentially active tectonic features which pose equally important earthquake hazards as does the Newport-Inglewood fault. To more adequately cover these adjacent faults, we have been systematically adding stations on land and offshore to close up the seismic monitoring gaps, including placing downhole seismometers to enhance the signal-to-noise ratio.

A seismic hazard analysis making use of all available seismic data from 1932 to the present has been made for both the Los Angeles basin area and the coastal zone of southern California. Maximum expected earthquake magnitudes are estimated from the historical seismicity and the mapped fault lengths. A strain release map has been prepared for the southern California coastal zone (Henyey and Teng, 1975).

Based on the strong motion data from the San Fernando earthquake and the subsurface geology from oil drilling data, a correlation analysis is made to study the effects of sediment thickness and basement topography on strong ground motions. The results of this analysis have been presented as a special technical report (Cerri and Teng, 1976). Making use of seismic data from networks in southern California, we have performed a thorough analysis of seismicity patterns and fault-plane solutions (Figure 1); compressional stress vectors have been derived (Buika and Teng, 1979). They are compared with the most recent known fault displacements in order to evaluate the regional stress field and relative hazards on the concerned faults in our monitoring area. Based on the recorded events, a travel-time analysis is made (McElrath and Teng, 1981) that derived the station delays as a function of epicentral distance and azimuth to earthquakes. An extensive program of 3-dimensional structural inversion of the Los Angeles basin is underway using the seismic data base gathered by this network. This program represents a forthcoming Ph.D. thesis which will be completed before the end of 1984.

RESEARCH AND DEVELOPMENT ON A NEW TELEPHONE TELEMETRY SYSTEM

There is an outstanding problem in modern seismic network operation utilizing telephone telemetry. The dynamic range of the telemetry link (VCO/Phone Line/Discriminator) is usually 45 dB or less. With the large dynamic ranges for sensors and for computer-based digital recording systems, the present telemetry link forms a bottleneck which severely limits the seismic signal flow. Oftentimes, the networks are tuned to the highest sensitivity permissible by the background noise in order to improve the detection threshold. The common results are: 1) clipping of signal amplitude begin to occur for local events larger than M3, and 2) extensive clipping appears for events larger than M4 in records from almost all network stations except the noisiest ones (see Figure 2 for example). This limitation presents a great shortcoming on the operation of modern telemetered seismic networks, as the waveform information is usually lost which otherwise can be extremely valuable for us to learn more about the source and structure. Therefore, despite the sophisticated digital recording of the entire seismogram, the usable information is mainly furnished at the point of the onset of the P wave. This limitation can be and must be overcome to remove this choking point of seismic data flow.

We are developing a new generation of seismic telemetry system, i.e., a new generation of smarter preamplifier/VCO-discriminator systems that not only permits a larger effective dynamic range (up to 120 dB) so as to keep all signals on scale, but also allows signal detection and some storage at the field site so that additional earthquake signals (say, all three components instead of one) can pass through a single \pm 125 Hz channel of transmission link. Large dynamic range telemetry systems do exist, but are expensive and require a large bandwidth only available for customized microwave links. The new seismic telemetry system we have in mind is one that can readily be adapted to the existing narrow band (400 Hz to 4,000 Hz) voice-grade telephone

circuit now in use*. The research seeks an economical and practical solution that would augment and optimize the dynamic range and the efficiency of the transmission link. Preliminary development work on this new telemetry system has been started at USC. Obviously, this system involves low power consumption μProcessor-based circuitry. We are confident that our system will accommodate 8-channel seismic signal flow. We plan to put one of our seismic data phone lines on the new telemetry system to fully field test it later this year. This development should also have important benefit to the current operation of other telemetered seismic networks.

REFERENCES

- Buika, J. A. and T. L. Teng, A seismicity study for portions of the Los Angeles Basin, Santa Monica Basin, and Santa Monica Mountains, California, U.S.C. Geophysical Laboratory Technical Report 79-9, 1979.
- Cerri, S. T. and T. L. Teng, Correlation of strong ground motion and local site geology in Los Angeles during the San Fernando earthquake, February, 1971, U.S.C. Geophysical Laboratory Technical Report 76-4, 1976.
- Heney, T. L. and T. L. Teng, Oil and tar seep studies on the shelves of southern California: III. Seismicity of the southern California coastal zone, U.S.C. Geophysical Laboratory Technical Report No. 75-4, 1975.

*FDM at 250 Hz per channel with 90 Hz guard band.

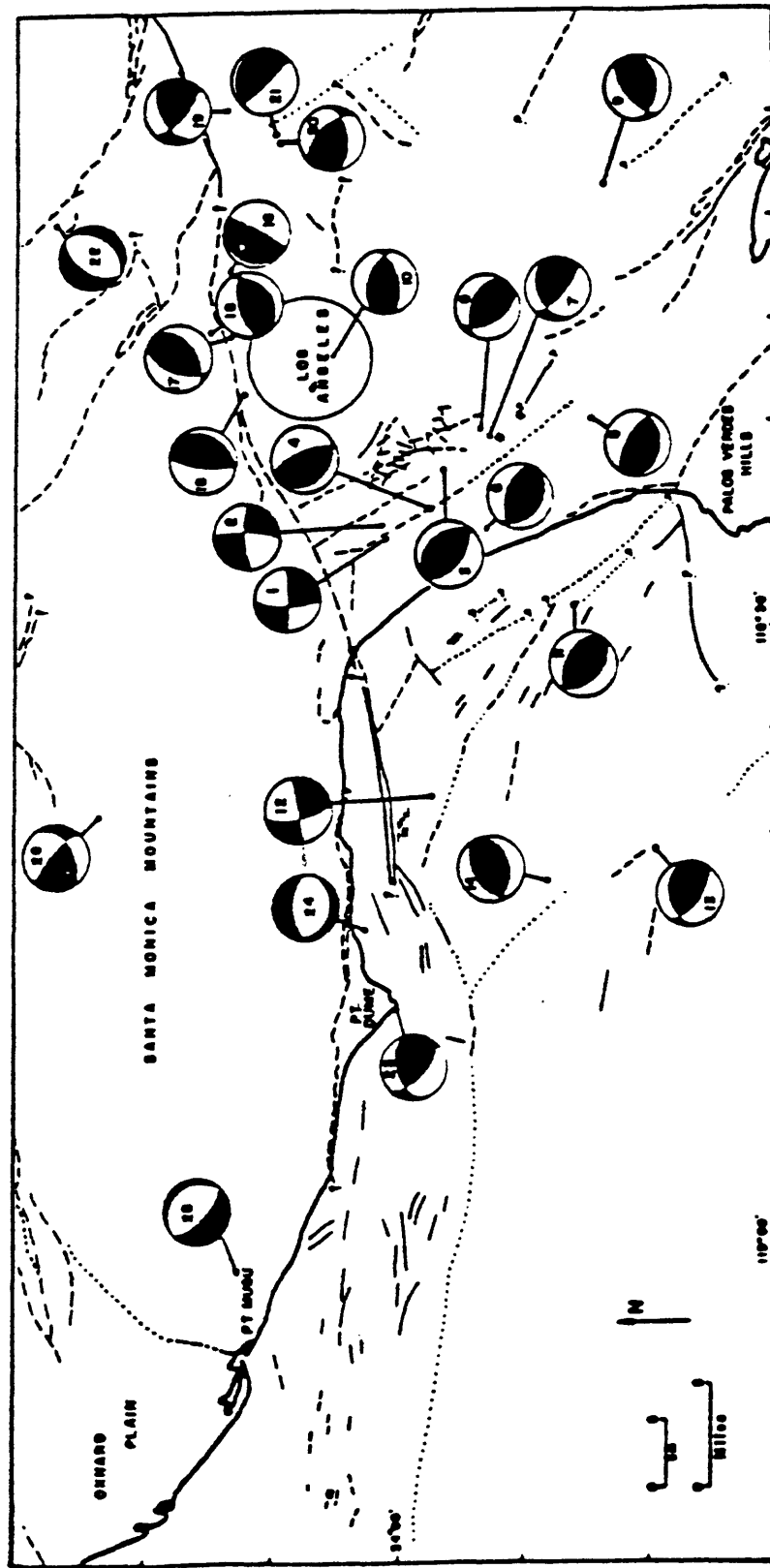


Figure 1. Fault-plane solution map for individual earthquakes, 1973-1976. Lower hemisphere projection; Black quadrants indicate compression; white quadrants indicate dilitation; from Buika and Teng (1979).

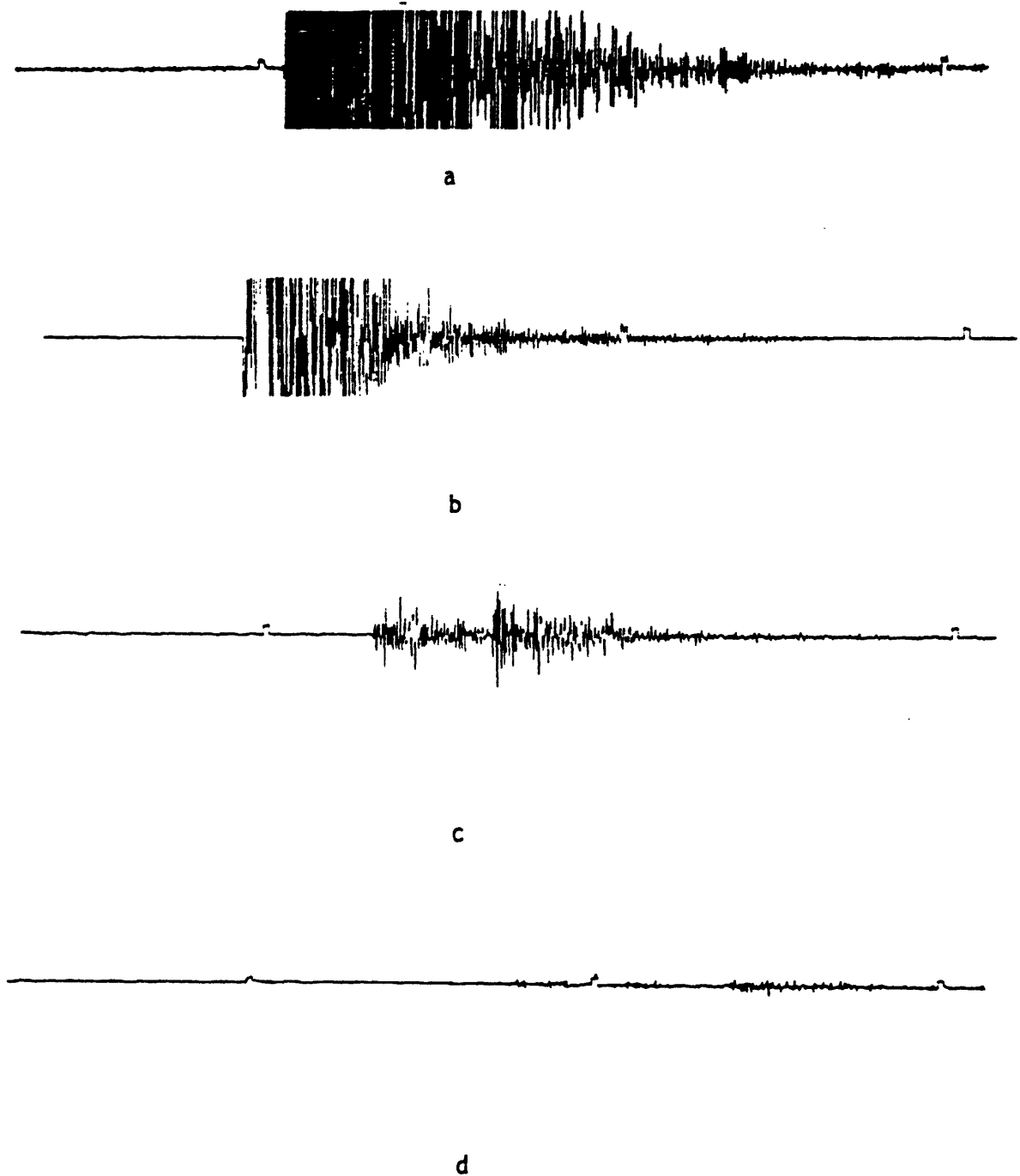


Figure 2 . a) Saturated waveform due to limited dynamic range.
b) Saturated waveform due to limited dynamic range.
c) Optimized recording full utilize the limited dynamic range.
d) Recording underutilize the limited dynamic range.

INTEGRATED STUDIES OF EARTHQUAKE POTENTIAL, PREDICTION, AND HAZARDS
IN THE WASATCH FRONT URBAN CORRIDOR AND ADJACENT
INTERMOUNTAIN SEISMIC BELT

14-08-0001-21856

W.J. ARABASZ, R.B. SMITH, J.C. PECHMANN, and W.D. RICHINS*

Department of Geology and Geophysics
University of Utah
Salt Lake City, Utah 84112
(801)581-6274

Investigations

1. Preliminary analysis of the aftershock sequence of the M_s 7.3 Borah Peak, Idaho, earthquake of October 28, 1983, based on both fixed- and portable-network recording, and implications for analogous events on the Wasatch Front.
2. Source properties of the M_s 7.3 Borah Peak earthquake from local and teleseismic data.
3. Pn travel-time variations in the Wasatch Front area from local and near-regional earthquakes, and implications for earthquake studies.
4. Swarm seismicity and deep hydraulic fracturing within 10 km of the southern Wasatch fault.
5. Instrumental calibration procedures for earthquake source studies.

Results

1. The M_s 7.3 Borah Peak earthquake occurred along a Holocene segment of the Lost River fault, a major Quaternary normal fault zone (Figure 1). Aftershocks located using a dense network of portable stations and a velocity model from nearby refraction profiles define a NW-trending 60 km-long aftershock zone that is 10 km wide and displaced approximately 7 km SW from the 34 km long surface fault. The entire aftershock zone became active immediately following the main shock. No aftershocks larger than M_1 5.8 have occurred. Hypocenters along the NW part of the aftershock zone extend to depths of approximately

*D. I. Doser and J. F. Peinado also contributed significantly to this project during the report period.

12 km, but do not show a planar distribution. Aftershocks in the SE part of the aftershock zone, however, define a plane that dips approximately 45° SW and intersects the surface near the fault scarp. Relatively few aftershocks occurred on the shallow part of the projected fault at depths less than about 4 km and relatively few aftershocks occurred within 6 km of the mainshock epicenter. The location of the mainshock (using well-located aftershock master events) relative to the surface faulting and the main aftershock zone suggests unilateral rupture propagation to the NW. Fault plane solutions for 39 aftershocks of $M > 3$ show a variety of fault orientations, but most indicate normal faulting along faults parallel to the main surface break or to W- to NW-striking fault splays near the NW end of the surface break. Vibroseis reflection data across the mainshock area reveal a complex structure at depths of 2 to 4 km that may relate to normal faulting in the vicinity of a pre-existing thrust. The mainshock nucleated at a depth of approximately 16 km, within a rheologically modeled brittle to ductile transition zone and near the depth of an inferred shear stress maximum.

Important characteristics of the Borah Peak earthquake and similarities between the Lost River and Wasatch fault zones that may influence our understanding of future large Wasatch Front earthquakes are: 1) segmentation of a major Quaternary fault zone with evidence of repeated Holocene displacement along a now active segment; 2) moderate-dip planar normal faulting; 3) nucleation of the large mainshocks at the maximum depth of seismicity; and 4) mainshock and aftershocks located several kilometers laterally offset from the surface fault trace. The position of a projected location of the mainshock-aftershock zone of a hypothetical Borah Peak-type earthquake on the Wasatch Front would be beneath the central or western parts of the deep alluviated valleys.

2. First-motion data from short-period body waves have been used to determine the focal mechanism for the Borah Peak mainshock (Figure 2). The azimuth of the 45° southwestward dipping nodal plane is 138° , consistent with the observed strike of surface faulting. The rake angle is -60° . Modeling of long-period body waves from the mainshock recorded at teleseismic distances gives a focal depth of 16 ± 4 km and a source time function of 12 seconds duration. The amplitudes of P, pP and sP phases obtained in the modeling process were used to invert for the unconstrained seismic moment tensor. The double couple component of the moment tensor (Figure 2) is essentially the same as the mechanism from the short-period first motion data. The average moment is 6.0×10^{26} dyne-cm and the stress drop is 50 bars.

3. Pn arrivals are frequently used in earthquake locations and focal mechanism determinations with the University of Utah seismic network because of the large station spacing and the broad region of coverage. An analysis of Pn travel-times from local and near-regional

earthquakes has therefore been undertaken in order to test the validity of our currently used Wasatch Front velocity model at Pn distances (greater than about 130 km). The travel times recorded out to about 250 km are consistent with velocity models derived from refraction data. These models feature a thin crust (25-28 km) and low upper mantle velocities (7.4-7.6 km/sec). However, at distances beyond 250 km the first arrivals have significantly higher apparent velocities (7.8-7.95 km/sec), indicating that the P-wave velocity increases to approximately 7.9 km/sec at a depth of about 40 km or more beneath the Wasatch Front. Travel-time residuals for this upper mantle arrival increase systematically from west to east across the array. The variation in residuals exceeds 1.5 seconds across central Utah. It is difficult to attribute more than about 0.5 seconds of these delays to lateral crustal velocity variations and crustal thickening across the Basin and Range-Colorado Plateau transition zone. Thus, this upper mantle discontinuity is inferred to have a significant eastward dip beneath the Wasatch Front.

4. In June-July 1982, earthquake swarms (M2.0 or less) were recorded originating within a few km of a deep exploration well (Chevron U.S.A. #1 Chriss Canyon, TD 5,344 m), coincidentally located within a temporary 10-station network. On April 16, 1982, an "acid-breakdown hydrofrac" had been made in the wellbore at a depth of 5,070 m using 4,000 gal of 28% HCl solution. Combining the hydrofrac and earthquake data provides the following information. An instantaneous shut-in pressure measured during the hydrofrac indicates an in situ minimum horizontal compressive stress of approximately 750 bars at 5,070 m depth. Methodology outlined, for example, by Zoback and Hickman (1982) suggests near-critical in situ stress differences at the hydrofrac depth for frictional sliding on optimally-oriented faults. The swarm earthquakes, accurately located with local velocity control, predominate at the level of the wellbore, and two-thirds cluster within 3.0 km map distance of the well bottom. Corresponding focal mechanisms based on both P-wave polarities and SV/P amplitude inversion indicate: normal faulting, a consistent northerly-trending nodal plane dipping steeply (72° - 86°)E, and near-horizontal T-axes trending WNW-ESE. Assuming causal connection between the swarm seismicity and pore-pressure changes due to fluid injection in the wellbore, distance-delay times suggest a bulk permeability of 10^{-1} to 10^0 mdarcy for pore-fluid diffusion.

5. An indirect approach to the problem of calibrating amplitude response for seismic network stations has been successfully tested using amplitude displacement spectra of initial P-waves from deep-focus teleseisms (M5.5 or greater). For a given teleseism the displacement spectra from a set of stations, corrected for instrument frequency response, are combined in the 1.6 to 3.2 Hz frequency band to form an average, which is then compared with individual spectra to yield relative gain values. Measurement of the absolute gain of one or more key stations allows calibration of the entire set. This

procedure is useful either for "bootstrap" calibration of a network or as a temporal check on the performance of previously calibrated stations. Results show consistent relative gains from one event to another. Relative gain from comparison of waveform amplitudes alone showed considerable scatter. Tests made with varying window length, from 1 to 2.5 sec, indicate that the displacement spectra are functions primarily of the station gain and the source; the inclusion of near-surface site reverberations in such a time window does not appear to alter the spectral ratios appreciably.

Reports and Publications

Arabasz, W. J., 1984, Swarm seismicity and deep hydraulic fracturing within 10 km of the southern Wasatch fault (abs.), Earthquake Notes 55 (1).

Doser, D. I., 1984, The 1959 Hebgen Lake, MT and the 1983 Borah Peak, ID Earthquakes: Examples of Large Normal Fault Events in the Intermountain Region (abs.), Earthquake Notes 55 (1).

Renggli, C. and Smith, R. B., 1984, Estimates of crustal extension for the Basin-Range/Southern San Andreas associated with active seismicity (abs.), Earthquake Notes 55 (1).

Richins, W. D., Smith, R. B., King, J. J., Langer, C. J., Meissner, C. W., Pechmann, J. C., Arabasz, W. J., and Zollweg, J. E., 1984, The 1983 Borah Peak, Idaho, earthquake: A progress report on the relationship of aftershocks to the mainshock, surface faulting, and regional tectonics (abs.), Earthquake Notes 55 (1).

Smith, R. B. and Bruhn, R. L., 1984, Intraplate extensional tectonics of the western U. S. Cordillera: Inferences on structural style from seismic reflection data, regional tectonics, and thermal-mechanical models of brittle/ductile deformation, J. Geophysical Research (in press).

Snay, R. A., Smith, R. B. and Soler, T., 1984, Horizontal strain across the Wasatch Front near Salt Lake City, Utah, J. Geophysical Research 89, p. 1113-1122.

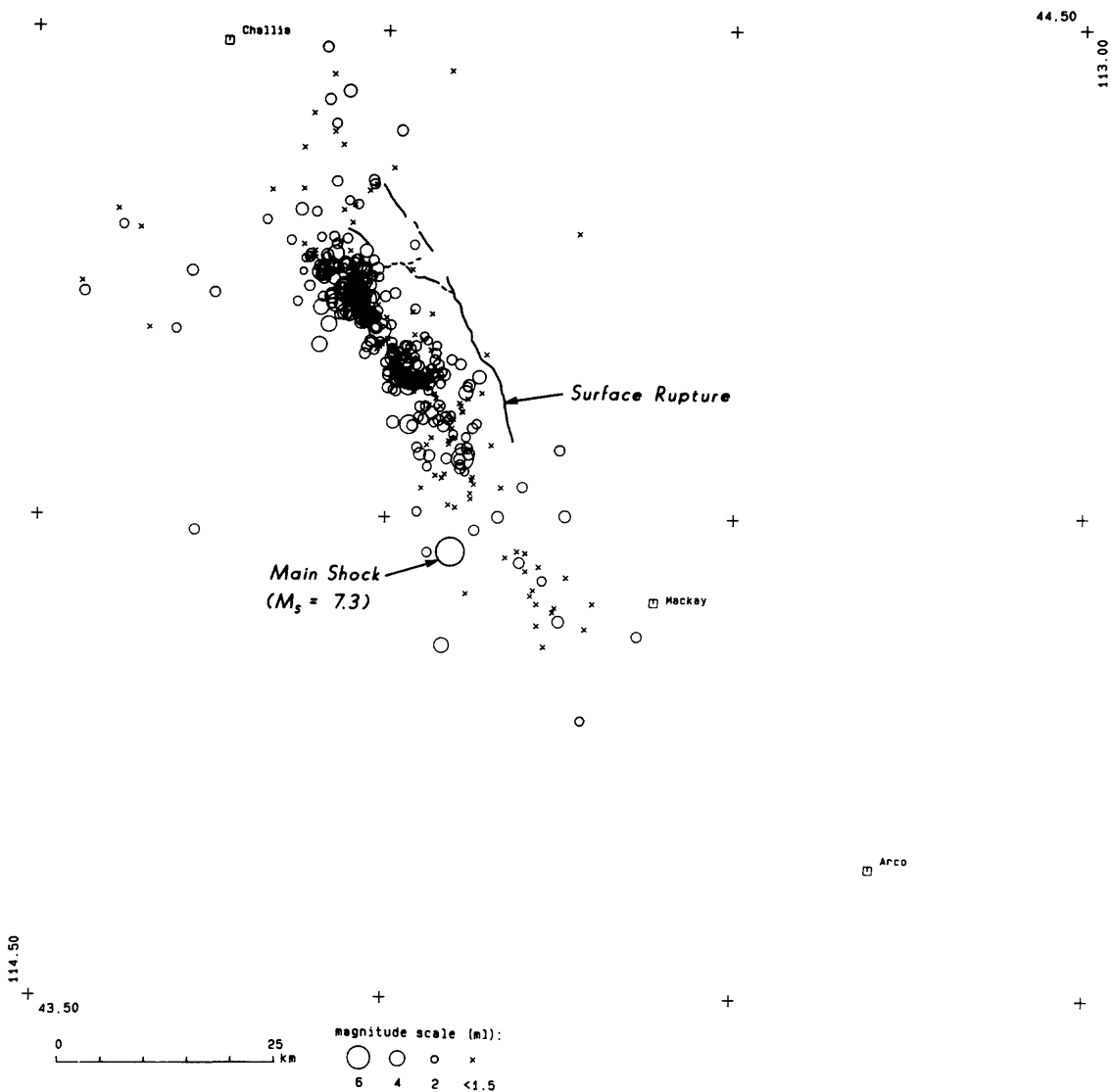
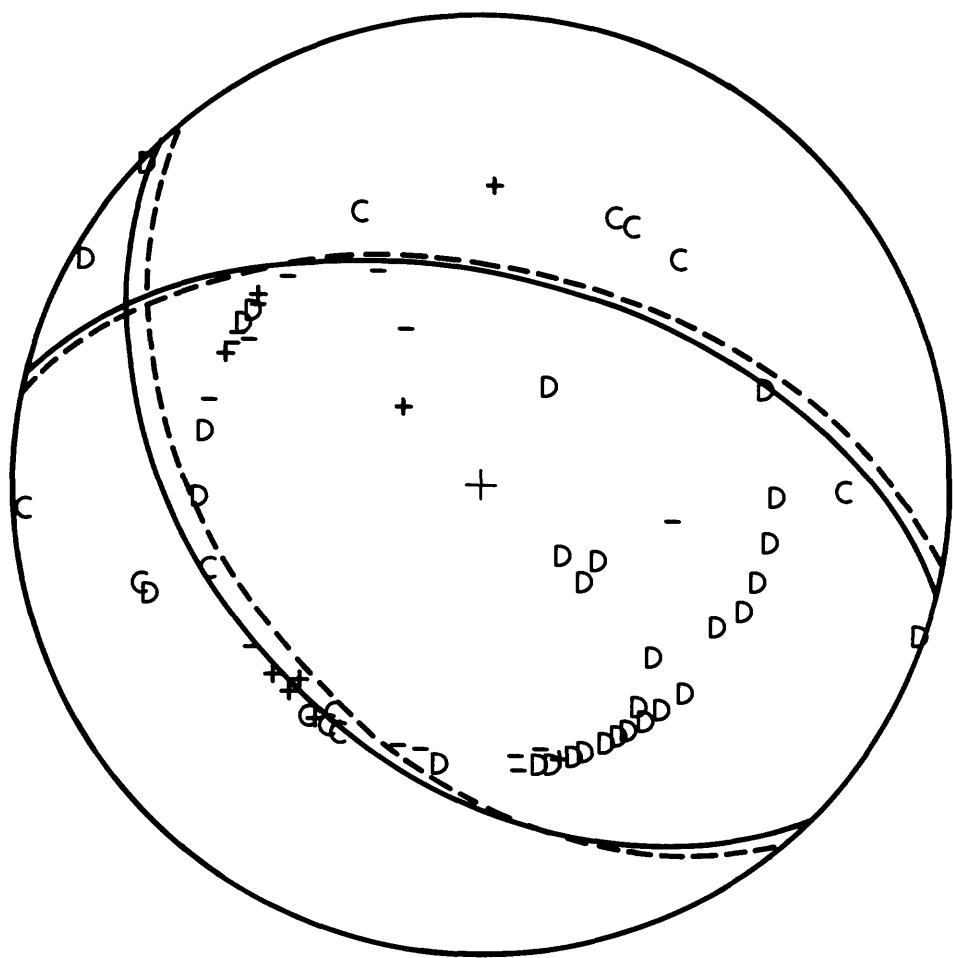


Figure 1. Map showing epicenters for the Borah Peak earthquake sequence, October 28 to November 19, 1983, and associated surface rupture.

BORAH PEAK MAINSHOCK
OCTOBER 28 1406



— Double couple component of
unconstrained moment tensor
- - - Fault plane solution

Figure 2. Focal mechanism for the Borah Peak earthquake from short-period local and teleseismic first motions (dashed nodal planes) and from moment-tensor inversion of long-period body waves (solid nodal planes).

NEOTECTONICS OF NEW ZEALAND: INSIGHT TO SAN ANDREAS
FAULT SYSTEM TECTONIC BEHAVIOR

14-08-0001-21882

William B. Bull and Peter L. K. Knuepfer
Geosciences Department
University of Arizona
Tucson, Arizona 85721

Bull: 602-621-2219; Knuepfer: 602-621-6006

INVESTIGATIONS

It is generally recognized that a critical aspect of seismic hazards is a thorough understanding of the geologic history of displacement across faults and folds as well as regional uplift and shear patterns. The late Quaternary history of a particular region is especially relevant in that most present-day movements on fault zones are consistent with latest Quaternary behavior on these same faults. So a consistent regional appraisal of late Quaternary earth deformation is a cornerstone of seismic hazards analysis.

1. Faulted Stream Terraces

The major strike-slip faults of the Alpine shear system, South Island, New Zealand (Figure 1) form a complex continental plate boundary as a trench-trench transform system. The Alpine fault and its splays in Marlborough (northeastern South Island) have a geometry very similar to the San Andreas fault system in southern California, and even in the San Francisco Bay region. Accordingly, an understanding of the temporal and spatial patterns of fault slip on these New Zealand faults and the associated regional deformational patterns can yield insight into the behavior of this complex plate boundary, and, by analogy, to the San Andreas fault system as well.

The faults of the Alpine shear system are ideally suited for studies of late Quaternary fault behavior, since each of the faults displaces several sequences of river terraces formed in the last 20,000 years or less. Many latest Pleistocene glacial moraines also are displaced. These moraines and terrace sequences preserve details of the history of latest Quaternary faulting, since older moraines and terraces are displaced by larger amounts than younger moraines and terraces. The purpose of our studies of faulted stream terraces and moraines has been to decipher details of the history of latest Quaternary slip across the complex continental Alpine shear system plate boundary.

This project is the second part of a New Zealand neotectonics study initiated in 1981-82 by the co-principal investigators. The scope of our studies of latest Quaternary slip across the Alpine shear system has involved two principal aspects: (1) measure latest Quaternary displacements at a large number of sites to obtain data that are really well-distributed and represent at least two sites on each major fault; (2) develop and/or improve on methods to date latest Quaternary surfaces that are displaced by active faults in New Zealand. In our desire to study many sites we have restricted ourselves to relatively accessible localities, many of which had already been mapped in differing detail by members of the New Zealand Geological Survey.

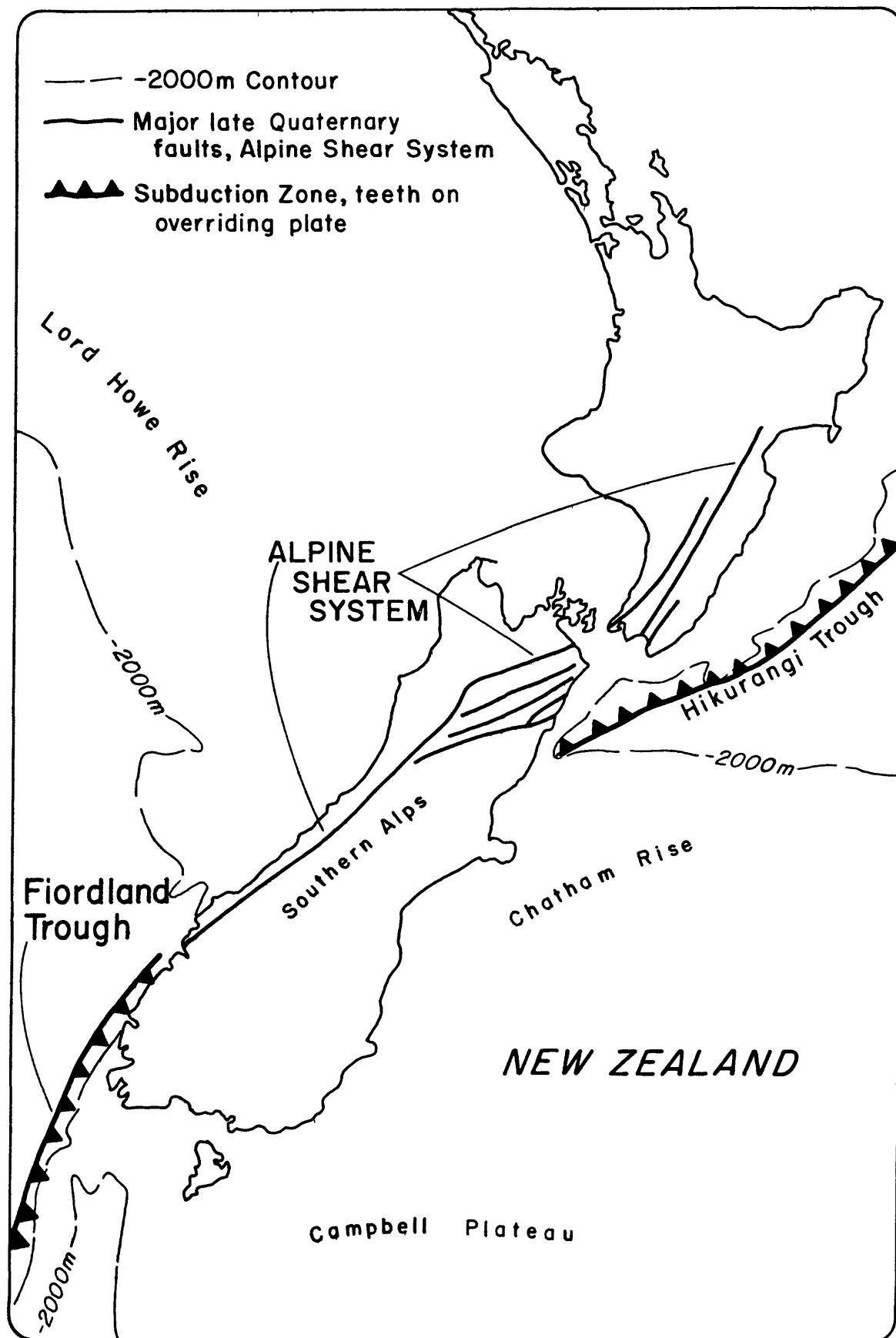


Figure 1.--Main active faults of the Alpine Shear System, New Zealand.

Our establishment of methods to date the terraces was motivated largely by the failure of ourselves and others in New Zealand to find suitable materials for radiocarbon dating at most sites. The coarse, cobbly nature of most of the stream deposits and the high energy of most New Zealand rivers combine to make preservation of charcoal, wood, or other datable materials the exception rather than the rule. Thus we have used indirect relative-absolute dating techniques calibrated at locations of known age as a basis for estimating ages of displaced geomorphic surfaces such as stream terraces or moraines. We emphasized two techniques: the thickness of weathering rinds developed in surface and/or subsurface cobbles of Torlesse graywacke; the morphologic and chemical properties of soils developed on geomorphic surfaces. Both of these techniques are calibrated by reference to sites of known radiocarbon age.

2. Uplifted Marine Terraces

The amounts and rates of downcutting by New Zealand rivers reflect the magnitudes and rates of ongoing uplift as well as climatically induced changes in discharge of water and sediment. However, it is the shore platforms that are present along much of the New Zealand coastline that provide data to assess late Quaternary uplift rates. They are geomorphic systems in equilibrium where a balance exists between available energy, sediment amount and size being transported across the platform, and hydraulic factors. Shore platforms typically form during relative high stands of sea level characterized by minor fluctuations, such as during the late Holocene. Subsequent decline of sea level terminates the construction of shore platforms and incorporates these coastal landforms into pre-existing fluvial systems.

Marine terrace time lines are directly tied to the chronology of major fluctuations of late Quaternary sea level. Thus it is the assumed worldwide general synchronicity of late Quaternary major high stands in glacio-eustatic sea level that is of paramount importance when using marine terraces to assess uplift rates. We believe that the flights of marine terraces on the New Zealand coastlines are part of an overall population of global marine terraces.

Materials for radiometric dating of the marine terraces are difficult to obtain for buried shore platforms. Entire flights of marine terraces along many coastlines lack either coral or volcanic materials that permit radiometric age determinations older than the upper limit of radiocarbon dating. However, when considered as sequences instead of single terraces, local flights may be correlated with the overall population of dated global marine terraces.

The objectives of this part of our investigation were to further develop and substantiate procedures for correlation of undated flights of marine terraces in New Zealand with the dated flights of terraces in New Guinea, which are regarded as being representative of the overall population of global marine terraces. Much of our recent field work concentrated on studies of exhumed shore platforms, remnants of degraded sea cliffs, and associated beach pebbles to altitudes of 2000 m at many locations within the Southern Alps.

RESULTS

1. Faulted Stream Terraces

We did field work in New Zealand from 30 November 1983 through 28 February 1984. Our studies of faults of the Alpine shear system involved three aspects:

1. Revisiting several sites first investigated in 1982 in order to map, sample soils, and/or sample rock weathering rinds.
2. Investigate additional fault study sites to obtain more complete coverage of the faults of interest, particularly emphasizing the obtaining of data from the main Alpine fault.
3. Obtain additional calibration localities in Marlborough for weathering-rind and soils analyses.

As a result of our 1983-84 field work we have expanded our number of fault study sites from 10 to 19; in addition 6 other locations were investigated but not used due to difficulties in interpretation, lack of suitability for dating techniques, etc. We have also expanded the number of calibration sites available for weathering-rind studies. When Chinn first described the systematic thickening of weathering rinds in graywacke cobbles from geomorphic surfaces, he had 10 sites as calibration points. Whitehouse and his coworkers expanded this number to 14. Our 4 additional sites corroborate the previously obtained data of Whitehouse and establish that rates of rock weathering in Marlborough are similar to other South Island study areas. These new data will be used to re-evaluate ages of faulted geomorphic surfaces and to provide the basis for slip-rate analyses.

We also obtained soil samples from 8 fault-study sites in order to assess time-dependent changes in soils morphology and chemistry. The results of these studies will be combined with the results of the weathering-rind studies to better constrain ages of faulted terraces, particularly along the Alpine fault where two well-studied chronosequences (Franz Josef and Reefton) are available for calibration.

2. Uplifted Marine Terraces

Flights of New Zealand marine terraces along coasts where uplift rates range from less than 0.5 mm/yr to 9 mm/yr can be correlated and dated by reference to the terraces in New Guinea dated in the age range of 30,000-340,000 years. The basis for the correlation is that unique differences in the number and altitudinal spacings of global marine terraces occur in a diagnostic manner for each uniform uplift rate. The procedure involves preparation of frequency-distribution plots, inferred uplift rate graphs, and altitude-age ratio graphs. The morphologies of landscape elements along the coasts and within the mountains of the Southern Alps are suggestive of remnants of formerly more extensive shore platforms associated with high stands of sea level. The most diagnostic landforms are notched spur ridges, flattening ridge crests and flat-topped ridges, accordant summits, and discordant saddles. Such landforms are present at all altitudes in the Southern Alps. The notched spur ridges at many localities clearly represent remnants

of exhumed shore platforms and their associated degraded sea cliffs. Late Quaternary glaciation has generally removed all traces of marine terrace remnants in the lower portions of the intervening valleys.

A further important line of evidence for the presence of uplifted marine terraces consists of rounded quartz pebbles. These have abrasion textures and impact marks that are identical to quartz pebbles on the modern high energy beaches along the northwest coast of the South Island. The rounded quartz pebbles are most commonly associated with landforms such as notched spur ridges; they occur at altitudes as high as 1800 m and are present on the summits along the main divide of the Southern Alps. Origins such as deposition by streams, weathering from in place quartz veins, and gastroliths of flightless birds such as the extinct moa seem highly improbable, given the range of locations in which we have found such pebbles associated with the characteristic landforms previously discussed. We conclude that these are uplifted beach pebbles.

Survey of helium in natural water wells and springs in southwest Montana
and Imperial Valley, California

Part VI - January 1 - December 31, 1983

W. P. Doering and Irving Friedman

U. S. Geological Survey, MS 963

Denver Federal Center

Denver, CO 80225

(303) 234-5531

9570-00382

Investigations

This report is of a continuing project begun in 1977 to evaluate a method to predict earthquakes. It involves a comparison of significant changes in helium found in natural water wells and springs with recorded earthquakes in the immediate vicinity of the wells or springs. A positive correlation was reported in the research done by Bulasevich and Bashorin (1974). Work in previous years on this project is reported by Doering and others (Doering and Friedman, 1980a, 1980b, 1982, 1983, and Doering and others, 1981).

Results

We received water samples from eight wells and four springs situated northwest of Yellowstone National Park and from four wells in the Imperial Valley of southern California. These sixteen stations located in the Hebgen Lake area of Montana and southern terminus of the San Andreas fault zone of California were chosen because the water contains measurable amounts of helium and they are in active seismic regions. We received samples from all but three of these stations during all of the year 1983. Table 1 gives a short description of these stations and Figures 1 and 2 shows their approximate location on maps.

The sample collectors withdraw about 9 milliliters of well or spring water into a plastic syringe and then injected it into a partially evacuated collection tube. A sample is usually taken once a day. When five tubes are thus filled they are mailed to the Geological Survey laboratory at the Denver Federal Center. There the gas in the ullage space above the water in the sample tube is extracted and analyzed for helium on a mass spectrometer. The method is described in Doering and others, 1981.

The analytical precision is $\pm 5\%$. An additional $\pm 15\%$ error is due to station variations due to water temperature changes, amount of water collected, and the method and daily time of sample collection. At the well stations the helium concentrations may be affected by the quantity of water being pumped just before the sample was taken. The daily record of the amount of helium present at each station is shown on Figures 3 through 19. Four scales are used on the graphs because there are large helium concentration differences between stations. There are a total of 8,340 individual analysis reported. Numerical (Julian) dates are given on these graphs but they may be converted to normally used calendar dates by use of Figure 20.

The National Earthquake Information Service located at Golden, Colorado reported six earthquakes having a magnitude greater than 3.5 that occurred in the reporting regions during 1983. Table 2 lists the date, epicenter location and magnitude of the two earthquakes that occurred in the Imperial Valley and

four earthquakes close to the Montana sampling network. These quakes are indicated by tick marks and labeled "EQ" on the dates of occurrence on the graphs of Figures 3 through 19.

Table 3 presents a summary of the helium data as related to changes in helium and earthquakes. These changes are listed by station number and Julian date. A + indicates there was a significant increase and a - indicates a significant decrease in helium beginning with the date shown and continuing for over 5 days. A significant change is defined as a change exceeding 20% of the amount present that continues for at least 5 days. The date of earthquakes are shown in column three. Column four shows the relationship of helium changes to earthquakes. A + indicates there was a change in helium preceding or about the same time as the occurrence of an earthquake. A - indicates there was a change in helium but no earthquake the preceding 30 days. At station 316 there was a sudden decrease in helium on day 146 (May 16) and a gradual increase beginning about day 314 (Nov. 10). This has occurred every year since 1980 when collecting was begun. These changes coincide with irrigation in the nearby fields.

Table 2.--Earthquakes in reporting areas in 1983

| Julian date | Calendar date | Latitude N. | Longitude W. | Region | Magnitude |
|-------------|---------------|-------------|--------------|------------------------------|-----------|
| 12 | Jan. 12 | 31.53 | 115.69 | S.W. of ElCentro, CA | 4.5 |
| 37 | Feb. 6 | 44.56 | 110.64 | N. of West Thumb, YNP, WY | 4.7 |
| 47 | Feb. 16 | 45.94 | 111.51 | Near Three Forks, MT | 3.7 |
| 194 | July 13 | 33.26 | 115.56 | N. of Calipatria, CA | 4.2 |
| 225 | Aug. 13 | 44.72 | 111.80 | W. of West Yellowstone, MT | 3.9 |
| 226 | Aug. 14 | 44.76 | 111.80 | W. of West Yellowstone, MT | 4.1 |

Table 3.--Dates of significant He changes and correlation with earthquakes

| Station No. | Julian date of start of significant He change (+increase, -decrease) | Date(s) of earthquake(s) | Significant He change and earthquake correlation (+ earthquake, - no earthquake) |
|-------------|--|--------------------------|--|
| 300 | | 37 | - |
| 300 | | 47 | - |
| 300 | 59+ | | - |
| 300 | | 225,226 | - |
| 301 | | 37 | - |
| 301 | | 47 | - |
| 301 | 162+ | | - |
| 301 | | 225,226 | - |
| 305 | 30+ | 37 | + |
| 305 | 34- | 37 | + |
| 305 | 40- | 47 | + |
| 307 | 37+ | 37 | + |
| 307 | 43- | 47 | + |
| 307 | 203- | 225,226 | + |
| 308 | 13+ | | - |
| 308 | 27- | 37 | + |
| 308 | | 47 | - |
| 308 | 52- | | - |
| 308 | 118- | | - |
| 308 | 128+ | | - |
| 308 | 224+ | 225,226 | + |
| 313 | 21- | 37 | + |
| 313 | 42- | 47 | + |
| 313 | 49- | | - |
| 313 | 181- | | - |
| 313 | | 225,226 | - |
| 314 | | 37 | - |
| 314 | | 47 | - |
| 314 | 58+ | | - |
| 314 | 182+ | | - |
| 314 | 214+ | 225,226 | + |

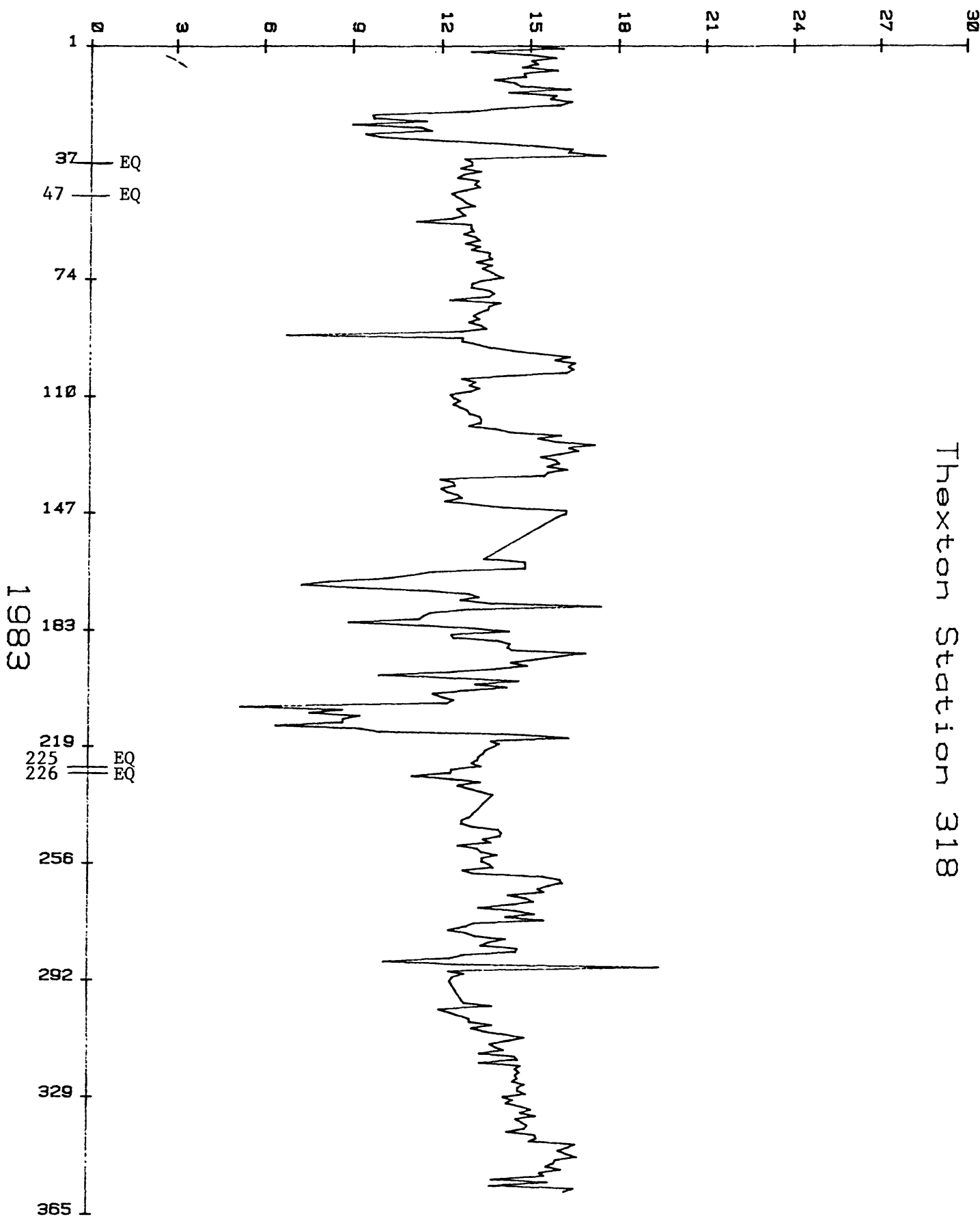
Table 3.--Dates of significant He changes and correlation with earthquakes, (Cont'd)

| Station No. | Julian date of start of significant He change (+increase, -decrease) | Date(s) of earthquake(s) | Significant He change and earthquake correlation (+ earthquake, - no earthquake) |
|-------------|--|--------------------------|--|
| 316 | | 37 | - |
| 316 | 45+ | 47 | + |
| 316 | 96+ | | - |
| 316 | 134- | | - |
| 316 | 146- | | - |
| 316 | | 225, 226 | - |
| 316 | 314+ | | - |
| 318 | 21- | 37 | + |
| 318 | 31- | 47 | + |
| 318 | 94+ | | - |
| 318 | 106- | | - |
| 318 | 122+ | | - |
| 318 | 138- | | - |
| 318 | 210- | 225, 226 | + |
| 318 | 221+ | 225, 226 | + |
| 318 | 291+ | | - |
| 321 | | 37 | - |
| 321 | | 47 | - |
| 321 | 218- | 225, 226 | + |
| 344 | | 12 | - |
| 344 | 116- | | - |
| 344 | 164+ | | - |
| 344 | | 194 | - |
| 344 | 205+ | | - |
| 348 | | 12 | - |
| 348 | 26+ | | - |
| 348 | 107- | | - |
| 348 | 177+ | | + |
| 348 | 190- | 194 | + |
| 348 | 227- | | - |
| 348 | 241+ | | - |
| 349 | 355 (1982)- | | - |
| 349 | 360 (1982)+ | 12 | + |
| 349 | 211+ | 194 | - |
| 349 | 271- | | - |
| 349 | 282+ | | - |

REFERENCES

- Bulashevich, Yu. P., and Bashorin, V. N., 1974, Combined use of helium surveying and seismic methods in the study of fault tectonics: *Geologiya; geofisika*, v. 15, p. 101-104.
- Doering, W. P. and Friedman, I., 1980a, Survey of helium in natural water wells and springs in southwest Montana and vicinity: U.S. Geological Survey Open-File Report 80-181, 42 p.
- Doering, W. P. and Friedman, I., 1980b, Survey of helium in natural water wells and springs in southwest Montana and vicinity, Part II-July 1-Dec. 31, 1979: U.S. Geological Survey Open-File Report 80-1257, 18 p.
- Doering, W. P., Friedman, I., and Veronda, G., 1981, Survey of helium in natural water wells and springs in southwest Montana and vicinity and Imperial Valley, California, Part III-Jan. 1-Dec. 31, 1980: U.S. Geological Survey Open-File Report 81-893, 58 p.
- Doering, W. P. and Friedman, I., 1982, Survey of helium in natural water wells and springs in southwest Montana and vicinity and Imperial Valley, California, Part IV-Jan. 1-Dec. 31, 1981: U. S. Geological Survey Open-File Report 81-486, 33 p.
- Doering, W. P. and Friedman, I., 1983, Survey of helium in natural water wells and springs in southwest Montana and Imperial Valley, California, Part V-Jan. 1-Dec. 31, 1982: U. S. Geological Survey Open-File Report 83-500, 32 p.
- U. S. Geological Survey, 1982, Preliminary determination of epicenters, No. 2-83 Feb. 2, 1983, No. 6-83 Mar. 2, 1983, No. 7-83 Mar. 10, 1983, No. 28-83 Aug. 3, 1983, No. 33-83 Sept. 9, 1983: U. S. Geological Survey National Earthquake Information Service.

HELIUM IN PPM/ML



Thexton Station 318

Figure 13.--Helium concentrations in water samples, Ennis, Montana.

Rodia Station 349

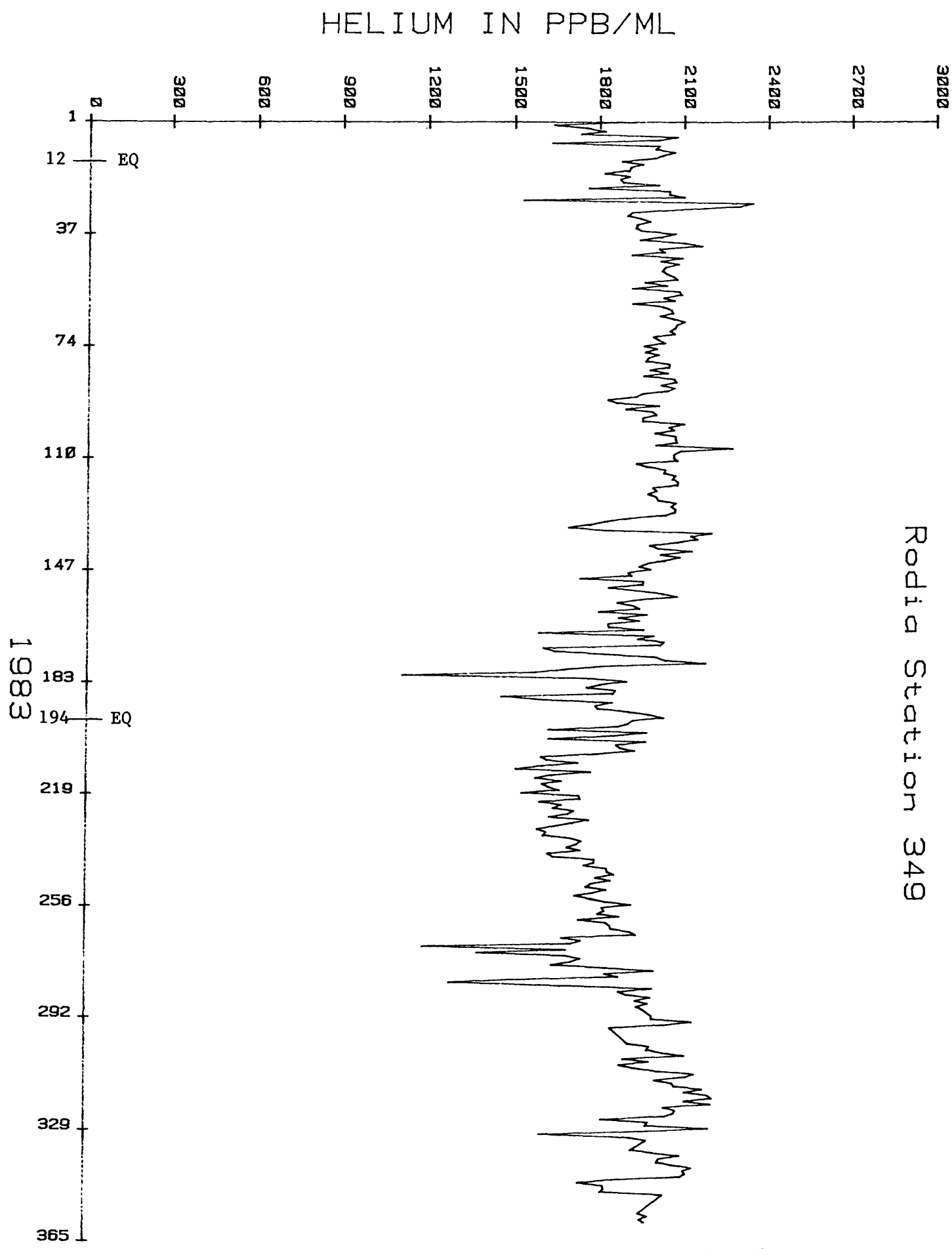


Figure 19.--Helium concentrations in water samples, Ocotillo, CA.

Global Seismology

9920-03684

E. R. Engdahl

Branch of Global Seismology and Geomagnetism
U.S. Geological Survey
Denver Federal Center
Box 25046, Mail Stop 967
Denver, Colorado 80225
(303) 234-4041

Investigations

1. Depth Phases. Establish criteria for the proper identification of depth phases from sub-oceanic subduction-zone earthquakes.
2. Earthquake Location in Island Arcs. Develop practical methods for accurately locating earthquakes in island arcs.
3. Subduction Zone Structure. Develop techniques to invert for subduction zone structure using seismic travel times.
4. Global Synthesis. Synthesize recent observational results on the seismicity of the earth and analyze this seismicity in light of current models of global tectonic processes.

Results

1. Depth Phases. Broadband data recorded by the Grafenberg array were used to study the frequency dependence of depth phases from moderate-sized earthquakes in the central Aleutians. It was found that in the presence of a water layer the short-period band is usually dominated by pwP energy and the long-period band by pP and sP energy. A technical article is being prepared on these findings.

Analysis of depth phases recorded both analog and digitally from a large set of moderate-sized central Aleutian earthquakes has been completed. Depths accurate to a few kilometers were determined for a large number of events by matching theoretical times of depth phases based on local structure to observed data. The new hypocenters provide a means to accurately locate the plate interface across the subduction zone. A journal article is in preparation.

2. Earthquake Location in Island Arcs. An extended data set of central Aleutian earthquakes, that includes events with well determined depths as previously described, has been relocated using the JHD approach. It is shown that by careful selection of observing stations, proper analysis of depth phases and the availability of local network calibration events, this approach can reduce hypocentral uncertainties to less than 15 kilometers over a broad region of the subduction zone. These results and their tectonic significance will be the subject of a paper to be prepared.
3. Subduction Zone Structure. A cooperative project with Dr. D. Gubbins at Cambridge University to jointly invert seismic travel times for hypocenters and for structure in the central Aleutian subduction zone has been undertaken.
4. Global Synthesis. A framework for this synthesis study has been developed.

Reports

Engdahl, E. R., Billington, S., and Dewey, J. W., 1984: Redefined spatial distribution of telesismically recorded earthquakes in the central Aleutian Islands, abstract submitted to the Anchorage Seismological Society of America meeting.

Seismic Hazard Studies, Anchorage

9950-03643

A. F. Espinosa
Branch of Engineering Geology and Tectonics
U.S. Geological Survey
Box 25046, MS 966, Denver Federal Center
Denver, CO 80225
(303) 234-5077

Investigations

1. A damage evaluation for the City of Anchorage, sustained from the 1964 Alaskan earthquake, is being performed with damage data which have not been published previously. This information and local surficial geological data is planned to be used in order to evaluate transfer function amplification curves in Anchorage and to ascertain any existing correlation between damage and soil conditions in the area.
2. A "completeness" of the seismicity catalog is being investigated in order to use lower magnitude thresholds in (a) spatial and magnitude-temporal distribution of shallow ($h < 33$ km) and intermediate ($34 < h < 100$ km) seismicity ($M_s > 5.5$) occurring within a specified area in the period of time which uses (a) historical and (b) instrumentally recorded earthquakes. b-values are being determined likewise for the region under study. This effort is part of the seismicity study being carried out in this project for the Anchorage and vicinity region in Alaska.
3. A surficial geologic map of the southeastern part of Anchorage and vicinity is being drawn. Geologic field data is being collected and mapped.
4. Three geological materials map for the municipality of Anchorage are being drawn.
5. A suite of seismicity maps and depth cross sections for the Anchorage and vicinity region in Alaska, are being plotted.

Reports

Bartsch-Winkler, S., and Schmoll, H. R., 1984, Guide to late Pleistocene and Holocene deposits of Turnagain Arm, Alaska: Alaskan Geological Society and Geological Society of America Bulletin, 90 p.

Espinosa, A. F., 1984, L_g -wave attenuation in contiguous United States [abs.]: EOS, American Geophysical Union Transactions, v. 65, no. 16, p. 233.

1984, Local magnitude determination using strong-motion horizontal accelerograms [abs.]: Seismological Society of America Annual Meeting, Anchorage, Alaska, May 30-June 1, 1984.

Espinosa, A. F., and Michael, J. A., 1984, Seismicity of the arctic and adjoining regions: U.S. Geological Survey Open-File Report 84-376, Lambert equal-area projection.

Schmoll, H. R., Yehle, L. A., Gardner, C. A., and Odum, J. K., 1984, Surficial geology and glacial stratigraphy within the Upper Cook Inlet Basin, Alaska: Alaskan Geological Society and Geological Society of America Bulletin, 89 p.

Detailed Analysis of 1906 Faulting
in Marin County, California

21242

N. T. Hall, W. R. Cotton, and E. A. Hay
Foothill-De Anza Community College District
Los Altos Hills, California 94022
(415) 948-8590

Investigation

The investigation is being focused on a 12 kilometer segment of the 1906 trace of the San Andreas fault. The research area lies between the Marin County localities of Dogtown and the Vedanta Retreat, and is an area where Holocene activity along the fault has occurred in a narrow zone. The investigation is designed to produce a set of detailed geologic and geomorphic maps of the seismotectonic features. This information will be augmented by the rich historic record of the 1906 faulting that was compiled by G. K. Gilbert shortly after the 1906 earthquake.

Results

1. All initial phase activities are complete. A total of 110 new stereoscopic photographs have been thoroughly studied in conjunction with careful field evaluation.
2. Thirteen (13) camera stations for G. K. Gilbert's 1906-1907 photographs of 1906 ruptures in the San Andreas fault zone have been located. We have taken modern photographs at each locality. Significant cultural and vegetative modifications are apparent.
3. Large scale topographic maps ($1'' = 100'$) are in preparation for three sites: 1) approximately one mile southeast of the Vedanta Retreat, 2) southeast of Five Brooks, and 3) west of the Randall trailhead. These maps will enable us to show the following with considerable accuracy: 1) the rupture traces of 1906; 2) additional traces active in Late Quaternary time; 3) camera stations for Gilbert's 1906-1907 photographs and other historic data; 4) fault-related geomorphic features; and 5) Holocene deposits associated with active faulting.

Reports

Hall, N. T., Hay, E. A., and Cotton, W. R., 1984, Problems in the application of ^{14}C dates to slip rate determinations of the San Andreas fault: Seismological Society of America, Abstracts and Program.

Investigation of Seismic Wave Propagation for
Determination of Crustal Structure

9950-01896

Samuel T. Harding
Branch of Engineering Geology and Tectonics
U.S. Geological Survey
Box 25046, MS 966, Denver Federal Center
Denver, CO 80225
(303) 234-5090/5087

Investigations

1. Conducted high-resolution seismic reflection surveys.
 - a. Across the Borah Peak earthquake fault scarp along the Double Springs Pass road.
 - b. Along the central Pacific railroad grade in Hansel Valley, Utah.
 - c. Along a line west of Becks Hot Springs in Salt Lake City, Utah.
2. Created synthetic seismogram for three deep wells in the Mississippi Embayment.

Results

1. These lines have been processed and are in the process of being interpreted. The line run from the interstate at Becks Hot Springs in Salt Lake City is shown in figure 1. CDP 1200 is at the intersection of the railroad tracks and Utah 249. CDP 1340 is at the intersection of Utah 249 and Redwood Drive. 1200 is at the east, and 1340 at the west end of the line.
2. The synthetic seismograms were used to interpret the reflection profiles recently purchased across the New Madrid fault zone.

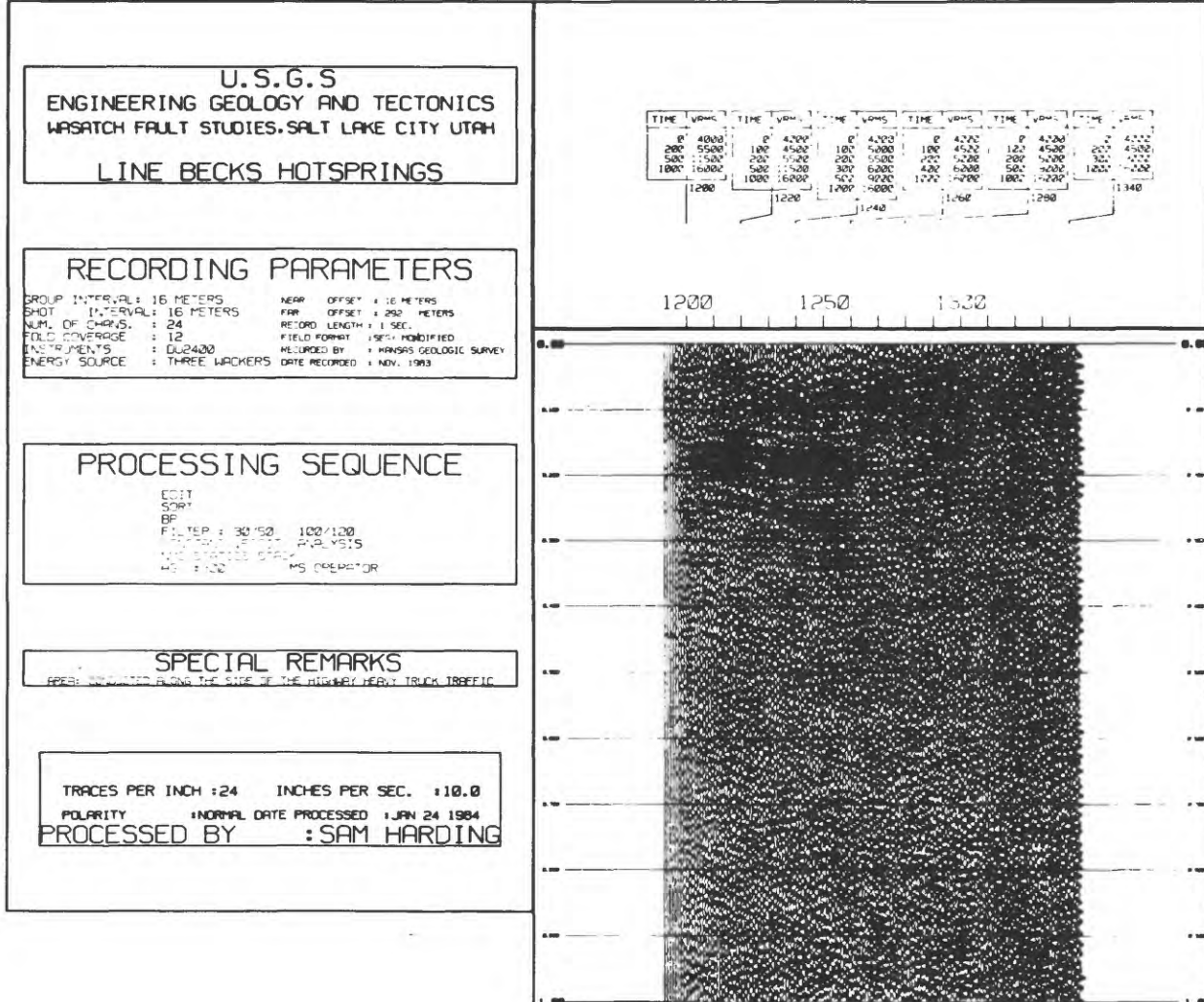


Figure 1.--High-resolution reflection line at Becks Hot Springs,
Salt Lake City, Utah.

Postglacial uplift in northeastern United States
9510-03207

Carl Koteff
U.S. Geological Survey
National Center, MS928
Reston, VA 22092
703/860-6503 FTS 928-6503

INVESTIGATIONS

Former glacial lake sites in the Connecticut River valley of New Hampshire and Vermont, the Champlain Valley in Vermont and New York, and the mid-Hudson River valley in New York were examined. Altitudes of topset-foreset contacts of deltas constructed in the former lakes were obtained in each of these areas. The topset-foreset contact is considered to be a reliable indicator of the former lake level to within one meter. Glaciomarine features in the Champlain Valley in Vermont also were examined.

RESULTS

The altitudes of topset-foreset contacts of the deltas provide a profile of significant postglacial crustal isostatic uplift of most of New England to the north-northwest, suggesting that the locus of depression caused by the last ice sheet (late Wisconsinan) was centered around Hudson Bay. This indicates that the ice sheet was not characterized by multi-centers at its maximum thickness, as proposed by several Canadian investigators, but rather the glacier's center was more of a saddle-shaped ridge over Hudson Bay, as proposed by Denton and Hughes (1981), and Walcott (1972).

Maximum uplift gradients are about 90 cm/km over most of New England. Thus northern areas of New England have been isostatically uplifted by over 300 meters during late glacial and postglacial time. Such a large amount of uplift indicates a thicker rather than thinner ice sheet model, perhaps more than 4000 meters thick at the center. A thicker ice sheet, in turn, suggests a greater rather than smaller eustatic sea-level drop of more than 135 meters at approximately 18,000 years B.P.

The uplift profile, more than 220 km long, obtained from the ice-marginal deltas is very straight, showing a tangent rather than being curved. The profile is also time-transgressive, that is, the southern end is older than the northern end by as much as 3000 years. The antiquity and straightness of the profile indicate two major conclusions. 1) Isostatic response of crustal uplift was delayed for about 5000 years, until about 13,000-14,000 years B.P. It has been suggested recently that as much as one half of the ice load had been removed by this time. Such a slow viscous response by the mantle is not yet clearly understood. 2) The isostatic crustal response was not affected in any measurable way by variations of lithologic or structural features of the crust. The profile crosses a number of lithologic and boundaries without any change in gradient.

REPORTS

Koteff, Carl, 1984, Debris source for meltwater deposits in New England [abs.]: Geological Society of America Abstracts with Programs, v. 16, no. 1, p. 28.

Determining Landslide Ages and Recurrence Intervals

9950-03789

Richard F. Madole
Branch of Engineering Geology and Tectonics
U.S. Geological Survey
Box 25046, MS 966, Denver Federal Center
Denver, CO 80225
(303) 234-3573

Investigations

Because this project has been in progress only a few months, study to date has been limited mainly to air photos. Besides selecting sites for detailed stratigraphic study during the summer of 1984, a comparison was made between landslides in several localities along the Wasatch Front and landslides in other localities in Utah and Colorado for which some age control exists. This comparison focused on the topographic expression of landslides as a function of age and on the relationships between landslide distribution, altitude, aspect, and age.

Results

Three conclusions can be drawn from the differences in the topographic expression and the altitude-aspect relations of the landslides studied.

1. The topographic expression of landslide deposits changes with time in a manner similar to that documented for glacial deposits. Landslide deposits of late Pleistocene age (10,000-15,000 B.P., for example) have a sharp, distinct, apparently little modified topographic expression similar to that of moraines of Pinedale age. Changes in morphology with increased age include (1) a decrease in relief, (2) progressive infilling of depressions, (3) a decrease in scarp slope angle, and (4) an increase in the width of the crests of ridges within the landslide deposits. As with glacial deposits, the topographic expression of landslides of a given age appear to be influenced by the lithology of the rocks composing them.
2. Crosscutting relations between landslide deposits and stream-terrace deposits containing the Lava Creek B volcanic ash (610 ka) indicate that some landslides retain topographic expression for longer than 610,000 years. Obviously, many landslides are relicts, products of environments different than those of the present. The tendency for relict landslides to accumulate in the landscape suggests that maps that show only the distribution of landslides, with little consideration given to age and origin, are likely to greatly overestimate the landslide hazard.
3. In many places, landslide distribution suggests that wetter climates of the past were the principal cause of landsliding. Landslides tend to be more common on north- and east-facing slopes than on south- and west-facing slopes. This relationship is not as evident at higher altitudes (greater than 2,600 m, for example) as it is at lower altitudes where the more arid climate of the present is less conducive to landsliding. With decreasing altitude, relict landslides appear to compose a greater percentage of the total number of landslides present.

Surficial Geology Along the Wasatch Front, Utah

Project: 9950-01622

Robert D. Miller
U.S. Geological Survey
Box 25046, Denver Federal Center, MS 903
Denver, CO 80225
Ph: (303) 234-2960

Continued preparation of text to accompany maps showing deposits grouped on the basis of texture along part of the Wasatch Front, Utah. The boundaries of the maps, already completed, coincide with the surficial geologic maps published as Miscellaneous Investigation Maps I-1198 and I-1477, which encompass areas along the Wasatch Front in Great Salt Lake Valley and Utah Valley. No additional field investigations were undertaken, and the text preparations included compilation of laboratory tests and evaluation of physical properties of the deposits.

Publications:

Miller, R. D., 1980, Surficial geologic map along part of the Wasatch Front, Salt Lake Valley, Utah: U.S. Geological Survey Miscellaneous Investigations Map I-1198, scale 1:100,000. [reprinted October 1983]

Miller, R. D., 1982, Surficial geologic map along part of the Wasatch Front, Great Salt Lake and Utah Lake Valleys, Utah: U.S. Geological Survey Miscellaneous Investigations Map I-1477, scale 1:100,000.

Stable Isotope Investigations of Fault Processes

9570-00383

James R. O'Neil

Branch of Isotope Geology

U.S. Geological Survey

345 Middlefield Road, MS 937

Menlo Park, CA 94025

Investigations

1. Deuterium and oxygen-18 analyses are made of well waters and springs sampled biweekly at several locations along the major fault systems in north-central California. The isotopic variations are correlated with variations in chemical compositions of the water and radon concentrations in soil gas in an attempt to identify possible geochemical precursors to seismic activity.
2. Concentrations and carbon isotopic compositions of CO_2 in soil gas from two locations in San Juan Bautista are measured weekly as a possible monitor for earthquake precursors.
3. Stable isotope compositions are measured of fault zone materials including mylonites, gouge and entrapped waters and clay materials in an attempt to understand the nature of water-rock interactions in fault systems and the temperatures generated during fault movement.

Results

Measurements were made of the contents of D, ^{18}O , and H_2O^+ in fault gouge collected over a depth of 400 meters in the San Andreas Fault near Hollister, California. The amounts and isotopic compositions of the pore fluids, also analyzed, suggest that formation waters from adjacent Franciscan rocks have migrated into the gouge and mixed with local meteoric water (Fig. 1). Thus the gouge is an open system permeable to fluid flow. This permeability has important implications concerning heat flow along the fault zone.

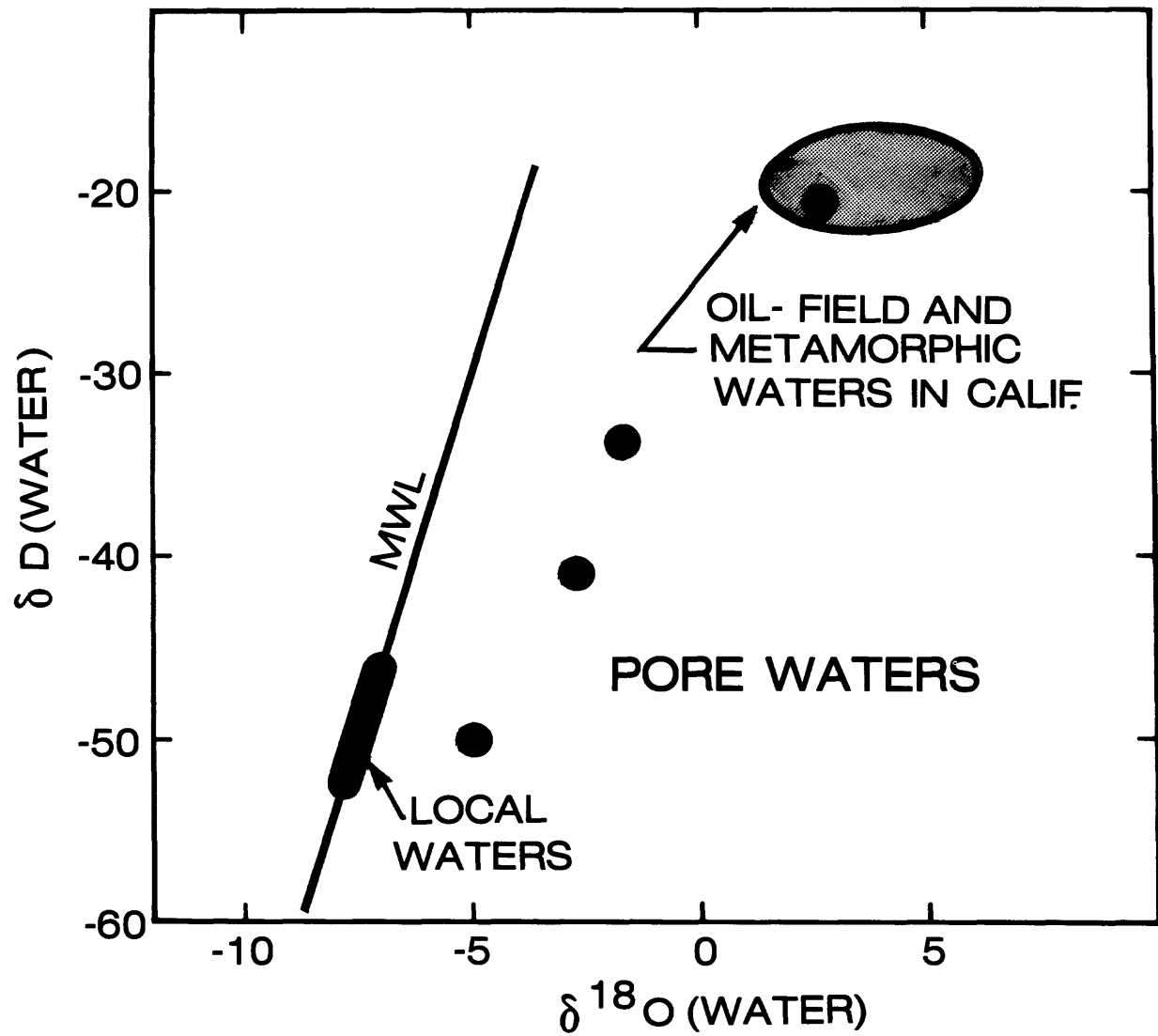
Analyses of the fault gouge itself gives information on the amounts, timing, and conditions of formations of the clay materials:

- (a) The gouge porosity of about 10 percent doesn't change significantly with depth.
- (b) Clay minerals constitute only about 42 percent of this gouge, previously considered to be composed dominantly of clay.
- (c) The bulk of the clays grew at a former time when climate or topography were different from those prevailing at the present location of the Gabilan Range.

Reports

O'Neil, James R. (1983), Water-rock interactions along active fault zones in California, Fourth International Symposium on Water-Rock Interaction (Extended Abstracts), p. 381-384.

O'Neil, James R. (1984) Water-rock interactions in fault gouge, Jour. Geophys. Res., in press.



Data Processing, Golden

9950-02088

Robert B. Park
Branch of Engineering Geology and Tectonics
U.S. Geological Survey
Box 25046, MS 966, Denver Federal Center
Denver, CO 80225
(303) 234-5070

Investigations

The purpose of this project is to provide the day to day management and systems maintenance and development for the Golden Data Processing Center. The center supports Golden based Office of Earthquakes, Volcanoes, and Engineering investigators with a variety of computer services. The systems include a PDP 11/70, several PDP 11/03's and PDP 11/23's, a VAX/780 and two PDP 11/34's. Total memory is 6.4 mbytes and disk space will be approximately 2.2 G bytes. Peripherals include four plotters, eight mag-tape units, an analog tape unit, five line printers, 5 CRT terminals with graphics and a Summagraphic digitizing table. Dial-up is available on all the major systems and hardwire lines are available for user terminals on the upper floors of the building. Users may access any of the systems through a Gandalf terminal switch. Operating systems used are RSX11 (11/34's), Unix (11/70), RT11 (LSI's) and VMS (VAX).

The three major systems are shared by the Branch of Global Seismicity and Geomagnetism and the Branch of Engineering Geology and Tectonics.

Results

Computation performed is primarily related to the Global Seismology and Hazards programs; however, work is also done for the Induced Seismicity and Prediction programs as well as for DARPA, ACDA, MMS, U.S. Bureau of Reclamation, and AFTAC among others.

In Global Seismology and Geomagnetism, the data center is central to nearly every project. The monitoring and reporting of seismic events by the National Earthquake Information Service is 100 percent supported by the center. Their products are, of course, a primary data source for international seismic research and have implications for hazard assessment and prediction research as well as nuclear test ban treaties. Digital time series analysis of Global Digital Seismograph Network data is also 100 percent supported by the data center. This data is used to augment NEIS activities as well as for research into routine estimation of earthquake source parameters. The data center is also intimately related to the automatic detection of events recorded by telemetered U.S. stations and the cataloging of U.S. seismicity, both under development.

In Engineering Geology and Tectonics, the data center supports research in assessing seismic risk and the construction of national risk maps. It also provides capability for digitizing analog chart recordings and maps as well as analog tape. Also, most if not all of the research computing related to the hazards program are supported by the data center.

The data center also supports equipment for online digital monitoring of Nevada seismicity. Also it provides capability for processing seismic data recorded on field analog and digital cassette tape in various formats. Under development is a portable microprocessor based system to be used by the field investigations group to do preliminary analysis and editing of temporary local networks and the GOES Satellite Event Detect System. Recent acquisitions include the replacement of the PDP 11/40 used for analog input with a PDP 11/34, expansion of the Nevada Network 11/34 for collection of Western Slope data for the U.S. Bureau of Reclamation, a second Versatec plotter and a Tektronix 4014 graphic system.

Northeastern U.S. seismicity and tectonics

9510-02388

Nicholas M. Ratcliffe

Branch of Eastern Regional Geology

MS 925, U.S. Geological Survey

Reston, VA 22092

(703) 860-6406

Investigations

1. Vibroseis profiling of Ramapo seismic zone in New York State (in cooperation with Virginia Polytechnic Institute and State University).
2. Detailed geologic mapping along routes chosen for Vibroseis profiles.
3. Examination of drill core and trenches across Mesozoic faults of the Ramapo fault system, and siting of drill holes for in-situ stress studies.

Results

1. Approximately 50 km of new 12-fold seismic reflection data were collected along a route extending from near Pound Ridge, N.Y., northwestward across the Hudson Highlands and into the lower Hudson River valley near Poughkeepsie, N.Y. The line crosses an area of the seismogenic Proterozoic Y basement rocks with well-located hypocenters at depth of 0 - 1 km in the west, to as deep as 12 km in the east. Preliminary interpretation of the migrated data suggests that reflectors associated with moderately steeply southeast dipping (35°) mylonite zones in basement rocks are detectable.
2. Geologic mapping of the northern Vibroseis route is 50% complete. Additional geologic mapping along Ramapo Vibroseis lines 1 (see previous report for index map) and 2 are also about 50% complete.
3. Five newly collected cores across the Ramapo fault near Riverdale, N.J., collected in cooperation with the New Jersey Department of Transportation completely recovered the fault zone along a 3 km length of the fault trace south of our Riverdale site. Detailed study of these cores reveals that the last recorded movement on the Ramapo fault surface was right-oblique normal faulting with typical Mesozoic mineralization. These results are consistent with our previous results from seven other sites along the Ramapo and Flemington faults (Mesozoic border faults) indicating that these northeast-striking, southeast-dipping gouge zones have not been reactivated as reverse faults in the current compressional stress field. Detailed studies of two deep 1,500 ft and 1,000 ft drill holes cored by the U.S. Nuclear Regulatory Commission for hydrofracturing have been completed. One of these deep drill holes at Annsville, N.Y., is located within Annsville earthquake swarm, where hypocenters have been accurately determined by Woodward-Clyde's 12-station network. Extensive Mesozoic brecciation is present at the 900 - 1,000 ft level and there is clear evidence of reactivation of Paleozoic mylonite zones as Mesozoic brittle faults in this area.

4. Additional Vibroseis profiles in New Jersey across the margin of the Newark Basin and in-situ stress measurements to be conducted by Mark Zoback in a 1-km-deep industry drill hole are being planned.

Reports

Stanley, R. S., and Ratcliffe, N. M., in press, Tectonic synthesis of the Taconic orogeny: New England Appalachians: Geological Society of America Bulletin.

Ratcliffe, N. M., and Burton, W. C., 1983, Brittle fault fabrics, mineralogy and geometry of the border faults of the Newark basin, New York - New Jersey, from drill-core information: Geological Society of America, Northeastern Section Meeting, Abstracts with Programs, v. 16., no. 1, p. 57.

Ratcliffe, N. M., 1983, Brittle-ductile transition zone in a Barrovian gradient: Implications for tectonic implacement of isograds: Geological Society of America, Northeastern Section Meeting, Abstracts with Programs, v. 16, no. 1, p. 57.

Burton, W., and Ratcliffe, N. M., Attitude movement history and structure of cataclastic rocks of the Flemington fault based on core drilling near Oldwick, New Jersey: U.S. Geological Survey Miscellaneous Field Survey Report.

Helium Monitoring for Earthquake Prediction
9570-01376
G. M. Reimer
U. S. Geological Survey, MS 963
Denver Federal Center
Denver, CO 80225
(303) 234-5531

Investigations

The variation of helium in soil-gas from sample collecting stations along the San Andreas Fault near San Benito, California has been observed to have a significant correlation to seismic activity recorded in the surrounding area. In addition to monitoring helium, an expanded effort is being planned to analyze for other gases, notably, nitrogen, oxygen, carbon dioxide and methane. This effort will hopefully provide information to understand the mechanisms for helium variations.

Results

Figure 1 shows the plot of the helium concentrations as a function of time. Table 1 lists the helium decrease beginning dates and dates of the nearby seismic activity. For this time period, May of 1979 to December of 1983, an empirical definition was developed to define a helium decrease and a corresponding earthquake. The criteria are as follows:

Two successive 4 ppb helium decreases from a 3-week moving average of all sample probes.

A 1.5 to 6.5 week leadtime from the beginning of the decrease until the occurrence of seismic activity.

An earthquake of magnitude 4(-0.2) occurring within a fixed distance from the center of the sample collection stations (an ellipse 160 x 80 km; the major axis parallels the San Andreas Fault).

Using these criteria, 15 helium decreases match 25 earthquakes. By considering some earthquakes as clusters, those that are not aftershocks but otherwise spatially or temporally related, the correlation is 15 of 18 earthquakes. Examples of clusters are the earthquakes identified as 81007-81015 and 80127-81062 in Table 1.

January 1, 1984 became the arbitrary date after which the empirically derived criteria would be applied to evaluate future correlations. Of particular note is the April M=6 earthquake near San Jose fit these criteria.

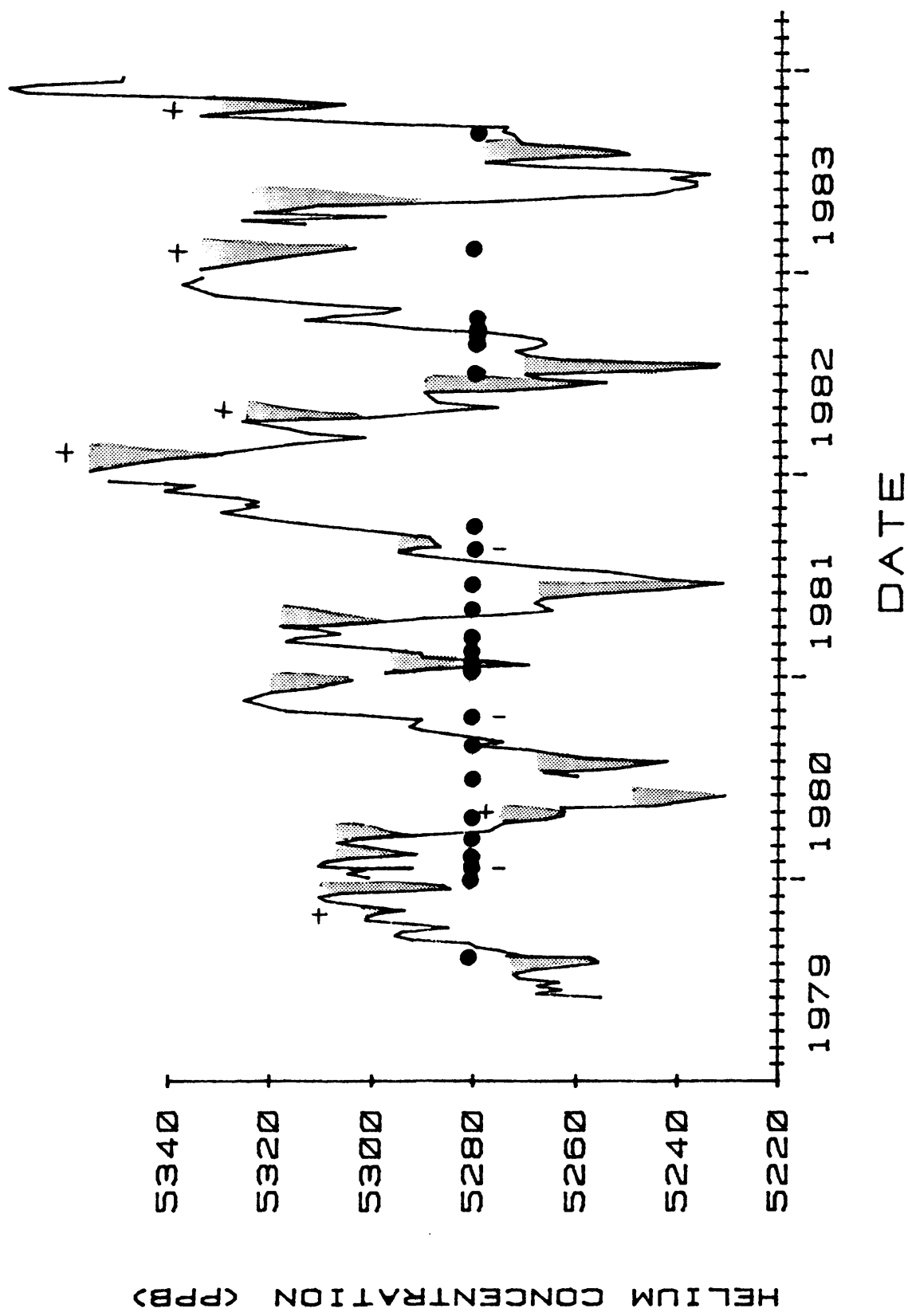
Reports

Reimer, G. M., 1983, Prediction of central California earthquakes from soil-gas helium fluctuations?, EOS, Transactions of the American Geophysical Union, v. 64, p. 757.

Table 1
 Date of the beginning of the helium decrease and corresponding earthquake data. The first two digits of the date are the year of the twentieth century and the last three digits represent the cumulative calendar day of that year. Tie lines represent clusters.

| Helium decrease date | Earthquake date | Location | | | Mag. |
|----------------------------|--------------------|----------|-----------|--|------|
| | | Lat. (N) | Long. (W) | | |
| 79192 | 79218 | 37.102 | 121.503 | | 5.9 |
| 79297 | | | | | |
| 79332 | 79358 | 36.975 | 122.272 | | 4.0 |
| | 80024 | 37.852 | 121.815 | | 5.5 |
| | 80027 | 37.737 | 121.740 | | 5.8 |
| 80030 | 80066 | 36.669 | 121.373 | | 4.0 |
| 80065 | 80104 | 36.762 | 121.548 | | 4.8 |
| 80100 | | | | | |
| 80128 | 80170 | 36.898 | 121.683 | | 4.1 |
| 80191 | 80236 | 37.569 | 121.672 | | 4.1 |
| | 80287 | 36.595 | 121.085 | | 4.1 |
| 80337 | 81007 | 36.866 | 121.630 | | 4.5 |
| | 81015 | 37.383 | 121.737 | | 4.8 |
| 80365 | 81027 | 36.843 | 121.633 | | 4.1 |
| | 81062 | 37.548 | 121.945 | | 4.4 |
| 81091 | 81115 | 37.090 | 121.885 | | 4.1 |
| 81141 | 81160 | 36.747 | 121.362 | | 4.2 |
| | 81226 | 36.773 | 121.293 | | 4.2 |
| 81224 | 81271 | 36.792 | 121.587 | | 3.9 |
| 82007 | | | | | |
| 82096 | | | | | |
| 82148 | 82170 | 36.530 | 121.073 | | 4.0 |
| 82180 | 82221 | 36.597 | 121.242 | | 4.5 |
| | 82230 | 37.025 | 121.745 | | 4.5 |
| | 82236 | 37.468 | 121.815 | | 4.0 |
| | 82240 | 37.845 | 121.782 | | 3.8 |
| | 82243 | 36.648 | 121.325 | | 4.0 |
| 82361 | 83036 | 36.680 | 120.855 | | 4.1 |
| 83108 | | | | | |
| 83199 | 83241 | 35.803 | 121.353 | | 5.4 |
| 83283 | | | | | |

Figure 1.--Helium soil-gas concentrations near San Benito, California from May 1979 to December 1983. Shaded areas are helium decreases, dots are earthquakes of M=4 or greater. + represents decreases without an earthquake following in 1.5 to 6.5 weeks. | indicates an earthquake without a preceding decrease. Date divisions are months. Breaks in the helium data line are periods when samples were not collected.



Rock Deformation

9950-00409

Eugene C. Robertson
Branch of Engineering Geology and Tectonics
U.S. Geological Survey
922 National Center
Reston, VA 22092
(703) 860-7404

Investigations

Quantitative studies of the relationship of displacement d on faults to the corresponding thickness t of gouge and breccia of the faults were completed and published. Measurements were obtained on faults observed underground in mines, at outcrops, and on laboratory specimens; about one-third of the data are from the technical literature.

Results

The d and t of faults observed underground in mines were obtained from geologic notes and maps of geological departments of mining companies in Butte, MT, Coeur d'Alene, ID, Magma, AZ, Alma, CO, and Kirkland Lake, Ontario. Only gouge and breccia are considered to make up the fault, and thicknesses of adjacent, jointed, undisplaced rock are not included, although sometimes not identified in the literature sources. Of the 49 data points and boxes which are plotted in Figure 1, 25 were obtained from faults in mines.

The three points and boxes at the lower left of Figure 1 are from laboratory studies of friction; rock cylinders with saw-cuts at various angles were compressed at room temperature under low confining pressure. The remaining 21 points and boxes are from observations at the earth's surface of normal and small thrust faults. No large strike-slip or overthrust faults are included because their d 's and t 's are poorly determined.

Assuming their logarithms are normally distributed, the points in Figure 1 have a high correlation coefficient, $r = 0.94$. Some of the scatter might be explained if each fault were studied more carefully; t might be too large because of including jointed rock with gouge and breccia, or t might be too small because splits of the fault were not included. Values of d may be in error because of uncertainty in the rake angle or in offset of indistinct or misidentified geologic features.

Confining pressure, water conditions, rock type, and history of deformation would affect d and t, and if understood, some of the scatter of points could probably be explained. A wide variety of igneous and sedimentary rocks were involved in the faults shown in Figure 1, which by its uniform trend of points indicates that the various rocks behave much alike in forming gouge and breccia. Limestone is an exception due to its ductility. A physical model for the brecciation process of continued production of gouge and breccia with continued displacement of a fault is described in Robertson (1982).

Reports

Robertson, E. C., 1982, Continuous formation of gouge and breccia during fault displacement, in R. E. Goodman and F. E. Heuze, editors, Proc. 23rd Symp. Rock Mechanics, Amer. Inst. Min. Met. Petrol. Engr., p. 397-404.

Robertson, E. C., 1983, Relationship of fault displacement to gouge and breccia thickness, Amer. Inst. Min. Met. Petrol. Engr., Mining Engineering, v. 35, no. 10, p. 1426-1432.

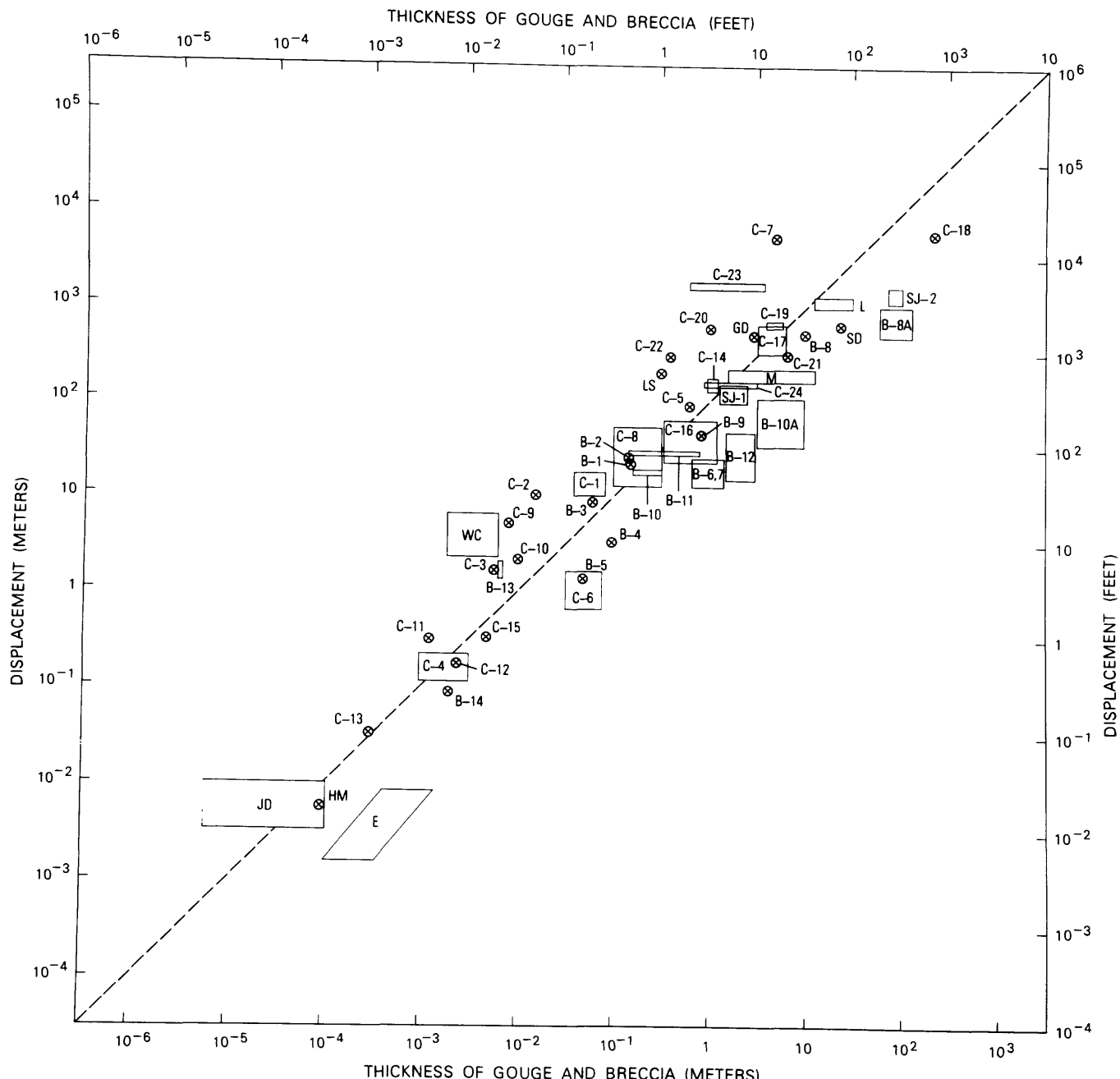


Figure 1. Fault displacement plotted against thickness of gouge and breccia of faults at the following localities: points "B", in mines at Butte, MT; points "C", in mines at Coeur d'Alene, ID; points "M", "L", and "LS", in mines in AZ, CO, and Ontario; points "JD", "HM", and "E", from laboratory data; remaining points, from surface observations in MT and NM. A trend line at a displacement-to-thickness ratio of 100 is shown.

Basement Tectonic Framework Studies
Southern Sierra Nevada, California

9910-02191

Donald C. Ross
Branch of Engineering Seismology and Geology
345 Middlefield Road, Mail Stop 977
Menlo Park, California 94025
(415) 323-8111, ext. 2341

Investigations

1. Petrographic study of basement rock samples to be submitted for 180 and Rb/Sr analyses.
2. Compilation of all sample data from the southern Sierra Nevada (north to lat. $36^{\circ}00'N$) on master set of 27 topographic quadrangles.
3. Preparation of a geologic map and accompanying report on the basement rock relations along the White Wolf, Breckenridge, and southern Kern Canyon faults, southern Sierra Nevada, California.
4. Preparation of petrographic summaries, compositional diagrams, and index maps for several granitic units of the southern Sierra Nevada.

Results

Several basement rock units show right-lateral strike-slip offset across a 200 km-long basement break in the Sierra Nevada batholith (the White Wolf-Breckenridge-Kern Canyon fault zone). This master crack in the batholith may have originated some 80 to 90 m.y. ago in response to a regional oroclinal flexure. The recent history of the southern part of this fault zone (White Wolf and Breckenridge faults) has produced fault displacements that contradict the offset pattern suggested by the basement rocks. The White Wolf fault has recently (1952) moved with a left-lateral and thrust sense, based on measurements of surface ruptures and fault plane solutions. Left-lateral offsets have also been noted in some subsurface formations in this area. The cause of this presumed change in fault style is not known, but northward impingement by the San Andreas fault on the northeast-trending White Wolf fault could cause left-lateral and thrust displacements on this old, right-lateral, basement crack. Present-day topography along the NNE-trending Breckenridge fault suggests that the most recent movements on this fault have been normal dip-slip displacement of more than 1,000 m. This style change is even more perplexing. The Breckenridge fault may now be responding to the stress pattern of late Cenozoic extension in this region. Thus, the old, right-lateral plane of weakness could now be behaving like a small Basin-Range normal fault.

Reports

- Ross, D. C., 1983, Generalized geologic map of the southern Sierra Nevada, California, showing the location of basement samples for which whole rock 180 O has been determined: U.S. Geological Survey Open-File Report 83-904, scale 1:250,000.
- (in press), Possible correlations of basement rocks across the San Andreas, San Gregorio-Hosgri, and Rinconada-Reliz-King City faults, California: U.S. Geological Survey Professional Paper 1317 (Director's approval, October, 1983).

Earthquake Hazard of the Red River Fault and
Related Faults Deduced from Geological Field Studies
in Western Yunnan Province, P.R.C.

14-08-0001-21289

Kerry Sieh
Division of Geological and Planetary Sciences 170-25
California Institute of Technology
Pasadena, CA 91125
(818) 356-6115

In the Spring of 1983, Ray Weldon and I went to Yunnan Province, China to study the Red River and related faults. A summary of our accomplishments in the field appeared in the a previous "Summaries..." volume.

Since our previous summary, we have (1) submitted most of the radiocarbon samples for analysis and (2) hosted 3 of our Chinese colleagues during a one-month visit to Caltech this Spring. The radiocarbon dates will be available by mid-summer, and analysis of the paleomagnetic samples was undertaken by the Chinese and Weldon during their one-month visit. The Chinese also brought a number of soil samples we collected from a faulted alluvial fan. The fan contains carbon that is currently being dated. Graduate student Emelia Burt will study the chemistry of these soils at the University of Maryland this summer. These data will enable us to begin to characterize the rate and nature of soil formation in southern China.

Seismicity and Tectonics

9920-01206

William Spence
 Branch of Global Seismology and Geomagnetism
 U. S. Geological Survey
 Denver Federal Center, MS 967
 Denver, Colorado 80225
 (303) 234-4041

Investigations.

Studies carried out under this project focus on detailed investigations of large earthquakes, aftershock series, tectonic problems, and earth structure. Studies in progress have the following objectives:

1. Provide tectonic setting for and analysis of the 1977 Sumba earthquake series (W. Spence).
2. Provide tectonic setting for and analysis of the 1974 Peru gap-filling earthquake (W. Spence, C. J. Langer, and J. N. Jordan).
3. Determine faulting parameters for aftershocks of the great (M_S 7.7) Colombia earthquake of December 1979 and infer rupture characteristics of the main shock (C. Mendoza).
4. Determine the maximum depth and degree of velocity anomaly beneath the Rio Grande Rift and Jemez Lineament by use of a 3-D, seismic ray-tracing methodology (W. Spence, R. S. Gross, and L. H. Jaksha).

Results.

1. The great ($M_0 = 4 \times 10^{28}$ dyne-cm), normal-faulting Sumba earthquake of 1977 occurred at the Java Trench, just west of the zone where the Australian continental lithosphere is in collision with the Java arc. Aftershocks of the Sumba earthquake have been relocated by the joint hypocenter method and occur in two zones: an east-west trending zone, mostly east of the main shock, and a triggered northwest-southeast-trending zone located about 180 km northwest of the main shock. Focal mechanism data for the aftershocks in the main shock zone and in the triggered zone combined with study of the detailed tectonic setting support the conclusion that both the Sumba main shock and the triggered group of earthquakes occurred directly as a result of slab pull. The main shock may be part of a continuing process of detachment of the subducted oceanic lithosphere from the Australian continental lithosphere, rather than being a simple plate-bending event.

2. The great 1974 Peru thrust earthquake (M_S 7.8, M_W 8.1) occurred in a documented seismic gap, between two earthquakes each with magnitude of about 8, occurring in 1940 and 1942. The stress release of the October 3, 1974, main shock and aftershocks occurred in a spatially and temporally irregular pattern. The multiple-rupture main shock produced a tsunami with wave heights of 0.6 ft at Hawaii and which was observed, for example, at Truk Island and at Crescent City. The aftershock series essentially was ended with the occurrence of a M_S 7.1 aftershock on November 9, 1974.
3. Three large earthquakes, occurring in 1942, 1958, and 1979, have reruptured the zone of the single great Colombia-Ecuador earthquake (M_S 8.6, M_W 8.8) of January 31, 1906. The last of these (December 12, 1979; M_S 7.7) ruptured the northernmost part of the 1906 rupture. This thrust earthquake was followed by numerous aftershocks as large as magnitude 5.5. A joint hypocenter relocation of these aftershocks indicates that most of them occurred at or near the interface between the Nazca plate and the overriding South American Plate. Long-period Love- and Raleigh-wave spectra in the 30-80 second band, as recorded by the Global Digital Seismograph Network, are being used to determine the fault parameters (strike, dip, and slip) at the corresponding source depths of many of these aftershocks. The procedure is to compare the observed spectra with a suite of theoretical source models until a best fit is obtained. The best fit is further constrained by taking ratios of the observed spectra to that of a standard, reference event. The latter procedure serves to remove perturbations of the observed spectra due to path effects. The final set of aftershock magnitudes, hypocenters, and faulting parameters will be used to infer the detailed rupture characteristics of the 1979 main shock and thus to provide insight into the nature of earthquake occurrence at this segment of plate convergence.
4. To a depth of about 160 km, the upper mantle P-wave velocity beneath the Rio Grande rift and Jemez lineament is 4-6 percent lower than beneath the High Plains Province. A 3-D, P-wave velocity inversion shows scant evidence for pronounced low P-wave velocity beneath the 240-km-long section of the Rio Grande rift covered by our array. However, the inversion shows a primary trend of 1-2 percent lower P-wave velocity underlying the northeast-trending Jemez lineament, down to a depth of about 160 km. The Jemez lineament is defined by extensive Pliocene-Pleistocene volcanics and late Quaternary faults. The upper mantle low-velocity segment beneath the Jemez lineament is at most 100 km wide and at least 150-200 km long, extending in our inversion from Mt. Taylor through the Jemez volcanic center and through the Rio Grande rift. A Backus-Gilbert resolution calculation indicates that these results are well-resolved.

Tectonic Analysis of Active Faults

9900-01270

Robert E. Wallace

Office of Earthquakes, Volcanoes and Engineering
345 Middlefield Road, MS 77
Menlo Park, California 94025
(415) 323-8111, ext. 2751

Investigations

1. Evaluation of fault scarps and tectonics of the central Nevada and eastern California seismic belts.
2. Active Tectonics--Impact on Society. A project under the auspices of the Geophysics Study Group, National Research Council, National Academy of Sciences.
3. International Geological Correlation Program - Active Faults of the World.
4. Investigation of active faults of Japan.

Results

1. Under the auspices of the Geophysics Study Group, National Research Council, National Academy of Science, a symposium on "Active Tectonics--Impact on Society" was held at the fall meeting of the American Geophysical Union. I served as chairman and organizer of the symposium, and am serving as editor of the NRC/NAS volume being prepared.
2. With the partial support of the Japanese Industrial and Technological Association, I spent six weeks as a guest of the Geological Survey of Japan examining active faults in western Japan. Among the faults examined were the Median Tectonic Line, the Yamasaki fault, Atera fault and Tana fault. All of these appear to have become active in late Quaternary time. All have recurrence intervals for large displacement events measured in many hundreds to several thousand years. Not all of the Median Tectonic Line is active, and the greatest strike-slip displacement is probably no more than a kilometer in central Shikoku.

Reports

Wallace, R. E., 1984, Variations in slip rates on faults in the Great Basin Province [Abs.]: Seismological Sociey of America, May 29-June 2, 1984, Anchorage, Alaska.

- Wallace, R. E., 1984, Fault scarps formed during the earthquakes of October 2, 1915, Pleasant Valley, Nevada, and some tectonic implications: U.S. Geological Survey Professional Paper 1274-A.
- Wallace, R. E., 1984, Eyewitness account of surface faulting during earthquake of October 28, 1983, Borah Peak, Idaho: Seismological Society of America Bulletin (in press).
- Wallace, R. E. and Whitney, R. A., 1984, Late Quaternary history of the Stillwater Seismic Gap, Nevada: Seismological Society of America, v. 74, n. 1, p. 301-314.
- Hanks, T. C., Bucknam, R. C., Lajoie, K. R., and Wallace, R. E., 1984, Modification of wave-cut and faulting-controlled landforms: Journal of Geophysical Research (in press).
- Hanks, T. C. and Wallace, R. E., 1984, Morphological analysis of the Lake Lahontan shoreline and Beachfront fault scarps, Pershing County, Nevada: Geology (in press).
- Schultz, S. S. and Wallace, R. E., 1984, The San Andreas fault.

Geophysical and Tectonic Investigations
of the Intermountain Seismic Belt

9930-02669

Mary Lou Zoback

U.S. Geological Survey

Branch of Seismology

345 Middlefield Road, Mail Stop 77

Menlo Park, California 94025

(415) 323-8111, ext. 2367

Investigations

- 1) Compilation and analysis of worldwide principal stress data.
- 2) Investigation of crust and upper mantle structure beneath the western United States using a combined analysis of gravity, seismic refraction, heat flow and surface elevation data.

Results

- 1) A file of principal stress data determined from focal mechanisms, in situ stress measurements, and geologic stress indicators, is being compiled. One data set covers the North American plate including oceanic areas and parts of the Pacific plate and includes the data from the conterminous United States compiled by Zoback and Zoback (JGR, 1980) as well as all new data published since that compilation. This data set was published in Zoback and others (1984). Stress data are also being compiled for the entire circum-Pacific region as part of the Circum-Pacific Geodynamic Map Series. Most data were obtained through collaboration with foreign scientists. However, some new stress orientations were determined for Szechwan, China from analysis of well bore breakouts measured on dipmeter logs provided by the Petroleum Corporation of the People's Republic of China.
- 2) An integrated analysis of gravity, seismic refraction, surface elevation and heat flow has been used to constrain crust and upper mantle structure beneath the western United States. A simple model in which the level of isostatic equilibrium lies at the base of a thermally defined lithosphere has been found to fit the data quite well. The model specifies surface elevation in terms of lithosphere buoyancy, which is a simple function of lithospheric thickness, the difference between mean lithosphere and asthenosphere density, and a constant related to the level to which asthenospheric material would rise if not overlain by lithosphere. This latter constant is obtained using a mid-ocean ridge as a standard mass column. The crustal component of lithosphere buoyancy is computed from density models derived from seismic refraction studies. Mantle lithosphere density is computed from thermal expansion using a mean lithospheric temperature which is derived from the lithosphere base temperature, (assumed to be 1350°C) and a crust-base temperature estimate from heat flow and heat production data. Lithospheric thicknesses computed from buoyancy considerations for different regions in the Western

United States are as follows: northern Basin and Range province, 55-65 km; southern Basin and Range province, 50-60 km; Colorado Plateau, 90-100 km; and the Southern Great Plains, 170 km. Four Long (1000-1500 km) gravity profiles have been constructed to check the results of this buoyancy-elevation model. All four profiles intersect near the center of the Colorado Plateau, two originate in the northern Basin and Range province and the other two cross the southern Basin and Range. The computed lithosphere thicknesses and densities are shown to provide an excellent fit to the gravity data and are also similar to thermal lithosphere thicknesses that would be predicted from a simple downward extrapolation of temperature gradients.

Reports

Zoback, M. L., 1984, State of lithospheric stress, in Drummond, K. J., Geodynamic Map of the Circum-Pacific Region, Northeast Quadrant, American Association of Petroleum Geologists, Tulsa, Oklahoma, scale 1:10,000,000.

Zoback, M. L., and Lachenbruch, A. H., 1984, Upper mantle structure beneath the western United States: Geological Society of America, Abstracts with Programs, Fall Meeting, (in press).

Zoback, M. L., Zoback, M. D., and Schiltz, M. E., 1984, Index of stress data for the North American and parts of the Pacific Plate: U.S. Geological Survey, Open-File Report, 84-157, 62p.

Surface Faulting Studies

9910-02677

M. G. Bonilla
Branch of Engineering Seismology and Geology
U. S. Geological Survey
345 Middlefield Road, MS 977
Menlo Park, CA 94025
(415) 323-8111, Ext. 2245

Investigations

1. Statistical data related to surface faulting.
2. Appearance of active faults in exploratory trenches.
3. Field investigations of surface faulting.

Results

1. Two manuscripts relating earthquake magnitude to rupture length and fault displacement at the ground surface were revised and prepared for publication.
2. The computer program to analyze the effect that material penetrated and fault displacement have on the visibility of faults in exploratory trenches was debugged by J.J. Lienkaemper. Galley proofs of a report on a trench across the 1915 Pleasant Valley, Nevada, fault were corrected.
3. With J.J. Leinkaemper, a field investigation was made of the October 1983 Idaho faulting with emphasis on fixing the limits of the surface rupture.
4. At the request of the U.S. Agency for International Development, a field examination was made of the epicentral area of the M_s 6.2 Guinea, West Africa, earthquake of December 22, 1983. This intraplate earthquake occurred in a part of Guinea where no previous earthquakes have been reported in either historical or instrumental records. About 275 people were killed, 1,000 injured, and 4,000 houses destroyed.

In collaboration with geologists of the Guinean Ministry of Mines and Geology, fresh surface faulting was identified and mapped in the period January 12 through January 28. The surface faulting extends discontinuously for about 9 km with a W.N.W. concave-south trend from 11.886° N., 13.394° W. to 11.912° N., 13.474° W. Displacement is consistently right lateral with a maximum right slip of at least 13 cm on the principal break. The maximum across the whole zone is no doubt greater, but could not be measured because no fences, roads, or straight paths crossed the whole zone. One segment of the fault has a small vertical component with the southwest side down.

The surface faulting is probably on the causative fault. The National Earthquake Information Service placed the epicenter at 11.950° N., 13.605° W., approximately on line with but 15 km west of the surface faulting. The distribution of damage suggests an epicenter near the

surface faulting rather than at the instrumental location and the distribution of rockfalls and liquefaction effects, to the extent known, is compatible with either location. For a strike-slip M_s 6.2 event the expected surface rupture length and maximum displacement, based on empirical data (Bonilla, Mark, and Lienkaemper report cited below), are 8 km and 0.8 m, respectively. C.J. Langer deployed a net of 11 seismographs in the area of the fault in mid-January. A preliminary examination by Langer of seismograms of several well-recorded aftershocks indicates, based on S-P times, that most of the aftershocks were probably originating on the fault defined by the surface faulting. The various kinds of evidence taken together strongly suggest that the surface faulting was on the fault that caused the earthquake.

The faulting followed preexisting fractures, lines of vegetation, and rare small scarps, but other topographic and geologic evidence of active faulting was not seen in the sections that were examined. This indicates that the faulting was on a preexisting fault, but one with a low slip rate.

Reports:

Bonilla, M.G., Villalobos, H.A., and Wallace, R.E., 1984, Exploratory trench across the Pleasant Valley fault, Nevada: *U.S. Geological Survey Professional Paper 1274-B*, in press.

Bonilla, M.G., Mark, R.K., and Lienkaemper, J.J., Statistical relations among earthquake magnitude, surface rupture length, and surface fault displacement. (Approved by Director).

Lienkaemper, J.J., Comparison of two surface-wave magnitude scales: M in Gutenberg and Richter (1954) and M_s of Preliminary Determination of Epicenters. (Approved by Director).

Soil-Structure and Structural Response Studies

9910-02760

A.G. Brady and G.N. Bycroft

Branch of Engineering Seismology and Geology
U.S. Geological Survey
345 Middlefield Road, MS 977
Menlo Park, California 94025
(415) 323-8111, ext. 2881

Investigations

1. Ambient (wind-excited) studies were completed, using temporary Sprengnether digital recorders, on the Great Western building in Berkeley, the Hayward City Hall, and the Palo Alto City Hall. Dynamic computer study of the Great Western building, Berkeley, confirms the mode shapes and frequencies seen in the ambient study. The Hayward City Hall test used the already permanently installed accelerometers. The Palo Alto City Hall test, using temporary accelerometers, is designed to allow comparison of the structure's dynamic characteristics before and after significant stiffening of the 8-story tower.
2. The investigation of time-dependent structural response has been concluded with a study of its application to the ductility requirements of structures during earthquakes.
3. Research on the effect of soil-structure interaction and differential ground motions on the motion of structures was continued. The effect of soil structure interaction on the recording of accelerograms has been studied further with a paper in preparation. Initial design of experiments to verify corrections of accelerograms for soil structure interactions was made. These experiments are to be made in conjunction with experiments planned by S.R.I. International, who will be testing an explosive device aimed at simulating earthquakes.

Results

1. The selected locations for temporary accelerometer placement for the ambient study at Great Western are confirmed as the desirable location for permanent instrumentation, which will be installed in FY 84. Three translational modes and one torsional mode of vibration are identified by ambient and dynamic computer studies. Structural behavior during a strong earthquake will involve all these modes.
2. The ductility factor for a specific structure during an earthquake is a measure of how much ductility is demanded of a structure during an earthquake, and may reach the value of four, for example, indicating that the inelastic displacements within the structure were four times larger than when the elastic limit was reached. The results of the described investigation on structural response indicate, for example, that on the average, such a structure will enter the inelastic regime not only once but for a total of eight cycles of response.

3. The differential array of accelerometers at Hollister, California was completed. An analytical solution to the impact of an elastic column on an elastic halfspace was developed. An analytical solution to the motion of a truncated wedge dam including soil structure interaction when subjected to simulated earthquakes was determined and it was shown that an optimum design is achieved when the trapezoidal section of the dam has the form of a triangle.

Reports

Bycroft, G.N., and Mork, P.N., Seismic Response of a Trapezoidal Section Dam Including Soil Structure Interaction, to be submitted to *The Journal of Earthquake Engineering and Structural Dynamics*.

Perez, V., and Brady, A.G., 1984, Reversing cyclic demands on structural ductility during earthquakes, *Proceedings of Applied Technology Council Seminar on Earthquake Ground Motion and Building Damage Potential*, San Francisco, in press.

Holocene and Quaternary Geologic Studies

9540-03787

Robert O. Castle
Branch of Western Regional Geology
345 Middlefield Road MS 975
Menlo Park, CA 94025
(415) 323-8111, ext. 2293

Investigations

1. Completed studies of uplift across the Long Valley caldera, California, during the period 1905-1983, with an emphasis on recent (post-1975) activity.
2. Continued investigations of the magnitude and predictability of the unequal refraction error in geodetic leveling based on an examination of the historic record and the results of several recent experimental studies.
3. Revised and corrected edited and reviewed versions, respectively, of reports on the southern California uplift and its early-20th-century analogue.

Results

1. Our examination of the results of repeated levelings through the Long Valley area indicate that the post-1975 uplift centering on the resurgent dome probably is unique within this century--certainly with respect to its magnitude. Although a dramatic and apparently aseismic down-to-the-northwest tilt of the order of 10 μ rad occurred over the reach between Toms Place and Lee Vining during the period 1914-1932, it was apparently of tectonic origin and cannot be directly associated with magmatic activity within the caldera.

Reports

Castle, R. O., Estrem, J. E., and Savage, J. C., Uplift across Long Valley caldera, California: 27 ms. p., 10 figs., 1 table (approved by Director); submitted to Journal of Geophysical Research.

Castle, R. O., Brown, B. W., Jr., Gilmore, T. D., Mark, R. K., and Wilson, R. C., 1983, An examination of the southern California field test for the systematic accumulation of the optical refraction error in geodetic leveling: Geophysical Research Letters, v. 10, no. 11, p. 1081-1084.

Castle, R. O., Church, J. P., Yerkes, R. F., and Manning, J. C., 1983, Historical surface deformation near Oildale, California: U.S. Geological Survey Professional Paper, 1245, 42 p.

Late Quaternary Slip Rates on Active Faults of California

9910-03554

Malcolm M. Clark
Branch of Engineering Seismology and Geology
345 Middlefield Road, MS 977
Menlo Park, CA 94025
(415) 323-8111, ext. 2591

Investigations

1. Compile a table and map (1:1,000,000) of late Quaternary slip rates for faults of California from published and unpublished data. The following U.S.G.S. geologists act as evaluators and compilers for specific regions: North Coast Ranges, J. J. Lienkaemper, K. R. Lajoie, K. K. Harms, J. D. Sims, J. A. Perkins; Transverse Ranges and L. A. Basin, J. I. Ziony, A. M. Sarna-Wojcicki, J. C. Matti, J. C. Tinsley; Peninsular Ranges, J. I. Ziony; Salton Trough, R. V. Sharp; Mojave Desert, Great Basin, and Eastern Sierra Nevada, M. M. Clark; Cascade-Modoc Plateau, K. K. Harms, and D. S. Harwood. Edited by K. K. Harms, J. J. Lienkaemper, M. M. Clark, and J. I. Ziony.
2. Detailed study of Nunez fault and local geology northwest of Coalinga to determine extent of fault and its history. Nine leveling lines across the fault were remeasured (Rymer, Harms, Lienkaemper, Clark).
3. Determine age of five nested fluvial terraces of Tres Pinos Creek at Calaveras fault, south of Hollister, California. Formation of these terraces is related to lateral and vertical displacement along the Calaveras fault. The investigation concentrates on detailed soil descriptions and analyses and will yield late Quaternary slip rates. The soils will also be useful in other slip-rate studies nearby and in the San Francisco Bay region. T. C. Hanks and R. E. Wallace will investigate the relation of inter-terrace scarp profiles to scarp age at this site (J. W. Harden, K. K. Harms, S. N. Hoose, M. M. Clark).
4. Help map and photograph surface ruptures of the October 28, 1983, Borah Peak, Idaho, earthquake (M. M. Clark).

Results

1. Our table and map of late Quaternary slip rates for faults of California, completed in January, 1984, will appear in successively revised editions as better data come forth and new sites are measured. Each contributor is responsible for compiling, calculating, interpreting, and evaluating the slip rates for all available sites within a specific geographic area of the State. We have tried to be both informative and judgmental about each slip rate. Where possible, we report or estimate minimum and maximum values of both slip and age of offset features as allowed by the measurements at each site. We then use the resulting range of values to calculate the probable range in slip rate. In addition, each contributor makes a qualitative estimate of the

reliability of the slip and age estimates on the basis of the data and methods used. Although our evaluations are individual and may be somewhat arbitrary, we believe that our informed opinions form a valuable part of the table. Sources and comments for each site will allow users to evaluate the original data and methods by which we or the quoted source derived the slip rates.

The resulting table lists about 150 entries showing consistent ranges of values for a given style of faulting within structural-physiographic provinces, but distinctly different values between some provinces and between different styles of faults in the same province.

2. The Nunez fault, which experienced surface rupture on June 11, 1983 in association with an aftershock of the Coalinga earthquake sequence, has an apparent total length of 4.2 km; 3.3 km of this length ruptured in 1983. The fault lies in Cretaceous fan deposits of the Great Valley sequence, which is locally broken by other short (<4 km) faults subparallel to the Nunez fault. Of interest for the history of movement along the Nunez fault is the presence of Quaternary terrace deposits that have been vertically offset about 17 m by movement on the Nunez fault. Age of the terrace deposit is unknown, but is inferred to correlate with a period of increased precipitation during the late Pleistocene.

Results from remeasurement of nine leveling lines across the Nunez fault indicate that afterslip has added to the total vertical displacement. In the last measurement period (July 27, 1983 to January 30, 1984) one line experienced 26 mm of vertical offset across the fault. Earlier statements, in Summaries of Technical Reports, volume XVII, indicated that vertical displacement measured on the leveling lines was due to renewed rupture of the fault by subsequent aftershocks $>M_L$ 5.0. However, in light of the last set of measurements, a different process is envisioned. The good fit of all leveling data and initial field measurements plotted on a logarithmic time scale indicates that all offset along the fault was probably due to initial rupture on June 11 and afterslip (with no contributions from subsequent aftershocks). Afterslip on the Nunez fault is one of the few cases of well-documented afterslip on a reverse fault.

3. During the late Pleistocene, Tres Pinos Creek produced at least three distinct nested terraces, which are composed of coarse gravels intermixed with fine sands overlain by well-sorted silts and sands. Soils developed in the upper 2-3 m suggest the major terraces are about 10-15, 30-60, and 80-100 thousand yr B.P. in age. Offset related to the youngest terrace infers that a major strand of the Calaveras fault has slipped at a rate of between 3 to 11 mm/yr during Holocene time. Vertical movement probably also occurred during this time.

4. Investigations by D. J. Ponti and M. M. Clark helped establish a southern limit of tectonic ruptures south of Elkhorn Creek. S. K. Plymell and Clark found and mapped diverging ruptures in Antelope Flat.

Reports

- Clark, M. M., Harms, K. K., Lienkaemper, J. J., Harwood, D. S., Lajoie, K. R., Matti, J. C., Perkins, J. A., Rymer, M. J., Sarna-Wojcicki, A. M., Sharp, R. V., Sims, J. D., Tinsley, J. C., Ziony, J. I., 1984, Preliminary slip-rate table and map of late-Quaternary faults of California: U.S. Geological Survey Open-File Report 84-106.
- Clark, M. M., Harms, K. K., Lienkaemper, J. J., and Ziony, J. I., 1984, Late-Quaternary slip-rates for California faults [abs.]: International Symposium on Recent Crustal Movement, February 9-14, 1984, Wellington, New Zealand.
- Clark, M. M., Harms, K. K., and Lienkaemper, J. J., 1984, Uncertainties in slip rates [abs.]: Earthquake Notes, v. 55, in press.
- Clark, M. M., Harms, K. K., Lienkaemper, J. J., and Ziony, J. I., 1984, Slip-rate table and map of late Quaternary faults of California [abs.]: Earthquake Notes, v. 55, in press.
- Harden, J. W., 1984, Techniques and uncertainties in using soil development for stratigraphic, geomorphic, and age analyses [abs.]: Earthquake Notes, v. 55, in press.
- Harms, K. K., Harden, J. W., Hoose, S. N., and Clark, M. M., 1984, Estimating slip rates along the Calaveras fault, California, using soil chronology and geometry of stream terraces [abs.]: Earthquake Notes, v. 55, in press.
- Lubetkin, Lester, and Clark, M. M., 1984, Inconsistent slip rates along the Lone Pine fault, Eastern California [abs.]: Earthquake Notes, v. 55, in press.
- Rymer, M. J., 1984, Constraints on slip and age determinations for estimation of late Quaternary activity on the Big Valley and Adobe Creek faults, Lake County, California [abs.]: Earthquake Notes, v. 55, in press.
- Rymer, M. J., Harms, K. K., Clark, M. M., and Lienkaemper, J. J., 1983, Surface faulting associated with an aftershock of the May 2, 1983 Coalinga, California, earthquake [abs.]: Transactions, American Geophysical Union, v. 64, p. 748.

Holocene Styles of Surface Faulting
Along the Creeping Segment of the
San Andreas Fault, San Juan Bautista

21335

W. R. Cotton, N. T. Hall, and E. A. Hay
Foothill-De Anza Community College District
Los Altos Hills, California 94022
(415) 948-8590

Investigation

This project is designed to recognize and evaluate localities along the creeping segment of the San Andreas fault capable of yielding information about 1) characteristics of the style of rupturing in a creeping segment (as opposed to locked segments), 2) slip rates for creep that extend back into pre-historic time, and 3) recurrence interval determinations if discrete rupture events are recognizable.

Results

1. All field work conducted as part of this investigation was summarized in Volume XVII of the Summaries of Technical Reports, December 1983.
2. Of attempts to age-date three paleostream channels located during trenching, only one radiocarbon age, 420 ± 90 years B.P., has thus far been determined. This age is for a cobble channel that is tectonically offset approximately 20 feet. Either the creep rate here was considerably slower prior to 1885 than it was since, or the age of 420 ± 90 years B.P. is much too old. Although we believe the latter to be most likely, several more charcoal samples are being evaluated in order to clarify the discrepancy between a well determined average creep rate of 34-35 mm/yr. since 1885 and the average value of less than 15 ± 15 mm/yr. indicated after dendrochronologic corrections are made for the age of 420 ± 90 years B.P.
3. Twenty (20) small charcoal samples are presently being evaluated by using the accelerator technique. Results are expected in June, 1984. Seven (7) of these are from the paleostream channels themselves, and thirteen (13) are from older fan sediments into which the channels were incised.

Reports

Hall, N. T.,¹⁴ Hay, E. A., and Cotton, W. R., 1984, Problems in the application of ¹⁴C dates to slip rate determinations of the San Andreas fault: Seismological Society of America, Abstracts and Program.

Seismic Hazard Investigations
in the Pacific Northwest

21861, 21862

R.S. Crosson
S.D. Malone
Geophysics Program
University of Washington
Seattle, WA 98195
(202) 543-8020

Investigations

1. Operation and routine preliminary analysis of the western Washington regional seismograph network.
2. Study of hypocenter mislocations for a regional or local seismograph network due to lateral or 3-dimensional structural variations and application to the Washington seismograph network.
3. Interpretation of Pn observations for both eastern and western Washington.
4. Development and implementation of automated processing for digital network data.
5. Crustal structure determination in the vicinity of Mt. St. Helens and in the greater Puget Sound region from earthquakes and explosions recorded digitally on the local and regional networks.
6. Locations, focal mechanisms and occurrence characteristics of subcrustal earthquakes beneath western Washington in relationship to possible active subduction.
7. Automated spectral analysis of digital seismic data for determination of source parameters for local earthquakes in the Pacific Northwest.

Results

1. Network operation for stations in western Washington, eastern Washington, and northern Oregon continued normally. No unusual regional earthquake activity was recorded outside of the Mt. St. Helens region. Some effort was expended to assist in recording aftershocks from the Borah Peak earthquake of October 28, 1983. In early February earthquake swarm activity at Mt. St. Helens increased to the point of creating an eruption alert; however the eruption was predominantly endogenous with only a small lobe being added to the composite dome. Again in late March, a dome building episode was accompanied by a significant increase in small earthquake activity.

2. A linearized travel-time prediction program for a layered structure with superimposed 3-dimensional slowness perturbations forms the basis for studying mislocation errors in structures with laterally varying velocity. Artificial data were generated with the 3-dimensional structure and relocated with a conventional layered model. Quantitative evaluation of the mislocation errors is possible and we have demonstrated, using the Bear Valley area as an example, that the predicted errors agree with observed errors. A preliminary evaluation of possible location errors for the Puget Sound region has been performed.

3. A joint P/S layered structure inversion program was developed to use earthquake and explosion arrival times for providing additional constraint on structure determination where high quality S arrivals are measured. This method uses coupled P and S models, and makes use of an independently determined VPVS ratio.

4. A new algorithm for phase picking has been developed and incorporated into an automated processing program for digital network data. Work is continuing to fully automate the network processing by providing additional feedback between the picking and locating elements. An important aspect of the automated processing is a quantitative and consistent estimate of phase picking errors, presently implemented for P waves only. All procedures are currently being run in test mode or utilized for special studies. We view these efforts as being important in the long range to improve the quantity, quality and consistency of network data analysis. In current work on structure inversion, for example, we are utilizing auto-picked phase data and we believe superior results are possible in comparison to hand picked data.

5. Using the joint P/S inversion program, crustal structure at Mt. St. Helens was inverted from both earthquake and explosion arrival times. The incorporation of S phases offers significantly greater stability to the modeling process than the use of P phases alone. Our final model indicates that the P velocity in the vicinity of St. Helens rises rapidly to about 6.1 km/sec at 1 km depth (very high shallow velocity) and then increases slowly in approximately a linear fashion to about 6.5 km/sec at 20 km depth. In comparison with the Puget Sound region, higher velocities are reached at shallower depths but mid-crustal values are lower. Digitally recorded network data are being assembled and reprocessed for crust and upper mantle structure inversion in the greater Puget Sound region. The structure inversion effort is preliminary to undertaking a careful analysis of deep earthquake seismicity.

6. Results from the Pn analysis reinforce the existence of significant differences in structure between eastern and western Washington. East of the Cascade Range, Pn velocity averages 8.18 ± 0.02 km/sec, whereas the average for western Washington is 7.77 ± 0.02 km/sec. Anisotropy appears to be significant east but relatively unimportant west of the Cascades. Calculated Moho dip east of the Cascades, assuming no lateral change in crustal velocity, is about 0.7 degree whereas the calculated regional dip for the west is about 2.1 degrees in a southeasterly direction. There is thus little evidence in the regional Pn data for Moho dip associated with a dipping slab

beneath western Washington.

7. Routines for determining seismic source parameters from digital seismic data are currently being implemented and tested. A synthetic source spectrum is fit to the amplitude density spectrum for P, S, and Coda waves corrected for instrument response and Q. All events located by the routine processing will ultimately have source parameters determined by this process. Obtaining and maintaining good station calibration is a major part of this effort.

Reports

Crosson, R.S., and D. Hesser, 1983, An algorithm for automated phase picking of digital seismograms from a regional network, (abs) EOS, 64, p 775.

Univ. of Wash. Geophysics Program, 1984, Seismicity of the Washington and Northern Oregon Cascades, October 1 through December 31, 1983, Quart. Tech. Rept. 83-D, 10p.

Wu, S., 1983, Earthquake mislocation due to lateral heterogeneity: M.S. Thesis, Univ. of Washington.

Wu, S., and R.S. Crosson, 1983, Effect of lateral heterogeneity on earthquake locations (abs), EOS, 64, p 775.

Zervas, C., 1984, A Time-Term analysis of Pn Velocities in Washington, M.S. Thesis, Univ. of Washington (in prep).

**Activity of the Santa Ynez Fault:
Continuation of Investigations**

Contract Number: 21367
Principal Investigators: Arthur C. Darrow
Dames & Moore
812 Anacapa Street, Suite A
Santa Barbara, California 93101
(805) 963-9676
and Arthur G. Sylvester
Department of Geological Sciences
University of California
Santa Barbara, California 93106
(805) 961-3471

Investigations

1. This study is a continuation of our previous investigations (Darrow and Sylvester, 1982) which demonstrated late Quaternary activity on the central reach of the Santa Ynez fault. In our current study we have excavated several trenches parallel and perpendicular to the fault (see Figure 1) in order to assess the magnitude, direction and timing of recent slip events on the fault.

Results

Detailed examination and logging of the faulting relationships exposed in the trenches allow the following interpretations:

1. The most recently active trace of the Santa Ynez fault offsets deposits of the first three emergent stream terraces of the Santa Ynez River.
2. Stream deposits in the present river channel are not offset by the fault.
3. Recent movements along the fault have been dominated by left separation.
4. Evaluation of a buried stream bank in the vicinity of the fault suggests a minimum of four meters of left separation in the latest Pleistocene and Holocene time.
5. A comparison of the soils developed on the stream terraces at the trenching site with well-dated terraces along the Ventura river suggests that the youngest terrace deposits offset by the fault are mid to late Holocene in age.

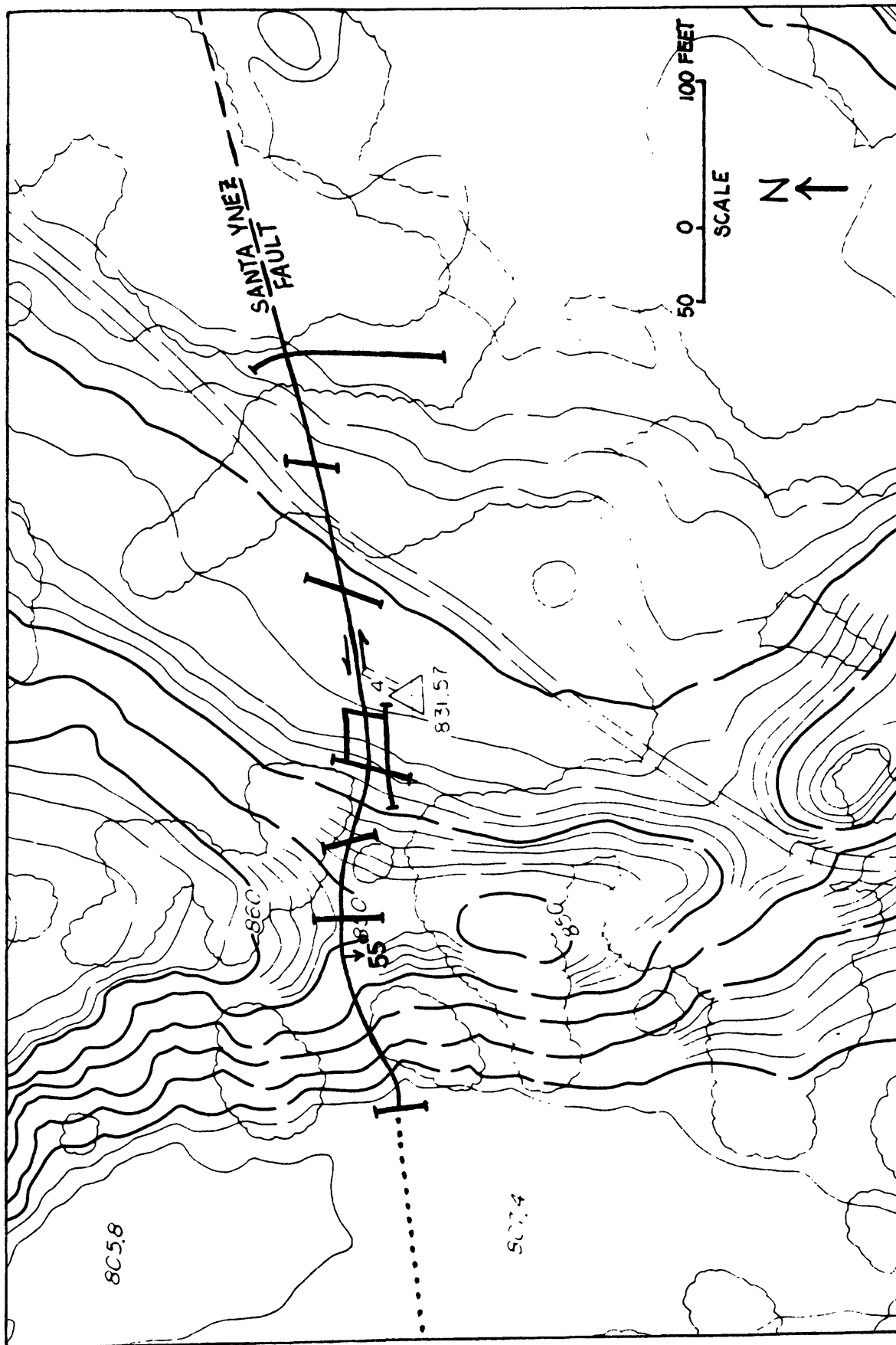


Figure 1. Trench Location Map

Tectonics of Central and Northern California

9910-01290

William P. Irwin
Branch of Engineering Seismology and Geology
U. S. Geological Survey
345 Middlefield Road
Menlo Park, CA 94025
415 323-8111, ext. 2065

Investigations

1. Tectonic accretion of allochthonous terranes of northern California, including delineation of plutonic belts through use of isotopic ages and other data, and integration of other tectonic features.
2. Utilization of aerial photography to correlate geologic features that were mapped along ground traverses made during the previous report period in the Rattlesnake Creek and Hayfork terranes of the Hyampom and Dubakella Mountain 15-minute quadrangles, southern Klamath Mountains.
3. Relations between seismicity and crustal out-gassing of carbon dioxide: collaboration with Ivan Barnes. Color proof for a map showing the global spatial relations between out-gassing of carbon dioxide and major zones of seismicity was approved for printing as an I-series map.
4. Paleomagnetic study of Permian and younger strata of the Eastern Klamath terrane: collaboration with E. A. Mankinen and C. S. Gromme.

Results

Much effort was made to determine the times of rotation of the Klamath terranes relative to the time of their accretion to North America. That relationship indicates whether the rotations occurred while the terranes were parts of oceanic plates or while part of the North American continent. The results of our studies suggest that nearly all the rotation of the Klamath terranes had occurred by Early Cretaceous time while the terranes were parts of oceanic plates. The plutonic belts and other components of the terranes must originally have been orientated much differently than now, relative to stable North America. Based on the available data, the primitive nucleus of the Klamath Mountains province, the Eastern Klamath terrane, was part of a volcanic island arc that faced SW during early Paleozoic time. Underplating of the Eastern Klamath terrane by hornblende and mica schists of the Central Metamorphic terrane was caused by subduction of a NE-moving plate beneath the arc during Devonian time. Deposition of a thick prism of flysch-like strata (Bragdon Formation) followed during Mississippian time, with volcanism (Baird Formation) becoming important again in Late Mississippian to Early Permian time. A

carbonate reef (McCloud Limestone) formed along the arc during Early Permian time and was partly contemporaneous with the Permian Dekkas Andesite and comagmatic plutons of the McCloud plutonic belt. The arc continued to face SW until latest Triassic or earliest Jurassic time, and then rotated approximately 50° clockwise to face westward during much of Early to Late Jurassic time. Volcanism and deposition continued in the Eastern Klamath terrane during the Early and Middle Jurassic. The Western Paleozoic and Triassic and the Western Jurassic terranes sequentially sutured to the developing W-facing Klamath terrane during the Middle and Late Jurassic, accompanied by intrusion of plutons. During latest Jurassic and possibly earliest Cretaceous time the arc rotated an additional 50° clockwise to attain nearly its present NW-facing orientation by the time it accreted to North America.

Reports

Irwin, W. P., 1983, Review of "Orogeny," Miyashiro, A., Aki, K., and Sengor, A. M. C., eds., Wiley: Precambrian Research, v. 23, p. 197-198.

Irwin, W. P., and Thurber, H. K., 1983, Agua Tibia Primitive Area, California, in Marsh, S. P., and others, eds., Wilderness mineral potential: U. S. Geological Survey Professional Paper 1300, p. 164-166.

Irwin, W. P., 1984, Preaccretion and postaccretion plutonic belts in allochthonous terranes of the Klamath Mountains, California and Oregon, in Howell, D. G., and others, eds., Proceedings of the circum-Pacific terrane conference, 1983: Stanford University Publications in the Geological Sciences, v. 18, p. 119-121.

Irwin, W. P., Mankinen, E. A., and Gromme, C. S., 1984, Paleomagnetism in the Klamath Mountains, California and Oregon, in Howell, D. G., and others, eds., Proceedings of the circum-Pacific terrane conference, 1983: Stanford University Publications in the Geological Sciences, v. 18, p. 122-125.

Anderson, R. E., Irwin, W. P., and Thenhaus, P. C., 1984, Southern Rocky Mountains seismic source zones--Summary of workshop convened January 23-24, 1980, in Thenhaus, P. C., ed., Summary of workshops concerning seismic source zones of the conterminous United States, convened by the U. S. Geological Survey, 1979-1980, Golden, Colorado: U. S. Geological Survey Circular 898, p. 14-19.

Blake, M. C., Jr., Harwood, D. S., Helly, E. J., Irwin, W. P., Jayko, A. S., and Jones, D. L., 1984, Preliminary geologic map of the Red Bluff 100,000 quadrangle, California: U. S. Geological Survey Open-File Map 84-105, with text, 22p.

Mankinen, E. A., Irwin, W. P., and Gromme, C. S., 1984, Tectonic rotations suggested by paleomagnetic studies of the Eastern Klamath terrane: Society of Economic Paleontologists and Mineralogists, Pacific Section, San Diego meeting, April 1984, abstract, in press.

Irwin, W. P., 1984, Plutonic belts in allochthonous terranes of the Klamath Mountains, California and Oregon: Geological Society of America, Program with Abstracts, Anchorage meeting, May 1984, in press.

Irwin, W. P., 1984, Age and tectonics of plutonic belts in accreted terranes of the Klamath Mountains, California and Oregon: AAPG terrane symposium volume, in press.

Mankinen, E. A., Irwin, W. P., and Gromme, C. S., 1984, Implications of paleomagnetism for the tectonic history of the Eastern Klamath and related terranes in California and Oregon, in Nilsen, Tor, ed., Field guide to the Hornbrook Formation: Society of Economic Paleontologists and Mineralogists, Pacific Section, in press.

Ground Response Along The Wasatch Front

9950-01919

Kenneth W. King
Branch of Engineering Geology and Tectonics
U.S. Geological Survey
Box 25046, MS 966, Denver Federal Center
Denver, CO 80225
(303) 234-5087

Investigations

The objective is to improve fundamental knowledge about how the ground response along the Wasatch Front is effected by local and regional geology. Response data have been acquired in the Salt Lake City, Ogden, Provo, Logan, and Cedar City areas. Preliminary soils and shallow unconsolidated sediment data are being correlated with the response data.

A cooperative agreement was signed with the Kansas Geological Survey. The cooperative investigation is to develop and test shallow P- and S-wave reflection techniques. The investigation is to take approximately 1 year at test sites in Kansas, Denver, and the Wasatch area.

The general goals and organization were worked out for the urban hazards investigation. A committee selected several types of seismic equipment for future site investigations. Specifications of several seismic systems were compared for future references.

The ground motion and urban hazard investigations in Salt Lake City were expanded to include strong motion studies. A cooperative strong motion program with the Utah Geological and Mineral Survey (UGMS) and the U.S. Geological Survey (USGS) was finalized.

A seismic study has been completed with the National Park Service. The study investigated the effects of induced seismic energy from road traffic and construction on adobe structures and archeological ruins.

Results

1. The activities in the Wasatch area are designed to prepare data reports and journal manuscripts. One publication is in the forthcoming Third International Conference on Microzonation. The Wasatch data report is complete and in CRT. A report on the results of the shallow-reflection program will be presented at the Urban Earthquake Hazards Evaluation Workshop.
2. All planned field equipment are under purchase contracts with delivery dates in June and August.
3. The preliminary experiments in the shallow-reflection program are very encouraging. A source has been developed which is low in acoustical wave energy and high in P and S energy in the 100-300 Hz band. A type site has

been selected, drilled, and logged. Preliminary work shows good reflections at approximately 10 m with resolutions of 1 m or less.

4. A network of strong-motion instruments was installed in the Salt Lake City area. The sites were selected by a cooperative effort between UGMS and USGS scientists and were selected accordingly to type and depth of underlying sediments.
5. Induced seismic motions were documented on adobe construction and analyzed. Preliminary reports were made to the Federal Highway Administration and the National Park Service.

Reports

Hays, W. W., and King, K. W., 1982, Zoning of the earthquake ground shaking hazard along the Wasatch fault zone, Utah [abs.]: International Conference on Microzonation, 3d, Seattle, July 1982.

King, K. W., 1982, A study of surface and subsurface ground motion at Calico Hills, Nevada Test Site: U.S. Geological Survey Open-File Report 82-1044, 19 p.

King, K. W., Hays, W. W., and McDermott, P. J., 1983 [1984], Wasatch front urban area seismic response data report: U.S. Geological Survey Open-File Report 83-452, 70 p. [in press].

Coastal Tectonics, Western U.S.

9910-01623

Kenneth R. Lajoie
Branch of Engineering Seismology and Geology
345 Middlefield Road, M/S 977
Menlo Park, CA 94025
(415) 323-8111, ext. 2642

Investigations

1. The objectives of this project are to determine patterns and rates of Quaternary crustal deformation and ground response in the coastal area of the western United States by mapping and dating marine terraces and associated marine and alluvial deposits, and evaluating geotechnical data from marine and alluvial deposits in deep sedimentary basins.

Project personnel are Dan Ponti, Scott Mathieson and Patricia McCrory.

Results

1. Matt Hageman (student supported by Project) mapped marine terrace at the mouth of Whale Gulch in northern California. Logs from basal alluvial deposits on wave-cut platform yield ^{14}C dates of 42, 45 and >57 ka B.P. The >57 ka indicates the underlying marine terrace is 60 ka or older. This terrace and its overlying deposits are similar to the terrace and deposits at Shelter cove about 7 km to the NW that were previously dated at 45 ka B.P.; the date from Whale Gulch implies that the date at Shelter Cove is incorrect. Also, a possible strand of the San Andreas fault was previously mapped in Whale Gulch. If this bedrock shear zone is a strand of the San Andreas fault, it has not moved in the past 60 ka because the overlying terrace deposits are not offset.
2. Pat McCrory is studying the Quaternary tectonic history of the southern Eel River sedimentary Basin north of Cape Mendocino in northern California by reconstructing basin depths using microfossils and mapping emergent terraces. The pattern of terrace deformation does not reflect the northward migration of the Mendocino triple junction.
3. A strand of the Newport-Inglewood fault exposed in trenches on the Huntington Beach Mesa (Woodward-Clyde Consultants) in southern California offset marine deposits we estimate to be 120 ka B.P. The marine deposits that cap this and adjacent Mesas correlated with the Palos Verdes sand on the first emergent terrace on the Palos Verdes Hills to the north. Deformation of this young marine deposit records the complex crustal movements (folding and faulting) in the Newport-Inglewood fault zone in the southern Los Angeles Basin over the past 120 ka.

4. Scott Mathieson and Dan Ponti assembled and began running an amino-acid laboratory to date marine shells along the west coast of the United States. Ponti is analyzing surface and subsurface fossil shells from marine deposits straddling the Palos Verdes fault and the Newport-Inglewood fault zone in the southern Los Angeles Basin to determine rates of fault displacement in this densely populated area. Initial results indicate that faulted marine deposits previously thought to be Palos Verdes Sand (120 ka B.P.) may be the uppermost San Pedro Sand (~200 ka B.P.). If this correlation is correct, the warm-temperature aspect of the fossil faunas in Palos Verdes Sand may not be stratigraphically diagnostic, as previously believed.
 5. Lajoie assembled slip rate data for coastal faults that were incorporated into a statewide compilation supervised by Malcolm Clark. Horizontal slip rates are difficult to establish because few datable topographic or stratigraphic features cross faults at high angles. Vertical separations across numerous faults are easier to establish, but these data may have little or no value in determining slip rates.
 6. Lajoie and Mathieson compiled data on coastal erosion in San Mateo County caused by heavy storms in January, 1983. The most severe erosion occurred on the north sides of promontories where little or no erosion had occurred in the past several decades. The slope failure that closed State Highway 1 at Devil's Slide was caused primarily by groundwater infiltration, not by wave erosion at the toe of the slope.
7. Attended Recent Crustal Movements Symposium in Wellington, New Zealand.
- A. With K. Berryman, A. Hull (New Zealand Geological Survey) and Y. Ota (Yokohama National University) visited numerous coastal sites on North Island to observe emergent Holocene terraces. A major problem is to differentiate between terraces produced by coseismic uplift events and storms. No concrete method has been devised to make this distinction, and no diagnostic test could be proposed. However, it appears that storm events are best preserved as beach ridges in embayments, and uplift events are best expressed as distinct terraces along open coastlines. However, beach ridges that record coseismic uplift events can form on open coasts, and even on exposed rocky headlands where wave erosion cannot cut a terrace. Here, the beach ridges (storm berms) form above the high tide line after the uplift event. Therefore, the oldest ^{14}C dates from such a berm date the preceding uplift event, and the youngest dates the uplift event that stranded the berm above the surf zone. Unfortunately, datable material is seldom found in storm berms, so there is little hope in radiometrically dating uplift events they record.

- B. Coverbed stratigraphy (primarily tephrachronology) plays an extremely important role in dating Pleistocene emergent marine terraces on North Island. The lack of tephra beds on marine terraces along the California coast is compensated for by the presence of datable marine fossils.

8. The rates of vertical crustal deformation is generally closely associated with the geologic processes producing that deformation. Along the central California coast, lateral tectonics dominate, and uplift rates are generally low (~ 0.3 m/ka). Here, uplift is probably related to regional mountain building processes, which include crustal thickening due to lateral compression. On local structures (folds and fault blocks) orthogonal to the direction of maximum crustal shortening, uplift rates may be very high (5-15 m/ka). The Ventura Avenue anticline is an example of a rapidly forming structure in an area of intense crustal shortening; Middleton in the Gulf of Alaska is another. In both areas, uplift rates are about 10 m/ka. These rates may be close to the upper limit of purely tectonic uplift. Intermediate, both in scale and rates of uplift, between these two processes are vertical crustal movements associated with directional changes in major structural patterns of elements, for example, the Mendocino triple junction in northern California and the big bend in the San Andreas fault in southern California. Rapid, short-term (episodic) and reversible regional vertical crustal movements (Palmdale Bulge) are associated with the Big Bend, but this sort of activity has not yet been detected in northern California. However, a narrow zone of rapid vertical structural movement, which includes the Ventura Avenue anticline, coincides with the southern boundary of the Palmdale Bulge, and emergent Holocene terraces record subregional uplift rates of 4.0 m/ka just south of the Mendocino triple junction. Uplift rates along the convergent subducting coastlines of Oregon and Washington vary from intermediate (3.0 m/ka) to low (0.0 m/ka). Landward tilt of emergent marine terraces locally in this area probably reflects the subduction process. In all the tectonic regimes outlined above, it is still not clear if vertical deformation takes place gradually or episodically, as by coseismic uplift; both processes may take place in different areas at the same time or at the same place at different times. The rapid, short-term vertical movements, such as those associated with the Palmdale Bulge, may be better indicators of long-term trends than of imminent seismicity. The most rapid vertical crustal movements recorded are those associated with volcanic edifices, for example, Iwo Jima Island, which has been rising at 10-20 cm/yr for 400 years (data of Kaizuka). It is not clear if the island has been rising episodically (the volcano is terraced) or gradually (the terraces may have been produced by storms), but it is clear that rapid vertical movements, which may be related to thermal expansion and contraction or other volcanic processes, are not necessarily indicators of imminent eruption. A major task in both the tectonic and volcanic problems is to recognize those vertical movements that are premonitory signals.

Reports

Lajoie, K. R., and Mathieson, S. A. (in press), Coastal erosion and hazards, San Mateo County, California, in *Coastal erosion in California*, ed. by G. Griggs: Orin Pilkey, publisher.

Lajoie, K. R., Sarna-Wojcicki, A. M., Kennedy, G. M., Mathieson, S. A., McCrory, P. A., 1983, Late Quaternary coastal tectonics of the Pacific Coast of the United States [abs.]: EOS. v. 64, no 45, p. 854.

Lajoie, K. R., Sarna-Wojcicki, A. M., Kennedy, G. M., Mathieson, S. A., McCrory, P. A., Morrison, S. O., and Stephens, T. A., 1983, Late Quaternary coastal tectonics of the Pacific Coast of the United States [abs.]: Abstracts of the International Symposium on Recent Crustal Movements of the Pacific Region, Wellington, New Zealand, February, 1984, p. 28.

Magnetostratigraphy and Paleomagnetism of the Saugus
Formation, Los Angeles County, California

Contract No. 14-08-0001-21219

Shaul Levi, Principal Investigator
Robert S. Yeats
College of Oceanography
Oregon State University
Corvallis, Oregon 97331
(503) 754-2912

The Saugus Formation is widely exposed in the East Ventura Basin in areas undergoing rapid urbanization north and west of Los Angeles (Figure 1). In the area of our study near Castaic Junction the Plio-Pleistocene Saugus Formation consists of nonmarine conglomerates, sandstones, silty sandstones, and sandy-siltstones.

The primary objective of our paleomagnetic investigation has been to identify dated magnetozones and geomagnetic reversal boundaries to more accurately date the Saugus sediments in this area. This would enable one to make correlations with other age calibrated sections of Saugus nearer to the Pacific coast and to determine average sedimentation rates and possibly detect changes of deposition with time. Furthermore, the magnetostratigraphy and paleomagnetism data could be used to estimate the rotation, tilting and translation of the Saugus, associated with major faulting and the tectonic activities in this region.

To establish a reference magnetostratigraphic section we sampled along the transmission line (TL) and the Santa Clara River (SCR) in the Castaic Junction oil field just north of Pico Canyon (Figure 2). The TL section consists of well exposed unfaulted homoclinal sedimentary beds dipping about 50° to the north-northeast. The SCR section exposes yet younger beds of the Saugus Formation which dip more gently (20° - 30°) to the northeast, and correlations between the TL and SCR sections are relatively unambiguous (Winterer and Durham, 1962; Figure 2).

Sites were selected at interbeds of the finer-grained sediments (siltstone, sandy siltstone, and silty sandstone), which are typically between 0.5 and 5 m thick. At each site three independently oriented hand samples were obtained. In the laboratory we cut two specimens from each hand sample, and at least two specimens from each site were demagnetized in progressively increasing alternating fields (AF), up to between 400 and 1000 Oersted, to isolate the primary remanence and to determine the blanket alternating fields for demagnetizing the remaining specimens at each site. At least four blanket AF levels were used for each specimen of every site. Figure 3 shows the behavior of two specimens during progressive AF demagnetization. The directions of both normal and reversely magnetized specimens are well clustered, suggesting that both contain only minor components of secondary remanence. The initial increase of the normalized intensity curve of the reversely

polarized specimen is commonly observed and is consistent with the overprinting influence of the present-day normal field. Figure 4 shows the stable directions (after AF demagnetization to 300 Oe) of all six specimens from two sites before and after bedding correction. The fact that the mean site directions prior to bedding corrections are clearly distinct from the mean Quaternary and the present field supports the interpretation that the stable direction predates folding.

Paleomagnetic directions were calculated when appropriate and the data were analyzed in two ways: (1) Each specimen was assigned equal weight; this usually resulted in data from two specimens per oriented sample and six specimens per site. (2) We combined the data of specimens from each oriented sample; thereby halving the number of independent vectors (N). The two methods yielded essentially identical directions. In most cases estimates for the precision parameter (k) increased significantly or hardly changed when N was halved; however, the radius of the 95 percent cone of confidence (α_{95}) usually increased or remained the same when N decreased. A total of 64 sites were sampled, of which 57 yielded polarity information, and 36 sites were suitable for obtaining the paleomagnetic direction.

The sampled sections are predominantly of reversed polarity containing dispersed normal beds, and capped by a sequence of normal polarity. An ash layer in the upper normal zone of the TL section is chemically very similar to the ~0.7 MY Bishop and Friant ashes (analysis by Sarna-Wojcicki, 1983). The chemistry of the ash bed together with the biostratigraphically determined Plio-Pleistocene age suggest that the Saugus in our sampling area was deposited during the Matuyama (reversed) and lower Brunhes (normal) epochs, and its bottom age is younger than 2.5 MY (Figure 5).

Site SCS 25 of the Santa Clara River section and site TL 54 of the transmission line section represent periods of normal polarity in the Matuyama epoch. These sites are shown stratigraphically in Figure 5, and they represent the deepest (oldest) normal polarity sites in their respective sections. If the normal site in the SCR section is assumed to belong to the Jaramillo event, then the resulting sedimentation rate between site SCS 25 and the Brunhes/Matuyama boundary is about 0.8 km/MY. Similarly, if the volcanic ash is assigned a 0.7 MY age and site TL 54 to the Olduvai event, the average sedimentation rate is 0.9 km/MY. The similarity in the average sedimentation rates of the SCR and TL sections lends some confidence to the otherwise rather arbitrary assignments of sites TL 54 and SCS 25 to the Olduvai and Jaramillo events, respectively. Furthermore, it is inferred from subsurface well data that the upper approximately 300 m of Saugus are covered by younger deposits in the study area and are unavailable for sampling. Hence, based on 0.9 km/MY sedimentation rate, the youngest Saugus was deposited about 0.1 to 0.2 MYBP (million years before present). The magnetostratigraphic data suggest that the Saugus in the TL section was folded during the past 1 MY with average tilting between 50°-60°/MY. In the SCR section the average rate of tilting is greater than 30°/MY during the past million years.

The mean paleomagnetic direction (inverted to normal polarity) of the Matuyama sites of both TL and SCR sections is $D=20^\circ$, $I=57^\circ$, $k=54$, $\alpha_{95}=4^\circ$, $N=27$. The mean direction of the Brunhes sites of both TL and SCR sections is $D=15^\circ$, $I=49^\circ$, $K=130$, $\alpha_{95}=5$, $N=9$ (Figure 6). The observed average inclination is not significantly different from that of the geocentric axial dipole of 54° . Hence, there is no evidence for north-south translation of the sampling location. The measured declination, however, indicates progressive clockwise rotation of the study area by about 30° since sometime in the Matuyama epoch ($t < 2.5$ MY).

References

- Winterer, E.L. and Durham, D.L., 1962. Geology of southeastern Ventura basin, Los Angeles County, California. U.S. Geological Survey Prof. Paper 334-H, p. 275-366.
- Mankinen, E.A. and Dalrymple, G.B., 1979. Revised geomagnetic polarity time scale for the interval 0 to 5 m.y.B.P., J. Geophys. Res., 84, p. 615-626.

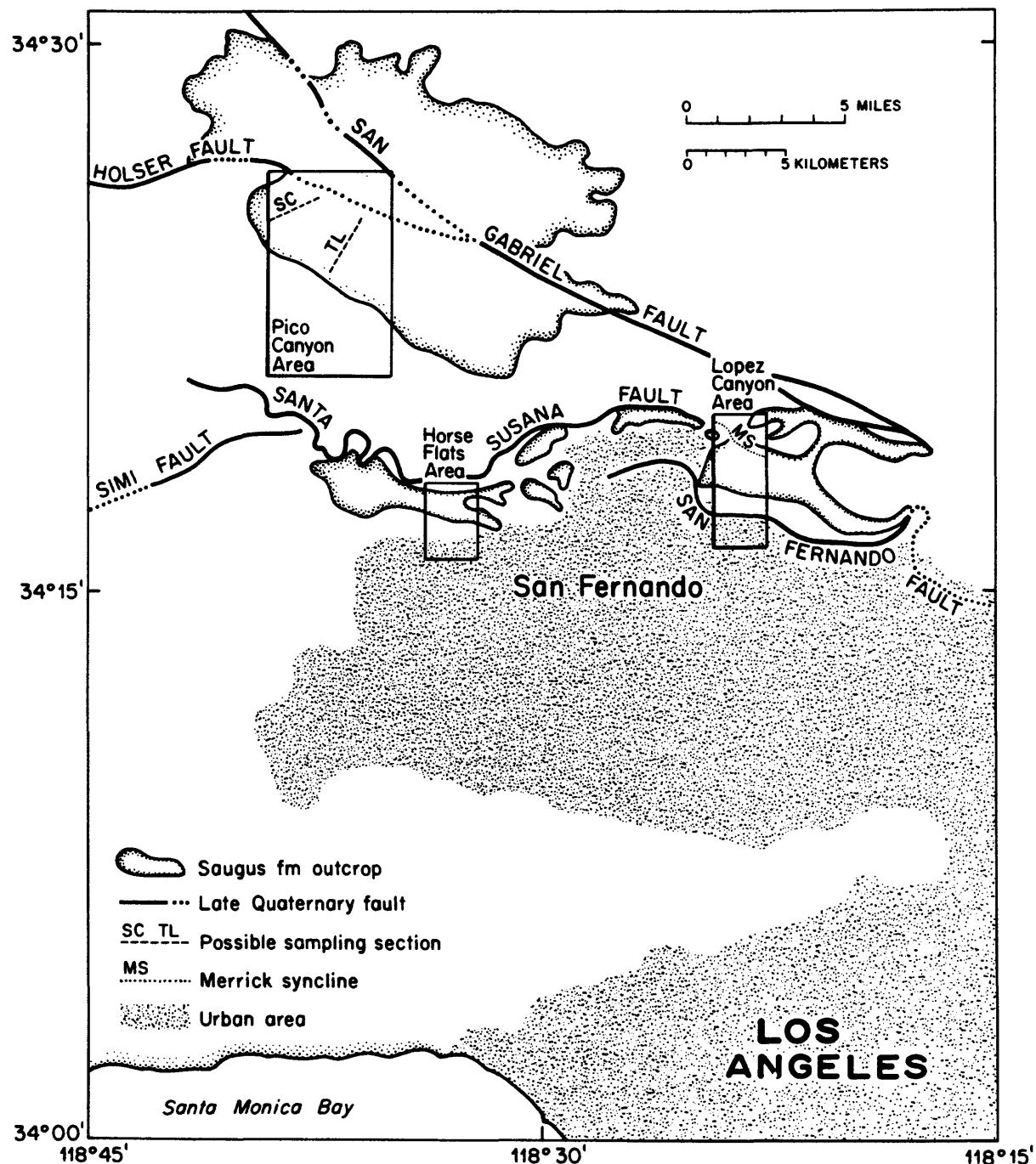


Figure 1. Location of Saugus outcrops in the east Ventura basin. The rectangles enclose regions where detailed magnetostratigraphic studies are planned. (SC = Santa Clara River section; TL = transmission line section; MS = Merrick syncline). Adapted from "Geologic Map of the San Gabriel Mountains, California: 1:250,000, by W. G. Bruer, California Division of Mines and Geology Bull. 196, 1975.

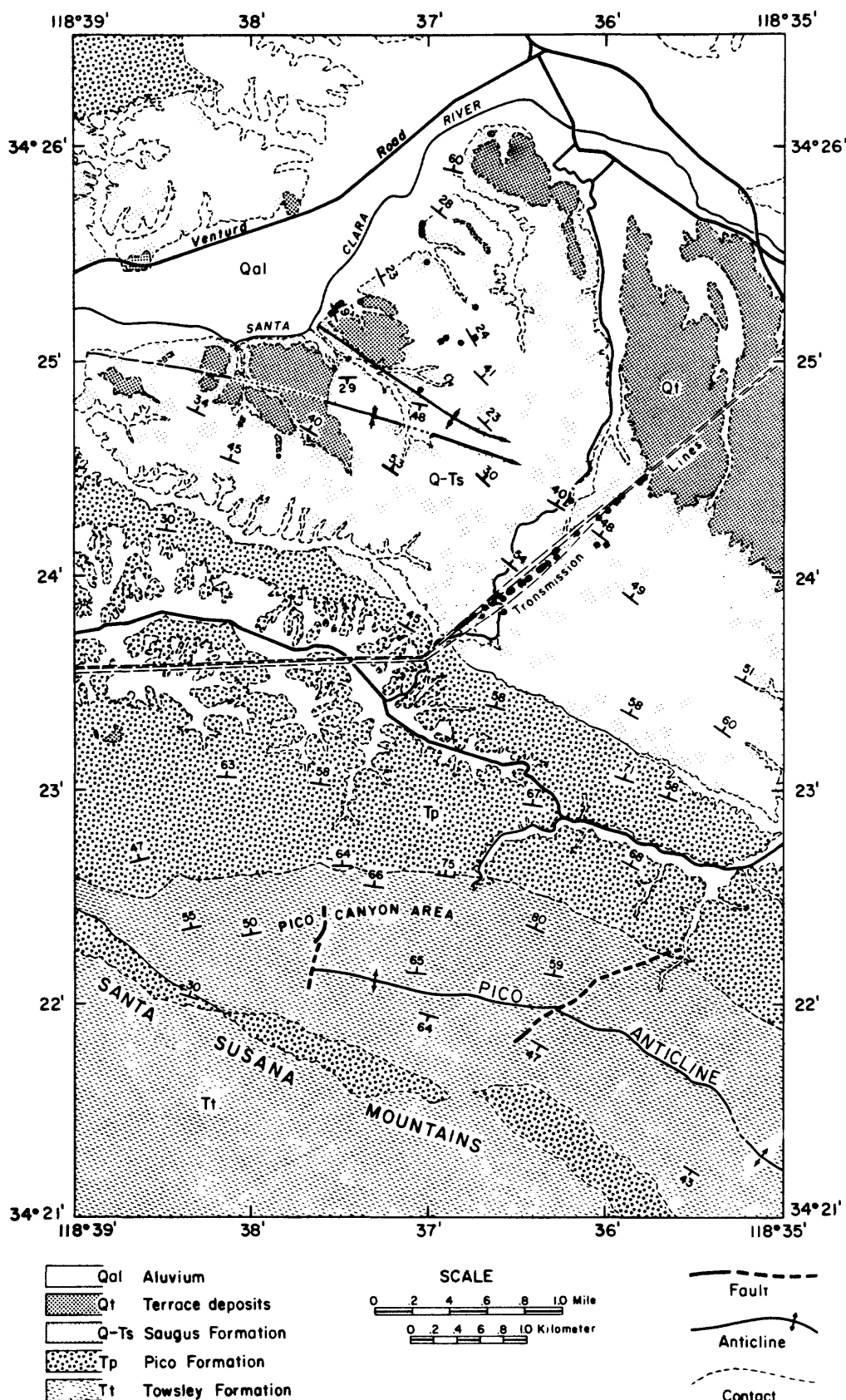


Figure 2. Geologic map of Castaic Junction/Pico Canyon area, showing the transmission line and Santa Clara River sections. Redrawn from "Geologic Map of part of the Ventura Basin, Los Angeles County, California: 1:24,000, Winterer and Durham, 1962. Closed circles represent paleomagnetic sites.

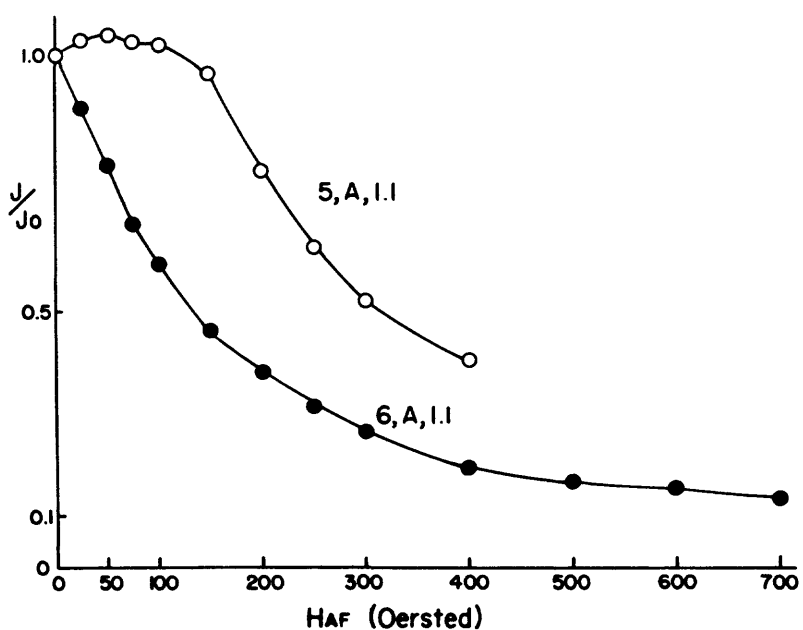
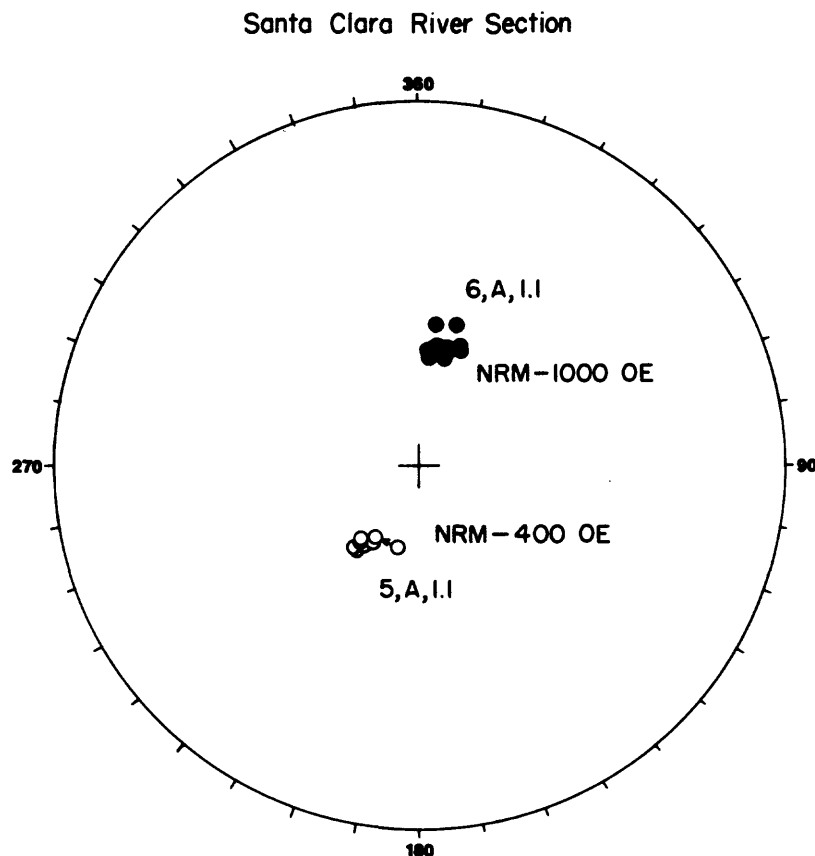


Figure 3. Behavior of the remanence vectors during progressive AF demagnetization of two specimens from a normal and a reversed site of the Santa Clara River Section. Closed (open) circles designate lower (upper) hemisphere inclinations.

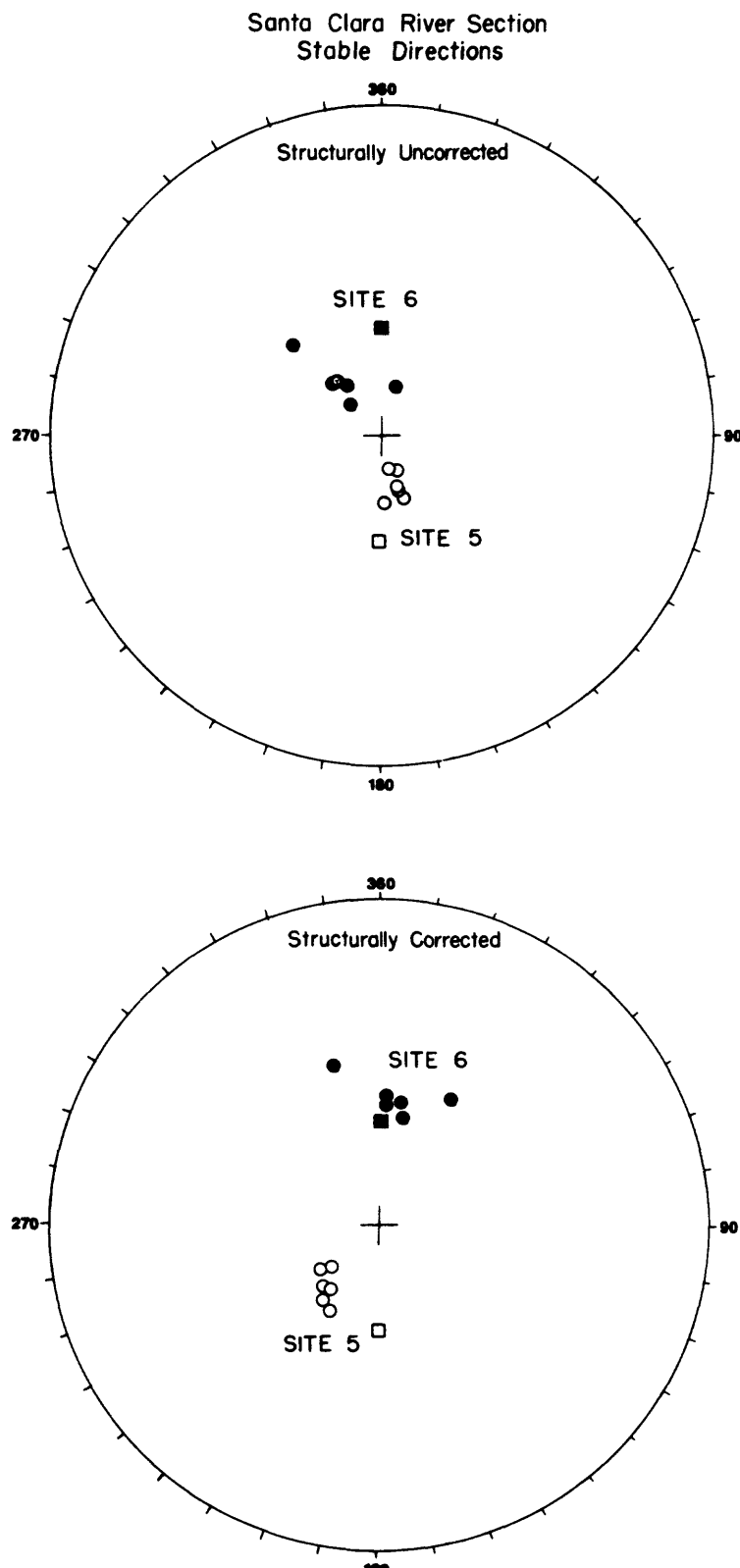


Figure 4. Stable remanence directions (after 300 Oe 'cleaning') of all specimens from sites S-5 and S-6 of the Santa Clara River Section before and after corrections for bedding attitudes: Closed (open) circles designate lower (upper) hemisphere inclinations. Squares represent the expected average remanence directions of the geocentric axial dipole.

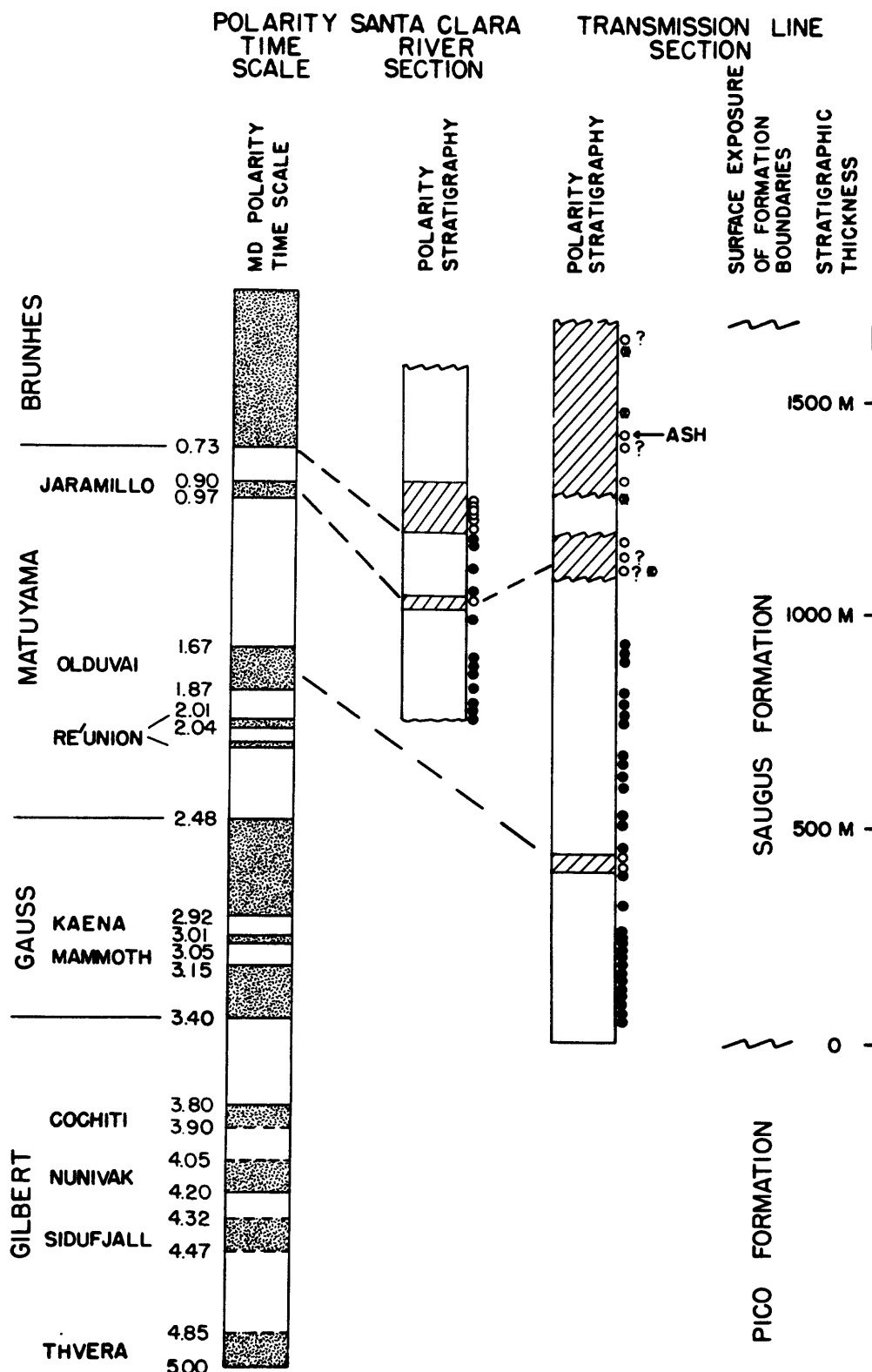


Figure 5. Magnetostратigraphy of the transmission line (TL) and Santa Clara River (SCR) sections and magnetic polarity time scale of Mankinen and Dalrymple (1979). Circles alongside the two stratigraphic columns indicate sampling sites of questionable (indeterminate) polarity.

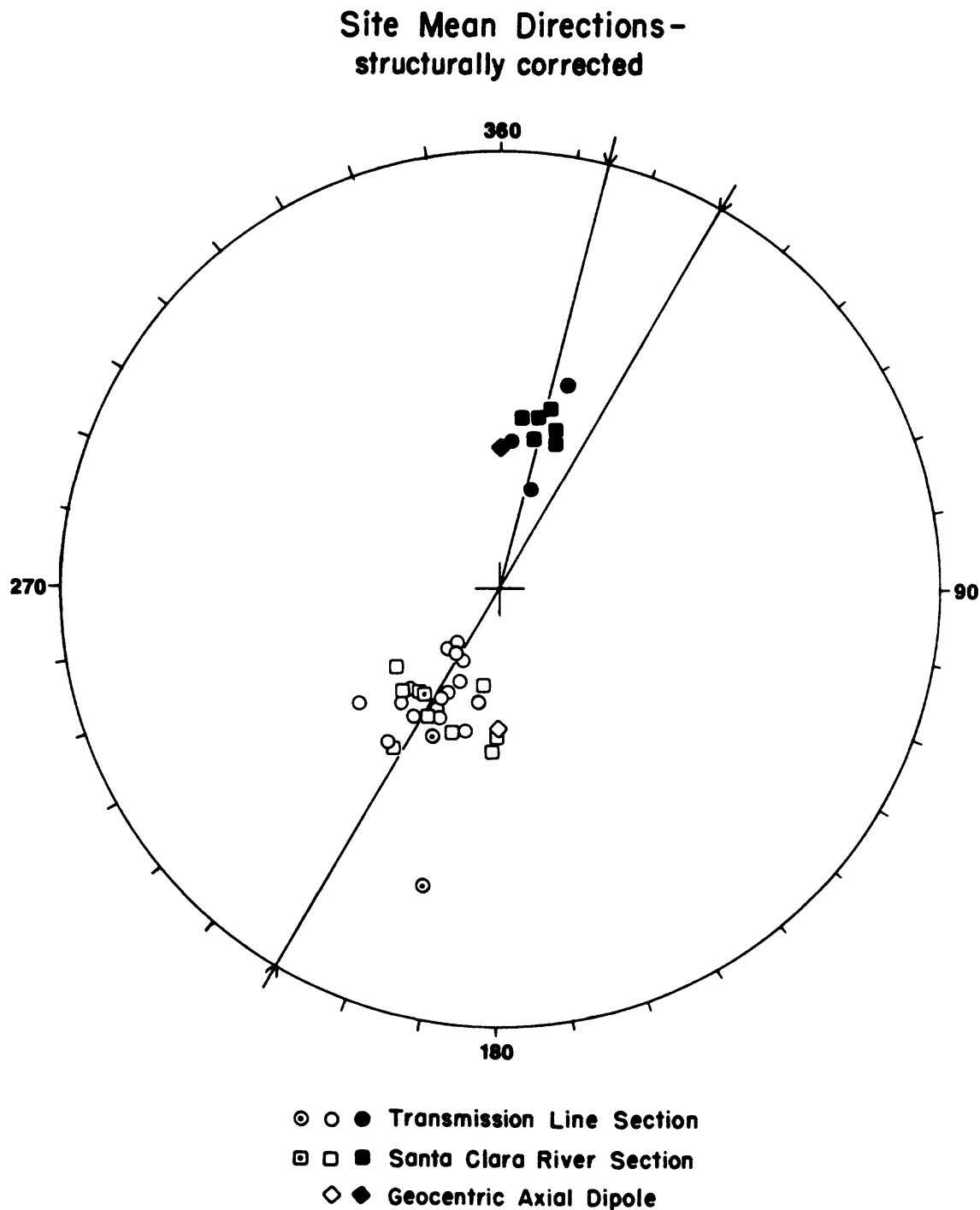


Figure 6. Paleomagnetic directions of Saugus sites. Closed/open symbols designate lower/upper hemisphere vectors. The two open symbols with central dots indicate normal Matuyama sites which were inverted through the origin to distinguish them from Brunhes data. Arrows along the circumference indicate the mean declination for Matuyama (30°) and Brunhes (15°) sites.

Earthquake Hazards Studies, Upper Santa Ana
Valley and Adjacent Areas, Southern California

9540-01616

Jonathan C. Matti
Branch of Western Regional Geology
U. S. Geological Survey
345 Middlefield Road, MS 975
Menlo Park, California 94025
(415) 323-8111 ext. 2358, 2353

Investigations

1. Studies of the Quaternary history of the upper Santa Ana River Valley. Emphasis currently is on: (a) generation of a liquefaction susceptibility map; and (b) the three-dimensional distribution of the valley fill and its lithologic, lithofacies, and pedogenic character.
2. Neotectonic studies of the Crafton Hills-Yucaipa Valley, Banning, and San Andreas fault zones. The study has focused on: (a) mapping fault strands that deform crystalline basement rocks, Tertiary sedimentary rocks, and Quaternary surficial units; (b) identification of Quaternary units to establish Quaternary depositional patterns and the relative ages of displacements along various fault strands; and (c) interpreting relationships between the Banning fault system and the south branch of the San Andreas fault.

Results

1. S. E. Carson and J. C. Matti are in the final stage of a liquefaction evaluation for the San Bernardino Valley. (1) Mapping of surficial materials for the Valley is complete, including reconnaissance studies of pedogenic soil profiles; (2) we have adopted a method for evaluating regional liquefaction susceptibility that incorporates site-specific techniques developed by H. Boulton Seed (UC, Berkeley) and his colleagues as well as regional techniques developed by T. L. Youd (USGS, Menlo Park) and his colleagues; (3) we have written an interactive computer program which utilizes our geotechnical and geological data base to identify areas of greater or lesser susceptibility to liquefaction, and which assesses the degree of susceptibility in terms of factors of safety; (4) Our preliminary calculations suggest that where ground water is shallow, many sites in the San Bernardino Valley are underlain by unconsolidated sediments that can become liquefiable under specific ground-shaking caused by earthquakes on the San Andreas ($M=8.0$), San Jacinto ($M=7.0$), and Cucamonga ($M=6.75$) faults.

2. J. C. Matti and J. W. Harden initiated a slip-rate study of the San Andreas fault in the vicinity of Yucaipa. Stratigraphic and geomorphic relations within this segment of the fault zone suggest that (1) the history of late Quaternary faulting along this reach of the San Andreas has been more complicated than further to the northwest in the vicinity of San Bernardino and Cajon Pass, and (2) the rate of late Quaternary slip in the vicinity of Yucaipa may be significantly less than the 25 mm/year documented in the Cajon Pass region. As discussed in our previous technical report (v. XVII), some

alluvial fans in the Yucaipa district that have been displaced by the San Andreas fault have recognizable source areas that may allow us to reconstruct the amount of right-lateral offset on various strands of the fault since deposition of the fans. We presently are evaluating soil-profile and clast-type data obtained from backhoe pits excavated on four different alluvial terraces. Preliminary results suggest that the late Quaternary slip rate is less than 25 mm/year.

Reports

Clark, M. M., Harms, K. K., Lienkaemper, J., Harwood, D. S., Lajoie, K. R., Matti, J. C., Perkins, J. A., Rymer, M. J., Sarna-Wojcicki, A. M., Sharp, R. V., Sims, J. D., Tinsley III, J. S., Ziony, J. I., Preliminary slip-rate table and map of Late-Quaternary faults of California: U.S. Geological Survey Open-File Report 84-106.

Mississippi Valley Seismotectonics

9950-01504

F. A. McKeown

Branch of Engineering Geology and Tectonics
U.S. Geological Survey
Box 25046, MS 966, Denver Federal Center
Denver, CO 80225
(303) 234-5087

Investigations

1. Processing and interpretation of seismic-reflection data recorded on the R/V Neecho on the Mississippi River.
2. Interpretation of 200 miles of conventional seismic-reflection profile data.
3. Quantitative geomorphic study of streams in the southeastern part of the Ozark uplift.
4. Analysis of level line data.

Results

1. Initial processing of the Mississippi River reflection data is complete, and interpretation of the first part of it for publication in the U.S. Geological Survey Miscellaneous Field Studies series is complete.
2. Preliminary correlations of the principal reflections on the record sections of the conventional reflection profile data were made. Utilizing those correlations and other signatures in the data a map of a highly disrupted zone was made. The disrupted zone correlates very closely with the distribution of seismicity in part of the New Madrid seismic zone and presumably is genetically related to the seismicity.
3. Interpretation of 70 stream profiles and data derived from the profiles is not complete but some tentative conclusions are as follows.
 - (a) Streams on the Salem Plateau commonly have steeper gradients and are less concave than streams draining from the Boston Mountains and Ouachita physiographic provinces even though the Salem Plateau has lower elevation and less relief than the latter provinces.
 - (b) The size of material in stream bottoms controls stream gradients much more than the kind of rock being eroded by a stream. This observation is in general agreement with other studies of stream gradients and with some theories of erosion.
 - (c) Meandering parts of streams, particularly on the Salem Plateau, commonly have steepest gradients, which is contradictory to most observations and theory of the meandering process. This could mean gradients have continued to increase since the meanders first developed, which was probably during the Tertiary Period.

(d) Streams draining the Salem Plateau enter the Mississippi embayment lowlands at a much higher elevation relative to Pleistocene base level than streams draining the Boston Mountains and Quachita provinces. This suggests that the Salem Plateau has not been eroded as deeply as the other provinces and has been uplifted more recently to account for the steeper gradients of the Plateau streams.

Consideration of a number of the quantitative measures of stream profiles suggests that the Salem Plateau may be rising relative to surrounding areas since the Tertiary Period. Many variables must still be considered, however, before quantitative differences in the stream profile data can be related to tectonic activity with some confidence.

4. Analyses of level line data resulted in identification of anomalous displacements along two level lines. One anomaly is conformable with the geologic evidence of the Lake County uplift in western Tennessee. The other anomaly is across the northern part of the Viburnum mineralized zone in the Ozark Mountains of central Missouri. It is unlikely that the Missouri anomaly is related to the mineralization. A tentative explanation is that the anomaly is related to solution of carbonate rocks.

EARTHQUAKE RESEARCH IN THE WESTERN GREAT BASIN

Contract 14-08-0001-21863

A.S. Ryall, U.R. Vetter, and E.J. Corbett
 Seismological Laboratory
 University of Nevada
 Reno, NV 89557-0018
 (702) 784-4975

Investigations

This program supports continued studies with research focused on: (1) seismicity and focal mechanisms associated with magma injection in Long Valley caldera; (2) geometry of magma bodies in Long Valley caldera; (3) stress changes associated with systematic changes in focal mechanism with depth in the Great Basin; (4) premonitory seismicity patterns preceding the 1980 Mammoth Lakes earthquakes; (5) precise relocation of the May 1980 Mammoth Lakes earthquake sequence. Progress in selected areas of this program is described below.

Results

A. Location of Magma Bodies in the western Great Basin

Detailed investigations of the anomalous seismic signals caused by magma bodies within Long Valley caldera have been published by Sanders (1984) and Sanders and Ryall (1983). The primary discriminant for paths through magma appears to be anomalously low (2-3 Hz) signal frequencies combined with the lack of an S-wave. Signals with anomalous characteristics are also observed for some earthquakes in the crustal block south of the caldera, recorded at stations to the east and northeast, indicating that magma may be present at least 10-12 km south of the caldera. The size of the attenuating bodies is of the order of a few kilometers and they appear to be located in a zone trending NW-SE. Epicenter maps and cross-sections for the Mammoth Lakes earthquake sequence indicate that the attenuating bodies are located in areas that have been aseismic during the 1979-1983 period. Another well-defined magma body is located northwest of Boundary Peak, at the north end of the White Mountains and about 50 km east of Long Valley caldera. Taken together these observations suggest that magma injection in the shallow crust may be a common feature of lithospheric extension in the western Great Basin.

B. Relocations of the 1980 Mammoth Lakes earthquake sequence

A recently completed Master's thesis by C.S. Lide has given new insight into the 1980 earthquake sequence. Lide (1984) used a simplified location program that uses a half-space velocity model and performs Geiger's inversion but without any data weighting. The program also calculates ray paths considering station elevations, to account for the rugged topography of the Sierra Nevada. It appears that these modifications have reduced location scatter due to instabilities introduced by the large number of uncontrollable parameters in the location program HYPO71, which was previously used. Lide derived the average crustal velocity from explosion data, chose a well-controlled earthquake for a master event and located all of his data relative to it. The most striking features of his locations (Figure 1) are two parallel zones of aftershocks that strike N20°E and dip vertically. These features are in agreement with the vertical strike-slip

focal mechanisms derived from short-period first-motion data for the three largest shocks ($M_L > 8$). However, they are at odds with the CLVD model currently adhered to by USGS scientists. These locations also indicate that the tectonic process was quite complex as many of the earthquakes occurred on other structural trends that are discussed in detail by Lide and Ryall (1984).

C. Reports

- Lide, C.S. (1984). Aftershocks of the May 1980 Mammoth Lakes earthquakes, M.S. thesis, Univ. Nevada.
- Lide, C.S. and A.S. Ryall (1984). Relationship between aftershock locations and mechanisms of the May, 1980 Mammoth Lakes earthquakes, U.S. Geological Survey Open-File Rpt, submitted.
- Ryall, A. and F. Ryall (1983). Spasmodic tremor and possible magma injection in Long Valley caldera, eastern California, *Science*, 219, 1432-1433.
- Ryall, A., U.R. Vetter, C.O. Sanders, and F.D. Ryall (1984). Seismological investigation of tectonic and magmatic processes in the Long Valley caldera, California, *Earthquakes Notes*, in press.
- Sanders, C.O. (1984). Location and configuration of magma bodies beneath Long Valley, California, determined from anomalous earthquake signals, *Jour. Geophys. Res.*, in press.
- Sanders, C.O. and F. Ryall (1983). Geometry of magma bodies beneath Long Valley, California, determined from anomalous earthquake signals, *Geophys. Res. Letters*, 10, 690-692.
- Vetter, U. and A. Ryall (1983). Systematic change of focal mechanism with depth in the western Great Basin, *Jour. Geophys. Res.*, 88, 8237-8250.
- Vetter, U.R. (1984). Focal mechanisms and crustal stress patterns in western Nevada and eastern California, *Annales Geophysicae*, in press.
- Vetter, U.R., A.S. Ryall and C.O. Sanders (1983). Seismological investigations of volcanic and tectonic processes in the western Great Basin, Nevada and eastern California, *Geothermal Resources Council, Special Rpt.* 13, 333-343.



Figure 1. Fault map of the Long Valley caldera showing 352 precisely located aftershocks (x's) that occurred from May 28 to July 31, 1980. The town of Mammoth Lakes is in the SW corner of the caldera and Lake Crowley lies astraddle the southeast margin of the caldera. From Lide (1984).

Salton Trough Tectonics and Quaternary Faulting

9910-01292

Robert V. Sharp

Branch of Engineering Seismology and Geology

U.S. Geological Survey

345 Middlefield Road, MS 977

Menlo Park, California 94025

(415) 323-8111, ext. 2596

Investigations

1. Monitoring near-field vertical deformation on the northern Imperial fault, Imperial Valley, California.
2. Post-seismic vertical deformation across the Lost River fault after the October 28, 1983 Idaho earthquake.
3. Trenching study of the Imperial fault, Imperial Valley, California.

Results

1. Vertical deformation of the ground surface along Harris Road since the 1979 Imperial Valley earthquake has generally slowed, but the profiles have usually indicated a concentration of slip (vertical component) in the uppermost 100 meters of the fault, according to elastic dislocation modeling. Between October and November 1983, a relatively large deformation event took place that was not associated with surface rupture; its deformation profile indicates subsurface dip slip of about 8 mm on the fault at depths between 130 m and 650 m. The form of the deformation profile also indicates an eastward steepening of dip of the fault to about 60 degrees for this slip depth. The rate of tilting of the ground surface near the fault between October and November 1983 was about 70 percent of that observed during the maximum tilting period observed between 9 and 6 months before the 1979 earthquake.
2. A 2.2 km-long leveling line was constructed and relevelled across the Lost River fault rupture at Willow Creek-Double Spring Pass Road during the first week of November. A 250 m line was also installed at Arentson Gulch. Relevelling of both lines indicated no significant increase in surface displacement at the fault trace for this period of time, but tilting of the lines suggested postseismic subsurface movement deeper than the length of our longest line on the downthrown side of the fault (1.44 km).
3. A new series of trenches on the Imperial fault have been cut at Heber Beach in order to search for a record of horizontal displacements older than 2500 years and to determine whether the slip history for a possibly creeping section of the fault is demonstrably different than that of the locked segment of the fault at the U.S.-Mexico border.

Reports

Clark, M. M., Harms, K. K., Lienkaemper, J. J., Harwood, D. S., Lajoie, K. R., Matti, J. C., Perkins, J. A., Rymer, M. J., Sarna-Wojcicki, A. M., Sharp, R. V., Tinsley, J. C., and Ziony, J. I., 1984, Preliminary map and table of slip-rate compilation for late Quaternary faults in California: *Seismological Society of America Bulletin*, Anchorage, Alaska.

**Late Holocene Behavior
San Andreas Fault**

14-08-0001-21275

Kerry Sieh
 Division of Geological and Planetary Sciences 170-25
 California Institute of Technology
 Pasadena, CA 91125
 (818) 356-6115

During the past six months, our work under this contract has progressed on two fronts. I and several others have studied excavations across the San Andreas fault at Indio, and Ray Weldon has been working on the ages of and relationships between the late Cenozoic sediments in the Cajon Pass region and integrating the results of this past 5 years of work in this area.

At the Indio site we are uncovering a fascinating late Holocene record of fault slippage. I expect this record will eventually yield dates and lateral offsets of prehistoric great earthquakes as detailed as the record at Pallett Creek. We have now nearly completed study of 2 of the four fault strands in the 50-m-wide fault zone. Both strands have slipped at least 3 times since 1400 A.D. Strike slip since 1700 A.D. has been 3 cm on one and 1 m on the other. Strike slip during an event in the late 17th century was 12 cm on one and 1.7 m on the other. Strike slip during an event in the 15th or 16th century was about 60 cm on one and an unknown, but large, amount on the other. I expect to resume work at this site in January 1985 and complete it by May of that year.

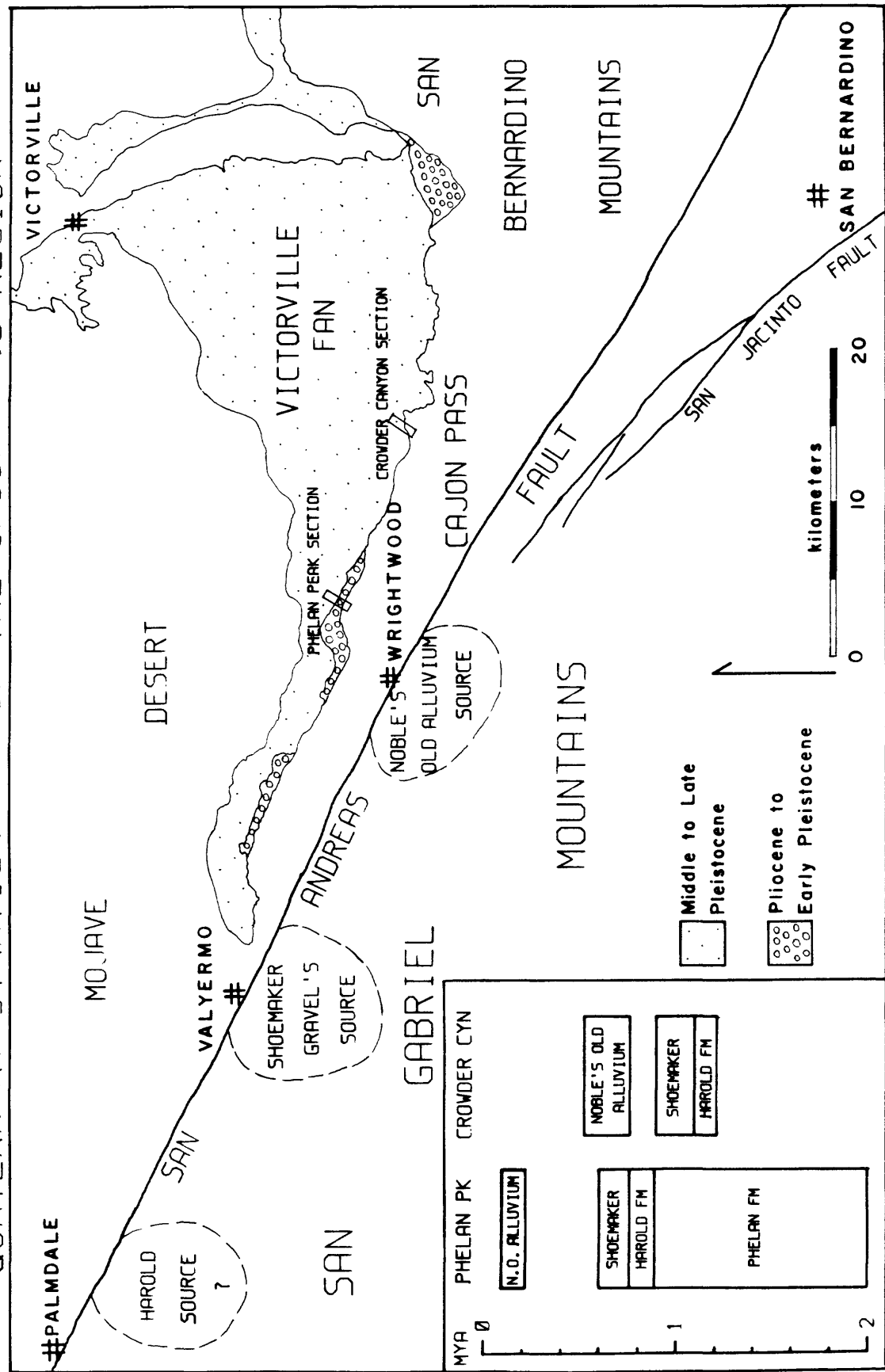
Ray Weldon is now wrapping up his Ph.D. work in the Cajon Pass region. Detailed mapping, coupled with new age determinations based on fossils, paleomagnetic stratigraphy, radiocarbon dates, and soils analyses, have led to a better understanding of the late Cenozoic stratigraphy and tectonics.

The type Crowder formation has been shown to be middle to late Miocene, overlapping in age with the Cajon Punchbowl sediments that were thought to underlie it. The sediments overlying the Punchbowl (and several major faults) have been shown to be Plio-Pleistocene in age and have been designated the Phelan Fm. The Phelan Fm overlies two early traces of the San Andreas system and records the onset of compressional tectonics associated with the San Andreas in the area about 4 million years ago. The Squaw Peak and Cajon Valley faults are proposed to be early traces of the San Andreas system and must have accumulated tens of kilometers of offset between 9 and 4 m.y. ago. The establishment of absolute age control in the Pleistocene Harold, Shoemaker Gravels, and Noble's Old Alluvium in Cajon Pass allows an estimate of the slip rate on the San Andreas system since the middle Pleistocene of about 3 to 4 cm/yr. More work is necessary to confirm the tentative age assignments and to better define the sources of these units across the San Andreas system. The proposed ages and matches are summarized on Figure 1.

Work on the late Pleistocene and Holocene history has centered on integrating and publishing earlier work on the slip rate and recurrence interval for the San Andreas fault, quantifying the stratigraphy with new radiocarbon samples, and developing a soils chronosequence with Les McFadden at the University of New Mexico. A paper on the slip rate and recurrence interval for the San Andreas fault has been submitted to the GSA Bulletin and is currently being revised. The slip rate has been tightly constrained to 24.5 ± 3.5 mm/yr and can be shown to be constant for the past 15,000 years (Figure 2).

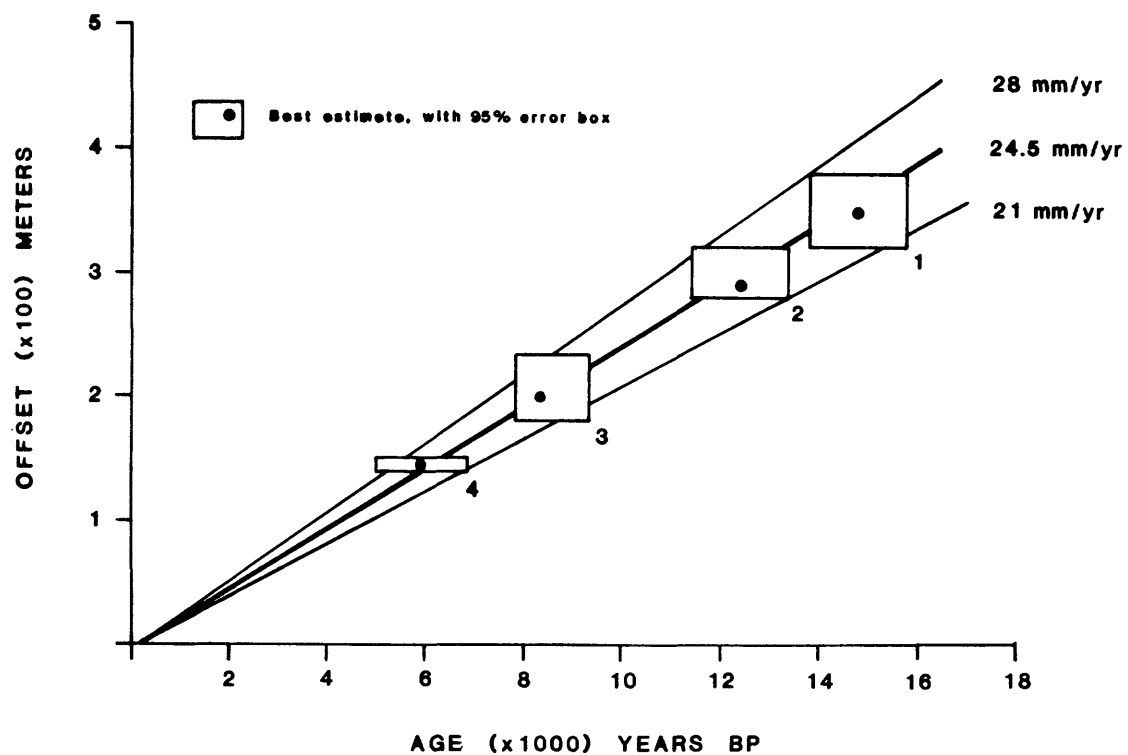
Fig 1

QUATERNARY STRATIGRAPHY OF THE CAJON PASS REGION



SLIP RATE ON THE SAN ANDREAS FAULT AT CAJON CREEK

Fig 2



Quaternary Framework for Earthquake Studies
Los Angeles, California

9540-01611

John C. Tinsley
Branch of Western Regional Geology
U. S. Geological Survey
345 Middlefield Road, MS 975
Menlo Park, California 94025
(415) 323-8111, x 2037

Investigations

1. Continued reviewing, preparing, and revising drafts of chapters for inclusion in the U.S. Geological Survey's forthcoming Professional Paper "Evaluating earthquake hazards in the Los Angeles region - an earth science perspective". (J. Tinsley)
2. Continued loading geotechnical data into the USGS VAX/computer (S. Wert, J. Tinsley, D. Ponti).
3. Visited the Nevada Test Site and inspected trenching operations investigating the Rock Valley Fault.

Results

1. Drafts of chapters are at the peer review stage of preparation.
2. Data base compilation is 90% complete in the Burbank and Van Nuys 7.5' quadrangles. Dan Ponti has completed a software package that permits us to check the digitized locations of boreholes and other data against selected hard-copy hand-plotted locations. We anticipate being fully able to manipulate the data base by early summer, 1984.
3. The inspection of the trench-logging operations proceeded smoothly and state-of-the-art logging techniques are being employed by USGS personnel studying the Rock Valley Fault.

Reports

Ponti, D. J. and Tinsley, J. C., 1984, Inherent uncertainties in Quaternary dating methods and slip-rate evaluations: Seismological Society of America, Abstracts with programs, (Anchorage, Alaska).

Rogers, A. M., Tinsley, J. C. and Borcherdt, R. D., 1984, Geographic variation in ground shaking as a function of changes in near-surface properties and geologic structure near Los Angeles, California: Proceedings of the 8th World Conference on Earthquake Engineering, San Francisco, California (Director's Approval, 1/84).

TECTONIC TILT MEASUREMENTS USING LAKE LEVELS: ALASKA

4-9950-02396

Kirk R. Vincent and Spencer H. Wood
Branch of Engineering Geology and Tectonics
U.S. Geological Survey
Mailing address: Boise State University
Boise, Idaho 83725
(208) 386-3629

Investigations

Measurements of land-surface tilt, made using water-level records of Kenai Lake in Alaska, are continuing to be evaluated as more data becomes available. During field work, water levels are recorded simultaneously at an array of stations (U77, BM1, Y11) on the lake. These records are surveyed into local bedrock reference points using precise level and rod. For periods of calm lake conditions; simultaneous water levels are taken from the charts, and the difference in relative elevation of reference points at each pair of sites calculated. A change in elevation difference through time is interpreted as tilting of the land-surface, or the result of erroneous data collected when the lake surface was temporarily inclined, during flood or by wind tides. Other errors include unstable reference points, surveying mistakes and vertical shifting of water-level recorder and stilling well.

This type of field data now spans 19 years, with the first value obtained in 1964, three and a half months after the March 27th earthquake. A value was also obtained in 1966. Since our involvement with the project in 1979, several elevation difference values for each of four field seasons have been collected. In addition, a new source of data has been discovered in the form of once-daily lake level measurements made at two points on the lake by other agencies. The Chugach Electric Association measures the lake level at the tail race of the Kenai Lake Power Plant (KLPP) for their own purposes. The water resources division of the USGS operates a stream gaging station near Cooper Landing (USGS) on the reach where lake water flows out and down the Kenai River. The period of simultaneous record starts in mid 1963 and continues to the present. We have in hand all available data.

Results

The elevation difference values collected in the field indicate significant tectonic tilting across Kenai Lake since the 1964 earthquake (figure 3). Regression lines fit to all of the values yields the following: During the period 1964 through 1983 tilting has occurred over a pivotal axis oriented N. 23° E., at a mean rate of .61 micro-radians per years (a 20-year total of 12.12 micro-radians) and down to the southeast. For geometric reasons the equation of change in elevation difference for the three sets of sites must be true - $\Delta(U77-BM1) + \Delta(Y11-BM1) = \Delta(U77-Y11)$. The measured values of 29.41 + 5.49 = 34.90 cm, which differs from the measured value for $\Delta(U77-Y11)$ of 35.17

cm by only 2.7 mm. This is remarkable considering the distance between U77 and Y11 is about 29.6 kilometers, and lends credence to the lake level technique.

The rate of tilt across the lake however, does not seem to have been constant, instead, it appears to have diminished through time. This is suggested by calculations, based on regression lines fit through all values within the period 1979 through 1983, which yielded a 5-year mean tilt rate of .316 micro-radians per year (a total of 1.58 micro-radians). The geometric equation of change in elevation differences for this period is $3.78 + 0.21 = 3.99$ cm, which differs from the measuring value for $\Delta(U77-Y11)$ of 4.63 cm by 6.4 mm. If the change of tilt rate through time is linear (figure 4), tilting just after the earthquake was on the order of one micro-radian per year.

1964 elevation difference values for KLPP and USGS sites are shown in figure 2. As a first approximation, all available difference values within a month were averaged, and plus and minus one standard deviation are shown as bars. These elevation difference values show a scatter of about 30 cm and are much more than an order of magnitude less precise than those mentioned above. Apparently the earthquake damaged the original stage reference as Water Resources moved the site within a few weeks of the earthquake. Unfortunately, they did not, or could not, precisely reference the old gage datum to the new gage datum. Hence, the values preceding the earthquake might be as much as 5 cm higher or lower on the graph. Although unclear in this figure, 1975 data (not shown) exhibit a strong relationship with lake level. Presumably water pours out of the lake with a different slope for high lake levels compared to that for low levels. During the winter the lake is low, freezes over and does not fluctuate much. Winter data may be the most reliable. The exceptionally high values during June and July of 1975 may be the result of aggradation or degradation of the river channel below the gaging station which could alter the river slope.

ELEVATION DIFFERENCE BETWEEN SITES, USING LAKE LEVELS,
AS A MEASURE OF TECTONIC TILT - KENAI LAKE, ALASKA

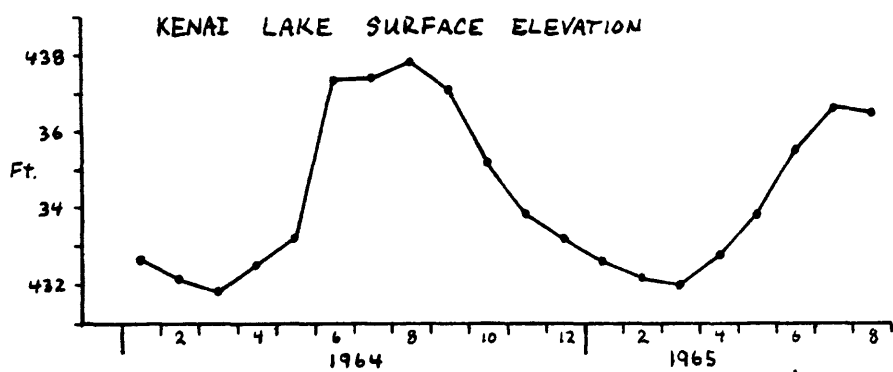
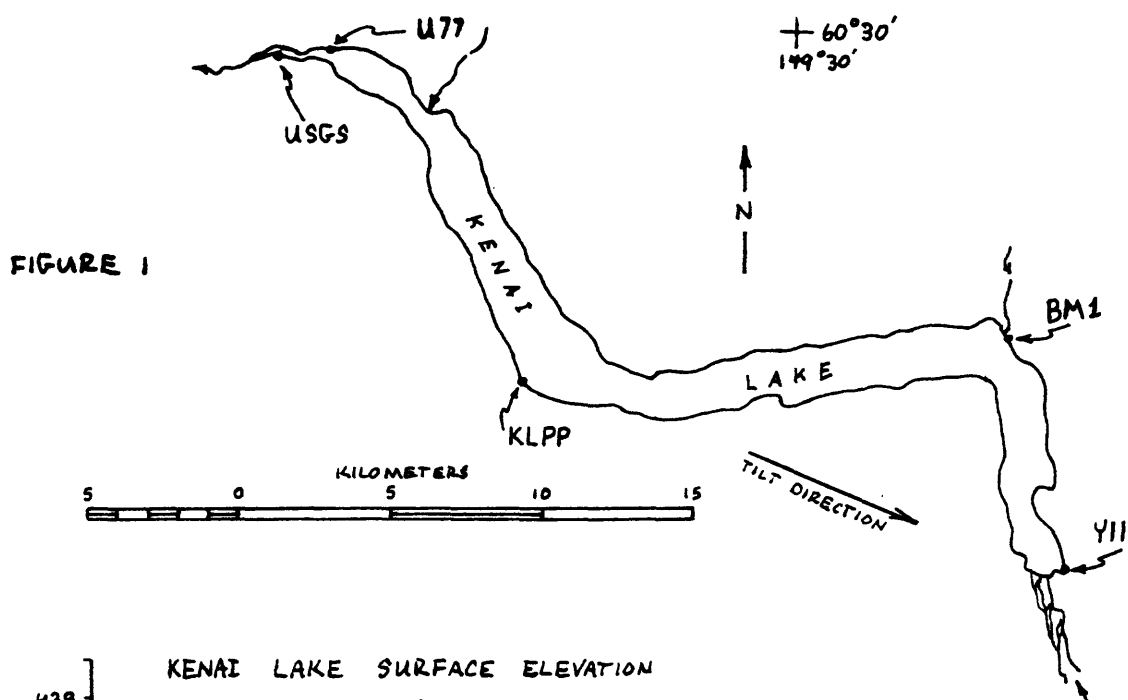
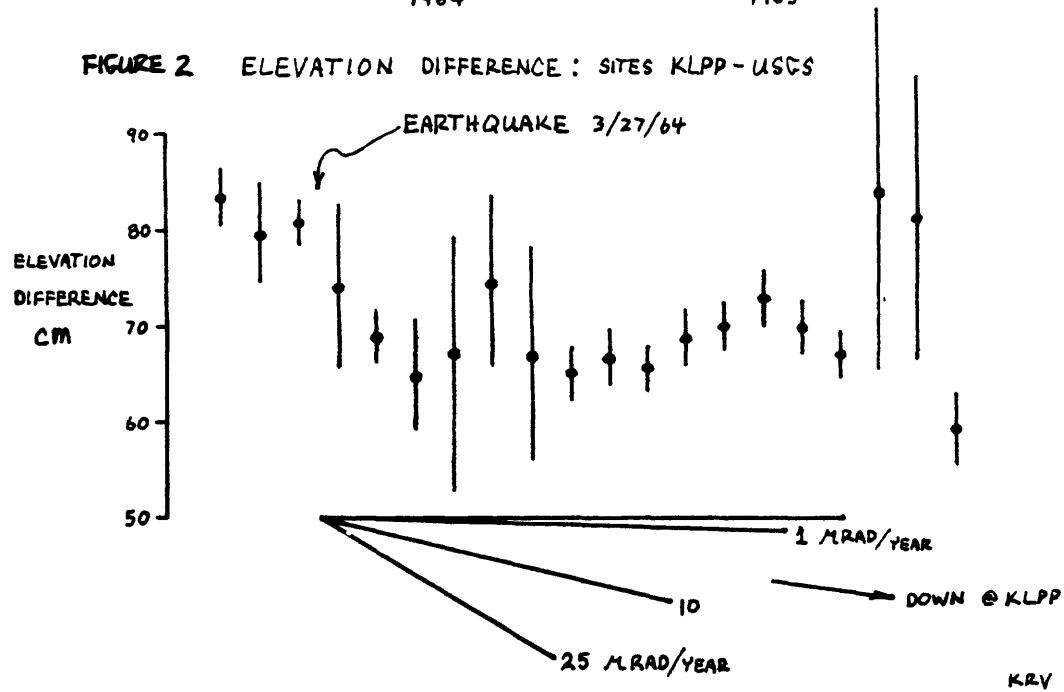
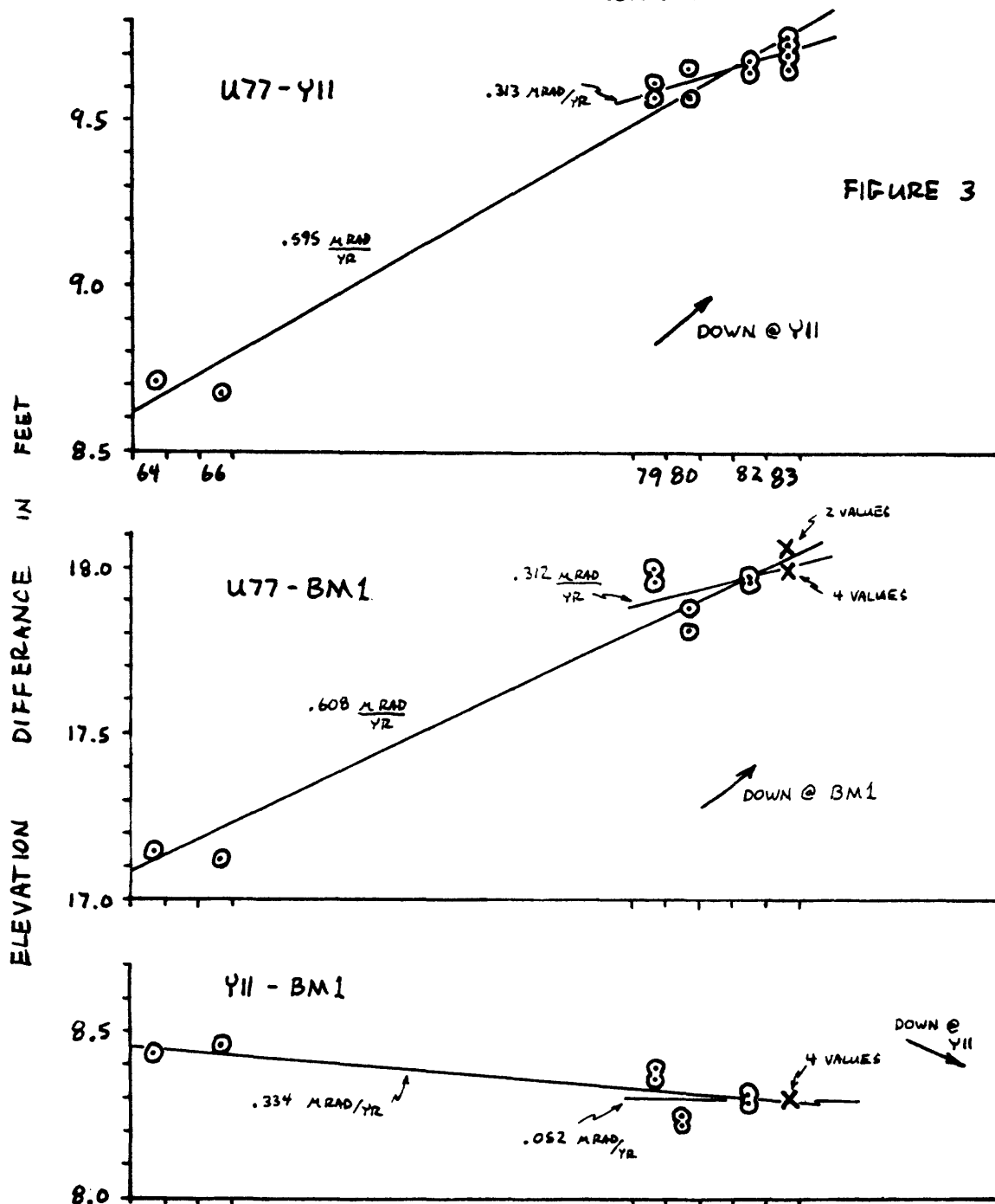


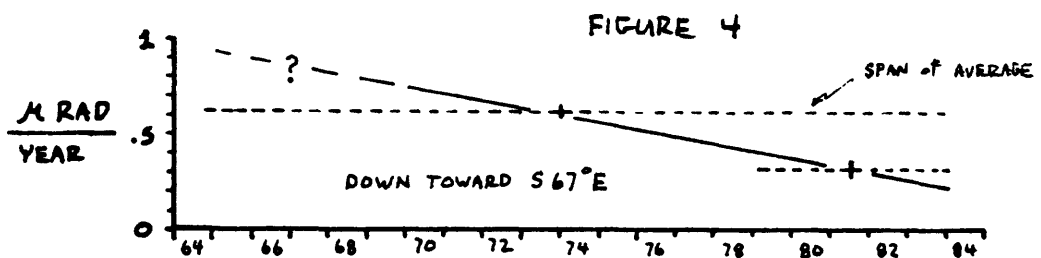
FIGURE 2 ELEVATION DIFFERENCE: SITES KLPP - USGS



ELEVATION DIFFERENCE BETWEEN SITES, USING LAKE LEVELS, AS A MEASURE OF TECTONIC TILT : KENAI LAKE ALASKA



TILT RATE SINCE THE 1964 EARTHQUAKE, ACROSS KENAI LAKE, AK.



KRV 4/84

Geothermal Seismotectonic Studies

9930-02097

Craig S. Weaver

Branch of Seismology
 U. S. Geological Survey
 Geophysics Program AK-50
 University of Washington
 Seattle, Washington 98195
 (206) 442-0627

Investigations

1. Continued analysis of the seismicity and volcanism patterns of the Pacific Northwest in an effort to develop an improved tectonic model that will be useful in updating earthquake hazards in the region. (Weaver, Michaelson, Yelin)
2. Continued acquisition of seismicity data along the Washington coast, directly above the interface between the North American plate and the subducting Juan de Fuca plate. (Weaver, Michaelson, UW contract)
3. Test the hypothesis: An area of crustal spreading exists in southwestern Washington between the St. Helens seismic zone to the northeast and a still poorly defined seismic zone that probably parallels the Portland Hills to the southwest. Both zones strike north-northeast, and are offset by about 40 km. The proposed opening is in a west-to-northwest direction. (Weaver, UW contract).
4. Continued seismic monitoring of the Mount St. Helens area, including Spirit Lake (where the stability of the debris dam formed on May 18, 1980 is an issue) and Elk Lake (where seismicity remains at elevated levels an elevated level 30 months after the February 14, 1981 earthquake). (Weaver, Grant, UW contract)
5. Relocation of the 1962 Portland, Oregon earthquake ($M_L=5.5$) and several earthquakes between 1958-1962 that occurred near Swift Reservoir (the largest event has an $M_L=5.1$). The events near Swift Reservoir were probably on the southern segment of the SHZ. (Grant, Weaver)

Results

1. Relocation of earthquakes in the greater Mount St. Helens area shows that a single fault zone, at least 20 km in length, may exist between the Elk Lake area and Mount St. Helens (Figure 1). In cross-sectional view, perpendicular to the nearly north-south strike of the fault, earthquakes from the Elk Lake aftershock zone plot directly on the deeper earthquakes (depths > 4 km) beneath Mount St. Helens (Figure 2). Previous work had suggested that the St. Helens seismic zone (of which the Elk Lake-Mount St. Helens zone is a part) might consist of shorter fault segments, with lengths similar to that observed from the Elk Lake aftershock sequence (5-10 km).
2. A re-analysis of teleseismic P-wave travel time residuals has been completed, giving more detailed resolution of upper mantle structure than earlier work. The results of a three-dimensional inversion resolves an east-dipping, N to NNW

striking, high-velocity zone, that is interpreted as the subducted Juan de Fuca plate. The high-velocity zone is characterized by 4-7% higher velocities than in the surrounding upper mantle. Although the shallow velocity structure is not well resolved from the inversion, from 50 to 250-300 km depth, the plate dips at a 40-45° angle beneath the Washington Cascade Range north of Mount Rainier. The plate plunges at a steeper (60-70°) angle beneath the Cascade Range in southern Washington and northern Oregon from 50 to 200 km depth (an example is shown in Figure 3). The structural transition from a shallow dipping plate in the north to a steeply dipping plate in the south, is proposed as a boundary between segments of the subducted Juan de Fuca plate. Major changes in the regional seismic activity and volcanism correlate with the surficial expression of this boundary, and may be a result of changes in the plate dip.

3. Earthquake focal mechanisms in the crust of the North American plate in northwestern Washington have previously been characterized by a bi-modal distribution of P-axis orientations: one group has nearly N-S and nearly horizontal P-axes, the second, smaller group exhibits a great deal of scatter in P-axis azimuths. Thus, the majority of P-axes in the crust of the Puget Sound region are not aligned in the direction of convergence between the Juan de Fuca and North American plates (northeast). These observations have lead to the suggestion that the subduction interface between the Juan de Fuca and North American plates might be unlocked, thus lessening the possibility of a great thrust earthquake on the interface. These observations have been compared with other Pacific rim subduction zones, known to have generated large magnitude thrust earthquakes, in terms of inferred stress directions and observed surficial strain in the overthrust plate. In SW Japan, which has the longest and best seismic and geodetic data set, P-axes have a large amount of scatter in their azimuthal orientations. Compressive strain axis orientations also exhibit a great deal of scatter and considerable spatial variation and in some areas do not agree with P-axis data. In Alaska and New Zealand there is both direct and indirect evidence that the stress and strain fields in overthrust plates can have significant spatial and temporal variations over a few decades of kilometers and years. The focal mechanism observations in northwestern Washington fit into the observed range of behavior of Pacific rim subduction zones known to generate large magnitude, shallow thrust earthquakes.

Reports

Weaver, C. S. and Smith, S. W., 1983, Regional tectonic and earthquake hazard implications of a crustal fault zone in southwestern Washington, *Journal of Geophysical Research*, v. 88, p. 10,371-10,383.

Grant, W. C., Weaver, C. S., and Zollweg, J. E., 1984, The February 14, 1981, Elk Lake Washington, earthquake sequence, *Bulletin of the Seismological Society of America*, v. 74, (in press).

Weaver, C. S. and Michaelson, C. A., 1983, Segmentation of the Juan de Fuca plate and volcanism in the Cascade Range, (abs): *EOS, Transactions, American Geophysical Union*, v. 45, p. 886.

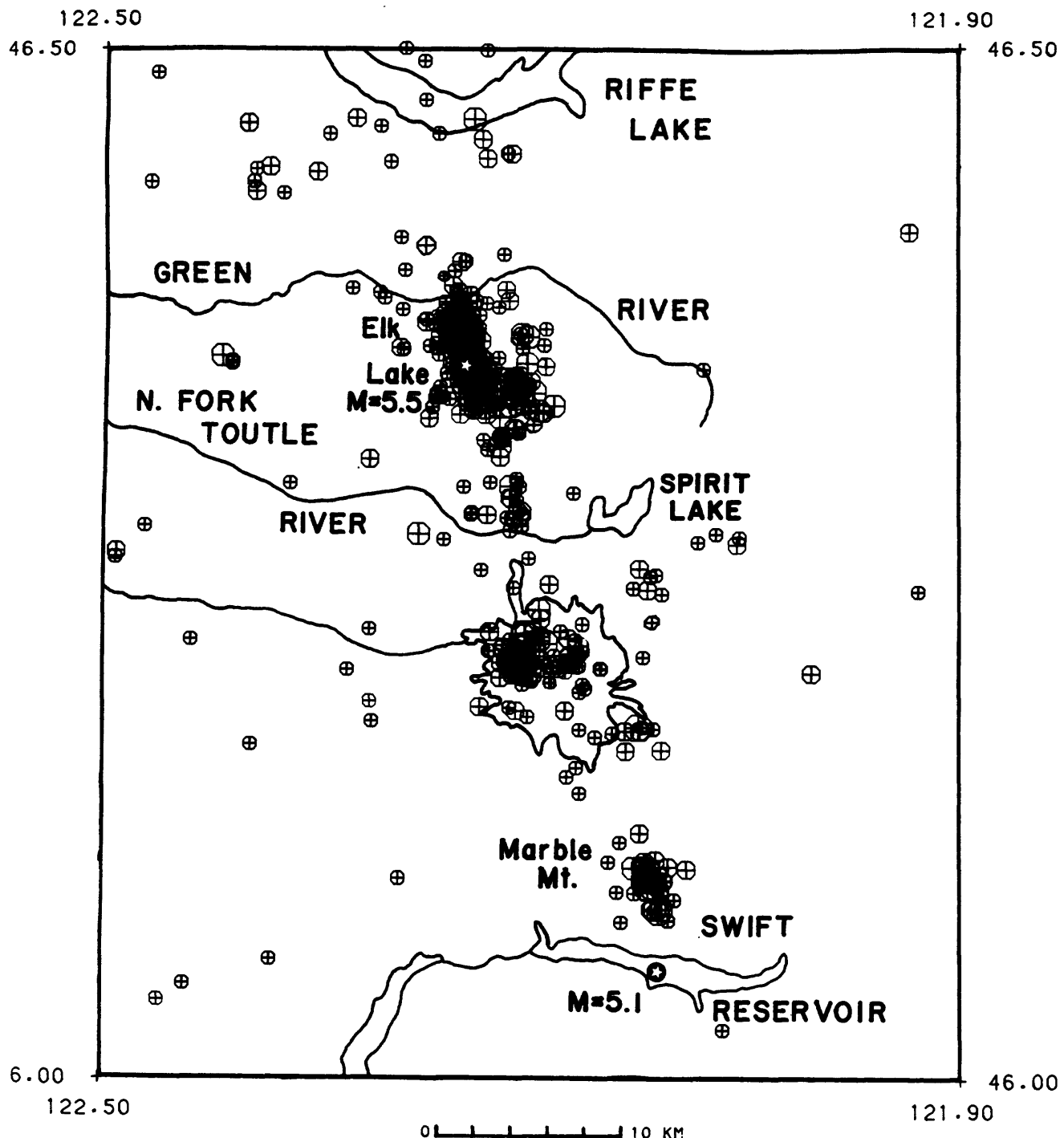


Figure 1: Relocated earthquakes near Mount St. Helens with magnitudes greater than 1.0 for the period 1980 to 1983. The cross section in Figure 2 is centered on Mount St. Helens. The magnitude 5.1 earthquake beneath Swift Reservoir occurred in 1961 and is being relocated.

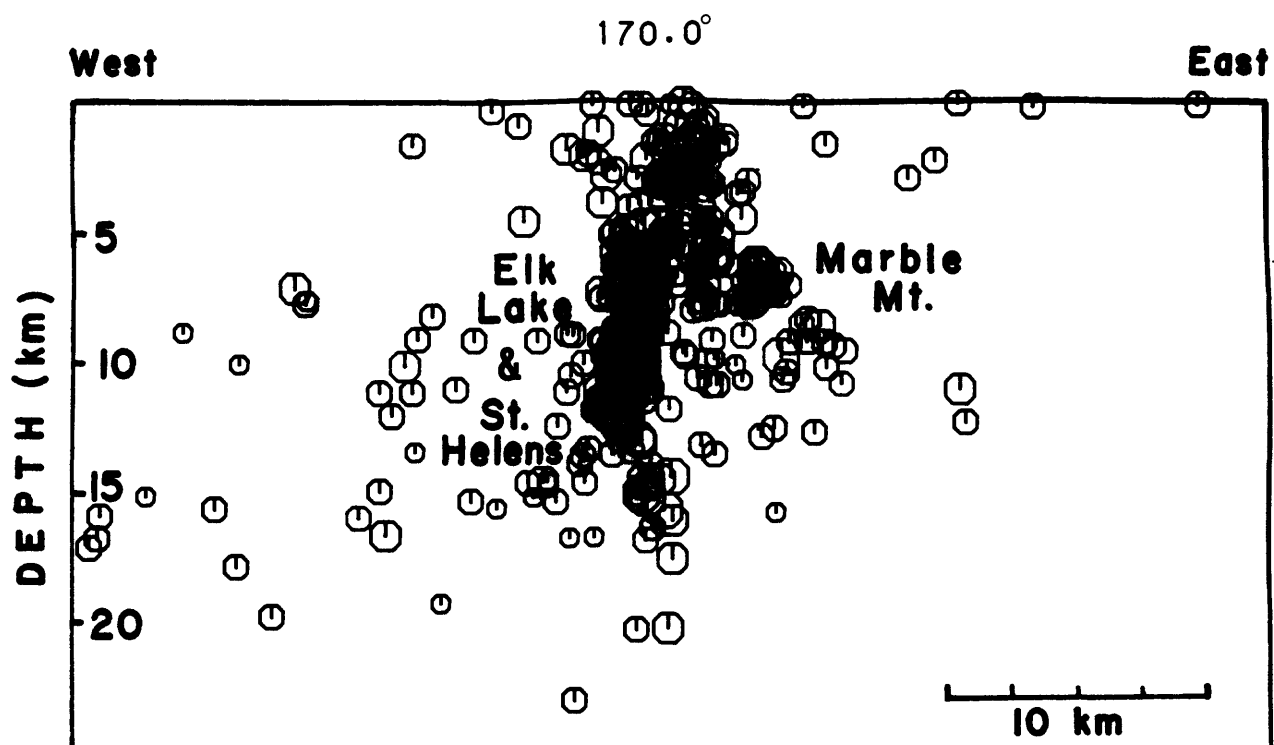


Figure 2: Cross section of relocated earthquakes shown in Figure 1. The Elk Lake aftershocks and the deeper earthquakes that have occurred directly beneath Mount St. Helens define a relatively sharp fault zone, about 2 1/2 km wide. The azimuth of view is 170°, with the earthquakes being projected onto a plane striking N. 80° W.

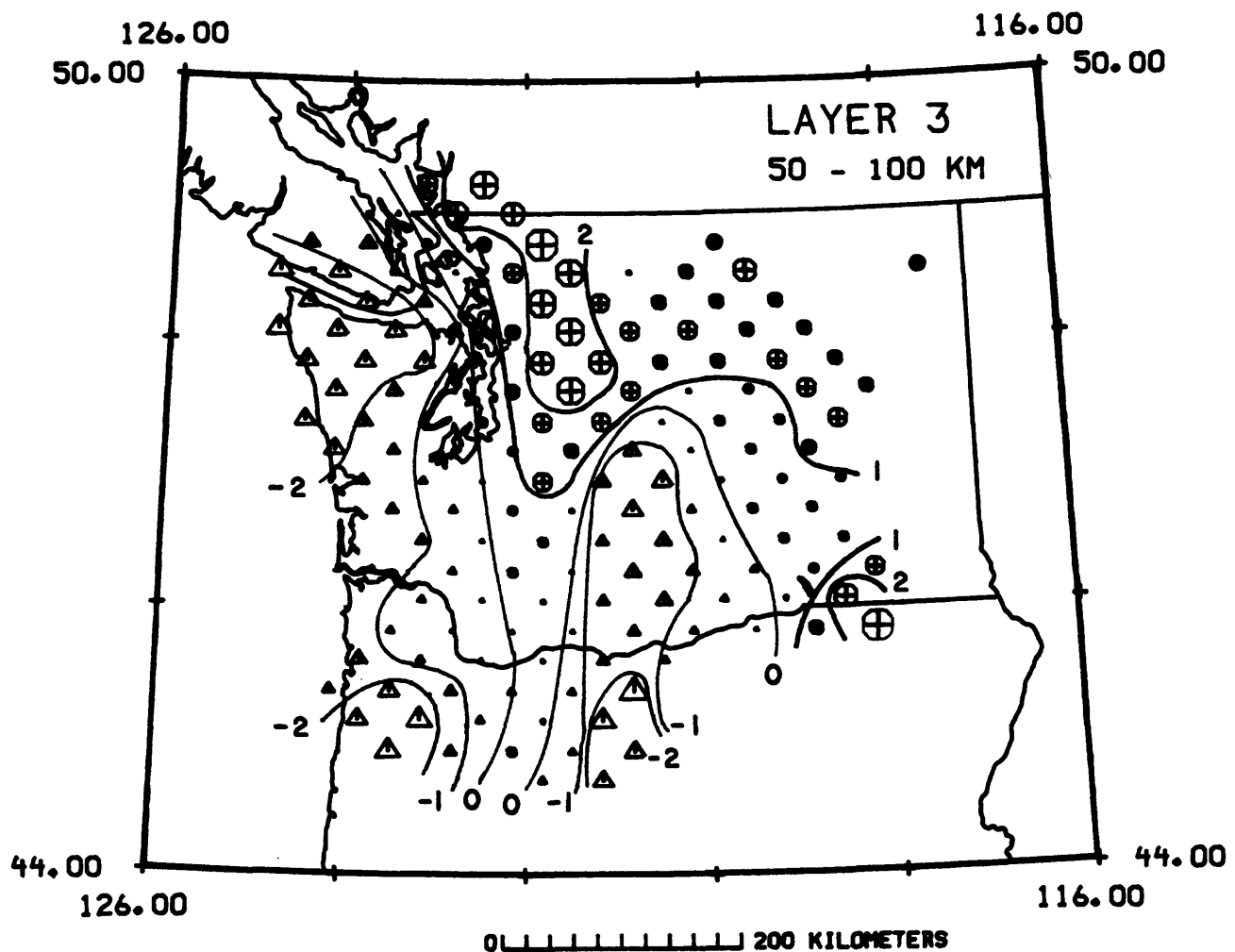


Figure 3. Contoured velocity perturbations from layer 3 of the teleseismic P-wave travel time inversion. The perturbations are in % of the mean velocity of layer 3. Circles and triangles represent high and low velocities respectively, with contours in 1% intervals. The N-S striking high-velocity zone at approximately 122°W longitude is interpreted as the position of the Juan de Fuca plate at 50-100 km depth.

Neotectonic Synthesis of U.S.

9540-02191

Carl M. Wentworth
Branch of Western Regional Geology
U.S. Geological Survey
345 Middlefield Road, MS 975
Menlo Park, California 94025
(415) 323-8111 ext. 2474

Investigations

1. Procurement of seismic reflection profiles across Coalinga nose in the vicinity of the Coalinga main shock of May 2, 1983: Two east-west reflection lines) that cross Coalinga nose north and south of the May 2 epicenter were purchased from Western Geophysical Company (lines SJ-3 and SJ-19 with lengths of 26.6 and 44.3 km). These are modern, 6-second Vibroseis lines that were collected with a frequency upsweep. This permitted correlation back into the sweep to obtain an additional 6 seconds of data.
2. Initial interpretation of SJ-19 as part of the development of velocity structure for use in reprocessing the 12-second record; coordination with the associated on-going refraction study of the same area by Allan Walter.
3. Collection and analysis of oil well records in the Coalinga area to (a) establish the stratigraphic framework within which other investigations must proceed, (b) define Tertiary structure, and (c) make stratigraphic identifications of events in the reflection records.
4. Study of the effects of various velocity structures and migration parameters on the shape and structural relations of Kettleman South Dome in migrating reflection profile SJ-6 (SJ-6 is described in Summaries of Technical Reports, vol. XV, p. 18-19 and in Wentworth and others, 1983x).

Results

1. Stratigraphy in Coalinga area: The stratigraphy in wells that define sections along the Coalinga Nose-Kettleman Hills-Lost Hills anticlinal trend and across Coalinga nose from within the Diablo Range to the middle of the San Joaquin Valley are used by Alan Bartow to describe the stratigraphic framework of the region and to infer relative sea-level history. Of particular interest are shoaling and local emergence of the Joaquin Ridge area in the early Tertiary, Miocene exposure of the New Idria serpentine diapir in the core of the Joaquin Ridge anticline from which debris slides carried serpentine debris into the shallow sea, and Pliocene initiation of Coalinga nose folding.
2. Stratigraphic identity of reflections in SJ-19: Clear reflections can be associated with the approximate tops of most of the principal stratigraphic units down to the top of the upper Cretaceous Panoche formation. At the west end of the record more than $2\frac{1}{2}$ seconds of layered

reflections dip eastward into the Pleasant Valley syncline and then gradually die out eastward beneath Coalinga nose. These events can represent a Great Valley sequence 6 or 7 km thick, which is nearly as thick as the section exposed to the west in the Diablo Range. Tentative identification - from distant wells and seismic refraction - of crystalline basement beneath Cretaceous strata 25 km east of the anticline suggests, in contrast, a Cretaceous section there that is only $1\frac{1}{2}$ km thick.

3. Structure in SJ-19: The nearly flat-lying sedimentary rocks beneath the western San Joaquin Valley rise westward in two steps onto Coalinga nose, drop back into the Pleasant Valley syncline and then rise into the Diablo Range to the west. Discontinuous deep events (3-5 s), presumably from layering in the Great Valley sequence, do not participate in the Coalinga nose folding that is evident higher in the record. The equivalent position of the hypocenter of the Coalinga main shock (6 km north of SJ-19) probably lies near the apparent base of layered reflections at a depth of 5-6 s.

4. SJ-6 migration: The limbs of Kettleman South Dome can be made to dip moderately to steeply or even be overturned, depending on selection of velocity structure and migration parameters. The geophysically most reasonable migration yields a steep-limbed fold and pulls reflections of the deep, gently west-dipping stratigraphic section in the San Joaquin Valley westward across beneath the anticline and upward into strong angular discordance with the west limb of the anticline. Thrusting is indicated, as concluded in Wentworth and others (1983x), but displacement may be quite limited.

Reports

Bartow, J. A., 1984, Cenozoic stratigraphy and geologic history of the Coalinga region, central California: chapter for USGS Coalinga professional paper on the Coalinga earthquakes, in peer review.

Wentworth, C. M., Walter, A. W., Bartow, J. A., and Zoback, M. D., 1983x, Evidence on the tectonic setting of the 1983 Coalinga earthquakes from deep reflection and refraction profiles across the southeastern end of Kettleman Hills, in Bennett, J. H., and Sherburne, R. W., eds., The 1983 Coalinga earthquakes: California Division of Mines and Geology Special Publication 66, p. 113-126.

Wentworth, C. M., Zoback, M. D., and Bartow, J. A., 1983, Thrust and reverse faults beneath the Kettleman Hills anticlinal trend, Coalinga earthquake region, California, inferred from deep seismic reflection data (abs.): Transactions, American Geophysical Union, EOS, v. 64, no. 45, Nov. 8, 1983, p. 747, Fall Meeting, San Francisco, December, 1983.

Wentworth, C. M., Walter, A. W., Zoback, M. D., and Blake, M. C., Jr., 1983, possible obduction of Franciscan assemblage, southeasternmost Diablo Range, California (abs.): Transactions, American Geophysical Union, EOS, v. 64, no. 45, Nov. 8, 1983, p. 868.

Wentworth, C. M., 1983, Reverse faulting as the source of earthquakes along the eastern seaboard of the United States: problems and needed research, in Hays, Walter, and Gori, P. L. (eds.), Proceedings of Conference XX, Workshop on the 1886 Charleston, South Carolina, earthquake and its implications for today: U.S. Geological Survey Open-File Report 83-843, p. 117-125.

-----1983, The changing tectonic basis for regulatory treatment of the 1886 Charleston, South Carolina, earthquake in the design of power reactors, in Hayes, Walter, and Gori, P. L. (eds.), Proceedings of Conference XX, Workshop on the 1886 Charleston, South Carolina, earthquake and its implications for today: U.S. Geological Survey Open-File Report 83-843, p. 266-275.

TECTONIC TILT MEASUREMENTS USING LAKE LEVELS: UTAH
4-9950-02396

Spencer H. Wood and Kirk R. Vincent
Branch of Engineering Geology and Tectonics
U.S. Geological Survey
Mailing address: Boise State University
Boise, Idaho 83725
(208) 386-3629

Investigations

1. Work continues on establishing a network of level lines and lake-level sites to monitor vertical tectonic deformation along the Wasatch Front. We report here the preliminary results from the first-order releveling by the National Geodetic Survey (NGS) from the Ogden, Utah area to Green River Wyoming. Leveling was completed over the interval 8/83 - 10/83. These elevations are differenced with recalculated elevations surveyed in 1958 by the NGS. The 1958 elevations were recalculated by John Till (NGS, Rockville) using the REDUC 4 program developed by Holdahl (1982) to estimate corrections for sight-line refraction and other systematic errors. Previous leveling along the segment of this line crossing the Wasatch fault had been done by the USGS in 1974 and 1979.
2. Lake level measurements have been made by temporary installations of mechanical recorders at several sites on the Great Salt Lake and on Utah Lake. These measurements are referenced to shoreline bench marks. Rising lake levels, storms, and vandalism have been a problem in maintaining these sites. All sites will have to be raised this year by establishing and leveling in new bench marks. We are in the process of assembling a digital data logger and pressure transducer system similar to one being used by Wayne Hamilton (National Park Service) on Yellowstone Lake. This system should resolve many of the problems we have previously had in maintaining a mechanical recorder on a stilling well out in the water. This system will be installed on the Farmington Bay body of water of the Great Salt Lake (Fig.1) to act as a continuous record of land-surface tilt of the lake shore within 3 km of the Wasatch Fault. Differencing and filtering digital data should permit resolution of movement between recorders of the order of 1 cm.

Results

The comparison of elevations obtained in 1983 by the NGS with those obtained in 1958 (recalculated with REDUC 4) by releveling from Ogden east to Evanston, Wyoming shows the pronounced down-to-west tilt is on the hanging-wall block of the Wasatch fault (Fig.2). Tilt amounts to about 10 cm over a distance of 12 km, or 9 microradians over a period of 25 years. The profiled apparent-elevation differences also show a slight tilting to the west of the foot-wall block and the entire line segment 100 km east of the fault to about Castle Rock, Utah. This slight tilt is about 0.4 microradians and may be within the range of possible systematic error and not significant.

The 1983 NGS survey relevelled the line of closely spaced bench marks in Weber Canyon established by the USGS in 1974 and last relevelled in 1979. The 1983 survey shows a 1 cm difference in elevation over a distance of 5 km on the line segment west of the fault, or a tilt of 3 microradians that developed in

the part of the hanging wall near the fault over a period of 4.4 years. This suggests an average tilt rate in the hanging wall of about 0.75 microradians per year over the period from 1979.4 - 1983.8 (Fig. 3a). Unfortunately bench marks at the west end of the line could not be recovered in 1983, so that this segment showing the steepest tilt between 1979 and 1983 does not give a complete picture of the deformation. New Class "A" bench marks were set near the Roy School in 1983 for future monitoring of the vertical deformation pattern west of the fault.

It is puzzling that the 1974.8 to 1978/79 comparison of USGS elevations in Weber Canyon show no significant tilt over a period of 4.6 years (Fig. 2b). Both surveys were run by the USGS topographic division for the purpose of monitoring vertical tectonic deformation across the Wasatch Fault. The only two possible explanations for the close agreement of the two sets of elevations obtained by the USGS parties are: (1) that vertical deformation occurs episodically along the fault zone, and the period 1974.8 to 1979.4 was a quiescent time, or (2) that the leveling procedures of the USGS and the NGS were sufficiently different that systematic errors may sometimes appear in comparisons of surveys by two different agencies, but may not appear in comparisons of surveys when the parties used identical methods and experienced similar conditions.

The question of serious systematic errors in the data sets through Weber Canyon is somewhat allayed by recalculation of the 1958 elevations using Holdahl's (1982) method of estimating refraction correction and also including new calibrations of the rods. Figure 3c shows that a difference of only 7 mm of apparent elevation change is generated by applying these corrections to the 1958 data; however, the estimated refraction correction is in the same sense as the corrected elevation change. As another check we intend to examine the near surface temperature gradients measured at every set-up in the autumn 1983 releveling along this route.

In the previous semi-annual report (Wood and Vincent, 1983, Fig. 2) we show a profile of elevation changes from data along the Wasatch Front between Ogden and Salt Lake City obtained by differencing the unadjusted elevations obtained in 1953 and 1967 by the NGS. R. Reilinger (written communication, 1984) has pointed out that the 1953 survey may have significant error that would not show up in loop closures, but does show up in calculating differences between the 1903 and 1967 surveys with the 1953 survey. The profiles of elevation change along the line are similar in magnitude, but opposite in sense suggesting error in the 1953 survey. This data set will be re-examined, and possibly short segments of the line that show an apparent tilt will be re-leveled to remove ambiguity in the future.

Another monitor line established in 1974 by the USGS for tectonic studies may also be partly leveled in the 1984-85 program. This line of closely spaced bench marks runs from Parleys Summit west through Salt Lake City along 21 Avenue South and crosses the East Bench branch of the Wasatch Fault near the Sugar House (Fig. 1).

All leveling data examined have been consistent in showing an apparent down-tilting to the west of about 11 cm, with most of the tilt on the hanging-wall side of the Wasatch Fault. If this can be interpreted as tectonic movement and strain accumulation on the fault, it appears that most of it developed between 1953 and 1974, that during the period from 1974 - 1979 the fault experienced little or no movement, and that movement resumed in the period 1979 to 1983. The earlier data (1903, 1953, 1958, and 1967) may always be questionable, because of possible systematic errors. Nevertheless, this earlier

data does yeild a consistant result. Furthermore, the sense and location of apparent movement is exactly what is expected of strain on the Wasatch Fault. If one accepts that the 1974 and 1979 elevations in Weber Canyon are valid (Fig. 3b), and that the latest survey in 1983 by the NGS is without significant error, then Fig. 3a would indicate that movement is continuing at a rate on the order of 0.75 microradians per year.

References cited

- Holdahl, S.R., 1982, Recomputation of vertical crustal motions near Palmdale, California, 1959-1975: Journal of Geophysical Research, v. 87, p. 9374-9388.
- Wood, S.H., and Vincent K. R., 1983, Tectonic tilt measurements using lake levels: Summaries of technical reports, Volume XVII, National Earthquake Hazards Reduction Program, December, 1983, U.S. Geological Survey Open-file Report 83-918, p. 52-55.

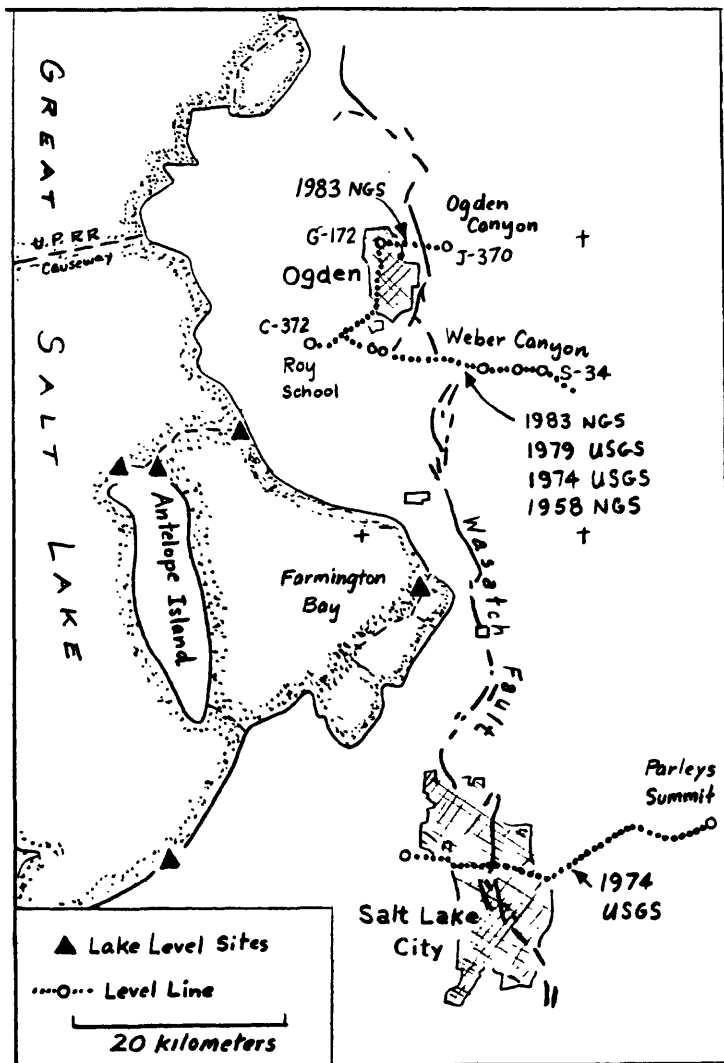


Figure 1. Network of level lines and lake-level sites for monitoring vertical tectonic movement along the Wasatch Front in the Salt Lake City - Ogden area. (Not shown on this map are the 1903, 1953, 1967 leveling-survey routes of the NGS that run north-south and just west of the fault.)

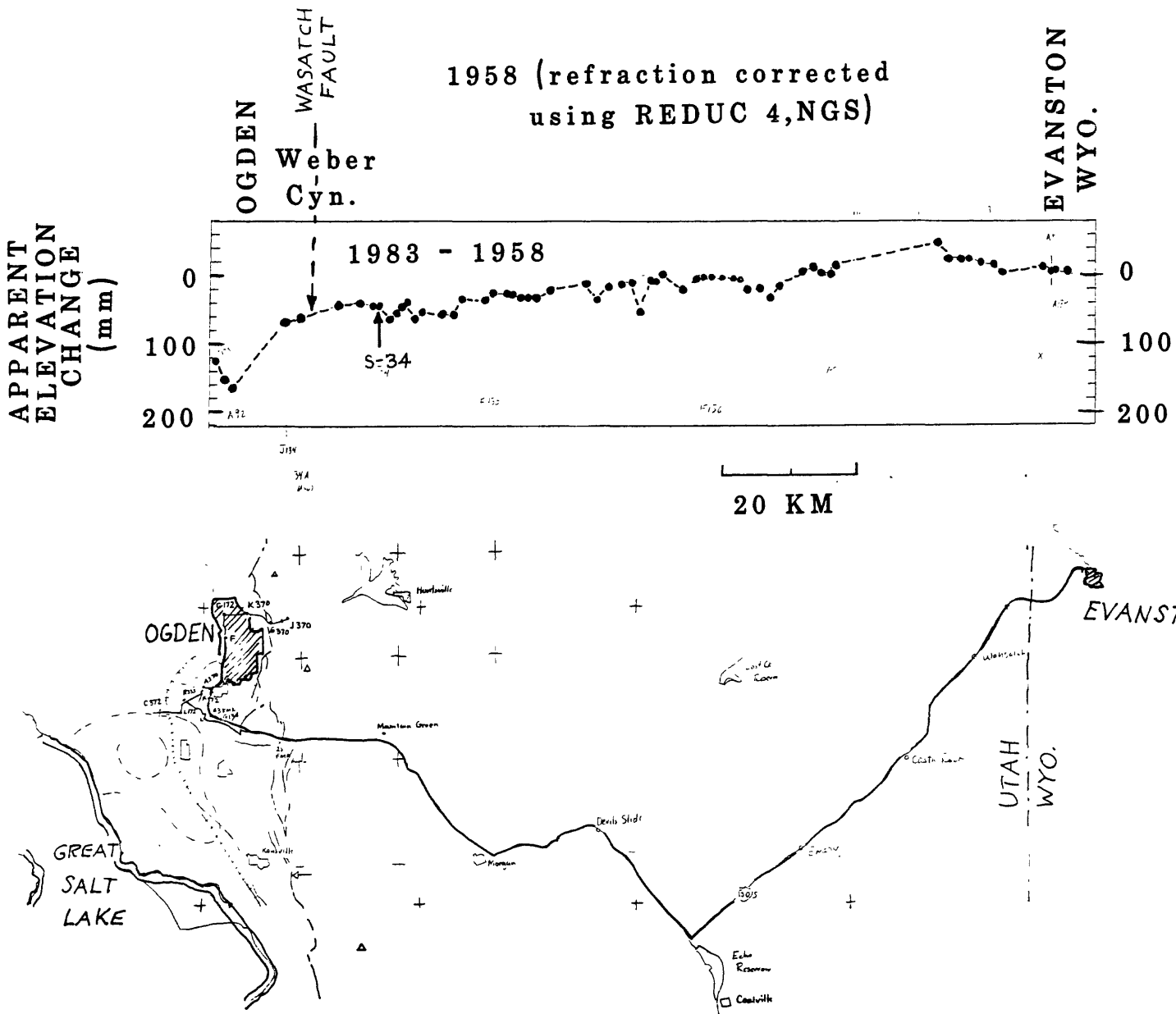


Figure 2. Profile of apparent elevation change with respect to bench mark S-34 near Mountain Green. The 1958 recalculated elevations are subtracted from the elevations determined by the 1983 NGS releveling. The line was re leveled from Ogden, Utah to Green River, Wyoming, but only the segment to Evanston, Wyo. is shown.

Releveling of Weber Canyon near Ogden

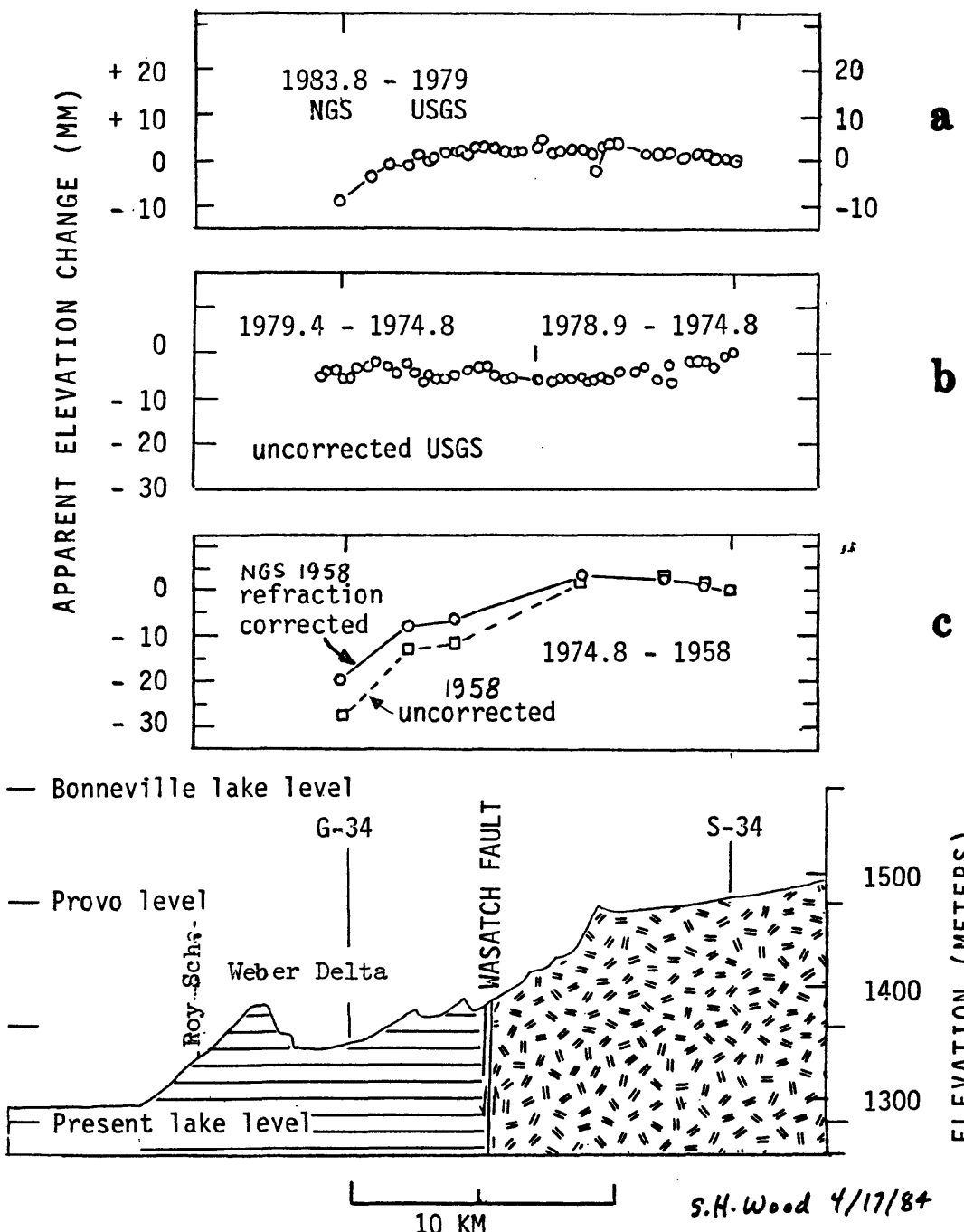


Figure 3. History of apparent elevation change across the Wasatch Fault in Weber Canyon. Elevation changes are referenced to bench mark S-34. (a) 1983.8 survey by NGS compared to the 1978/79 USGS survey. USGS work has not been recalculated for estimated refraction error, or rod calibration error. (b) 1978/79 survey compared to the 1974 USGS survey. Neither survey has been recalculated. (c) 1974.8 USGS survey compared to the 1958 NGS survey. The original comparison (before recalculation) is shown with boxes. The comparison with the recalculated 1958 elevations is shown with circle points.

Potentially Active Reverse Faults of Eastern Ventura Basin,
Los Angeles County, California

USGS Contract No. 14-08-0001-21279

Robert S. Yeats
Department of Geology
Oregon State University
Corvallis, Oregon 97331-5506
(503) 754-2484

Investigations

Field work is now completed, and cross sections and maps are being prepared for the final report. The maps (1:24,000) are to be submitted for open file by USGS.

Results

The Saugus Formation is involved in faulting and folding throughout the area, although faulting and folding of similar structural style predates Saugus deposition. Field mapping has not found evidence of tectonic topography as youthful as that associated with the San Cayetano and Oak Ridge faults which extend into the area.

Earthquake Hazards Studies, Metropolitan Los Angeles-
Western Transverse Ranges Region

9540-02907

R. F. Yerkes
 Branch of Western Regional Geology
 U. S. Geological Survey
 345 Middlefield Road, MS 975
 Menlo Park, California 94025
 (415) 323-8111 ext. 2350

Investigations and results

1. Historic earthquake data (W. H. K. Lee). Continued organizing and merging phase data from several sources into common format.

2. Earthquake hazard studies (Yerkes). Continued evaluating well data for evidence of abnormally high fluid pressures, southern San Joaquin Valley. Much of San Joaquin Valley south of lat 36.80° N. is underlain at shallow depths by deposits with fluid pressure/depth ratios near or above 0.5 psi/ft; the ratios generally increase with depth and structural penetration; they are relatively high along the Lost Hills-Kettleman Hills trend and extend through Coalinga Nose, site of the 1983 earthquakes, to Joaquin Ridge. Pressure/depth plots from about 300 wells show an average ratio of about 0.6 psi/ft, a lower bound somewhat above hydrostatic (0.47 psi/ft), and an upper bound exceeding 0.9 psi/ft. Below about 3 km the ratio commonly increases with depth at rates greater than 1.00 psi/ft; the depth limit of such pressures is not known, but they extend to the limit of drilling, about 6.5 km. The "high-pressure" wells are located southwest of the valley axis; no wells are known to bottom in Franciscan rocks, but a few that bottom in non-Franciscan basement show high-pressure gradients above or near the top-basement contact. Sonic logs for a few modern, deep wells all show abrupt reversals in the velocity/depth gradient at the top of the "high-pressure" (≥ 0.61 psi/ft) zone, and where well data coincide with seismic refraction/reflection profiles, the top of the zone marks the top of a seismic low-velocity zone. Genesis and source of the high pressures are unknown, but all data are consistent with their being present in Franciscan-Great Valley rocks at seismic depths below Coalinga Nose.

Joined Paul Segall in evaluating stress and fluid-pressure changes associated with oil-field operations at Coalinga (reported by Segall, OEVE).

3. Quaternary stratigraphy, chronology, and tectonics, Ventura area
 (A.M. Sarna-Wojcicki)

Continued feasibility study of using oxygen-isotope analysis of foraminifers in on-land Quaternary marine sections in order to (1) improve existing age control for these sections through correlation with deep-sea secular oxygen-isotope variations, and (2) derive a detailed climatic history that can be correlated to non-marine sections in the Western United States.

Analysis of seven samples of tests of Uvigerina peregrina, obtained from sites in the Balcom Canyon-Santa Paula Creek area east of Ventura, indicate that (1) the isotopic compositions of the foraminifera have not been affected by post-depositional or meteoric alteration, as can be seen from the uniform and low negative delta ^{13}C values, and (2) the range of delta ^{18}O values (table 1) is in general agreement with that observed in deep-sea cores for the time span studied.

These results invite continuing with the next phase of the study, a collection of samples from the Balcom Canyon section at intervals of about 4 m, corresponding, by our calculations, to about 4,500 yrs of time for each interval. (Study in cooperation with Kristine McDougall, B. P. & S., Menlo Park, and R. K. Matthews, Brown University).

Reports

Clark, M. M., Harms, K. K., Lienkaemper, J. J., Harwood, D. S., Lajoie, K. R., Matti, J. C., Perkins, J. A., Rymer, M. J., Sarna-Wojcicki, A. M., Sharp, R. V. Sims, J. D., Tinsley, J. C., III, and Ziony, J. I., 1984, Preliminary slip-rate tables and map of late-Quaternary faults of California: U.S. Geological Survey Open-File Report 84-106.

Sarna-Wojcicki, A. M., Bowman, H. R., Meyer, C. E., Russell, P. C., Woodward, M. J., McCoy, Gail, Rowe, J. J., Jr., Baedecker, P. A., Asaro, Frank, and Michael, Helen, 1984, Chemical analyses, correlations, and ages of upper Pliocene and Pleistocene ash layers of east-central and southern California: U.S. Geological Survey Professional Paper 1293, 40 p.

Sarna-Wojcicki, A. M., Champion, D. E., and Davis, J. O., 1983, Holocene volcanism in the conterminous United States and the role of silicic volcanic ash layers in correlation of latest-Pleistocene and Holocene deposits, in H. E. Wright, ed., "Late Quaternary Environments of the United States", v. 2, University of Minnesota Press, p. 52-77.

Segall, P., Reasenberg, P., and Yerkes, R. F., 1983, Crustal stress changes and subsidence resulting from subsurface fluid withdrawal in the epicentral region of the 1983 Coalinga earthquake: EOS, Vol. 64, No. 45, p. 747-748.

Segall, P., and Yerkes, R.F., Stress and fluid pressure changes associated with oil field operations: A critical assessment of effects in the focal region of the 1983 Coalinga earthquake: prepared and submitted for U.S. Geological Survey Professional Paper on the earthquake.

Yerkes, R. F., and Williams, K. M., 1983, Shallow stress changes due to withdrawal of liquid from oil fields in the Coalinga area, California: California Division of Mines and Geology, Special Publication 66, p. 195-199.

Yerkes, R. F., Levine, Paia, and others, Abnormally high fluid pressures and the Coalinga earthquakes: preliminary report prepared for "Redbook" Workshop on Coalinga earthquake.

Table 1. Oxygen and carbon isotope delta values (relative to standard PDB) for samples of Uvigerina peregrina from the Balcom Canyon section, Ventura area, California.

| <u>Sample</u> | $\delta^{13}\text{C}$ % rel. PDB | $\delta^{18}\text{O}$ % rel. PDB |
|---------------|----------------------------------|----------------------------------|
| Pico 163A | -1.23 | +2.39 |
| Pico 167 | -1.39 | +2.51 |
| Pico 168 | -1.22 | +1.78 |
| Pico 169 | -1.28 | +2.69 |
| Pico 170 | -1.29 | +2.17 |
| Pico 171 | -1.56 | +2.66 |
| Pico 172 | -1.51 | +2.91 |

Regional Syntheses of Earthquake Hazards in Southern California

9910-03012

Joseph I. Ziony
Branch of Engineering Seismology and Geology
U.S. Geological Survey
345 Middlefield Road, MS 977
Menlo Park, California 94025
(415) 323-8111, ext. 2944

Investigations

1. Analysis of the geologic and seismologic character of late Quaternary faults of the Los Angeles region, as determined from published and unpublished sources and from limited field investigations, continued. Our emphasis is on obtaining: (a) quantitative data on offsets of deposits or geomorphic features younger than about 700,000 years in order to provide a reasonably uniform basis for estimating rates of geologically recent slip along individual faults, and (b) geologic constraints on the recurrence of large earthquakes. The long-term objectives are to estimate the relative activity of these faults, and, where possible, their earthquake and surface faulting potential.
2. Coordination of the preparation of a professional paper on the earthquake hazards of the Los Angeles region continued. This comprehensive report will summarize the current methods and conclusions of USGS investigators concerning the major earthquake-hazard factors for the region.

Results

A comprehensive report on the geologically controlled earthquake hazards of the Los Angeles region, containing new or improved methods for predicting their areal extent and severity, has completed technical review and is being submitted for publication in 1985 as a Geological Survey Professional Paper. The report, *Evaluating Earthquake Hazards in the Los Angeles Region--An Earth-Science Perspective*, contains the following chapters:

Introduction, by J. I. Ziony and W. J. Kockelman

Geologic setting, by R. F. Yerkes

Evaluating earthquake and surface-faulting potential, by
J. I. Ziony and R. F. Yerkes

Predicting earthquake ground motion--an introduction, by
R. D. Borcherdt

*Mapping Quaternary sedimentary deposits for areal
variations in shaking response*, by J. C. Tinsley
and T. E. Fumal

Mapping shear-wave velocities of near-surface geologic materials,
by T. E. Fumal and J. C. Tinsley

Predicting seismic intensities, by J. F. Evernden

Predictive mapping of earthquake ground motion by W. B. Joyner
and T. E. Fumal

Predicting relative shaking response, by A. M. Rogers,
J. C. Tinsley, and R. D. Borcherdt

Predicting time histories of ground motion, by P. A. Spudich
and S. H. Hartzell

Evaluating liquefaction potential, by J. C. Tinsley, T. L. Youd,
D. M. Perkins, and A.T.F. Chen

Estimating areal limits on earthquake-induced landsliding,
by R. C. Wilson and D. K. Keefer

Identifying active faults and potentially unstable slopes offshore,
by S. H. Clarke, Jr., H. G. Greene, and M. P. Kennedy

Evaluating the tsunami potential, by D. S. McCulloch

*Predicted geologic and seismologic effects of a postulated magnitude 6.5
earthquake along the northern part of the Newport-Inglewood zone*, by
J. I. Zony, J. F. Evernden, T. E. Fumal, E. L. Harp, S. H. Hartzell,
W. B. Joyner, D. K. Keefer, P. A. Spudich, J. C. Tinsley, R. F.
Yerkes, and T. L. Youd

Using earth-science information for earthquake-hazard reduction,
by W. J. Kockelman

The following is the abstract for the Professional Paper:

ABSTRACT

Potentially damaging earthquakes are inevitable within the Los Angeles region, but the hazards caused by them can be predicted in order to provide a basis for reducing damage and loss. This volume identifies the principal geologically controlled earthquake hazards of the region (surface faulting, strong shaking, ground failure, and tsunamis), summarizes methods for characterizing their extent and severity, and suggests opportunities for reducing earthquake hazards.

Two families of active faults generate earthquakes in the Los Angeles region: northwest-trending faults, such as the San Andreas, with chiefly horizontal slip, and west-trending faults of the Transverse Ranges with chiefly vertical slip. Faults in these two systems have produced more than 40 damaging earthquakes since 1800. Ninety-five faults have slipped in late Quaternary time (approximately the past 700,000 years) and are judged capable of generating future large earthquakes and displacing the ground surface. Average rates of late Quaternary slip or separation along these faults provide an index of their relative activity. The San Andreas and San Jacinto faults have slip rates measured in tens of millimeters per year, but most other faults have rates of about 1 mm/yr or less. Intermediate rates of as much as 6 mm/yr characterize a belt of Transverse Ranges faults that extend from near Santa Barbara to near San Bernardino. The dimensions of the late Quaternary faults provide a basis for estimating the largest size of future earthquakes likely to occur in the Los Angeles region: moment magnitude (M) 8 for the San Andreas; M 7 for the other northwest-trending elements of that fault system; and M 7.5 for the Transverse Ranges faults. Geologic and seismologic evidence along these faults, however, suggests that appropriate earthquakes for planning and design purposes for non-critical facilities are M 8 for the San Andreas; M 7 for the San Jacinto; M 6.5 for other northwest-trending faults; and M 6.5-7 for the Transverse Ranges faults. The geologic record indicates that parts of the San Andreas and San Jacinto faults have generated major earthquakes with repeat times of several tens to a few hundred years. In contrast, the geologic evidence at points along other active faults suggests repeat times measured in many hundreds to several thousands of years. The

distribution and character of late Quaternary surface faulting permit estimation of the likely location, style, and amount of future surface displacements.

An extensive body of geologic and geotechnical information is used to evaluate areal differences in future levels of shaking. Bedrock and alluvial deposits are differentiated according to the physical properties that control shaking response; maps of these properties are prepared by analyzing existing geologic and soils maps, the geomorphology of surficial units, and geotechnical data obtained from boreholes. The shear-wave velocities of near-surface geologic units must be estimated for some methods of evaluating shaking potential. Regional-scale maps of highly generalized shear-wave velocity groups, based on the age and texture of exposed geologic units and on a simple two-dimensional model of Quaternary sediment distribution, provide a first approximation of the areal variability in shaking response. More accurate depictions of near-surface shear-wave velocity useful for predicting ground-motion parameters take into account the thickness of the Quaternary deposits, vertical variations in sediment type, and the correlation of shear-wave velocity with standard-penetration resistance of different sediments. A map of the upper Santa Ana River Valley showing shear-waves velocities to depths equal to one-quarter wave length of a one-second shear wave demonstrates the latter mapping procedure.

Four methods are presented for predicting the distribution and strength of shaking from future earthquakes. These techniques use different measures of strong-motion severity: seismic intensities, peak horizontal acceleration and velocity (or response spectral values), amplification factors relative to ground motion on bedrock, and time histories of ground motion.

Maps of predicted seismic intensities for the Los Angeles region are useful for emergency-preparedness planning and for estimating losses from future earthquakes. Comparison of observed intensities from the 1971 San Fernando earthquake with strong-motion records indicates that intensity correlates directly with expected levels of shaking in the range from 0.5 to 3 hertz (periods of approximately 0.3s to 2s), frequencies of concern to ordinary structures. A computer-based technique for predicting earthquake intensities incorporates: (1) a numerical model of the earthquake source; (2) a mathematical expression for the rate of attenuation in the crust of the region; (3) an empirical correlation of geologic ground conditions with differences of expected intensity; and (4) a digitized map of geologic ground conditions for the area studied. To demonstrate the method, predicted intensities are mapped for postulated earthquakes along the San Andreas, San Jacinto, Newport-Inglewood, Pitas Point-Ventura, Elsinore (Glen Ivy), and Raymond faults; the calculated maximum intensities highlight those parts of the region that have a significant shaking hazard. This technique of predicting intensities can be extended to estimate losses from future earthquakes by incorporating empirical correlations between observed intensities and percentage of damage experienced by various types of structures. A comparison of predicted losses to wood-frame construction for various possible California earthquakes shows that earthquakes of about M 6.5 in the Los Angeles basin would cause much greater damage than an earthquake of about M 8.0 on the closest part of the San Andreas fault.

Predictive mapping of peak horizontal acceleration and velocity, and of horizontal response spectral values, provides an appraisal of areal shaking potential that is useful for engineering design and for building codes. The technique relies upon equations that are derived from regression analyses of an extensive set of strong-motion records. These equations link the ground-motion parameters to earthquake magnitude, source distance, and site conditions. The site effect can be expressed in terms of the shear-wave velocities of near-surface geologic materials. Thus, predictive maps of ground-motion values for a single postulated earthquake can be made by applying the predictive equations and by taking into account the areal differences in shear-wave velocities. The uncertainty associated with the frequency of occurrence and size of future earthquakes from multiple potential sources can be evaluated by a newly developed approach that incorporates fault slip rates to compute the ground motion that will be exceeded at a specified annual probability. Predictive maps for the Upper Santa Ana River Valley illustrate this method by showing the areal distribution of ground-motion values exceeded at a return period of 500 years for future large earthquakes on the San Andreas, San Jacinto, and Cucamonga faults.

Areal variations in shaking potential also are estimated by comparing measurements of ground motions from distant underground nuclear explosions recorded at 98 sites in the Los Angeles region. Because local ground response from these low-strain signals correctly predicts ground-motion amplification for higher strain levels caused by nearby large earthquakes, the data provide a way of assigning amplification factors relative to shaking on crystalline bedrock. At periods less than 0.5 s, the most pronounced differences in observed site response correlate with differences in sediment void ratio, thickness of surficial deposits, and depth to basement rocks; resonant effects with large amplifications over narrow frequency bands are observed for sites underlain by Holocene deposits 10-20 m thick. At periods greater than 0.5 s, the most important geologic factors are depth to basement rocks and thickness of Quaternary sediments. By comparing the recorded motions with what is known about geologic conditions at each site, the principal factors that affect amplification are grouped, and distinctive types of sites are identified through cluster analysis. These site types become the basis for predictive mapping of relative shaking response. To demonstrate the mapping procedure, the areal distribution of expected amplification factors for part of the Los Angeles basin is shown for three period-bands (3.3-10 s; 0.5-3.3s; and 0.2-0.5s); locally, the spectral amplification is predicted to be as great as 6 1/2 times the shaking levels on crystalline bedrock.

Earthquake-resistant design of critical structures commonly requires elaborate estimates of the characteristics of ground motion at a particular site. Time histories of ground motion from postulated earthquakes are predicted by assuming how each point on a slipping fault might be displaced, determining the ground motions caused by each point, and then summing the ground motion contributions from each point to obtain the total motion at a given distant site. The method depends upon assumptions concerning: (1) the detailed character of the expected rupture propagation, and (2) the velocity structure of the Earth's crust in the region analyzed. The time history of ground motion caused by slip of a single point on a fault is called a Green's function. Green's functions can be determined theoretically by solving the wave equation in a model of the crust, or they may be obtained empirically by using recordings of small earthquakes in the desired crustal structure. Simplifying methods of computing Green's functions economically are reviewed.

Secondary geologic effects such as liquefaction within the alluvial basins and landsliding within the upland areas can be expected to result from strong shaking during future earthquakes. Liquefaction potential is evaluated by preparing two types of maps--one showing the susceptibility of sediments to liquefy with shaking and the other expressing the probabilities that critical levels of shaking for liquefaction will be attained. Areas of susceptible sediments are delineated by analyzing the physical properties of the late Quaternary alluvial deposits, grouping these according to their probable content of clay-free sand or silt, and determining whether these deposits are saturated with ground water at depths less than about 15 m. Holocene sediments, especially those deposited during the past few hundred years, are the most susceptible to liquefaction-related ground failure; these materials are mapped on the basis of soil-profile development, geomorphic expression, and geotechnical properties such as standard penetration resistance. Areas of the Los Angeles region deemed most vulnerable to liquefaction during future earthquakes include the flood plains of the Los Angeles, Santa Ana, and San Gabriel Rivers; parts of the San Fernando Valley and the Oxnard Plain; coastal and harbor areas of Long Beach and Marina Del Rey; and in flood control basins. The opportunity for liquefaction at a site containing susceptible sediments can be estimated by considering the earthquake potential and by applying an empirically determined relationship between earthquake magnitude and the limiting distances for liquefaction-related ground failure. Regional liquefaction opportunity is mapped by summing for points on a map the expected annual rates of occurrence of magnitude 5 or greater earthquakes from those fault sources that influence each point. Most of the region will experience ground shaking sufficient to cause liquefaction in susceptible sediments on an average of once every 33 years.

The extent and severity of future earthquake-induced slope failure can be fully evaluated only when detailed information on the geologic and topographic controls on slope stability is available. Such information is not yet complete for the Los Angeles region. However, a twofold approach has been developed to assess, for postulated earthquakes of specified size, the areal limits of earthquake-triggered landslides. The maximum distance from an earthquake source at which various classes of landslides can occur (given susceptible slopes) is estimated from correlations based on a worldwide data set for historical earthquakes that have triggered landslides. The probability distribution of threshold levels of shaking capable of triggering slope failure then can be mapped by extending the Newmark method of slope-stability analysis; the probabilistic procedure depends upon newly established correlations between earthquake magnitude, critical displacement of a slope, and the intensity of shaking for a given earthquake-source distance. Using these relations, the likelihood for slope failures from a postulated earthquake is evaluated for an example site in the Santa Monica Mountains.

Faults and zones of potential slope instability on the sea floor off the Los Angeles region have been identified and evaluated by specialized remote-sensing methods. Acoustic reflection profiles reveal those faults that offset late Quaternary sediments of the sea floor; the profiles also show potentially unstable slopes on which subaqueous sediment slides, mass flows, and gas-charged sediments occur. A regional analysis of these profiles indicates offshore counterparts to the onshore faults of the San Andreas system and the Transverse Ranges. Many of these offshore faults may generate large earthquakes and offset the sea floor. Scattered zones as large as 60 km² of

seafloor sliding are mapped along the outer edge of the Santa Monica and San Pedro shelves and cover several hundred km² in the central Santa Barbara basin. Furthermore, potentially unstable gas-charged sediments apparently are widespread across the Santa Monica and San Pedro basins. Some zones of sea-floor instability could fail during shaking from nearby large earthquakes.

The ocean-side setting poses a threat of tsunamis to coastal areas, although the hazard in the Los Angeles region is much less than for many other regions along the circum-Pacific border. Methods are available to predict tsunami wave heights and frequency of occurrence resulting from both distant and local sources and a number of these are summarized. A review of predictive models for distantly generated tsunamis indicates that wave heights of 2 m are exceeded on the average of once every 500 years, except locally along Santa Monica and San Pedro Bays and near Ventura, where wave heights of 3 m are exceeded on the average of once every 500 years. A preliminary appraisal of the potential for locally generated tsunamis suggests that wave run-up heights as great as 4-6 m could be caused by faulting of the sea floor in the Santa Barbara Channel; wave run-up heights no greater than 2-3 m are estimated for the dominantly strike-slip faults further south. Earthquake-triggered seafloor slides with the dimensions observed in the offshore region are unlikely to cause tsunamis.

As a demonstration of the various hazard-evaluation methods discussed in this volume, the geologically controlled effects expected from a postulated M 6.5 earthquake along the northern part of the Newport-Inglewood fault zone are evaluated. Predicted effects include: (1) secondary faulting (normal-oblique slip) at the ground surface along one or more late Quaternary faults exposed in the Baldwin and Rosecrans Hills. Possible subsurface slip along reverse faults at the north end of the Dominguez Hills; (2) shaking intensities of Modified Mercalli intensity VII distributed widely throughout the Los Angeles basin and the San Fernando Valley, with scattered areas of intensity VIII to distances of 18 km from the main fault; (3) shaking lasting about 10 to 15 seconds. Peak ground motion values will be about 0.4 g acceleration, 90-100 cm/s velocity, 1.2 g pseudo-acceleration response, and 160-180 cm/s pseudo-velocity response near the earthquake source zone. Peak ground velocity values at the northwest end of the fault zone will be higher than to the southeast if the subsurface tectonic rupture propagates northwestward from the postulated epicenter; (4) liquefaction in highly susceptible, water-saturated, clay-free Holocene alluvial sediments as distant as 18 km from the earthquake source zone. Rock/soil falls and slides will be the most common earthquake-triggered slope failures and will occur chiefly in upland areas within about 40 km of the earthquake source zone; and (6) minor harmonic waves (seiches) in enclosed small bodies of water.

The use of earth-science information such as that described here is illustrated by five examples of specific earthquake-related problems faced by decision makers in southern California. These include: anticipating damage to critical facilities; adopting seismic safety plans; strengthening highway bridges; regulating development in areas of potential surface faulting; and strengthening or removing unsafe masonry buildings. These examples show what geologic and seismologic information was used and the actions taken to reduce the hazard. They demonstrate that effective measures for reducing future earthquake losses can result where adequate scientific data and interpretations are available and are thoughtfully applied by engineers, planners, and others who are responsible for public safety.

Department of Earth and Planetary Sciences
Massachusetts Institute of Technology
Cambridge, Massachusetts 02139
Contract No. 14-08-0001-G-885
Principal Investigator K. Aki
Co-Investigator S. Ellis
(617) 253-3381

P-1

Theory and Strategy of Earthquake Prediction

Extensive studies of local earthquake S coda (Aki, 1969; Aki and Chouet, 1975; Rautian and Khalturin, 1978; Tsujiura, 1978) have shown that the following two well-established features of local earthquake S coda are very useful tools for quantitative studies of small-scale heterogeneities in the earth. The first feature is its independence on the source-receiver path. The second feature is the regional change of its apparent Q^{-1} between stable and active tectonic areas at frequencies around $0.5 \sim 1.0$ Hz (Aki, 1981). Aki (1984) further suggested, on the basis of many observations, that the time-varying local earthquake coda Q may be an earthquake precursor. Thus, the purpose of the present study is to focus on the investigation of the time-varying quality factor. We studied local earthquake coda Q in different oceanic areas, young and old. An advantage of the coda Q as a precursor is its complete coverage of a large area in detecting the change of the heterogeneous structure of an earthquake source region which is responsible for precursory phenomena (Aki, 1984).

In a detailed study of scattering and attenuation of shear waves of numerous local earthquakes in central Japan and other areas (Aki, 1980a, 1980b), an interesting phenomenon that the Q^{-1} values of shear waves at period around 1 s varies from place to place by an order of magnitude showing a strong correlation with the intensity of current tectonic activity was noticed. This phenomenon was also confirmed by the Q values of coda and S waves from Central Asia (Rautian and Khalturin, 1978). Moreover, Singh and Herrmann (1983) obtained a contour map of crustal Q values (frequency $f = 1$ Hz) for the entire United States based on a scattering model to explain the coda waves of local and near regional earthquakes. They found a gradual increase of Q values from the lowest around $140 \sim 200$ in the western United States to the maximum around 1300 in the central United States. The correlation between tectonic activity and Q value at 1 Hz is very impressive. However, detailed short-period attenuation observations from the ocean floor, young or old, are lacking. We hope that the present study will be complementary to earlier studies on the continents.

Unfortunately, we still cannot take advantage of digital records for our particular purpose, because only a few stations of the Global Digital Seismograph Network (GDSN) are located in the ocean (Engdahl et al., 1982). We have chosen three WWSSN stations in the ocean. They are Guam on Mariana Islands, Galapagos Islands of Ecuador, and Akureyri on Iceland. Guam is on the Philippine plate near the Mariana trench; it belongs to the oldest, coldest oceanic lithosphere. The Galapagos Islands are located near the ridge between the Cocos and Nazca plates, and Akureyri is near the ridge in the North Atlantic Ocean; thus both of these sites belong to the youngest, hottest oceanic lithosphere. We digitized the records of 22 earthquakes, of which 10 are from Akureyri, 4 from the Galapagos Islands, and 8 from Guam. All these earthquakes are local earthquakes relative to these stations. All the earthquakes chosen are smaller than 5.0 in magnitude, to ensure that the effect of the source spectrum can be ignored (Herrmann, 1980).

After interpolation, we used a well-developed program by S. Phillips of MIT for calculating Q values. This program is based on the formulation of a single isotropic scattering approximation (Sato, 1977) which can be used for the near source case.

The preliminary results are (1) Q increases with frequency for all three areas investigated; (2) at frequency $f = 1$ Hz, the average Q value in Akureyri is nearly twice as large as the average value in Guam (180:110); and

(3) the Q values obtained are low in comparison with those obtained from the stable part of continents. It is possible that Q values do not vary as much from place to place on the ocean floor as they do on continents.

References

- Aki, K. (1969). Analysis of the seismic coda of local earthquakes as scattered waves, J. Geophys. Res., 74, 615-631.
- Aki, K. (1980a). Attenuation of shear-waves in the lithosphere for frequencies from 0.05 to 25 Hz, Phys. Earth Planet. Inter., 21, 50-60.
- Aki, K. (1980b). Scattering and attenuation of shear waves in the lithosphere, J. Geophys. Res., 85, 6496-6504.
- Aki, K. (1981). Scattering and attenuation of high-frequency body waves (1-25 Hz) in the lithosphere, Phys. Earth Planet. Inter., 26, 241-243.
- Aki, K. (1984). Theory of earthquake prediction with special reference to monitoring of the quality factor of lithosphere by the coda method, Proceedings of the U.S.-Japan Symposium on Earthquake Prediction, Nov. 1983, in press.
- Aki, K., and B. Chouet (1975). Origin of coda waves: Source, attenuation and scattering effects, J. Geophys. Res., 80, 3322-3342.
- Engdahl, E.R., J. Peterson, and N.A. Ursini (1982). Global digital networks - current status and future directions, Bull. Seism. Soc. Am., 72, 5243-5259.
- Hermann, R.B. (1980). Q estimates using the coda of local earthquakes, Bull. Seism. Soc. Am., 70, 447-468.
- Rautian, T.G., and V.I. Khalturin (1978). The use of coda for determination of the earthquake source spectrum, Bull. Seism. Soc. Am., 68, 923-948.
- Sato, H. (1977). Energy propagation including scattering effects single isotropic scattering approximation, J. Phys. Earth, 25, 27-41.
- Singh, S., and R.B. Herrmann (1983). Regionalization of crustal coda Q in the continental United States, J. Geophys. Res., 88, 527-538.
- Tsujiura, M. (1978). Spectral analysis of the coda waves from local earthquakes, Bull. Earthquake Res. Inst., Tokyo Univ., 53, 1-48.

On-Line Seismic Processing

9970-02940

Rex Allen
Branch of Seismology
U.S. Geological Survey
345 Middlefield Road, MS 77
Menlo Park, California 94025
(415) 323-8111 ext 2240

Investigations and Results

The Menlo Park real-time processor continues as a major component of the CALNET data processing effort. In addition to the 256-station machine which has been in operation for several years, we have installed another consisting of 72 stations in an effort to cover more of the telemetered network while development proceeds on the Mark II RTP.

Performance of the RTP has been satisfactory in many respects, but many additional features have been suggested which are not possible to include in the current version because of limitations inherent in the hardware (at present the processors running the picker algorithm are operating at a duty cycle of about 92%). Inclusion of additional filtering or of specialized detection algorithms for processing teleseisms or S-arrivals are examples of the kind of enhanced performance we would like to include. The use of a high-level language, preferably FORTRAN, in place of assembly language in most parts of the picker will make the machine more generally useful in different locations, since the people actually using the machine will be able easily to modify the algorithms for their special purposes. The desired performance improvements dictated the use of one of the much more powerful microprocessors which have recently become available. After careful evaluation of the available microprocessors we have selected one, the 68000, that we believe will make possible the addition of desired features as well as allowing the use of a high-level language for most of the picker operation. This is currently carried out entirely in assembly language in the 9900 processor. The 68000 is several times faster than the 9900 for our application, and should allow the desired improvements.

A development system has been purchased and program development is proceeding on the new picker software. We expect an operating prototype to be ready for evaluation later this year.

Regional and Local Hazards Mapping in the Eastern Great Basin

9950-01738

R. Ernest Anderson
Branch of Engineering Geology and Tectonics
U.S. Geological Survey
Box 25046, MS 966, Denver Federal Center
Denver, CO 80225
(303) 234-5109

Investigations

1. Study the surface effects of the October 28, 1983, Borah Peak earthquake in central Idaho (A. J. Crone and M. N. Machette).
2. Continue paleostress studies in central Utah using fault-slip data collected from exposed faults (R. E. Anderson and T. P. Barnhard).
3. Begin evaluation of proposed segmentation of seismogenic structure along the Wasatch Front (R. L. Wheeler).
4. Complete the reports left over from project 02653 (Structural Framework of Eastern U.S. Seismic Zones) (R. L. Wheeler).

Results

1. Ms 7.3 Borah Peak earthquake that struck central Idaho on October 28, 1983, was one of the strongest historic earthquakes in the intermountain seismic belt. Much of the 34-km-long, northwest-trending zone of fault scarps and surface ruptures that formed during the earthquake follows Holocene and upper Pleistocene scarps of the Lost River fault. The throw along the new fault scarps averages 0.8 m, exceeds 1.0 m along 43 percent of their length, and is as much as 2.7 m along the broad and complex zone of deformation in the southern section. The net slip was normal sinstral having an average of 17 cm lateral slip for every 100 cm of dip slip. The preferred nodal plane from the focal mechanism strikes N. 28° W. and dips 60° SW., and suggests a larger component of strike slip than does the geologic data.
2. Fault-slip studies from the east margin of the transition zone between the Great Basin and Colorado Plateau in central Utah indicate a neotectonic(?) least compressive principal stress (σ_3) orientation at azimuth 110° - 115° . This orientation is displaced clockwise 10° - 15° from the perpendicular to the average trend of major normal faults in the surrounding portion of the transition zone. These normal faults had major displacements in Pliocene and Pleistocene time. The neotectonic(?) σ_3 is displaced clockwise 20° - 25° from an east-west σ_3 inferred for Pliocene time (ca. 4 m.y.) from dike strikes on the adjacent Colorado Plateau, and about 90° from a σ_3 orientation of inferred Miocene age deduced from slip on an areally restricted group of faults on the adjacent Colorado Plateau. A clockwise Neogene rotation of σ_3 for the eastern transition zone and adjacent Colorado Plateau in central Utah is suggested but not proven.

3. Two weeks of reconnaissance fieldwork in the Wasatch Range and literature review suggest that detailed and systematic studies of joint intensities and relative ages can provide a means for highlighting contrasts in deformational history. Such contrasts may aid in understanding how preexisting structures affect segmentation of the Wasatch Front.
4. Joints are the most ubiquitous rock structure, and record much of the brittle history of a rock mass. However, most methods used to infer the sequence of jointing are without strong foundation. A few field geologists have used, with great and productive success, methods that were developed mostly in research of ceramics. Unfortunately, their reports are not widely available. A short review by Wheeler summarizes and extends their methods, and will be submitted to a journal read by most field geologists.

Reports

Bollinger, G. A., and Wheeler, R. L., 1983a, The Charleston, South Carolina, seismogenic zone--terrane decoupling and horizontal versus vertical source geometry, in Hays, W. W., and Gori, P. L., eds., and Kitzmiller, Carla, compiler, A workshop on The 1886 Charleston, South Carolina, earthquake and its implications for today, Charleston, South Carolina, May 23-26, 1983, Proceedings: U.S. Geological Survey Open-File Report 83-843, p. 132-136.

1983b, Seismicity, tectonics, and seismic hazard in the southeastern United States, in Hays, W. W., and Gori, P. L., eds., and Kitzmiller, Carla, compiler, A workshop on The 1886 Charleston, South Carolina, earthquake and its implications for today, Charleston, South Carolina, May 23-26, 1983, Proceedings: U.S. Geological Survey Open-File Report 83-843, p. 367-370.

Wheeler, R. L., 1983a, Is South Carolina seismically active on a northwestward projection of the Blake Spur fracture zone?, in Hays, W. W., and Gori, P. L., eds., and Kitzmiller, Carla, compiler, A workshop on The 1886 Charleston, South Carolina, earthquake and its implications for today, Charleston, South Carolina, May 23-26, 1983, Proceedings: U.S. Geological Survey Open-File Report 83-843, p. 150-163.

1983b, Linesmanship and the practice of linear geo-art--Discussion: Geological Society of America Bulletin, v. 94, p. 1377-1379.

Seismological Data Processing

9930-03354

Barbara Bekins

Branch of Seismology
U.S. Geological Survey
345 Middlefield Rd. MS 977
Menlo Park, California, 94025
(415) 323-8111 ext. 2965

Investigations

Computer data processing is absolutely necessary in modern seismological research; digital seismic data can be analyzed in no other way, and problems of earthquakes and seismic wave propagation usually require numerical solution. On the other hand, the interface between computers and people usually makes data processing unnecessarily difficult. The purpose of this project is to develop and operate a simple, powerful, well human-engineered computer data processing system and to write general application programs to meet the needs of scientists in the earthquake prediction program and monitor earthquakes in northern California. This goal includes maintaining the ability to transfer data and programs over a network and the ability to share data and programs with external contractors.

Results

The PDP11-70 UNIX system has continued to operate smoothly, and performs a large amount of computing for program projects. Some current statistics:

| | |
|--------|------------------------------------|
| 194 | registered users |
| 779223 | 1024-byte disk storage blocks used |
| 110 | login sessions per weekday |

Recent events of particular importance include:

The real-time Ppicker is operating smoothly. It has been augmented with a graphics program which plots the events as they occur on a color monitor. The Unix networking capabilities have been used daily to transfer data processed by a portable Ppicker system at the University of Utah.

A program has been written to translate *BTRANS* tapes digitized on the Data General Eclipse system to a convenient format for input to the *Spires* database system at SLAC.

The Operating system has been updated to perform bad block forwarding on all disk drives. This is especially important since most of our disk storage is now of the winchester type. This means that the disk cannot be removed and reconditioned because of a few bad blocks. Instead, this software transparently replaces a bad block with another from a pool of reserved replacement blocks.

A new Vax 11/750 computer has arrived and been installed. Two 400 Mbyte winchester disks and a controller purchased from System Industries and a new tape drive with 6250 density capability have also been installed. The tape drive is dual ported to the realtime 11/44

Seismic Network processing system. A Berkeley 4.2 UNIX system is running on the Vax system and all user accounts from the 11/70 have been installed. Some major application programs have been brought over from the 11/70 including geoplot, hypo71x, and select. Arrangements with Digital Equipment Corporation, System Industries and Computer Marketing Associates have been made to transfer equipment from the 11/70 to the Vax. In addition equipment upgrades have been performed where necessary. New IMSL software for Berkeley UNIX on the Vax has been purchased.

Crustal Deformation Measurement in Alaskan Seismic Gaps:
Yakataga and the Shumagin Islands

USGS-14-08-0001-21246

Roger Bilham and John Beavan
Lamont-Doherty Geological Observatory of Columbia University
Palisades, New York 10964
(914) 359-2900

Investigations

1. Nine short (\approx 1 km) level lines are measured approximately annually within the Shumagin Islands seismic gap, Alaska. Surface tilt data are interpreted in terms of tectonic deformation at the Pacific-North American plate boundary.
2. Four sea-level gauges are operated in the Shumagins to measure vertical deformation associated with the Aleutian subduction zone.
3. A prototype pore-pressure gauge was installed on Unga Island in the Shumagins in a preliminary attempt to monitor volumetric strain changes in the region. A correlation between pore-pressure and volumetric strain is known to be high in sealed aquifers at seismic periods and poor in leaky aquifers subjected to long period strains. Correlations between pore-pressure and tidal strain, atmospheric pressure and rainfall are being investigated. (Funding by Lamont-Doherty grant.)
4. Because of the occurrence of several moderate earthquakes at the ends of the Yakataga seismic gap during the summer of 1983, the LDGO and USGS level lines at Cape Yakataga were remeasured. The opportunity was taken to level geodetically some terraces at Icy Bay in order to settle a dispute about the height of the terraces above sea-level (see Jacoby and Ulan, 1983).

Results

1. The levelling results show a steady tilt down towards the trench at about $0.6 \mu\text{rad yr}^{-1}$ between 1972 and 1983, interrupted by a tilt reversal of about $5 \mu\text{rad}$ magnitude between 1978 and 1980 (Figures 1 and 2). This is interpreted as due to a reverse slip of about 80 cm magnitude on the plate interface at \approx 20 to \approx 70 km depths between 1978 and 1980 (see Reports). The SIM and SMH lines show signals due to the February 14, 1983 earthquakes just 15 km south of Simeonof Island. The other lines are too remote to have recorded significant tilts.
2. One of the three sea-level gauges installed in June 1982 ran all year, and a second ran until April 1983. The failures were due only to exhausted batteries. Three of the four gauges installed in July 1983 are still operating (late November 1983). Several of the pressure gauges and all the electronics in the field have been recalibrated.

brated to check for zero drift, gain changes and non-linearity. The data suggest that we can measure long-term sea-level to ± 3 cm, better than we had previously anticipated. The resolution of the gauges is such that we have detected coherent waves between gauges 40 km apart with amplitudes of 0.3 mm at 28 minute periods.

3. A Paroscientific Digiquartz Depth Sensor (#8270) with a range of 0-2.7 MPa was embedded at a depth of 40 m in a 2 m section of sand within a 10 cm diameter unlined borehole. Although the borehole was partly backfilled with bentonite pellets and the 10 m lined surface section is capped, it is clear from the data that hydraulic conduits from the surface to the borehole exist that are active during heavy rain. The sensor is approximately 30 m below the water-table on the island and 203 m above sea-level. Attempts to install the sensor at a greater depth were frustrated by partial blockage of the hole during installation. Pressure and temperature data are transmitted as 12 minute averages via the GOES satellite. A tidal signal with an amplitude of about 200 Pa peak-to-peak is superimposed on longer period fluctuations lasting several weeks with amplitudes of several KPa presumably related to rainfall. The resolution of the system is approximately 1 Pa.

4. The Lamont-Doherty 2 km N25°E level line at Cape Yakataga was remeasured in July 1983. The line showed a tilt of $1.4 \pm 0.7 \mu\text{rad}$ down towards the north between 1979 and 1983. We also remeasured the USGS level network, previously measured by Prescott, Savage and others in 1974, 1975, 1979 and 1980. Our measurements were transmitted to USGS and they give tilt results consistent with those of the Lamont line (W. Prescott, pers. comm., November 1983).

References

Jacoby, G. C., and L. Ulan, Tree ring indications of uplift at Icy Cape, Alaska, related to 1899 earthquakes, J. Geophys. Res., 88, B11, 9305-9313, 1983.

Reports

Beavan, J., R. Bilham, and K. Hurst, Coherent tilt signals observed in the Shumagin Islands seismic gap (Abstract), EOS, Trans. AGU, 64, 258, 1983.

Beavan, J., R. Bilham, and K. Hurst, Coherent tilt signals observed in the Shumagin seismic gap: Detection of time-dependent subduction at depth, J. Geophys. Res., in press, 1983.

Beavan, J., E. Hauksson, K. Jacob, R. Bilham, J. Armbruster, and T. Johnson, Aseismic deformation in the Shumagin Islands seismic gap, Alaska, 5th Annual NASA Geodynamics Conference, Washington, D.C., January 24-28, 1983.

Beavan, J., E. Hauksson, S. R. McNutt, K. Jacob, and R. Bilham, Tilt and seismicity changes in the Shumagin seismic gap, Science, 222, 322-325, 1983.

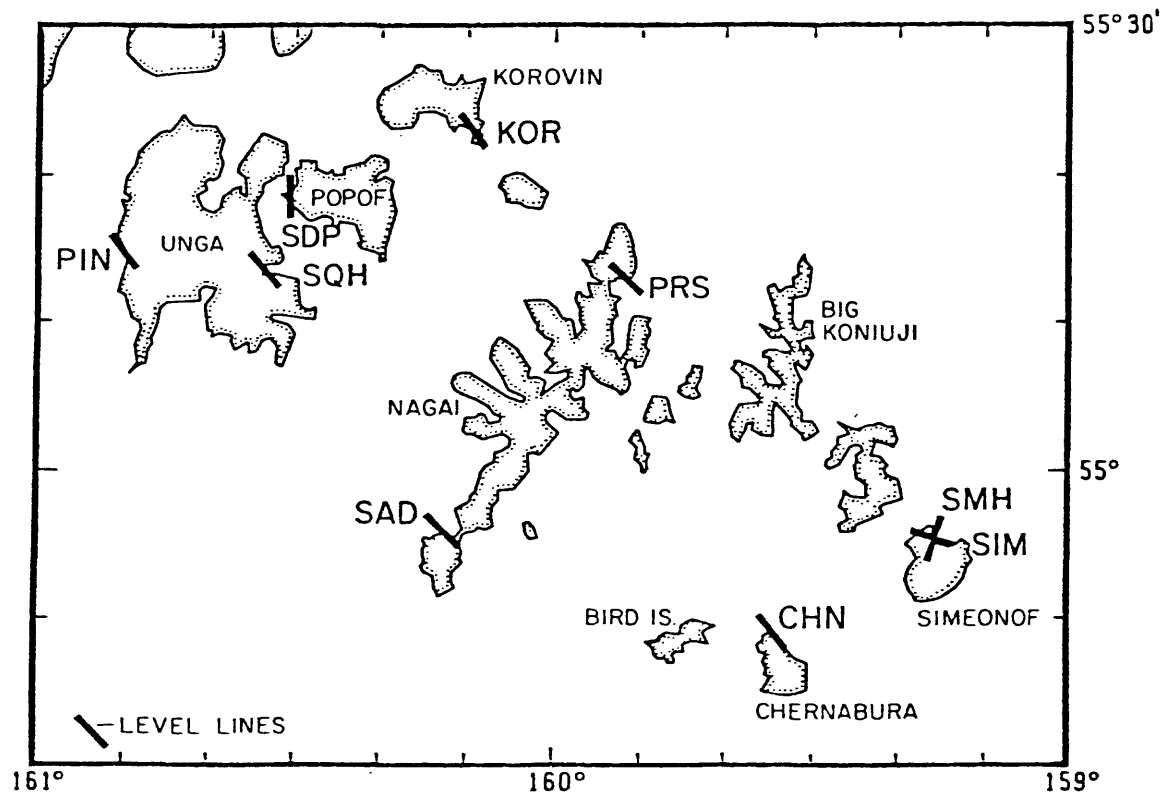


Figure 1. Locations and directions of Shumagin Island level lines.

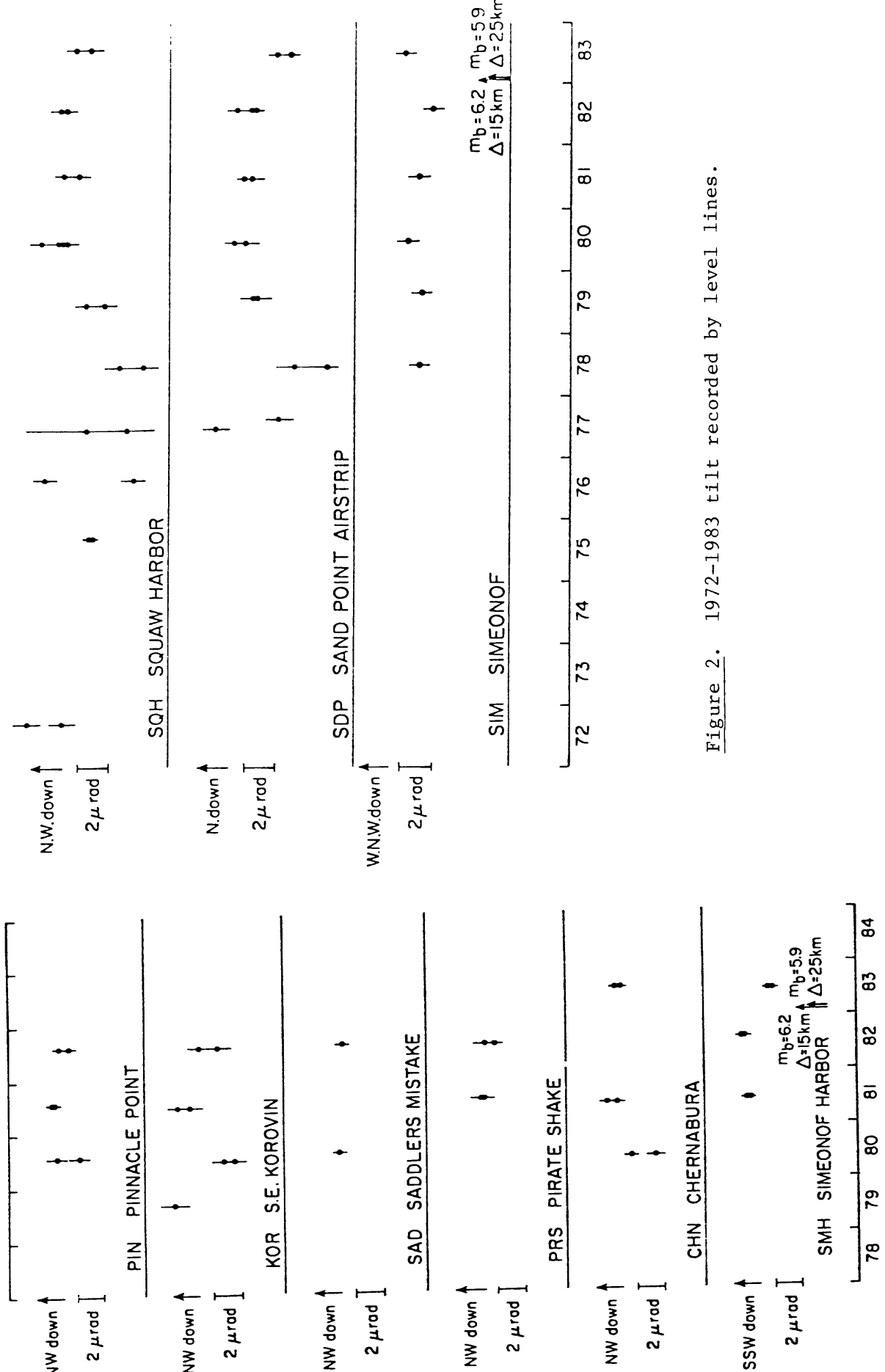


Figure 2. 1972-1983 tilt recorded by level lines.

Remote Monitoring of Source Parameters for Seismic Precursors

9920-02383

George L. Choy
Branch of Global Seismology and Geomagnetism
U.S. Geological Survey
Denver Federal Center, MS 967
Denver, Colorado 80225
(303) 234-4041

Investigations

1. Rupture process of moderate-sized earthquakes. We are applying methods of seismogram synthesis to study the rupture characteristics of the Coalinga earthquake of May 2, 1983 and the Yemen earthquake of December 13, 1982.
2. Rupture process of large earthquakes. We are applying methods of generating waveforms that incorporate source complexity to the study of the rupture process of large complex earthquakes (magnitude greater than 7.0).

Results

1. From broadband waveforms we have determined the depth, focal mechanism, moment and associated stresses of the Yemen and Coalinga earthquakes. Both events were complex ruptures. The Coalinga earthquake consisted of two events rupturing en echelon fault planes. The Yemen earthquake consisted of two events rupturing along the same fault plane. The resolution that can be achieved with broadband data indicates that in general moderate-sized earthquakes can exhibit complex behavior.
2. We have resolved the details of the large (MS 7.8) Samoa earthquake of September 1, 1981. The earthquake occurred in two stages, rupturing two separate faults in an en echelon pattern. The first stage consisted of a cluster of three events. The second stage consisted of four events linearly aligned.

Reports

Choy, G. L., 1983, Broadband body wave analysis of the complex rupture process of the Samoa earthquake of September 1, 1981: Journal of Geophysical Research, submitted.

Choy, G. L., 1984, Source parameters of the Coalinga, California earthquake of May 2, 1983 inferred from broadband body waves: U.S. Geological Survey Professional Paper, submitted.

Earth Structure and its Effects Upon Seismic Wave Propagation

9920-01736

George L. Choy
Branch of Global Seismology and Geomagnetism
U.S. Geological Survey
Denver Federal Center, MS 967
Denver, Colorado 80225
(303) 234-4041

Investigations

1. Use of body wave pulse shapes to infer earth structure. Many studies of earth structure have dismissed the effects of source finiteness and source complexity as secondary to propagation effects. We have been developing methods of generating synthetic waveforms that can incorporate the frequency-dependent effects of source directivity and multiple rupture as well as the effects of propagation through the earth. We are using these methods to examine the possible bias in determining earth structure that results from neglect of actual source functions.
2. Source parameters from GDSN data. Extract source parameters from digitally recorded data of the GDSN by determining corrections to waveforms to distinguish source effects from propagation effects.

Results

1. Detailed studies of the rupture process using broadband body waves indicates that moderate-sized earthquakes (mb between 5.8 and 6.5) can rupture in complex fashion. Besides some shallow earthquakes (the Coalinga earthquake of 2 May 1983 and the Yemen event of 13 December 1982) we have looked at 20 deep earthquakes. Only about one of every ten deep events generated simple waveforms. All other events had varying degrees of complexity.
2. After correcting broadband waveforms for propagation effects, we were able to detail source parameters for earthquakes in Samoa (September 1, 1981; MS 7.8) and Yemen (December 13, 1982; MS 6.0). Stations at distances for body waves that were diffracted, that interacted with the earth's core and that touched internal caustics provided crucial azimuthal control on the rupture processes.

Reports

- Choy, G. L., 1983, Broadband body wave analysis of the complex rupture process of the Samoa earthquake of September 1, 1981: Journal of Geophysical Research, submitted.
- Choy, G. L., 1984, FWT (Full Wave Theory) Documentation, in Documentation of Earthquake Algorithms, World Data Center A for Solid Earth Physics.

Central California Network Operations

9930-01891

Wes Hall

OFFICE OF EARTHQUAKES, VOLCANOES AND ENGINEERING
Branch of Seismology
345 Middlefield Road, Mail Stop 77
Menlo Park, California 94025
(415) 323-8111, ext. 2509

Investigations

1. Maintenance and recording of 387 seismograph stations, located in northern California, Central California and Oregon. The area covered is approximately 83,000 square miles.

Results

1. Consolidated the number of developorders from 15 machines to 10.
2. Wired 72 seismic stations to prototype RTP.
3. Completed installation of microwave equipment at Mission Peak, Fremont Peak, and Menlo Park.
4. Completed wire listings which show signal paths from all discriminator outputs to the inputs of the RTP and 1144 computer.
5. Replaced all Develco discriminators (72 each) with J110 20Hz cutoff filters.
6. Began recording dilitometers at Gold Hill.
7. Installed two new permanent stations (Ponciano Ridge and Stover Mountain).

NORTHWEST U.S. SUBDUCTION ZONE SEISMIC RISK ASSESSMENT
4-9930-03790

Thomas H. Heaton and Stephen H. Hartzell
Branch of Seismology
U.S. Geological Survey
Calif. Inst. of Technology 252-21
Pasadena, CA 91125
(818) 356-6956

Current evidence indicates a convergence rate of approximately 4 cm/yr between the Juan de Fuca and North American plates. However, there is disagreement over the degree of coupling (seismic slip/total slip) between the plates. If there is good coupling, then the area is poised for a major earthquake.

INVESTIGATIONS

1. The first phase of the work is a comparative study of subduction in the northwestern United States with other world wide subduction zones. Due to the lack of large historic earthquakes in the Pacific Northwest, the seismic risk is evaluated by drawing analogies with other subduction zones having similar characteristics. Physical parameters which are considered include; a) plate age, b) convergence rate, c) shallow seismicity, d) trench bathymetry and gravity, and e) rupture complexity.
2. Plans call for a cooperative study with Japanese scientists to look at the coastal terraces in Washington and Oregon. These terraces may offer important constraints on the size and repeat time of major subduction zone earthquakes.
3. Using the information obtained from investigations 1 and 2, the potential source characteristics are estimated for a subduction zone earthquake in the northwestern United States. These characteristics include a) fault dimensions, b) stress drop, and c) rupture heterogeneity.
4. The final phase of the project is the estimation of potential strong ground motion and tsunami hazard based on the results of the above investigations.

RESULTS

1. The young age of the subducting Juan de Fuca plate (10-15 my) is consistent with strong coupling due to the lower density and buoyancy of young crust. Other areas of the world where a young plate is being subducted include South Chile, Colombia, Alaska, Nankai Trough (S.E. Japan), and Mexico. All these areas have been the sites of

major earthquakes. On the other hand, a very young plate may have too high a temperature and too low a strength to support large earthquakes.

2. The subduction rate for Juan de Fuca appears to be 3 to 4 cm/yr which is a moderate rate on a world wide average. Higher rates of subduction also appear to increase the coupling and make a major earthquake more likely.
3. The shallow seismicity associated with the subducting plate in Washington and Oregon is very low. Typical old ocean subduction zones with low coupling such as Marianas, Tonga-Kermadec, and New Hebrides have a much higher level of small shallow earthquakes. There is some evidence that strongly coupled zones such as Chile, Colombia, Alaska, Nankai Trough, (Washington?) are characterized by quiescence.
4. Trench bathymetry and gravity for Washington and Oregon is typical of a young subduction zone and have a striking resemblance to South Chile, Alaska, and the Nankai Trough.
5. The characterization of the rupture heterogeneity is an important component of both the comparison of different subduction zones and the computation of response spectra for the Washington-Oregon area. After considering different data sets, the Caltech, 1-90 Benioff seismometer records were selected to characterize the rupture heterogeneity of large, shallow thrust earthquakes from different subduction zones. The 1-90 instrument was chosen because of its broad bandwidth and long history of operation. Records from the 63 largest, shallow, thrust earthquakes that have occurred in the circum Pacific since 1938 have been collected and their P-waves digitized. Time functions for these events have been computed using a constrained, least-squares inversion. The time functions computed resolve considerable details (variations with durations down to one second), reflecting the broad bandwidth of the instrument. These time functions show considerable variation from event to event, but there are also systematics in pulse widths and roughness between different trenches which are being evaluated.
6. Fourier power spectra have been computed for the P-wavetrains of the 63 large subduction zone earthquakes studied. These spectra yield information about the nature of the spectral scaling relationships for large earthquakes. The average spectral fall off between 30 sec and 2 sec for all the events is $\omega^{-1.5}$. This result may be adjusted following an evaluation of the effect of the free-surface reflection phase on the spectrum.
7. Using the age-rate relationship vs. maximum magnitude obtained by Ruff and Kanamori (1980), the maximum projected earthquake is 8.4 (M_w). The worst case model of good coupling everywhere with a convergence rate of 4 cm/yr and assuming the total area of the Juan de Fuca - North America convergence zone were to rupture in one event (approximately 600 km by 200 km), would produce a magnitude 9.0 (M_w) earthquake. Some data currently under evaluation, suggests that the plate boundary is segmented with different degrees of coupling on

each segment. If two segments exist, and only one ruptures at a time, the maximum magnitude earthquake is about 8.7 (M_W).

PUBLICATIONS AND REFERENCES

- Hartzell, S.H., and T.H. Heaton (1984). Estimating the source parameters for a major subduction zone earthquake in the Pacific Northwest, Earthquake Notes, vol. 55, no. 1.
- Heaton, T.H., and H. Kanamori (1984). Seismic potential associated with subduction in the northwestern United States, Bull. Seism. Soc. Am., in press.
- Ruff, L., and H. Kanamori (1980). Seismicity and the subduction process, Phys. Earth. Pl. Inter., 23, 240-252.

LOW FREQUENCY DATA NETWORK

9960-01189

J. Herriot, K. Breckenridge, S. Silverman
U.S. Geological Survey
Branch of Tectonophysics
345 Middlefield Road, MS/977
Menlo Park, California 94025
415-323-8111, ext. 2932

Investigations

1. Real-time monitoring, analysis, and interpretation of tilt, strain, creep, magnetic, and other data within the San Andreas fault system and other areas for the purpose of understanding and anticipating crustal deformation and failure.
2. Compilation and maintenance of long-term data sets free of telemetry-induced errors for each of the low frequency instruments in the network.
3. Development and implementation of graphical display systems for the purpose of monitoring seismic and surface deformation activity in real-time.
4. Installation of satellite-based telemetry system for reliable real-time reporting and archiving of crustal deformation data.

Results

1. Data from low frequency instruments in southern and central California have been collected and archived using the Low Frequency Data System. In the six months three million measurements from 125 channels have been received and subsequently transmitted on the Low Frequency 11/44 UNIX computer for archival and analysis.
2. A major effort of the project has been to provide real-time monitoring of designated suites of instruments, in particular, geographical areas. Terminals are dedicated to real-time color graphics displays of seismic data plotted in map or cross-sectional view or low frequency data plotted as a time series. During periods of high seismicity these displays are particularly helpful in watching seismic trends. This system was appreciated in the recent Morgan Hill earthquake.

3. In November Stan Silverman went to Reston to install the real-time graphics monitoring system there. Thus seismic activity at Mammoth and other active areas can now be displayed directly in Reston.
4. Work continues on a "creep alarm" system. When finished, creep events will be detected automatically as they occur and personnel can be contacted by radio pager or "beeper".
5. New software was written to improve access to the Low Frequency data set for the uninitiated. Our goal is to facilitate access to the data without requiring and special training on our tools.
6. The project continues to operate a configuration of one PDP 11/44 computer running the UNIX operating system and two PDP 11/03 running real-time data collection software. This 11/44 has been operational as our analysis machine with less than 1% down time. The two 11/03 machines operate redundantly for robustness. Accordingly, our real-time collection has had 0% down time.
7. An additional DEC PDP 11/23 computer is being added to the present configuration for the purpose of collecting satellite telemetry data. The 11/23 system is for satellite telemetry what the 11/03 systems are for telephone-based telemetry. Once fully operational the 11/23 system will be made redundant.
8. A 5-meter satellite receiver dish was installed in Menlo Park for retrieval of real-time surface deformation data from Alaska to California, even the South Pacific islands. The GOES-6 geostationary satellite together with transmit and receive stations makes possible a greatly improved telemetry system. This new system has provided enhanced data quality as well as more flexibility in locating instruments over the old telephone-based telemetry system.
9. Software has been developed to control and collect data from the newly installed ground receiving station in Menlo Park. The project has developed special purpose table-driven software which is very flexible with regard to adding and changing instrument and platform configurations while still being efficient on a small PDP 11/23 computer.
10. The data from the network have been made available to investigators in real-time. Data only minutes old can be plotted. Events such as creep events can be monitored while they are still in progress.

11. The working prediction group of the Branch has made extensive use of the timely plots which are produced routinely by the project.
12. The project continues to develop color graphics and color hardcopy capabilities for use in real-time seismic displays. Using the advanced graphics software with color graphics devices we have demonstrated our real-time seismic and low frequency data monitoring ability to visiting government officials, scientific investigators, and public interest groups.
13. In October Jim Herriot lead a four person team to install real-time seismic and related software on a PDP 11/44 computer in China for the Beijing Seismic Network.

Data Processing Section

4-9920-02217

John P. Hoffman

Branch of Global Seismology and Geomagnetism
U. S. Geological Survey
Albuquerque Seismological Laboratory
Building 10002, Kirtland AFB-East
Albuquerque, New Mexico 87115
(505) 844-4637

Investigations

1. Data Management Center for the China Digital Seismograph Network: Data processing equipment necessary to process the station tapes from the China network must be purchased, assembled, and completely tested prior to shipment. Software programs required to read the station tapes and to assemble the data into network-day tapes must be written and tested at the Albuquerque Seismological Laboratory before the hardware is shipped.
2. Data Processing for the Global Digital Seismograph Network: All of the digital data received from the global network and other contributing stations are reviewed and checked for quality.
3. Network-Day Tape Program: Data from the global network of stations are assembled into network-day tapes which are distributed to regional data centers and other Government agencies.
4. Event Detection Program: This program has been revised and upgraded, and will be used on the China Digital Seismograph Network.

Results

1. Data Management Center for the China Digital Seismograph Network: Most of the hardware for the data management center has been received at the Albuquerque Seismological Laboratory. All the necessary support equipment including the uninterruptable power supply system, tape storage racks, batteries, plus all necessary supplies, have also been received and are being organized for surface shipment to China. Export licenses for the hardware have been received, and we are awaiting approval for training the Chinese technicians in the maintenance and repair of the computer system. This training is scheduled to start in June 1984, and two of the Chinese will receive their training at the Digital Equipment Corporation in Menard, Massachusetts.
2. Data Processing for the Global Digital Seismograph Network: During the past six months, 626 digital tapes (213 SRO/ASRO, 346 DWWSSN, and 67 RSTN) from the global network and other contribution stations were edited, checked for quality, corrected when feasible, and archived at the Albuquerque Seismological Laboratory (ASL). The global network is now comprised of 11 SRO stations, 4 ASRO stations, and 15 DWWSSN stations, which comprise the Global Digital Seismograph Network (GDSN) and are supported by the ASL. In addition, there are six contributing stations which include Glen Almond, Canada, and the five RSTN stations installed and supported by Sandia National Laboratories.

3. Network-Day Tape Program: The Network-Day Tape Program is a continuing program which assembles all of the data recorded by the Global Digital Seismograph Network plus the contributing stations for a specific calendar day onto one magnetic tape. This tape includes all the necessary station parameters, calibration data, frequency response, and time correction information for each station in the network. A fourth edition of the Network-Day Tape Newsletter containing information on all of the global stations and on the Network-Day Tape was distributed in November 1983. These newsletters are published twice a year and copies are forwarded to all digital data users. A surplus PDP 11/70 computer system was received from the Defense Advanced Research Projects Agency (DARPA) and was installed in November 1983. A new version of the unit operating system has been installed in the 11/70 and the system is presently being used to process station tapes, copy network-day tapes, and for the development of new software.

4. Event Detection Program: The short period event detector algorithm that has been installed at the SRO and ASRO stations is being written in C language for implementation on the systems that will be installed in China. Murdock and Hutt presented a short paper on the algorithm at a recent symposium that was held in Albuquerque. The paper gave experiences of several investigators who have implemented the algorithm at other institutions.

Reports

1. Murdock, James N. and Charles R. Hutt, 1984, An Algorithm That Detects and Analyzes Earthquake Signals - A Fast Signal Detector and Analyzer. Sixth Annual Ideas in Science and Engineering Symposium of the Institute of Electrical and Electronic Engineers, Albuquerque, New Mexico, 5 pages.

2. Newsletter:

Hoffman, J. P., R. Buland, and M. Zirbes, Network-Day Tape Newsletter, November 1984, V. 2, No. 2, 6 pp., available from Albuquerque Seismological Laboratory, Albuquerque, New Mexico.

SEARCH FOR PRECURSORS TO EARTHQUAKES IN THE VANUATU
ISLAND ARC BY MONITORING TILT AND SEISMICITY

14-08-0001-G-822

Bryan L. Isacks
Department of Geological Sciences
Cornell University
Ithaca, NY 14853
(607)256-2307

Investigations

During the period between Oct. 1, 1983 and March 31, 1984 the network of seismograph stations and tiltmeters continued to operate in the central Vanuatu (New Hebrides) island arc. The network includes twenty seismograph stations distributed along 500 km of the arc, seven bubble-level tiltmeter stations, two periodically leveled arrays of benchmarks (1 km aperture), and a 100 m two-component long baseline water-tube tiltmeter. Our investigations include continued examination of the tilt data for possible earthquake related signals, continued development of the water-tube tiltmeter, and detailed studies of the evolving pattern of seismicity recorded by the seismograph network. The most important sequence so far captured includes three magnitude (Ms) 6 events and one magnitude 7 event. These events occurred between 1978 and 1981 in a coherent, spatially progressive sequence located between Efate and Malekula Islands.

Results

1. The six month period covered by this report was one of the quietest during the past $5\frac{1}{2}$ years. The largest shallow events within the network included four magnitude (mb) 5 events in the region of Efate Island. The three events for which we have at this point received data were not associated with particularly remarkable aftershock sequences, and produced only the usual site-related coseismic transients on the tiltmeters. The long baseline tiltmeter operated well after G. Hade's work on it during August-September, 1983. Relevelling of the Devils Point benchmark array on Efate Island in November, 1983 showed no significant tilt change, a result that continues the pattern of stability that followed the large ramp-like tilt signal that occurred during 1977-1978. That signal may have been a precursor to the 1978-1981 sequence.

2. Analysis of the seismicity data for the 1978-1981 episode was focussed on developing less subjective methods for describing the time-space development of seismicity, especially in relation to the detection of swarms and the description of the time-space evolution of aftershock sequences. With the huge numbers of events accumulating, the standard dot plots of epicenters are not able to show effectively the very intense and spatially concentrated zones of seismicity that have emerged. In general the dot plots give only a very qualitative, low dynamic range indication of the seismicity pattern. Counting events within a temporal and spatial grid is particularly amenable to computation and graphical output with a computer. With a gridding system we have established an average spatial pattern of seismicity against which swarm or aftershock activity can be more objectively detected. Reanalysis of

the spatially expanding aftershock zones of the 1978-1981 events, done in a less subjective fashion than before, shows that although the spatial expansion remains a characteristic feature, it appears to be more a secondary peripheral diffusion of seismicity than a major expansion of the rupture zone. More striking in the aftershock sequences is the very coherent sequential activation and reactivation of specific small epicentral areas. These areas are also activated in swarms and foreshock sequences, and probably represent specific structural features of the interplate boundary that may produce spatial heterogeneity in stress accumulation and in the ratio of seismic versus aseismic interplate slippage.

Another clear result for the Efate region is that the swarms, aftershock sequences and inferred rupture zones of the larger events tend to occur in the shallow part of the interplate boundary, while a more continuous background level of seismicity is characteristic of the deeper part of the interplate boundary and adjacent parts of the interacting plates. This down-dip seismicity may reflect creep along the plate boundary below a shallower level of seismic stick-slip behavior.

3. Detailed study of the spatial distribution and focal mechanisms of hypocenters beneath southern Malekula Island, in the area of a possible major gap along the arc, shows a volume of seismicity around the interplate boundary with complex spatially variable focal mechanism orientations. Previous analysis based on HYPO71 locations has been redone with HYPOINVERSE. Refined determinations of the Vp/Vs ratios, study of the precision of relative locations, and study of the effect of velocity models on focal mechanism determination have been done. The complexities in the seismicity beneath southern Malekula, suggestive of a "locked" segment of the plate boundary, remain.

Reports

Marthelot, J.-M., J.-L. Chatelain, B.L. Isacks, R.K. Cardwell, and E. Coudert, "Seismicity and Attenuation in the Central Vanuatu (New Hebrides) Islands: A New Interpretation of the Effect of Subducting the D'Entre-casteaux Fracture Zone", submitted to J. Geophys. Res., 1984.

Analysis of Seismic Data from the Shumagin Seismic Gap, Alaska

USGS-14-08-0001-21299

Klaus H. Jacob

Lamont-Doherty Geological Observatory of Columbia University
Palisades, New York 10964
(914) 359-2900Investigations

Digitally recorded seismic data from the Shumagin seismic gap in the eastern Aleutian arc, Alaska, are analyzed for detecting space-time variations in seismicity, focal mechanisms, and of dynamic faulting parameters that could be precursory to a major earthquake expected in this seismic gap. The seismic results obtained from the network data are being integrated with crustal deformation data that are independently collected, with volcanicity data of nearby Aleutian volcanoes, and with teleseismic information, to identify basic tectonic processes which may be potentially precursory to a great earthquake.

Results

1. Conditional Long-Term Probabilities. An analysis of the recurrence periods of historic earthquakes in the Aleutian arc (Jacob, 1984) has been completed and allows estimates of the basic conditional long-term probabilities for great earthquakes ($M_w \geq 7.8$) in the Shumagin seismic gap and all other major plate boundary segments of the Aleutian arc between 164°E and 140°W, including three other potential seismic gaps in the Yakataga, Unalaska and Kommandorski segments. Results indicate (Figure 1) that for the 20-year period 1983 to 2003 the Shumagin Gap has a 30 to 99% conditional probability to rupture in one or several great earthquakes. This is one of the highest known probability levels for future great earthquakes anywhere in the U.S. Long-term probabilities for the Yakataga, Unalaska (less certain), and Kommandorski Islands seismic gaps are only slightly less than that of the Shumagins, but are much higher (i.e., >30%) than for arc segments that broke more recently in 1965, 1964 and 1957 in which the conditional probabilities for great earthquakes during the same time period (1983-2003) measure all less than 20%. The large uncertainty margin (e.g., 30 to 99% for the Shumagins) stems from the relatively short historic record of Aleutian seismicity (<~200 years) and from the uncertainty whether recurrence periods are normally, log-normally or statistically otherwise distributed.

2. Seismicity Patterns. The seismicity patterns earlier detected (see Beavan et al., 1983; Hauksson et al., 1984) are essentially confirmed by recent analyses and show the following features: (a) Network data (Figure 2) yield relatively high levels of seismicity near the down-dip end of the main thrust zone (~40 km). Below that depth intra-plate seismicity in the dipping plate is moderately high to depths of ~100 km, and above that depth (40 to 0 km) moderately high activity is concentrated on a steeply dipping feature above the

'aseismic front' that cuts through the overriding plate (near the center of section C-C', Figure 2). The shallow portion of the gently dipping main thrust zone located between the 'aseismic front' and the trench remains relatively quiescent. (b) The long-term teleseismic pattern for the period 1963 to 1983 (Figure 3) conforms to that seen by the network data. It may be loosely described as resembling an often quoted 'doughnut-pattern', although the pattern is only more or less developed depending on the cut-off level of the magnitudes considered. (c) The previously reported coincidence in 1978 to 1980 of a reversal in crustal tilt, rise in overall network seismicity rates, and lack of volcanicity of Pavlof Volcano with a deep-seated (30-80 km), mostly aseismic slip event (of \approx 80 cm amplitude; Beavan et al., 1983), has now been shown to also coincide with a clustering of unusual seismicity at depth ($>$ 100 km) within the descending slab directly beneath Pavlof Volcano which remained volcanically quiescent at the time of the deep seismicity (Figure 4). In addition, focal mechanisms in the descending slab at depth from about 40 to 100 km reversed polarity thus indicating a temporal reversal of slab stresses during the anomalous slip event. The slip event at depth is believed to have brought the shallow unbroken thrust zone closer to failure.

References

- Beavan, J., E. Hauksson, S.R. McNutt, R. Bilham, and K.H. Jacob, Tilt and seismicity changes in the Shumagin seismic gap, Science, 222, 322-325, 1983.
- Hauksson, E., J. Armbruster, and S. Dobbs, Seismicity patterns (1963-1983) as stress indicators in the Shumagin seismic gap, Alaska, Bull. Seismol. Soc. Am., in press, 1984.
- Jacob, K., Estimates of long-term probabilities for future great earthquakes in the Aleutians, Geophys. Res. Lett., 11, no. 4, in press, 1984.

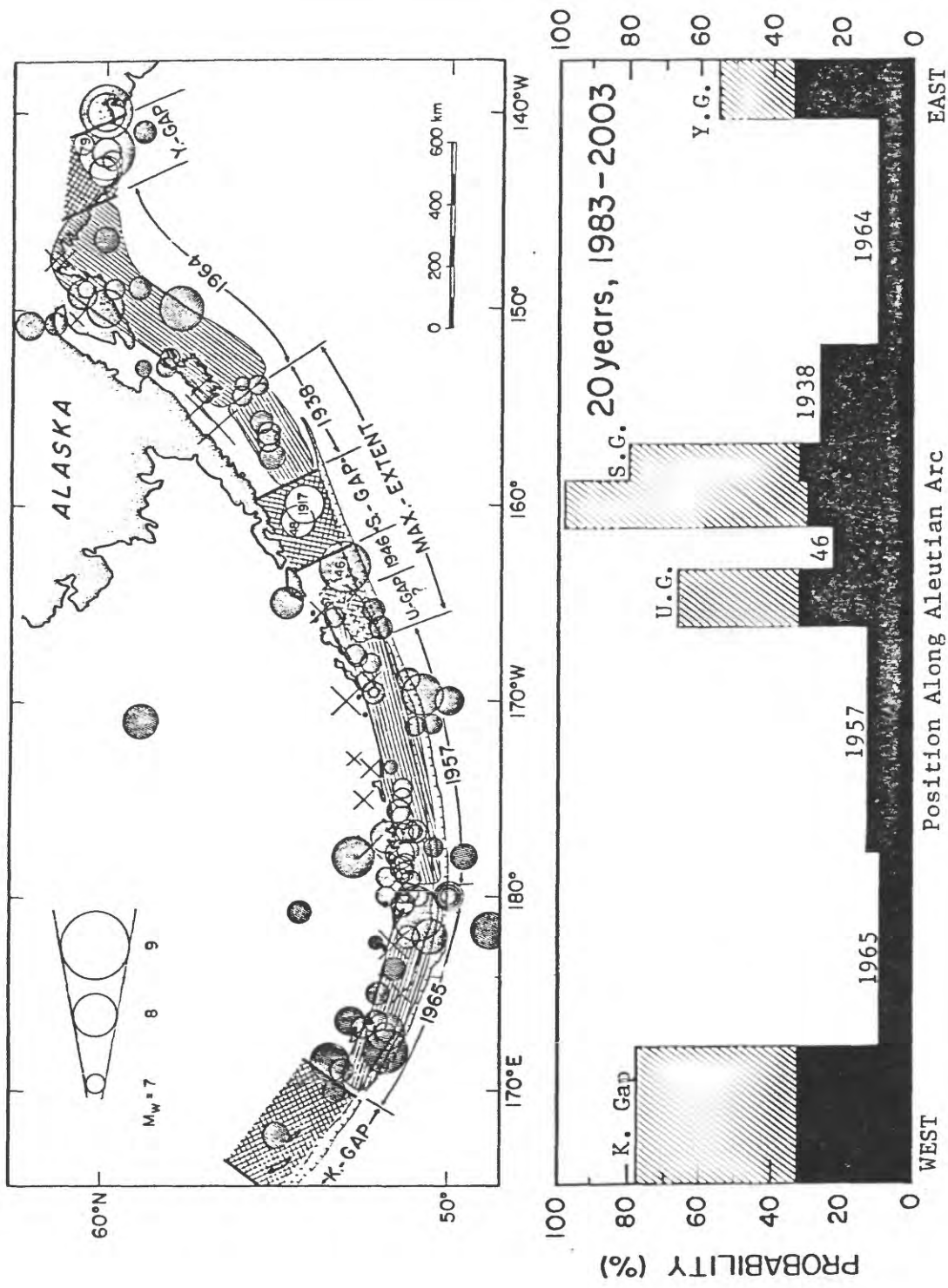


Figure 1. Top: New compilation of large ($M > 7$) earthquakes since 1898, recent great rupture zones, and seismic gaps. Bottom: Probability for a great ($M > 8$) earthquake to occur in the next 20 years (1983-2003) as a function of position along arc. Hatching indicates values for normally distributed, and solid symbols, those for log-normally distributed recurrence periods (Jacob, 1984).

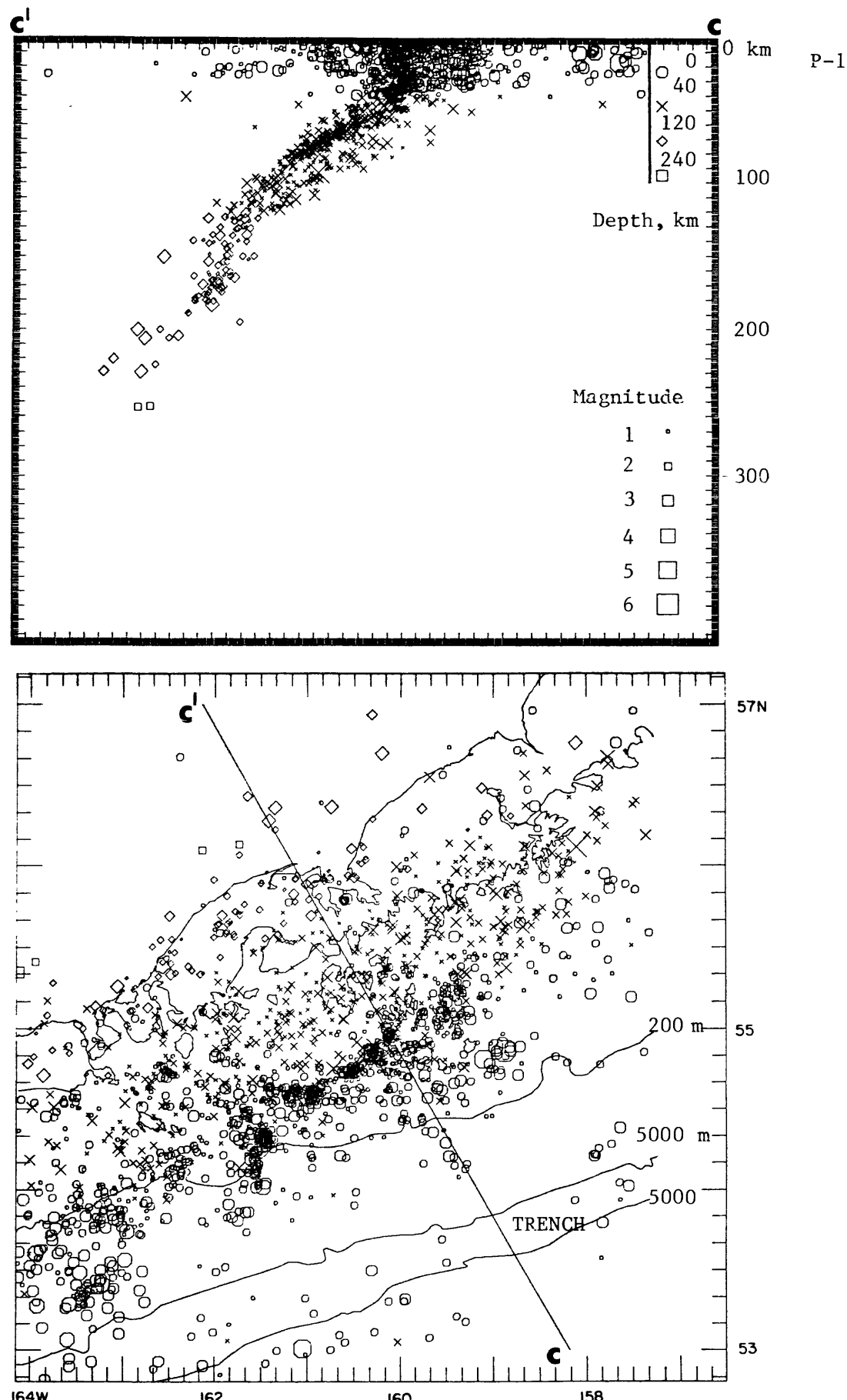


Figure 2. Recent seismicity (1979.0 to 1983.6) located by the Shumagin seismic network in profile (top) and map view (bottom). No vertical exaggeration in profile.

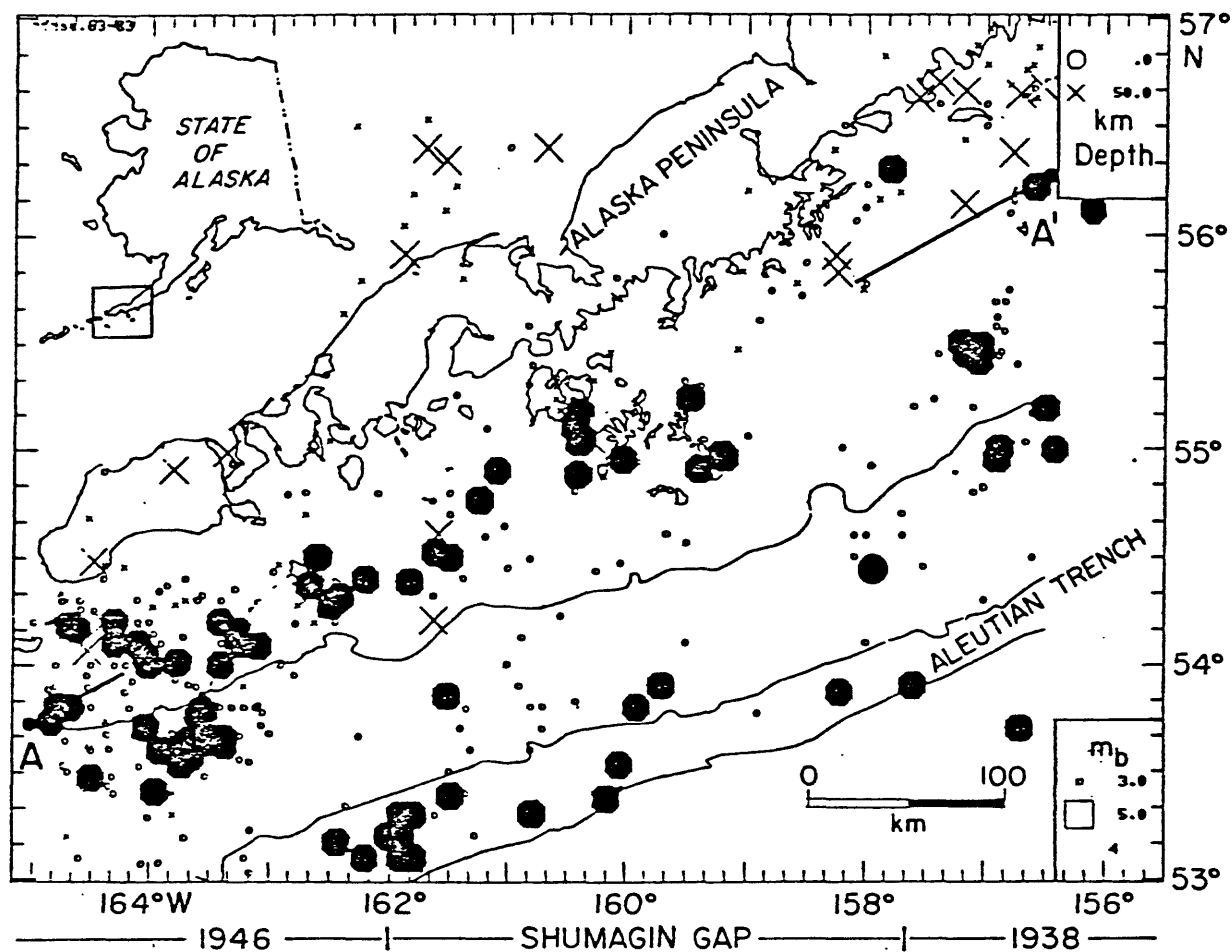


Figure 3. Teleseismic seismicity (from NOAA and PDE files) for the Shumagin Islands region from 1963-1983. Shallow earthquakes (depth \leq 50 km) of m_b $>$ 5.0 are shown as large black symbols and smaller earthquakes (m_b \leq 5.0) are shown as open symbols. A high level of earthquake activity surrounds the main thrust zone.

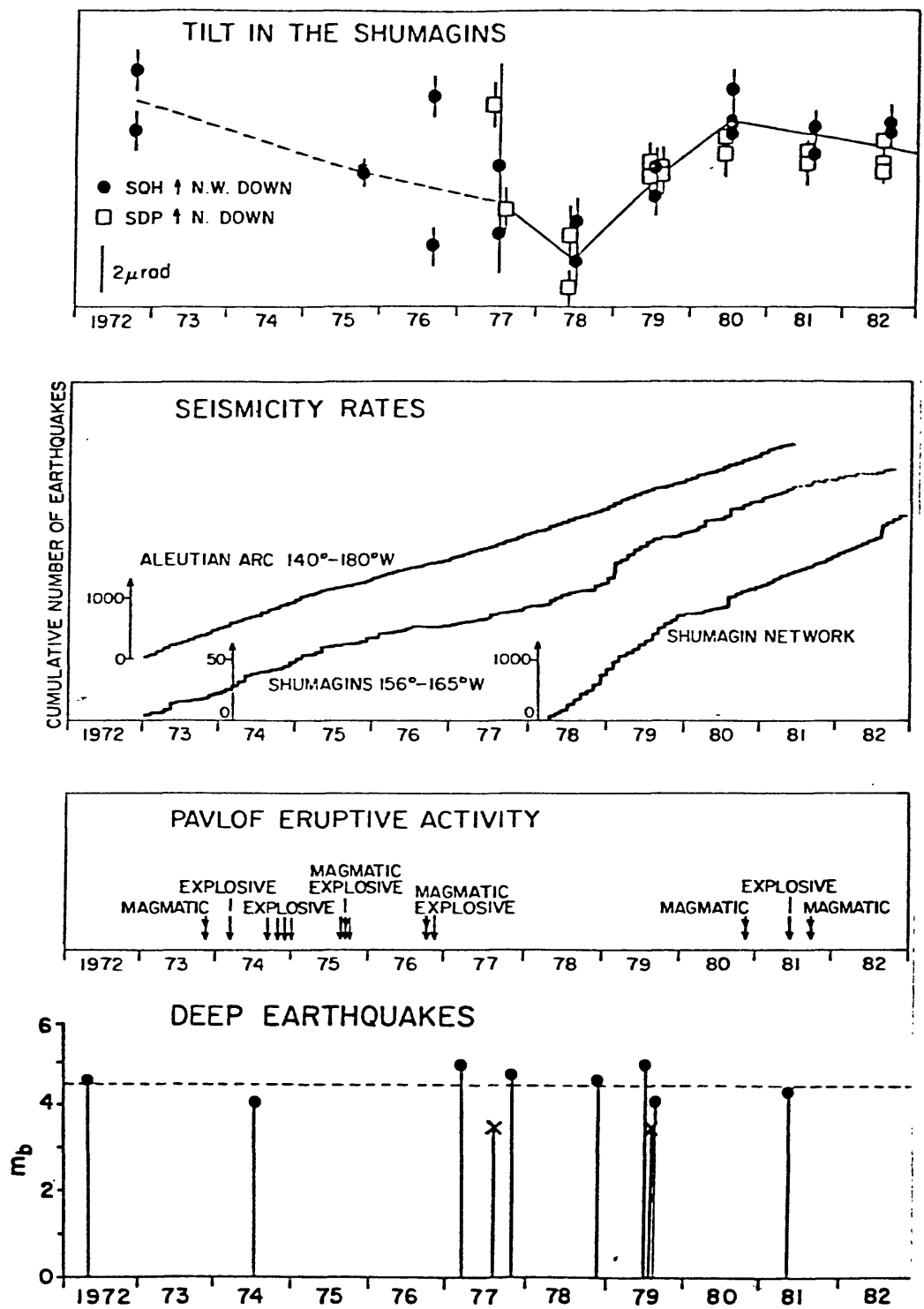


Figure 4. Comparison of (a) tilt, (b) seismicity rates, (c) eruptivity of Pavlof Volcano, and (d) occurrence of deep earthquakes in the Shumagins versus time. Note the erratic behavior between about 1977 and 1980 of virtually all quantities monitored in the Shumagins only.

Socorro Magma Bodies

4-9920-03379

Lawrence H. Jaksha
 Branch of Global Seismology and Geomagnetism
 U.S. Geological Survey
 Albuquerque Seismological Laboratory
 Building 10002, Kirtland AFB-East
 Albuquerque, New Mexico 87115
 (505) 844-4637

Investigations

1. Albuquerque Basin Seismicity
2. San Acacia Earthquake
3. Source Parameters
4. Q
5. Crustal Structure
6. Instrumentation

Results

1. The last two widely felt earthquakes in Albuquerque occurred on November 28, 1970, and January 4, 1971. These events have been reanalyzed with the following results: The two earthquakes occurred in almost the same place; the epicentral distance is 25.3 km from station ALQ for the November 28 shock and 25.5 km for the January 4 shock. The epicenters are at 35.1 N, 106.7 W. A composite fault plane solution suggests strike-slip faulting on a fault striking N20°E and dipping 60°W. The fault plane solution is not well constrained.

A first draft of a report summarizing USGS seismicity studies near Albuquerque is being drafted.

2. Steve Jarpe has completed his analysis of the M_L 4.0 earthquake that occurred near San Acacia in March 1983. The earthquake sequence contained about 300 shocks in the three-week study period. Well located earthquakes had focal depths between 5 and 8 km. The 30 best hypocenter locations define a planar area striking NNW and dipping 50°NE. This plane is in good agreement with the fault plane solution for the main shock, which suggested normal faulting on a generally N-S striking fault. The entire sequence was located in the center of surface uplift defined by level-line data.

3. John Ake is studying 2 earthquake swarms (> 700 events that were observed near Socorro in 1983. Cross correlation of P-phase wave forms for events up to magnitude 1.2 reveal duplicate phases. The first zero crossing is constant at 0.36 ± 0.003 . This observation will allow calculations for rupture duration, source radius, and stress drop for earthquakes in the swarm with magnitudes above 1.2.

4. Phil Carpenter has determined apparent Q for upper crustal rocks near Socorro by studying the spectra of ~ 400 digitally recorded earthquakes in the magnitude range -0.8 to 1.2. He found Q values of less than 50 for most Phanerozoic rock sections. The average Q's for the Socorro area is greater than 500; but localized zones of lower Q, possibly related to magmatic intrusions, were located.

5. Our paper summarizing crustal structure in northwestern New Mexico was revised after review by the B.S.S.A. and was accepted for publication.

A feasibility study for determining crustal structure along a line between Datil, New Mexico, and Flagstaff, Arizona, using explosions as energy sources is being done. A field trip to locate prospective sites and arrange for timing shots in coal and copper mines is planned for this summer.

6. In October, field recording units were deployed for large explosions at White Sands Missile Range and Kirtland Air Force Base.

In January, field recorders were installed at and around Gran Quivira National Monument to monitor a micro-earthquake swarm.

During February and March, a series of 1,000 lb. bombs were exploded underground at Kirtland Air Force Base. We recorded the shots along a 25 km long line in the Rio Grande rift.

Reports

1. Jaksha, L. H., and Evans, D. H., 1984, Reconnaissance Seismic Refraction - Reflection Studies in Northwestern New Mexico, Bulletin of the Seismological Society of America, (in press).
2. Wong, I.G., Cash, D. J., and Jaksha, L. H., 1984, The Crownpoint, New Mexico, Earthquakes of 1976 and 1977, Bulletin of the Seismological Society of America, (in review).

Instrument Development and Quality Control

9930-01726

E. Gray Jensen
Branch of Seismology
U.S. Geological Survey
345 Middlefield Road - MS 977
Menlo Park, California 94025
(415) 323-8111, ext. 2050

Investigations

This project supports other projects in the Office of Earthquakes, Volcanoes, and Engineering by designing and developing new instrumentation and by evaluating and improving existing equipment in order to maintain high quality in the data acquired by the Office. During this period some personnel from this project were assigned to other projects on a part-time basis.

Results

With the assistance of this project the first two links of microwave transmission system for seismic telemetry has been installed. These links from Fremont Peak to Monument Peak and from Monument Peak to our Menlo Park office are currently operational and should soon be carrying seismic data. This project also participated in the preparation, testing and installation of an automatic seismic network event digitizing system employing a PDP 11/44 computer in the People's Republic of China. In addition a time comparison circuit has been designed which will allow portable seismic event recorders in the PRC to be synchronized with radio time.

A member of this project traveled to Guatemala to reestablish and rehabilitate a seismic network consisting of about 20 stations. Following the Idaho earthquake support in the form of deployment or maintenance was provided for the GEOS, 5-day and Seismic Cassette Recorders. Testing and evaluation of various types of timing and positioning systems including Omega, Loran-C and Transit satellite systems has been performed to determine suitability seismic field use.

A circuit for measuring and displaying time difference of IRIG-E and WWVB time codes on 5-day tape playback equipment was designed and is operating well. A special, stable VCO was installed at the Gold Hill dilatometer site to allow telemetry of very long period data. Technical assistance has been provided in selecting and acquiring HF radio communications equipment for use in the Mammoth Lakes area. Emergency generator backup power is now installed on the RTP as well as the Low Frequency Telemetry computer.

An Ethernet system has been installed which allows communication between Office VAX computers and will soon be connected to systems

outside the Office. In addition numerous terminal lines and port connections have been added. Ongoing maintenance has been performed for the Seismic Cassette Recorders, radon equipment, film digitizers and various other equipment. During this period 200 discriminators were tuned and tested, 100 radio units were repaired and 80 seismometers were calibrated.

Southern California Cooperative Seismic Network

4-9930-01174

Carl Johnson
Branch of Seismology
U.S. Geological Survey
Seismological Laboratory 252-21
Pasadena, California 91125
(818) 356-6957

Investigations

1. Operation and maintenance of the southern California seismic network continued through the reporting period without significant failure. At present 248 instruments are telemetered to Caltech for analysis including two new stations (CBK and CMPV).
2. Routine processing using stations of the southern California cooperative seismic network was continued for the period October through March 1983. Routine analysis includes the timing of phases, event location and preliminary catalog production using the newly developed CUSP analysis system.
3. We model the performance of a hypothetical system to provide short-term warning (less than several minutes) of imminent strong ground motion from significant earthquakes. In large earthquakes of great rupture length, significant damage often occurs at large distances from the epicenter. It is theoretically possible to construct a system that would almost instantaneously detect the occurrence of strong ground motion in the epicentral area of significant earthquakes. This information would then be broadcast to areas that may be strongly shaken when seismic energy propagates to them. Automated safety responses could then be initiated before the occurrence of strong shaking. For example, there is evidence that the great 1857 California earthquake initiated in the vicinity of Parkfield which is located 275 km northwest of metropolitan Los Angeles. Thus, significant shaking in the Los Angeles region probably did not occur for at least a minute after the origin time of the earthquake. We compute the distribution of warning time as a function of the severity of ground shaking from a hypothetical collection of earthquakes having a normal magnitude-frequency relationship.

Results

1. The CUSP off-line network processing software used by C.I.T. for routine processing was expanded to include the creation of ASCII formatted card image monthly phase tapes (access tapes).
2. We conclude that significant warning times are likely for areas that

are strongly shaken in very large earthquakes. However, we find that relatively frequent, short-rupture length, moderate-sized earthquakes are the most likely origin of ground acceleration levels of about 0.2 G. Thus, of the areas to receive this level of shaking, less than 50% can expect warning times of great than 5 seconds. However, large areas of very strong shaking, are only produced by very large earthquakes. Of the area expected to experience ground accelerations of 0.6 G, at least 50% can expect a warning time of over 20 seconds.

Publications

Heaton, T.H., and S.H. Hartzell (1984). Modeling the warning times produced by a hypothetical seismic early warning system, Earthquake Notes, vol. 55, No. 1.

SEISMIC PARAMETERS OF THE ARKANSAS EARTHQUAKE SWARM

14-08-0001-21245

A. C. Johnston and A. G. Metzger
 Tennessee Earthquake Information Center
 Memphis State University
 Memphis, TN 38152
 (901)-454-2007

INVESTIGATIONS AND RESULTS

The Arkansas swarm began on January 12, 1982, close to the town of Enola, Arkansas, about 50 km north of Little Rock, and approximately 165 km southwest of the New Madrid seismic zone. Over 30,000 earthquakes have been recorded by the Tennessee Earthquake Information Center's (TEIC) temporary seismic network since the swarm initiated, and activity continues to the present. In this project we concentrated on a detailed study of the 88 events digitally recorded during a period from June 24 to July 5, 1982, in a cooperative project of TEIC and USGS. From the seismic data alone we are not able to answer the question of why and how the Arkansas swarm began. However, several points of interest have been developed in this preliminary analysis.

(a). The source volume of the swarm is small, about 45 km^3 . The episodic nature of swarm activity indicates a periodic and very localized accumulation and relaxation of stress within small volumes inside the source zone. It seems unlikely that this region is a candidate for a major earthquake (e.g. magnitude 6.0 or greater) because of the small source volume, the inferred highly fractured nature of the source volume, and the shallow depth of the swarm.

(b). The V_p/V_s ratios of the 88 events determined from Wadati plots fluctuate in a range from as low as 1.59 to as high as 1.78 (and nearly 1.90 for individual ray paths). Most of the best determined V_p/V_s values fall around 1.67 to 1.70, which is lower than the 1.78 recommended in HYP071 (Lee and Lahr, 1975) and the 1.73 representative of Poissonian solids. Also the V_p/V_s values show very clear spatial and temporal variations during this 12-day period. The introduction of open fractures into previously competent material decreases the V_p/V_s ratio. Because of the great number of microearthquakes during the past two years ($>30,000$ in a 45 km^3 volume or roughly a "density" of >650 earthquakes/ km^3) we expect that the rock of the swarm source volume must be highly fractured. If a highly fractured region were saturated with less rigid materials such as water or even magma an increased V_p/V_s would result. Closing of pre-existing cracks also would increase V_p/V_s . We conclude from the high V_p/V_s variability in the Enola region that extensive fracturing is present, and these cracks can either close or resaturate on a very short time scale (hours).

(c). Anomalous negative P and S travel time residuals are found along the path immediately north of the center of the swarm toward the station MHC about one day prior to the major 3.8 event. Also V_p/V_s for this path increases to 1.80-1.90 during this period. The negative travel time residuals indicate that both P and S waves are traveling faster toward station MHC than to all the other stations. Therefore we suggest that a small region of anomalous seismic wave velocities must have formed about one day before the 3.8 event at shallow depth (probably less than 4 km) very close to station MHC.

This anomalous zone is located in the compressional quadrant of the focal mechanism for the anomalous events (mechanisms 4,5,6,7, Fig. 1). Local re-orientation of the prevailing NE-SW compressive stress in this region may result from the seismic strain induced by nearby earthquake sequences or perhaps by the strain build up for the impending M3.8 event. The stress re-orientation causes cracks to close in the anomalous zone; therefore seismic wave velocities increase dramatically. The process of concentration and relaxation of the stress field may repeat and migrate throughout the swarm region resulting in the episodic sequences of swarm activity. The observations presented here are strictly qualitative and short term. We are not able to answer whether the velocity variations observed for this sequence are typical for the swarm area or unique for the time period we analyzed.

(d). Two strong secondary arrivals are clear, especially on seismograms recorded at MHC. These secondary arrivals can be seen most clearly on the vertical component seismograms and sometimes even show larger amplitude than the first P arrival. They are very easily misidentified as S arrivals if only vertical component seismograms are available. Four inferences that can be drawn from the study of these two secondary arrivals are listed below. (1). The fact that these two secondary arrivals are most prominent on vertical component seismograms suggests that they must be P waves. (2). That their amplitudes are sometimes larger than the first P arrival indicates that they are not reflected P waves. (3). The epicentral distances to station MHC (from 2 to 4 km) are in general less than the focal depths (from 4 to 7 km), which suggest that these two arrivals are not refracted waves from horizontal layer interfaces. (4). The steeply incident ray paths from earthquakes to MHC eliminate the possibility that seismic phase conversion can occur at the horizontal interfaces between the layers above the hypocenters. Study of the nature of these two arrivals is still under investigation. However, it is clear that they must be S to P converted phases from two deep discontinuities.

(e). The hypocenters clustered tightly as earthquake sequences and migrated within a volume of about 45 km³ as the activity developed during this 12-day period. Composite focal mechanisms for groups of earthquakes closely related in time and space all indicate predominantly strike-slip faulting on NNE or ESE fault planes (see Figure). These focal mechanisms yield stress axis orientation consistent with those obtained in the New Madrid seismic zone (e.g. Herrmann and Canas, 1978) about 165 km to the northeast. Thus the Arkansas swarm region is subject to a similar stress regime as the nearby New Madrid zone; however, the two zones are unrelated in terms of geologic crustal structure. No surface faulting was reported in the swarm region. Focal depths of the 88 events presented in this study range from 4 km to 7 km, which extends from the lower sedimentary layers into the basement rock.

REPORTS AND PUBLICATIONS

A summary of the early phases of this project may be found in USGS Open-File Report 83-918, 1983.

Chiu, J.M., A.C. Johnston, A.G. Metzger, L.Haar and J. Fletcher, Analysis of Analog and Digital Records of the 1982 Arkansas Earthquake Swarm, accepted for publication, Bull. Seismo. Soc. Amer., 1984.

Gracey, G.D., J.M. Chiu, and A.C. Johnston (1984). Focal Mechanism and Seismic Wave Velocity Studies of the Arkansas Earthquake Swarm, EOS Trans. Amer. Geophys. Union (abstr.), 65, 16, p. 241.

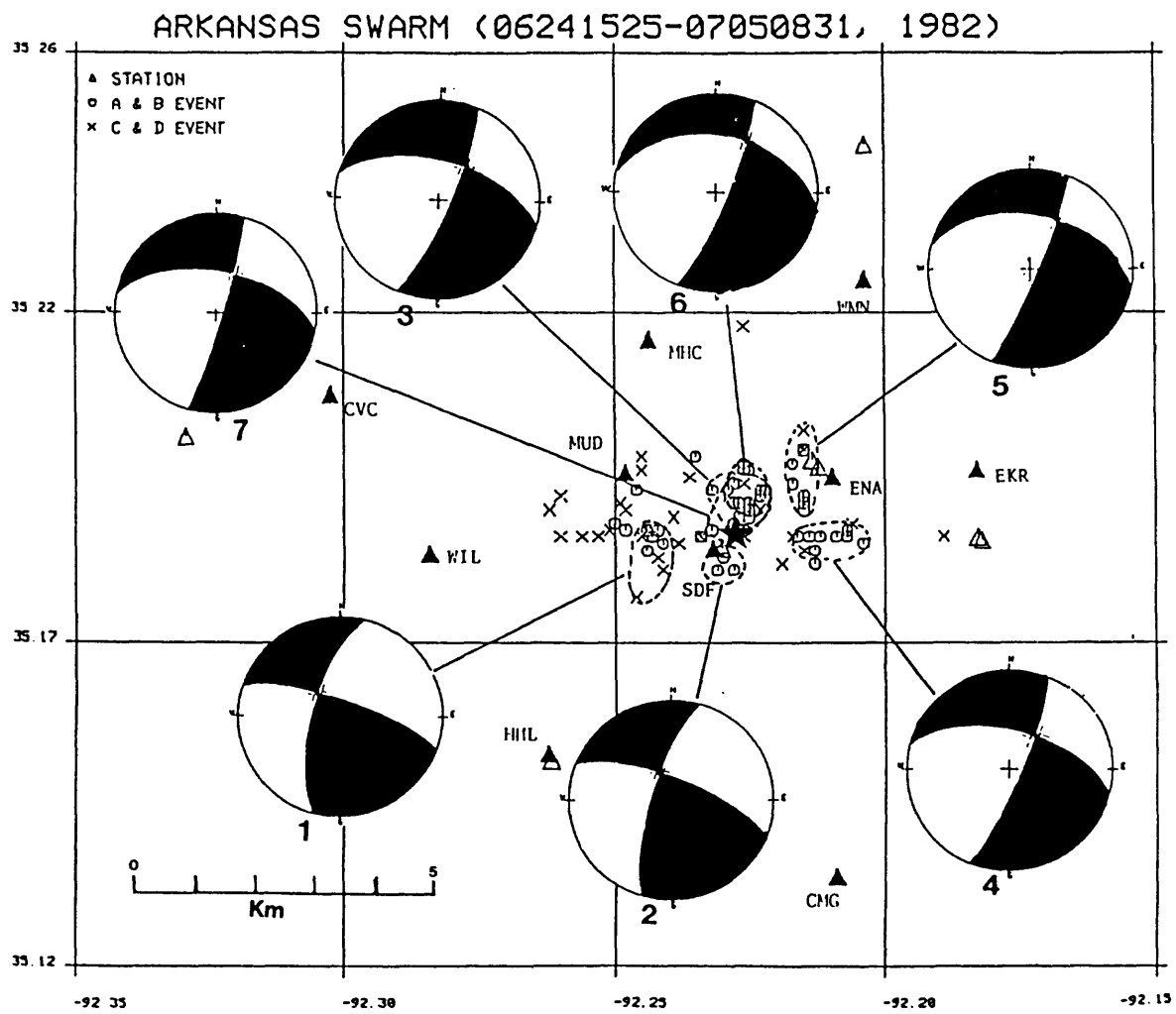


Figure 1. Summary of the composite focal mechanism for seven group of events that occurred during a period from June 24 to July 5, 1982 in the Arkansas swarm region.

TILT, STRAIN, AND MAGNETIC MEASUREMENTS

9960-02114

M.J.S. Johnston, R. Mueller, C. Mortensen
D. Myren, A. Jones and V. Keller
Branch of Tectonophysics
U.S. Geological Survey
345 Middlefield Road, MS/77
Menlo Park, California 94025
(415) 323-8111, ext. 2132

Investigations

1. To investigate the mechanics of failure of crustal materials using deephole and surface strainmeters, tiltmeters and arrays of absolute magnetometers.
2. To investigate real-time records of these and other parameters for indications of incipient failure of the earth's crust.

Results

1. Surface observations of aseismic fault displacement (fault creep) exhibit episodic behavior (creep events) whose sources are typically limited in extent and complex in character. Strain, tilt and displacement data obtained near and across the fault segments where these events are occurring indicate that they are triggered by deeper slip of longer duration. The apparent rupture velocities obtained by replicating the strain data with simple quasistatic models of the deep creep are about 1 km/day or less. These are much slower than the inferred slip or rupture velocities obtained from creep onset times at adjacent creepmeters and could explain the general correspondence over periods of months between higher than normal average creep and higher rates of bution episodes with timescales of several weeks resulting from deep creep is easily detected with small 2-dimensional arrays of low-noise borehole strainmeters or from continuous cross-fault displacement data at 0.01 ppm sensitivity on 1 to 5 km lines. Routine detection and quantification of these episodes could allow prediction of related moderate magnitude earthquakes, at least in the creeping/locked transition zones at Parkfield and San Juan Bautista on the San Andreas fault.
2. Magnetic fields were recorded at five sites on Mt. St. Helens over a 20 day period, which included a dome

extrusion-eruption of the volcano. Two of the magnetometers located in the crater measured reversible magnetic changes, which correspond to fluctuations in tilt measured nearby. However, the correlation is highly nonlinear. Electric fields were measured on the east flank of the volcano near its summit to search for electrokinetic effects. They show no correlation with the magnetic changes and in the long term are uncorrelated with eruptive activity. Our favoured interpretation of the magnetic changes is that they result from piezomagnetic changes in the magnetization of the volcano induced by eruption stresses. Their reversibility rules out pressure induced magnetization as the dominant mechanism and places an upper limit of $\sigma \sim 300$ bars on the stresses. The limited spatial extent of the magnetic anomaly field places the source of stress at shallow depth beneath the crater floor consistent with models based on strain data.

3. Seven to ten years of data from a large magnetometer array throughout central and southern California is used to define the characteristics of secular variation of the earth's geomagnetic field across this zone. During this period, a well determined rate of secular variation can be obtained at each location by simple linear least-square fits to the data but these rates vary from site to site. Least-square surface fits to the rate data indicates secular variation decreases in a general south-easterly direction from -45.0 nT/a near San Francisco to -54.0 nT/a near the Mexican border. Deviations of as much as 1.0 nT/yr occur on scales of a few tens of kilometers. This results from differences in local induction and remanent magnetization and may be corrected by determination of a site transfer function. When compared with IGRF and other techniques for predicting secular variation at this location, discrepancies in both amplitude and mean isogram directions of 10 nT/a and 30° , respectively, occur. Correction for site response appears necessary at observations where local magnetization response can bias estimates of secular variation.
4. In an attempt to observe magnetic events related to changes in crustal stress, the U.S. Geological Survey has operated a network of proton magnetometers (PMs) near active faults in California for the past decade. We present different data taken simultaneously using self-calibrating rubidium magnetometers (SCRs) and PMs colocated at two of these sites. Over a 13-km baseline the SCR data are up to a factor of 10 quieter for periods less than one hour, but the PM and SCR data are both dominated by external geomagnetic noise for longer periods. In Colorado, SCR data were observed on a 13-km baseline and were processed using a

noise reduction technique. For periods longer than one hour, the residuals were a factor of four quieter than the USGS PM instrument noise levels. A comparison of SCR and PM differences over a short baseline shows that the SCR differences are 30 dB quieter than the PM instrument noise level for periods less than one hour. These results indicate that the detection threshold for typical USGS PM data is significantly limited by instrument noise in California for periods ranging up to one hour, and for longer periods in Colorado.

Reports

- (P) Davis, P. M., and Johnston, M. J. S., 1983, Localized geomagnetic Field Changes Near Active Faults in California 1974-1980: *Journal of Geophysical Research*, v. 88, 9452-9460.
- (P) Davis, P. M., Pierce, D. R., McPherron, R. L., Dzurisin, D., Murray, T., Johnston, M. J. S., and Mueller, R. J., 1984, A Volcano-Magnetic Observation on Mount St. Helens, Washington: *Geophysical Research Letters*, v. 11, 225-229.
- (P) Johnston, M. J. S., Mueller, R. J., Ware, R., and Davis, P. M., 1983, Precision of Magnetic Measurements in a Tectonically Active Region: *Journal of Geomagnetism and Geoelectricity* [in press].
- (O) Dvorak, J., Okamura, A. T., Johnston, M. J. S., Mortensen, C. E., Mueller, R. J., and Furukawa, 1983, Tiltmeter and Magnetometer Measurements of Mt. St. Helens, Washington: 1980-1981: U.S. Geological Survey Open-File Report 84-164.
- (P) Ware, R. H., Johnston, M. J. S., and Mueller, R. J., 1984, The Detection Threshold for Short Period Seismomagnetic Events: *Journal of Geomagnetism and Geoelectricity*, [in press].
- (A) Johnston, M. J. S., 1983, The Approach to Catastrophic Crustal Failure--Inference From Two Earthquakes with $M_L > 6.5$: *EOS (Trans. Am. Geophys. Un.)*, v. 64, p. 749.
- (A) Johnston, M. J. S., Chen, Z., Jiang, K., Mueller, R. J., Keller, V. G., and Zhan, Z., 1983, Magnetic and Fault Crossing Geodetic Arrays in the Peoples Republic of China, *EOS (Trans. Am. Geophys. Un.)*, v. 64, p. 856.

- (A) Jones, A. C., and Johnston, M. J. S., 1983, Continuous Strain Measurements at the Presidio, California: 1973-1983: EOS (Trans. Am. Geophys. Un.) v. 64, p. 841.
- (A) Johnston, M. J. S., 1984, Deep Creep: Earthquake Notes, [in press].
- (A) Johnston, M. J. S., Silverman, S. A., and Breckenridge, K., 1984, Secular Variations and its Variations, EOS (Trans. Am. Geophys. Un.), v. 65, 203.

Earthquakes and the Statistics of Crustal Heterogeneity

9930-03008

Bruce R. Julian

Branch of Seismology
U.S. Geological Survey
345 Middlefield Road - MS77
Menlo Park, California 94025
(415) 323-8111 ext. 2931

Investigations

Both the initiation and the stopping of earthquake ruptures are controlled by spatial heterogeneity of the mechanical properties and stress within the earth. Ruptures begin at points where the stress exceeds the strength of the rocks, and propagate until an extended region ("asperity") where the strength exceeds the pre-stress is able to stop rupture growth. The rupture termination process has the greater potential for earthquake prediction, because it controls earthquake size and because it involves a larger, and thus more easily studied, volume within the earth. Knowledge of the distribution of mechanical properties and the stress orientation and magnitude may enable one to anticipate conditions favoring extended rupture propagation. For instance, changes in the slope of the earthquake frequency-magnitude curve ("b-slope"), which have been suggested to be earthquake precursors and which often occur at the time of large earthquakes, are probably caused by an interaction between the stress field and the distribution of heterogeneities within the earth.

The purpose of this project is to develop techniques for determining the small-scale distributions of stress and mechanical properties in the earth. The distributions of elastic moduli and density are the easiest things to determine, using scattered seismic waves. Earthquake mechanisms can be used to infer stress orientation, but with a larger degree of non-uniqueness. Some important questions to be answered are:

- ** How strong are the heterogeneities as functions of length scale?
- ** How do the length scales vary with direction?
- ** What statistical correlations exist between heterogeneities of different parameters?
- ** How do the heterogeneities vary with depth and from region to region?

Scattered seismic waves provide the best data bearing on these questions. They can be used to determine the three-dimensional

spatial power spectra and cross-spectra of heterogeneities in elastic moduli and density in regions from which scattering can be observed. The observations must, however, be made with seismometer arrays to enable propagation direction to be determined. Three-component observations would also be helpful for identifying and separating different wave types and modes of propagation.

The stress within the crust is more difficult to study. Direct observations require deep boreholes and are much too expensive to be practical for mapping small-scale variations. Earthquake mechanisms, on the other hand, are easily studied and reflect the stress orientation and, less directly, its magnitude, but are often not uniquely determined by available data.

This investigation uses earthquake mechanisms and the scattering of seismic waves as tools for studying crustal heterogeneity.

Results

Dike-intrusion earthquake mechanisms

During the last six months further investigations have been conducted, in cooperation with Dr. Stuart Sipkin of the Branch of Global Seismology, into the processes responsible for the non-double-couple mechanisms of many of the earthquakes that have occurred since 1978 in and near Long Valley caldera. A paper on this work was presented in December at the 1983 Western National meeting of the AGU, which was held in San Francisco.

Most investigators now agree that several of the largest Long Valley caldera earthquakes of May, 1980 had non-double-couple earthquake mechanisms. A controversy has arisen, however, about the physical process responsible for these unusual mechanisms: are they caused by accidental occurrence of pairs of earthquakes at nearly the same time, or are they caused by a process (for example tensile failure at high fluid pressure) whose equivalent force system is inherently not a double couple? Most project work during the last 6 months has been aimed at answering this question.

Waveform modelling - The results of inversion of digitally-recorded long-period waveforms do not support the multiple-event hypothesis. Derived source-time functions show no indication of double peaks, which would be expected if the earthquakes are multiple events. Even more convincingly, the moment tensors show no significant change in orientation with time. Analysis of other earthquakes, such as the May 1983 Coalinga event, has shown that changes in fault orientation of as little as 10° can easily be detected. The multiple-event hypothesis is also inconsistent with synthetic broad-band waveforms constructed by deconvolving long- and short-period digital data: for one non-double-couple event in particular (which occurred at 1450 UTC on May 17, 1980) the broad-band waveforms are strikingly simple, and not at all like those expected for a multiple event.

Dynamics of fluid-driven cracks - Aki has recently pointed out an apparent inconsistency in the interpretation of the Long Valley caldera earthquakes in terms of tensile failure. The first motions expected from such a source should be compressive everywhere, whereas the observed first motions are rarefactional in a band of the focal sphere centered on the plane of the inferred crack. Aki suggested that the true first motions would be very small over this part of the focal sphere, and that a later, much larger compression might be mistakenly identified as the first motion. Aki supported this idea with data that showed that the arrival times reported for signals with compressive first motion directions are systematically earlier than the times for rarefactional signals. To better understand this question, we have conducted finite-difference numerical calculations of the dynamics of an extending fluid-filled crack. We find that the far-field signals do indeed consist of a small high-frequency compression followed by a lower-frequency rarefaction, much as Aki predicted they would. We plan to conduct a detailed comparison of the observed waveforms with those predicted for a fluid-driven crack, taking into account crustal reverberations and seismograph response.

Dilatometer installation - In order to gather data bearing on the earthquake mechanisms, a Sacks-Evertson dilatometer was installed last fall near the Devil's Postpile, immediately southwest of Long Valley caldera. As soon as roads in the area are cleared of snow (expected by mid-June), a small building will be constructed and electronic recording equipment will be installed. This instrument will provide high-sensitivity measurements of areal strain changes, and can also be used as a high-quality seismometer. Such instruments have proven useful for monitoring dike propagation in Japan, Iceland and other volcanic areas.

Earthquake location - A new computer program for has been written that uses seismic-wave arrival data to estimating the locations and origin times of earthquakes. This program offers several operational advantages over those previously available: it is small enough to run on a small minicomputer and still allow space for several hundred readings; it allows users easily to change computational algorithms, earth models, etc.; it will require little or no modification to run on virtually any type of computer; and it is about ten times faster than other programs in current use. The program also offers several important seismological advantages: it provides confidence regions for earthquake locations that are much more realistic than those normally available, which are based on unreasonable assumptions about the sources of error; it can deal with multi-branched travel-time curves, thus taking advantage of the information contained in later arrivals and aiding in correctly associating these arrivals with earthquakes; and it is capable of using array slowness and azimuth data, as well as arrival times. A open-file report describing the use of the program is planned, as is a scientific paper on technical aspects of estimating earthquake location.

Reports

B. R. Julian and S. W. Sipkin, Earthquake processes in the Long Valley caldera area, California (abstract) EOS, v. 64, no. 45, p. 890.

Seismic Study on Rupture of Seismic Gaps

Contract No. 14-08-0001-G-814

Hiroo Kanamori

Seismological Laboratory, California Institute of Technology
Pasadena, California 91125 (818-356-6914)

Investigations

The 1983 Akita-Oki Earthquake ($M_w = 7.8$) and Its Implications for Systematics of Subduction Earthquakes

Results

Ruff and Kanamori (1980) found an empirical relation between the magnitude of the characteristic earthquake for a given subduction zone, the convergence rate V and the age of the subducting plate T . The relation is:

$$M'_w = -0.00953T + 1.143V + 8.01 \quad (1)$$

(T in M year, V in cm/year), where M'_w is the magnitude of the characteristic earthquake for each subduction zone.

Figure 1 shows the relation between M'_w predicted by this relation and that observed for various subduction zones. The magnitude can be predicted reasonably well from the plate parameters V and T . Although the empirical relation is valid for the ranges of V and T used to construct it, its applicability to plate boundaries with extreme values of V and T is somewhat questionable. For example, when the subducting plate is very young, it may not be mechanically competent enough to cause large earthquakes. If the convergence is very slow, the repeat time is very long and the plate boundary becomes essentially aseismic. Hence, it is important to know the ranges of V and T where this empirical relation is valid.

Heaton and Kanamori (1984) applied relation (1) to the Juan de Fuca subduction zone in the Pacific Northwest. The Juan de Fuca subduction zone has a slow convergence rate, about 3.5 cm/year, and a very young, 15 M years, subducting plate (Figure 3). Empirical relation (1) would predict an M'_w of about 8.4.

In order to investigate the applicability of empirical relation (1) to subduction zones with a very slow convergence rate and a young subducting plate, we examined the mechanism of the 1983 Akita-Oki, Japan, earthquake (May 26, 1983, 02^h 59^m 59.6^s, UT, 40.482°N, 139.102°E, 24 km, $m_b = 6.8$, $M_s = 7.7$). This earthquake is unique because most large earthquakes in Japan occur on the Pacific coast side and large events seldom occur on the Japan Sea side. In fact, for at least the past 400 years, no large earthquake is known to have occurred near the epicenter of the Akita-Oki earthquake.

We used long-period (256 sec) surface waves recorded at IDA (International Deployment of Accelerographs) and GDSN (Global Digital

Seismographic Network) stations. Twenty-eight Rayleigh-wave phases and twelve Love-wave phases are inverted to determine the mechanism. Since the first-motion data reported by Shimazaki and Mori (1983), Takahashi et al. (1983), Tohoku University and Hirosaki University (1983) and Ishikawa et al. (1983) indicate a dip angle ranging from 25° to 34° , we constrained the dip angle to be 30° and inverted the data to determine the strike, slip angle and the seismic moment. The result is shown in Figure 2. This solution is constrained very well by the data and agrees well with the solutions by other investigators. The mechanism is almost pure dip slip on a plane dipping 30° E or 60° W, with a seismic moment $M_0 = 5.9 \times 10^{27}$ dyne-cm ($M_w = 7.8$). The distribution of the aftershocks determined by Sato et al. (1984) suggests that the plane dipping 20° to 30° E is the fault plane. However, Suyehiro et al. (1984) caution that the results obtained from the ocean bottom seismograph network do not provide conclusive evidence for this choice of the fault plane. If the dip angle is different from 30° , the moment should be changed to $M_0 \sin 60^\circ / \sin 2\delta$, where δ is the dip angle.

Recently several investigators (Nakamura, 1983; Kobayashi, 1983; Seno and Eguchi, 1983) suggest that the plate boundary between the Eurasia and North American plates lies along the Japan Sea coast (see Figure 2). According to this model, northern Honshu, Hokkaido and Sakhalin are on the North American plate. If this geometry is correct, then the global plate model RM2 of Minster and Jordan (1978) implies convergence at the rate of 1.1 cm/year in the direction of $N84^\circ$ W at the epicenter of the Akita-Oki earthquake. This direction is very close to our preferred slip direction of the Akita-Oki earthquake. Thus the location and the geometry of the Akita-Oki earthquake are consistent with the idea that the present-day boundary between the Eurasia and North American plates is along the Japan Sea coast. In this case, the Akita-Oki earthquake can be considered as a subduction event that occurred on a very young (15 M years) and slowly-converging (1.1 cm/year) plate boundary.

Applying empirical relation (1) to Japan-Sea plate boundary we obtain $M'_w = 8.0$ assuming $V = 1.1$ cm/year and $T = 15$ M years. This compares well with the observed magnitude of the Akita-Oki event. The good agreement between the predicted and observed magnitudes suggests that the empirical relation is valid for subduction zones with very small T and V such as the Juan de Fuca subduction zone, Pacific Northwest.

Reports and Publications

Heaton, T. H. and H. Kanamori, Seismic potential associated with subduction in the Northwestern United States, Bull. Seismol. Soc. Am., 74, in press, 1984.

Kanamori, Hiroo and Luciana Astiz, The Akita-Oki Earthquake ($M_w = 7.8$) implications for systematics of subduction earthquakes. Submitted to Earthquake Prediction Research, April 26, 1984.

Ruff, L. and H. Kanamori, Seismicity and the subduction process, Phys. Earth Planet. Inter., 23, 240-252, 1980.

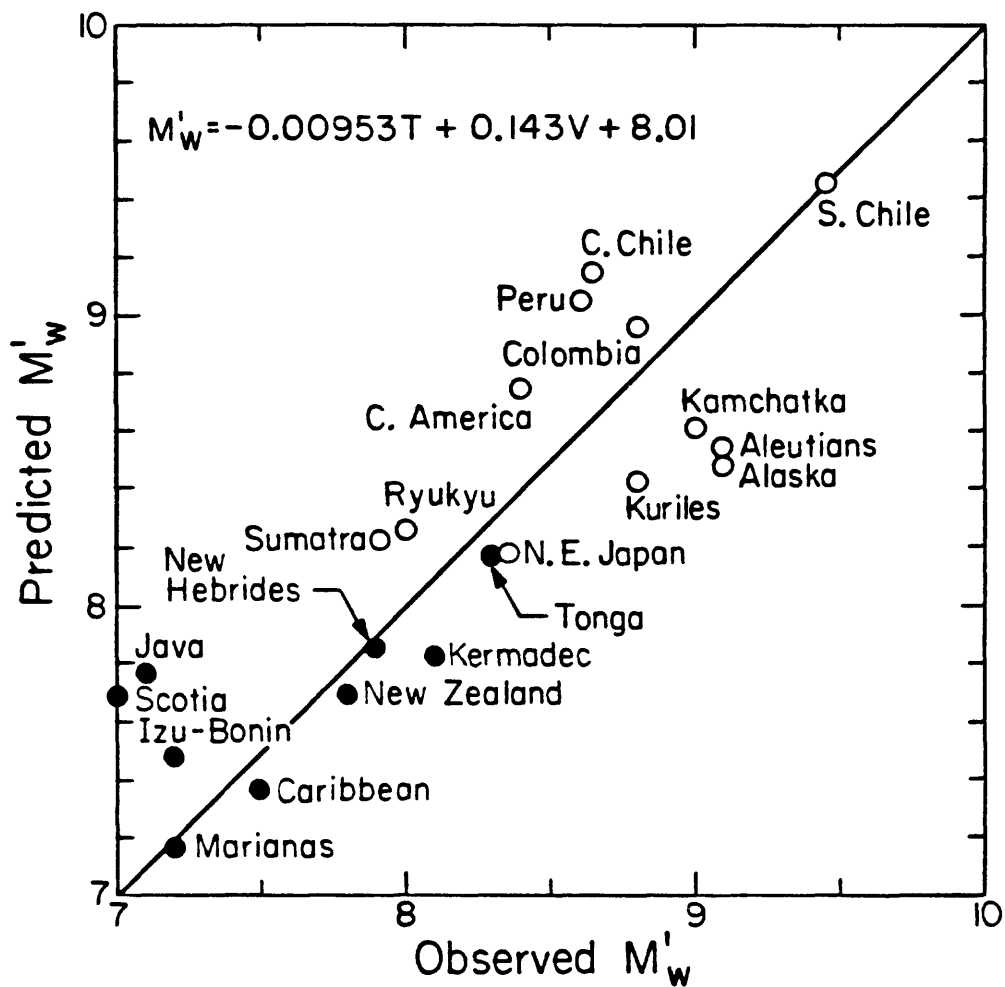


Figure 1. The magnitude of the characteristic earthquake for various subduction zones. The vertical axis: Predicted values from the convergence rate V(cm/year) and the age of the subducting slab T(M years). Horizontal axis: Observed values. (Ruff and Kanamori, 1980, Kanamori, 1983). The closed and open symbols denote subduction zones with and without active back-arc opening respectively.

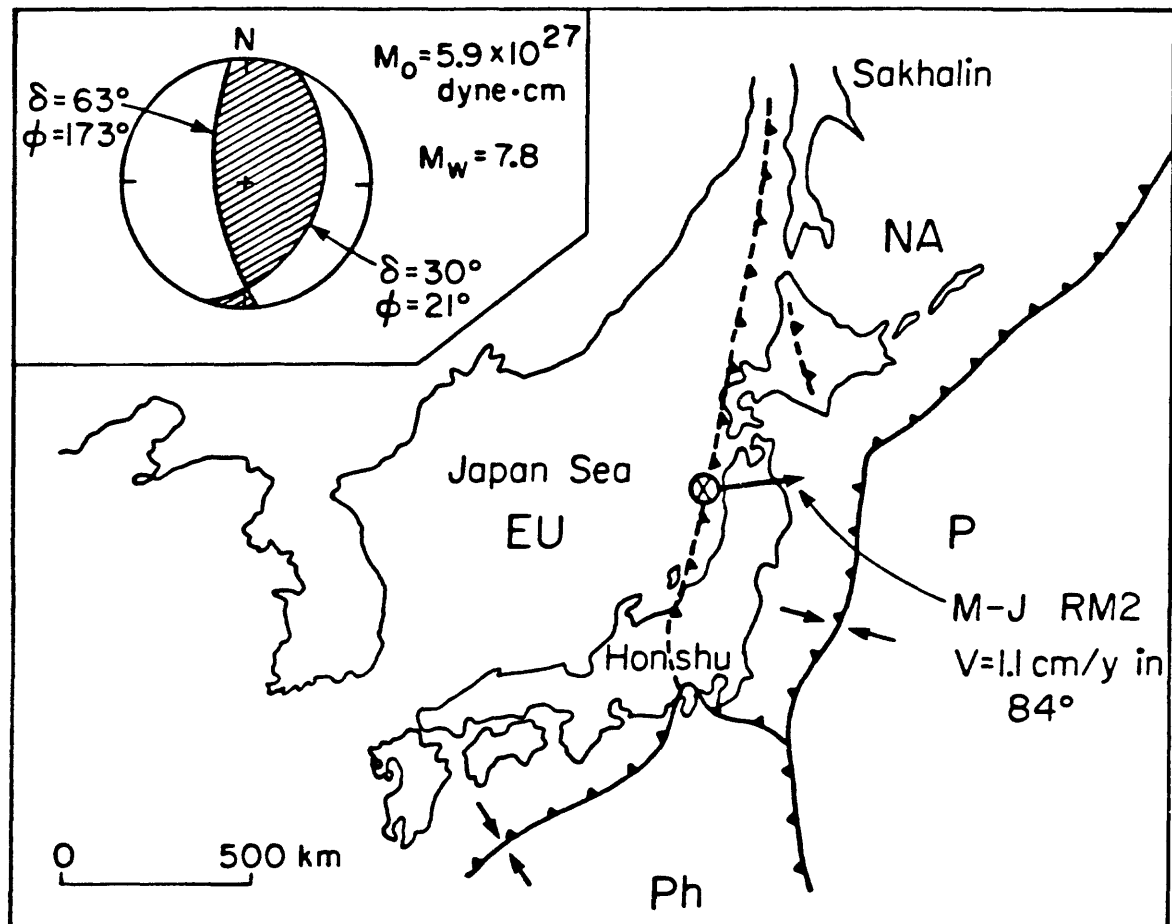


Figure 2. Schematic figure showing the plate geometry in the Northern Japan. The epicenter of the 1983 Akita-Oki earthquake is shown by a circled x. The inset shows the mechanism (lower focal sphere in Wulff projection) of the 1983 Akita-Oki earthquake. The convergence rate and the direction at the epicenter predicted by Model RM2 of Minster and Jordan (1978) are shown.

SEISMICITY, TOPOGRAPHY AND PRE-EARTHQUAKE
LOADING PROCESSES ALONG THE SAN ANDREAS SYSTEM

Contract No. 14-08-0001-21282

John Kelleher
REDWOOD RESEARCH, INC.
San Mateo, CA 94401
(415) 342-8276

Investigations

Research supported under this contract includes a) an investigation into the relationship between topographic features and the locations of larger strike-slip earthquakes along the San Andreas system b) a study of the depth distribution of events along the San Andreas system. Some evidence suggests a time-dependent component to deeper earthquakes ($h \geq 10$ km) whereby the distribution of deeper events may be an important indication of regional stress accumulation. c) continued study of the patterns of seismic activity which precede larger strike-slip earthquakes.

Results

The major result to date concerns the regularities observed in the patterns of seismicity preceding strike-slip earthquakes. An increasing number of examples have been found in which the mainshock is preceded by a migration of seismic activity approximately in the direction of maximum compressive stress, and toward the rupture surface. In addition comparable patterns have been found before thrust-type earthquakes within the overthrusting blocks. The examples are not numerous enough to suggest a process which universally precedes earthquakes. Rather the evidence suggests that some earthquakes may be preceded by a geometrically simple pattern of seismicity which may be recognizable. A further implication is that some strike-slip and thrust-type earthquakes may have more in common than do strike-slip events as a class.

Our tentative interpretation is that the stress accumulation process which precedes these earthquakes and generates the seismicity patterns may itself be simple geometrically. Furthermore, this simple geometry stress accumulation may not always be expressed seismically and therefore may occur more commonly than the relatively few examples of seismicity referred to above.

The examples cited above are virtually all characterized by the presence of strong faulting or other structures transverse to the fault surface of the main rupture. Thus, the simple geometry of stress accumulation may be present and controlled by the mechanical coupling of the blocks on either side of the fault surface of the mainshock.

FAULT MECHANICS AND CHEMISTRY

9960-01485

C.-Y. King
Branch of Tectonophysics
U.S. Geological Survey
345 Middlefield Road, MS/977
Menlo Park, California 94025
(415) 323-8111, ext. 2706

Investigations

1. Water temperature and radon content were continuously monitored at two water wells in San Juan Bautista, California.
2. Water level was continuously recorded at seven other wells.
3. Water samples were periodically taken from most of these wells for chemical analyses.
4. Radon content of ground gas was continuously monitored at three sites (Melendy Ranch, Limekiln A well and Cienega Winery) along the San Andreas fault in the Bear Valley area, California.
5. Slip events generated along a laboratory faulting model were studied.

Results

Predictability of large slip events along a laboratory fault --

Long sequences of slip events of various sizes have been generated along a laboratory fault model consisting of spring-connected masses that are elastically driven to slide on a frictional surface. Large slip events commonly occur when sufficient strain is built up simultaneously on most masses along a long segment of the fault, whereas smaller events occur when fewer masses are stressed to comparable levels. The occurrence of large events is preceded by a lag in slippage of most masses behind expected average values and by frequent occurrence of smaller events. Thus, the occurrence time of large events is easily predictable, whereas their size is not. The recurrence intervals between large events vary widely and are not a useful means for large-event prediction.

Reports

King, C.-Y., 1983, Impulsive radon emanation on a creeping fault [Abst.], EOS, Trans. Am. Geophys. Un., vol. 64, p. 758.

King, C.-Y., 1984, Predictability of large slip events along a laboratory fault [Abst.], Earthquake Notes, in press.

King, C.-Y., 1984, Hydrological and geochemical approaches to earthquake prediction in the United States of America [Abst.], 27th International Geological Congress.

PREDICTION METHODOLOGY FOR SUBDUCTION ZONE EARTHQUAKES,
CENTRAL ALEUTIAN ISLANDS

Contract No. 14-08-0001-21230 and Grant No. 14-08-0001-G881

Carl Kisslinger and Selena Billington
 Cooperative Institute for Research in Environmental Sciences
 Campus Box 449, University of Colorado
 Boulder, Colorado 80309

(303) 492-8028

Current Quiescence within the Adak Seismic Zone

A period of pronounced reduction in the rate of occurrence of earthquakes in all magnitude bands, within the Adak Seismic Zone (175° - 178.5° along the Aleutian arc) started in September, 1982. The observed drops in activity, based on the data set provided by the Adak Network, are:

| | |
|-----------------|---|
| M_D 1.6 - 2.2 | July '81 - Aug '82, 36 ± 7 per month |
| | Oct '82 - Dec '83, 15 ± 3.5 per month |
| M_D 2.3 - 3.0 | July '81 - Aug '82, 15 ± 5 per month |
| | Oct '82 - Dec '83, 5 ± 3 per month |
| $M_D > 3.0$ | July '81 - Aug '82, 8 ± 3 per month |
| | Oct '82 - Dec '83, 3 ± 2 per month |

In each magnitude range the drop that started sometime in September 1982 was about 60%.

A variety of tests have been made to determine whether this decrease in the number of events located by the network is due to a change in the detection and location capability of the network itself. Various stations, or components at a station, drop out from time to time. The fact that the drop in rate of occurrence is very similar in all magnitude bands, including the largest earthquakes, is our best evidence that the rate decrease is real.

One independent check that we have is the number of earthquakes reported in the USGS PDE reports. The events in this listing are independent of the Adak Network. The PDE reports show a sharp drop in the rate of activity starting in September, 1982, with a gradual return toward the normal background rate (one or two of these teleseisms per month) starting in March 1983. The PDE show one event in January, 1984, none in February or March, and one in early April, the most recent report available.

The data indicate that a period of seismic quiescence began within the Adak Seismic Zone in September 1982 and continues to the present, punctuated by intervals of somewhat higher activity. The question is whether this behavior is precursory to a strong earthquake in the near future. The only similar pattern since 1965 was seen in the PDE data by Habermann, starting in 1968 and terminating with the two magnitude 7 events in early 1971. The absence of

teleseismically-locatable events in the Adak Canyon region from 1971 to June 1982 had attracted our attention to this place as a likely site for a major earthquake. The outbreak of activity in subregion SW2, reported in earlier technical summaries, has led us to conclude that this subregion has some characteristics of an asperity on the thrust zone that may be approaching failure (Bowman and Kisslinger, 1984b).

Only time will provide the final answer as to whether the observed quiescence and other anomalous behavior are precursory. The previous teleseismic quiescence associated with an Adak Canyon earthquake lasted just over three years. Our present conclusion is that the totality of evidence suggests an enhanced likelihood of a magnitude 7 earthquake in the Adak Canyon region, perhaps nucleating within SW2, at 176.75°W longitude, within the next 12 to 15 months.

Teleseismic JHD Study

In collaboration with E. R. Engdahl and J. W. Dewey (both with the U.S.G.S. Branch of Global Seismology), we are very carefully relocating a set of teleseismically well-recorded earthquakes which occurred over the time period 1965-1982 between 172°W and 179°W longitude. Two major stages are involved in this procedure: first, the depths of selected calibration events are carefully determined; and second, the relocated hypocenters for those calibration events are used in the method of Joint Hypocenter Determination (JHD) to relocate the complete set of events.

(1) Depths of about 60 events have now been individually determined, using primarily depth phases read specifically for this study. Ray tracing through a two-dimensional velocity model of the central Aleutians was used to compute predicted arrivals for source-receiver pairs, and these were used to unravel the identification of observed short-period depth phases as pP (the sediment-water reflection), pwP (the water-surface reflection), or sP. In general, the best agreement between predicted and observed arrival times of depth phases is seen for events south of the main thrust zone; here exceptional agreement is often seen and within the reliability of the velocity structure, depths can be constrained to within 2 km. For most cases for events within the main thrust zone, focal depths can be estimated with an uncertainty of less than 5 km.

(2) Calibration events for the JHD process are being relocated using depths determined from the teleseismic depth phases and with arrival time data from both teleseismic and local stations. When these locations are completed, the entire teleseismic data set (several hundred events) will be relocated with these calibration events. Preliminary relocations suggest that the 100-km contour of the steeply-dipping Benioff zone between 177°W and 173°W longitude is continuous beneath the right-lateral offset of about 40 km in the line of volcanoes near 173°W, where the Amlia fracture zone is being subducted.

Shallow Earthquakes Seaward of the Main Thrust Zone

South of the central Aleutians there is a group of shallow-focus earthquakes, seaward of and spatially separated from the main zone of shallow interplate earthquakes. Almost all of these earthquakes are located either under Hawley Ridge (a major forearc bathymetric structure) or under its extension to the east and west. Hypocenters for these earthquakes were determined from the Adak network data for the period from 1975 through December, 1983, and from preliminary Joint Hypocenter Determinations of teleseismically-recorded events for the period 1964 through 1982.

In contrast to earthquakes in the main thrust zone farther to the north, the "Hawley Ridge" earthquakes occur in temporal swarms, each swarm with tightly clustered epicenters. Moreover, the data suggest that the temporal swarms occur episodically, with individual sources becoming activated at roughly five-year intervals.

Teleseismic focal mechanism solutions for four of these events are thrust mechanisms, with thrusting occurring either on a very shallow-northwest-dipping plane or on a very steep, southeast-dipping plane. Local P-wave first motion data have been composited for two of spatial clusters. In one case all of the observed arrivals are compressional, in the other they are all dilational. The take-off angles to the local stations are not well-known, so that the strongest conclusion that can be made about these data are the events within each cluster probably all had the same focal mechanism.

Depths have been individually determined for four of the teleseismically-recorded earthquakes using careful interpretation of short-period depth phases. Two of the events are clearly at about 17 km depth, and the best interpretation of the depth of the other two is also at about 17 km.

The teleseismic focal mechanism solutions and hypocenter depth determinations suggest that the earthquakes under Hawley Ridge and its extension to the east and west are occurring on the plate boundary trenchward of the main thrust zone. One possible explanation for the occurrence of earthquakes under the ridge but not between the ridge and the main thrust zone might be that the load of the ridge on the plate interface causes increased friction at the fault, making this the site of episodic earthquakes.

Publications

Billington, S., and J. R. Bowman, Interplate earthquakes seaward of the main thrust zone in the Central Aleutian Islands region (abstract), **EOS**, 64, 768, 1984.

Bowman, J. R., and C. Kisslinger, A test of foreshock occurrence in the Central Aleutian island arc, **Bull. Seism. Soc. Amer.**, 74, 181-197, 1984.

Bowman, J. R., and C. Kisslinger, Seismicity associated with a cluster of earthquakes of $m_b \geq 4.5$ near Adak, Alaska: Evidence for an asperity?, submitted for publication to **Bull. Seism. Soc. Amer.**, 1984.

Toth, T., and C. Kisslinger, Revised focal depths and velocity model for local earthquakes in the Adak seismic zone, in press, **Bull. Seism. Soc. Amer.**, August, 1984.

Alaska Seismic Studies

9930-01162

John C. Lahr
Christopher D. Stephens
Branch of Seismology
U. S. Geological Survey
345 Middlefield Road, MS 977
Menlo Park, California 94025
(415) 323-8111, Ext 2510

Investigations

- 1) Continued collection and analysis of data from the high-gain short-period seismic network extending across southern Alaska from Juneau to Cook Inlet and inland across the Chugach Mountains.
- 2) With funding from the Division of Geological and Geophysical Surveys of the State of Alaska, continued operation of four seismic stations in the northern Prince William Sound region which experienced two magnitude 6 earthquakes last summer.
- 3) Continued monitoring of the region around the proposed Bradley Lake hydroelectric project on the Kenai Peninsula, a cooperative effort with the Alaska Power Authority.
- 4) Cooperated with the Engineering Seismology and Geology Branch in operating strong motion accelerographs in the vicinity of the seismic network, including 13 between Icy Bay and Cordova in the area of the Yakataga seismic gap. Fourteen accelerographs are connected to the high-gain station telemetry network so that absolute trigger times can be obtained.

Results

- 1) During the past six months data processing has remained on schedule. Preliminary hypocenters have been determined for 2263 earthquakes that occurred between August 1983 and January 1984 (Figure 1). Twenty-five events of magnitude 4 m_b and larger occurred during this time, including a 6.2 m_b shock on September 7 near Columbia Bay (Page and others, 1984). The September shock was located 30 km deep near the southwest end of the aftershock zone of a magnitude 6.1 m_b event that occurred in July 1983. Aftershocks of the September event were located within an approximately equidimensional zone about 9 km across that did not overlap significantly with the July sequence. The focal mechanisms for both the July and September shocks determined from regional and teleseismic P-wave first-motions and the distributions of aftershocks indicate normal faulting on a steeply northwestward-dipping plane. Both events are inferred to occur within the subducted Pacific plate. Other notable events include a magnitude 5.0 m_b event that occurred southwest of

Montague Island, and a 4.9 m_b shock that occurred near the southwest edge of Icy Bay outside of the immediate aftershock zone of St. Elias earthquake, but within an area that has been seismically active since at least 1974 when the network was installed.

- 2) The 1979 St. Elias earthquake ($7.1 M_s$) that occurred beneath the Chugach-St. Elias Mountains north of Icy Bay was a shallow, low-angle thrust event that accommodated convergence between the Pacific and North American plates. An important question concerning this event is, on what fault or faults did the rupture occur? Page and others (1982) studied aftershocks recorded by a small array of temporary seismographs deployed near the center of the aftershock zone about six months after the mainshock. They showed that beneath the array the events were confined to a planar, subhorizontal zone less than 2 km thick at a depth of 10 to 15 km. In October 1983 the station AGA was installed by Agassiz Lakes to obtain additional information about the depth distribution of the continuing activity southwest of the area of the temporary array. Well-located hypocenters constrained by P- and S-arrivals recorded at AGA indicate that the upper surface of the zone defined by Page and others (1982) extends beneath AGA at a depth of about 10 km. However, several shocks of magnitude 2 and less had S-P intervals between 1.0 and 1.5 sec and were clearly located above the main thrust zone. The epicenters of most of the shallower events were located within a small area intersected by the Chaix Hill fault. Although limited accuracy of the hypocenters and lack of information about the subsurface geometries of mapped faults preclude associating the activity with a particular fault, this observation indicates that faults within the upper crust are seismically active.
- 3) Seismograms of crustal and Benioff-zone earthquakes in the vicinity of Mt. Spurr were examined for anomalous character that might indicate source or propagation path effects associated with this active volcano. Since late 1981, three vertical component seismographs have been operating within 20 km of the volcano summit. The stations lie east or southeast of the summit and form a triangle with sides of 9-14 km. The closest neighboring stations are at distances beyond 60 km. Although the sparse distribution of stations hampers the identification of anomalous seismograms, the records examined to date suggest two significant features. First, seismograms from the three stations near Mt. Spurr exhibit distinctive low frequency (2-4 Hz), ringing (typically more than 4 cycles) P and S phases from shocks occurring at depths of 30 to 40 km beneath the stations. Second, signals recorded at CRP, the station closest to the 1953 eruptive center, seem to be attenuated, particularly at high frequencies, for many but not all shocks. The available data are not sufficient either to resolve whether the low-frequency, ringing seismograms result from a source or propagation effect, or to relate the attenuation at CRP to a particular distribution of attenuating material.
- 4) Two stations, CNP (China Poot) and SDE (Sadie Cove), were installed southeast of Kachemak Bay on the southern Kenai Peninsula to investigate

the nature of a concentration of shallow crustal activity that has been observed previously in this area (Stephens, and others, 1983). The earlier activity had an apparent southeast-northwest trend that crossed the mapped surface trace of the northeast-trending Border Ranges (Seldovia Bay) fault. Between August 1983 and January 1984, twelve crustal earthquakes of magnitude 2 and smaller were located in the area and were recorded at both CNP and SDE and had at least one S-P interval measured at one of these two stations. The depths of these events range from 5 to 13 km. The epicenters clearly occur within a northwest-striking zone about 12 km long and 2 or 3 km wide, but this distribution appears to consist of at least two smaller clusters. Although the northwest trend in the distribution of activity may be indicative of a buried structure with a similar orientation, the available seismic data are not sufficient to resolve the orientations of the causative faults.

- 5) J. Rogers completed design and construction of a prototype earthquake event logging device (ELOG). Using a FORTH program running on an RCA COSMAC computer, the ELOG detects earthquake P-arrivals and records their onset time and polarity on a cassette tape. The prototype ELOG will be deployed in Alaska for a few months this summer for testing. Design goals include logging of P- and S-phases along with duration and amplitude. Current drain will be low enough to allow remote battery operation for 1 year. The ELOG will be ideally suited for locally augmenting at relatively low cost a sparse regional telemetry network for special detailed studies.

References cited

- Page, R. A., Hassler, M. H., Stephens, C. D., and Criley, E. E., 1982, Focal depths of aftershocks of the 1979 St. Elias, Alaska, earthquake [abs.], EOS, Transactions of the American Geophysical Union, v. 63, n. 45, p. 1039.
- Page, R. A., Stephens, C. D., Fogelman, K. A., and Maley, R. P., 1984, The Columbia Bay, Alaska, earthquakes of 1983, in, The United States Geological Survey in Alaska, Accomplishments during 1983, U.S. Geological Survey Circular (in prep.).
- Stephens, C. D., Lahr, J. C., Page, R. A., and Rogers, J. A., 1983, Review of earthquake activity and current status of seismic monitoring in the region of the Bradley Lake Hydroelectric Project, southern Kenai Peninsula, Alaska: December 1981 - May 1983, U.S. Geological Survey Open-File Report 83-744, 29 p.

Reports

- Fogelman, K. A. and Rogers, J. A., 1984, Regional earthquake monitoring in Southern Alaska, 1971-83 [abs.], Earthquake Notes, Eastern Section, Seismological Society of America (in press).

Fogleman, K. A., Stephens, C. D., and Lahr, J. C., 1983, Recent seismicity in and around the Yakataga seismic gap, southern Alaska [abs.], EOS, v. 64, p. 768.

Lahr, J. C., Stephens, C. D., and Page, R. A., 1984, Resolution of seismic source zones in the Anchorage area, Alaska [abs.], Earthquake Notes, Eastern Section, Seismological Society of America (in press).

Page, R. A., 1984, Seismological aspects of the great 1964 Alaska Earthquake [abs.], Earthquake Notes, Eastern Section, Seismological Society of America (in press).

Pelton, J. R., and Page, R. A., 1984, Focal depth estimates for selected Alaskan teleseisms [abs.], Earthquake Notes, Eastern Section, Seismological Society of America (in press).

Stephens, C. D., Fogleman, K. A., Lahr, J. C., and Page, R. A., 1984, The Wrangell Benioff zone, southern Alaska, Geology, (in press).

Stephens, C. D., Page, R. A., and Lahr, J. C., 1984, Variations in the style of convergence across southern Alaska inferred from regional seismic data [abs.], Earthquake Notes, Eastern Section, Seismological Society of America (in press).

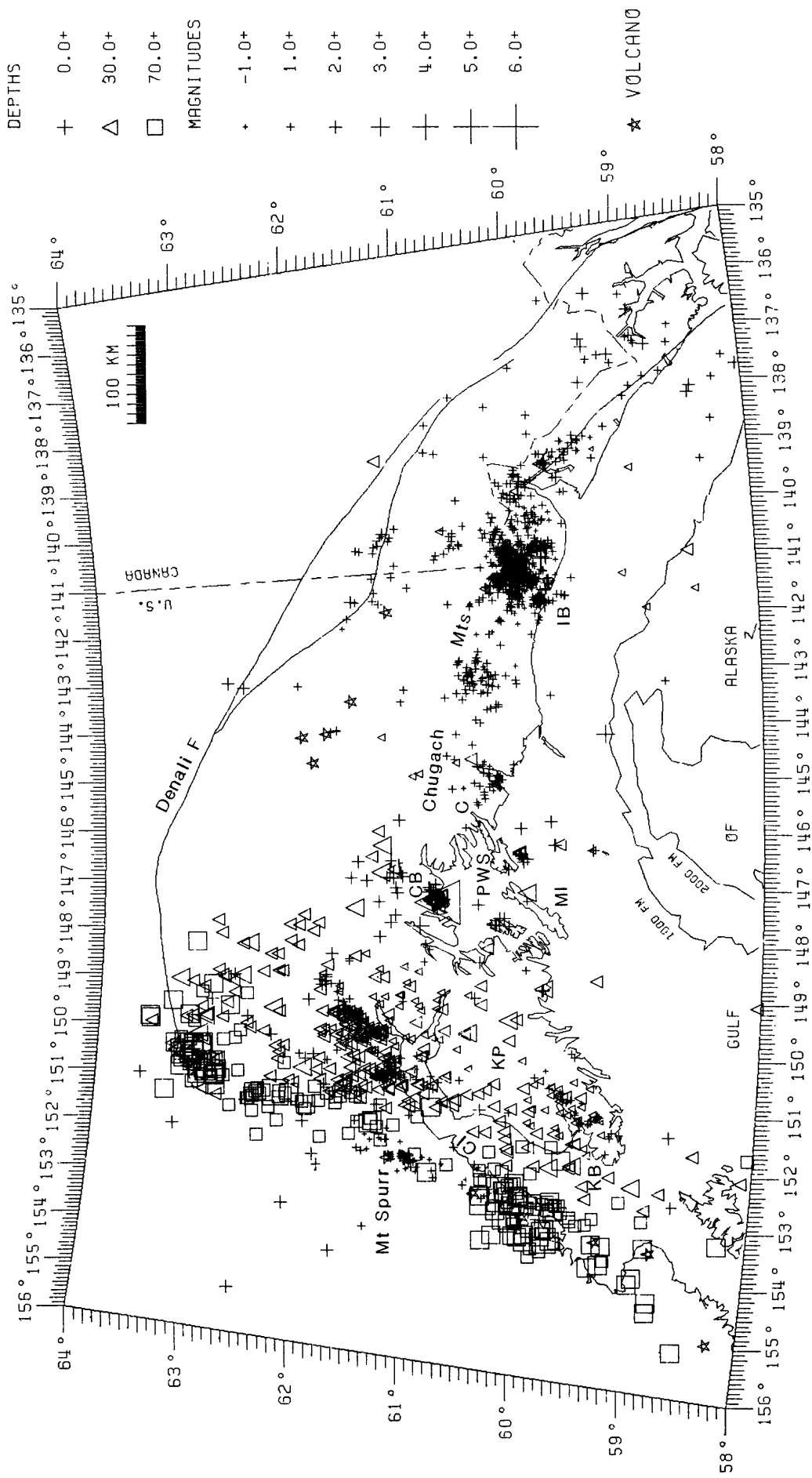


Figure 1. Epicenters of 2263 earthquakes that occurred in southern Alaska between August 1983 and January 1984 and were located by the USGS regional seismograph network. Magnitudes are determined from coda duration or maximum amplitude. Apparent high rates of shallow activity east of Prince William Sound (PWS) and around southern Kenai Peninsula (KP) and northern Cook Inlet (CI) are due to emphasis placed on locating smaller earthquakes in these areas. C - Cordova; CB - epicenter of September 7, 1983 Columbia Bay shock; IB - Icy Bay; KB - Kachemak Bay; MI - Montague Island.

Seismological Field Investigations

9950-01539

C. J. Langer

Branch of Engineering Geology and Tectonics
U. S. Geological Survey
Denver Federal Center, MS 966
Denver, CO 80225
(303) 234-5091

Investigations

1. The 1983 Borah Peak, Idaho earthquake aftershock study--regional investigation of aftershocks resulting from $M_s = 7.3$ earthquake of October 28, 1983.
2. The 1983 Guinea, West Africa earthquake aftershock study--regional investigation of aftershocks resulting from $M_s = 6.2$ earthquake of December 22, 1983.

Results

1. Data obtained from a dense network of portable, short-period seismographs were used to locate about 400 aftershocks of the Borah Peak, Idaho earthquake of October 28, 1983.

These events occurred during a three-week period of time following the main shock and extend in an elongated pattern striking roughly N25°W. Length of the principal aftershock zone is approximately 75 km, and it has a width of some 15 km. Aftershock depths range from near surface to 13 km with the greatest number being concentrated in the interval between 5 and 11 km. The distribution of aftershocks in both space and time indicate a highly complex relationship to the local geology and tectonics.

2. In response to the Guinea, West Africa earthquake of December 22, 1983, C. J. Langer traveled to Guinea in January, 1984, and installed an 11-station network of portable, short-period seismographs which operated for a period of about two weeks. The area enclosed by the network was essentially bounded between latitudes 11°45'N and 12°00'N, and longitudes 13°20'W and 13°35'W. Preliminary results indicate that the aftershock pattern projects roughly east-west through the middle of the network, is about 20-km long, 8-km wide, and the hypocentral depths extend from near-surface to roughly 16 km. Refer to the report by M. G. Bonilla for details on the geology.

GEODETIC STRAIN MONITORING

9960-02156

John Langbein
Branch of Tectonophysics
U.S. Geological Survey
345 Middlefield Road, MS/977
Menlo Park, California 94025
(415-323-8111, ext. 2038)

Investigations

Two-color laser geodimeters are used to survey, repeatedly, geodetic networks within selected regions of California that are tectonically active. This distance measuring instrument has a precision of 0.1 to 0.2 ppm of the total length.

Results

1) During the period from January to March, 1984, frequent measurements have been made of the distances on 11 baselines within the southern moat of the Long Valley caldera. To accomplish these measurements during the winter months, an observatory was constructed over the monument Casa to house the 2-color geodimeter. Also, seven retroreflectors were installed into sheds so that line-length measurements could be made to these remote locations. The remaining 4 monuments were located along the major highways in the area. Figures 1 and 2 shows the baseline locations and line-length changes measured. The program of measurements commenced in June, 1983 from the central site at Casa. The data has been adjusted for an apparent change in the instrument length due to component failures in the portable two-color geodimeter that occurred in September and October, 1983. Preliminary modeling of the data indicates that the strain is not uniform and that volumetric expansion at two points at depth is a possible explanation of the observations. The first source is located 5.5 km beneath Casa Diablo Hot Springs and expands at a rate of $1.4 \times 10^{-3} \text{ km}^3/\text{year}$. The location of the second source is not well defined, but if it is located 9 km beneath Smokey Bear Flat, then it would be expanding at $17 \times 10^{-3} \text{ km}^3/\text{year}$.

2) Twice weekly measurements of the distances of the 11 baseline network at Pearblossom, California have been made during the last 6 months using the prototype 2-color geodimeter in cooperation with Dr. L. E. Slater of CIRSES. The strain changes for the last 3-1/2 years are plotted in Figure 3 for a coordinate system oriented normal and parallel to the local strike of the San Andreas fault ($N65^\circ W$). During the year from

April, 1983 to April, 1984, the following extension strain rates have been inferred from the data;

normal strain: -0.26 ± 0.08 ppm/year
 parallel strain: -0.24 ± 0.07 ppm/year
 dextral shear strain: 0.19 ± 0.05 ppm/year

The non-zero amount of strain for the normal and parallel components represent fluctuations about their secular trends of nearly zero for the 3-1/2 years of this experiment. The 0.2 ppm/year rate of shear strain is a continuation of its nominal rate.

In mid-March, the CIRES geodimeter was moved to Parkfield, California. Future measurements of line-lengths at Pearblossom will continue at monthly intervals with the portable two-color geodimeter.

3) Due to the possibility of either component failures or instrumental drift, simultaneous measurements of several baselines using both the CIRES geodimeter and the portable geodimeter have been done periodically. These measurements were initiated in August, 1983, and continued in December, 1983 and March 1984. The data for the first interval indicated that the portable instrument showed an apparent lengthening relative to the CIRES geodimeter of 0.4 ppm of the total line-length under measurement. We have attributed this change to the failure and subsequent replacement of two key components in the portable instrument. During the second interval from December to March, no change in relative lengths of the instruments could be detected at the 0.1 ppm level.

4) Due to several component failures in the portable 2-color geodimeter that was purchased in 1980, we returned it to Terra Technology for repair. A contract has been awarded to the factory to repair the blue laser, crystal modulator, microwave power amplifier and a few items that are covered under the instrument's warranty. The instrument should be delivered in the early part of the summer, 1984.

5) Spectral analysis of the initial 15 months of the 2-color geodimeter data from Pearblossom reveals a gaussian probability distribution of data residuals about a linear trend for periods less than 50 days for some of the baselines. At longer periods, the probability distribution is not gaussian and has a characteristic that tends to increase the apparent variance of the data. This is consistent with variations in the strain rate which, for example, is reported in item 1. If only the gaussian part the line-length data is examined, then the statistical errors in the observations can be represented in the form of $(a^2 + b^2 l^2)^{1/2}$ where $a = 0.3$ mm, $b = 0.12$ ppm and l

is the baseline length. The data used in this analysis were measurements made by the Cires instrument. From other measurements at Pearblossom using the portable instrument, the "b" term may be 20 to 40% larger than reported above.

REPORTS

- (A) Linker, M. F., Langbein, J., and McGarr, A., 1983, Two-color geodimeter, measurements of crustal deformation at Long Valley, California: Initial Results (abs): EOS (American Geophysical Union Transactions), v. 64, no. 45, p. 841.
- (A) Langbein, J. O., Linker, M. F., McGarr, A., and Slater, L. E., 1983, Two-color geodimeter measurements of crustal strain accumulation near Palmdale, California: Comparisons with gravity and meteorological data (abs): EOS (American Geophysical Union Transactions), v. 64, no. 45, p. 841.
- (A) Langbein, J., Linker, M. F., McGarr, A., and Slater, L. E., 1984, Two-color geodimeter measurements of crustal deformation near Palmdale and Long Valley, California (abs): International Symposium on recent crustal movements of the Pacific region [in press].

Figure 1. Location of the baselines in the Long Valley caldera that are routinely measured with the two-color geodimeter from the monument at Casa.

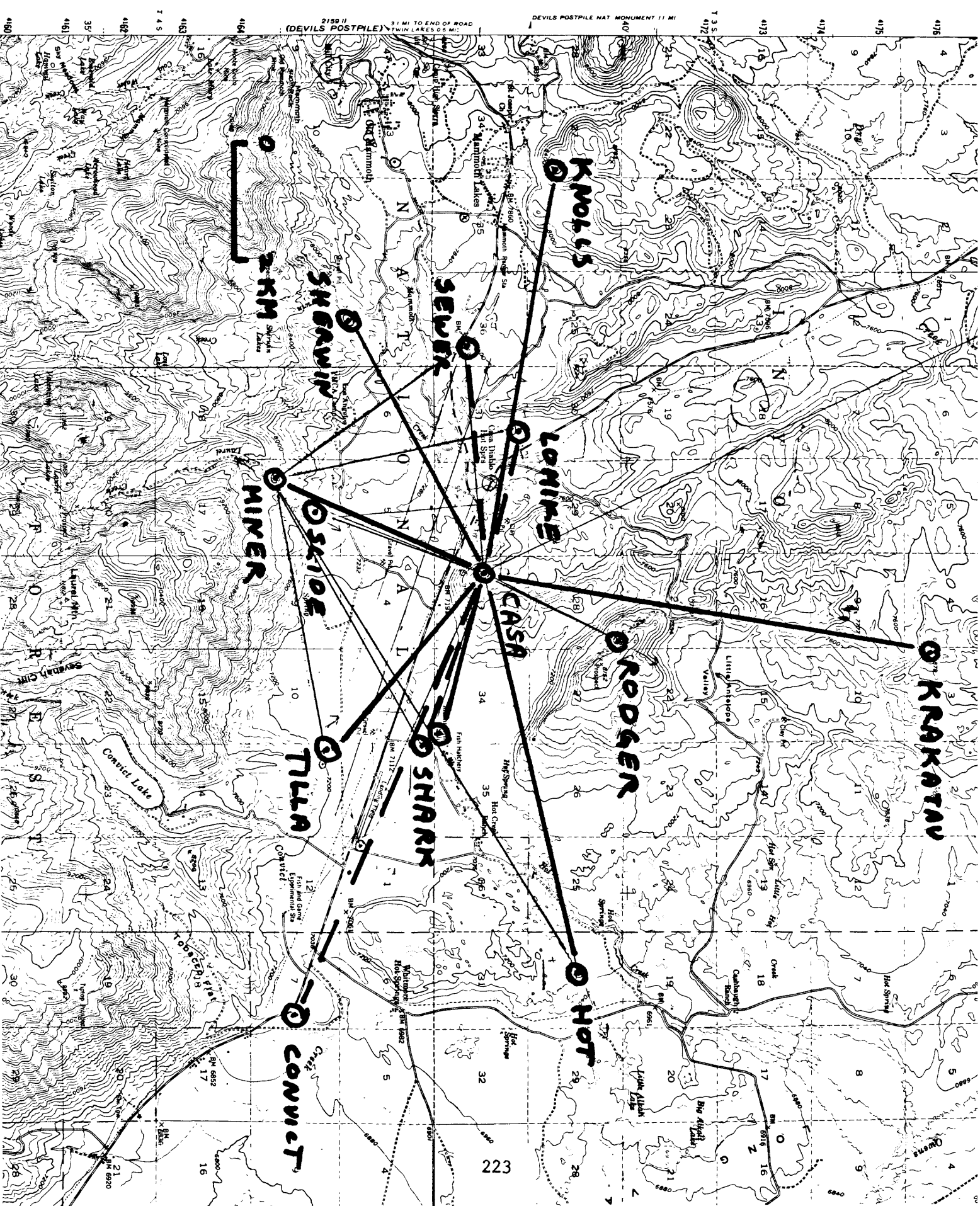


Figure 2a. Line-length changes in mm measured with a two-color geodimeter.
 Data for baselines using portable retroreflectors.

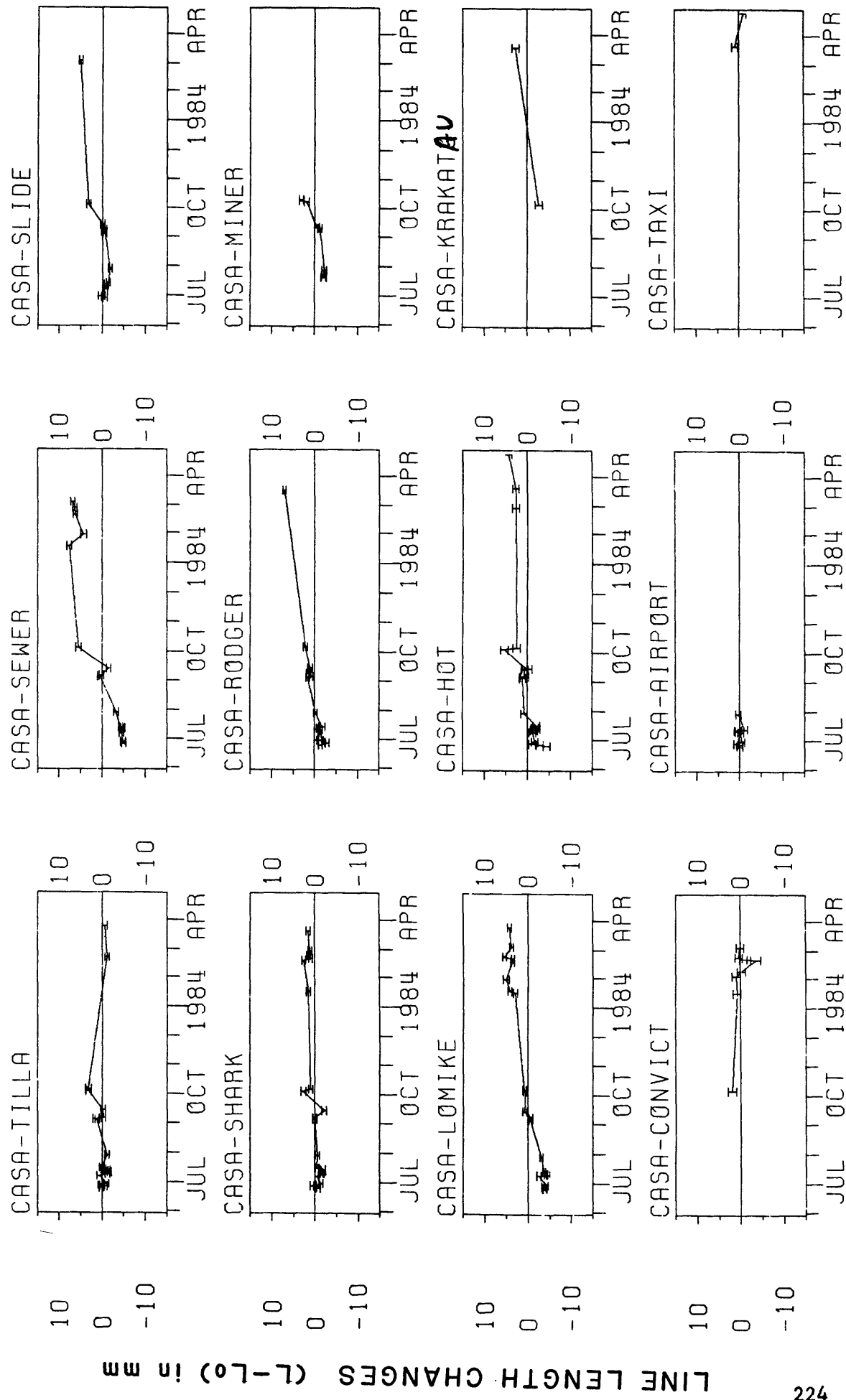
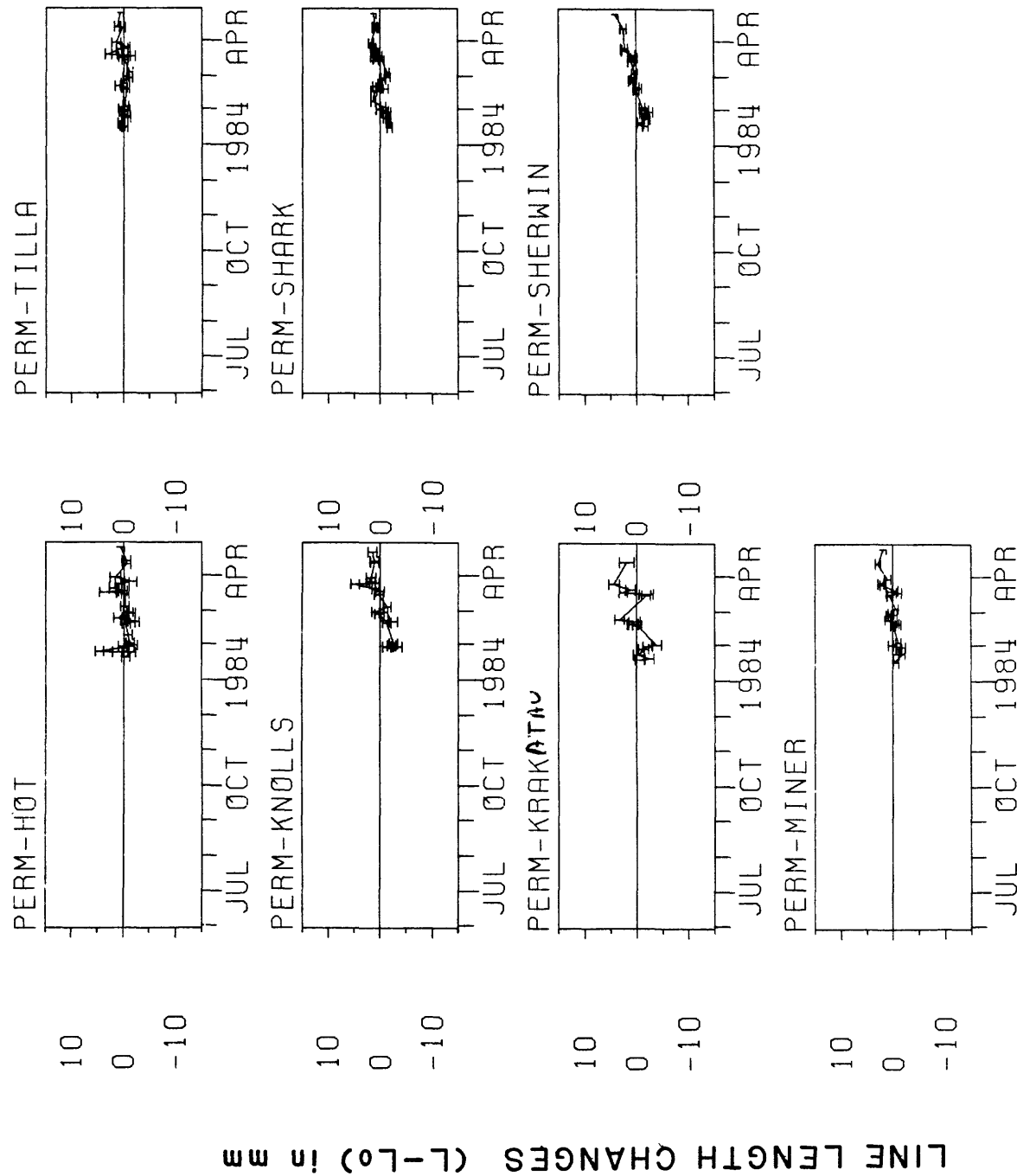


Figure 2b. Line-length changes in mm measured with a two-color geodimeter. Data for baselines using permanent retroreflectors.



STRAIN CHANGES in PPM

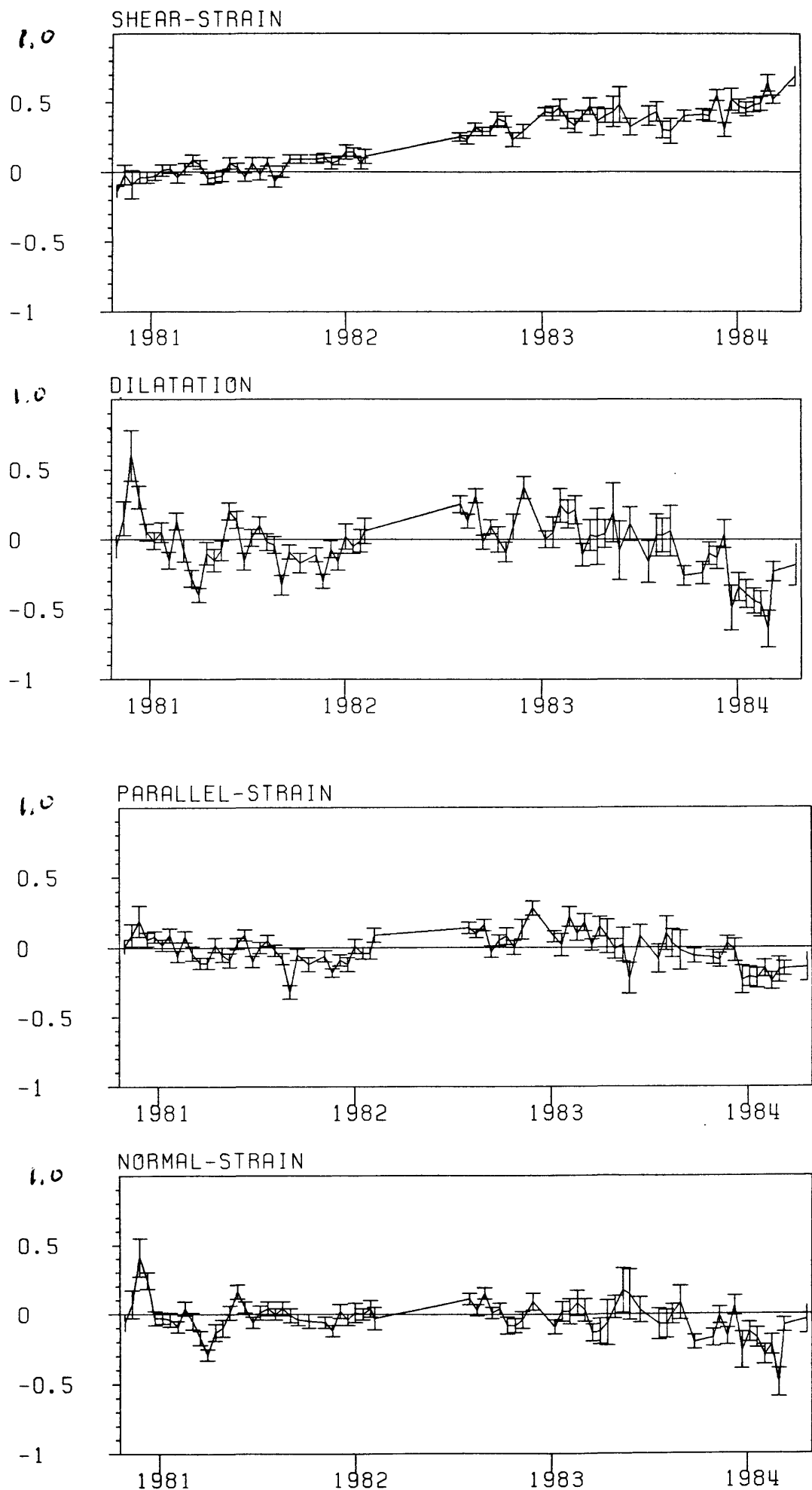


Figure 3. Strain changes that have been inferred from line-length measurements near Pearblossom, California. The strain components represent extension parallel and normal to the local strike of the San Andreas fault (N65°W). The shear strain is the dextral shear and is plotted as a tensor quantity.

Microearthquake Data Analysis

9930-01173

W. H. K. Lee
Office of Earthquakes, Volcanoes, and Engineering
Branch of Seismology
345 Middlefield Road, MS 977
Menlo Park, California 94025
(415) 323-8111, Ext 2630

Investigations

The primary focus of this project is the development of state-of-the-art computation methods for analysis of data from microearthquake networks. For the past six months I have been recovering from my illness and mostly working part-time.

A computer-based system for organizing earthquake-related data has been put into routine operation. This system edits, archives, and backups earthquake data sets, and allows users to query and retrieve archived data sets. During the past six months, about 200 data sets have been edited and archived.

Results

Three data libraries were set up within the USGS Earthquake Data Archive. In the General Library, we archive data sets as received. Unfortunately, most data sets we received do not have all the information necessary to use them. Thus, a lot of time was spent in gathering the necessary information from various sources and incorporating them into the data sets. About 140 data sets have been archived. These data sets contain the following major items: (1) hypocenter data files from the International Seismological Center, (2) hypocenter and phase data files from Caltech, and (3) digital waveform data from the Salmon nuclear explosion as recorded by the USGS.

In order to search data sets by their individual records, we must have labels (or indexes) at the record level. The Standardized Library is introduced to store data sets that are coded according to our standardized structure and recommended formats. For the most frequently used data sets, we have written conversion programs to translate data sets in the General Library to the equivalent data sets in the Standardized Library. About 60 data sets have been archived this way; they contain (1) hypocenter data files from the International Seismological Center, (2) hypocenter and phase data files from Caltech, and (3) hypocenter and phase data files from USC.

We are also in the process of setting up a Waveform Library to deal with the voluminous digital seismic data.

Reports

Blumling, P., Mooney, W. D., and Lee, W. H. K., 1983, Structure of the southern calaveras fault zone, central California, (Abstract), EOS, 64, p. 762.

Northern and Central California Seismic Network Processing

9930-01160

Fredrick W. Lester
Branch of Seismology
U.S. Geological Survey
345 Middlefeld Road M/S 977
Menlo Park, California 94025
(415) 323-8111, ext. 2149

Investigations

1. Signals from 433 stations of the multipurpose Northern and Central California Seismic Network (Calnet) are telemetered continuously to the central laboratory facility in Menlo Park where they are recorded, reduced, and analyzed to determine the origin times, magnitudes, and hypocenters of the earthquakes that occur in or near the network. Data on these events are presented in the forms of lists, computer tape and mass data files, and maps to summarize the seismic history of the region and to provide the basin data for further research in seismicity, earthquake hazards, and earthquake mechanics and prediction. A magnetic tape library of "dubbed" unprocessed records of the network for significant local earthquakes and teleseisms is maintained to facilitate futher detailed studies of crust and upper mantle structure and physical properties, and of the mechanics of earthquake sources.
2. Project personnel also conducted investigations of significant earthquakes or earthquake sequences that occurred in northern and central California.
3. Quarterly reports were prepared on seismic activity around Lake Shasta, Warm Springs Dam, the Auburn Dam site and New Melones Dam for the appropriate funding agencies.

Results

1. Figure 1 shows the seismic activity of Northern and Central California for the period October 1, 1983 through March 31, 1984. The 8442 earthquakes plotted are all reliable locations using 4 or more phase readings in the solution. The phase readings were obtained either by hand timing or by the Real Time Picker (RTP) or they are a combination of both sources. The Coast Ranges have been screened for quarrys and those data have been eliminated. Identification of quarrys in the Sierra Nevada Foothills is a constant problem so that all quarry data have not yet been eliminated from the catalog. We feel that the catalog of location data maintained by Calnet is relatively complete for earthquakes M 1.5 and larger.
2. Processing of data for the first half of calendar years 1978 and 1983 is nearly complete and those data will be open-filed in the summer of 1984.

3. Investigations into the cause of the May 2, 1983, magnitude 6.5 earthquake that occurred near Coalinga are currently underway. To date there have been more than 8000 aftershocks, the largest of which was a magnitude 6.2 event. Data from 7 to 10 aftershocks per day are currently being processed. Results and conclusions from this investigation will be included in an U.S.G.S. Professional Paper to be published in the spring of 1985.
4. As a result of the Volcano Hazards Notice released on May 27, 1982, for the Long Valley caldera (LVC) area of eastern California special attention has been placed on the monitoring of seismic activity. Since October 1, 1983, 1737 earthquakes have been located in this region. Most of the earthquakes have been located outside the caldera in a broad zone extending 20 to 25 kilometers to the south.

Seismic activity within the caldera has been characterized by low level seismicity which is occasionally punctuated by small swarms. These swarms last only a few minutes and produce a few tens of events, most of which are less than magnitude 1.0. The largest events in LVC for the report period were two magnitude 3.2 events, one in November in the south moat area, 7 kilometers southeast of Mammoth Lakes and the other in February under Mammoth Mountain.

5. On January 23, 1984 a moderate earthquake (M_L 5.0) occurred 25 kilometers south of Monterey. It was followed by 38 aftershocks, the largest of which was magnitude 4.6. This aftershock occurred 79 minutes after the main shock, in essentially the same location. A focal mechanism for the main shock and the location of the main shock and aftershocks indicate that right lateral strike-slip movement probably occurred on the northwest trending Palo-Colorado Fault. These events occurred in an area where there has been little seismic activity in the last 10 years.
6. Focal mechanisms based on first motion directions were determined for six of the largest earthquakes that occurred near the coast of California between Santa Barbara and Monterey from 1978 to 1984. For this study appropriate records from both the northern California and southern California telemetered networks were played back from magnetic tape and were read for P-wave onset times and first motion directions, S-wave onset times (when legible), and maximum wave amplitudes and associated periods. Hypocenter determinations were based primarily on P-wave onset times and were calculated by the program HYPO 71 (Lee and Lahr, 1975). The crustal model used for each event was adjusted in an iterative process wherein it was sought to minimize the root-mean-square of onset time residuals as well as to separate the fields of compressions and dilatations of the first motion plots to permit double couple focal mechanism solutions. Except for one earthquake, which occurred in a region of very abrupt lateral variation in the thickness of the low speed sedimentary section, station time corrections were all set equal to zero in the determination of hypocenters. Magnitudes were computed (by HYPO 71) from maximum amplitudes and associated periods by reducing the recorded amplitudes to equivalent Wood-Anderson amplitudes, which were then used with Richter's zero-magnitude-earthquake amplitude versus distance relationship to determine the magnitudes.

The focal plane solutions of the earthquakes show a steady change in character in accordance with the location of the earthquakes. For the choices of fault planes selected, the corresponding progression in style of faulting from south to north is from left lateral reverse oblique, through simple reverse, to right lateral reverse oblique, and finally to right lateral strike slip. The three southernmost earthquakes, which lie in the Transverse Ranges, resulted from predominantly reverse faulting. The southernmost of the northern three quakes results from oblique faulting with nearly equal reverse and right lateral components. The two northernmost quakes resulted from nearly pure right lateral strike slip faulting.

7. A report indicating the seismic activity for October through December 1983 around Lake Shasta, Auburn dam site, and the New Melones Dam has been sent to the Bureau of Reclamation and one is being prepared for January through March 1984. No unusual or significant activity has occurred in any of these areas during those time periods.

A report indicating seismic activity around Warm Springs Dam for October through December 1983 has been sent to the Corps of Engineers. One is being prepared for January through March 1984. No unusual or significant activity has occurred in this area during these time periods.

Reports

Cockerham, R. S., 1983, Evidence for a 180-km-long subducted slab beneath northern California, BSSA (in press).

Eaton, J. P., Cockerham, R. S., and Lester, F. W., 1983, Study of the May 2, 1983 Coalinga earthquake and its aftershocks, based on the U.S. Geological Survey seismic network in northern California in California Division of Mines and Geology Special Publication 66, p. 261-268.

Savage, J. C., and Cockerham, R. S., 1983, Earthquake swarm in Long Valley caldera, California, January 1983: Evidence for dike intrusion, JGR (in press).

NORTHERN CALIFORNIA SEISMICITY

OCTOBER 1983 - MARCH 1984

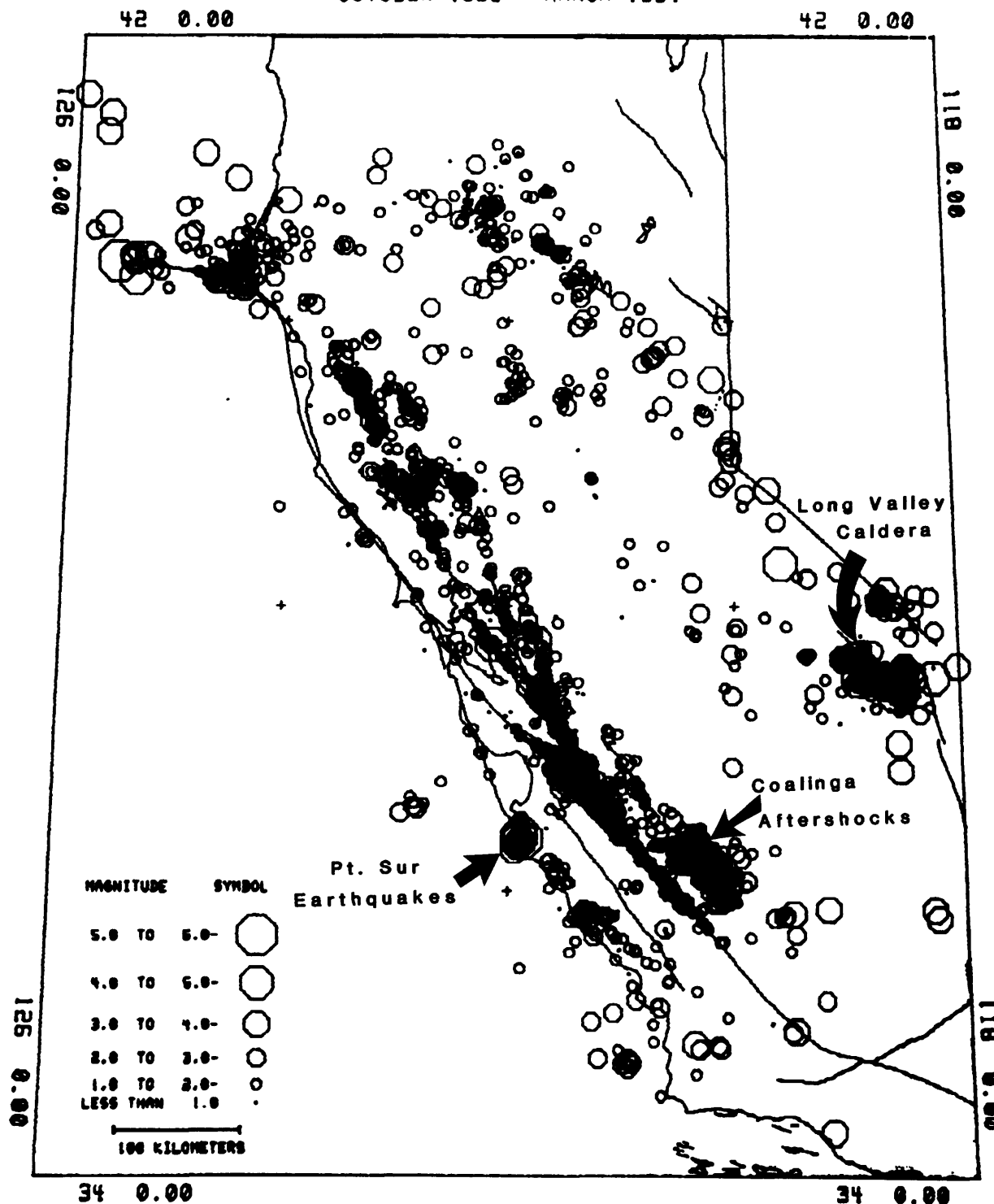


FIGURE 1

FAULT ZONE TECTONICS

9960-01188

Gerald M. Mavko, Beth D. Brown, Sandra S. Schulz
Branch of Tectonophysics
U.S. Geological Survey
345 Middlefield Road, MS/977
Menlo Park, California 94025
(415) 323-8111 x 2763

Investigations

1. Directed maintenance of creepmeter arrays in California.
2. Updated archived creep data on PDP 11/44 computer.
3. Continued to work on developing experimental procedures aimed at an operational prediction program.
4. Maintained and upgraded earthquake alinement array network on central and northern California faults. Expanded existing network to include selected southern California faults.
5. Monitored effects on April 24, 1984, Morgan Hill earthquake on creep near Hollister.
6. Submitted for publication results of study on the effects of the 1983 Coalinga earthquake on central California creepmeters along the San Andreas fault.

Results

1. Currently 28 extension creepmeters operate; 20 of the 28 have on-site strip recorders; and 18 of the 20 are telemetered to Menlo Park (locations shown on Figure 1).
2. Fault creep data from all 28 USGS creepmeter sites on the San Andreas, Hayward and Calaveras faults have been updated (through January 1984) and stored in digital form (1 sample/day).
3. A computer program was completed to process the new alinement array data. A computer program to perform statistical manipulations on long-term creep data was begun.
4. Currently 24 alinement arrays (locations shown in Figures 2, 3) have been established and surveyed across active faults in California. New arrays were installed at Middle Mountain near Parkfield on the San Andreas fault, and in

the San Felipe Valley near San Jose on the Calaveras fault. Each site will be remeasured approximately every 90-120 days. The arrays will be used for siting and checking creepmeters as well as for monitoring fault creep where creepmeters are impractical or logically impossible. Expansion of the alinement network will continue as is practical. Results are being computed and analyzed.

5. USGS creepmeters on both the Calaveras and San Andreas faults near Hollister recorded small right-lateral steps of from 0.11 to 0.33 mm at the time of the Morgan Hill earthquake (magnitude 6.2) on April 24, 1984. The earthquake occurred in an area not covered by our network, and the closest creepmeter was Shore Road (SHR1), 50 km distant (Figure 4). Nevertheless, 22 minutes after a small right-lateral coseismic step, SHR1 began a 12.9 mm creep event, one of the largest continuous events seen in 15 years of data from the network. The event had a rise time of 2 hours with a gradual decay over the next 16 hours, and was followed by a return to slight right-lateral creep (Figure 5).

SHR1 also responded to the August 6, 1979, magnitude 5.9 Coyote Lake earthquake 15 km distant. This response ended a three-year lag in movement at the station. However, no similar long-term lag preceded the April 24 earthquake.

Reports

Mavko, Gerald M., Sandra S. Schulz, and Beth D. Brown, Effects of the 1983 Coalinga, California, earthquake on creep along the San Andreas fault (submitted to BSSA, January, 1984).

Schulz, Sandra S., Gerald M. Mavko, Beth D. Brown, Response of creepmeters on the San Andreas fault near Parkfield to the May 2, 1983, Coalinga earthquake (submitted to USGS Professional Paper on Coalinga Earthquake, April, 1984).

stns -> only

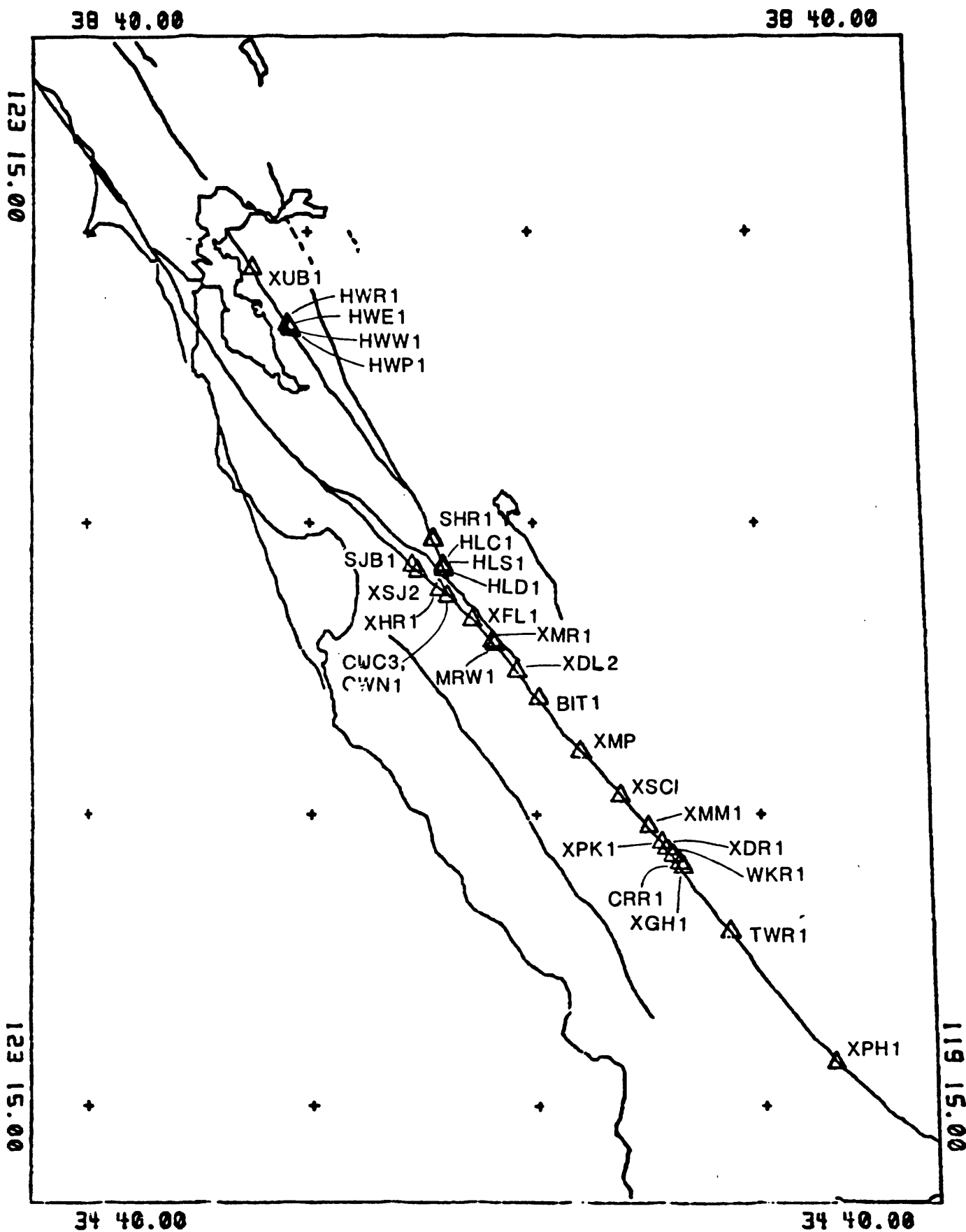


FIGURE 1

stns → only

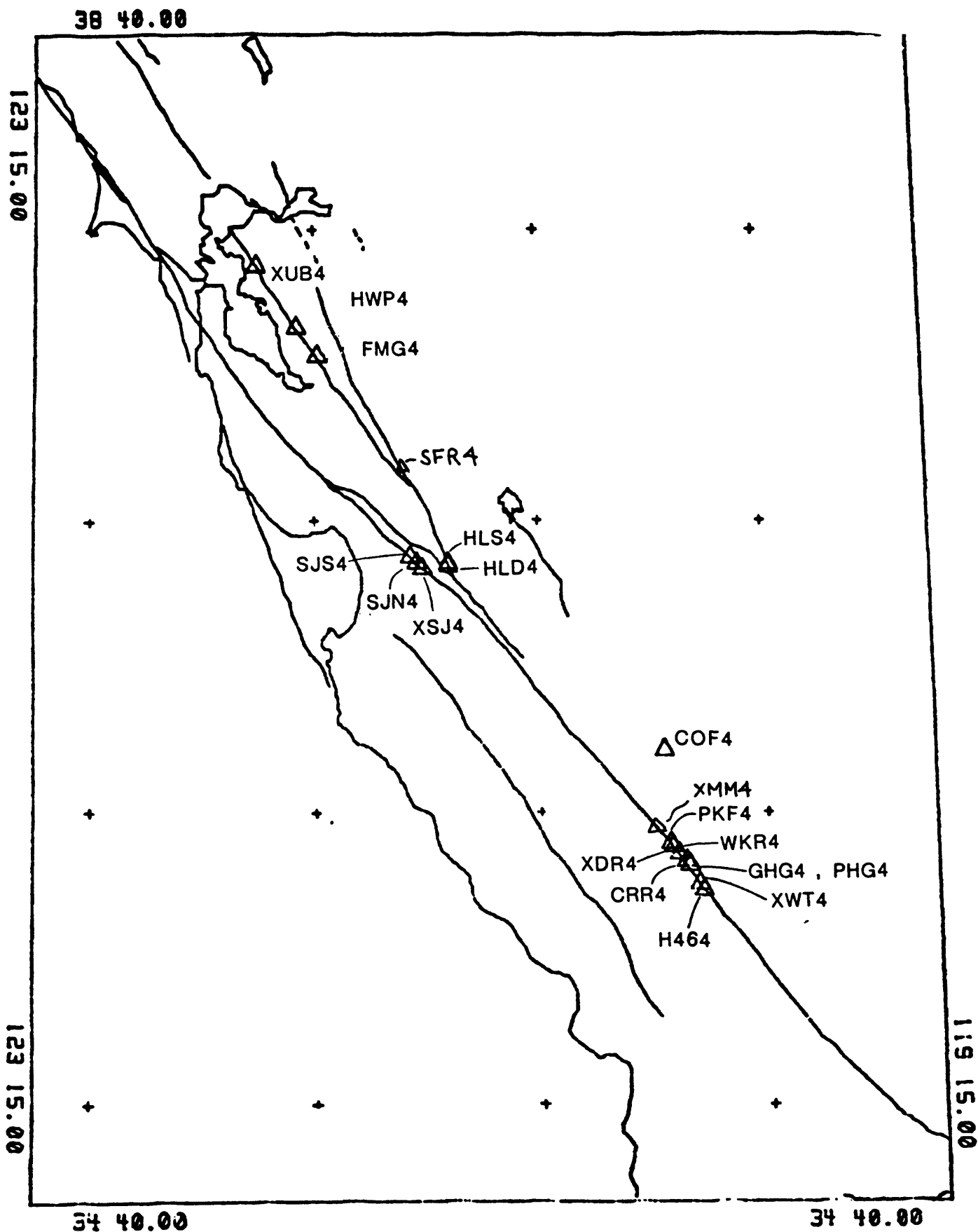


FIGURE 2

U.S.G.S THEODOLITE ALIGNMENT ARRAYS ACROSS MAJOR FAULTS IN
CENTRAL AND NORTHERN CALIFORNIA

IMPERIAL COUNTY

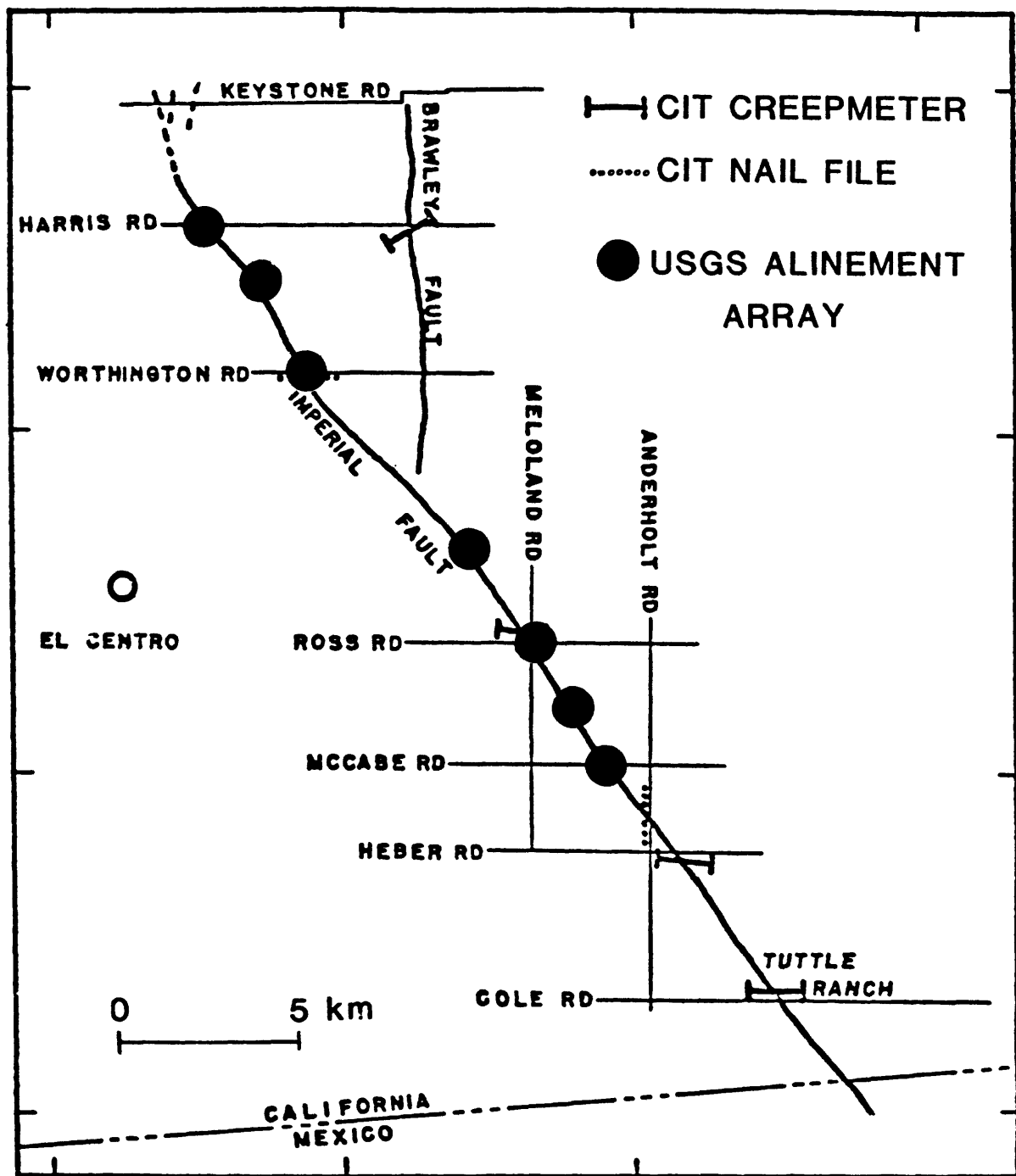


FIGURE 3

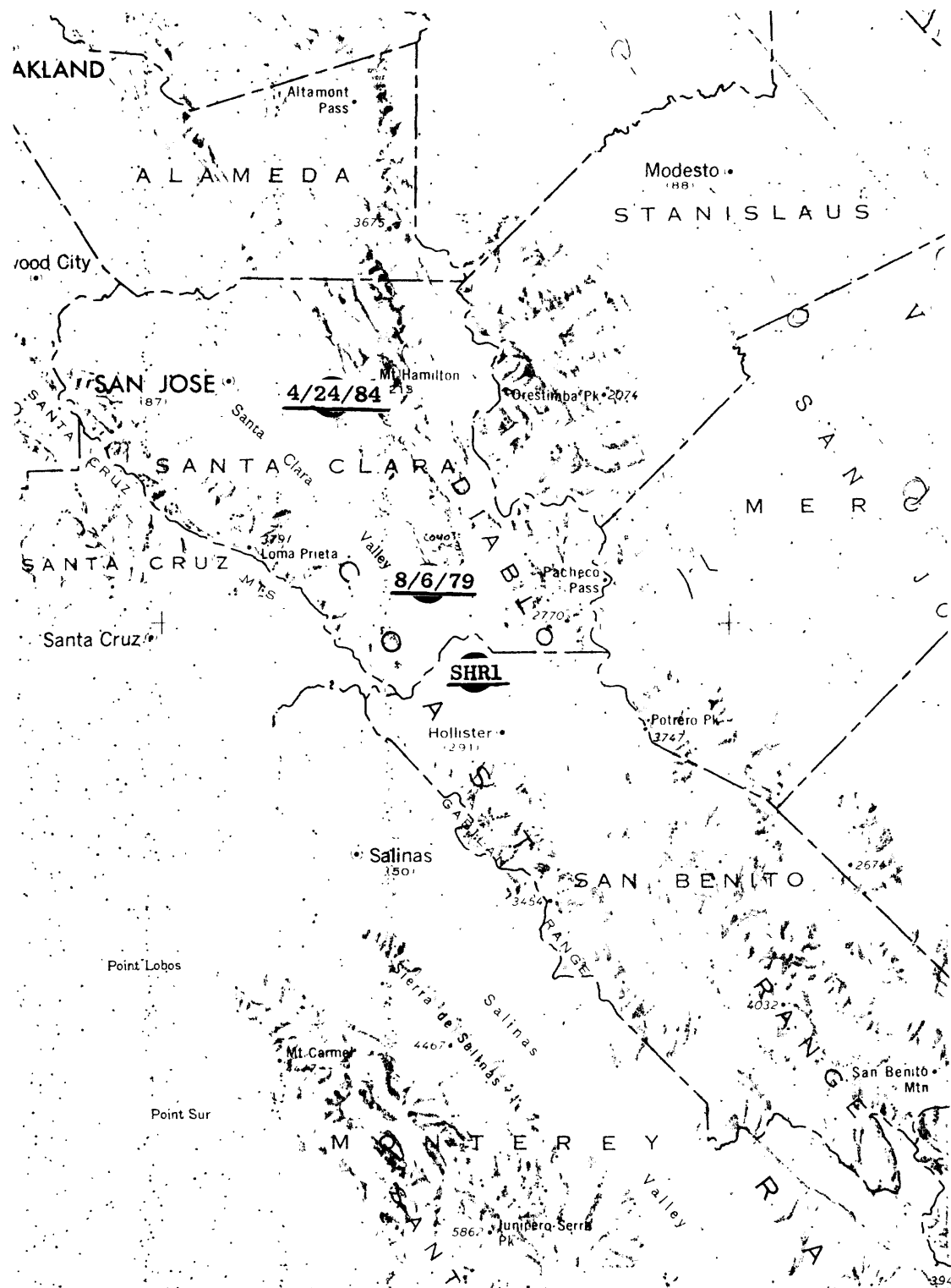
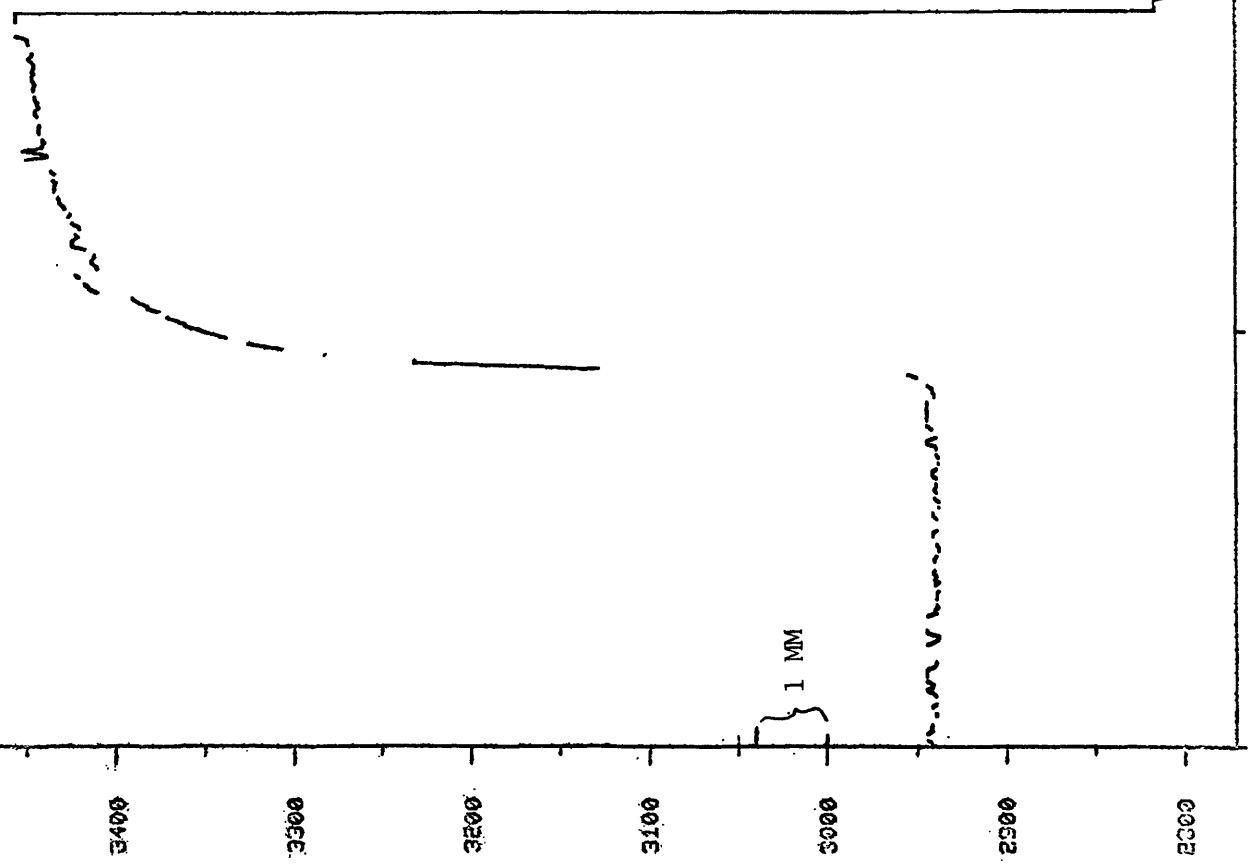


FIGURE 4

0 10 20 30 40 50 km



$$\begin{aligned} & \frac{3446}{-2944} \\ & \hline & 55 \div 9.13 = .071 \\ & = 12.9 \text{ mm} \end{aligned}$$

28

27

26

25

24

FIGURE 5

EXPERIMENTAL TILT AND STRAIN INSTRUMENTATION

9960-01801

C.E. Mortensen
Branch of Tectonophysics
U.S. Geological Survey
345 Middlefield Road, MS/977
Menlo Park, California 94025
(415) 323-8111, ext. 2583

Investigations

1. A direct readout ground station that receives telemetered data through the GOES West satellite has been procured from Sutron Corporation. A dish antenna five meters in diameter has been installed in the parking lot south of Building 8. Two coaxial cables carrying the down-converted satellite frequency and a reference frequency led into Building 7 to a set of demodulators and a multiplexer. The demodulated signals are fed to an 1123 computer that has been programmed by Jim Herriot to perform various data handling, storage and test functions as well as control the multiplexer. Currently the system is being run on the 1144 computer while the 1123 is being debugged.

Twenty-five Data Collection Platforms (DCPs) have also been procured from Sutron and are scheduled for delivery in May. The DCPs will collect data from a variety of sensors, digitize the data with 13-bit resolution and transmit through the GOES West satellite directly to the ground station in Menlo Park. We have worked out an agreement with the National Environmental Satellite, Data, and Information Service (NESDIS) whereby we will operate for a two-year trial period on an exclusively assigned channel. During this period we plan to demonstrate the feasibility of sampling and transmitting data at 10-minute intervals. This will result in a high-capacity system for telemetering data from a wide variety of geophysical sensors in nearly real time. Currently the direct readout ground station is recording data from 40 instrument sites transmitted at 3-hour intervals.

2. A heavy pier has been designed, in consultation with Jim Savage, John Langbein, and Mark Linker, to serve as a monument for the collimating reflector used by the 2-color laser experiment. Two such piers were installed in November, as part of the Long Valley 2-color net, by Savage, Liechti and Mortensen. Fifteen additional piers were procured by Mortensen, and he spent a week in January

installing two of these monuments in the Parkfield region with Bob Burford. In March and April, Rich Liechti spent three weeks with Burford installing eight more monuments.

In consultation with Linker and Langbein, the 2-color reflector has been redesigned. Parts have been ordered for a prototype.

3. A network of alinement arrays installed following the Imperial Valley earthquake of 15 October 1979 ($M=6.7$) by Harsh was resurveyed by Harsh in February 1984. The purpose of the resurvey was to provide additional geodetic control over a region identified by Bob Sharp as undergoing deformation.
4. Networks of tiltmeters, creepmeters and shallow strainmeters have been maintained in various regions of interest in California. A network of 14 tiltmeters located at 7 sites monitor crustal deformation within the Long Valley caldera. Other tiltmeters are located in the San Juan Bautista and Parkfield regions. Creepmeters are located along the Hayward, Calaveras and San Andreas faults from Berkeley to Parkfield and shallow strainmeters are located in the Parkfield region. Observatory type tiltmeters and strainmeters are located at the Presidio in San Francisco and a tiltmeter in the Byerley Seismographic Vault at Berkeley. Data from all these instruments are telemetered using 12-bit digital telemetry via phonelines and radio links to Menlo Park.
5. A set of five portable magnetometer systems have been assembled for Malcolm Johnston, who will be delivering them to the Chinese.
6. Vince Keller and Rich Liechti helped Doug Myren install a new dilatometer at Mammoth Lakes and maintain existing instruments near San Juan Bautista, near Parkfield and in the Mojave Desert.
7. After a hiatus in activity while a new student was sought for the project, the radio emissions experiment of the Naval Postgraduate School, Monterey, has been revived. All the equipment is tested and ready and field sites have been selected.

Results

1. Preliminary data from tiltmeters located within the Long Valley caldera show no significant tilt episodes over periods of minutes to several days since data were first recorded in September 1983. The tiltmeter data are of

sufficient quality that large tilt episodes having amplitudes on the order of 10 microradians and periods in the range of tens of minutes to days, as might be expected in the case of a dike intrusion, should be easily detected.

MAGNETIC FIELD OBSERVATIONS

9960-03814
 R. J. Mueller
 Branch of Tectonophysics
 U.S. Geological Survey
 345 Middlefield Road, MS/977
 Menlo Park, CA 94025
 (415) 323-8111 ext. 2533

INVESTIGATIONS

- 1) Investigation of total field magnetic intensity measurements and their relation to seismicity and strain observations along active faults in Central and Southern California.
- 2) Recording and processing of synchronous 10 minute magnetic field data and maintenance of the 25 station telemetered magnetometer network and telemetry system in Central and Southern California.
- 3) Processing and analysis of on-site recorded data from the 64 station portable magnetometer network in California.

RESULTS

1) A linear regression of differential proton magnetometer measurements at distances from a few meters to 50 kilometers indicates a standard deviation of hourly means that varies with site separation as $\sigma = a + bd$ where $a = 0.007 \pm 0.02$ nT, $b = 0.01 \pm 0.003$ nT/Km and d is the site separation in kilometers (figure 1). At a few meters separation, at sites with low cultural noise in both seismically active and inactive regions, the standard deviation of hourly mean data range from 0.09 and 0.15 nT for instruments with 0.25 nT sensitivity and from 0.07 and 0.08 nT for instruments with 0.125 nT sensitivity. The least-count noise contributions are expected to be less than 0.07 nT and 0.03 nT, respectively, while undetermined instrument noise appears to contribute 0.05 nT. Instrument temperature sensitivity does not exceed 0.001 nT/ $^{\circ}$ C over a range from -6 $^{\circ}$ C to 21 $^{\circ}$ C. For typical site separations of 10 to 15 Km throughout the San Andreas fault, estimates of σ for hourly mean data range from 0.15 to 0.3 nT depending on local magnetization characteristics.

To determine measurement precision at high frequencies (> 4 c.p.d.) we have compared data from U.S.G.S. operated proton precession magnetometers (PMs) with collocated self-calibrating rubidium magnetometers (SCRs) operated by R. H.

Ware from CIRES, University of Colorado. The SCRs have better sensitivity and higher accuracy than the PMs. Exact comparison of data from the two types of instruments is not possible due to the inherent differences in their measuring techniques. The SCR instruments measured the field continuously, and average over a selected period while the PM instruments measure the field during a 1.5 second period at selected intervals greater than 7.5 seconds.

The SCRs and PMs were operated at sites separated by 13 Km along the San Andreas fault in Central California. The PMs recorded 1.5 second averages at a 15-second interval and the SCRs recorded continuous 10-second averages. The power spectral density for both data (figure 2) indicate the SCRs exceed the resolution of the 0.125 nT PMs by up to an order-of-magnitude for periods less than 2 minutes (720 cycles/day). Both systems are equivalent at periods greater than 3.5 minutes (420 cycles/day).

The optimum designed network for the PM instruments would be 5 to 6 Km site separations and a 3 to 4 minute sample interval. The present U.S.G.S. magnetometer network has a typical site separation of 10 to 15 Km and a 10 minute sample interval which is a suitable compromise to allow greater regional coverage, and to reduce data storage and processing.

2) Vince Keller has completed construction of five on-site magnetometer systems. These systems and laser distance measuring equipment are to be furnished to the Peoples Republic of China as part of the current exchange program. The equipment will be operated by Chinese scientists in an effort to monitor crustal deformation near the northern end of the Red River fault in Yunnan, Province and near the Da chang fault near Beijing.

3) We have completed conversion of 19 of the 25 telemetered magnetometer stations to solar charged battery systems. The conversion will enable lower station maintenance, lower operating costs, and the ability to power satellite telemetry.

4) A third telemetered magnetometer station was installed in the Long Valley region. The station is located 15 Km SE of the Long Valley caldera at a previous portable magnetometer location. The station is intended as a reference to the two telemetered stations operating inside the caldera.

REPORTS

Davis, P. M., Pierce, D. R., McPherron, R. L., Dzurisin, D., Murray, T., Johnston, M. J. S., and Mueller, R. J., A volcano-magnetic observation on Mount St. Helens, Washington: Geophys. Res. Lett., vol. 11, no. 3, pp. 225-228, 1984.

Ware, R. H., Johnston, M. J. S., and Mueller, R. J., The detection threshold for tectonomagnetic events: J. Geomag. Geoelec., in press, 1984.

Johnston, M. J. S., Mueller, R. J., and Davis, P. M., Precision of magnetic measurements in a tectonically active region: J. Geophys. Res., in press, 1984.

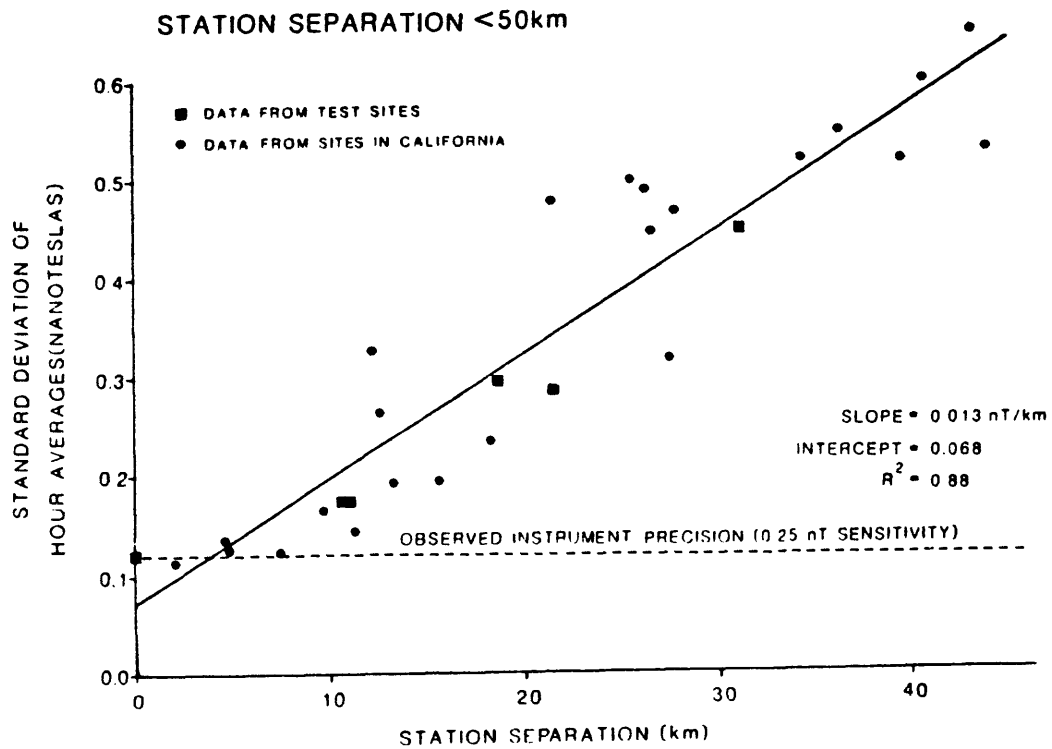


Figure 1. Summary plot showing the increase in standard deviation of hourly averages of all field differences with increasing station separation up to 50 Km.

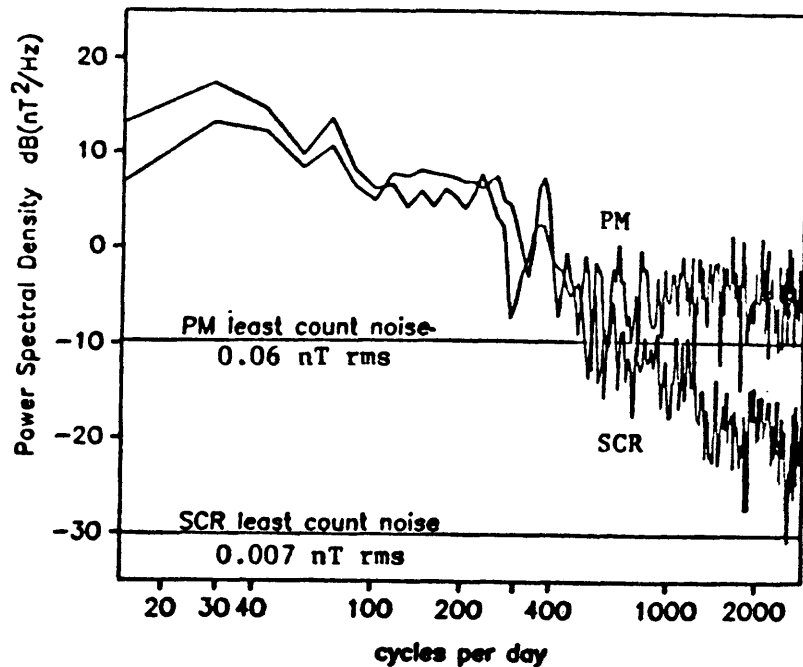


Figure 2. Power spectral density of magnetic field differences over a 13 Km baseline. The 0.125 nT least count PM data were observed every 15 seconds. The SCR data are consecutive 10-second field averages.

Dilatometer Network Operations

9960-03815

G. Douglas Myren
Branch of Tectonophysics
U.S. Geological Survey
345 Middlefield Road, MS/977
Menlo Park, California 94025
415-323-8111, ext. 2705

Investigations

1. In October of 1983 dilatometer's were installed at Devils Postpile near Mammoth Lakes and Devils Punchbowl near Pearblossom, California in the Mojave Desert.

The hole for the Mammoth instrument was drilled by a crew headed by Dave Wylie and John Singer of the Water Resources Division out of Santa Barbara. Alan Linde from Carnegie Institute and Doug Myren looked at core samples taken from a granite hole drilled in 1973 by the U.S.G.S. Geothermal Project. From these cores a site was picked 50-100 ft from this hole and drilled to a depth of 560 feet. An instrument of Y4 the normal sensitivity was installed at a depth of 520' by Alan Linde, Doug Myren, Bob Mueller, and Rich Liechti.

Shortly after this installation a 606' hole was drilled in Devils Punchbowl sandstone near Pearblossom, California by a crew from the Geologic Division, Tectonics Branch, headed by Dennis Styles. This instrument of normal sensitivity was installed at a depth of 577' by Alan Linde, Doug Myren, Dennis Styles, and the drill crew.

Holes at both locations were cemented to the surface. Telephone lines were ordered and the instruments were allowed to cure.

The Mammoth Lakes instrument will be telemetered in the summer of 1984 after snow melts and the Pearblossom instrument will be operating by the end of May.

In November enclosures were ordered and electronics tested for installation at Searle Road and Gold Hill for telemetering of data to Menlo Park of those instruments installed in July and August of 1983.

These instruments were put on line with barometric pressure in December 1983 and January 1984 and by February the bugs

were worked out of the electronics.

In late February the electronics at instruments in the Mojave were changed to a more temperature stable, and more environmentally sound package. At this same time crystal-air, which is believed to have water in the cable head, was rewired by Doug Myren and Malcolm Johnston with Carnegie supplied electronics and is now transmitting both strain and downhole pressure.

In March after calibration of new DC/DC regulated power sources, Gold Hill 1 and 2, Searle, and Echo Valley were put on Solar power. The instruments in the Mojave will also be put on solar power.

Also in March Fred Fischer assembled and calibrated 2VCO's for telemetering of short-period seismic data from Gold 1 and 2. Doug Myren put these in and after some telephone line problems finally calibrated these through the system (on site dilatometer electronics, VCO, telephone line, discriminator, tape). Both lab and field calibrations agreed.

Ongoing paper change, electronics trouble-shooting, telephone line problems and general maintenance were done during this time.

Malcolm Johnston and Roger Borcherdt attached a GEOS seismic data retrieval system to the Searle Road instrument and were able to better define the sensitivity range of the Searle Road dilatometer and determine the frequency spectrum of the short-period notchfilter.

Information is now being gathered for siting of 3 additional instruments in Parkfield for late July of 1984.

Results

Data from existing sites is being reduced by Malcolm Johnston and Al Lindh.

Post-Earthquake Shaking Effects and Fault Creep

9910-03027

Robert Nason
Branch of Engineering Seismology and Geology
U. S. Geological Survey, MS-977
345 Middlefield Road
Menlo Park, California 94025

Investigations

1. Analysis of the seismic intensity effects of the 1906 California earthquake has continued, particularly for improved reliability of intensity indicators with regard to the seismic shaking.

Results

1. It appears that the highest reliability occurs in the statistical damage to the many chimneys in large towns.
2. Good data on chimney damage is available for 41 large towns in the 1906 earthquake, located both on bedrock and in alluvial valleys.
3. The data show that within 20 km of the fault, the statistical chimney damage was as great or greater at towns in the bedrock hills than at towns in the alluvial valleys.
4. At more than 20 km from the fault, the statistical chimney damage was somewhat greater in the alluvial valleys than in the bedrock hills.

Reports

None.

Global Seismograph Network Evaluation and Development

4-9920-02384

Jon Peterson
Branch of Global Seismology and Geomagnetism
U.S. Geological Survey
Building 10002, Kirtland AFB-East
Albuquerque, New Mexico 87115
(505) 844-4637

Investigations

Work contained in accordance with the Protocol Agreement between the State Seismological Bureau (SSB) of the People's Republic of China and the U.S. Geological Survey (USGS), in which the USGS is assisting in the establishment of the China Digital Seismograph Network (CDSN).

Results

Meetings of USGS and SSB technical personnel were held in Beijing to coordinate activities. Several of the station sites (Beijing, Urumqi, Lanzhou, and Mudanjiang) were visited to inspect facilities and meet station personnel. A location was selected for the borehole at Lanzhou. Preliminary design work was completed and contracts have been awarded for hardware for five data systems, the data management system, and a depot maintenance center. Assembly of a demonstration system is underway. Export licenses have been received for the equipment. Plans for the second half of the fiscal year include the final assembly and testing of the demonstration system and data management system, training of SSB personnel in the United States, and assembly of four additional field systems.

CRUSTAL STRAIN

9960-01187

W.H. Prescott, J.C. Savage, M. Lisowski, and N. King
Branch of Tectonophysics
U.S. Geological Survey
345 Middlefield Road, MS/977
Menlo Park, California 94025
(415) 323-8111, ext. 2701

Investigations

The principal subject of investigation was the analysis of deformation in a number of tectonically active areas in the western United States.

1. Morgan Hill, California Earthquake of 24 April 1984

The epicenter of the Hall's Valley earthquake of 24 April 1984 was within 5 km of one end of a geodetic line that has been measured monthly during the past two years. There were measurements of the line length 1 day and 8 days prior to the earthquake. None of the preearthquake measurements is unusual. Dislocation modeling of the rupture surface suggests that less than 70 mm of preseismic slip could have occurred on the rupture surface prior to the earthquake. A small aperture geodetic network located 5 km northwest of the epicenter was observed 2 weeks prior to the event. It indicated no detectable preseismic surface slip had occurred. A dislocation model for the earthquake suggests that the event involved about 420 mm of slip on a surface defined by the aftershocks. Slip on the fault near the surface in Hall's Valley during the event was at most about 8 mm. As of the first week in May no detectable postseismic slip has been observed either at depth or at the surface.

2. Time History of the Line Llagas to Sheep

A geodolite line between station Llagas near Morgan Hill, California and station Sheep near Coyote Lake, California has observations spanning both the 1979 Coyote Lake earthquake and the 1984 Morgan Hill earthquake (Figure). A coseismic step of 10 mm occurred during the Coyote Lake earthquake. During the 18 months following the earthquake the line changed by a further 35 mm before slowing down to approximately its pre-Coyote Lake rate. During the Morgan Hill earthquake the line changed by 20 mm. It is too soon to know what the post-Morgan Hill effects will be. This

record as well as data from short range networks (Lisowski and King, unpub. ms.) make it clear that slip, probably in the upper part of the fault plane, occurred at a decreasing rate for more than one year after the 1979 Coyote Lake earthquake. No unusual signals were detected prior to either earthquake.

3. Deformation in the White Mountain Seismic Gap, California-Nevada, 1972-1982

A 100 km by 4 km trilateration network extending from Bishop, California, to near Hawthorne, Nevada, crosses the east end of the Long Valley caldera, site of renewed magma inflation in the 1979-1980 interval, and spans most of the White Mountain seismic gap. The network was surveyed in 1972, 1973, 1976, 1979, 1980, and 1982. The 1980 survey seems to have a -0.5 ppm scale error, presumably due to instrument miscalibration. Leveling surveys across the caldera have been run in 1932, 1957, 1975, 1980, 1982, and 1983. Interpretation of the observed deformation is complicated by the May, 1980, Mammoth Lakes earthquake sequence (four earthquakes $M_L > 6$) just south of the caldera. Most of the deformation can be accounted for by 0.10 to 0.15 km³ expansion of a magma chamber 8 to 10 km beneath the resurgent dome within the Long Valley caldera sometime between July 1979 and September 1980 with an additional expansion of perhaps 0.05 km³ between September 1980 and July 1982. Minor normal slip (0.11 m) on the Hilton Creek fault is also required. Additional sources of deformation within the aftershock area of the Mammoth Lakes earthquake sequence are required to fit the observed horizontal deformation. About 1 m of right-lateral slip on each of three 10 km square faults provides the required additional horizontal deformation for the 1979-1982 interval. The faults extend WNW from the epicenters of the first, third, and fourth main events in the Mammoth Lakes sequence; the second event in that sequence lies on the same fault as the first event. The same model with less slip on the three strike-slip faults provides adequate fits to the 1979-1980 and 1980-1982 deformation. Other sources within the aftershock zone could probably explain the residual deformation as well, but it does appear that inflation of a magma chamber beneath the resurgent dome is required in any model.

4. Monitoring Deformation in the Long Valley Caldera, Eastern California, 1983-1984

Deformation in the Long Valley caldera has been monitored since October 1983 by monthly surveys of five, L-shaped, 1-km aperture leveling arrays and three, 10-km-long,

geodimeter lines. No significant ($\pm 2\mu\text{rad}$) tilt has accumulated in any of the leveling arrays in the six-month interval. The geodimeter lines extend from a hill near Casa Diablo Hot Springs to the top of Mammoth Mountain, (12.1 km WSW) to Lookout Mountain (10.4 km NNW), and to a point along Highway 395 (8.2 km ESE). An airplane is flown along these lines at the time of ranging to measure temperature and humidity required for the refractivity correction. The only significant line-length change occurs on the line to Lookout Mountain which appears to be lengthening at the rate of 40 mm/a.

5. Deformation in the "Big Bend" Region of the San Andreas Fault, 1973-1983

Analysis of data from a large trilateration network shows strain differences between the northwest section spanned by the Garlock fault, and the southeast section spanned by the San Andreas fault. For the northwest section, principal strain rates are $\dot{\epsilon}_1 = 0.11 \pm 0.02 \mu\text{strain/yr}$ and $\dot{\epsilon}_2 = -0.06 \pm 0.02 \mu\text{strain/yr}$, with the 1 axis directed N93°E. For the southeast section, principal strain rates are $\dot{\epsilon}_1 = 0.14 \pm 0.02 \mu\text{strain/yr}$ and $\dot{\epsilon}_2 = -0.16 \pm 0.02 \mu\text{strain/yr}$, with the 1 axis directed N73°E. The best fitting dislocation model requires 20 mm/yr slip at depth on the San Andreas fault and 8 mm/yr slip at depth on the Garlock fault, below 15 km in both cases. However, locking depth is not well-constrained by this data, and other depths would fit almost as well.

6. Deformation in the Central Mojave Desert, 1979-1983

A trilateration network spans late-Cenozoic right-lateral strike-slip faults in the Mojave Desert block in California. Dokka, 1983, reports 9.8 - 12.2 km cumulative right-lateral displacement across the Camp Rock and Calico faults over the past 20 million years. Analysis of trilateration data shows no clear pattern of displacement and overall strain rates are negligible. However, there is a marginally significant increase in fault-parallel right-lateral shear between early and late 1980.

7. Deformation near Parkfield, California, 1970-1983

The Parkfield, California region is the transition zone between the central creeping section of the San Andreas fault and the southern locked zone. Data from small and large aperture trilateration networks allows us to distinguish the effects of creep and slip at depth. Surface slip decreases to the southeast from 22 mm/yr near Slack Canyon, at a rate of about 1/2 mm/yr/km. Shear strain

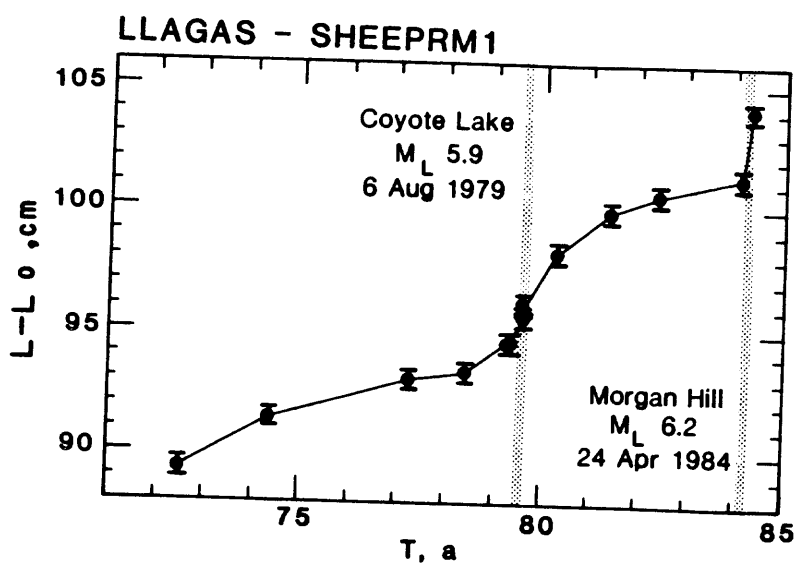
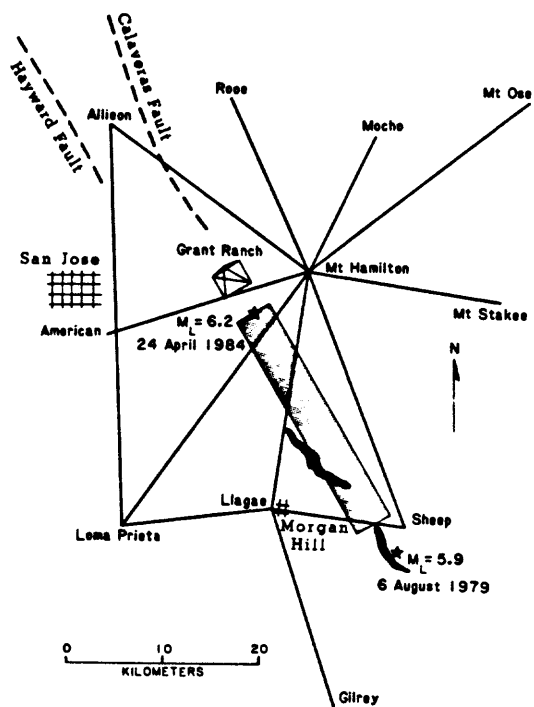
rates from two broadscale trilateration networks, one in the transition zone where creep dies out and the other in the locked zone, fit the same profile of fault-parallel shear. The shear strain rate decreases as distance from the fault increases, and the values are consistent with 32 mm/yr slip at depth below 16 km. The depth agrees well with the deepest earthquake depths. The slip rate is consistent with estimates of relative plate motion in the creeping zone, which is presumably the rate of deep slip as well since no strain is observed in the creeping section. Thus this result suggests a simple model of constant deep slip through the creeping section, transition zone, and locked section.

Reports

Savage, J. C., Local gravity anomalies produced by dislocation sources, J. Geophys. Res., 89, 1945-1952, 1984.

Savage, J. C., Precision of Geodolite surveys: A reply to Jackson and Cheng, J. Geophys. Res., 88, 10478-10484, 1983.

King, N. E. and J. C. Savage, Regional deformation near Palm-dale, California, 1973-1983, J. Geophys. Res., 89, 2471-2477, 1984.



Seismic Studies of Fault Mechanics

9930-02103

Paul A. Reasenberg
U. S. Geological Survey
345 Middlefield Road, Mail Stop 977
Menlo Park, California 94025
(415) 323-8111, ext. 2049

Investigations

1. Analysis of the second-order moment (2-point correlation function) of the U. S. Geological Survey's central California earthquake catalog for the period 1969-1982 continued.
2. Analysis of the hypocentral distribution and fault-plane solutions of aftershocks of the M 6.5 earthquake near Coalinga, California, (May 2, 1983) continued.

Results

1. In the previous report we described an investigation into the structure of the second-order moment of central California seismicity. With the aftershocks in the catalog removed, the second-order moment was found to be consistent with a catalog Poissonian in time. We have since determined that the catalog's second-order moment (with the aftershocks removed) is consistent with a random spatial distribution as well. Space-time correlations are apparently absent. A crucial step in obtaining these statistics was the identification of the aftershocks. A new method was applied that recognizes clusters in space-time of any "shape", size and duration. A simple 2-event interaction model provides a basis for associations between proximate events; each resulting cluster is treated as statistically dependant on its mainshock. This method is efficient (fewer than half the events in the catalog are identified as dependant), and complete (essentially all two-point correllation is removed).
2. In the previous report we presented results from a preliminary study of the hypocentral distribution during the first 10 days of the 1983 Coalinga, Ca. earthquake sequence obtained from local (CALNET) P-wave arrival times. During the period covered by this report we began a more thorough study of the faulting surfaces activated during the entire 1983 sequence. We are using a) CALNET local P-wave arrivals at 24 stations within an 80-km radius; b) P-wave arrivals from 12 portable 3-component seismographs installed within 4 days after the mainshock within a 30-km radius; c) S-P times read from 11 portable digital (GEOS) wideband seismographs located directly above the aftershock zone. Using the combined data we are now in the process of obtaining hypocentral solutions with better depth control, and modeling the fault-plane orientations.

In order to obtain P-wave arrival times and first-motions from the vast amount of recorded portable instrument analog data, an analog tape playback system was fashioned and interfaced with an Allen/Ellis microprocessor picker (RTP). The system automatically reads analog tapes at 20 times real-time and provides precise P-wave arrivals and usefully accurate first-motion polarities.

Global Digital Network Operations

4-9920-02398

Robert D. Reynolds
Branch of Global Seismology and Geomagnetism
U. S. Geological Survey
Albuquerque Seismological Laboratory
Building 10002, Kirtland AFB-East
Albuquerque, New Mexico 87115
(505) 844-4637

Investigations

The Global Network Operations continued to provide technical and operational support to the SRO/ASRO/DWWSSN observatories which include operating supplies, replacement parts, repair service, redesign of equipment, training and on-site maintenance, recalibration and installation. Maintenance is performed at locations as required when the problem cannot be resolved by the station personnel. One digital technician was added to the Bendix O&M contract during this period to perform repair of replaceable modules. This brings the personnel level to a team leader, 3 field engineers, and a digital technician.

The DEC LA-12 matrix printers were shipped and installed at all SRO/ASRO stations. Assembly of modification kits was started for the SRO enhancement program. These kits will contain hardware and software for addition of two short period horizontal channels and the removal of six second notch from the long period filters.

The following station maintenance activity was accomplished:

ANMO - Albuquerque - SRO

Two maintenance visits

ANTO - Ankara, Turkey - SRO

Two maintenance visits

BCAO - Bangui, Central African Republic - SRO

One maintenance visit

CHTO - Chiang Mai, Thailand - SRO

Two maintenance visits

MAJO - Matsushiro, Japan - ASRO

One maintenance visit

SHIO - Shillong, India - SRO

One maintenance visit

TATO - Taipei, Taiwan - SRO

One maintenance visit

DWWSSN

SLR - Silverton, South Africa
One maintenance visit

ASL Repair Facility

A minimum amount of routine repair was done during this period due to maximum effort being performed in field work. Most of the repair facility effort was directed to testing and shipping the DEC LA-12 printers and S.P. filters.

Special Activity

The Global Telemetered Seismic Network (GTSN) noise survey started in the previous reporting period was completed in November 1983. The purpose of this survey was to find potential GTSN locations in South Africa, Kenya, and Ivory Coast.

Preliminary equipment determinations were done to resolve what is necessary to convert the WWSSN station at Scott Base, Antarctica, (SBA) from photographic data recording to helicorder (heated pen) recording.

Results

The digital network continues with a combined total of 30 SRO/ASRO/DWWSSN stations. The maximum effort is now to perform as much on-site maintenance and training as possible to provide the most quality digital data for the worldwide digital data base.

Project title: Systems Analysis of Geologic Rate Processes
Project number: 9980-02798
Principal
Investigators: Herbert R. Shaw and Anne E. Gartner
Name and address: U.S. Geological Survey
IGP Branch, MS 910
345 Middlefield Road
Telephone number: 415 323 8111 X 4169, 4170

Investigations:

Work continued on manuscript to compare Quaternary faulting rates and seismic moments in the United States and Japan. This work discusses the relationship between intraplate seismicity and density of Quaternary faulting according to the maximum moment model (Wesnousky and others, 1983). This model postulates that the seismic moment on a fault is released periodically in earthquakes of a characteristic size, M_0^{max} and that M_0^{max} is directly related to the length of the pre-existing fault. An important consequence of this fault model, if valid, is that earthquake frequency distributions for a region is a function of the regional patterns of fault length and slip rates. Data used in the analysis are from Open File Report 81-946 (Shaw and others, 1981) and Wesnousky and others (1982, 1983).

Shaw, H. R., A. E. Gartner, and F. Lusso, 1981, Statistical data for movements on young faults of the conterminous United States; paleoseismic implications and regional earthquake forecasting: U.S. Geological Survey Open File Report 81-946, 353 p.

Wesnousky, S. G., C. H. Scholz, and K. Shinazaki, 1982, Deformation of an island arc: Rates of moment release and crustal shortening in intraplate Japan determined from seismicity and Quaternary fault data: J. Geophys. Res., 87, p. 6829-6852.

Wesnousky, S. G., C. H. Scholz, K. Shimazaki, and T. Matsuda, 1983, Earthquake frequency distribution and the mechanics of faulting, J. Geophys. Res. 88, p. 9331-9340.

Consolidated Digital Recording and Analysis

9930-03412

Sam W. Stewart
Branch of Seismology
U.S. Geological Survey
345 Middlefield Road MS-977
Menlo Park, California 94025
(415) 323-8111 Ext. 2577

Investigations

The goal is to operate, on a routine and reliable basis, a computer-automated system that will detect and process earthquakes occurring within the USGS Central California Earthquake Network (also known as CALNET). Presently, the output from more than 425 short-period seismic stations is telemetered to a central recording point in Menlo Park, California. Two DEC PDP11/44 computers are used on this project (see Figure). The 11/44A is dedicated to the task of online, realtime detection of earthquakes and storing the waveforms for later analysis. The 11/44B is used for offline processing and archiving of earthquakes. Both computers have a 512 channel analog-to-digital converter, so the 11/44B can serve as backup to the online system whenever necessary.

Both computers use the RSX11M-PLUS (v2.1) operating system. Software has been developed largely by Carl Johnson in Pasadena, but with considerable modification by Peter Johnson, Bob Dollar and myself, to meet Menlo Park's specific needs. Our applications are all written in Fortran-77, but with heavy use of system functions unique to the RSX operating system.

Results

1. We point to January 3, 1984 as the day that the entire system became operational, though considerable software modification continues. At present 438 channels are being digitized at a rate of 100 Hertz per channel. For the three month period January-March we processed about 3700 events thru the system; this does not include noise events, which are discarded. We wrote about 65 archive tapes. These tapes contain the digitized waveform data, in binary format. Seismicity during this period was relatively low.

2. In order to minimize the number of false triggers that can be generated in monitoring a large network, the online system requires that small, overlapping subnets be defined. Typically, a subnet consists of 6-15 neighboring stations, and 4 to 6 station 'triggers' within a subnet are required for a subnet to be declared in a 'triggered' state. When a subnet is in a 'triggered' state, then the raw digitized waveform data for the entire network are saved on disk. We have divided CALNET into approximately 75 subnets. By comparing our detection summaries with those obtained by detailed visual

scanning of the Develocorder films, we have a basis for comparison of detection performance. This comparison technique has resulted in considerable refinement in our subnet definitions, and improvement in our detection capability.

3. Absolute time (UTC) to 0.01 seconds is maintained thru four separate sources. First, the serial analog signals from WWVB radio transmission and IRIG-E from an in-house time code generator (TCG) are digitized along with the incoming seismic data. There are software routines to decode these. Further, these digitized time series are always archived with the seismic traces. A third time base is derived from the parallel IRIG-E time code that is also generated by the TCG. This parallel time code is read whenever an event is detected, and the time is included in the header information associated with the event. This is known as a 'time stamp' for each event. A fourth time base is maintained simply by having a long-word integer counter that increments by one for each online buffer that is filled. This serves as a continuity check for the three, more precise time bases just described.

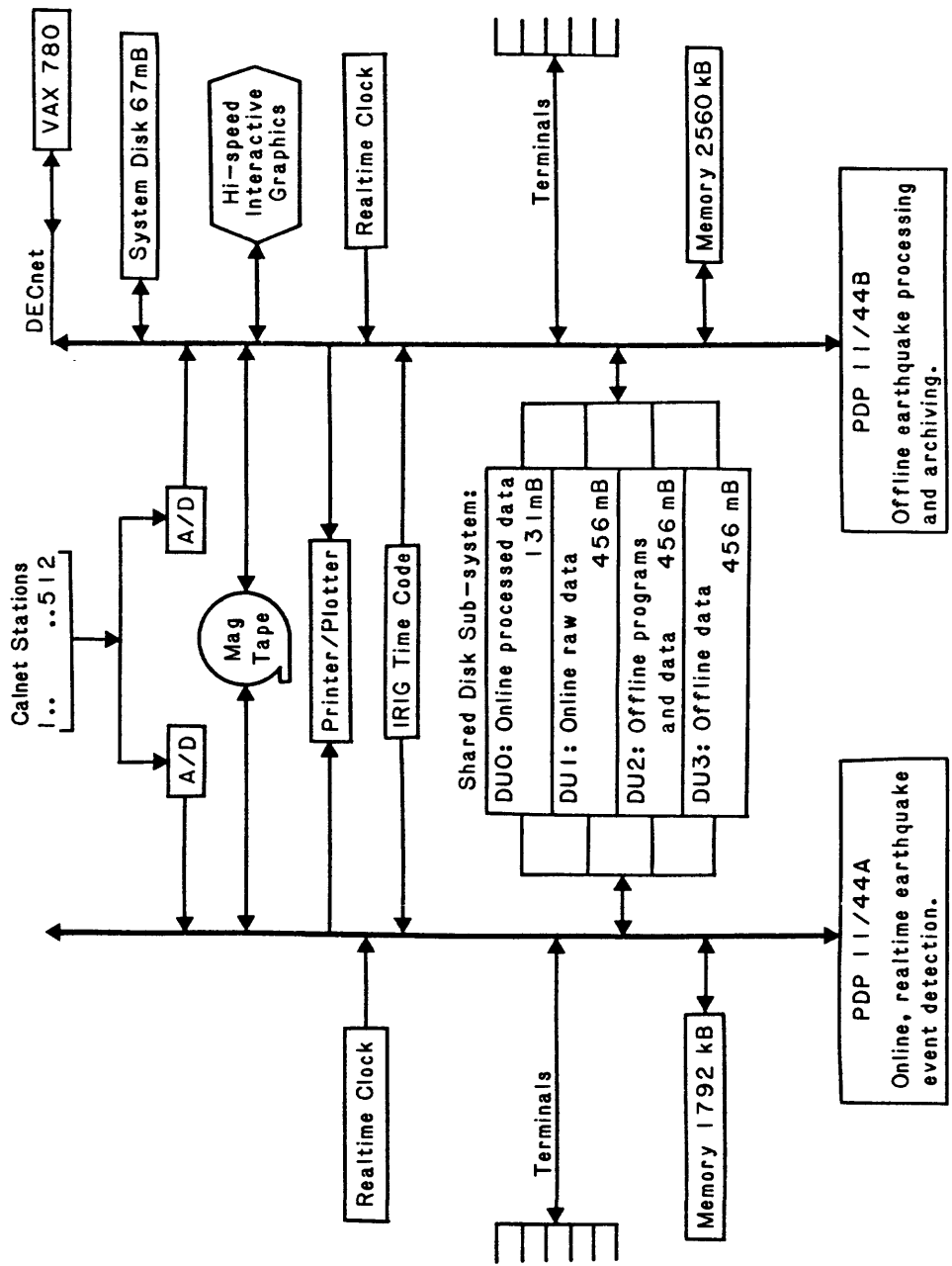
4. A major modification was made to the online system, in effect doing some pre-processing in its 'spare' time that previously was done by the offline system. It turns out that, during periods of normal seismicity, there is 'spare time' available. Because of this change, there is a noticeable increase in the thruput rate of data in the offline system. Briefly, the change may be described as follows:

Referring to the attached figure, disk DU1: accumulates the raw, unprocessed detected events. This disk is large enough to hold about 60 minutes total of data, before it starts to overwrite itself. Disk DUO: is considerably smaller. A transfer program was written (RRUN) that examines each raw event, one at a time. The program demultiplexes the raw data, deletes those traces that are not energetic, computes simple trace parameters such as bias and average amplitudes, decodes the serial time codes WWVB and IRIG-E, and sets up the appropriate files (on DUO:) to be ready for timing and further processing on the offline system. The RRUN program typically reduces the number of seismic traces from the 438 being digitized to less than 100, or even less than 50. As often as necessary, usually once or twice a day, the processed data on disk DUO: are copied onto disk DU3:, at which time they are available for the offline processing operations.

5. During periods of unusually high seismic activity, such as swarms or aftershock sequences, the RRUN program falls behind, and the raw data disk (DU1:) is in danger of being overwritten. A program was written (MFLING) that writes the raw event data out to magnetic tape. The 125 IPS speed of the tape drive is just fast enough that it is possible to keep up with the large number of raw detected events being written to DU1: (This writing process may have to be kept up around the clock; so far this hasn't happened.) When the seismic activity subsides, then these MFLING tapes can be read into the offline computer, where there are programs to process the events on them and prepare them for timing and archiving.

Reports

None.



Hardware Configuration for Earthquake Processing System
(Stewart 9930-03412)

National Earthquake Catalog

9920-02648

J. N. Taggart

Branch of Global Seismology and Geomagnetism
U.S. Geological Survey
Denver Federal Center, MS 967
Denver, Colorado 80225
(303) 234-5079

Investigations

1. Completed a compilation of intensity data for southern California earthquakes, 1932-1975.
2. Continued the development of an annotated bibliography of references on California earthquakes.
3. Completed a compilation of instrumentally recorded California earthquakes ($M = 5$, and larger) for 1910-present.
4. Completed a data base of historical and teleseismically recorded Alaskan earthquakes, 1786-1980.
5. Continued the development of a computer program with numerous data options for joint or relative magnitude determinations.

Results

1. Carol Thomasson and James Taggart verified, corrected and added intensity data to a Cal Tech compilation of 22,000 southern California earthquakes for 1932-1975. Corrections, mainly to intensify values, were made to 680 events and intensity values were added to 650 other events. The approximate origin times of several thousand additional earthquakes felt in California also were entered into the file. The file is now the most accurate and complete listing available of instrumentally recorded southern California earthquakes for this time interval.
2. Karen Meagher continued to develop an annotated bibliography of references to instrumentally recorded California earthquakes ($M = 5$, or larger) that occurred from 1910 to the present. The bibliography, doubly listed by source or author and chronologically by earthquake, highlights important references and also identifies poorly known sources of information.
3. Meagher completed a compilation of event and phase data for instrumentally recorded California earthquakes ($M = 5$, and larger) for 1910-present. Excluding offshore events, the list probably is complete at $M = 6$, and larger, for that entire range of time, and at $M = 5$, and larger, since 1930.
4. Taggart and Thomasson completed the compilation of a database of historical and teleseismically recorded Alaska earthquakes, covering the period from 1786-1982. The database contains listings of 17,700 events with separate references and estimated uncertainties for all parameters. The database also contains 11,200 duplicate listings, which can be used for statistical comparisons with the primary listings. Listings of 12,000 small earthquakes, located with data from regional networks, currently are available for merging into the database file.

5. Taggart continued the development of a computer program for the determination of joint and relative magnitudes of earthquake swarms or aftershock sequences. The attenuation model and joint magnitude technique of von Seggern Bulletin Seismological Society of America, 1973, p. 827) are used to estimate station and event corrections, attenuation coefficient and constant term for limited or non-uniform data sets. Several optional substitutions of calibration corrections or standardized attenuation coefficients provide flexibility, simplify the normal equations, and reduce standard errors compared with uncorrected data.

GEODETIC MODELING AND MONITORING

9960-01488

Wayne Thatcher
Branch of Tectonophysics
U.S. Geological Survey
345 Middlefield Road, MS/977
Menlo Park, California 94025
(415) 323-8111, ext. 2120

Investigations

Analysis and interpretation of repeated geodetic survey measurements relevant to earthquake-related deformation processes operative at or near major plate boundaries. Principal recent activities have been:

1. A study of Quaternary and modern deformation produced by earthquakes near Coalinga, California and a comparison with similar earthquakes in fold/thrust belts elsewhere in the world.
2. A review of the role of geodetic survey measurements in the study of active tectonic processes and the relation of these present-day measurements to geological measures of recent deformation.

Results

1. The 2 May 1983 Coalinga, California, $M_s = 6.5$ earthquake failed to rupture through surface deposits and, instead, elastically folded the top few kilometers of the crust. We estimate the subsurface rate of fault slip and the earthquake repeat time from seismic, geodetic, and geologic data, and show that other thrust faults concealed beneath active folds have generated earthquakes of $M_s \leq 7.5$. (R.S. Stein and G.C.P. King).
2. The cyclic buildup and release of strain across major faults can be monitored over the short-term (years or less) using ultra-precise modern techniques, and longer term movements can frequently be determined by utilizing the historic record of measurements, which in many active regions extend back into the late 19th century. Since about 1970, annual laser ranging surveys in the western U.S. and Alaska have delineated the pattern and current rates of deformation in these seismically active regions and begun to provide accurate fault slip rates to compare with late Holocene geological estimates. The imperfect

balance between interseismic strain buildup and coseismic strain release introduces a component of permanent deformation into the earthquake cycle that under favorable conditions can be estimated geodetically, providing another link between present-day movements and those preserved in the recent geologic record. Examples include tectonically elevated former shorelines related to great interplate thrust earthquakes and deformed river terraces observed in intra-plate reverse faulting environments. Despite the relative uniformity of longer term deformation rates, accumulating evidence indicates considerable short-term irregularity, at least in some regions. Perhaps the best documented example comes from southern California, where rapid, correlated changes among gravity, elevation, and horizontal strain measurements have recently been observed. (W. Thatcher)

Reports

- Thatcher, W., and J. B. Rundle, 1984, A viscoelastic coupling model for the cyclic deformation due to periodically repeated earthquakes at subduction zones, J. Geophys. Res., 89, in press.
- Thatcher, W. and N. Fujita, 1984, Deformation of the Mikita Rhombus: Strain buildup following the 1923 Kanto earthquake, Central Honshu, Japan, J. Geophys. Res., 89, in press.
- Thatcher, W., 1984, The earthquake deformation cycle, recurrence, and the time predictable model, J. Geophys. Res., 89, in press.
- Thatcher, W., 1984, The earthquake deformation cycle at the Nankai Trough, Southwest Japan, J. Geophys. Res., 89, in press.
- Thatcher, W., 1984, Geodetic measurement of active tectonic processes, in Active Tectonics - Impact on Society, National Research Council, Washington, D.C., submitted.
- Stein, R. S., 1983, Reverse slip on a buried fault during the 2 May 1983 Coalinga earthquake: Evidence from Geodetic elevation changes, The 1983 Coalinga, California Earthquake: California Div. Mines & Geol. Spec. Pub. 66, Sacramento, 151-164.
- King, G. and R. S. Stein, 1983, Surface folding, river terrace deformation rate and earthquake repeat time in a reverse faulting environment: The Coalinga, California earthquake of May 2, 1983, ibid, 165-176.
- McTigue, D. F., and R. S. Stein, Topographic amplification of tectonic displacement: Implications for geodetic measurement of strain changes, J. Geophys. Res., 89, 1123-1131.
- Stein, R.S. and G.C.P. King, 1984, Seismic potential revealed by surface folding: The 1983 Coalinga, California, earthquake, Science, in press.

Stein, R.S., 1984, Comment on "The impact of refraction correction on leveling interpretations in southern California" by William E. Strange, J. Geophys. Res., 89, 559-561.

Abstracts

- Thatcher, W., 1983, Geodetic measurement of active tectonic processes, EOS, 65, 859.
- Thatcher, W., 1983, Earthquake deformation cycle, recurrence an the time predictable model, EOS, 65, 842.
- Stein, R. S., 1983, The 2 May 1983 Coalinga Earthquake: Evidence for reverse slip on a buried fault from geodetic elevation changes, EOS, 65, 748.
- King, G. and R. S. Stein, 1983, Surface folding, river terrace deformation rate and earthquake repeat time: The Coalinga, California, Earthquake of May, 1983, EOS, 65, 749.
- Stein, R. S., 1983, Historical vertical deformation in southern California: Removal of systematic errors in geodetic leveling, Canadian Geophys. Union Annual Meeting, Program with abstracts, 8.
- Stein, R. S., 1983, Implications of off-fault aftershocks for pre-earthquake stress, ibid.

Development of General Earthquake Observation System

9910-03009

John Van Schaack
Branch of Engineering Seismology and Geology
U.S. Geological Survey
345 Middlefield Road, MS 977
Menlo Park, California 94025
(415) 323-8111, ext. 2584

Investigations

The objectives of this program are to complete the assembly, testing, and documentation of the General Earthquake Observation System (GEOS). An expanded memory is being developed for an enhanced detection program. A digital-to-analog board is being developed to replace the analog-to-digital board. With a change in the program a recording system can be made into a playback system.

Results

Sixteen systems have been tested and are now operational. Another nine systems are approximately 90% complete. Seven GEOS systems were deployed near Mammoth Lakes in January 1983. These systems were operated with both force balance accelerometers and velocity sensors. Record quality was very good and indicated that the instruments were operating near their maximum dynamic range of 96Db.

Reports

None.

Field Experiment Operations

9930-01170

John Van Schaack
Branch of Seismology
U. S. Geological Survey
345 Middlefield Road MS/77
Menlo Park, California 94025
(415) 323-8111, ext. 2584

Investigations

This project performs a broad range of management, maintenance, field operation, and record keeping tasks in support of seismology and tectonophysics networks and field experiments. Seismic field systems that it maintains in a state of readiness and deploys and operates in the field (in cooperation with user projects) include:

- a. 5-day recorder portable seismic systems.
- b. Smoked paper-recorder portable seismic systems.
- c. "Cassette" seismic refraction trucks.
- d. Portable digital event recorders.

This project is responsible for obtaining the required permits from private landowners and public agencies for installation and operation of network sensors and for the conduct of a variety of field experiments including seismic refraction profiling aftershock recording, teleseism P-delay studies, volcano monitoring, etc.

This project also has the responsibility for managing all radio telemetry frequency authorizations for the Office of Earthquakes, Volcanoes and Engineering and its contractors.

ResultsSeismic Refraction

60 seismic cassette recorders were deployed across Yellowstone Park to record aftershocks from the October 28, 1983 Idaho earthquake. The information from these recordings is being used in a P-delay study of Yellowstone Park area.

Telemetry Networks

A seismic telemetry network was installed around the epicenter of the Oct. 28, 1983 Idaho earthquake. The network consisted of 6 single component stations telemetered by radio to two phone drops then to the University of Utah at Salt Lake City. Two links in the Microwave backbone network for geophysical data telemetry have been completed and tested. Three more links are being installed and will be complete in July 1984.

Portable networks

Six 5-day recorders were operated near Lake Isabella California during October 1983 during a series of earthquakes in the area. Ten 5-day recorders were operated around the Idaho earthquake for 3 weeks during November 1983. 6 recorders were also deployed following the Morgan Hill earthquake of April 23, 1984.

Data Processing Center Operations

9930-01499

John Van Schaack
Branch of Network Operations
U.S. Geological Survey
345 Middlefield Road - MS-977
Menlo Park, California 94025
(415) 323-8111, ext. 2584

Investigations

This project has general housekeeping, maintenance and management authority over the Earthquake Prediction Data Processing Center. Its specific responsibilities include

1. day-to-day operation and performance quality assurance of 5 network tape recorders,
2. day-to-day management, operation, maintenance, and performance quality assurance of 2 analog tape playback stations,
3. day-to-day management, operation, maintenance and performance quality assurance of the USGS telemetered seismic network event library tape-dubbing facility (for California, Alaska, Hawaii, Oregon, and Yellowstone National Park), and
4. projection of usage of critical supplies, replacement parts, etc., maintenance of accurate inventories of supplies and parts on hand, and uninterrupted operation of the Data Processing Center.

Results

Procedures and staff for fulfilling assigned responsibilities have been developed, and the Data Processing Center is operating smoothly and serving a large variety of scientific user projects.

Exploiting the Precision Inherent in NAVSTAR/GPS Geodetic Measurements

14-08-000121378

Randolph H. Ware

Cooperative Institute for Research in Environmental Sciences
University of Colorado, Box 449
Boulder, CO 80309
(303) 492-8028

Investigations

The NAVSTAR/Global Positioning System (GPS) can be used to make high accuracy relative crustal measurements. However, water vapor radiometers (WVRs) will be needed in most cases to achieve the full accuracy inherent in the GPS system (Bossler et al., 1980; Larden and Bender, 1984). We have carried out the first experiments using WVRs with GPS receivers. Two WVRs measured the integrated water vapor along the line-of-sight to NAVSTAR satellites at both ends of a 22-km baseline near Boulder, Colorado. Path corrections to GPS phase measurements were computed from the WVR data. Baseline coordinates computed using water vapor path corrections based on surface meteorological data are compared to results computed using WVR path corrections.

History

The plan was to coordinate an experiment using WVRs operated by NOAA and dual frequency GPS receivers (Macrometers, Texas Instruments Geostars, and JPL's Series or Series-X). The use of the WVRs was set for July, 1983, and preliminary arrangements were made for the receivers. In June 1983 we learned that only single frequency Macrometers would be available, as a result of delays in the final development of the other receivers. We had hoped to use dual-frequency receivers to reduce errors from ionospheric refractivity. However, we decided to proceed as the WVRs would not be available again until summer of 1984, and we expected that useful data could be obtained using the single-frequency Macrometers. Benchmarks were installed by the National Geodetic Survey near Boulder and Erie. A relatively short (22-km) baseline was chosen as a best guess toward a length that would allow WVR corrections to be significant compared to errors resulting from ionospheric refraction and satellite orbit uncertainties.

The present constellation of five NAVSTAR satellites appears four minutes earlier each day and is visible for several hours. An advantage of performing the experiment in July was that the constellation was visible during the early evening. At that time thunderstorms often occur, causing local variability in water vapor, thereby increasing the magnitude of WVR corrections.

Instrumentation

Two WVRs developed by the Boulder NOAA Laboratories measured the water vapor path delay to one centimeter accuracy (Hogg et al., 1983). They were located within 50 m of the Macrometer receivers. The total angular aperture of the WVRs is 5°. The calibration of the WVRs and the water vapor computations were carried out by NOAA. The WVRs, which are normally used for meteorological studies, are housed in forty-foot trailer vans. They were pointed toward each satellite every fifteen minutes. This

allowed two minutes to change the pointing and one minute of observation for each of the five satellites. David C. Hogg and Jack Snider of NOAA assisted with the set up, execution, analysis, and interpretation of the experiment. Larry Slater, Max Wyss, Chris Roecken (all from Cires), and Roger Bilham (Lamont) assisted with the operation of the WVRs. Will Prescott (USGS) and Tom Yunck (JPL) were present during the experiment, offering valuable advice and information.

The single-frequency Macrometers were operated by the National Geodetic Survey at the Boulder and Erie sites. NGS provided spline function fits to the WVR data and computed baseline coordinates using the receiver data alone and also the receiver data corrected by WVR data. Clyde Goad of NGS assisted with the execution, analysis, and interpretation of the experiment.

Discussion

Excess path errors computed from the WVR data are shown for two evenings of measurements in Figures 1 and 2. The zenith precipitable water vapor (the depth of liquid water that would result if all the water vapor in a vertical column were condensed) during the experiment ranged from about 2 to 3 cm. The excess path error is obtained by multiplying the line-of-sight water vapor by a factor of 6.5 (Hogg et al., 1981). The general sloping curvature seen in Figures 1 and 2 is caused by the change of water vapor with elevation angle as the satellites track across the sky at 30° per hour. Short-term variations in line-of-sight water vapor resulting primarily from local thunderstorm activity are also present. The dependence of excess path on elevation angle can be clearly seen in Figure 3. Short-term variations in excess path up to 15 cm are also seen.

Included in Figures 1 and 2 are the differences in excess path between the sites at Boulder and Erie. The Boulder site has an excess path that averages about 4 cm greater than Erie. This can affect the computed baseline coordinates, as seen in Table 1. These relative coordinates are based on initial computations. Three days of data were analyzed, but only on Julian Day 200 were the receiver and WVR data more or less complete, including three hours of observations. JD 199 includes 70 minutes and JD 198 includes 90 minutes of simultaneous WVR and receiver data.

Two separate computer programs were used. The Macrometrics software computed double differences (Bock et al., 1983) and uses the North American Datum, 1927 (NAD27). The NGS software computed triple differences (Goad and Remondi, 1983) and uses the World Geodetic System, 1972 (WGS72). Triple differences for JD 198 have not yet been computed. For the 22-km baseline in this experiment, the use of different (NAD27 and WGS72) ellipsoids should have a negligible affect on the computed relative coordinates.

Computations were carried out using all of the receiver data with no WVR corrections, and for the subsets where receiver and WVR data were available. For this subset, coordinates were computed with WVR corrections and with no WVR corrections.

It is clear that more measurements, preferably using dual-frequency receivers and additional analysis are needed to answer the questions raised by this first experiment. However, in the light of this qualifying statement, the following comments may be useful:

- The double and triple difference computations give results that vary by some 10 cm for the elevation and north-south coordinates, using identical receiver data and no WVR corrections. This lack of agreement should be studied.

- WVR corrections result in an apparent 8-cm decrease in relative elevation between Boulder and Erie on the two days that were computed. Assuming that satellites were viewed at an elevation angle of 30° on the average (a reasonable assumption, considering Figures 1, 2, and 3), the correction for an additional excess path of 4 cm for the Boulder site would cause a decrease in the relative elevation of $(4 \text{ cm})/\cos(30^\circ) = 8 \text{ cm}$. Therefore, the 4-cm average additional excess path for the Boulder site is consistent with the 8-cm decrease in relative elevation.
- The N-S and E-W coordinate changes after WVR correction are variable in sign and magnitude. This is expected from local variations in water vapor associated with thunderstorms. The additional 4 cm average excess path observed from the Boulder site would not affect the horizontal coordinates (constant excess paths to satellites toward the east and west, for example, would tend to cancel).

Some of the questions that have been raised by this attempt to correct GPS baseline measurements using WVRs can be addressed by computer simulations. We intend to use simulations to study the affects of excess path offset at one site, and excess path variations vs. time and azimuth.

References

- Bock, Y., R. I. Abbot, C. C. Counselman, S. A. Gourevitch, R. W. King, and A. P. Paradis, Geodetic Accuracy of the Macrometer Model V-1000, **IUGG General Assembly**, Hamburg, Aug. 15-27, 1983.
- Bossler, J. D., C. C. Goad, and P. L. Bender, Using the Global Positioning System (GPS) for geodetic positioning, **Bull. Geod.**, **54**, 553-563, 1980.
- Goad, C., and B. W. Remondi, Initial relative positioning results using the Global Positioning System, **IUGG General Assembly**, Hamburg, Aug. 15-27, 1983.
- Hogg, D. C., F. O. Guiraud, and M. T. Decker, Measurement of excess radio transmission length on Earth-space paths, **Astron. Astrophys.**, **9**, 304-307, 1981.
- Hogg, D. C., F. O. Guiraud, J. B. Snider, M. T. Decker and E. R. Westwater, A steerable dual-channel microwave radiometer for measurement of water vapor in the troposphere, **Journal of Applied Meteorology**, **22**, 789-806, 1983.
- Larden, D. R., and P. L. Bender, Expected accuracy of geodetic baseline determinations using the GPS reconstructed carrier phase method, in preparation, 1984.

Table 1. Relative Coordinates of the Boulder - Erie Sites

| <u>Julian date</u> | <u>data set (minutes)</u> | <u>soft-ware</u> | <u>relative water vapor correction</u> | <u>elevation (cm) +11 m</u> | <u>north-south (cm) +2058 m</u> | <u>east-west (cm) +21,979 m</u> |
|--------------------|---------------------------|------------------|--|-----------------------------|---------------------------------|---------------------------------|
| 198 | 100 | Macrometrics | no | 57.4 | 44.4 | 102.0 |
| 199 | 140 | Macrometrics | no | 54.6 | 42.0 | 83.0 |
| 199 | 140 | NGS | no | 45.8 | 55.7 | 74.3 |
| 199 | 70 | NGS | WVR | 37.2 | 55.9 | 59.8 |
| 199 | 70 | NGS | no | 45.5 | 54.6 | 78.1 |
| 200 | 180 | Macrometrics | no | 55.9 | 40.3 | 75.0 |
| 200 | 180 | NGS | no | 40.7 | 55.4 | 72.1 |
| 200 | 170 | NGS | WVR | 33.3 | 56.2 | 71.4 |
| 200 | 170 | NGS | no | 41.1 | 55.5 | 73.9 |

The Macrometrics software calculated double differences and uses the North American Datum, 1927.

The NGS software calculated triple differences and uses the World Geodetic System, 1972.

Lines that are grouped together used the same data set.

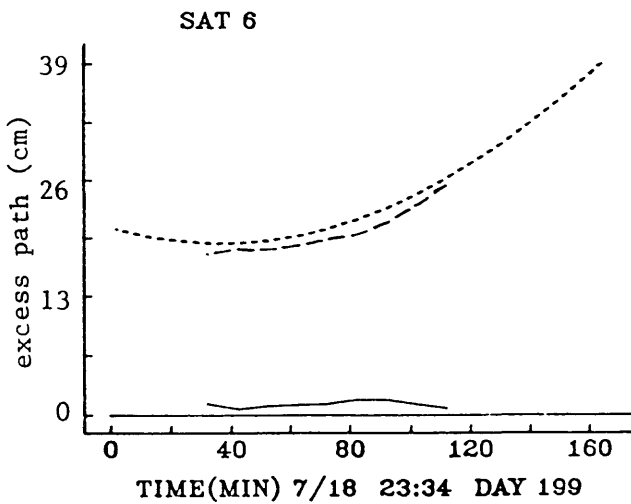
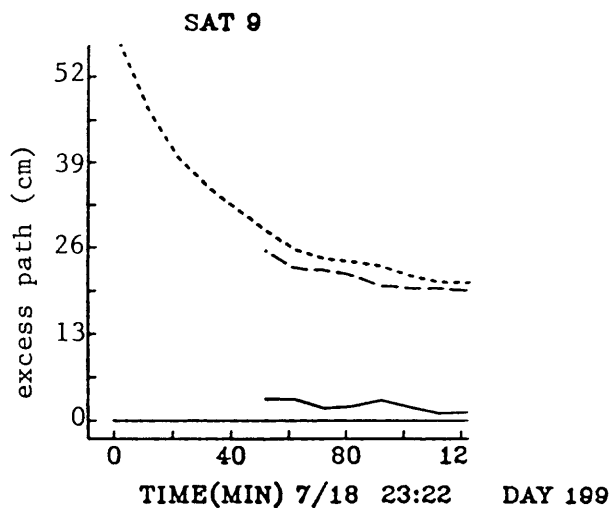
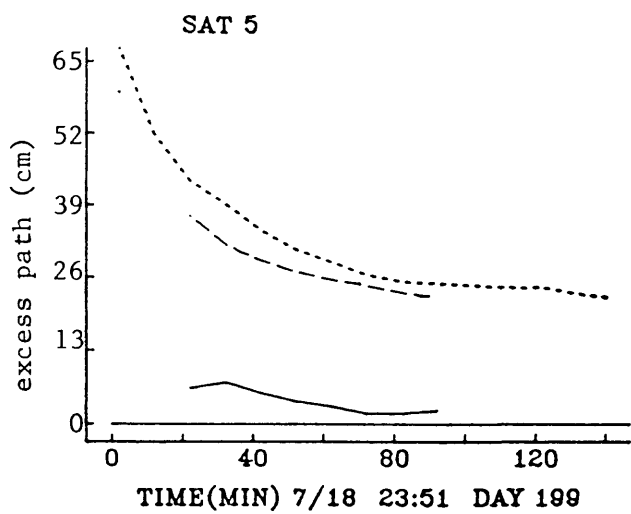
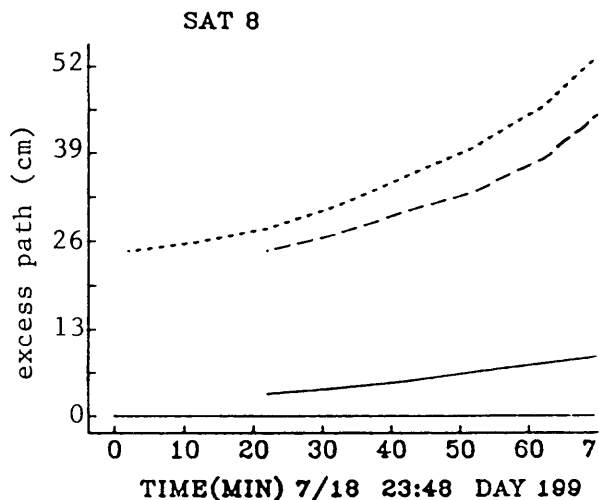
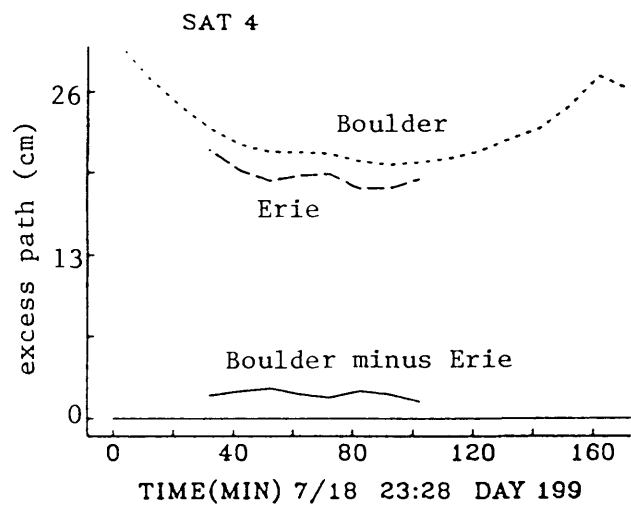


Figure 1. Spline fits of WVR data for the Boulder and Erie sites. The excess path for Boulder minus Erie is also shown.

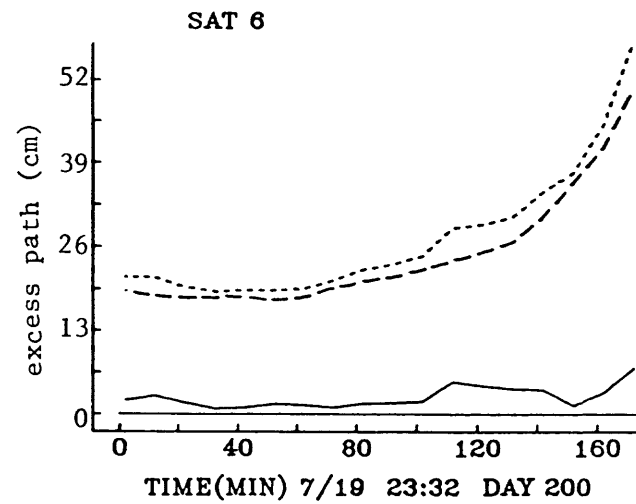
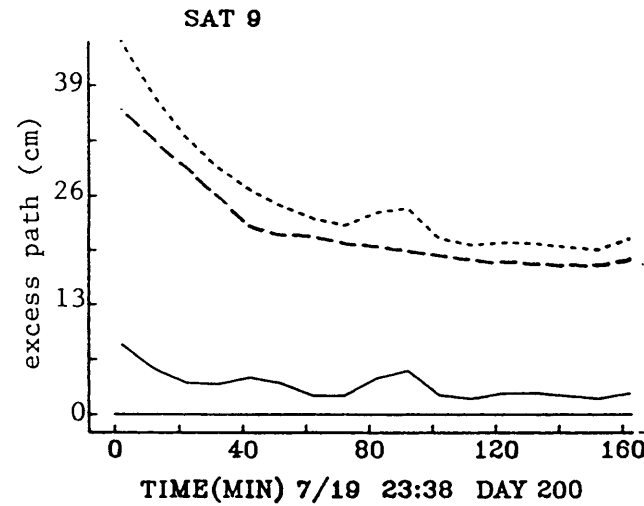
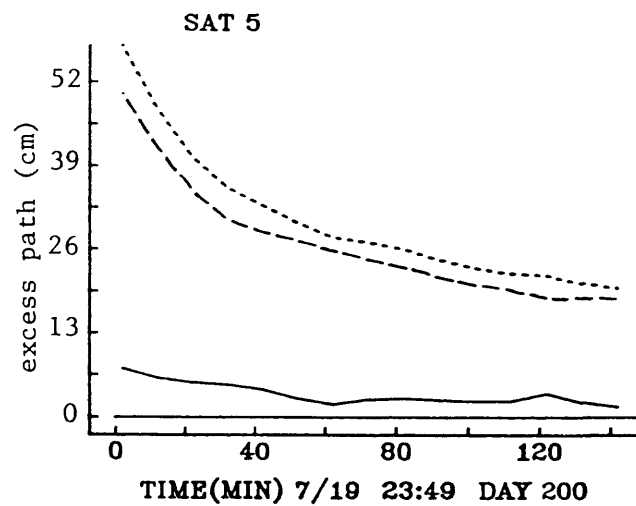
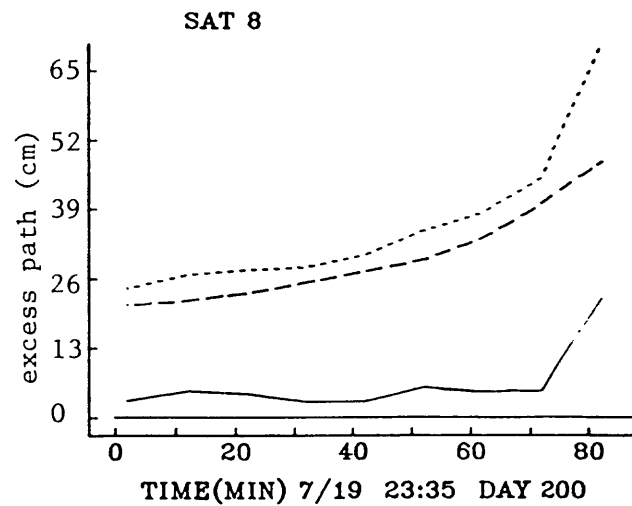
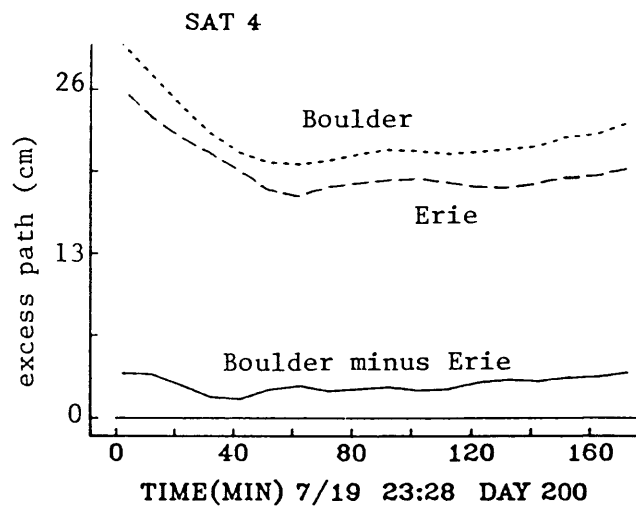


Figure 2. Spline fits of WVR data for the Boulder and Erie sites on July 19, 1983. The excess path difference between the Boulder and Erie sites is also shown along the line-of-site to each satellite. Clyde Goad of NGS provided the plots. The sweeping curves are a result of the changing elevation angle as each satellite tracks across the sky. The "bumps" result from local variations in water vapor.

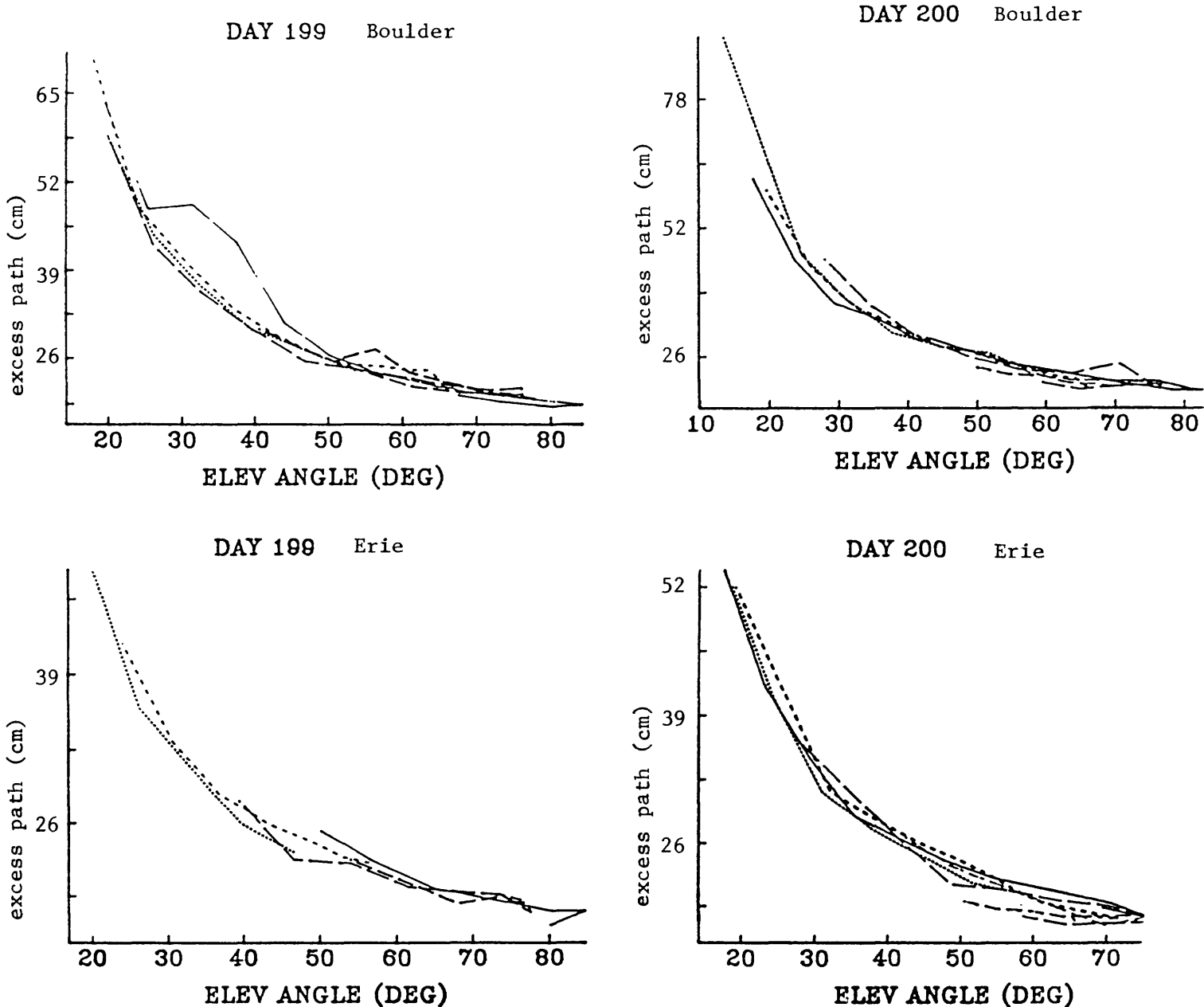


Figure 3. Excess path to NAVSTAR satellites as seen from the Boulder and Erie sites as a function of elevation angle. On Julian Day 199 from Boulder, the excess path to one satellite is 15 cm larger than the excess path to the other satellites at the same elevation angle.

Seismicity and Structure of the San Pablo Bay-Suisin Bay
Seismic Gap from Calnet and Explosion Data

9930-02938

David H. Warren
Branch of Seismology
U.S. Geological Survey
345 Middlefield Road M/S 977
Menlo Park, California 94025
(415) 323-8111, ext. 2531

Investigations

Stereographic plots were made of the 1977 deep earthquake swarm just east of Suisin Bay.

A major effort was made to complete the Willits aftershock study

Results

The earthquake swarm just east of Suisin Bay is a very tight cluster extending from 14 to 19 km in depth and 2 km in width. The axis dips to the northeast at a high angle. It is located just north of a branch of the Antioch Fault.

First motion plots showing fault mechanisms were previously made for the 1977 swarms. They show a strike slip mechanism and an orientation consistent with that of the Antioch Fault.

Reports

Warren, D. H., Scofield, C., and Bufe, C. G., Aftershocks of the November 22, 1977 earthquake at Willits, California: Activity on the Maacama Fault: to be submitted to the Bulletin of Seismological Society of America (Director's approval 4/12/84).

Earthquake Process
9930-03483
Robert L. Wesson
Branch of Seismology
U.S. Geological Survey
922 National Center
Reston, Virginia 22092
703/860-7481

Investigations

1. Analysis of theoretical and numerical models of the processes active in fault zones leading to large earthquakes.
2. Analysis of seismological and other geophysical data pertinent to the understanding of the processes leading to large earthquakes.

Results

Both the spatial expansion of aftershock zones and the continuation of displacement--as "afterslip"--are commonly observed following moderate and larger strike-slip earthquakes in California. Because the aftershock zones expand very rapidly in the first hours following a mainshock, then more slowly, space-time characteristics are best studied using plots of position in space vs log time. Aftershock zones typically expand along strike in both directions away from the mainshock. Commonly, the expansion of the zone will be retarded for a period; however, following one or more larger aftershocks on the limit of the zone, the aftershock zone will "breakout" and the expansion of the zone will resume. Aftershock zones of some earthquakes clearly expand downward, a few expand upward. Afterslip--commonly characterized by a law of the form displacement = $a + b \log(t)$ --in some instances seems to be controlled by these "breakouts." These observations suggest that a process of "progressive failure" continues in the fault zone following the mainshock.

Surficial observations of active faults and geologic observations of fault zones in deep mines and tunnels, suggest that a reasonable geologic model of an active fault at seismogenic depths would involve a fault zone of highly fractured rock hundreds to thousands of meters wide, including branching and anastomosing faults typically associated with zones of plastic, clay-like gouge up to tens of meters thick, and zones of pervasively sheared rock up to hundreds of meters wide. A previously proposed "patch" model of the fault zone is elaborated to suggest that portions of the fault surface (or volume) identified by the hypocenters of mainshocks and aftershocks are characterized by frictional failure criteria. Intervening portions of the fault zone are characterized by a low-temperature creep phenomenon, perhaps associated with the quasi-plastic deformation of plastic, clayey fault gouge. A simple semiquantitative numerical model based on the assumptions that the mainshock represents frictional failure of a large (strong) patch, followed by quasi-plastic deformation--afterslip--in the fault zone "matrix" and frictional failure on smaller (weaker) patches--aftershocks--reproduces the observed characteristics of the expansion of aftershock zones and afterslip.

Central American Seismic Studies
9930-01163

Randall A. White
David H. Harlow
Branch of Seismology
345 Middlefield Road, Mail Stop 77
Menlo Park, California 94025

Investigations

A network of 6 seismic stations were installed in near Guatemala City in February of 1975. By itself the network is adequate for locating events along the western half of the Motagua fault. In order to study the micro-seismicity of the entire Motagua fault region immediately prior to the Guatemala Earthquake of February 4, 1976 (M_w 7.5), these data were combined with S-P data from three low-gain seismographs in El Salvador. No seismograph network has ever been closer to the epicenter of such a large strike-slip event before the fact, thus these data present a unique opportunity to look for microseismicity patterns that may have had predictive value, or that at least may tell us something new about the processes that occur during this critical stage of the the earthquake cycle. Also records from a Weichert's Seismograph that has operated in Guatemala for decades, have been located and are being analyzed in order to extend the time period of the data set for $M_L > 4$ events.

Results

- 1) During the 15 years before February 4, 1976, no onset of precursory moderate seismicity ($M_L > 4$) is observable in the region. In fact, a decrease in the number of events/year in 1975 is marginally significant.
- 2) Events of $M_L > 4$ appear to have concentrated somewhat near the eventual epicenter and near the point of greatest observed surface slippage, about 100 km to the west.
- 3) During the 9 months prior to the February 4, 1976, for which micro-seismicity data ($M_L 2$ to 4) are available, most of the seismicity occurs as small swarms along the volcanic chain. This seems typical of other volcanic arcs and there is probably nothing significant here of predictive value.
- 4) The rest of the superficial micro-seismicity during these 9 months describes a loose oval about the eventual surface rupture. Two of the largest events, of $M_L > 4.5$, occurred near the eventual epicenter, one on January 26, just a week before the earthquake. The only other event to occur along the fault during the week the earthquake, was a small felt event of about $M_L 2.5$ on February 3 near the point of highest observed surface rupture, about 100 km west of the epicenter.
- 5) There were no significant changes in the level of micro-seismicity during the 9 months prior to the earthquake, for the fault zone as a whole.
- 6) During the two years prior to 1976, six moderate events occurred very near the epicenter of the main event and these are being carefully relocated and examined. Large differences are apparent in aftershock production between some of these events. This may be related to differences in locations along the fault with respect to the eventual epicenter.

Recognition of Individual Earthquakes on Thrust Faults (New Zealand)

USGS Contract No. 14-08-0001-21379

Robert S. Yeats
Department of Geology
Oregon State University
Corvallis, Oregon 97331-5506
(503) 754-2484

Kelvin R. Berryman, Sarah Beanland
Earth Deformation Section
New Zealand Geological Survey, D.S.I.R.
P.O. Box 30368
Lower Hutt, New Zealand
(644) 699-059

Investigations

1. Trenching of late Quaternary active reverse faults in central Otago was completed in early April. Two peat beds that place some constraint on the time of faulting were sampled for ^{14}C dating by the Institute of Nuclear Sciences, D.S.I.R.

2. Field work on flexural-slip faults in the Grey-Inangahua basin was completed in March.

Results

1. Prior to this study, extensive bulldozer trenching had been done on the Dunstan and Pisa faults in central Otago. In November, trenching was carried out on the Nevis fault zone in the Upper Nevis and Lower Nevis basins. In March and April, trenches were cut in the Cardrona fault zone, and additional trenching comes out at the Dunstan fault.

All these faults are predominantly reverse-slip, with relatively little strike-slip component. Each fault zone contains individual strands which dip east and others which dip west. For the Dunstan fault, which marks the general tectonic boundary between the Dunstan Range and the Manuherikia basin, this means that some faults dip toward the range and others dip away from the range. The only historic faulting which shows this pattern is that accompanying the Tabas-i-Golshan, Iran earthquake reported by Berberian (1979, BSSA 69:1851-1887).

2. We are now evaluating information on reverse-fault recurrence intervals in central Otago (low instrumental and historical seismicity) and in northwest Nelson (high instrumental and historical seismicity). Our preliminary indications are that the recurrence intervals are similar in both areas, despite the great contrast in seismicity.

3. In the Grey-Inangahua basin, outwash gravels $>150,000$ years old overlie folded Miocene-Pleistocene strata unconformably. Flexural-slip faulting of the gravels accompanied late-stage folding of the subjacent strata, in part after the old outwash surface had been abandoned for a lower, younger stream course.

Larger fault scarps facing up the former depositional slope are ungullied whereas fault scarps facing down the former slope are extensively gullied. If the fault scarps formed by slow, aseismic creep, the local drainage on the outwash surface should be able to maintain itself across the growing scarps, even though the main drainage had abandoned this surface. Instead, the drainage is defeated at the base of the scarps, suggesting that the scarps formed instantaneously, accompanying earthquakes. If the flexural-slip faults are coseismic, then the folding to which they are genetically related must be coseismic as well.

Reports:

Beanland, Sarah, 1984, Late Quaternary deformation along the Dunstan fault, central Otago, New Zealand, in Proceedings of the International Symposium on Recent Crustal Movements of the Pacific Region: Royal Society of N.Z., in review.

Berryman, K., 1984, Late Quaternary tectonics in New Zealand, in Walcott, R. I., compiler, An introduction to the Recent crustal movements of New Zealand: Royal Society of N.Z. Misc. Series 7, p. 91-107.

Wood, P. R., compiler, 1984, Guidebook to the South Island scientific excursions, International Symposium on Recent Crustal Movements of the Pacific Region: Royal Society of N.Z. Misc. Series 9, 149 p.

Yeats, R. S., 1984, Active faults related to folding, in Wallace, R. E., editor, Active Tectonics--Impact on Society: National Research Council Studies in Geophysics, in review.

Yeats, R. S., 1984, Faults related to folding, with examples from New Zealand, in Proceedings of the International Symposium on Recent Crustal Movements of the Pacific Region: Royal Society of N.Z., in review.

ANALYSIS OF CENTRAL CALIFORNIA NETWORK DATA

AND EARTHQUAKE PREDICTION

U.S.G.S. Contract Number 14-08-0001-21292

Principle Investigator: Keiiti Aki

Massachusetts Institute of Technology

77 Massachusetts Ave., Cambridge, MA 02139 (617)253-6397

The Site Effect on Coda Waves

Coda wave data from sixteen California earthquakes have been processed to study the site effect variation. Each earthquake has been recorded by a subset of over 150 vertical component Calnet stations lying in the Coast Range province, between San Francisco and San Luis Obispo. The essentials of the calculation will be described, followed by a discussion of the results.

Method for Calculating the Site Effect

Over 700 codas were processed and inverted simultaneously to obtain sets of coda source factors for center frequencies 1.5, 3, 6, 9, 12, 18, and 24 hz. The coda source factors contain information about the source and site effects on coda excitation. They are separated as follows:

$$s_0 = \langle \ln D_{ij} \rangle_i \rangle_j$$

$$r_j = \langle \ln D_{ij} - s_0 \rangle_i$$

where D_{ij} is the natural logarithm of the coda source factor of event i at station j , corrected to a reference source. These r_j are plotted in map view for center frequencies 1.5, 3, 6, and 12 hz., (Figures 1a-d). These maps were produced by the Comtal image processor at the MIT Earth Resources Laboratory. The radius of influence of a single measurement varies inversely as the station density, and does not exceed 20 km. Station locations are also plotted for reference. The standard errors of the r_j average less than 5% of the total variation at 1.5 hz. Roecker(1981), and this study (Figure 2) have shown that Q_c can vary with the lapse time over which the coda is measured. Since constant Q_c is assumed here, this effect should contribute to our errors. In the future this will be corrected for by inverting coda decay data grouped by lapse time. Undetected glitches and small events occurring in the coda may also contribute to the error.

The Site Effect in the Southern Coast Ranges

As seen by Aki(1969), considerable variation in the site amplification effect of coda waves is observed in the California Coast Ranges (Figures 1a-d). At 1.5 hz. there is a factor of twenty difference in amplitude between the highest and lowest measurements. In order to interpret the site effect, USGS quadrangle geology maps were examined, a simplified map can be found in figure 6. At 1.5 hz. site amplification is found to depend on surface geology; high amplification is strongly associated with young, usually upper Tertiary or Quaternary sediments. Prominent highs are located: 1) near Hollister (Plio-Pleistocene sediments), 2) near Watsonville (Quaternary sediments), 3) directly east of the San Francisco Bay area (upper Tertiary marine sediments), 4) in the Santa Cruz Mountains (Pliocene marine sediments) and 5) between the Salinas River Valley and the San Andreas fault zone, south of the Gabilan Range (Pliocene marine and Plio-Pleistocene sediments). Low site amplification is found where stations are located on one of the two basement core complexes found in the area. These are the Franciscan formation, composed of Jurassic

and Cretaceous meta-sediments, mostly greywackes, and the granite-metamorphic basement of the Salinian block. The most prominent low is found over the Gabilan Range granites. The Franciscan is responsible for almost all low measurements to the northeast of the San Andreas, and to the southwest of the Nacimiento faults. This includes 2 stations at the south end of the San Francisco Bay, one of which is situated in a borehole at -180 m. Moderate site amplification is usually associated with Miocene or older marine sediments, including Cretaceous Great Valley Sequence rocks; amplification generally varying inversely with age. Aki (1969) ascribed his site effect variation at 2.5 hz. to the impedance effect. This conclusion is qualitatively supported by the results at 1.5 hz. presented above.

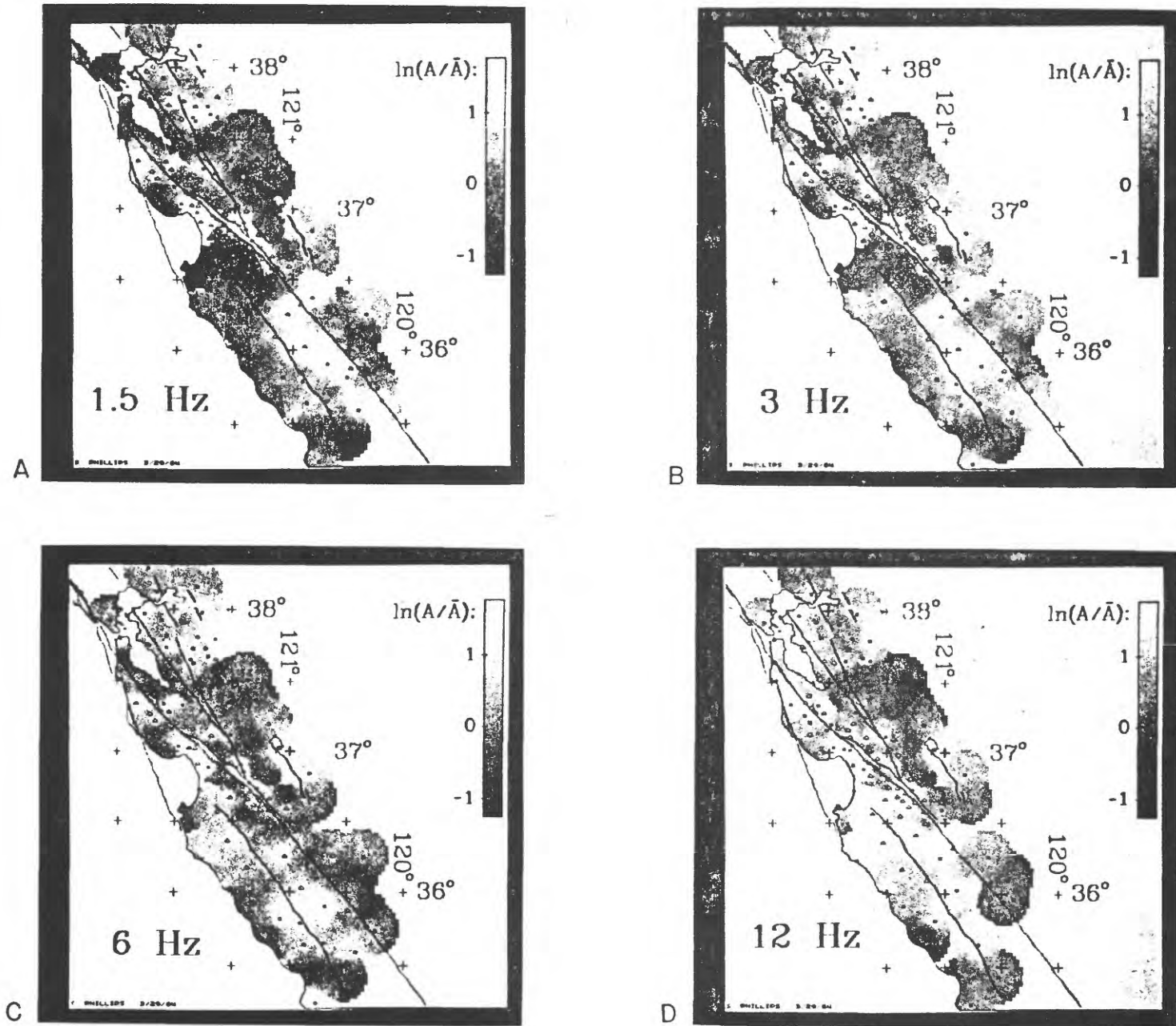
At higher frequencies, the site amplification pattern changes. The most obvious change can be seen throughout the Gabilan region where a well defined low gradually turns moderate to high as frequency increases. This is reminiscent of a observation made by Hudson(1972), at granite and sediment sites in Pasadena during the San Fernando earthquake. Lower near site attenuation in the granites is most likely responsible for this effect, which is also reflected in the lack of high frequency observations at young sediment sites. Some elements of the site amplification pattern are stable. The high regions at 1.5 hz. remain moderate to high, although muted, and represented by gradually fewer and poorer measurements. Most sites located on Fransican basement remain low.

It is apparent that near surface impedance and attenuation are major factors governing site amplification. Impedance is more important at low frequencies, while attenuation becomes important as frequency increases. Since the Calnet stations are sited selectively on the "hardest" (high impedance, low attenuation) rock in a given area, we expect our site amplification map to represent a lower bound at frequencies where impedance is the dominant factor. Likewise, our map represents an upper bound at frequencies where attenuation is dominant.

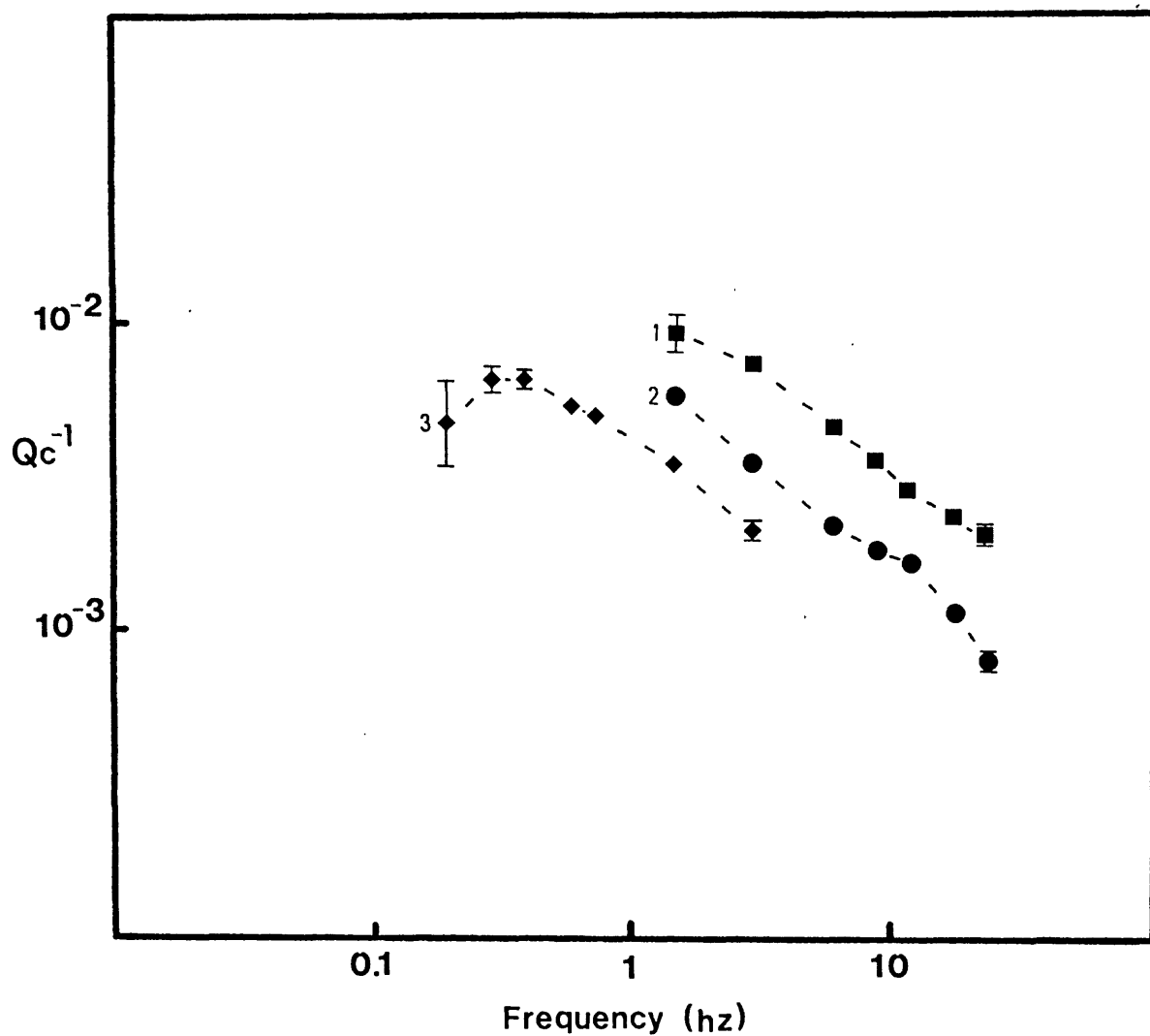
The impedance-attenuation coupling also offers some interesting modeling possibilities. Near surface Q could be constrained given initial knowledge of density and velocity. Also, temporal changes in the site effect could give information complementary to coda wave Q measurements which are being looked into as a possible earthquake prediction tool (Jin, 1984).

References

- Aki, K., Analysis of the seismic coda of local earthquakes as scattered waves, *J. Geophys. Res.*, 74, 615-631, 1969.
- Hudson, D.E., Local distribution of strong earthquake ground motion, *Bull. Seis. Soc. Am.*, 62, 1765-1786, 1972.
- Jin, A., Temporal change in coda Q before the Tangshan earthquake of 1976, submitted to *J. Geophys. Res.*, 1984.
- Roecker, S.W., Seismicity and tectonics of the Pamir-Hindu Kush region of Central Asia, *Ph.D. thesis, M.I.T., Cambridge*, 1981.

**Figure 1**

Maps of site amplification for frequencies 1.5-12 hz. Each station has a radius of influence of ≤ 20 km., depending on the local station density; $1/(distance\ to\ station)^2$ weighting has been applied. Triangles represent stations for which 3 or more codas were measured, otherwise squares are used.

**Figure 2**

Q_c measurements showing the effect of lapse time: 1) ~200 codas recorded in the Coyote Lake area, magnitudes 1.5-2.0; codas were measured over lapse times 5-35 s., 2) >700 codas from the 16 events used in the Coast Range site effect study, magnitudes 2.5-3.0, lapse times 20-100 s., 3) >30 codas from the Coyote Lake earthquake, magnitude 5.9, lapse times 100-300 s. Error bars represent twice the standard error of Q_c^{-1} . No error is indicated if it is smaller than the symbol size.

Creep and Strain Studies in Southern California

Contract No. 14-08-0001-21212

Clarence R. Allen and Kerry E. Sieh
Seismological Laboratory, California Institute of Technology
Pasadena, California 91125 (818-356-6904)

Investigations

This semi-annual report summary covers the six-month period from 1 October 1983 to 31 March 1984. The contract's purpose is to monitor creepmeters, displacement meters, and alignment arrays across active faults in the southern California region. Primary emphasis focuses on faults in the Imperial and Coachella Valleys.

During the reporting period, resurveys of theodolite alignment arrays were carried out at ALL AMERICAN CANAL, ANZA, BAILEYS WELL, DILLON ROAD, INDIO HILLS, HIGHWAY 80, PALLET CREEK, SUPERSTITION HILLS, UNA LAKE, and KEYSTONE ROAD. In addition, nail-file arrays were resurveyed at ANDER-HOLT ROAD, ROSS ROAD, and WORTHINGTON ROAD, and creepmeters were serviced at HARRIS ROAD, HEBER ROAD, NORTHSORE, MECCA BEACH, ROSS ROAD, SUPERSTITION HILLS, AND TUTTLE RANCH.

Results

No unusual or startling events were detected during the reporting period. Creep activity and inactivity were compatible with the long-term results summarized in the previous semi-annual report. During the reporting period a manuscript was completed detailing the 16 years of measurements: Louie, J. N., Allen, C. R., Johnson, D. C., Haase, P. C., and Cohn, S. T., "Fault slip in southern California." The abstract of this paper, along with one of its tables and one figure, are reproduced below.

Measurements of slip on major faults in southern California have been carried out over the past 16 years using principally theodolite alignment arrays and taut-wire extensometers. They provide geodetic control within a few hundred meters of the fault traces, which complements measurements made by other techniques at larger distances. Approximately constant slip rates varying from 1 to 6 mm/yr over periods of several years have been found for the southwestern portion of the Garlock fault, the Banning and San Andreas faults in the Coachella Valley, the Coyote Creek fault, and an unnamed fault 20 km west of El Centro. These slip rates are typically an order of magnitude below displacement rates that have been geodetically measured between points at greater distances from the fault traces. Exponentially decaying postseismic slip in the horizontal and vertical directions due to the 1979 Imperial Valley earthquake has also been measured. Analysis of seismic activity adjacent to slipping faults has shown that accumulated seismic moment is insufficient to explain either the constant or the decaying postseismic slip. Seismic activity removed from slipping faults may be driving their relatively aseismic motion.

Table 1

| Array | Fault | Period | Slip Rate | cor. | samples | ang. |
|---------------|--------------|-------------|-----------|------|---------|-------|
| | | | mm/yr | r | n | omit. |
| Baileys Well | Coyote Creek | 6/71-8/82 | 5.8 | 0.97 | 189 | 3 |
| Devers Hill | Banning | 10/72-11/82 | 2.0 | 0.64 | 69 | 0 |
| Dillon Road | San Andreas | 4/79-11/82 | 0.7 | 0.70 | 35 | 10 |
| | | 4/70-6/77 | 3.0 | 0.85 | 18 | 0 |
| Dixieland | unnamed | 1/71-7/76 | 4.5 | 0.81 | 63 | 0 |
| Indio Hills | San Andreas | 6/77-11/82 | 1.8 | 0.60 | 58 | 0 |
| | | 4/70-6/77 | 1.4 | 0.99 | 12 | 6 |
| North Shore | San Andreas | 8/70-10/72 | 1.2 | 0.65 | 8 | 0 |
| Rand | Garlock | 11/71-2/83 | 0.0 | 0.00 | 120 | 65 |
| Red Canyon | San Andreas | 6/77-5/83 | 3.1 | 0.81 | 44 | 2 |
| | | 5/67-5/83 | 1.7 | 0.88 | 80 | 0 |
| Sta. Ana Wash | San Andreas | 1/73-12/81 | 0.0 | 0.02 | 40 | 4 |

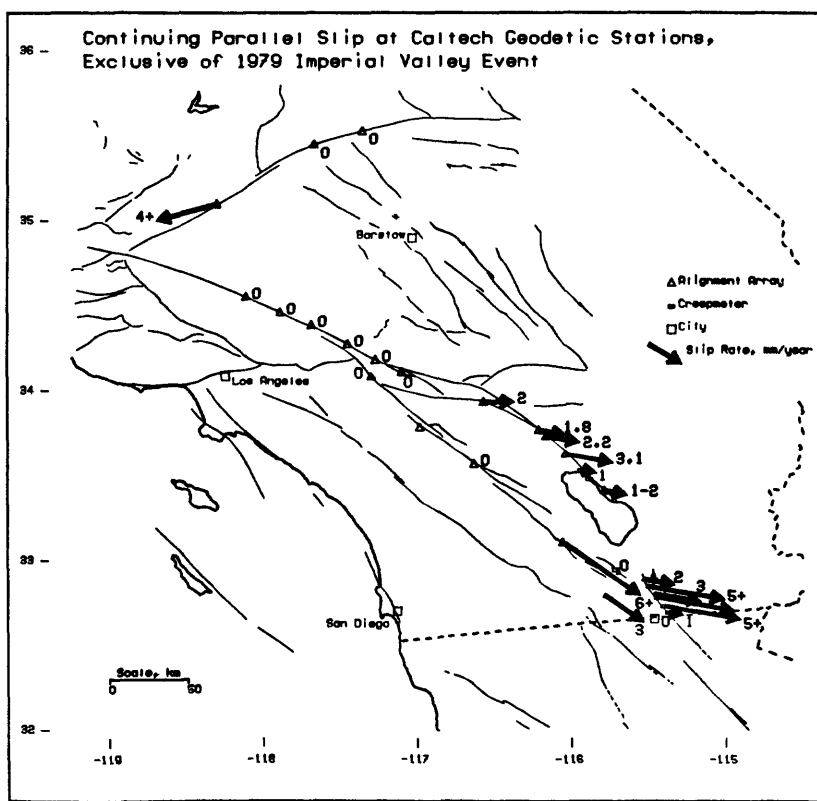


Fig. 1.--Map summarizing observations in southern California of fault slip rates not associated with earthquakes showing surface rupture. All motion is assumed to be parallel to the fault traces; the arrows are oriented only for pictorial convenience and have lengths proportional to the slip rates. Note the faults on which no slip is discernible.

CONTINUED OPERATION OF STRESSMETER NET ALONG
ACTIVE FAULTS IN SOUTHERN CALIFORNIA

Contract #14-08-0001-21868

BRUCE R. CLARK
Leighton and Associates, Inc.
1151 Duryea Avenue
Irvine, California 92714
(714) 250-1421

Investigations

- A. Continue to monitor the Net of fourteen stations along the San Andreas, San Jacinto, and Sierra Madre faults for small stress changes using vibrating-wire Stressmeters.
- B. Develop methods of increasing the sensitivity and depth of emplacement of vibrating-wire sensors.

Results

A. Continued Monitoring

- I. Long-term trends of stress levels are generally consistent with expected tectonic trends at a number of sites. At the Valyermo Array #1 (Figure 1) in a strike-slip setting, the maximum shear stress increase is on a vertical plane in a right-lateral sense, subparallel to the local trace of the San Andreas fault. At San Antonio Dam Array #1 (Figure 2), the maximum shear stress increase is on an east-west plane dipping north (or south) subparallel to the traces of the nearby Sierra Madre fault zone.
2. The long-term trends of the younger arrays are beginning to track the older arrays more faithfully. For example, the Valyermo Array #2 (Figure 1) is starting to show a small stress increase on the north-south sensor after a few years of "relaxing".
3. Both Valyermo and San Antonio Dam recorded a significant stress change accompanying a very low pressure storm front in March 1983. There were no other short-term anomalies in the past year. It is interesting that not all sensors recovered from the barometric event. The dip in the San Antonio Dam #1 EW record (Figure 2) in late 1983 and early 1984 is thought to be an internal sensor malfunction.

4. There appear to be good sites and bad sites for detecting true ground strains or stress changes from boreholes, and the site quality cannot be determined on the basis of surface geology or drilling logs. Causes of a "bad site" may include ground water flow, highly fractured rock, varied lithology, or decoupled bedrock. Increasing the depth of burial helps, but even deep arrays can be noisy, and costs increase dramatically with depth. This implies that we need to deploy arrays widely and be prepared to abandon some.

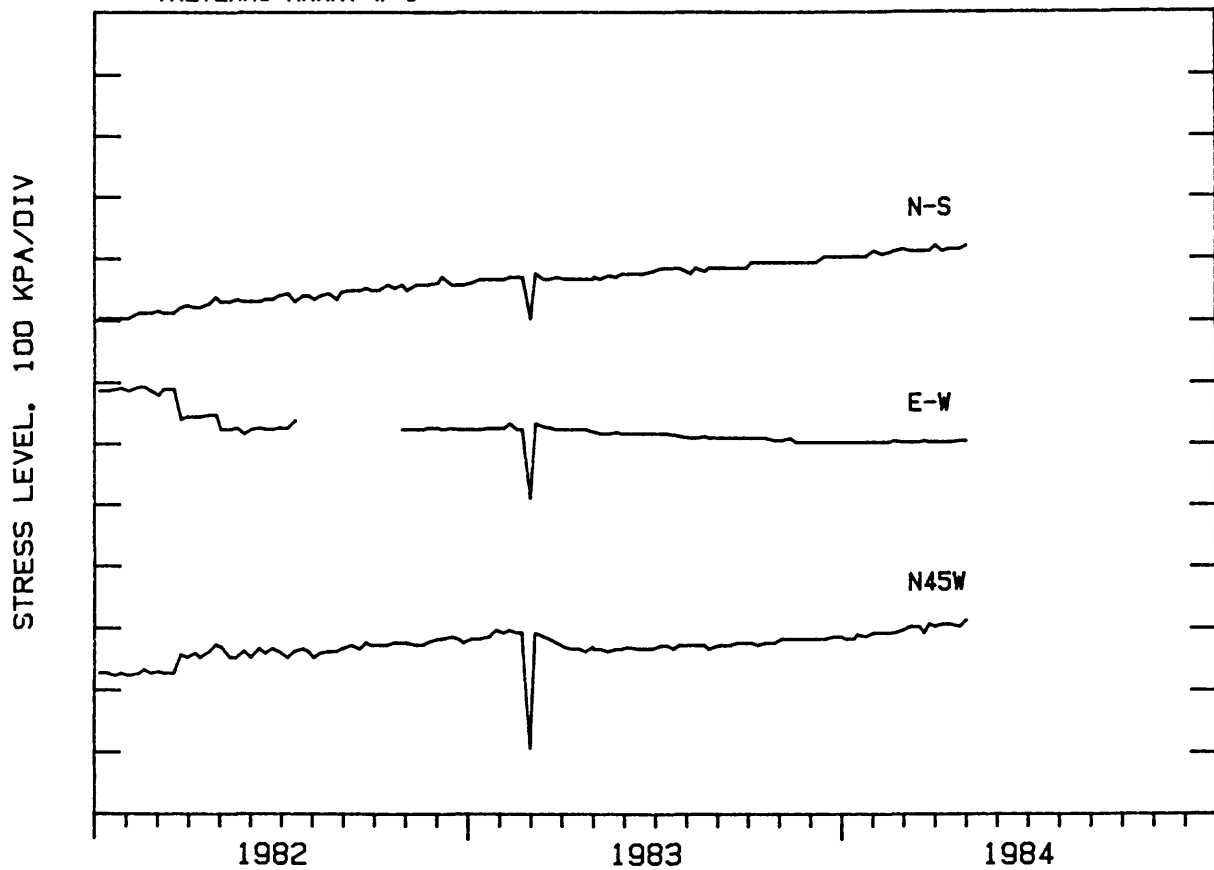
B. New Methods of Emplacement

1. During 1983, we developed and installed a new vibrating-wire Stressmeter (VWS)-based Strain Cell in which the Stressmeter is used as the sensor unit in a Strain Cell consisting of opposed plates of about 100 cm^2 area. The new Strain Cell responds to strain changes of approximately 10^{-8} over a usable range of about 4×10^{-6} . It is grouted into place in standard 15 cm boreholes to depths of at least 60 m.
2. Calibration of the Strain Cell can be checked in the field using the earth tides. The cells are no longer rigid inclusions in this configuration, and strains can be interpreted directly, although for comparison purposes we still convert to stress levels.
3. Initial results come from an array of six sensors installed at a depth of 60 m at Pinyon Flat in late October 1983. Laboratory sensitivities are 0.05 to 0.18 kPa/unit of readout. After the initial curing of the grout, the sensors have given very consistent results at a much higher sensitivity (Figure 3). The initial rise in the records in Figure 3 is due to curing of the grout. Note the change in scale of Figure 3 from Figures 1 and 2.
4. Only limited earth-tide data are available yet. Continued recording problems in this first array preclude our obtaining long records of readings at a reasonable data rate. However, the initial results continue to look good. At a new array scheduled for installation in June, we should be able to correct the electrical grounding problems being encountered in the first array.

Reports

- I. Clark, B. R., 1983, New high-sensitivity Stressmeter installation for ground stress monitoring: EOS, v. 64, p. 862.

VALYERMO ARRAY # 1



VALYERMO ARRAY # 2

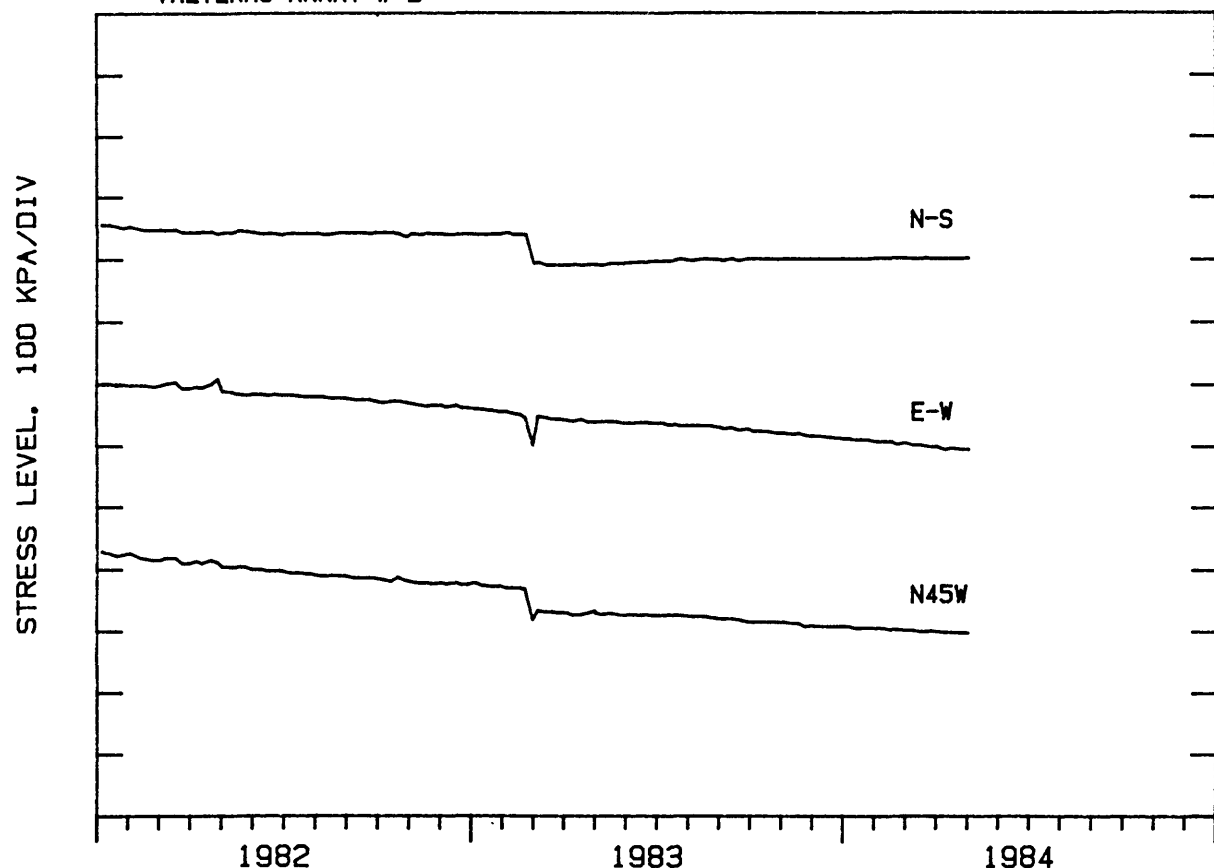


FIGURE 1. Current Records for Valyermo Stressmeter Arrays

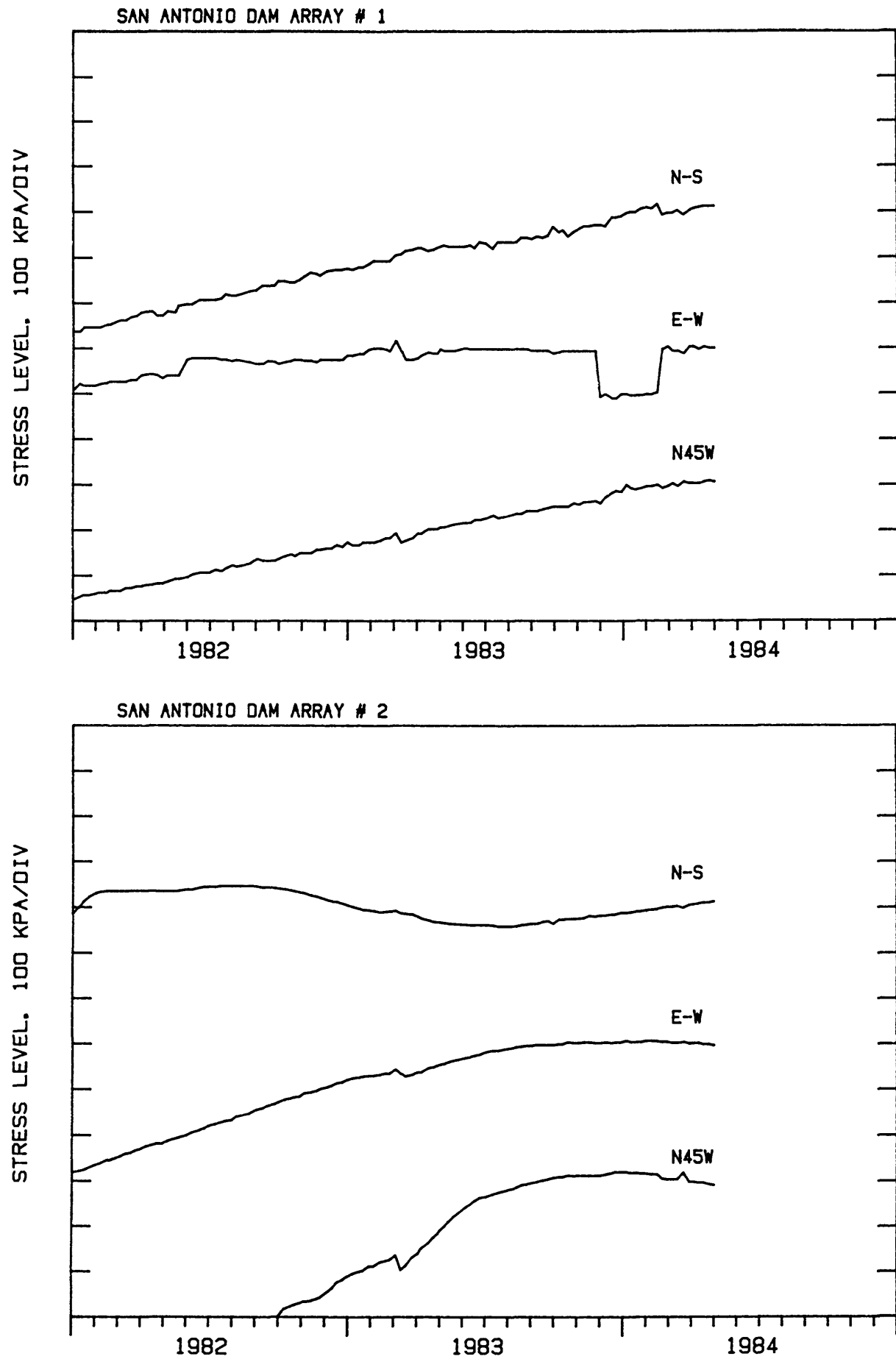


FIGURE 2. Current Records for San Antonio Dam Stressmeter Arrays

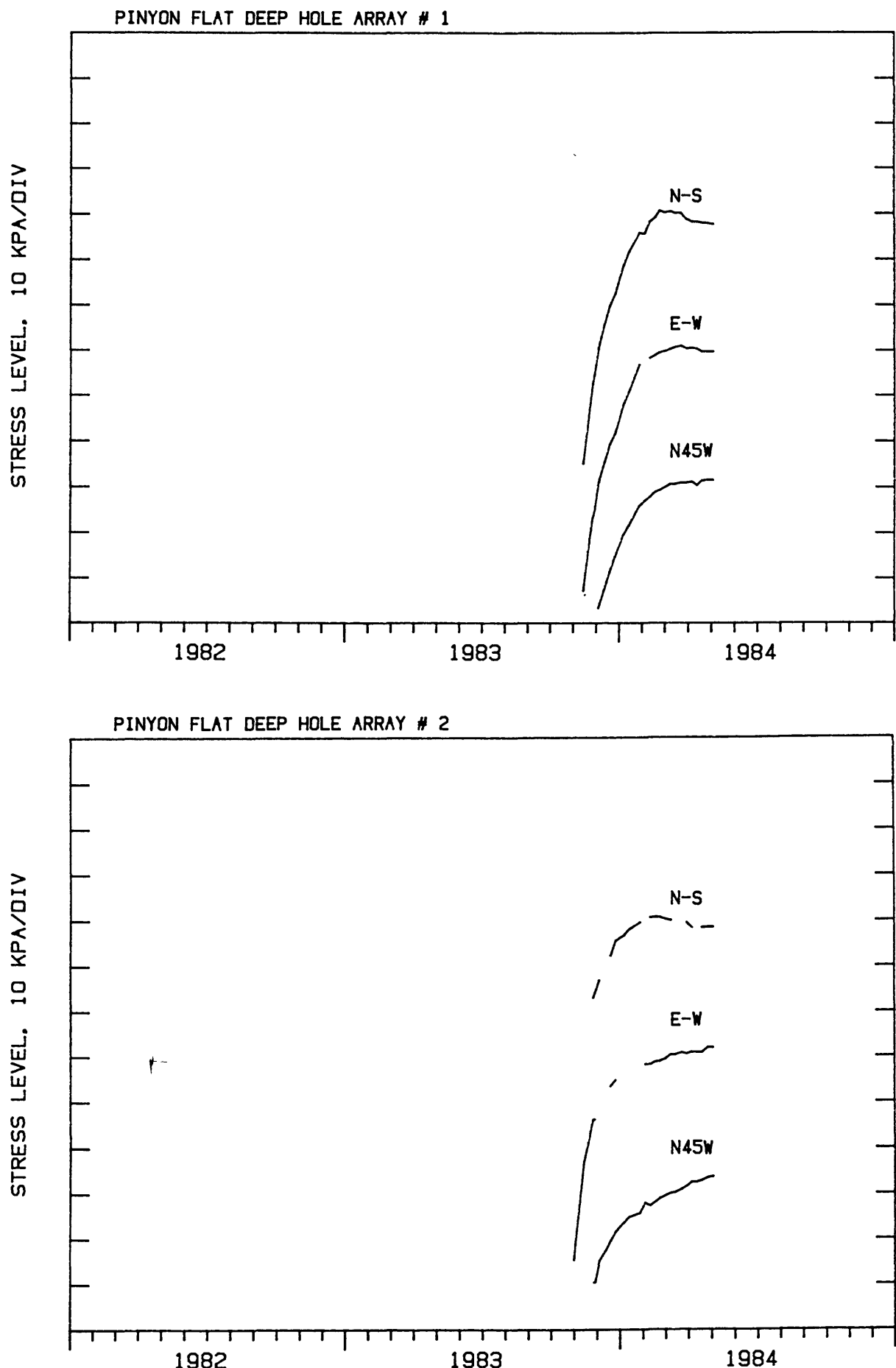


FIGURE 3. Current Records for Pinyon Flat Deep Hole Arrays.
Note expanded vertical scale.

Theodolite Measurements of Creep Rates
on San Francisco Bay Region Faults

Contract No. 14-08-0001-21260

Jon S. Galehouse
San Francisco State University
San Francisco, CA 94132
(415) 469-1204

We began measuring creep rates on San Francisco Bay region faults in September 1979. Amount of slip is determined by noting changes in angles between sets of measurements taken across a fault at different times. This triangulation method uses a theodolite set up over a fixed point used as an instrument station on one side of a fault, a traverse target set up over another fixed point used as an orientation station on the same side of the fault as the theodolite, and a second traverse target set up over a fixed point on the opposite side of the fault. The theodolite is used to measure the angle formed by the three fixed points to the nearest tenth of a second. Each day that a measurement set is done, the angle is measured 12 times and the average determined. The amount of slip between measurements can be calculated trigonometrically using the change in average angle.

We presently have theodolite measurement sites at 20 localities on faults in the Bay region. Most of the distances between our fixed points on opposite sides of the various faults range from 75-215 meters; consequently, we can monitor a much wider slip zone than can be done using standard creepmeters. The precision of our measurement method is such that we can detect with confidence any movement more than a millimeter or two between successive measurement days. We remeasure most of our sites about once every two months.

The following is a brief summary of our results thus far:

Seal Cove-San Gregorio fault - We began our measurements on the Seal Cove fault in Princeton, San Mateo County, in November 1979. For the next 4.2 years, the Seal Cove fault showed net movement at a rate of slightly less than a millimeter per year in a right-lateral sense. However, details regarding whether the tectonic slip is steady or episodic are difficult to ascertain because of seasonal effects involving apparent left-lateral slip that occur toward the end of each calendar year.

Various logistic problems have occurred at our site across the San Gregorio fault near Pescadero in San Mateo County. Since May 1982, we have only remeasured the site four times and results indicate a rate of about three millimeters per year displacement in a right-lateral sense.

San Andreas fault - In more than four years since March 1980 when we began our measurements across the San Andreas fault in South San Francisco, virtually no net slip has occurred. This indicates that the San Andreas fault is locked in the San Francisco area. Our site in the Point Arena area has averaged slightly more than one millimeter per year of right-lateral slip in the three years from January 1981 to January 1984.

Calaveras fault - We have three measurement sites across the Calaveras fault and the nature and amount of movement are different at all three. We began monitoring our site within the City of Hollister in September 1979. Slip along this segment of the Calaveras fault is quite episodic, with times of relatively rapid right-lateral movement alternating with times of little net movement. In the three years from September 1979 to September 1982, the fault moved at a rate of nearly one centimeter per year in a right-lateral sense. However, in more than 1.6 years from September 1982 until 25 April 1984 (the day after the 6.2 magnitude Morgan Hill earthquake on the Calaveras fault) the fault in Hollister has shown virtually no net movement.

At our site across the Calaveras fault on Wright Road just 2.3 kilometers northwest of our site within the City of Hollister, the slip is much more steady than episodic. In more than 4.5 years from October 1979 until 25 April 1984, the Calaveras fault at this site has been moving at a rate of about 13 millimeters per year in a right-lateral sense, the fastest rate of movement of any of our sites in the San Francisco Bay region.

U.S.G.S. creepmeter results in the Hollister area are quite similar to our theodolite results. Creepmeters also show a faster rate of movement at sites on the Calaveras fault just north of Hollister than at sites within the City of Hollister itself.

The rate of movement is much lower at our site in San Ramon, near the northwesterly terminus of the Calaveras fault. Only about one millimeter per year of right-lateral slip has occurred during the past three and one-half years.

The epicenter of the 24 April 1984 Morgan Hill earthquake occurred on the Calaveras fault between our Hollister area sites which are southeast of the epicenter and our San Ramon site which is northwest of it. No surface displacement associated with the earthquake appears to have occurred at any of our three sites.

Rodgers Creek fault - In more than 3.7 years since we began our measurements on the Rodgers Creek fault in Santa Rosa in August 1980, there has been an overall net right-lateral slip of about five millimeters. However, our results also show large variations in the amounts and directions of movement from one measurement day to another which are probably due to seasonal and/or gravity-controlled mass movement effects, not tectonic slip.

West Napa fault - In the 3.8 years since we began our measurements on the West Napa fault in the City of Napa in July 1980, there has been an overall net left-lateral movement of about five millimeters. Similarly to our results for the Rodgers Creek fault, however, large variations up to nearly a centimeter have occurred in both a right-lateral and a left-lateral sense between measurement days. The magnitude of these nontectonic effects is obscuring any tectonic slip that may be occurring. We hope that continued monitoring of these North Bay faults over a longer period of time will help clarify the situation.

Hayward fault - We began our measurements on the Hayward fault in late September 1979 at sites in Fremont and Union City. During the past 4.6 years (through early May 1984), the average rate of right-lateral slip has been about 5.2 millimeters per year in Fremont and about 4.3 millimeters per year in Union City.

We began measuring two sites within the City of Hayward in June 1980. In the nearly 3.8 years since then (to April 1984), the average rate of right-lateral movement has been about 5.1 and about 4.3 millimeters per year.

We began measurements in San Pablo near the northwestern end of the Hayward fault in August 1980. For the past 3.6 years (to April 1984), the average rate of movement has been about 4.3 millimeters per year in a right-lateral sense. However, superposed on this overall slip rate are changes between some measurement days of up to nearly a centimeter in either a right-lateral or a left-lateral sense. Right-lateral slip tends to be measured during the first half of a calendar year and left-lateral during the second half.

Our theodolite triangulation results for the Hayward fault are quite comparable to those determined by U.S.G.S. creepmeters. The Hayward fault appears to be creeping at a rate of about four to five millimeters per year, making it the second fastest creeping fault in the San Francisco Bay region. Only the Calaveras fault in the Hollister area is moving faster.

Concord fault - We began our measurements at two sites on the Concord fault in the City of Concord in September 1979. Both sites showed about a centimeter of right-lateral slip during October and November 1979, perhaps the greatest amount of movement in a short period of time on this fault in the past two decades. In the 4.3 years since this rapid slip, both sites have shown additional right-lateral movement at a rate of only about one millimeter per year.

Antioch fault - We began our measurements at the more southeasterly of two original sites on the Antioch fault in the City of Antioch in January 1980. During the next 27 months, we measured a net right-lateral displacement of nearly two centimeters. However, large changes in both a right-lateral and a left-lateral sense occurred between

measurement days. Three times left-lateral displacement occurred toward the end of one calendar year and/or beginning of the next. We abandoned this site in April 1982 because of logistic problems and relocated it just southeast of the City of Antioch in November 1982. In the 1.5 years until May 1984, the fault at this new site has had a net movement of about two millimeters in a right-lateral sense.

The more northwesterly of our original sites on the Antioch fault is located where the fault zone appears to be less specifically delineated. In the four years from May 1980 to May 1984, we have measured an average of about a millimeter per year of left-lateral slip. Much subsidence and mass movement creep appear to be occurring both inside and outside the Antioch fault zone and it is probable that these non-tectonic movements have influenced our theodolite results. However, a recent trench across the Antioch fault within the City of Antioch showed soil horizons also offset in an apparent left-lateral sense.

Support of the Southern California
Geophysical Data and Analysis Center

14-08-0001-21216

David G. Harkrider
Seismological Laboratory, 252-21
California Institute of Technology
Pasadena, California 91125

This report covers the six-month period from October 1, 1983 to April 1, 1984.

Goals

1. This contract supports the data collecting and processing activities of the CEDAR (Caltech Earthquake Detection and Recording) and CROSS (Caltech Remote Observatory Support System) systems at the Seismological Laboratory.

Results

1. CEDAR

The CEDAR system was originally developed and supported by this contract and its predecessors (contracts #14-08-0001-16629, 17642, 18330, and 19267), and is now an element of the joint USGS-Caltech SCARLET system (Southern California Array for Research on Local Earthquakes and Teleseisms). Its product is a component of the results produced by the contract "Southern California Seismic Arrays", contract #14-08-0001-21209, i.e., the recording and processing of earthquake data effecting a digitized data base of seismic events stored on "Archive" 800 PBI magnetic tapes.

2. CROSS

This contract supplies continuing operational support for CROSS developed under the predecessor contracts (given above). During this reporting period fourteen data login (TIM) units have been maintained on site.

Stations currently in operation:

| SITE LOCATION | TYPE OF MEASUREMENT | PRINCIPAL INVESTIGATOR |
|----------------------|------------------------------|---------------------------|
| Anza (AZ) | water well | Lamar/Merifield |
| Caltech campus (RO) | tilt | T. Ahrens |
| Hollister (HO) | tellurics | T. A. Madden |
| Kresge Lab. (KR) | tilt | Test site |
| Lake Hughes (LH) | tilt, meteorology | T. Ahrens, T. Henyey |
| Palmdale (PD) | tellurics | T. A. Madden |
| Palmdale (PM) | water well baro. pressure | Lamar/Merifield |
| Palmdale (GP) | water well | Lamar/Merifield |
| Palmdale (AQ) | water well | Lamar/Merifield |
| Octillo Wells (OW) | water well | Lamar/Merifield |
| Borrego Springs (BS) | water well | Lamar/Merifield |
| Pallett Creek (PC) | water well | Lamar/Merifield |
| Mecca Beach (MC) | tilt, creep | C. Allen |
| Dalton tunnel (DT) | tilt, meteorology | T. Ahrens |

Note: Some sites listed in previous reports have been removed from service by the P.I.s for operational reasons.

The data at these Southern California sites are collected once or twice a day via a telephone telemetry polling procedure and are being accumulated as a data base on the Caltech Seismological Laboratory PRIME computing system. For non-Caltech investigators the data is made available on hard copy, magnetic tape or via a modem port into the PRIME computer through which investigators may transmit the data to devices at their location by telephone.

DEEPWELL STUDIES ALONG THE SOUTHERN SAN ANDREAS FAULT
14-08-0001-21879

T. L. Henyey and S. P. Lund
Center for Earth Science
University of Southern California
Los Angeles, California 90089-0741
(213) 743-6123

INVESTIGATIONS

Over the past few years, we have reclaimed a set of abandoned wells in the western Mojave Block in which to monitor groundwater variations. The wells are located (Figure 1) in a variety of geologic terranes and range from 500' to 5500' in depth; they were selected from a much larger well population after extensive investigations and work-over operations by commercial rigs. Security and environmental housings have been placed at most well-heads, and in some cases, AC power and telemetry lines installed. We have developed a set of downhole sensors for use in these wells, with emphasis on the following points:

- (1) deployment in deep as opposed to shallow wells;
- (2) compatibility with multiple sensors down-hole;
- (3) long term down-hole service;
- (4) high resolution and low drift.

RESULTS

Figure 1 shows an overview of the water level response across the Palmdale Deepwell Array for the last three years. Note specifically the changing pattern of water level response from the northwest to the southeast. Figure 2 shows the relationship of three months of water level data in the Crystalaire well to the dilatational tides and atmospheric pressure. Figure 3 shows the spectra of the atmospheric pressure, water level and barometric pressure for the same three month period.

Variability in the raw data, due primarily to barometric pressure changes and solid earth tides, tend to mask any short term anomalies due to tectonically induced strain, unless they were abnormally large or short in duration (~ 1 hr. or less). Furthermore, longer term strain changes with time constants from a few days to one year are difficult to separate from rainfall effects. The rainfall effects include long relaxation times which can be on the order of 6 months or more depending on the actual mechanism by which rainfall is communicated to the water table (or air/water interface in the borehole).

It is interesting to note, in spite of these potential problems, that the Fairmont, Skelton and Del Sur wells (northwest of Palmdale along the SAF) all show a continuing long term change in water level while wells to the SE of Palmdale along the fault (Anaverde, Crystalaire, Chief Paduke and Phelan) respond to seasonal rainfall but recover to a reasonably stable baseline.

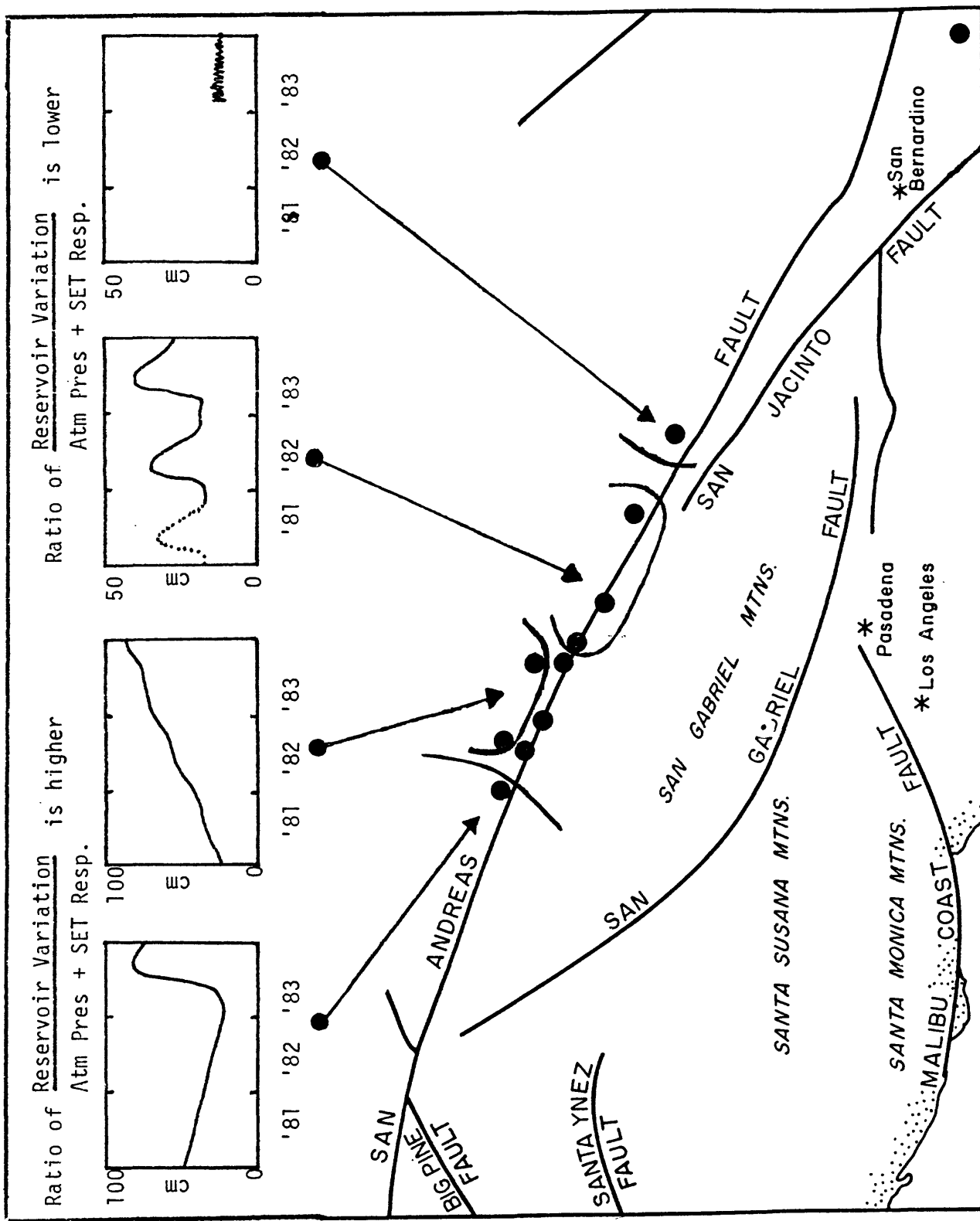


Figure 1: Generalized water level variation along the length of the Palmdale Deepwell Array.

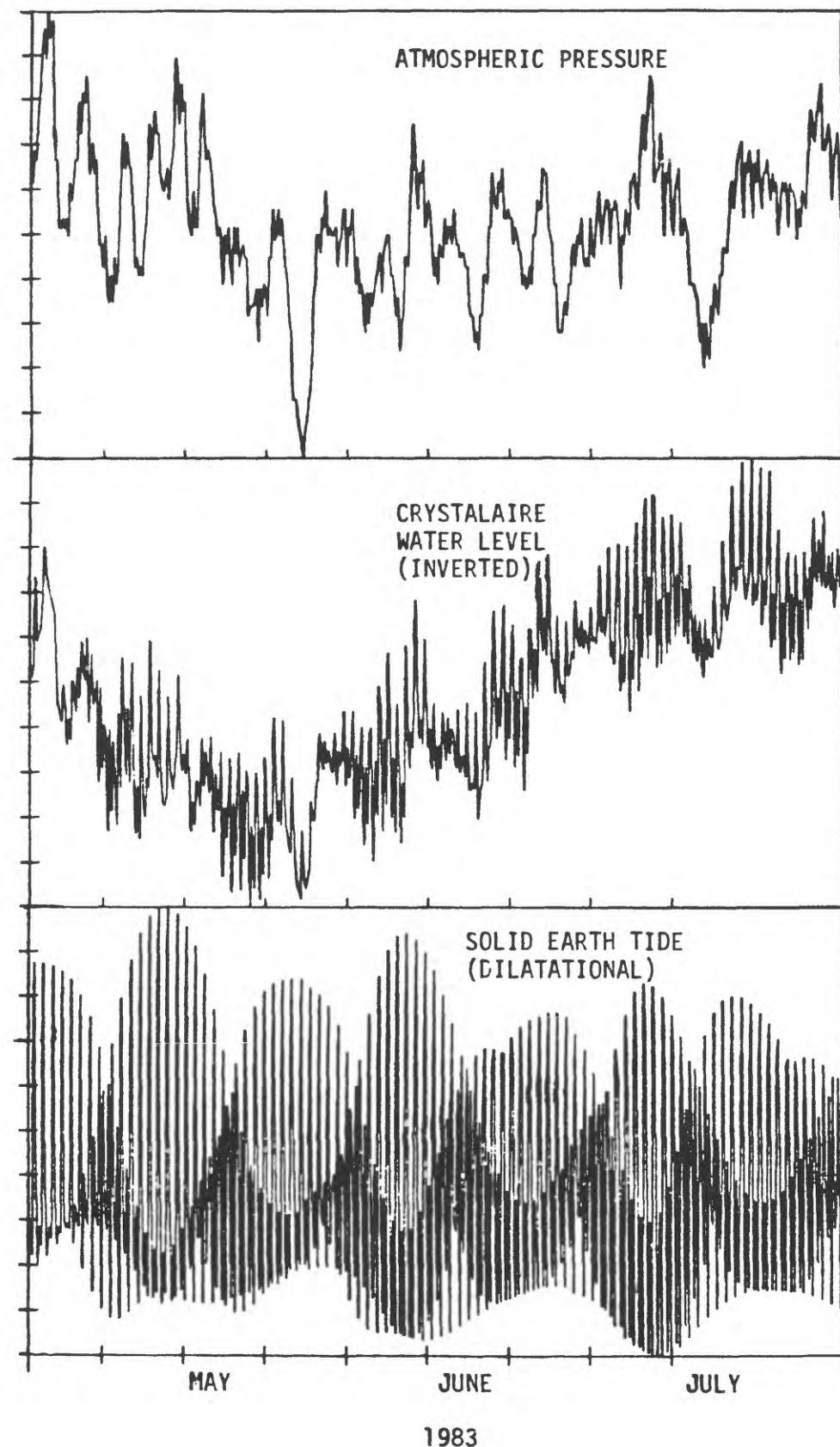


Figure 2. A comparison of the water-level response at Crystalaire with the atmospheric pressure and solid-earth tidal forcing functions.

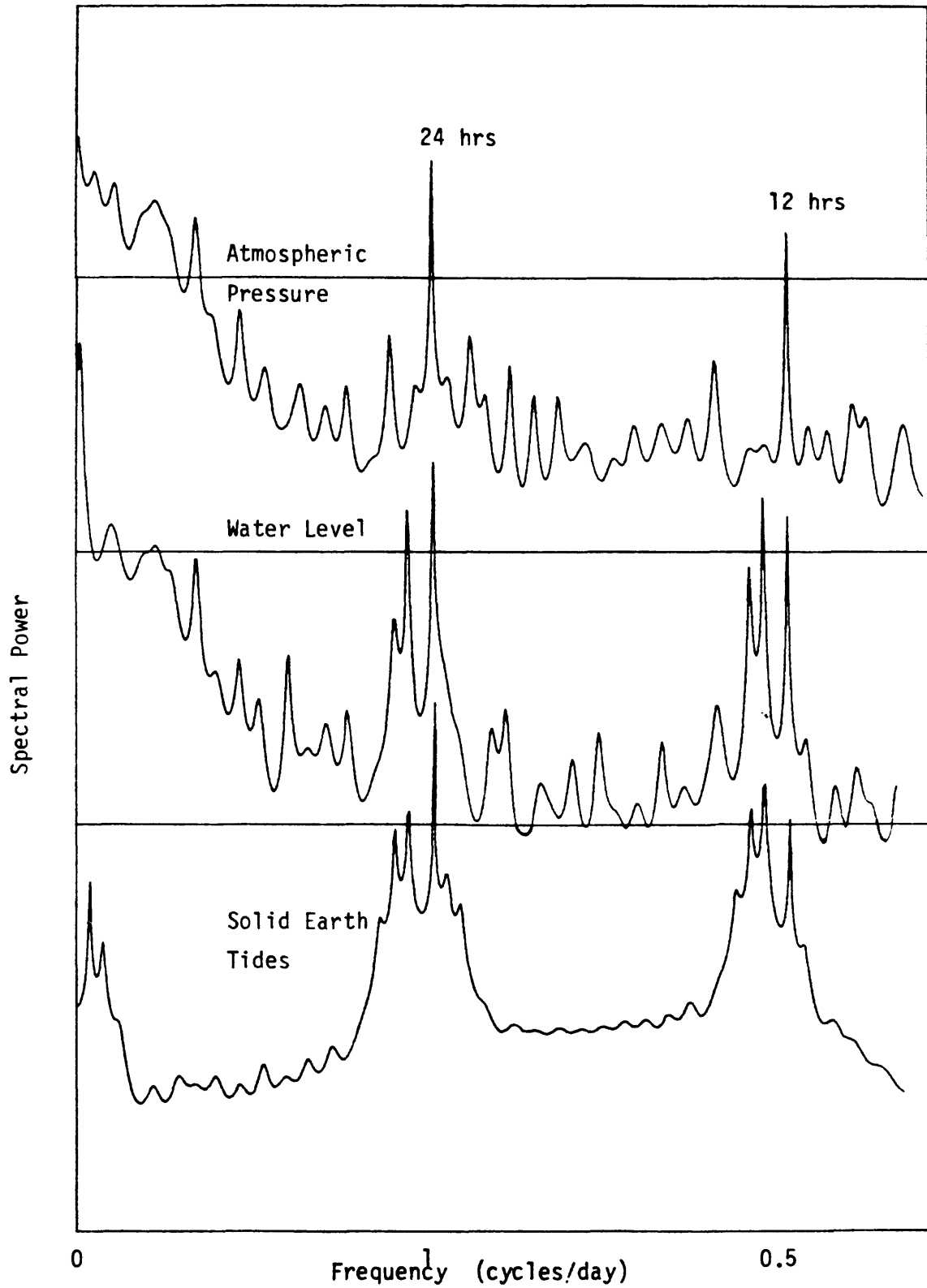


Figure 3. MEM spectra of the waveforms shown in Figure 5. Note the strong correlation between the water-level spectrum and the solid-earth tidal spectrum at periods shorter than 2 days. Likewise note the strong correlation between the water-level spectrum and atmospheric-pressure spectrum at periods greater than 2 days.

San Andreas Earthquake
9380-03074

Robert C. Jachens and Carter W. Roberts
Branch of Geophysics
U.S. Geological Survey, MS 989
Menlo Park, CA 94025
(415) 323-8111, x4248

Investigations

- 1) Remeasured southern California precision gravity base station network.
- 2) Remeasured gravity station at Holcomb Ridge 2-color geodimeter observatory to check for correlation with dilatation anomaly seen in strain observations.
- 3) Analyzed temporal and areal gravity data from Long Valley, California.

Results

- 1) Data from temporal gravity measurements at Tejon Pass, Palmdale, Cajon Pass, and Glendale in November 1983 and February 1984 show a continuing pattern of low amplitude ($20 \mu\text{Gal}$ peak-to-peak) short wavelength (1-2 year) variations that have been seen since late 1976.
- 2) Gravity measurements have been made at the Holcomb Ridge 2-color geodimeter observatory since late 1982 for the purpose of testing the correlation between gravity change and areal strain. Although the gravity changes since the first survey have been small, they display a regular decrease with time during a period when the strain data indicate areal compression. The sign of the relationship between areal strain and gravity change at Holcomb Ridge is the same as that seen earlier at three other locations along the San Andreas fault but the amplitude of the ratio $\delta g/\delta \epsilon$ is smaller than previously measured.
- 3) Recent temporal gravity surveys at Long Valley indicate that gravity changes over the interval June 1982-July 1984 resulted both from crustal deformation and from changes in water table elevation. After correcting for variations in water table elevation, the gravity data covering the 1982-1983 uplift indicate a gravity change/elevation change ratio of about $-2.5 \mu\text{Gal/cm}$. This value suggests that magma intrusion accompanied the uplift. Gravity measurements at a few stations near Casa Diablo Hot Springs taken in June 1982, September 1982, January 1983 (during the south moat earthquake swarm), and July 1983 suggest that the 1982-1983 uplift accumulated after the earthquake swarm. A leveling survey conducted by the Los Angeles Department of Water and Power about two weeks after the swarm detected the uplift. Therefore, the combined data sets suggest that the uplift accumulated immediately after the swarm.

Reports

- 1) Langbein, J. O., Linker, M. F., McGarr, A., and Jachens, R. C., 1983, Two-color geodimeter measurements of crustal strain accumulation near Palmdale, California: Comparisons with gravity and meteorological data: *Transactions American Geophysical Union*, v. 64, p. 841.
- 2) Jachens, R. C., and Roberts, C. W., 1984, Gravity investigations at Long Valley Caldera, California, in *Proceedings of Conference, Active Tectonic and Magmatic Processes in Long Valley Caldera, Eastern California*: U.S. Geological Survey Open-File Report (in press).

Earthquake and Seismicity Research Using SCARLET and CEDAR

Contract No. 14-08-0001-21210

Hiroo Kanamori, Clarence R. Allen, Robert W. Clayton
 Seismological Laboratory, California Institute of Technology
 Pasadena, California 91125 (818-356-6914)

Investigations

- 1) Seismic evidence for a slab beneath southern California.
- 2) Pn travel times in southern California.

Results

Humphreys et al. (1984) performed a detailed tomographic inversion of teleseismic P delays recorded by the Southern California Array and found two prominent features beneath the region (Figure 1). The first is a vertical slab-like wedge directly beneath the Transverse Ranges that is 2-3% faster than the surrounding region. This feature deepens to the east, attaining a maximum depth of about 250 km beneath the San Bernardino Mountains. The spatial association of the Transverse Ranges with the velocity anomaly below can be explained by lithospheric convergence in the region of the Big Bend of the San Andreas Fault, and the subduction of sub-crustal lithosphere. The second feature is a major zone of low velocity material (>2% slow) under the Salton Trough rift valley, extending to a depth of about 125 km.

A tomographic back-projection method was applied to invert about 10,000 teleseismic P delays. The algorithm used was a modified form of an Algebraic Reconstruction Technique (ART) used in medical X-ray imaging. A deconvolution with an empirically estimated point spread function was also applied to help in the focusing of the image.

Hearn (1984) analyzed Pn travel times in southern California. The Pn arrivals recorded from the southern California array have been used to demonstrate regional variations in crustal thickness and Pn velocity and to investigate the presence of anisotropy in the mantle. Over 2800 travel times were used in the analysis. The classical time term method was extended to allow the Moho velocity to vary in a block-type structure. The statistical F test shows these effects to be significant. Crustal delays determined depend on both crustal velocities and Moho depth. The Ventura and Los Angeles basins have sediment delays which indicate sediment thicknesses near 10 km. The Moho depth itself varies by 10 km over southern California with a mean of about 29 km. Slightly thicker crust is prevalent in the northwestern corner of the array near the Southern Coast Ranges. Five kilometers of rapid thinning between the coast and the Channel Islands is shown by a sharp gradient in the delay times. Normal crustal thicknesses occur over the rest of the array except for the area east of the Salton Trough, where an anomalously thick crust of 22 km exists. This area extends from near the plate boundary into Arizona. While the Peninsular Ranges and the San Bernardino Mountains have

small roots, the San Gabriel Mountains have none. Pn velocities range from 7.6 to 8.2 km/s within the array. High velocities are found in the Mojave and offshore regions. Low velocities are found in the Peninsular Ranges and the Transverse Ranges. The analysis supports a mean anisotropy of 0.15 km/s with the fast direction at N 75° W. This value represents an average of a parameter that varies considerably in the region.

Reports and Publications

Hearn, Thomas M., Pn travel times in southern California, Jour. Geophys. Res., 89, No. B3, 1843-1855, 1984.

Humphreys, Eugene, Robert W. Clayton, and Bradford H. Hager, A tomographic image of mantle structure beneath southern California. Submitted to Geophysical Research Letters, January 10, 1984.

Webb, Terry H. and Hiroo Kanamori, Earthquake focal mechanism near the southern San Andreas fault, Seismological Society of America, Spring Meeting, Anchorage, Alaska, May 30, 1984.

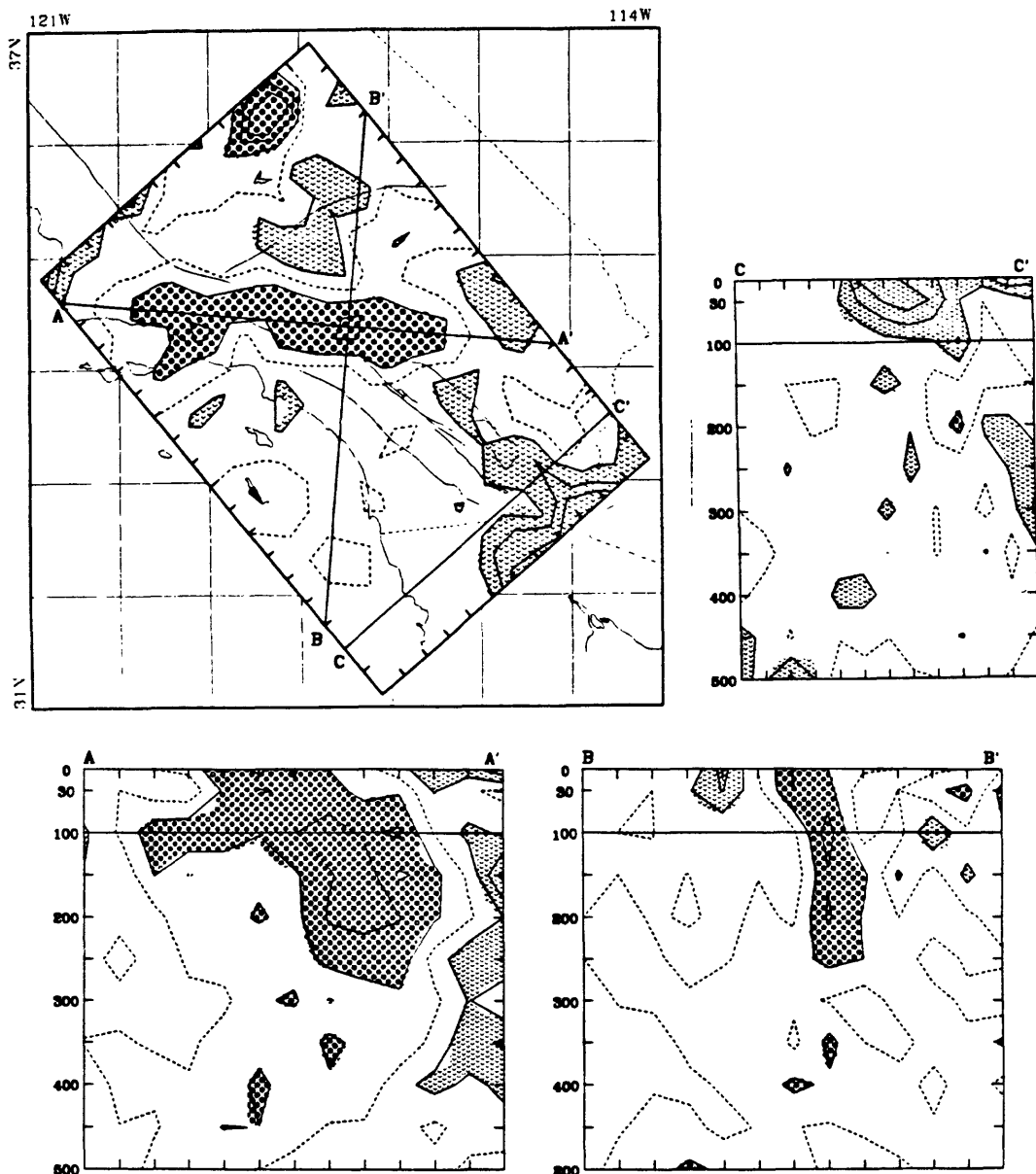


Figure 1. Results of the inversion of teleseismic P-delays. In the upper-left panel a horizontal section at a depth of 100 km is shown superimposed on a location map of southern California. The locations are shown for the three cross-sections (A-A', B-B', and C-C') that are displayed in the other panels. The tick marks surrounding the horizontal section show the locations of the block centers used in the inversion. All panels are displayed with no relative exaggeration. The contour interval is 1.5% relative velocity deviations, with >1.5% indicated by dotted areas and <-1.5% by the hatched areas. The zero contour is dashed. In the lower-left panel a W E cross-section (A-A') through the Transverse Range anomaly is shown. In this projection the anomaly appears as a wedge-like feature that is deeper on the eastern side. A S N cross-section (B-B') through the Transverse Range anomaly is shown in the lower-right panel. The anomaly appears as a slab-like feature that dips slightly to the north. In the upper-right panel a SW NE cross-section through the Salton Trough anomaly is shown. The anomaly is about 2-4% slow and extends down to 75-125 km.

HYDROLOGICAL/GEOCHEMICAL MONITORING ALONG SAN ANDREAS
AND SAN JACINTO FAULTS, SOUTHERN CALIFORNIA,
DURING FIRST HALF OF FISCAL YEAR 1984

Contract 14-08-0001-21859

D. L. Lamar and P. M. Merifield
Lamar-Merifield Geologists, Inc.
1318 Second Street, Suite 25
Santa Monica, California 90401
(213) 395-4528

Investigations

Water levels in more than thirty wells along the San Andreas and San Jacinto fault zones were monitored during the current reporting period. Water levels in five wells, barometric pressure at three wells, and temperature and conductivity at one well were monitored by TIM units operating on the Caltech Remote Observatory Support System (CROSS). The changeover from CROSS to a telemetry system utilizing Enviro-Labs, Inc. data loggers (Model DL-120-MCP) and our office computer has been initiated; two wells are currently operating in the new mode.

Another nine wells were monitored continuously with Stevens Type F recorders, two being maintained by W. R. Moyle, Jr. of the Geological Survey. The remaining wells were probed primarily monthly, but in a few cases weekly, semiweekly, or daily with the aid of volunteers. Temperature, salinity, and conductivity were measured in ten selected wells at the time the water-level charts were changed.

Results

Precipitation during the winter months of 1983-84 was less than normal. Most well hydrographs showed little or no response to the winter rains, for example, the hydrograph in Fig. 1. No anomalous water-level changes have been identified in the long-term hydrographs. Moreover, wells that are considered good strain meters because of their response to earth tides and diurnal barometric pressure variations (see, for example, Fig. 2) have not shown anomalous fluctuations that could be interpreted as strain events.

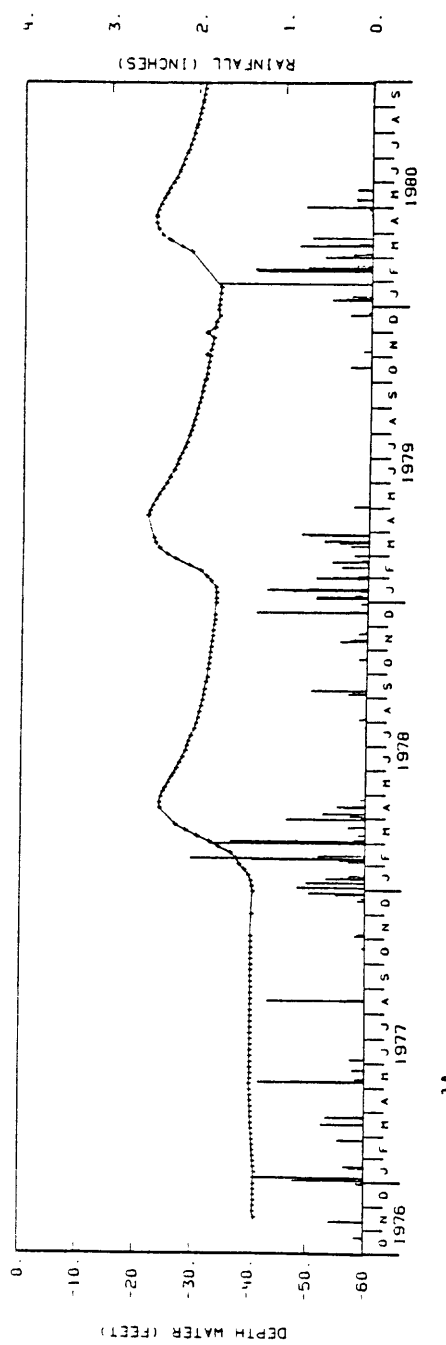


FIGURE 1A -- WEEKLY OBSERVATIONS OF WATER LEVEL (•) AND RAINFALL (.) IN WELL NUMBER 05N12W-14C01 DURING 1976-1980 PALMDALE AREA SEASONAL RAINFALL AT ADJACENT STATIONS IN INCHES ACROSS TOP

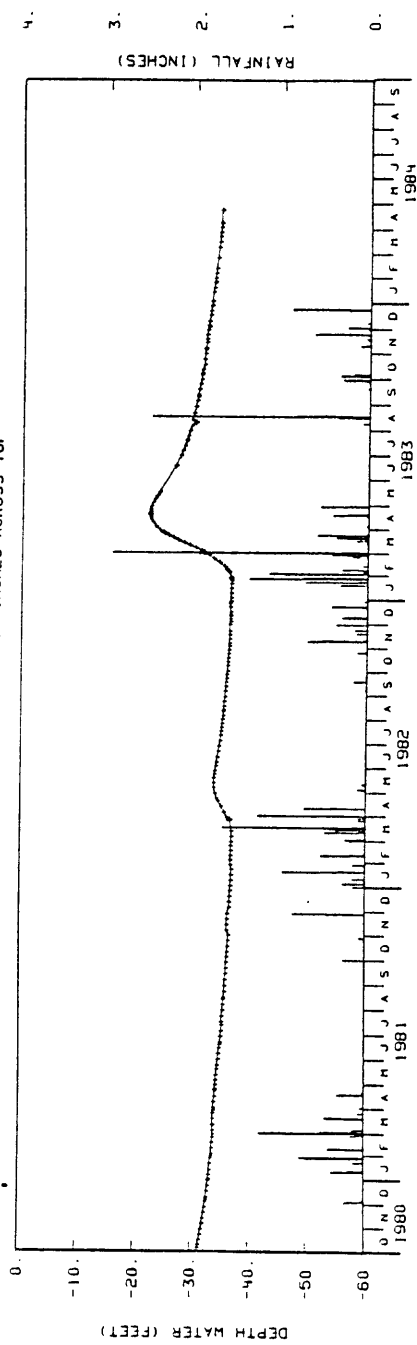


FIGURE 1B -- WEEKLY OBSERVATIONS OF WATER LEVEL (•) AND RAINFALL (.) IN WELL NUMBER 05N12W-14C01 DURING 1980-1984 PALMDALE AREA SEASONAL RAINFALL AT ADJACENT STATIONS IN INCHES ACROSS TOP

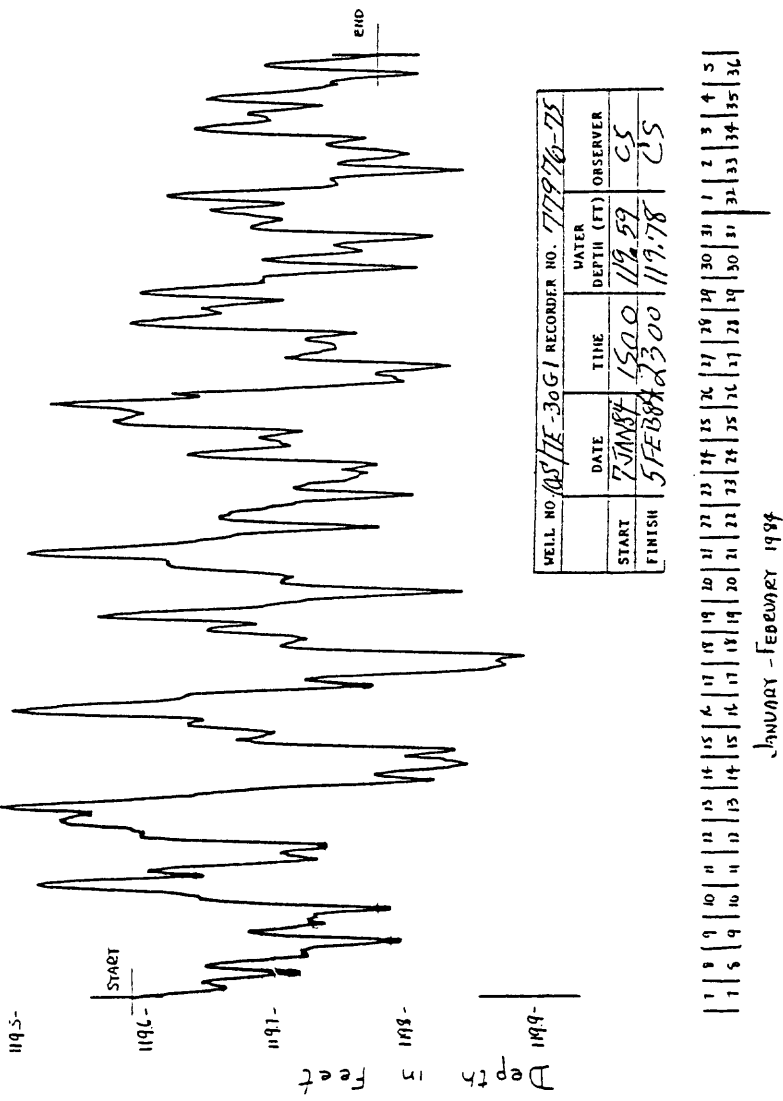


Fig. 2 - Stevens record for well 10S/7E-30G1, Borrego Valley, 7 Jan to 5 Feb 1984

CARBON FIBER STRAINMETER STUDIES
IN SOUTHERN CALIFORNIA
14-08-0001-21240

Peter C. Leary
Center for Earth Science
University of Southern California
Los Angeles, CA 90089-0741
(213) 743-8034

The southern California strainmeter network comprises instruments designed at Cambridge and improved by Roger Bilham (King and Bilham, 1976). The strainmeter installation consists of two piers firmly anchored to the ground at points 20 meters or more apart, and connected by a multistranded length of molecular carbon fiber. The carbon fiber is kept under tension by a weighted arm on a pivot. Displacement of the arm is recorded by an LVDT at a resolution of 1 micron. The strain sensitivity of the undisturbed instrument is about 10^{-9} . Long term drift due to fatigue in the fiber is about $10^{-7}/\text{year}$. The instrument is capable of returning a well resolved solid earth tide signal.

For fault zone strain studies, the desirable distribution of these instruments would have been near the fault. However, shielding the strainmeter from surface disturbances by placing them in tunnels took priority over proximity to the fault. The present array of sites is, therefore, dictated by available tunnel locations (Figure 1). Of these sites BQ has been operating since 1979, the DT site since mid-1980, and the remaining sites since mid-1981.

The experience gained in these years indicate that near surface temperature and particularly precipitation strain effects dominate the strain record of the 20 meter carbon fiber instruments even when they are placed in tunnels. Season temperature and precipitation strain cycles of $1/2$ to $3/2 \times 10^{-6}$ are a factor of ten larger than the secular trend of fault zone strain build-up. Short term rainfall effects dot the strain records. These surface effects register 10 to 100 times the plausible levels of short term tectonic strain, and remain the only transient strain signal that could be called "coherent" across the strainmeter network.

There is probably little hope for obtaining information to correct the strain record for local strain effects. The problem is that an instrument that is 20 meters deep in the crust senses surface effects at the 20 meter scale length. Monitoring the tilt of the strainmeter piers, for instance, would provide a corrective factor for strain at the one meter scale length. Strain noise at one meter is, however, probably unrelated to strain noise at 20 meters. Unless the strainmeter is longer than it is deep, local effects cannot be efficiently compensated for by short baseline secondary strain, tilt, or pore pressure data.

The role of short baseline, continuously recording instruments should not be discounted. By very closely examining the records of the USGS creepmeter near Palmdale, i.e. treating the creepmeter as if it were a strainmeter, Leary and Malin (1984) have been able to show that the nominally locked portion of the San Andreas fault underwent a series of at least four 20 micron dislocations in very close temporal association with local seismicity during the time of the 1979 Palmdale trilateration strain anomaly (Figure 2). Between February and October, 1979, the USGS Palmdale geodimeter net showed a marked E-W tensional strain anomaly (Savage *et al.*, 1981). Subsequent analyses of nearby trilateration, leveling and gravity networks tend to support the Palmdale anomaly (Jachens *et al.*, 1983) and local seismic events have been shown to undergo a change in focal mechanism from thrust to strike-slip during this period in 1979 (Sauber *et al.*, 1983). The nearest strainmeter to the fault zone that was operational in 1979 showed no evidence of strain associated with this deformation.

Without the temporal and spatial details of a continuously recording strain instrument network, the strain anomaly is very poorly defined. In contrast, from the limited observations of the one available creepmeter qua strainmeter (Figure 2), it is seen that, i) at least some of the strain was concentrated in the January, February and March period of 1979; ii) the strain preceded the earthquakes, as if the latter occurred only as local stress hangups to a larger scale deformation, and iii) because the Homestead Valley earthquake (March 15, 1979) was also preceded by a creepmeter slip event, it is sensible to incorporate this earthquake into a larger picture of regional strain associated with the trilateration strain event and other regionally distributed displacement sensors (Leary and Malin, 1984). The continuously recording short baseline record is incomplete because only a single instrument was operating. Moreover, because there are no off-trace strainmeters there is no depth profile of the slip detected on the fault trace. It was demonstrated by Goultby and Gilman (1978) that slip 500 meters deep could be well resolved by off-fault strainmeters. Judging from their results, deeper slip planes could be resolved if such slip occurred during the 1979 event.

With a complete set of strain sensing short baseline instruments on and near the fault, the active surface trace of the fault could be determined and the equivalent earthquake magnitude of "slow earthquake" deformational events such as occurred in early 1979 could be ascertained. This information could then be translated into amplitude and time resolution levels of monitoring sensitivity required to detect plausible precursory events on the locked San Andreas fault. For instance, if we follow the creepmeter slip data as interpreted by Leary and Malin (1984) and incorporate the M=5.0 Homestead Valley earthquake into the 1979 strain event on the San Andreas fault, we can say that precursory and co-seismic strain associated with M=5 earthquake was not detected by presently arrayed strainmeters, but that such strain would be detectable by surface sited near-fault strain instruments.

REFERENCES

- Goultby, N. R. and R. Gilman, Repeated creep events on the San Andreas fault near Parkfield, California, recorded by a strainmeter array, JGR, 83, no. B11, November 10, 1978.
- Jachens, R. C., W. Thatcher, C. W. Roberts, R. S. Stein, Correlation of changes in gravity, elevation, and strain in southern California, Science 219, p. 1215, 11 March 1983.
- King, G. and R. Bilham, A geophysical wire strainmeter, BSSA, 66, no. 6, December 1976.
- Leary, P. C. and P. E. Malin, Ground deformation events preceding the Homestead Valley earthquakes, BSSA, 1984, in press.
- Savage, J., W. Prescott, M. Lisowski, and N. King, et al., Strain accumulation in southern California, 1973-1980, JGR, 86, 1981.
- Sauber, J., K. McNally, J. Pechmann, and H. Kanomori, Seismicity near Palmdale, California, and its relation to strain changes, JGR, 88, no. B3, March 10, 1983.

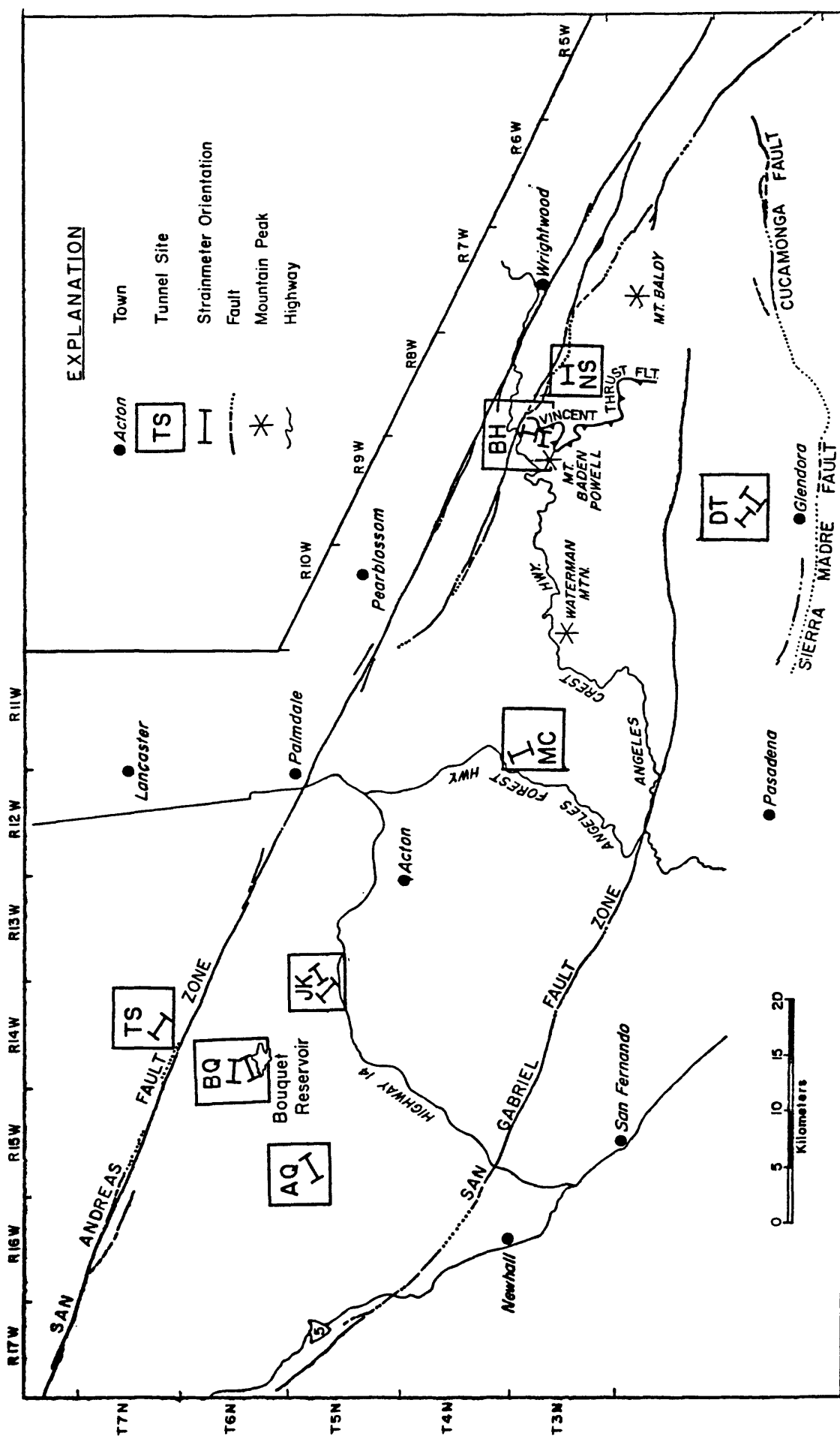


Figure 1. Distribution of carbon fiber strainmeters in southern California; active sites are TS, BQ, JK, and DT.

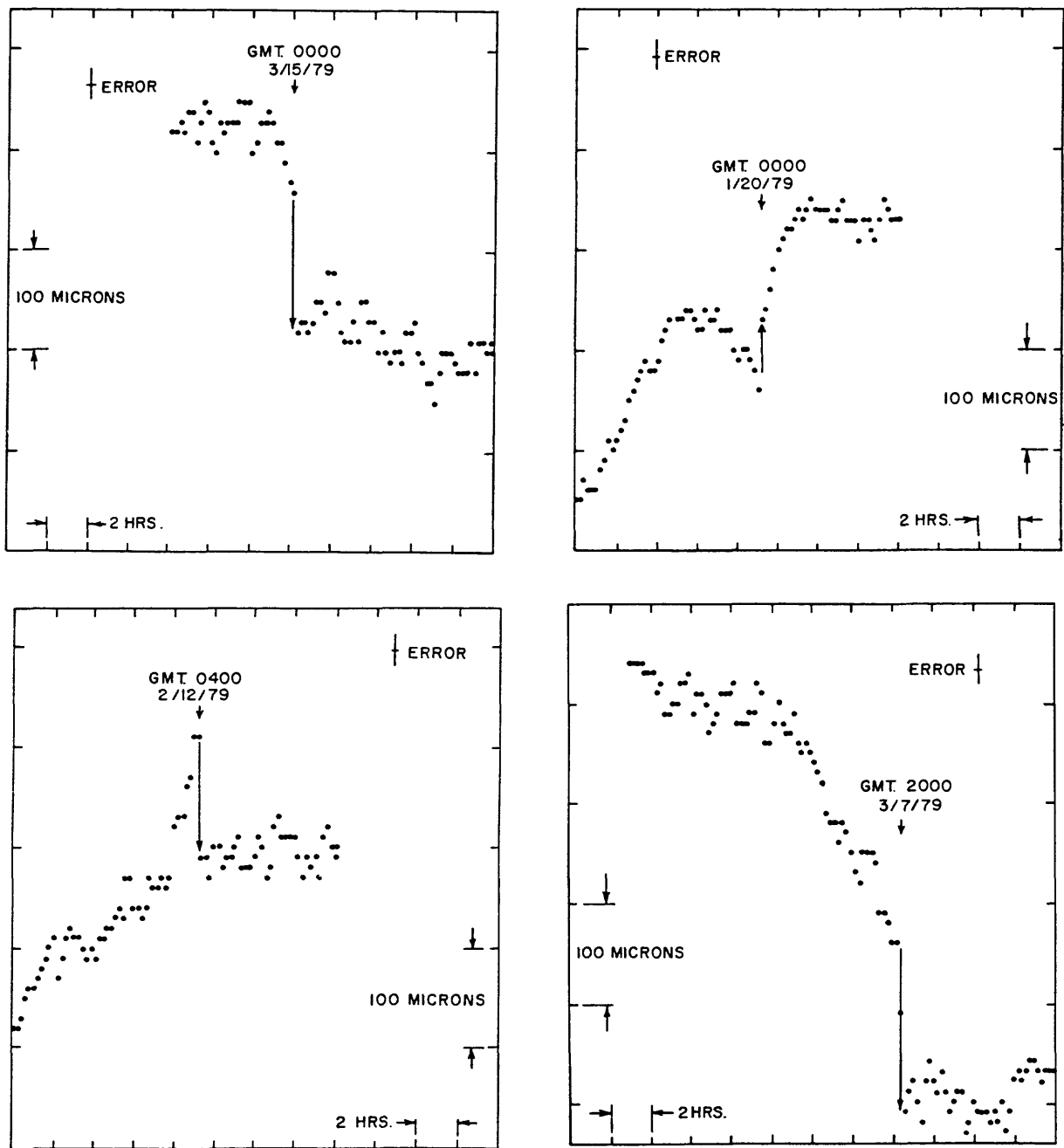


Figure 2. Creepmeter steps in the analog record for 11-30-78 to 3-22-79 for USGS instrument XWR1 near Palmdale, CA. Vertical scale is given in microns as measured by traveling stage microscope under which records were digitized. 200 microns on the analog chart correspond to 20 microns relative pier displacement. Extension is down. A, B, and C are creep steps preceding earthquakes; D is the step prior to the Homestead Valley earthquake.

Parkfield Seismicity Project

9930-02098

Allan G. Lindh
Branch of Seismology
U. S. Geological Survey
345 Middlefield Road M/S 977
Menlo Park, California 94025
(415) 323-8111, ext. 2042

Investigations

Work continued on Parkfield, long-term earthquake probabilities along the San Andreas systems, automatic processing of real-time seismic data, digital magnitudes for real time systems, and next-generation micro-processors for real time systems.

Results

Lindh, A. G., and Ellsworth, W. L., (1984), Long Term Probabilities for Large Earthquakes on the San Andreas Fault System, JGR (in press).

In-Situ Seismic Wave Velocity Monitoring

14-08-0001- 21222

T.V. McEvilly

R. Clymer

Seismographic Station

Department of Geology and Geophysics

University of California

Berkeley, California 94720

(415) 642-3977

Investigations

On-going monitoring of first-arrival travel times on 8 paths and down-hole times at 7 boreholes at sites adjacent to the San Andreas fault in central California (Figure 1) continued through this report period. One measurement was made of deep reflections in the vicinity of Bear Valley. Measurements are made with a Vibroseis® system.

Results

Repeated measurements indicate a travel-time precision below 1 msec for first arrivals. Travel times on monitoring paths have followed smooth trajectories that primarily represent seasonal variations of several msec of very near-surface origin. Borehole data sets, collected at most sites, have been used to develop preliminary corrections to remove the near-surface effects. We see a stability of about 1 msec in the corrected travel-time data, shown in Figures 2 and 3. After 3.5 years of monitoring, it is now evident that there is a similarity of data sets from paths that share a common vibrator site. We suspect this is indicative of incomplete removal of near-surface variations occurring at the source end of each path.

Monitoring of deep crustal reflections in the Bear Valley area has continued to proceed slowly, due to severe cultural noise and the present necessity to temporarily install the long geophone array for each measurement. In the one recording session of this report period, measurements were compatible with a precision of several msec in the travel time of individual extrema (10^{-4} to 10^{-3} of travel time), and showed no significant change in travel time from the measurement made in December '82.

Equipment

In the spring and early summer, we were forced to move the recording-truck systems to a new vehicle. A new cassette-based recording system allowing phone-line transmission of field data to a computer in Berkeley was installed at this time, and functioned well for the remainder of the field season.

Data collection during this period was slowed by frequent intermittent failures of the vibrator control system and the correlator.

Future Operations

To cut costs, the field crew was permanently disbanded in January '84. For the remainder of this fiscal year, we expect to make quarterly measurements, replacing the full-time field crew with the project scientist and a temporary hire.

* Conoco

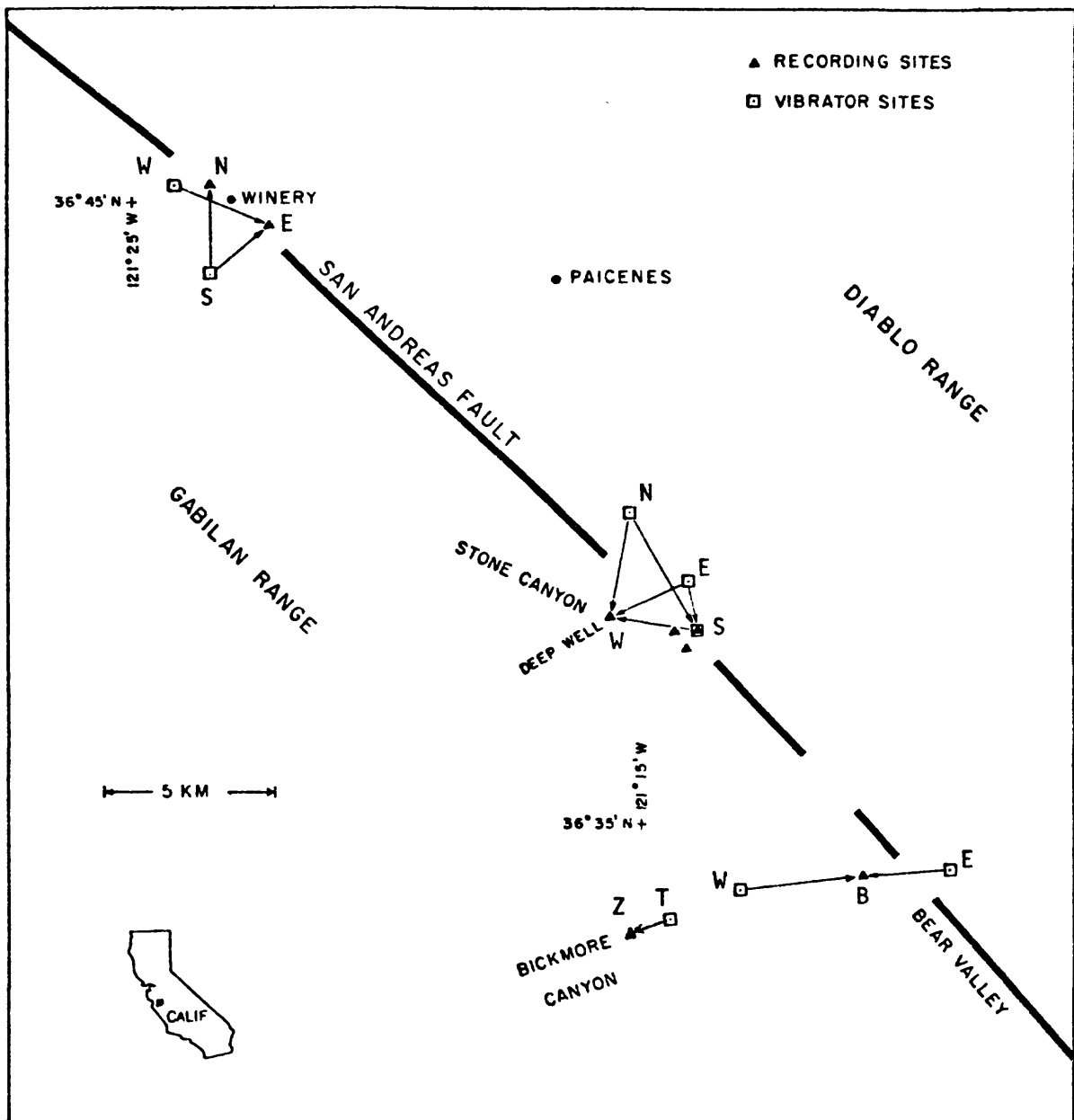


FIGURE 1. Source and receiver sites, Winery, Stone Canyon and Bickmore Canyon areas.

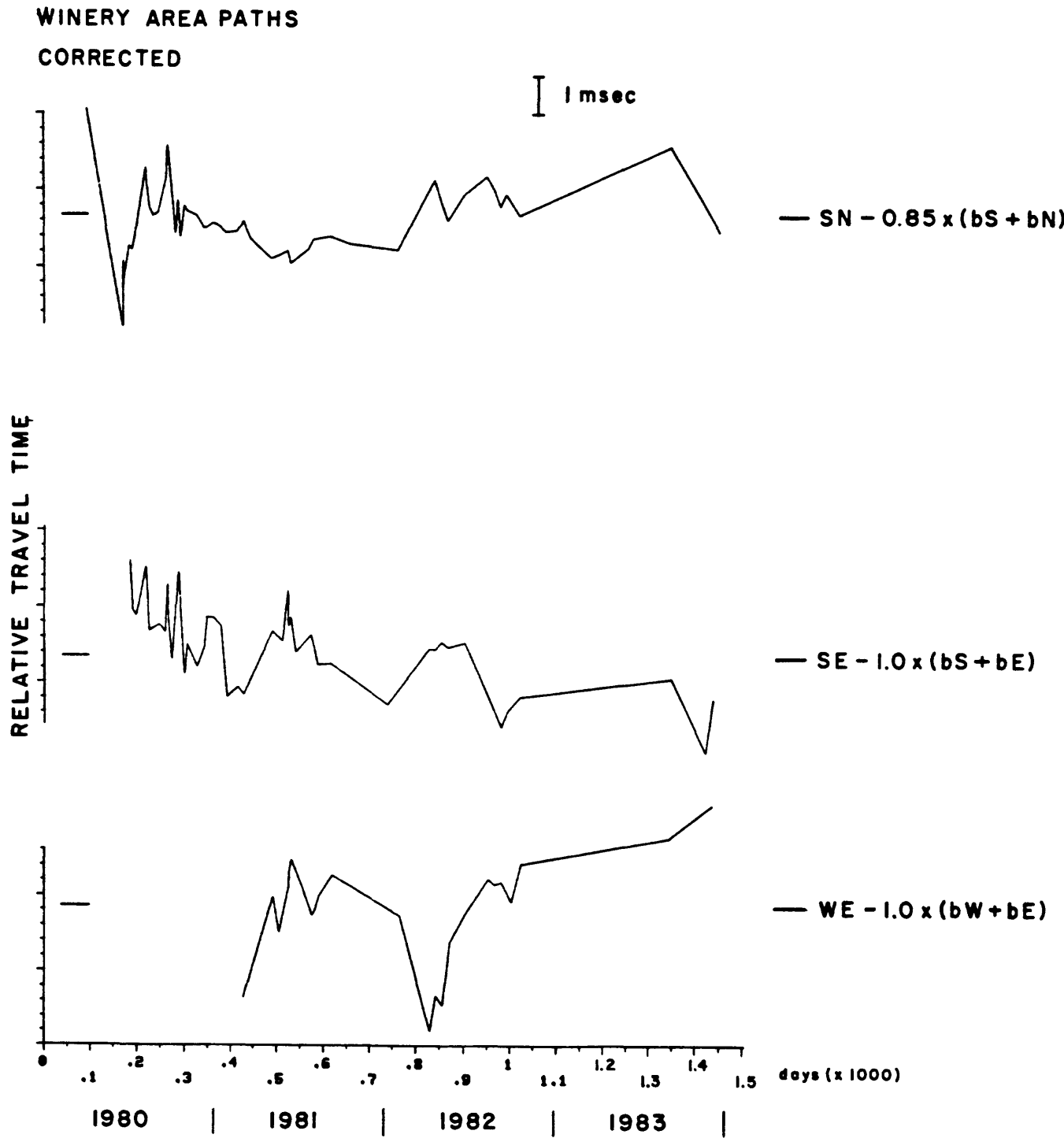


Figure 2. Winery area, seasonally-corrected data.

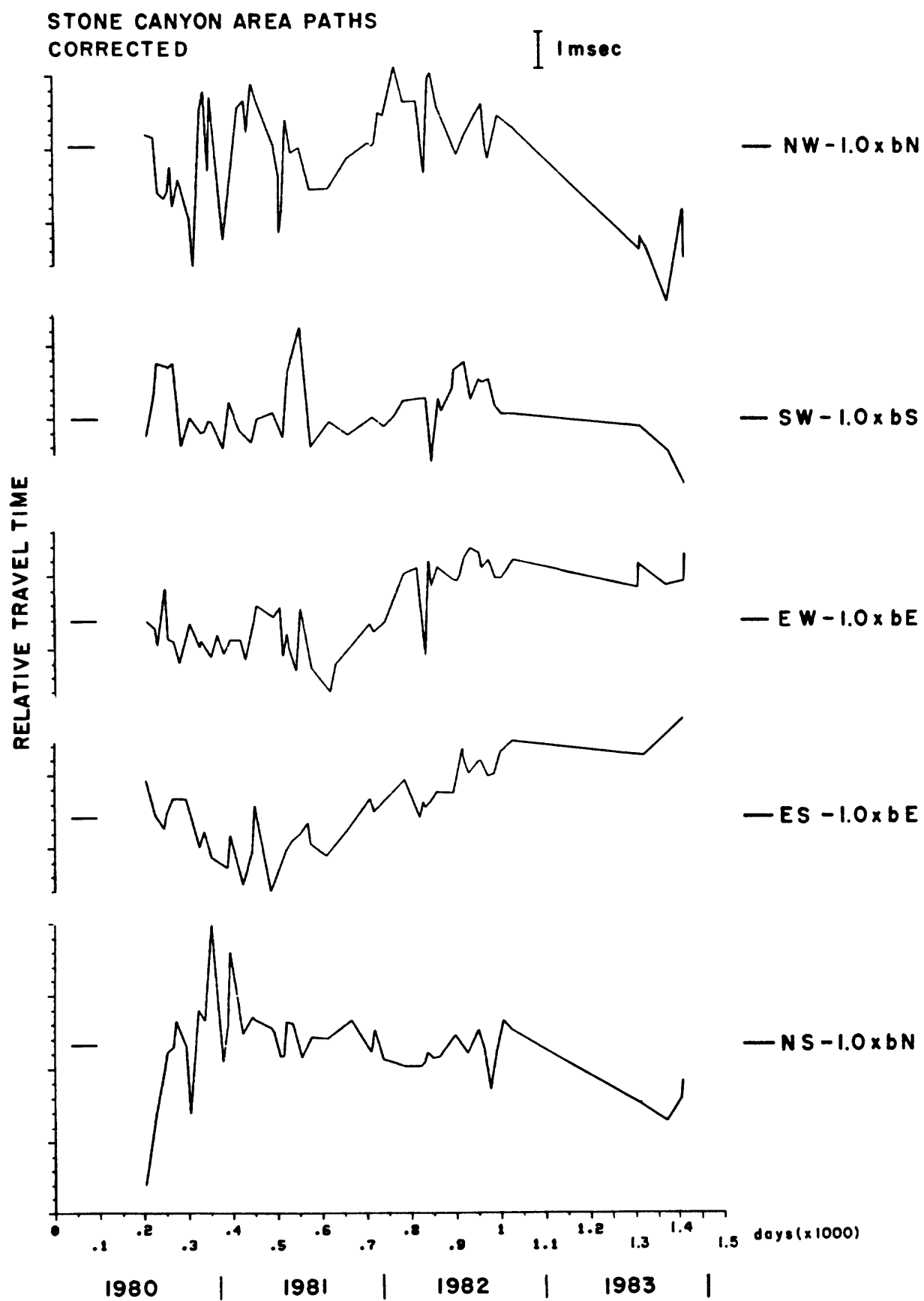


Figure 3. Stone Canyon area, seasonally corrected data.

Summary of Semi-Annual Technical Report

Tiltmeter and Earthquake Prediction Program in S. California and at Adak, AK

14-08-0001-212441

Sean-Thomas Morrissey

Rene Rodriguez

Department of Earth and Atmospheric Sciences
P.O. Box 8099 - Laclede Station
St. Louis, MO 63156
(314) 658-3129

I: Task 1: The Tiltmeter System

Objective: To continue to improve the performance of bubble sensor tiltmeter systems and to investigate other sensor systems for use in moderate depth boreholes, seeking relatively low-cost, readily deployed instrumentation.

Accomplishments: The new electronics system for the bubble sensor tiltmeter continues to perform well at 14 installations. With the thermal problems relegated to the bubble and its mount, it is now possible to test the bubbles for relative gain and stability by operating them on the floor of the Tyson vault on telescope mirror blanks (25 cm diameter, 3 meter radius of curvature). Recording is ± 4 ppm and, since the vault has large thermoelastic noises, short term agreement between "good" bubbles is readily apparent. The new electronics has greatly increased the signal/noise ratio of the observed solid earth tide (with ocean load) at Adak. Figure 1 shows the power spectral densities of two of the instruments, where the power of the tides is easily 20 db above the earth noise. hence the amplitude of the tides involved would be greater than 40 db above the background (this is raw, unfiltered data).

Another accomplishment is the beginning of the design and construction of the proposed simple pendulum tiltmeter with a variable reluctance transducer. A crude operational conceptual realization of the transducer has been built to test the linearity of the device. It is a bi-axial transducer that senses the pendulum mass position via orthogonal inductive bridges. As opposed to LVDT-based concepts, this system is sensitive only to the position of the cylindrical mass, and is inherently insensitive to either the length or the rotation of the pendulum. Figure 2 is a plot of the linearity of one axis of the transducer. The cyclic variations from the straight line are due to eccentricities in the machined threads of the differential micrometer used. The linearity extends over 1 mm with expansion of the electronic zeroing capability. The transducer is pin-compatible with the present new electronics for the electrolytic bubble sensor, with only a minor change of the electronic zeroing system. The transducer and 50 cm pendulum will fit inside the new tapered cast stainless steel housing that is being used with the Autonetics bubble. Tests of the prototype (with bubble-sensor electronics settings) give an output of 200mv/micro-radian.

II: Task 2: The Installation Method

Objective: To improve the installation methods for borehole instruments, with a goal of installing them as deep as 100 meters.

Accomplishments: The instruments are not ready for installation in the Mojave yet; considerable preparation of the data systems has to be done, but it is nearing completion. However, the new cable-controlled installation system is ready for testing at CCMO (when the rains end), and it will allow much more reliability and confidence in the installation process. The warp-drive tool allows electrical motor driven pre-leveling of the downhole package prior to packing in the bonded sand. It has a range of 5° and a control to 1μ radian. It includes electronic coarse level indicators, and optical orientation to the surface. The installation pre-leveling system, TV camera, etc., are all removed from the hole once installation is complete. It is anticipated that the data from 10 meter holes in the Mojave will be notably more stable than that from 1-2 meter holes at Adak.

Task 3: The Digital Data System

Objective: To continue to develop and operate a digital data acquisition system to acquire geodetic data and to thoroughly monitor the environment of the instrument installations.

Accomplishments: The eight tiltmeters and 5 14-channel digitizers at Adak are continuing to be run as long as the P.I. has to go there to service the Cires seismic network. The program also includes comparison of electronic tide gauges with a standard NOAA recording unit. Two of the Adak digitizers were ruined in the lightning strike last January, and may be irreparable because they are older electronics. New digitizer options are being investigated, especially the possibility of getting 16-bit rather than 12-bit data. All of the telemetry lines at Adak were equipped with lightning suppressors. The data base is essentially uninterrupted since August 1980, and amounts to over 75 mbytes of raw data. A removable 80 mbyte disk for processing the data on the DEC 11/70 is essential. A multi-tasking system for the receive/logging/de-logging microcomputer has been developed to avoid the expense of having to have separate micros to do each task.

Task 4: Data Interpretation

Objective: To process the digital data and make efforts to remove the environmental noise from the data, so as to establish the intrinsic long term stability of the tiltmeters. Various analysis techniques are then utilized to present the data in the meaningful formats such that any precursory tilt events would become evident.

Accomplishments: Acting on a suggestion that using only hourly data samples, which were filled in by repetition where missing for an hour or two, was seriously aliasing or distorting the data, a new pre-processor system was developed. It uses a C program to insure time continuity of the raw 10 minute data (by repeating as necessary), then low pass filters the result, then decimates it to exact hourly values. It made

the data look better, but did not improve the power spectra or other studies at all; conversely, it was time consuming and used a lot of disk space.

Various efforts are underway to remove the environment from the raw data. FFT conversions to the frequency domain for direct deconvolution were unstable, so convolutions of the environmental noise (tide, temperature, heat flow, etc.) plus an inferred DC tilt to produce data that modeled observed data have been done. The preliminary efforts show DC tilts that agree remarkably between the four tiltmeters used, showing a mean tilt of 5 ± 1.75 ppm/yr down to the west and 0.55 ± 0.09 ppm/yr down to the south for March 1983 through January 1984. If this data are supported by further analysis, they will be reported later.

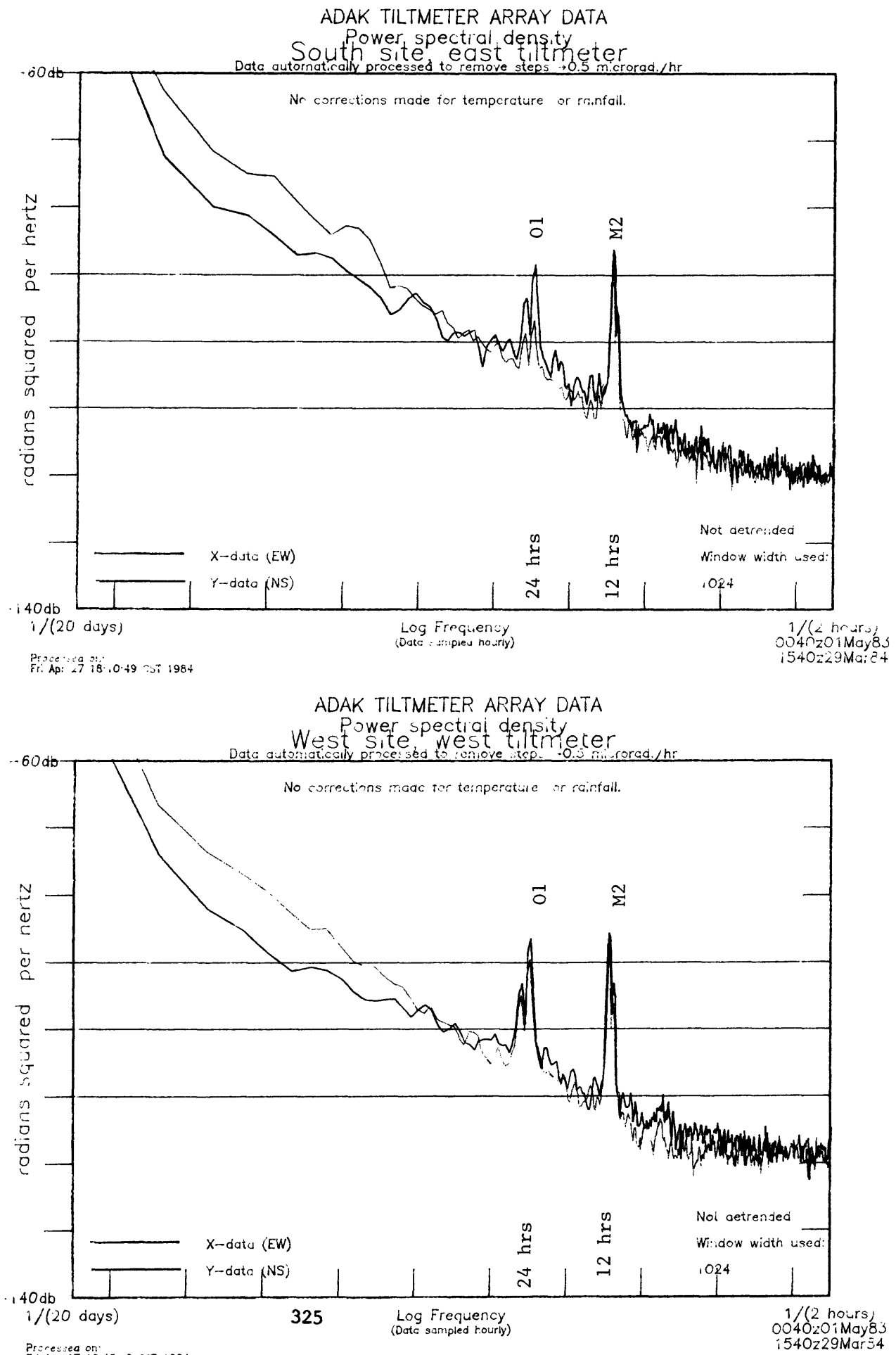
An alternative approach has been to make a simple linear thermal correction to the data, under the assumption that with the new electronics, most of the drift is due to thermal effects on the bubble sensor. Figure 3 is a sample of the corrected data from the west site at Adak. (The WE-Y is missing due to a connector failure.) The coherence spectra of the WE-X and WW-X is nearly unity from the nyquist (2 hours) to the cutoff (42 days). Other sites are poorer and should be relocated to hard rock sites, but program cutbacks prevent it.

There have been a number of strong local quakes, but no coherent coseismic tilt data as reported for six previous events. A relocation of the coherent coseismic events by Cires places all of them at the top of the semi-aseismic portion of the downgoing slab, further suggesting that they are large aseismic slip events. No work on modeling them as such has been done. In another study, the data from the water tide gauges was analyzed for coherence and linear trend. The coherence is unity at the tidal and barometric cycles, but some minor underlying temperature differences remain. A significant linear trend was found, but must be supported by further evidence before it is reported.

Sean-Thomas Morrissey
9 May 1984

Figure 1: Power spectral density of two Adak tiltmeters.

P-2



TRANSDUCER TEST DATA

back out from 1mm, ac zero to sum. jct.

12Apr84b

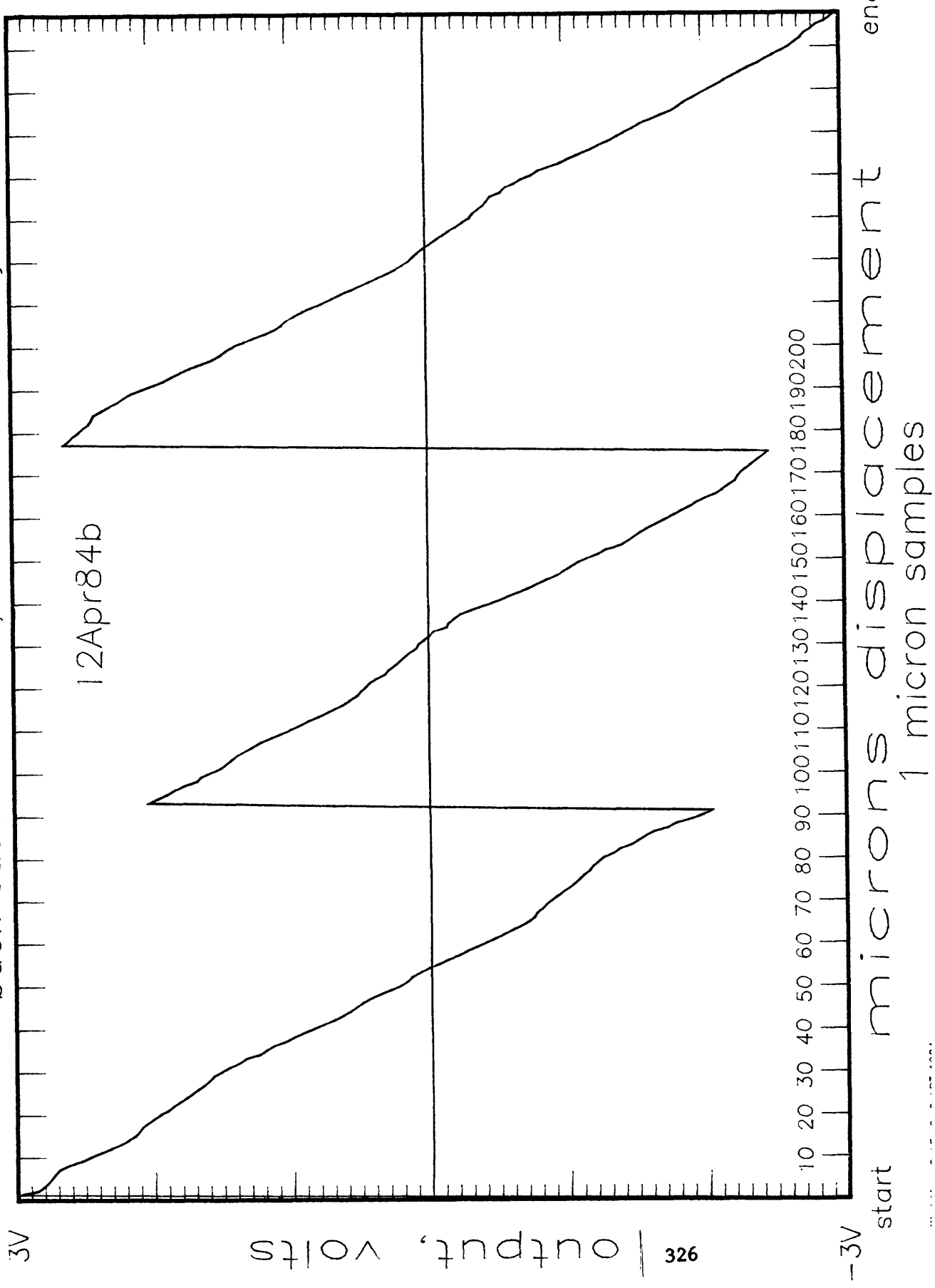
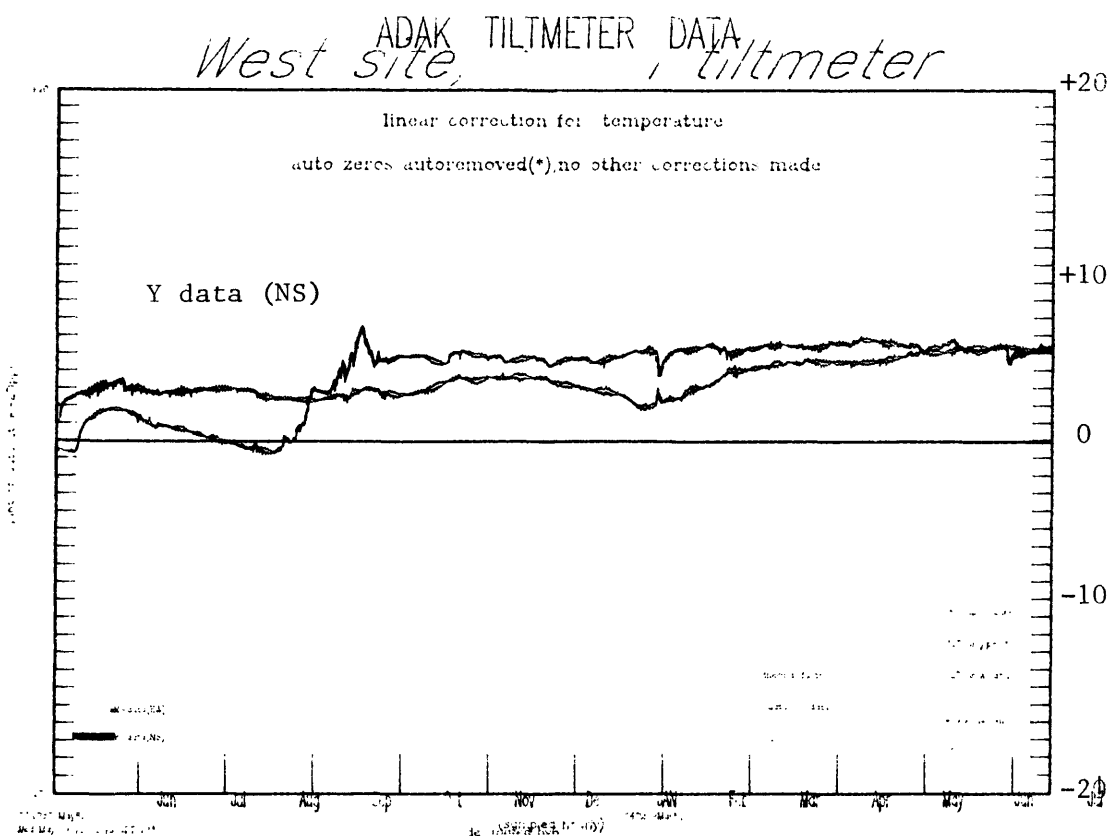
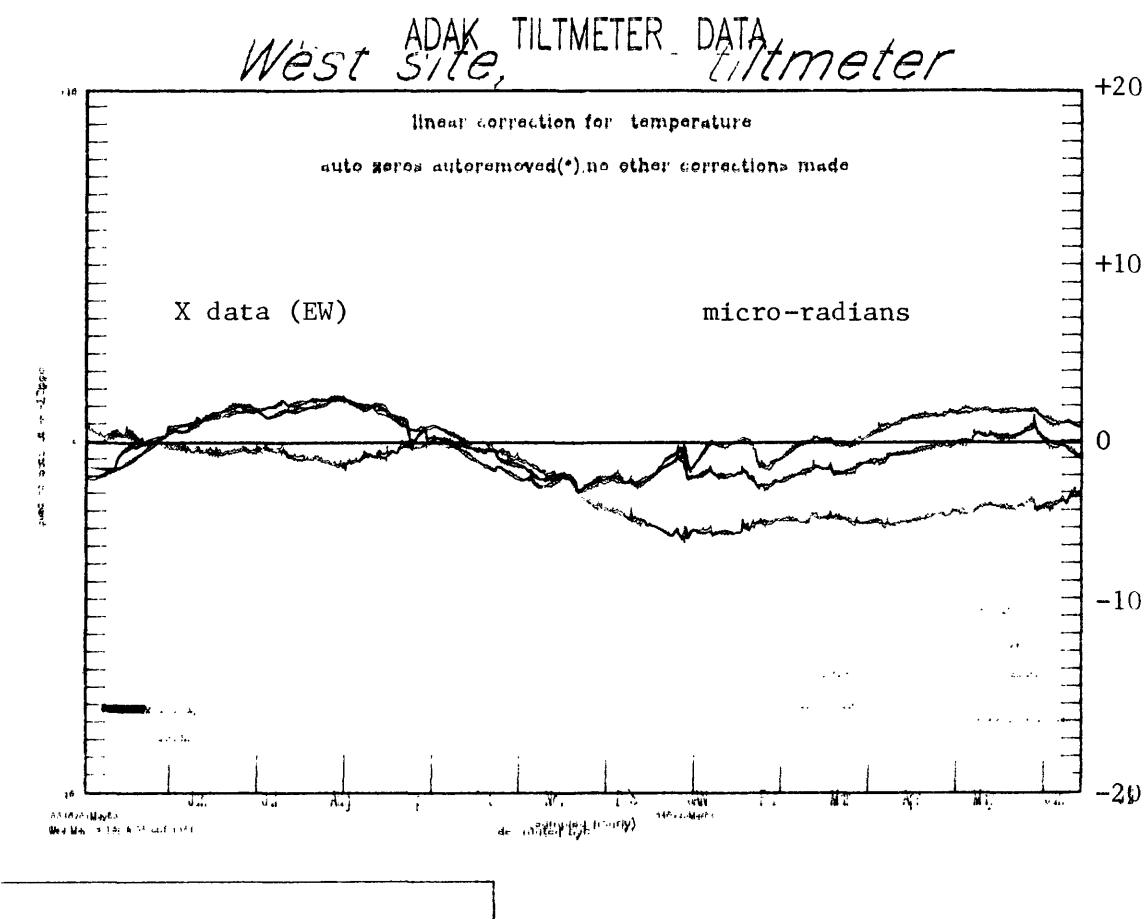


Figure 2: linearity of output of new variable reluctance P-2 transducer for pendulum tiltmeter. Cyclic variations are from error of differential micrometer. This is low level output; high level is 200mv/micro-radian with 50cm pendulum.

Figure 3: Linear thermal correction of Adak west site data.

P-2



THE EXTENSION AND OPERATION OF A COMPUTER-CONTROLLED MONITORING NETWORK
FOR RADON AND OTHER GEOCHEMICAL PRECURSORS, AND LABORATORY STUDIES ON
SEISMO-GEOCHEMICAL PRECURSORS

14-08-0001-21268

M.H. Shapiro, A. Rice, J.D. Melvin, and T.A. Tombrello
Div. of Physics, Mathematics, and Astronomy - Caltech
Pasadena, CA 91125
(818) 356-4277

INVESTIGATIONS

Since the last reporting period we have continued to monitor radon, thoron, and environmental variables at all network sites except for Santa Anita where the borehole is dry. A new site at Acton was completed early this year to provide coverage of the San Andreas between existing stations at Lake Hughes and Lytle Creek. In addition to radon and thoron, carbon dioxide and hydrogen are monitored at several network stations. Borehole water level now is measured at all sites except for Anza and Ft. Tejon. (At these sites radon is monitored from pumped wells.) Water temperature is monitored at all sites.

Several techniques including cross-correlation, pattern recognition, fourier transformation, and multiple regression analysis are being used to identify non-tectonic environmental noise in the radon data. A paper describing preliminary results from this effort has been prepared.

RESULTS

Radon levels have been within normal limits at all but two stations during the past year or more. The two sites where radon data are outside normal limits are Alandale and Stone Canyon. The Alandale site is undergoing a "carbon-dioxide" event similar to those which took place at Lake Hughes in two prior years. This is a non-tectonic environmental effect which occurs at a few network sites when the borehole water level drops and carbon dioxide concentration reaches saturation. Carbon dioxide bubbling, modulated by barometric pressure changes, scour radon from the aquifer. This type of event is readily identified by the close correlation between radon level, carbon dioxide level, and barometric pressure.

At Stone Canyon a somewhat unusual change in radon level began early in March 1984. It coincides with a small change in borehole water level (possibly driven by a much larger change in reservoir level at the nearby Stone Canyon Reservoir). There is a correlation with barometric pressure that is higher than normal for this site, but not as high as that found at Alandale or Lake Hughes during "carbon-dioxide" events. We suspect that a gas component is now present in the Stone Canyon borehole; however, this has not yet been confirmed. A continuous carbon dioxide monitor will be installed at the site shortly. Stone Canyon is near the northern end of the Newport-Inglewood fault, and several small earthquakes have occurred along this fault during the past two months. The level of activity, however, is not unusually high. At this time the change in radon level at Stone Canyon has not been classified as "anomalous".

CALTECH ARCHIVE RADON DATA

P-2

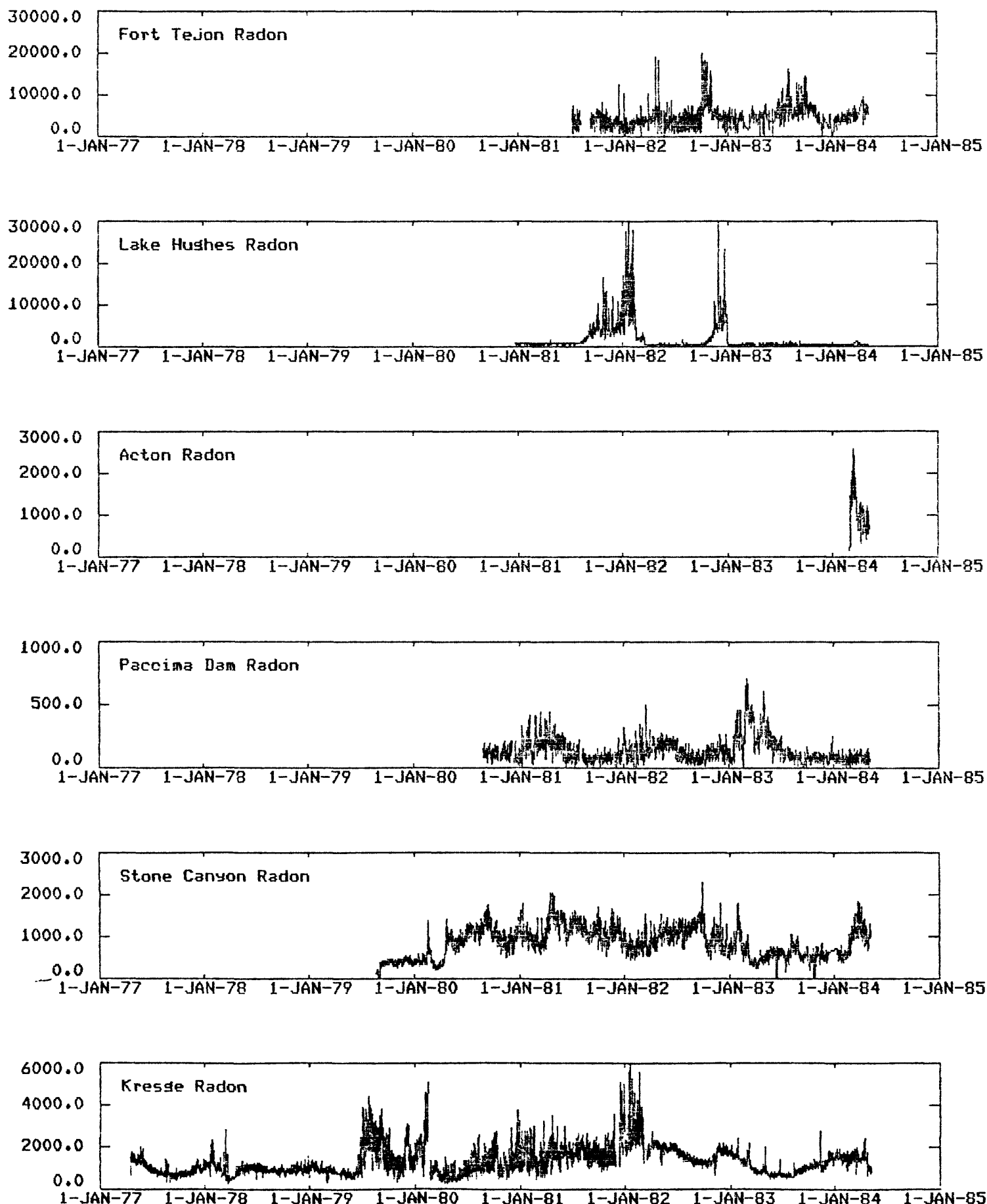


Figure 1a.

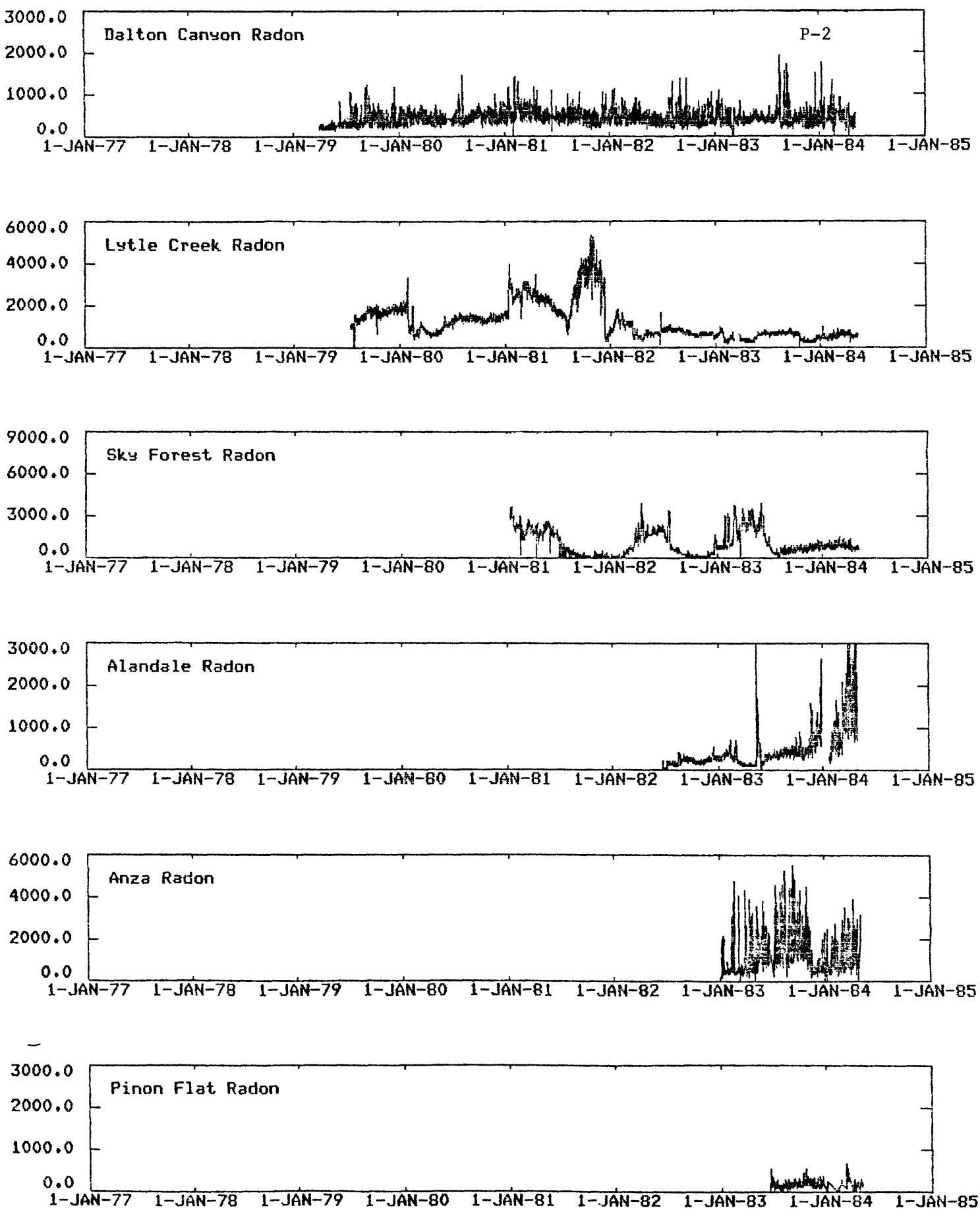


Figure 1b.

CALTECH ARCHIVE WATER LEVEL DATA

P-2

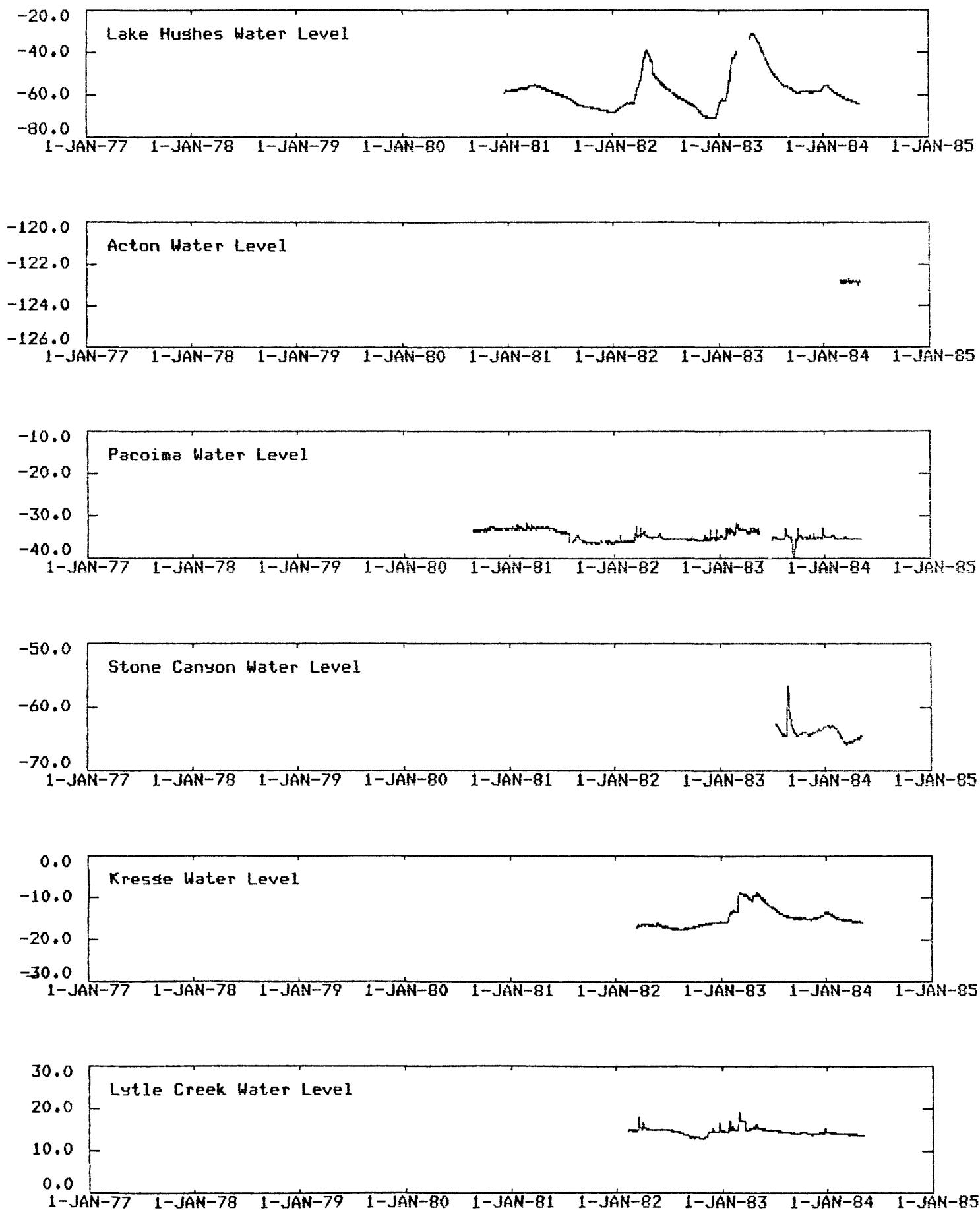


Figure 2a.

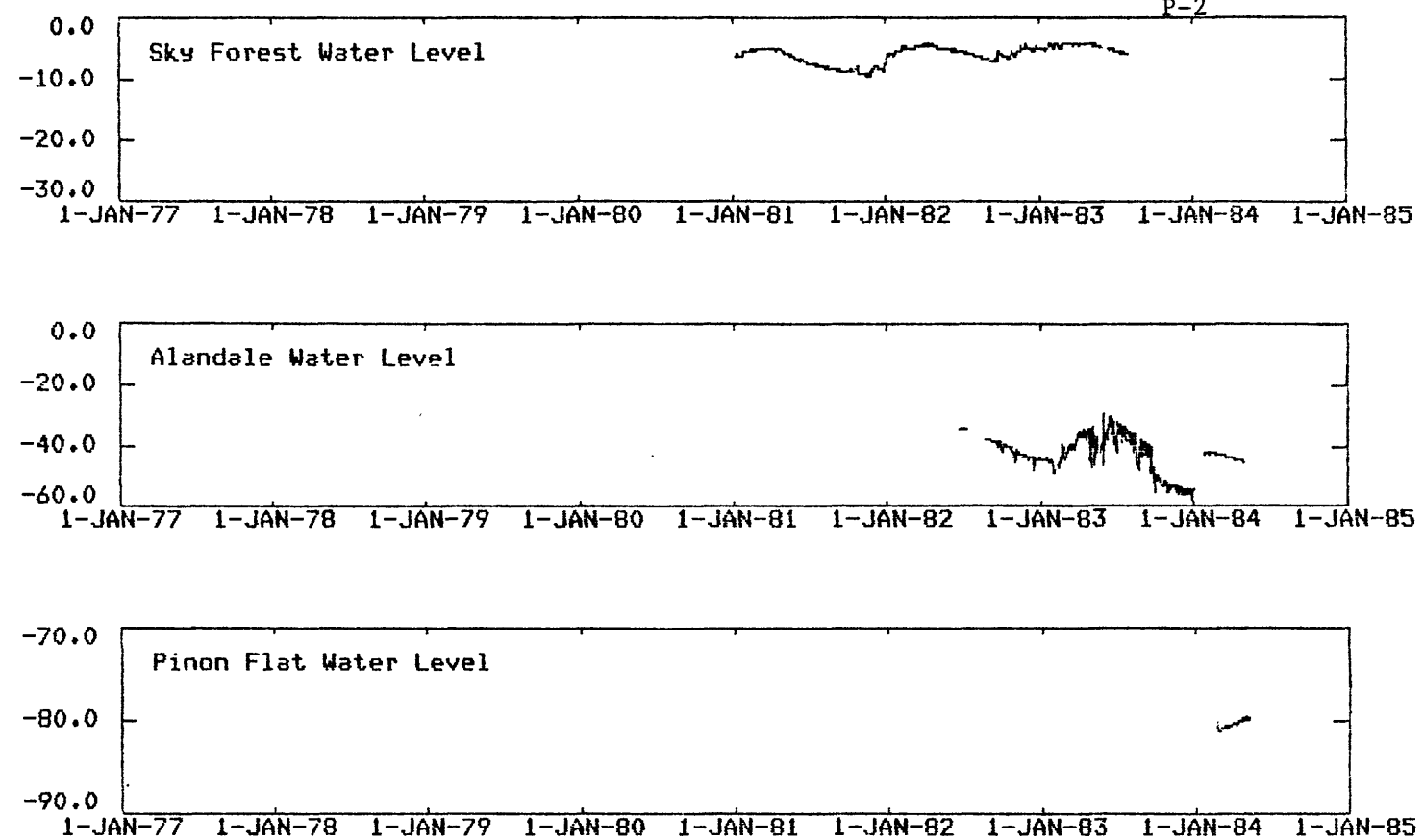
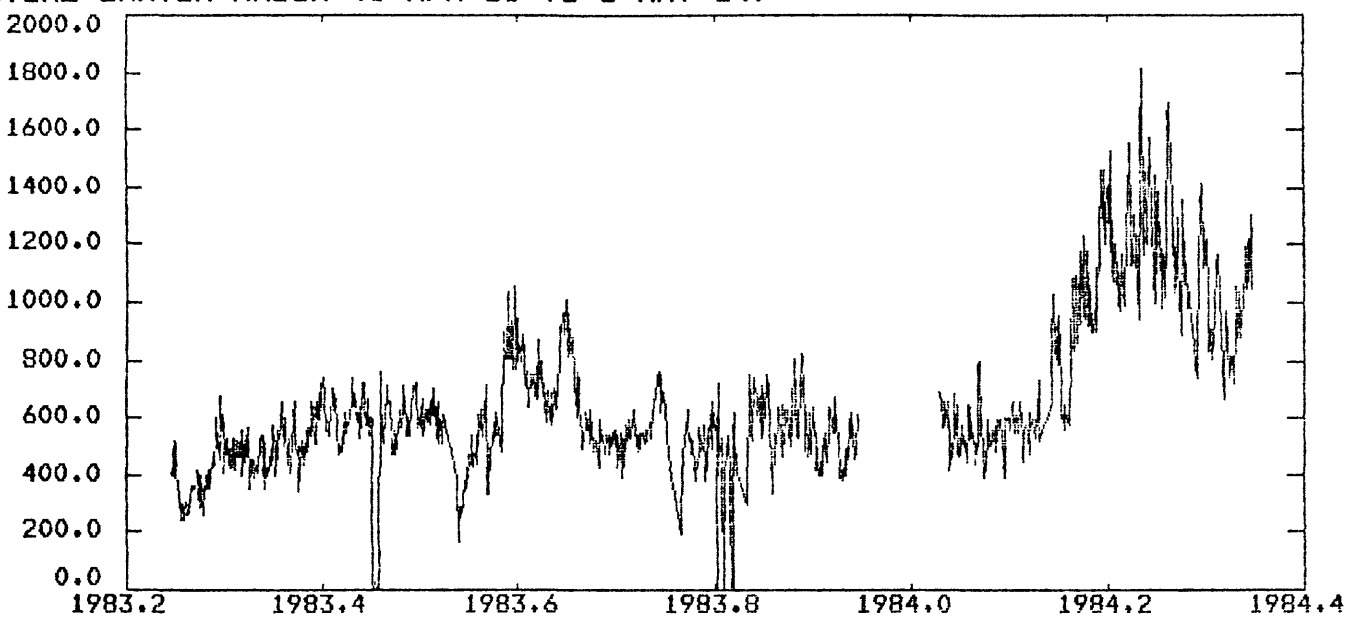


Figure 2b.

STONE CANYON RADON (1-APR-83 TO 6-MAY-84)



STONE CANYON WATER LEVEL

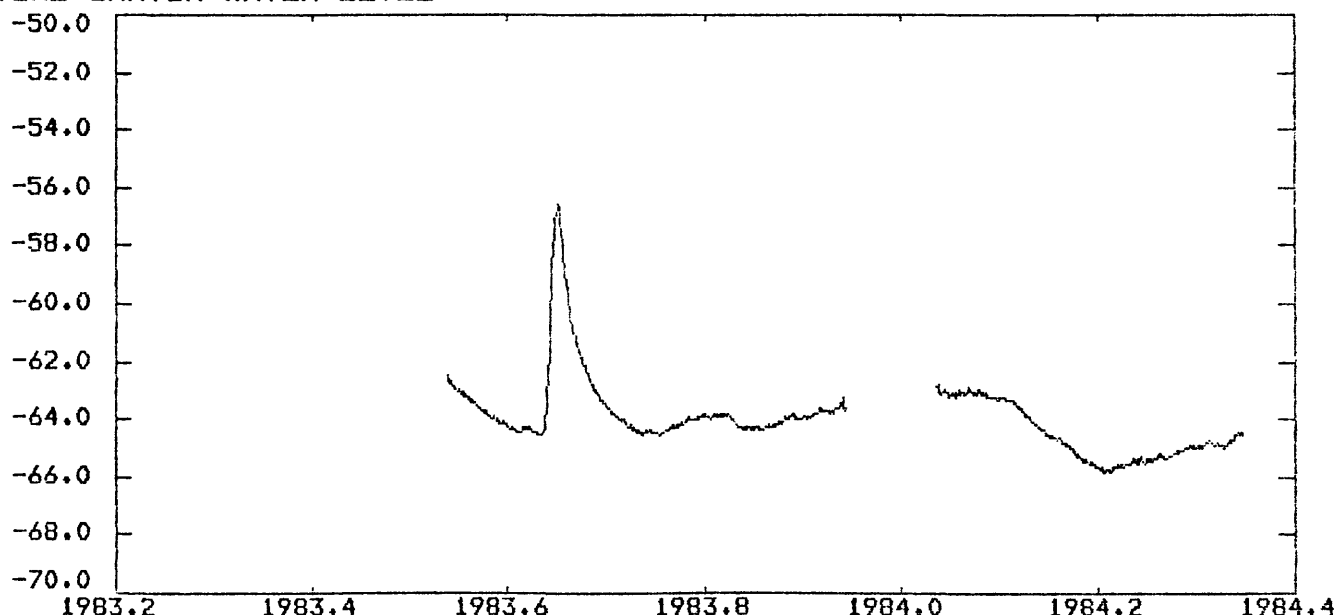


Figure 3.

REPORTS

Recognition of environmentally caused variations in radon time series. M.H. Shapiro, A. Rice, M.H. Mendenhall, J.D. Melvin and T.A. Tombrello, Caltech preprint BB-15 (April, 1984) and submitted to PAGEOPH. (A preliminary version of this paper was presented at the Fall Meeting of the AGU.)

A CRUSTAL DEFORMATION OBSERVATORY NEAR THE SAN ANDREAS FAULT
IN CENTRAL CALIFORNIA

21300

LARRY E. SLATER
CIRES
University of Colorado
Boulder, Colorado 80309
(303) 492-8028

Investigations

1. A cooperative crustal deformation study between U.S. Geological Survey and University of Colorado was concluded in early 1984. The study utilized the CIRES multiwavelength EDM to monitor 13 lines in a radial geodetic array near Pearblossom, California.
2. We are establishing a similar geodetic array near Parkfield, in central California.
3. Some of the error sources in multiwavelength EDM measurements have been identified and we are attempting to minimize or eliminate same.

Results

1. The CIRES multiwavelength EDM instrument was moved to a location near Pearblossom, in southern California, during October 1980. An array of 13 lines, straddling the San Andreas fault, was established in the region. The lines ranged from 3 to 8 km in length and radiated from the central instrument site. This portion of the San Andreas fault is within the 1857 rupture and shows little or no surface slip. The entire data set, consisting of over 3000 line length measurements has been analyzed with the assumption of uniform strain within the network. The strain components parallel and normal to the local trace of the fault show substantial departures from the long-term trends. The amplitude of these fluctuations approach 0.5 microstrain for the normal component. The time behavior and amplitude of these fluctuations are similar to those observed at the Hollister site. Of course, it is the dilatational strain measurements that are most susceptible to any type of scale error, either instrumental or atmospheric in nature. These possible causes of the fluctuations were investigated in detail and we do not believe that scale error is responsible for them.
2. The region near Parkfield should provide further insight into the nature of episodic fault behavior. The San Andreas fault to the south of Parkfield appears to be locked while the portion of the fault to the north exhibits aseismic surface slip as large as 3 cm/a.

The instrument site is located at the central point in the array approximately 1 km south of the town of Parkfield. The array straddles the San Andreas fault with the instrument site approximately 100 m west of the fault trace near benchmark CARR. The array consists of approximately a dozen lines at present which are positioned in such a fashion as to allow the determination of the strain components on each side of the fault, the slip on the fault, and test the uniformity of strain within this transition region. The array also is located near the center of the 1966 Parkfield earthquake rupture zone. Most of the lines within the array are approximately 5 km in length so we expect to achieve sub-millimeter precision in our measurements. We also plan to establish 2 lines near the San Andreas fault to the north where we will use the ratio technique to determine changes in shear strain near the fault trace. We hope to be able to monitor changes in shear strain to better than 1 part in 10 million.

3. The goal of this research project is to precisely monitor strain changes in the Parkfield region. The accomplishment of this goal will depend on the measurement of line lengths within the array. There are several possible causes for a change in line length; among them, 1) real tectonic deformation, 2) apparent changes due to instrument problems, 3) apparent changes due to errors in measuring the atmospheric parameters, and 4) local soil instability, benchmark instability, or poor instrument-retro location over the benchmarks. Potential error sources 2) and 4) are best minimized by periodic instrument calibration, operator care in instrument and retro set-up and frequent checks, and were local soil or benchmark stability is questioned, either select another site or install multiple benchmarks several meters apart. The separation of error source 3) from real deformation 1) is the most difficult problem. Recent studies suggest at least a partial solution to the problem. Figure 1 shows some of the results of that study. A series of benchmarks were placed along a long, straight, level line. The distance between adjacent benchmarks ranged from 50 m to approximately 1 km. These benchmarks were measured with the multiwavelength EDM instrument on 2 consecutive evenings during each of 2 surveys. The modulation frequencies were recorded as well as the distances during the surveys so we could calculate the relative position change of the benchmarks by the ratio technique as well as from the measured distances. It is obvious in Figure 1 that large changes (approx. 1 ppm) are common along the line of benchmarks. The problem, if only the distance determinations are available, is to determine whether these changes are real or simply due to errors in monitoring the atmosphere. We can see in Figure 1 that both the distance changes and the ratio determinations agree well with each other. Since the ratio determinations do not require any atmospheric measurements we can conclude that the changes measured between the benchmarks are not due to errors in monitoring the atmosphere, they are either real changes along the line or the retro reoccupation of the benchmarks was careless. Later tests proved the latter was the case.

Reports

Langbein, J., M.F. Linker, A. McGarr and L.E. Slater, 1984, Two-colour geodimeter measurements of crustal deformation near Palmdale and Long Valley, California. International Symposium on Recent Crustal Movements of the Pacific Region, Wellington, New Zealand.

Slater, L.E., 1984, Improving multiwavelength EDM instrument precision. International Symposium on Recent Crustal Movements of the Pacific Region, Wellington, New Zealand.

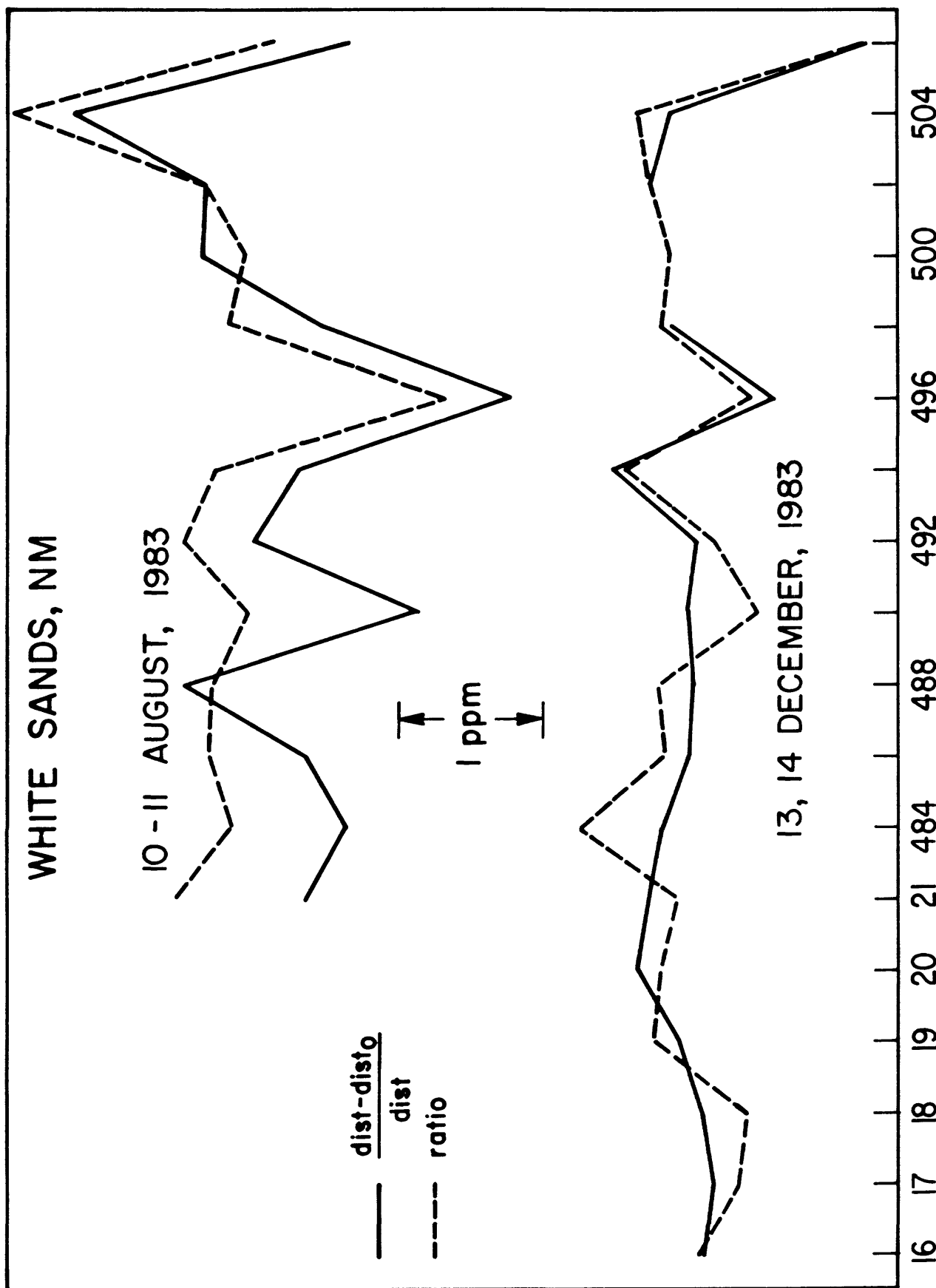


Fig. 1. Results of 2 surveys using multiwavelength EDM instrument. The solid line lines represent the normalized distance change between consecutive days along lines to benchmarks indicated on the horizontal axis. Dashed lines represent results obtained from ratio technique.

Nearfield Geodetic Investigations of
Crustal Movements, Southern California

Contract No. USDI-USGS 14-08-0001-21218

Arthur G. Sylvester
Department of Geological Sciences, and
Marine Science Institute
University of California
Santa Barbara, California 93106
(805) 961-3156

Investigations

Precise releveling of 4 lines of permanent benchmarks across three faults in Death Valley and across one line on the San Jacinto fault at Anza. Releveled and realigned a leveling-alignment array across the San Andreas fault near Frazier Park in response to concern about nearby aqueduct break.

Results

No variations in height in Death Valley since last resurvey in 1978, and therefore none since the lines were established in 1970.

No variations in height at Anza since last resurvey in September, 1983, and none since the line was established in January 1981.

No height variations or horizontal offsets near Frazier Park since last resurvey in September 1983, and therefore none since the array was established in February, 1977, except for previously reported motion of a class B rod mark located right in the trace of the 1857 surface rupture of the San Andreas fault. That mark did not move since the previous resurvey.

Crustal Deformation Observatory, Part B:
Precise Leveling

Contract No. USDI-USGS 14-08-0001-21234

Arthur G. Sylvester
Department of Geological Sciences, and
Marine Science Institute
University of California
Santa Barbara, California 93106
(805) 961-3156

Investigations

One complete resurvey of leveling array at Pinyon Flat, the first complete winter survey we have performed there in 16 separate surveys.

Results

No significant variations observed. The resurvey yields still one data point to a burgeoning data set which shows the details of motions of different kinds of benchmarks, as well as surveys at different times of the year under different meteorological conditions.

GROUNDWATER RADON STUDIES FOR EARTHQUAKE PRECURSORS
14-08-0001-21193

Ta-liang Teng
Center for Earth Science
University of Southern California
Los Angeles, California 90089-0741
(213) 743-6124

The U.S.C. radon monitoring program began in 1974 and has now developed into a multifaceted program consisting of three principal experiments. Two major efforts have been made in the program during the past two years. One is the installation of seven continuous groundwater radon monitors. This change of emphasis, from discrete to continuous monitors, results from the writer's findings during his visits to China where many reported radon anomalies before large earthquakes are found to be spike-like with short duration (about a day or so). If radon anomalies of similar nature were to occur in California, they might easily be missed by a practice of weekly or monthly sampling. The second change is the augmentation (being completed in FY 1984) of the monitoring activity to include studies of other parameters associated with the groundwater hydrology; these include temperature, conductivity and pH value. This additional effort should increase our insight into the mechanisms responsible for radon fluctuations.

The three principal experiments on radon and water chemistry ongoing at U.S.C. include:

1. Groundwater Radon Content Monitoring Network (Discrete Samples)

We have established a 14-station groundwater radon sampling network covering much of the extended southern California uplift area. The monitoring area covers much of the southern California uplift, particularly along a segment of the "locked" San Andreas fault from Gorman to San Bernardino. Weekly sampling is maintained, with the first station having been monitored since October 1974. Six liquid nitrogen cold-trap radon extraction systems and a dual-channel scintillation counter have been constructed in our laboratory to handle the routine analysis. Radium standards are available for counting system calibration. Efforts are made to correlate the groundwater radon results with nearby earthquake occurrences, as well as with meteorological variations (Teng et al., 1981).

2. Design, Construction and Deployment of Continuous Radon Monitor (CRM)

To augment our capability on the groundwater radon content monitoring, we have been actively pursuing the design, construction, and field deployment of continuous radon monitors (CRMs). These CRM units are field-worthy and give reliable radon measurements of sufficient precision. Figure 1 gives the records of two CRMs installed at the same site (Haskell Ranch); over an eighteen-month test period the radon measurements track each other faithfully, giving a high degree of measurement reliability and repeatability. The field data have been calibrated against laboratory measurements using the cold-trap α -counting method that gives high measurement resolution. The transformation of the prototype into well packaged CRM units has been successfully accomplished. The CRM unit consists of a flushing probe, an α -scintillation probe, a counting, calculating, and printing (CCP) circuit, and a printer/recorder with absolute time base. The entire package weighs less than 20 lbs, and the recorder can accommodate two more analog inputs in addition to the radon counting. These two inputs can be temperature, barometric pressure, pH value, conductivity or any parameters deemed useful alongside with radon monitoring. The CRM is packaged in a 15" x 12" x 10" fiberglass carrying case and can run on either AC or DC. Currently, seven groundwater sampling sites in the southern California uplift area are deployed with the CRM units, they are: Arrowhead Hotspring (two units monitoring two different springs), Haskell Ranch, Wrightwood, Seminole Hotspring, Warm Spring and Encino Hotspring. Although the CRMs were only recently installed, a typical data plot is given in Figure 2. Radon values are taken and recorded automatically (programmable) on an hourly basis, with daily average also printed on the record.

3. Monitoring of Other Groundwater Parameters

Variations in groundwater radon concentrations may be caused by mixing waters from different strata. This could occur through environmentally controlled mechanisms such as rainfall, or through stress-related mechanisms such as rock fracturing. We have monitored the concentration of several ionic constituents (Na, K, Ca, Mg, Cl) in groundwater samples to search for covariance with radon (Hammond et al., 1981). These analyses can provide insight into the mechanisms which may cause radon concentrations to fluctuate.

REFERENCES

- Hammond, D. E., T. L. Teng, L. Miller, and G. Haraguchi, A Search for Co-Variance Among Seismicity, Groundwater Chemistry, and Groundwater Radon in southern California, *Geophysical Research Letters*, vol. 8, no. 5, p. 445-448, 1981.
- Teng, T. L., L. F. Sun, and J. K. McRaney, Correlation of Groundwater Radon Anomalies with Earthquakes in the Greater Palmdale Bulge Area, *Geophysical Research Letters*, vol. 8, no. 5, p. 441-444.

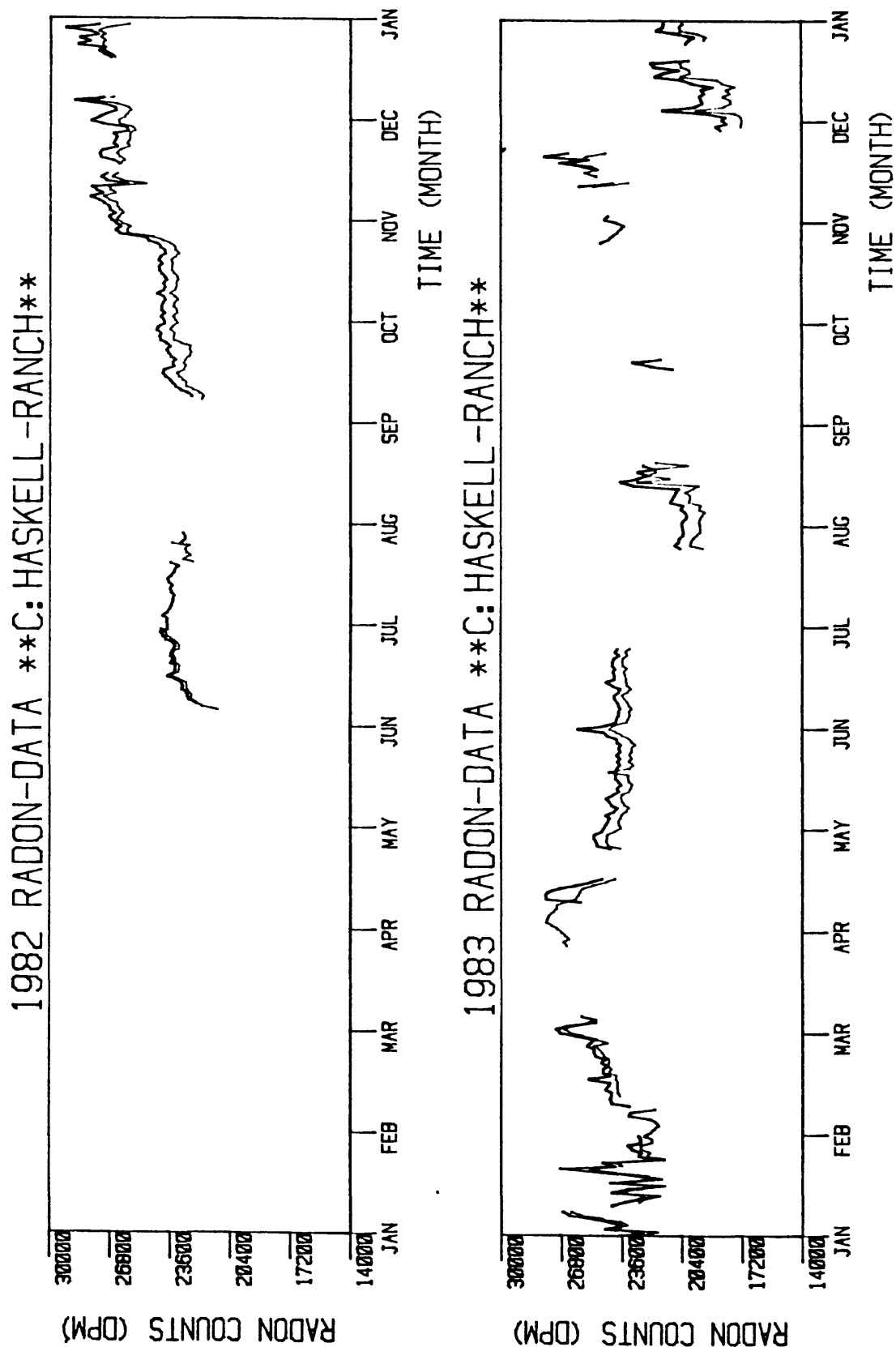


Figure 1

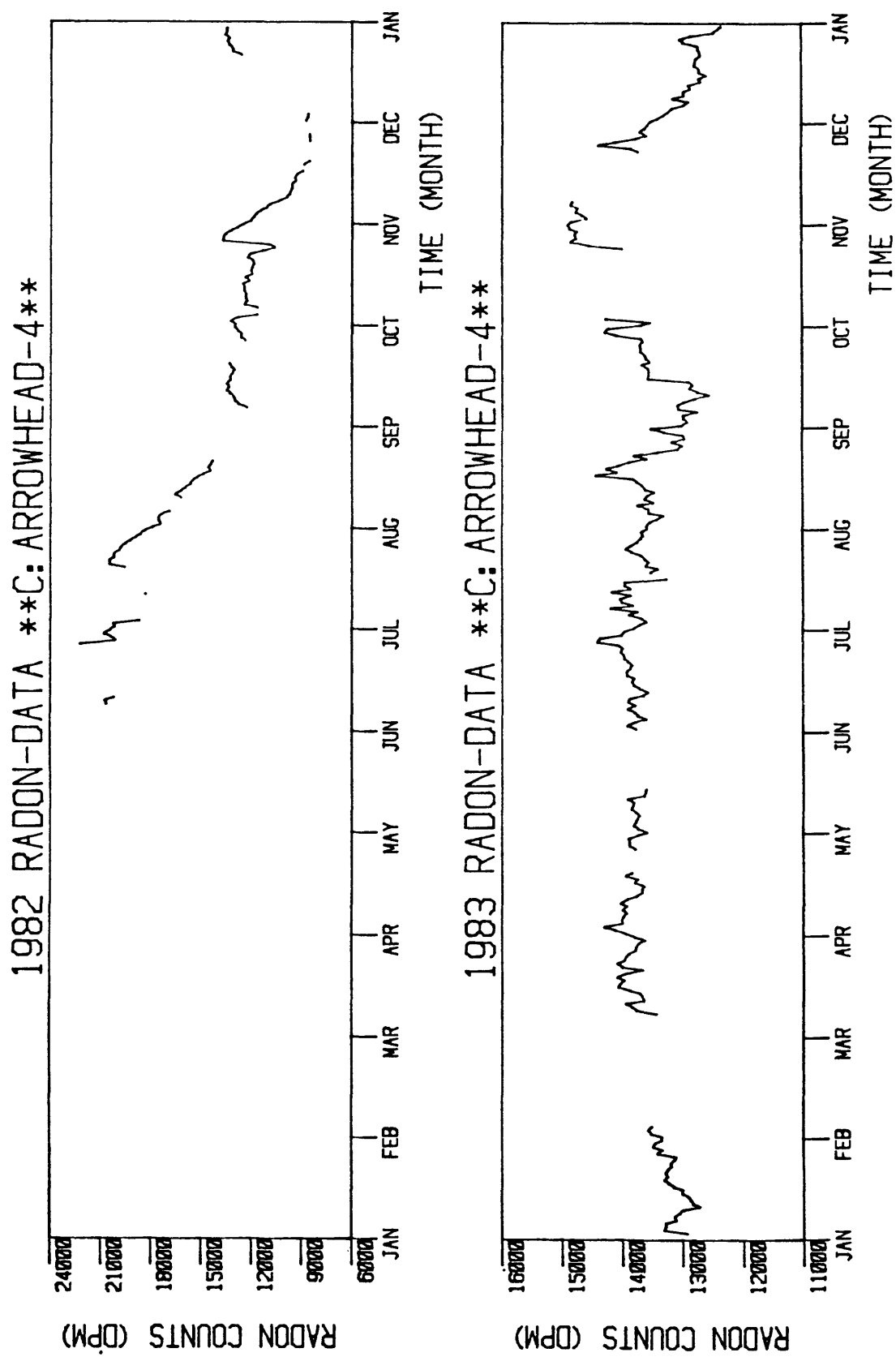


Figure 2

Crustal Deformation Observatory

Part D

May 1983 through October 1983

14-08-0001-21254

Frank Wyatt and Duncan Agnew

Institute of Geophysics & Planetary Physics

Scripps Institution of Oceanography

University of California, San Diego

La Jolla, CA 92093

(619) 452-2019

Results

CDO Program:

1. Air Force Geophysics Laboratory. Continued testing of the intermediate-depth borehole tiltmeter operated by the AFGL established unambiguously the nature of a serious down-hole electronics malfunction. Plans have been made to recover the instrument and recalibrate the biaxial sensors to an accuracy of 1 percent for secular and tidal tilt studies.
2. Cambridge University. The differential-pressure tiltmeter developed at Cambridge University did not require any servicing during this period. The short period noise which had come to dominate the recent records, is generally subsiding.
3. CIRES. Protective sheds were constructed this summer to reduce environmental variations within the end-building instrument enclosures. Initial measurements from the two-fluid tilt transducer are to be conducted in 1984.
4. Lamont-Doherty Geological Observatory. A number of unfortunate circumstances resulted in a significant loss of data from this high-quality tiltmeter. Principally, a pair of hard-sealed He-Ne lasers, whose lifetime should exceed two years, began to fail after only six months of operation. Discovery of this problem led to a prolonged round of musical lasers with the manufacturer. Records from the latest three months are quite encouraging.
5. University of California, Los Angeles. The most recent data edited by Calum Macdonald (segment #17--1982:270 to 1983:81) shows the response of the three continuously recording long baselength tiltmeters at Piñon Flat Observatory to the most severe winter at the site since 1970. Generally the instruments, including their interface to the near-surface material, behaved rather well.
6. University of California, Santa Barbara. In August 1983, the entire array of benchmarks at Piñon Flat Observatory, including those on the long-fluid tiltmeters and the absolute gravity monument were surveyed by the UC Santa Barbara team.

7. University of California, San Diego. During the summer, large A-frame sheds were fabricated above the end vaults of the long baselength tiltmeter. Periodic analysis of the records from this instrument show tilt rate of less than .25 μ rad/yr. Figure 1 shows the benchmark-corrected tilt records for this instrument and the Cambridge and Lamont-Doherty instruments for most of 1983.

Projects Related to the CDO Program:

1. California Institute of Technology. In June 1983, a continuously recording radon monitor was installed in borehole CIB. Data from this transducer are telemetered directly to Los Angeles over a phone line on a daily basis.
2. Carnegie Institute of Washington. The combination of battery failures and a month-long period of intense lightning storm activity introduced a large number of brief interruptions in the records from the three volumetric strainmeters (CIA, CIB, and CIC). Overall, these borehole transducers continue to show a gradual reduction of ambient noise levels.
3. CIRES. In July 1983, a survey gravimeter measurement was made at the absolute gravity monument by Jim Whitcomb.
4. Leighton and Associates. Early this fall a new 62 m borehole was drilled for a vertical array of high-sensitivity relative stressmeters. The transducers were installed shortly thereafter.
5. NASA/NGS - National Crustal Monument Network. Don Acres and a team from NGS completed a local survey of the six NCMN monuments during a visit to the site this past June. In October 1983, both NGS and JPL personnel were present for a series of VLBI measurements using the prominent MV-3 transportable antenna.
6. University of California, San Diego. As part of his experimental program to monitor well gases, Yu-Chia Chung has installed a prototype gauge in borehole CIB, in parallel with an existing radon monitor operated by the California Institute of Technology.
7. University of California, San Diego. Mark Zumberge conducted the initial testing of his new absolute gravity meter in September. When fully calibrated this transducer will yield measurements of gravity accuracy to 8 digits (3 cm). A study of the water table has been underway to correct for apparent elevation changes corresponding to the changes in the ground water.
8. University of Queensland. Numerous surveys were made in boreholes UQA and UQB by teams from the U.S. Geological Survey in anticipation of installing a pair of linear borehole strainmeters developed by Mick Gladwin. Because of instability in the borehole walls of UQA, a decision was reached to install only one instrument at this time. This work was completed in September 1983. Data from this transducer are telemetered via satellite to Menlo Park.

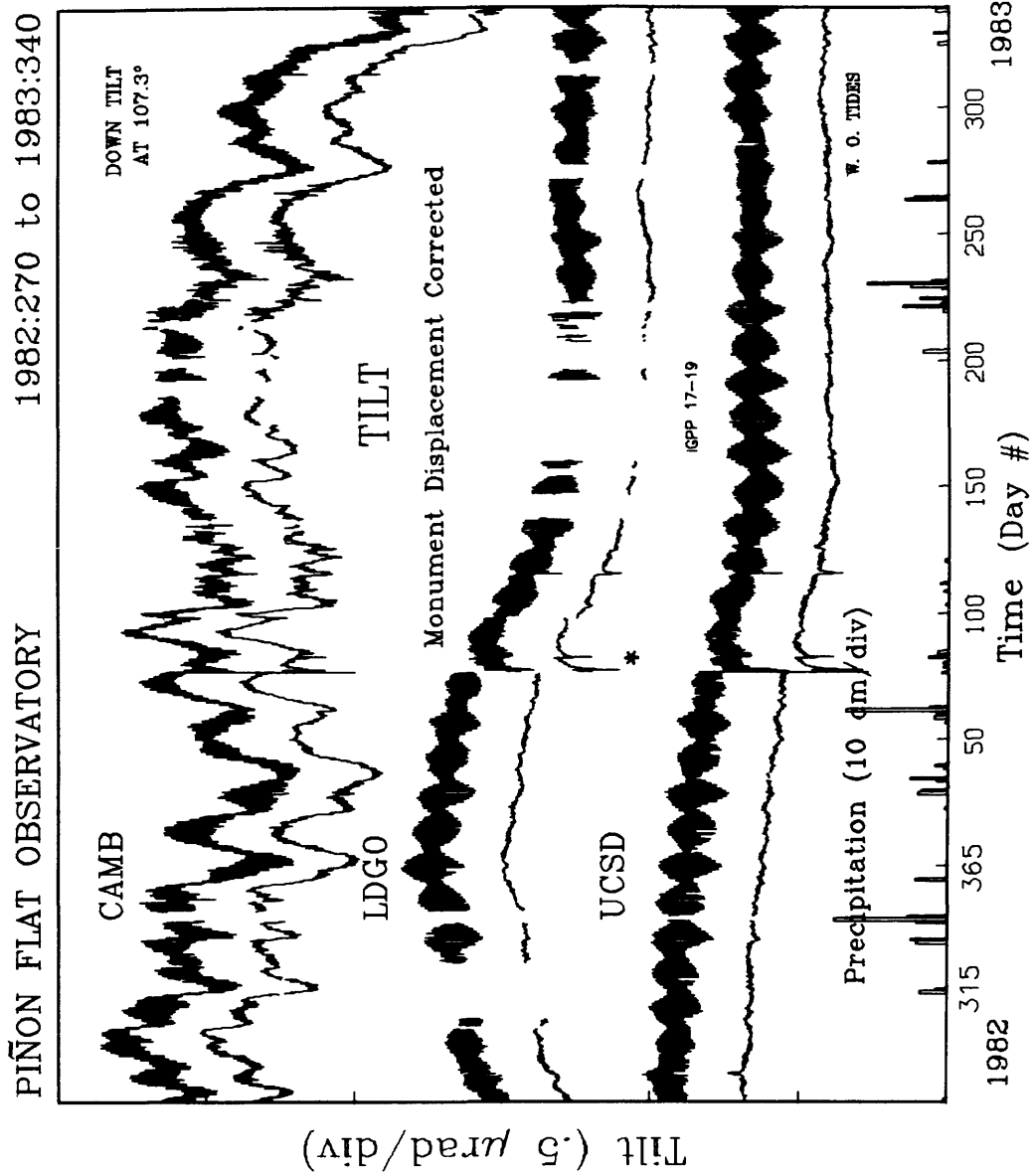


Figure 1.

Studies of the Seismic and Crustal Deformation Patterns
of an Active Fault: Piñon Flat Observatory

14-08-0001-21270

Frank Wyatt, Duncan Carr Agnew, Jonathan Berger
Institute of Geophysics & Planetary Physics
Scripps Institution of Oceanography
University of California, San Diego
La Jolla, CA 92093
(619) 452-2019

Introduction

This contract supports the ongoing research program at Piñon Flat Observatory. The objectives of this program are: 1) To provide a common location with shared facilities for research on, and the development of, precision geophysical instruments; 2) To establish the accuracy with which each of these instruments measures different geophysical quantities by operating the best available reference standards; 3) To monitor reliably the state of strain in the lithosphere near the observatory, a region of imminent seismic activity.

Results

As part of our continuing efforts to upgrade the instrumentation at PFO, a second optical anchor was installed at the southeast end of the NW-SE strainmeter in late 1983. Figure 1 presents some data from this strainmeter, including both of the optical anchor correction series and the corrected strain (with the tides removed). Although this record is quite short, the magnitude of the SE LOA correction, when extrapolated to a year, is significant; it alone accounts for nearly an order of magnitude greater strain rate than that deduced geodetically for this azimuth (.01 $\mu\epsilon/a$). As we anticipated, the SE LOA results are crucial to an accurate measure of the strain. However, the trend of the corrected NW-SE strain (-.26 $\mu\epsilon/a$) remains large. Now that the motions of the end monuments are being recorded, we have begun an examination of the optical length standards used in these strainmeters. Preliminary studies in 1981 showed that our quartz Fabry-Perot resonators may be unstable at a level of .6 $\mu\epsilon/a$; for the resonator used in the NW-SE strainmeter we found a frequency drift corresponding to a strain of -.34 $\mu\epsilon/a$, more than enough to explain the trend found above after applying the monument corrections. Under NSF sponsorship, we plan to monitor the frequency stability of all the lasers at PFO relative to an atomic wavelength standard to investigate this problem.

Both optical anchors on the long fluid tiltmeter were completed in October 1982; Figure 2 presents a year (1982:270-1983:240) of data from this instrument, including the anchor corrections. Fortunately, we

finished assembling these anchors before the intense rainstorms of the winter of 1982. Up to that time the reference monuments had shown very little instability. Within a three-month period, beginning just before 1983, the vaults flooded repeatedly, causing the east end monument to move up about .75 mm; the west one moved only .2 mm, causing an apparent tilt down to the WNW of 1 μ rad. Correcting for the differential motion yields the bottom trace. Examination of the tiltmeter series has already provided us with some clues about the sources of noise in this corrected record. The abrupt downward spikes show times when the water table under the west end of the instrument was drawn down by as much as 64 m during drilling operations nearby. This caused the closure of a large horizontal fracture 100 m below the west end of the tiltmeter, giving rise to a displacement of that end which creates an apparent tilt. Because natural water level fluctuations over the past few years have been less than 5 m, their effect should be small enough not to cause an appreciable error signal. However, we do not know anything about the possible size of a similar effect at the east end of the tiltmeter (or for that matter on either end of any other tiltmeter in the world). If this effect of subsurface cracks is common, the secular trend in the tilt data may reflect an uplift at the east end in response to the heavy rain of this period. The long-term fluctuations observed on the corrected tilt series are comparable to those seen on the quietest of the strainmeters.

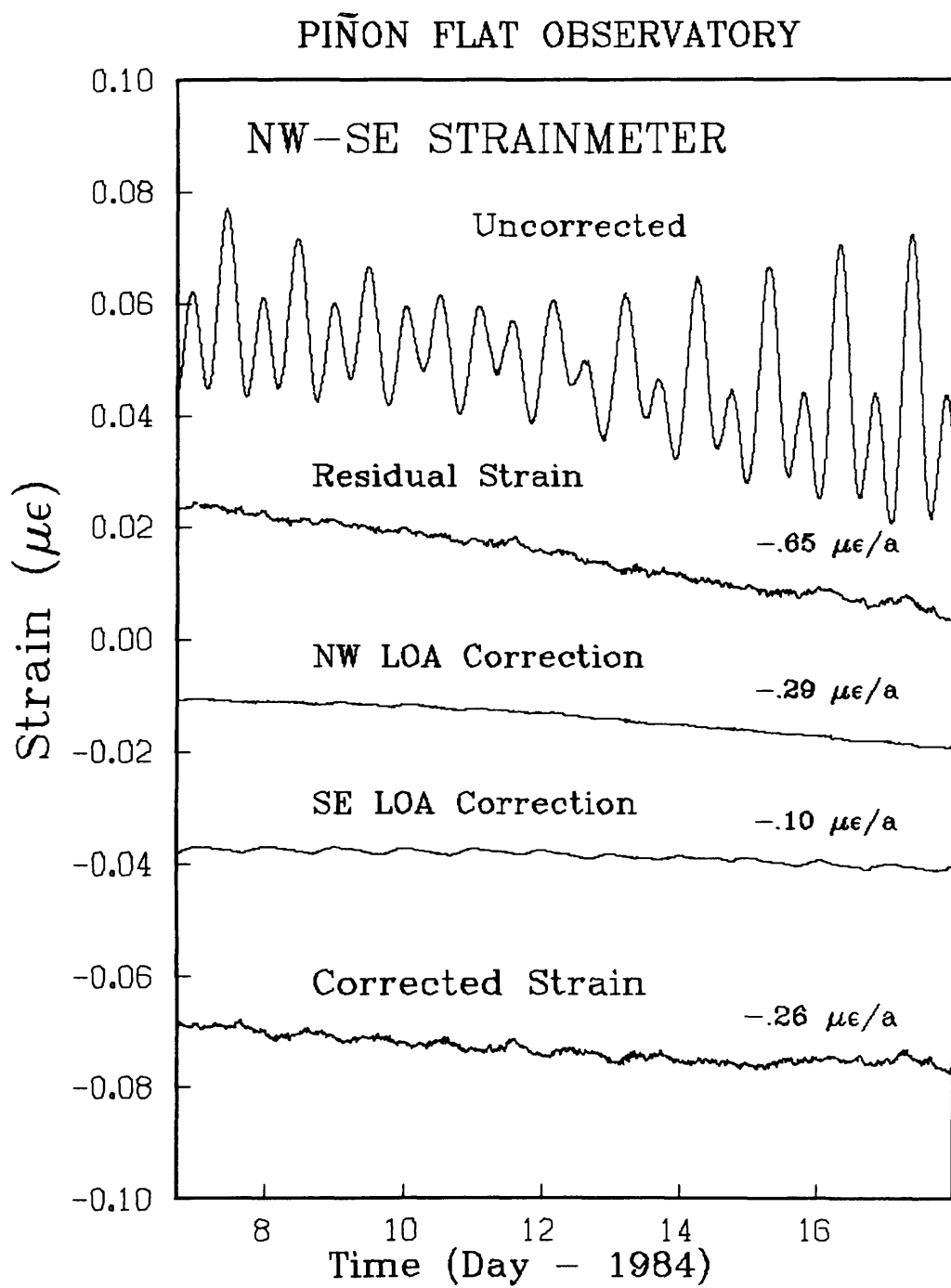


Figure 1

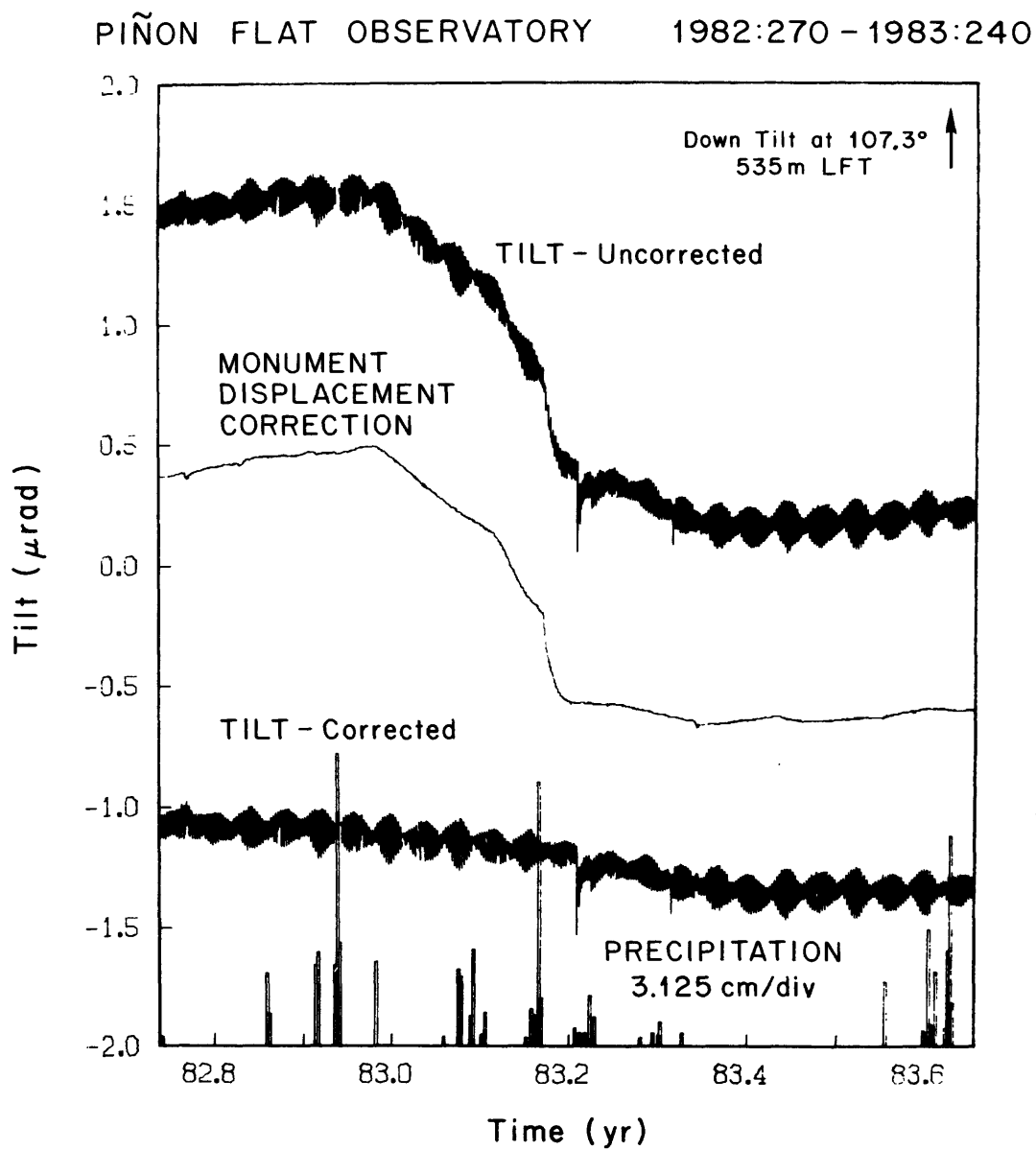


Figure 2

Digital Signal Processing of Seismic Data

9930-02101

W. H. Bakun
 U. S. Geological Survey
 345 Middlefield Road M/S 977
 Menlo Park, California 94025
 (415) 323-8111, ext. 2777

Investigations

Local magnitude M_L , seismic moment M_0 , and USGS central California seismic network (CALNET) coda durations τ were studied to develop consistent size scales for earthquakes in central California.

Accomplishments

1) Empirical formulae to estimate M_L and M_0 from τ as well as a technique to estimate M_0 from the coda-duration magnitudes M_D already published in the USGS preliminary catalogs have been obtained. Amplitudes recorded on Wood-Anderson seismograms (real and synthetic) indicate that for epicentral distance $\Delta \leq 475$ km, $-\log A_0 = \log (R/100) + 0.00301(R - 100) + 3$, where R hypocentral distance. For $30 \leq \Delta \leq 475$ km, these $-\log A_0$ are within 0.15 of Richter's values for southern California. For $0 \leq \Delta \leq 30$ km, Richter's values are significantly smaller than those obtained here.

Results

Bakun, W. H., 1984, Seismic Moments, Local Magnitudes, and Coda Duration Magnitudes for Earthquakes in Central California, Seismological Society of America Bulletin, v. 74, no. 2, p. 439-458.

Bakun, W. H., 1983, Magnitudes and moments of duration (abs.): EOS, American Geophysical Union Transactions, v. 64, no. 45, p. 765.

Scofield, C. P., W. H. Bakun, and A. G. Lindh, (1983), The $M_L = 5.4$ Idria, California, earthquake of October 25, 1982, (abs.): EOS, American Geophysical Union Transactions, v. 64, no. 45, p. 748.

Bakun, W. H., 1984, Magnitudes and moments of duration, Seismological Society of American Bulletin, (in press).

Lindh, A. G., W. H. Bakun, W. Ellsworth and M. E. O'Neill (1983), Long term probability estimates and an earthquake prediction experiment along the San Andreas fault system, (abs.): EOS, American Geophysical Union Transactions, v. 64, no. 45, p. 761.

Lindh, A. G., R. Allen, C. Johnson, J. Ellis, W. Bakun, D. Oppenheimer, and K. Poliakoff, 1983, Real time processor magnitudes (abs.): EOS, American Geophysical Union Transactions, v. 64, no. 45, p. 775.

Bakun, W. H., and W. B. Joyner, (1984). The M_L scale in central California, (abs.): Earthquake Notes, v. 55, no. 1, p. 13.

Bakun, W. H., and W. B. Joyner (1984). The M_L scale in central California, Seismological Society of America Bulletin, in press.

Bakun, W. H., and M. McLaren (1984). Microearthquakes and the nature of the creeping-to-locked transition of the San Andreas fault zone near San Juan Bautista, California, Seismological Society of America Bulletin, vol. 74, no. 1, pp. 235-254.

ROCK MECHANICS

9960-01179

James Byerlee
U.S. Geological Survey
Branch of Tectonophysics
345 Middlefield Road, MS/77
Menlo Park, California 94025
(415) 323-8111, ext. 2453

Investigations

Laboratory experiments are being carried out to study the physical properties of rocks at elevated confining pressure, pore pressure and temperature. The goal is to obtain data that will help us to determine what causes earthquakes and whether we can predict or control them.

Results

We have subjected samples of Westerly granite and Berea sandstone, saturated with $0.01M\text{ KCl}_{aq}$, to confining pressures of from 0.5 to 200 MPa. At each confining pressure, the complex resistivity of the samples was measured over a frequency range of 10^{-3} to 10^6 Hz. The observed increases in real resistivity with confining pressure at 1 Hz were 1,420% and 30% for the granite and sandstone, respectively. The equivalent real conductivity and real relative permittivity of the granite and sandstone decreased with pressure, although the changes observed in the granite exceeded those in the sand-stone. Conductivity decreased 3 times faster than permittivity in the granite, but at the same rate as permittivity in the sandstone. This result is consistent with a model in which conductivity is controlled by the interconnected paths available to the electrolyte in the rock pores, whereas permittivity (over this frequency range) is due primarily to boundary-layer effects at the grain-electrolyte interfaces.

Reports

D. Lockner and J. Byerlee, 1984, Complex resistivity of rock at elevated pressures, E.O.S. Trans. Am. Geophys. Union, v. 65, no. 16, p. 283.

PERMEABILITY OF FAULT ZONES

9960-02733

James Byerlee
Branch of Tectonophysics
U.S. Geological Survey
345 Middlefield Road, MS/77
Menlo Park, California 94025
(415) 323-8111, ext. 2453

Investigations

Laboratory studies of the permeability of rocks are carried out to provide information that will assist us in evaluating whether in a given region, fluid can migrate to a sufficient depth during the life-time of a reservoir to trigger a large destructive earthquake.

Results

Changes with time of the permeability and fluid chemistry of tuff have been measured in samples subjected to a temperature gradient. Initial permeabilities range from 3 to 65 microdarcys and there was little or no change in flow rate with time. The discharge fluid was near neutral pH that differed only slightly from the initial groundwater composition.

Reports

D. Moore, C. Morrow and J. Byerlee, 1984, Changes in permeability and fluid chemistry of the Topopah spring member of the Paintbrush Tuff when held in a temperature gradient, U.S.G.S. Open-File Report 84-273.

INVESTIGATION OF RADON AND HELIUM AS POSSIBLE
FLUID-PHASE PRECURSORS TO EARTHQUAKES

14-08-0001-21186

Y. CHUNG

Scripps Institution of Oceanography
University of California, San Diego
La Jolla, California 92093
(619) 452-6621

Investigations

1. Monitoring radon, helium, and other geochemical parameters in a southern California network of thermal springs and wells along the San Andreas, San Jacinto, and Elsinore faults, to study possible precursory effects correlated with earthquakes.
2. A general study of the relationships between these components, their origin, and variations due to flow rate changes, seasonal effects, atmospheric contributions, and crustal and mantle sources.
3. Continuous radon monitoring at network sites with field-installed Continuous Radon Monitors (CRMs) for possible short-term anomalies that may be precursory to earthquakes.
4. Comparison of long-term variations between the CRM and the discrete data.
5. Comparison between the CRM and Caltech Radon-Thoron Monitor data obtained at Pinon Flat for compatibility study.

Results

1. Discrete sampling at our southern California network sites for analyses of radon and helium continues at monthly intervals. No major earthquakes were reported in our network area during the past six months. However, many earthquakes with $M \geq 3$ occurred in the San Bernardino, Ocotillo Wells and Brawley areas. During mid-1983, four shocks ($M = 3.0-3.5$) occurred in the San Bernardino area within 20 km from the Arrowhead site. These shocks were preceded by a gradual radon and helium increase which reached a maximum (~60% above the baseline level) in May and June 1983. Both radon and helium have since fluctuated above their baselines with a similar pattern. On December 29, a shock ($M = 3.6$) took place near the converging area between the Banning and San Jacinto faults, only 9 km away from Arrowhead. This event was preceded by another radon and helium peak. Radon and helium were linearly correlated at Arrowhead. An earthquake swarm ($M = 3.0, 3.5, 3.3, 3.1$) occurred at the northern end of the Imperial fault north of Brawley on

November 15, 1983. No radon anomaly was observed at the Niland Slab Well, located 24 km northeast of the epicenter. However, a 30% radon increase was observed prior to this swarm at the Hot Mineral Well, 45 km north of the epicenter. At both sites helium shows a gradual decrease of about 30% during mid- and late-1983. At Hot Mineral Well, the well head pressure and water temperature have dropped significantly in recent months. The temperature dropped from the "plateau" at 70°C (1982 to 1983) to 61°C in March 1984. The February and March radon values were extremely high (~60% above the baseline) probably due to an increase of the gas bubbles in the samples. One week after the March collection, the well water turned muddy for one day, according to the spa keeper, but no nearby earthquakes were noticed.

2. From September to December 1983, six shocks with $M \geq 3$ were registered at the same location ($33^{\circ}03'N$, $116^{\circ}11'W$). This epicenter was located at 11 km southwest of the Robison's Well (in Ocotillo Wells) and 16 km northeast of the Agua Caliente sites. At Robison's Well, helium has been fluctuating since early 1983, in contrast to a fairly constant level before 1983. A 50% increase in radon was observed on the December 1983 sample. A similar pattern of radon and helium variations was also observed at the Indian Canyon site, along the San Jacinto fault, and at Agua Caliente, along the Elsinore fault. At Agua Caliente, radon increased by 20% in September but returned to the baseline after October 1983. Helium also increased by 20% in September but decreased to a minimum (~50% below the baseline) during the December collection, which was followed by an earthquake ($M = 3.5$) 5 days later at 1.3 km away from Agua Caliente. These features seem to suggest some precursory effects.
3. Except for a few data gaps, the CRMs have been working at the field quite well since 1983. At Arrowhead Springs, the CRM data accumulated since October 1983 have remained at the baseline level with fluctuations within $\pm 5\%$. The rapid increase (~10% in 5 days) began in late February 1983 which was reported previously was not observed in 1984. This increase was clearly not seasonal. At Murrieta Springs a 15% increase over the presumed baseline was observed within a week in late January 1984. Since then the radon has remained at this increased level with fluctuations less than $\pm 4\%$. This new level is quite close to the "plateau" level observed from May to September 1983. The 1983 CRM variations at Arrowhead and Murrieta are described and discussed in a paper to be published in Pure and Applied Geophysics. The Pinon Flat data are discussed in item 5.
4. The CRM and discrete radon data at the Arrowhead and Murrieta sites could be compared by either their time-series variations or variations of the ratio between them. Correlation between the two sets of data in time-series is not clear at present mainly due to the

dramatic difference in time scale. At Arrowhead, the gradual radon increase in discrete data in early 1983 to a maximum in May ($\sim 60\%$) was compared to a moderate CRM increase ($\sim 10\%$) in February and a flat plateau from March until July 1983 when the instrument malfunctioned. After a 2 month data gap, the CRM data accumulated after September 1983 indicated a return to the baseline while the discrete data showed fluctuations at a higher level after the May maximum. At Murrieta the discrete data displayed fluctuations of about $\pm 10\%$ along the baseline for 1983 and early 1984 while the CRM data clearly indicated variations at two levels: the higher level being 15-20% above the lower level. The high level was seen from May to September and after January 1984; the low level was seen from November 1983 to January 1984. Since the CRM monitors the gas-phase radon while the discrete measurements are for the dissolved radon, the ratio between the two sets of data after proper normalization (to a constant volume basis) gives a measure of the partition or distribution of radon between the two phases in the hot springs. The ratio as a distribution coefficient can be compared with that expected from the radon solubility at the spring water temperature. At both sites only about five percent of radon is in the dissolved phase, much lower than that expected from radon solubility. The variations of the ratio are about $\pm 10\%$ for Arrowhead and $\pm 15\%$ for Murrieta, comparable to the variations of the discrete data. Variations of the ratio for 1983 were discussed in the previous data summary report. Additional data obtained from 1984 are in line with those of 1983.

5. The CRM data from Pinon Flat indicate a decreasing trend during November and December 1983. This trend is reflected somewhat in the Caltech data, but with 3 weeks offset in time. The 1984 data fluctuated with large amplitudes ($\pm 45\%$) probably because of plumbing and other changes made by the Caltech group on their monitor. As the counting level was so low (~ 2 to 5 times the background level) it appears that no significant or meaningful variations could be obtained. Correlation between the CRM and Caltech data in time series could not be established on the basis of the data accumulated from the past 9 months. The Pinon Flat monitoring experiment was terminated in March 1984. The CRM unit is now re-located at the Fountain of Youth spa near the Hot Mineral Well.

Reports

- Y. Chung, Radon variations at Arrowhead and Murrieta Springs: Continuous and discrete measurements, Pure and Applied Geophysics (in press).

Mechanics of Earthquake Faulting

9960-01182

James H. Dieterich
U.S. Geological Survey
Branch of Tectonophysics
345 Middlefield Road, MS/977
Menlo Park, California 94025
415-323-8111, ext. 2573

Investigations

Constitutive Law for Dynamic Faulting Calculations

Data from large scale fault instability experiments were systematically analysed to evaluate different constitutive laws for use in dynamic fault calculations. Results of this study will be used for detailed rupture propagation and ground motion calculations.

Nucleation and Triggering of Earthquakes

Analysis was begun of the processes associated with the nucleation and triggering of unstable earthquake slip on a fault patch. Of particular interest in this investigation are the relationships between the occurrence of a stress step (such as might be caused by a fore-shock or mainshock) and time-delayed earthquake slip following the stress step. In addition, the conditions under which tidal triggering of earthquakes would or would not be evident were studied.

Deformation Mechanics of Active Volcanoes

Finite element codes were extensively modified and updated to permit analysis of caldera formation and rift expansion by either the independent or combined effects of magma injection/withdrawal and faulting.

Results

Constitutive Law for Dynamic Fault Calculations

Records of local fault stress and slip velocity from numerous experiments in a large scale laboratory faulting experiment were analysed to evaluate fault constitutive laws prior to and during unstable rupture propagation. Parameters that were used in the evaluation include premonitory slip velocity, dynamic slip velocity, the magnitude of the stress increase ahead of the propagating

rupture, the magnitude of the stress drop behind the rupture front and displacement weakening. Constitutive laws with velocity dependence that employ a state variable to represent history effects reproduce the characteristics of quasi-static fault slip and the propagating dynamic unstable slip. Comparison of specific state variable laws proposed by Dieterich and by Ruina indicates that the former can accurately represent the data over the full range of quasi-static and dynamic conditions (up to a 10^6 variation of slip velocity) while the latter tends to predict stress changes that are too large by about a factor of two or more under the dynamic conditions.

Nucleation and Triggering of Earthquakes

State variable constitutive laws with velocity dependency have been used in time-marching computations with a simple model that approximates conditions for slip on a fault patch. For a patch much larger than a critical radius, any initial stress, τ_i , above a critical stress, τ_c , results in accelerating slip leading to instability. Following a step in stress, $\Delta\tau = \tau_i - \tau_c$, the logarithm of the time to unstable fault slip decreases as $\Delta\tau$ is increased. The time to unstable slip following the stress step shows a direct linear scaling with the magnitude of the velocity-dependent coefficient in the constitutive law. As the velocity coefficient goes to zero, there is no delay between the time the critical stress is reached and the onset of unstable slip. Preliminary results indicate that if the velocity coefficient for natural faults has values similar to laboratory measured values then tidal triggering of earthquakes should be observable only if the total stress on natural faults is 1.0 MPa or less. Conversely, if the velocity coefficient of natural faults is significantly less than that observed in the laboratory, then tidal triggering of earthquakes should be observable at higher total shear stresses.

Using laboratory derived constitutive parameters extrapolated to time intervals characteristic of earthquake faulting (10^7 seconds or longer) the time delay from application of the stress step to unstable slip varies from 1 to 10^7 seconds (or longer) depending on the magnitude of $\Delta\tau$. It is speculated that this delayed failure may be an important process in controlling the timing of a mainshock following a foreshock, or in controlling aftershock sequences. Displacements during the accelerating slip that leads to instability are proportional to the displacement weakening parameter, d_c , in the constitutive law. The duration of stable slip is independent of d_c . Unless d_c for earthquake faults is significantly larger than that

observed on simulated faults in the laboratory, premonitory displacements prior to earthquakes may be too small to detect directly using current strain observation methods. Estimates from natural faults suggest that d_c may, in some cases, be significantly greater than laboratory measurements indicate.

Deformation Mechanics of Active Volcanoes

Updating of existing finite element codes and development of new codes, during the report period progressed and is nearly complete. The codes now incorporate more accurate high-order elements and fault elements and are capable of representing gravity loading effects and generalized interactions between magma reservoirs and fault slip. The codes will be applied to analysis of deformation data particularly at Kilauea.

Reports

Dieterich, J.H., 1983, Overview of Earthquake Prediction in the United States, Abstracts for: U.S.-Japan Seminar on Practical Approaches to Earthquake Prediction and Warning, p. 3-4.

Dieterich, J.H. and Conrad, G., 1984, Effect of Humidity on Time- and Velocity-Dependent Friction, Jour. of Geophys. Res., in press, 23 p.

Okubo, P.G., and Dieterich, J.H., 1984, Effect of Physical Fault Properties on Frictional Instabilities Produced on Simulated Faults, Jour. Geophys. Res., in press, 50 p.

In Situ Stress Measurements

9960-01184

John H. Healy
Branch of Tectonophysics
U.S. Geological Survey
345 Middlefield Road MS 977
Menlo Park, CA 94025
415/323-8111, ext. 2535

Investigations and Results

During this reporting period, we have completed the following tasks related to our areas of investigation:

1. A major part of our effort has been in site selection and drilling of holes for instrument emplacement related to earthquake prediction. Holes were drilled at San Juan Bautista and the Devil's Punchbowl for installation of the Carnegie Institute's Sacks-type volumetric strainmeters. The holes were logged and cemented as necessary for suitable instrument installation.

Cuttings that had been collected and stored over the past 5 years from these and previous instrument holes in California were analyzed petrographically and lithologic descriptions were written.

2. Ten weeks during November, December, and January were spent in the field at the Nevada Test Site. This work included field testing and calibration of pressure systems, televIEWer logging in hole USW G-3 and the lower part of hole Ue25p-1, and hydraulic fracturing stress measurements in these two holes. Analysis of this data was begun during this reporting period. Preliminary results show that the direction of least horizontal stress in these two holes is N60°W to N65°W, based on the orientations of drilling-induced hydraulic fractures in hole USW G-3 and the orientations of borehole breakouts in the lowermost carbonate units in hole Ue25p-1. These results agree closely with previous results from Yucca Mountain. The least horizontal principal stress in hole USW G-3 is low compared to the vertical stress, similar to previous results from holes USW G-1 and USW G-2. The horizontal stresses in hole Ue25p-1 appear to be higher in magnitude (closer to the magnitudes of the vertical stress).

Due to the higher stresses in hole Ue25p-1 and the extreme impermeability of the volcanic units in hole USW G-3, some difficulties were encountered with operation of the TAM International resettable packers. We have continued to work with TAM International on improvements for this resettable packer system. During a trip to TAM in April, an improved design was agreed upon. This modification will be manufactured and tested this spring and summer.

Open-file reports describing previous results from holes USW G-1 and USW G-2 were completed during this reporting period.

3. Continued monitoring of the Hi Vista well for tidal response has provided more data to support our previous observations that this hole and similar isolated deep fractures are potentially very useful in earthquake prediction. Computer programs were developed to remove tidal response from this data and analyze the power spectra of the signals. Work on temperature oscillations due to convection in deep boreholes was presented in a seminar at the Petroleum Engineering Department of Stanford University.

Data from Hi Vista and other wells drilled along the San Andreas fault zone were analyzed for trends in physical properties and in situ stress conditions, and results were presented at a special session on fault zone drilling at the Fall AGU meeting.

4. Some time was spent on meetings with the Nuclear Regulatory Commission and other groups involved in the Nevada Nuclear Waste Storage Investigations Program. Quality assurance procedures relating to the NNWSI work were updated and instruments were factory calibrated to meet NNWSI QA standards.
5. As part of a continuing program of cooperation with the People's Republic of China, some individuals in our group participated in hydraulic fracturing stress measurements in the Kunming province of China during October and November 1983. One of the Chinese scientists involved with this project came as a visiting scientist to Menlo Park. He and others have spent time processing the Chinese borehole data and developing computer systems and other equipment for use in China.
6. We have completed the design and assembly of a real-time seismic data acquisition and processing system for the Kingdom of Jordan, as part of a cooperative program between Jordan and the USGS.
7. Progress was made on the design and testing of a smaller computer system for the hydrofrac logging truck. Some of the components were purchased during this reporting period, but much of the work is continuing on into the next reporting period. This system, based on the Hewlett-Packard HP85 minicomputer and associated peripherals, is capable of recording pressure and flow data at a rate of 2 samples per second on two separate channels. The data are stored on cassette tape and can be plotted in the field, making this a compact and versatile system for field use.
8. Substantial effort was devoted to developing a calibration procedure for pressure recorders, pressure testing of equipment for hydraulic fracturing tests, and redesigning all working components of the hydrofrac system for surface pressures of 3000 to 6000 psi. Substitute components were obtained for operation at surface pressures to 10000 psi. This system is now in full working order and will greatly increase the range of depths to which we can conduct hydraulic fracturing tests.
9. Laboratory investigations of the process of initiation and development of borehole breakouts were completed. These studies were conducted in an attempt to quantify the possibility of using borehole breakouts as

indicators of relative stress magnitudes. Results show that the process of breakout formation is a complex one involving the formation of both shear and tensile fractures at the borehole wall. Breakout size varies considerably for a given applied stress, so that breakout shape is not likely to be a useful indicator of relative stress magnitudes.

Reports

- Fuis, G. S., Mooney, W. D., Healy, J. H., McMechan, G. A., and Lutter, W. J., 1984, A seismic refraction survey of the Imperial Valley Region, California: *Journal of Geophysical Research*, v. 89, no. B2, p. 1165-1189.
- Ginzburg, A., Mooney, W. D., Walter, A. W., Lutter, W. J., and Healy, J. H., 1983, Deep structure of the northern Mississippi Embayment: The American Association of Petroleum Geologists, v. 67, no. 11, p. 2031-2046.
- Healy, J. H., Hickman, S. H., Zoback, M. D., and Ellis, W. L., 1984, Report on televiewer log and stress measurements in core hole USW-G1, Nevada Test Site, December 13-22, 1981: U.S. Geological Survey Open-File Report 84-15, 51 pp.
- Hickman, S. H., Healy, J. H., and Zoback M. D., 1984, In situ stress, natural fracture distribution, and borehole elongation in the Auburn geothermal well, Auburn, New York.
- Mooney, W. D., Fuis, G. S., and Healy, J. H., 1984, Seismic refraction studies of a sedimentary basin, southern California, USA: Methods and results: submitted to *Journal of the Association of Exploration Geophysicists*.
- Stock, J. M., Healy, J. H., and Hickman, S. H., 1984, Report on televiewer log and stress measurements in core hole USW-G2, Nevada Test Site, U.S. Geological Survey Open-File Report.
- Urban, T. C. and Healy, J. H., 1983, Monitoring fluid pressure in fractures for earthquake prediction: EOS, *Transactions of the American Geophysical Union*.
- Zoback, M. D., Healy, J. H., Zoback, M. L., and Prescott, W., 1983, In situ stress and faulting: (abs) IUGG Meeting.

Experimental Rock Mechanics

9960-01180

Stephen Kirby
Branch of Tectonophysics
U.S. Geological Survey, MS/977
345 Middlefield Road
Menlo Park, California 94025
(415) 323-8111, Ext. 2872

Investigations

We continue our research on the rheology of the lithosphere and the strength of rocks and minerals of the continental crust and upper mantle. This work focuses on establishing the laws governing flow and to estimate stress differences that can be supported within the earth.

Results

It has recently been emphasized that the shear stresses sustained by the upper 20 kilometers of the crust are governed by the pore pressure (the effective stress phenomenon) and by the chemical interactions between aqueous fluids and rocks, interactions that lead to a variety of processes that reduce rock strength [Kirby, 1983, 1984; Kirby and Scholz, 1984]. One of these processes is the reduction in the plastic yield strength of silicates, termed hydrolytic weakening. We recently have shown that molecular water, incorporated in the crystal structure, is the weakening species in quartz [Aines, Kirby and Rossman, 1983, 1984]. How is molecular water taken up by quartz in the crust? We have identified four uptake mechanisms that operate in the laboratory: (1) Intracrystalline diffusion, as suggested by $H_2^{18}O$ -diffusion studies; (2) Diffusion aided by microfracture, which reduces the diffusive path length; (3) Rapid crystal growth in hydrothermal fluids; (4) Sweeping by grain boundary migration during recrystallization or solid-state grain growth [Kirby and Kronenberg, 1984]. All of these processes appear to be aided by high water pressure and are likely to be important in strain localization in crustal shear zones. We are investigating these possibilities by determining the water concentrations in feldspar and quartz in the shear zones in granitic rocks from the Sierra Nevada studied by Paul Segall. Using a new Fourier-transform infrared spectrometer, we have been able to determine water concentrations as low as 100 ppm in quartz grains from the undeformed granodiorite. This is a major experimental breakthrough because it permits us to evaluate quantitatively the contribution of hydrolytic weakening in naturally deformed rocks.

Kirby contributed a paper to the 6th Annual Texas A&M Geodynamic Symposium titled, "Deformation Processes and Rheologies of Mafic and Ultramafic Rocks: Relevance to the Collisional Tectonics Regime," where he reviewed the existing knowledge on the rheological structure of the continental lithosphere. Two major conclusions were made: that the Moho is likely to be a rheological as well as a chemical boundary and that strain localization in shear zones may be important phenomena in the deep crust and upper mantle.

Reports

- Aines, R. D., Kirby, S. H., and Rossman, G. R., Hydrogen speciation in synthetic quartz and its relevance to hydrolytic weakening, *Trans. Amer. Geophys. Union*, 64, 839, 1983.
- Aines, R. D., Kirby, S. H., and Rossman, G. R., Hydrogen speciation in synthetic quartz, *Phys. and Chem. Miner.* (In Press), 1984.
- Kirby, S. H., Rheology of the lithosphere, *Rev. Geophys. Space Phys.*, 21, 1458-1487, 1983.
- Kirby, S. H., Introduction and digest to the special issue on the chemical effects of water on the deformation and strengths of rocks, *Jour. Geophys. Res.*, 89, (In Press), 1984.
- Kirby, S. H., and Kronenberg, A. K., Hydrolytic weakening in quartz: uptake of molecular water and the role of microfracturing, *Trans. Am. Geophys. Union*, 65, 277, 1984.
- Kirby, S. H., and McCormick, J. W., Inelastic properties of rocks and minerals: strength and rheology, in R. S. Carmichael, ed., *Handbook of Physical Properties of Rocks*, v. 3, (In Press), 1984.
- Kronenberg, A. K., and Kirby, S. H., Electrical conductivity of quartz: time dependence and transition in ionic charge carriers, *Trans. Am. Geophys. Union*, 65, 277, 1984.
- Lee, R. W., and Kirby, S. H., Experimental deformation of topaz crystals: possible embrittlement by intracrystalline water, *Jour. Geophys. Res.*, 89, (In Press), 1984.
- Linker, M. F., Kirby, S. H., Ord, A., and Christie, J. M., Effects of compression direction on the plasticity and rheology of hydrolytically-weakened synthetic quartz crystals, *Jour. Geophys. Res.*, 89, (In Press), 1984.

LABORATORY EXPERIMENTS OF WAVE PROPAGATION
IN ANELASTIC MEDIA

9910-02413

Hsi-Ping Liu and Louis Peselnick
Branch of Engineering Seismology and Geology
U. S. Geological Survey
345 Middlefield Road, Mail Stop 977
Menlo Park, California 94025
(415)-323-8111 ext. 2731

Investigations:

1. Model experiments investigating the effects of anelasticity on travel time and amplitude in seismic wave propagation.
2. Development of an apparatus for determining Young's modulus of rocks subject to quasi-static small strain (10^{-8}). The objectives are (1) to investigate dispersion effects, specifically to compare 'zero-frequency' small strain elastic moduli of rocks with measurements from dynamic methods, and (2) to investigate small strain, quasi-static anisotropic elastic properties of rocks in terms of crack orientation and fabric.
3. Continuing data analysis for the effect of tidal stress on seismic travel times.

Results:

1. The internal friction of several materials have been determined in search of a suitable modeling material for anelastic wave propagation experiments at ~ 1 MHz. Figure 1 shows the experimental arrangement which is capable of measuring both the internal friction and velocity of the sample material. The solids investigated (Lead, $Q = 300$; A Neoprene Rubber, $Q > 500$; Plexiglas, $Q > 500$; Copper, $Q > 500$) showed internal friction values too low, and therefore unsuitable for modeling seismic wave attenuation. Measurements are currently being carried out on thixotropic materials and on highly viscous fluids in order to find a suitable modeling medium.
2. A calibration experiment on the quasi-static, 10^{-8} strain Young's modulus apparatus was made on an aluminum sample. The Young's modulus of this sample was determined from ultrasonic P and S velocities. Agreement between the 'static' and dynamic measurements were within 10 percent. The difference is a result of non-uniform stress in the sample. An improved version of the 'static' apparatus has been designed for uniform loading on the sample.
3. Data analysis is continuing on the effects of tidal stress on seismic travel time from eight 12-hour experiments carried out in Hollister, California and one 36-hour experiment carried out in North Chelmsford, Massachusetts. Phase velocities of 8 extrema in the wave train generated by air-gun shots starting from the first arrival are included in the analysis.

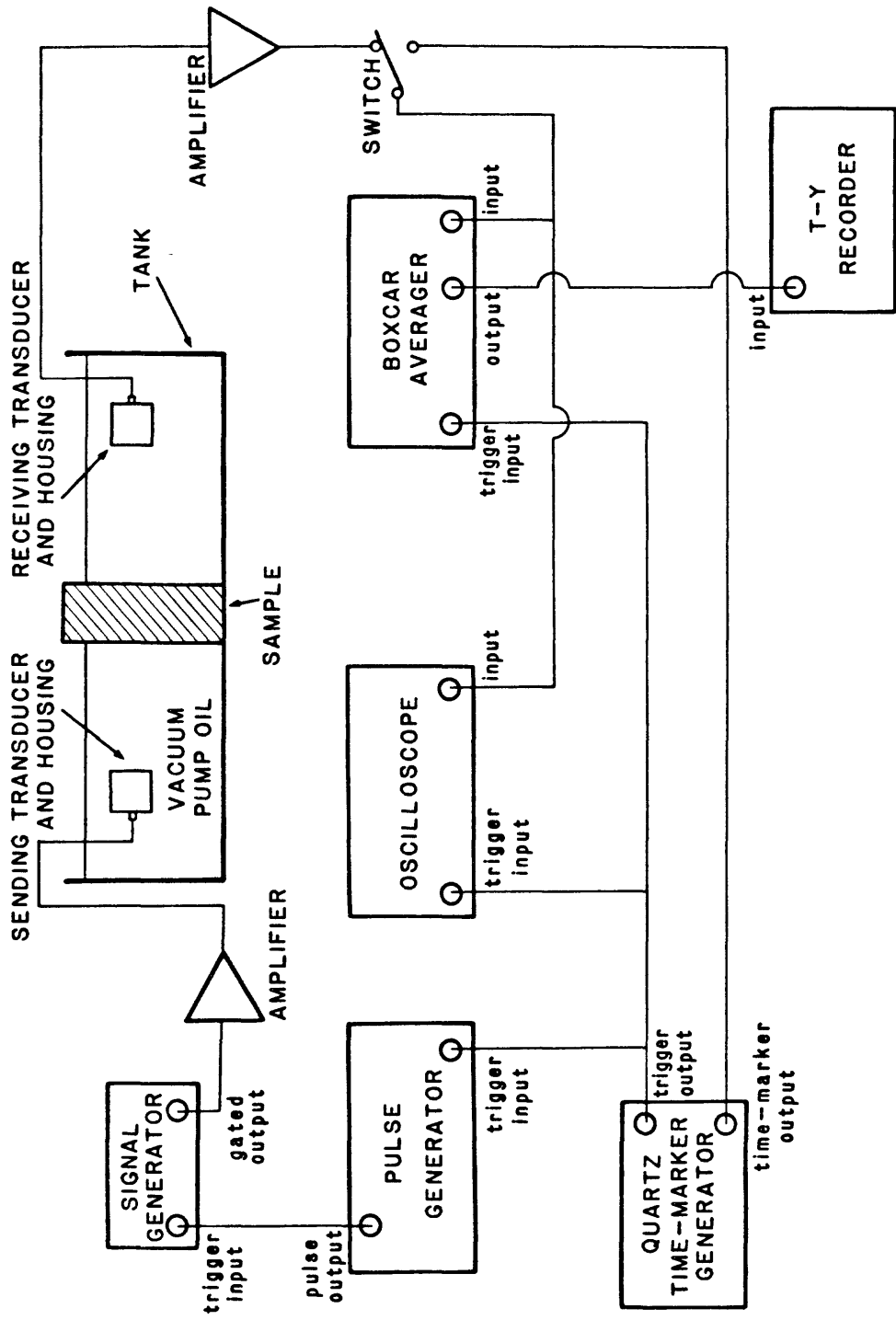


Figure 1. Schematic drawing showing experimental arrangement for the measurement of ultrasonic internal friction and velocity of solids and liquids. Two or more samples of the same material but of different thicknesses are placed individually between the sending and receiving transducers. The difference in travel times and amplitudes yield the velocity and internal friction respectively.

Active Seismology in Fault Zones

9930-02102

Walter D. Mooney
Gary S. Fuis
U. S. Geological Survey
Branch of Seismology
345 Middlefield Road, Mail Stop 977
Menlo Park, California 94025
(415) 323-8111, ext. 2569

Investigations Undertaken

- 1) Final manuscript preparation of a 1981 seismic refraction experiment in northeastern California (Zucca, Fuis, Catchings, Milkereit and Mooney).
- 2) Continued time-term analysis of a 1979 seismic refraction experiment in the Imperial Valley region, California (Kohler and Fuis).
- 3) Analysis of earthquake aftershock and seismic-refraction data in the Coalinga, California, region following the May 2, 1983, earthquake, M 6.5 (Fuis and Walter).
- 4) Field planning of 1983 seismic-refraction experiment in southern Alaska--the first project in a multi-year Trans-Alaska Crustal Transect (TACT) program (Fuis, Mooney, Page, Criley).
- 5) Continued analysis of seismic refraction and reflection data from central California (Walter, C. Wentworth, and others.)

Results

- 1) In 1981, the U. S. Geological Survey conducted a seismic-refraction experiment in northeastern California that included 95-km-long north-south lines in the Klamath Mountains (KM) and on the Modoc Plateau (MP), and a 275-km-long east-west line from the KM to the California-Nevada state line. Instrument spacing average 1 km, and shotpoint spacing 50 km. The KM and MP lines yielded the simplest models. The KM line is underlain by relatively flat high-velocity layers (6.1, 6.5, 6.7, and 7.0 kms) with low-velocity layers between them. Layer thicknesses range from 1 to 3 km; the 7.0-km/s-velocity layer is 14 km deep. The MP line is underlain by 4-1/2 km of relatively low-velocity (3.5-4.5 km/s) material over a 6.2 km/s-velocity basement.
- 2) The U.S. Geological Survey conducted an extensive seismic refraction survey in the Imperial Valley region of California in 1979. We analyzed five refraction profiles, modeled an existing gravity profile across the Salton Trough, constructed a basement depth map, and produced a structure and tectonic summary map of the Imperial Valley region. Results are itemized:

- 1) The models for the refraction profiles have in common a sedimentary layer ($V_p = 1.8\text{--}5.0 \text{ km/s}$), a "transition" zone ($V_p = 5.0\text{--}5.65 \text{ km/s}$), a basement ($V_p = 5.65 \text{ km/s}$ in Imperial Valley, 5.9 km/s on West Mesa), and subbasement ($V_p = 7.2 \text{ km/s}$, only well documented in Imperial Valley).
- 2) The sedimentary layer ranges in thickness along the axis of the Salton Trough from 3.7 km (Salton Sea) to 4.8 km (U.S.-Mexican border). On West Mesa it ranges from 0-3.5 km.
- 3) The "transition" zone is about 1 km thick in most places. In Imperial Valley, there are no marked velocity discontinuities in this zone between the sedimentary layer and basement. On West Mesa, however, there is a discontinuity at the top of this zone.
- 4) There are apparently two types of basement. On West Mesa, basement is crystalline igneous and metamorphic rocks. In Imperial Valley, beneath 5-6 km of sedimentary rocks (including the "transition" zone), basement is likely to be mostly lower-greenschist-facies metasedimentary rocks.
- 5) The subbasement, or lower crust, ranges in depth along the axis of the Salton Trough from 16 km (Salton Sea) to 10 km (U.S. Mexican border). Gravity modeling indicates that this layer deepens and (or) pinches out beneath the bordering mesas and mountain ranges. Based on its high velocity and the presence of intrusive basaltic rocks in the sedimentary section in the Imperial Valley, the subbasement is thought to be a mafic intrusive complex similar to oceanic middle crust.
- 6) The Imperial Valley (and also East Mesa) is underlain by a geologic section consisting of sedimentary rocks, metasedimentary rocks, and mafic intrusive rocks, according to our interpretation, all of which are late Cenozoic in age. West of the Imperial Valley-East Mesa region, West Mesa and the Peninsular Ranges are underlain mostly by pre-Cenozoic crystalline rocks, as are the Chocolate Mountains, east of the Imperial Valley-East Mesa region.
- 7) Certain block motions can be inferred from the configuration of the suture between new and old crust. A block between the San Jacinto fault zone and Elsinore fault appears to have moved about 50 km northwestward from the Cerro Prieto spreading center, and a block between the San Jacinto fault zone and San Andreas fault appears to have moved 25-45 km northwestward from the Brawley spreading center. Spreading at the Brawley spreading center may be asymmetrical.

Thus, new crust is forming in the Salton Trough as rifting occurs: Mafic igneous rocks intrude the lower crust as the rift opens, and sedimentary rocks are deposited in the rift basin. Rifting and intrusion produce high heat flow, metamorphosing the sedimentary rocks to relatively shallow depth in the rift basin.

- 3) The U.S.G.S. conducted a seismic-refraction experiment in the Coalinga area shortly after the May 2, 1983, $M = 6.5$ earthquake in order to obtain a better knowledge of the crustal velocity structure near Coalinga.

The experiment consisted on two phases of data acquisition. In the first phase, aftershocks were recorded along two profiles crossing the epicentral region of the May 2 earthquake. A NW-SE profile extended from the epicentral region along the syncline west of the Kettleman Hills, and an E-W profile extended from the interior of the Diablo

Range across the epicentral region into the San Joaquin Valley. A total of 120 analog-tape-recording, single-vertical component seismographs were used to record aftershocks. On the night following the main shock, the seismographs were deployed at 1-km spacing along the NW-SE profile. Two days later, the seismographs were re-deployed at .5-km spacing along the E-W profile. For both deployments, four 13-minute time intervals were recorded.

In May and June of 1983, the second phase of the refraction experiment used the same instruments to record nine shots along approximately the same profiles as the aftershock profiles. Four shots were recorded along the E-W profile and five shots along the NW-SE profile. Fortunately, a M=2.5 aftershock was also recorded along the NW-SE shot profile.

From the known surface geology, available well logs, and seismic reflection records, geologic cross-sections were derived along the 1983 Coalinga refraction profiles to provide constraints for the on-going velocity modeling of the refraction data. Preliminary modeling of the refraction data has shown that in certain places along the profile, velocity inversions are observed in either or both the Tertiary and Cretaceous sediments. These velocity inversions are not continuous along the length of the profiles; they appear to be structurally controlled, perhaps, localized by folds and faults in the area. The depths calculated in the refraction modeling for the tops of some of the inversions correlate with the depths found for the tops of zones of high-pore pressure in nearby wells (R. Yerkes, WRG).

For 19 Coalinga aftershocks recorded along the 1983 Coalinga refraction profiles, the P-phase arrivals at stations surrounding the epicentral region were timed and then used to locate the aftershock events. Six events located closest to the profile lines were selected for digitization in record section format. Because most of the refraction shots had a poor signal-to-noise ratio beyond 30 km from the shotpoints, the earthquake record sections will provide added constraints on the velocity structure below the Coalinga earthquake hypocenters.

- 4) In 1984 the USGS will conduct an extensive seismic refraction experiment in southern Alaska, as the first major project of the Trans-Alaska Crustal Transect (TACT) program. TACT's a multi-year, multi-disciplinary effort to investigate the crustal structure along a route paralleling the Alaska oil pipeline. The program includes many investigations including seismic refraction, seismic reflection, geologic mapping, and gravity and aeromagnetic studies. The 1984 seismic refraction experiment will consist of four profiles designed to investigate in various ways the accreted terranes of southern Alaska and their sutures, including the current Benioff zone(s) extending northwestward under the Kenai Peninsular and northward under the Wrangell volcanoes, and the active Denali fault zone. One profile extends along the Glenn Highway from Tahneta Pass to Mentasta Pass near the Denali fault (225 km), crossing the Peninsular and Wrangellia terranes more or less diagonally; shotpoint spacing will average about 45 km. A second profile extends southward along the Richardson Highway from the Denali fault to the Tiekel River

and thence cross-country to the Tasuuna River (260 km), crossing numerous terranes roughly perpendicular to strike. Shotpoint spacing will average 25 km to deal with expected rapid near-surface velocity variation in this direction. A third profile extends eastward cross-country from Valdez to the Tana River (200 km) sampling the Chugach terrane parallel to strike.

- 5) Preliminary interpretation of seismic reflection and refraction profiles across the southeastern end of Kettleman Hills, 65 km southeast of the Coalinga epicentral area, suggests that presence of both northeast-dipping reverse faults and southwest-dipping thrust fault beneath the Kettleman Hills anticline. Two deep reverse faults are inferred to dip steeply northeastward beneath the anticline and offset basement at a depth of about 9 km. One of these faults is aligned with a shallow northeast-dipping reverse fault in the southwest limb of the anticline that offsets upper Miocene strata about 200 m; we assume that these two faults are connected. The reverse faults have an orientation beneath the anticline approximately equivalent to that of one plane of the focal mechanism solution for the Coalinga main shock, which is the plane preferred from surface deformation studies.

The thrust fault is inferred to dip gently southwestward from 3 km beneath the north-east limb of the anticline to a depth of 10 km beneath the Diablo Range. The thrust shows about 10 km of post-late Miocene dip slip that has repeated the Tertiary and upper Mesozoic section and the underlying Franciscan essemblage.

Mafic basement unconformably underlying the Great Valley sequence beneath the San Joaquin plunges southwestward at 40° to a depth of 15 km beneath the Diablo Range, rather than following the base of the Great Valley sequence up to the surface. If this is a single, continuous basement surface, as eastward-thinning wedge of Franciscan rock is defined that lies between the basement and the overlying Great Valley sequence. Farther east, however, the Great Valley sequence was deposited directly on the same mafic basement.

Reports

Andrews, M. C., Mooney, W. D., and Meyer, R. P., The relocation of microearthquakes in the northern Mississippi Embayment, Jour. of Geophy. Res. (submitted).

Blumling, P., Mooney, W. D., and Lee, W. H. K., Crustal structure of the southern Calaveras fault zone, central California, from seismic refraction investigations, Bull. Seis. Soc. Am. (in press).

Fuis, G. S., Mooney, W. D., Healy, J. H., McMechan, G. A., and Lutter, W., 1982, Crustal structure of the Imperial Valley region, in The Imperial Valley Earthquake of 1979: U.S. Geological Survey Professional Paper 1254, p. 64.

Fuis, G. S. and Kohler, W. M., 1984, Crustal structure and tectonics of the Imperial Valley region, California, Soc. Econ. Paleontologists and Mineralogists, Pacific Section, p. 1-14.

- Fuis, G. S., Zucca, J. J., Mooney, W. D., and Milkereit, B., A geologic interpretation of seismic-refraction results in northeastern California: Geol. Soc. Am., in press.
- Milkereit, B., Mooney, W. D., and Kohler, W. M., Tau-p inversion for laterally-varying structure, Geophy. Jour. Royal Astr. Soc., in press.
- Mooney, W. D., Andrews, M. C., Ginzburg, A., Peters, D. A., and Hamilton, R. M., 1983, Crustal structure of the northern Mississippi Embayment and a comparison with other Continental rift zones: Tectonophysics, v. 94, 327-348.
- Mooney, W. D., and Colburn, R. H., A seismic-refraction profile across the San Andreas Sargent, and Calaveras faults, west-central California, Bull. Seis. Soc. Am., in press.
- Mooney, W. D., Fuis, G. S., and Healy, J. H., 1984, Seismic refraction studies of a sedimentary basin, southern California, USA: Methods and results, Journal of Exploration Geophysics Hyderabad, India.
- Mooney, W. D., Gettings, M. E., Blank, H. R., and Healy, J. H., Saudi Arabian seismic-refraction profile: A travelttime interpretation of crustal and upper-mantle structure (Tectonophysics, in press).
- Mooney, W. D., and Prodehl, C., Preceedings of the IASPEI Workshop on the interpretation of the 1978 Saudi Arabian refraction profile (USGS circular, in press).
- Walter, A. W., and Mooney, W. D., 1983, Preliminary report on the crustal report on the crustal velocity structure near Coalinga, California, as determined from seismic refraction surveys in the region (Calif. Div. Mines and Geol. Spec. Report 66, p. 127-136.
- Wentworth, C. M., Walter, A. W., Bartow, J. A., and Zoback, M. D., Evidence on the tectonic setting of the 1983 Coalinga earthquakes from deep reflection and refraction profiles across the southeastern end of the Kittleman Hills, (Calif. Div. Mines and Geol. Spec. Rept. 66, p. 113-126.
- Zucca, J. J., Fuis, G. S., Milkereit, B., Mooney, W. D., and Catchings, R. D., Crustal structure of northeast California from seismic refraction data: Jour. Geophy. Res., in press.

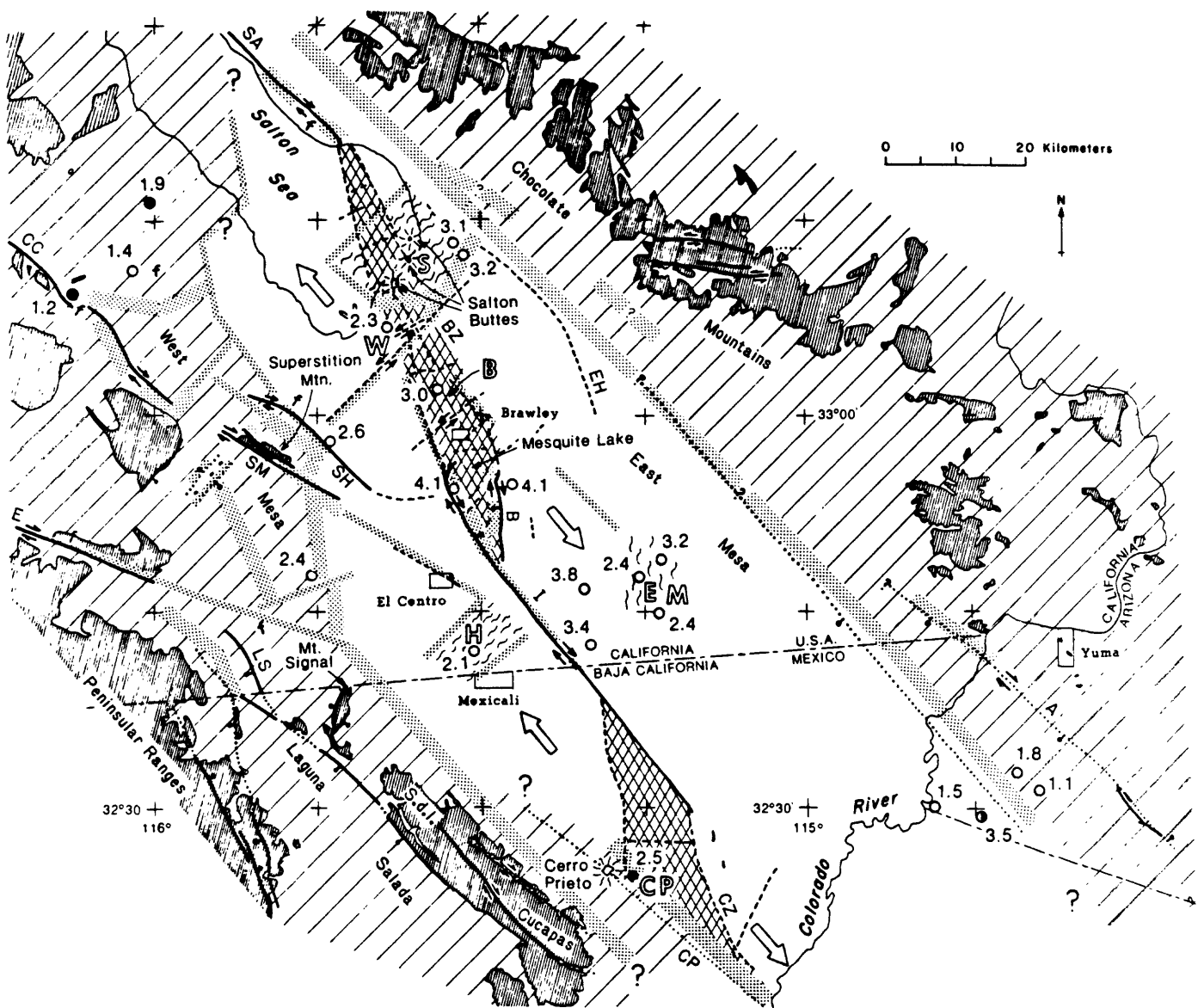


Figure 1. Structure and tectonic summary map. Zones of high (greater than 16 percent) gradient on basement depth map are indicated here by wide stippled lineaments of different lengths. Other selected linear features on basement depth map are indicated here by narrow stippled lineaments. Faults, seismicity lineaments, and geothermal areas are reproduced from fig. 5. "f" refers to areas of Cenozoic folding and (or) reverse faulting. Similar information in Mexico and southwest Arizona comes from Gastil and others (1971), Mattick and others (1973), Reed (1975), Johnson and Hutton (1982), James J. Lienkaemper (oral commun., 1984). Abbreviations in Mexico are CZ, Cerro Prieto seismic zone; CP, Cerro Prieto geothermal area and Cerro Prieto fault; S.d.l. Cucapas, Sierra de los Cucapas. Seismic zones are crosshatched. Apparent basement shallowing under Salton Sea, Heber, and East Mesa geothermal fields is indicated by wavy lines. Circles with numbers denote wells and depths in km. Solid circles penetrate crystalline rocks. Open circles penetrate only Cenozoic sedimentary rocks. Half-filled circle in Arizona penetrates numerous Miocene basaltic dikes(?) near base. Outcrops of pre-Cenozoic crystalline basement are indicated by closely spaced lines; locally include Tertiary intrusive rocks. Inferred extent of crystalline basement beneath Cenozoic sedimentary rocks is indicated by widely spaced lines, queried where there is little data. Direction of spreading from Brawley and Cerro Prieto spreading centers is indicated by large open arrows. From Fuis and Kohler, 1984.

COUPLED DEFORMATION - PORE FLUID DIFFUSION EFFECTS
IN FAULT RUPTURE

14-08-0001-21818

John W. Rudnicki
Department of Civil Engineering
Northwestern University
Evanston, Illinois 60201
(312)-492-3411

Investigations

1. Effects of coupled deformation - diffusion on water well level changes due to propagating creep events.
2. Dilatant hardening effects on precursory processes.
3. Coupled deformation - diffusion effects accompanying slip on impermeable fault zones.

Results

1. Our results in this area are summarized in the following abstract from publication 3 listed below:

"Water well level fluctuations associated with episodic creep are studied using a coupled deformation-diffusion solution for the pore pressure produced by a plane strain shear dislocation moving steadily at a speed V in a linear elastic, saturated porous medium. For large $Vr/2c$, where r is distance from the dislocation and c is diffusivity, the solution approaches the form of the uncoupled elastic solution used by Wesson (1981) to analyze water level changes due to creep events. The differences between the two solutions are significant within 10 diffusion lengths ($20V/c$) from the fault plane. More specifically, the pore pressure predicted by the coupled solution reverses sign behind the dislocation and is much smaller in magnitude than that predicted by the uncoupled solution. For an undrained Poisson's ratio of 0.3, Skempton's coefficient of 0.8 and a shear modulus of 30 GPa, the coupled solution predicts a peak pore pressure change of 13.7 kPa (137 mbar) per millimeter of slip for $V = 1 \text{ km/day}$ and $c = 1.0 \text{ m}^2/\text{s}$. The spectrum of the coupled solution is limited to a band of frequencies, centered at a value proportional to V and approximately inversely proportional to the distance from the observation point to the fault plane. Thus, close to the fault plane, the frequency band occupied by the coupled solution may lie above the

range at which water wells can respond. The coupled solution is used to interpret the same creep-associated water level change observed by Johnson (1973) and modeled by Wesson (1981) using the uncoupled solution. Although there are uncertainties in rock material properties and in the speed of the creep event, the coupled solution predicts a water level change comparable in magnitude to the observed change."

2. Some earlier work in this area is summarized in the following Abstract from publication 4 below:

"This study examines the effects of dilatant hardening on the development of concentrated shear deformation. Specifically, the analysis considers the shear of an inelastically deforming rock mass containing a weakened layer of width h . The presence of the weakened layer causes localization instability, characterized by an unbounded ratio of a strain increment in the weakened layer to that in the farfield, to occur earlier than it would be predicted from the response of the material surrounding the embedded layer. The development of instability depends on the relative rate of imposed shear strain γ_∞ and the time scale of fluid mass exchange between the layers, h^2/c , where c is an effective diffusivity. In the limit $\gamma_\infty h^2/c \rightarrow 0$, the pressure in the weakened layer is equal to that in the surrounding material and localization instability occurs at the peak of the drained response curve. For finite $\gamma_\infty h^2/c$, instability is delayed until the material in the weakened layer has been driven to the peak of its undrained, dilatantly hardened response curve. The time delay between final instability and the time at which the weakened layer passes the peak of its drained stress strain curve is called the precursor time t_{pr} because rapid straining of the weakened layer occurs during this period. For small $\gamma_\infty h^2/c$, as appropriate for tectonic applications and most laboratory experiments, a nonlinear asymptotic analysis predicts that

$$t_{pr} = (\alpha h^2/c)^{2/3} (\lambda/\gamma_\infty)^{1/3} \Delta^{-1/6}$$

where λ is the half-width of the peak of the stress strain curve, Δ is the difference in the peak stresses of the layers divided by λ times the elastic shear modulus and α is a nondimensional measure of the strength of dilatant hardening. For a wide range of numerical values, the precursor times are very short: less than few hours for tectonic strain rates and less than a few tens of seconds for typical laboratory strain-rates."

The work in publication 4 indicated that the stabilization times associated with dilatant hardening effects on the development of concentrated shear deformation are very short for deformation rates typical of both laboratory experiments and tectonic straining. The predictions for laboratory strain-rates are in contrast to the observations of Martin (1980) on pore fluid stabilization of failure in Westerly granite: Martin observed stabilization times on the order of several minutes. To resolve this discrepancy, we are investigating the possibility that additional stabilization results from dilatant uplift and cracking associated with frictional sliding after deformation has localized into a narrow fault zone. Preliminary results, based on a very simple model of a slab bounded by a frictional surface and

assuming steady state flow conditions, indicate delay times more comparable to those observed by Martin.

3. Existing solutions for coupled deformation-diffusion effects accompanying fault slip (Booker, 1974; Rice and Cleary, 1976) or shear fault propagation (Rice and Simons, 1976) impose zero pore pressure change on the fault plane. Consequently, they are most appropriate for application to permeable fault zones. Because many fault zones contain large amounts of fine particles and clay gauge, they are relatively impermeable. We have recently obtained solutions for suddenly introduced and steadily propagating shear dislocations on an impermeable fault plane in a fluid-saturated rock mass. The solutions are considerably different than those for permeable faults. In particular, the spatial dependence of the stresses and pore pressure is much different. The solution for the pore pressure change due to a steadily propagating shear dislocation has been used to complement our results in publication 3. In contrast to the results for the permeable fault plane, the pore pressure change for steadily propagating slip on an impermeable plane does not reverse sign behind the dislocation and decays more slowly in magnitude with distance away from the fault plane.

References

- Booker, J.R., J. Geophys. Res., 79, 2037-2044, 1974.
 Martin, R.J., III, Geophys. Res. Letters, 7, 404-406, 1980.
 Rice, J.R. and M.P. Cleary, Rev. Geophys. Space Phys., 14, 227-241, 1976.
 Rice, J.R. and D.A. Simons, J. Geophys. Res., 81, 5322-5334, 1976.
 Wesson, R.L., J. Geophys. Res., 86, 9259-9267, 1981.

Publications

1. Rudnicki, J.W., Effect of pore fluid diffusion on deformation and failure of rock, to appear in Mechanics of Geomaterials (edited by Z.P. Bazant), Proceedings of the IUTAM William Prager Symposium on Mechanics of Geomaterials: Rocks, Concretes, Soils, September 11-15, 1983, Northwestern University, Evanston, IL. Publication by John Wiley, Ltd., London, expected in 1984.
2. Roeloffs, E. and J.W. Rudnicki, Coupled Deformation-Diffusion Effects on Water Level Changes Due to Propagating Creep Events, (Abstract), EOS, Trans. Am. Geophys. Union, 64, 851, 1983.

3. Roeloffs, E. and J.W. Rudnicki, Coupled Deformation-Fluid Diffusion Effects on Pore Pressure Due to Propagating Creep Events, submitted to PAGEOPH for special volume on Earthquake Hydrology and Chemistry, ed. by C.-Y. King, 1984.
4. Rudnicki, J.W., Effects of dilatant hardening on the development of concentrated shear deformation in fissured rock masses, submitted to J. Geophys. Res., 1984.

Heat Flow and Tectonic Studies

9960-01176

John H. Sass
 Branch of Tectonophysics
 U.S. Geological Survey
 2255 North Gemini Drive
 Flagstaff, AZ 86001
 (602) 527-7726
 FTS: 765-7226

Arthur H. Lachenbruch
 Branch of Tectonophysics
 U.S. Geological Survey
 345 Middlefield Road
 Menlo Park, CA 94025
 (415) 323-8111, ext. 2272
 FTS: 467-2272

Investigations:

1. Heat flow and tectonics, general: Recent generalizations concerning heat flow versus age and the relation between stable continental and stable oceanic geotherms were examined critically from a regional rather than a global viewpoint.
2. Heat flow and tectonics of the Western United States: Additional thermal data were obtained from the southern Sierra Nevada, Yucca Mountain, near Parkfield, near Mammoth Lakes, the Vekol Valley in Arizona, and at the USBR's Brantley Dam site near Carlsbad, New Mexico. Four heat-flow wells were drilled in the northeastern Mojave - Southern Death Valley region. A major interpretive effort concerning the thermal and tectonic regime of the Salton Trough continued.
3. Heat flow and tectonics of Alaska: Velocity, density, and porosity logs for about 2 dozen wells in the National Petroleum Reserve, Alaska, were digitized in an attempt to establish an empirical relationship among these parameters and the ~600 determinations of thermal conductivity obtained from these wells. Refinement of heat-flow estimates continued.
4. Thermal studies related to nuclear waste isolation: Topography, well locations, static water level and isotherms, were plotted on several profiles from the Yucca Mountain area (Figure 1) in an attempt to discern systematic trends related to the thermal-hydrologic regime of the candidate high-level waste repository and the region surrounding it.
5. Thermal conductivity measurement: A systematic evaluation of line-source techniques for measuring thermal conductivity was carried out.

Results:

1. Heat flow and tectonics, general: It is well established that there is a close relation between heat flow and age of the crust in most oceanic regions. There is also a suggestion of a general decline in mean continental heat flow with age when the global data set is viewed as a whole, even though there is large scatter, particularly within areas active during the Cenozoic. Many recent reviews have elevated the latter observation to the status of established fact and some reviews have attempted to establish that there is

equivalence between the thermal regimes of old continental and old oceanic regions. When the global heat-flow data set is studied critically on a region-by-region basis, it becomes clear that, because of the complex thermal history of continental lithosphere and the large and laterally variable radiogenic component of continental heat flow, no general relation between heat flow and age can be established and geotherms beneath stable continental blocks are generally different from those beneath old ocean basins.

2. Heat flow and tectonics of the Western United States: A combination of *in situ* and conventional heat-flow determinations, re-evaluation of some published data, and estimates from gradient wells and from two deep test wells resulted in a total of 322 heat-flow determinations for the unconsolidated sediments of the Imperial Valley. Temperature gradients from industry gradient wells were combined with the regional mean of 93 *in situ* determinations of thermal conductivity ($1.88 \text{ W m}^{-1} \text{ K}^{-1} = 0.34 \text{ SD}$) to obtain heat-flow estimates. The availability of a suite of drill cuttings from a 2.5 km test well at El Centro together with a suite of geophysical logs including velocity and porosity logs allowed an independent test of the empirical Goss-Combs relations between thermal conductivity and seismic velocity and density. The relations fit very well at the high-velocity high-conductivity ($>2.5 \text{ km s}^{-1}, >1.7 \text{ W m}^{-1} \text{ K}^{-1}$) end, but require modification for lower velocities and conductivities, where Goss and Combs had no data. To take account of an irregular geographical distribution of data, heat-flow data were averaged within $3' \times 3'$ ($\sim 5 \times 5 \text{ km}$) elements; the mean of 100 such elements was $166 \text{ mW m}^{-2} \pm 97$ (SD). If the ten elements with average heat flows $>280 \text{ mW m}^{-2}$ (associated in each instance with known near-surface hydrothermal convection systems) are excluded, the overall mean conductive heat flow for the Imperial Valley portion of the Salton Trough is $139 \text{ mW m}^{-2} \pm 46$ (SD) which is the heat flow that would be observed if the region were in a thermal steady state with the temperature at the base of the crust near the mantle solidus.

Measurements of gravity and crustal seismic velocity indicate that the upper crust of the Salton Trough is composed largely of recent sediments and the lower crust of gabbroic material from the mantle, and that they are in isostatic balance with the surface at sea level. These observations in turn suggest a simple mechanical model wherein an extending crust is intruded or underplated by gabbroic magma from the mantle while subsidence is accompanied by rapid sedimentation that keeps the surface at sea level and isostatic balance is maintained. Over the past 4 to 5 m.y., the Salton Trough can be viewed as having undergone distributed extension at a uniform average rate. If the basalt supply is proportional to the spreading rate as it is at ocean ridges, the crustal thickness will approach a stationary value at which intrusion and sedimentation will compensate for thinning and their relative rates will be determined by isostacy. For the ratio of sedimentation to intrusion required by isostatic balance, increasing the extension rate has little effect on heat flow because it increases effects of the heating by intrusion and cooling by sedimentation in a compensating manner. Thus for a wide range of extension rates, the heat flow is close to the static value (with crust base at the solidus) and this explains why that is the measured value in spite of evidence for rapid extension.

Extension rate can be estimated by applying a second boundary condition at the base of the crust, namely that the conductive heat flow there be negligible. Physically this is expected if the uppermost mantle is a zone of melt separation where the gradient is buffered by latent heat. On the basis of this criterion, we expect average extension rates in the Salton Trough of a few tens of percent per m.y. ($\sim 10^{-14} \text{ sec}^{-1}$). With the extensional strain rates suggested by heat balance, and total pull-apart velocities approaching the Pacific-America relative plate velocity, the length of the actively extending region of the basin would be ~ 150 km which is a reasonable result. Extension of this region during the opening of the Gulf of California with sedimentary and magmatic additions as described by our idealized models can account for formation of the deep sedimentary basin observed, and for the major findings from gravity, seismic refraction, heat flow, and plate tectonics in the Salton Trough region.

3. Heat flow and tectonics of Alaska: Estimates of formation conductivity for rocks in the National Petroleum Reserve Alaska are being refined, resulting in changes of the corresponding heat-flow estimates obtained from near-equilibrium bottom-hole temperatures from some two dozen wells. These still preliminary results indicate a systematic increase in heat flow from about 50 mW m^{-2} on the North Slope of the Brooks Range to $>70 \text{ mW m}^{-2}$ along the Arctic Coastal Plain. Climatological and permafrost studies are continuing.

An attempt was made to establish a Goss-Combs type empirical correlation among thermal conductivity, porosity, density and compressional wave velocity. Although good correlations were established for a few individual wells, the coefficients varied considerably among wells and the overall correlation was poor, and the attempt to interpolate among wells with spotty thermal conductivity data using other geophysical logs was abandoned.

4. Thermal studies related to Nuclear Waste Isolation: Heat-flow measurements in tuffs near Yucca Mountain, Nevada (Figure 1) reveal a thermal regime dominated by non-conductive processes in the upper kilometer and conductive, but laterally variable heat flow in the volcanic rocks below depths of a kilometer. We have attributed the latter to water movement in the underlying Paleozoic carbonate rocks. In recent measurements in a hole (Ue25-P-1) that penetrated such rocks, active water circulation was confirmed by the anomalous thermal conditions observed.

5. Thermal conductivity measurement: For the conventional needle probe, the standard mode (line source in an infinite medium) is achieved simply by inserting the probe into unconsolidated material or into a hole drilled in harder material. A halfspace mode is achieved by embedding the needle probe in an epoxy material of low thermal conductivity ($<0.2 \text{ Wm}^{-1} \text{ K}^{-1}$) and grinding the material away until the needle is flush with a flat surface. The sample to be measured is placed on the halfspace surface, and the conductivity is measured in the usual way. Either configuration is capable of yielding values of thermal conductivity of consolidated rocks comparable in accuracy to values obtained with the steady-state, divided-bar technique most commonly used for these rocks. The line-source techniques are of particular advantage for materials that prove difficult to machine into the cylindrical disk specimens required for the steady-state apparatus. The halfspace probe

is of additional value for rocks that are too friable to machine, but too hard to allow the drilling of the long, small diameter (38×1 mm) holes required for the standard application of the needle probe.

Reports:

Bills, D. J., and Sass, J. H., 1984, Hydrologic and near-surface thermal regimes of the San Francisco volcanic field: U.S. Geological Survey Professional Paper, in press.

Chapman, D. S., Howell, J., and Sass, J. H., 1984, A note on drillhole depths required for reliable heat flow determinations: Tectonophysics, v. 103, p. 11-18.

Lachenbruch, A. H., Sass, J. H., Galanis, S. P., Jr., and Marshall, B. V., 1983, Heat flow, crustal extension, and sedimentation in the Salton Trough: EOS, v. 64, p. 836.

Lachenbruch, A. H., Sass, J. H., Lawver, L. A., Brewer, M. C., and Moses, T. H., Jr., 1984, Depth and temperature of permafrost on the Alaskan Arctic Slope: U.S. Geological Survey Professional Paper, in press.

Morgan, P., and Sass, J. H., 1984, Thermal regime of the continental lithosphere: Journal of Geodynamics, in press.

Pollack, H. N., and Sass, J. H., 1984, Thermal regime of the lithosphere, in Haenel, R., Rybach, L., and Stegema, L., eds., Handbook of Terrestrial Heat-Flow Density Determination (Guidelines and recommendations of the International Heat Flow Commission), in press.

Sass, J. H., Stone, C., and Munroe, R. J., 1984, Thermal conductivity determinations on solid rock--A comparison between a steady-state divided-bar apparatus and a commercial transient line-source device: Journal of Volcanology and Geothermal Research, v. 20, p. 145-153.

Sass, J. H., Kennelly, J. P., Jr., Smith, E. P., and Wendt, W. E., 1984, Laboratory line-source methods for the measurement of thermal conductivity of rocks near room temperature: U.S. Geological Survey Open-File Report 84-91, 21 p.

Sass, J. H., Lawver, L. A., and Munroe, R. J., A heat-flow reconnaissance of southeastern Alaska: Approved - October 21, 1983.

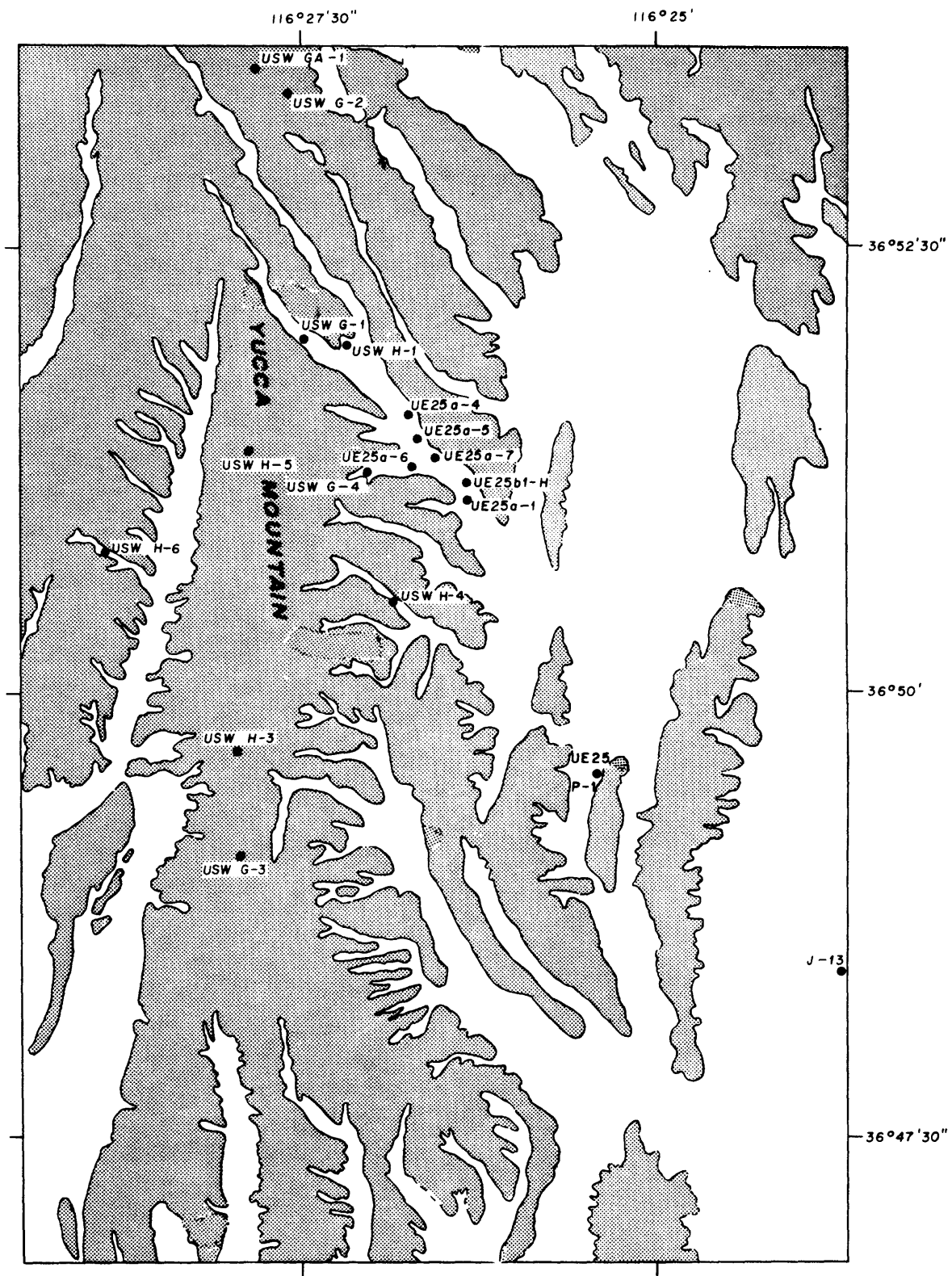


Figure 1. Sketch map showing the relative positions of test wells at Yucca Mountain.

Mechanics of Geologic Structures
Associated with Faulting

9960-02112

Paul Segall and David D. Pollard
Branch of Tectonophysics
U.S. Geological Survey
345 Middlefield Road, MS/977
Menlo Park, California 94025

Investigations

1. Analysis of the effects of fluid injection and extraction on stresses and pore pressures acting in the focal region of the 1983 Coalinga earthquake.
2. Field and theoretical analysis of the mechanics of igneous dike propagation.

Results

1. The proximity of the May 2, 1983 Coalinga earthquake to active oil fields on Anticline Ridge led to speculation that the earthquake might have been triggered by oil field operations. Elsewhere, earthquakes have been associated with pore-pressure increases resulting from fluid injection and also with subsidence resulting from fluid extraction. Simple calculations show that shales, which underlie the oil producing strata, hydraulically isolate the oil field from the earthquake focal region. The large volumes of fluid extracted from the oil fields caused a 50 percent decline in reservoir pressures from 1938 to 1983. These observations appear to rule out substantial increases in pore pressure at focal depths due to fluid injection. A theoretical method, based on Biot's constitutive theory for fluid-infiltrated elastic media, is used to evaluate the change in stresses acting in the focal region resulting from fluid extraction in the overlying oil fields. As an independent check on the method, the subsidence of the earth's surface in response to fluid withdrawal is also calculated and compared with measured elevation changes of Anticline Ridge. The producing horizons are taken to be horizontal permeable layers, bounded above and below by impermeable horizons. Strains within the producing layers are related to extraction-induced changes in pore-fluid mass. Contraction of the producing layers causes the free surface to subside and strains the elastic surroundings. The calculated subsidence rate of Anticline Ridge between 1933 and 1972 is 3 mm/yr, in good agreement with the

measured subsidence rate of 3.3 ± 0.7 mm/yr. Calculated pore pressure changes in the deepest producing zone also compare well with observed changes in reservoir pressure. The sign of the shear stress changes induced by extraction favor reverse slip on the fault. Stress magnitudes range from 0.02 MPa (0.2 bar) at a depth of 11 km, to 0.05 MPa (0.5 bar) at 4 km. The induced normal stresses are compressive across the fault, inhibiting slip. The net effect of fluid extraction is to weakly inhibit slip near the hypocenter and to weakly favor slip at shallower depths.

2. Dike emplacement and propagation involves a number of complex processes. In so far as dikes act like pressurized cracks, dilation induces tensile stresses in the host rocks near the dike tip. These tensile stresses could promote the formation of vertical joints near the dike tip. The joints weaken the host rock and could provide a pathway for flow of the magma. They will also affect the cooling history of the intrusion and local hydrothermal circulation. The strength of the stress concentration near the dike tip is proportional to the square root of the quantity dike half-height divided by radial distance from the tip $(a/r)^{1/2}$. We use the criterion that tensile stress must exceed tensile strength to estimate a distance from the tip over which joints might form: this distance ranges from 0.0001 a to 0.02 a . For a dike from 1 to 10 km high this analysis suggests joints may form at distances as great as 10 to 100 m from the tip. The concentration of tensile stress is not centered on the tip, but forms two lobes that spread outward to either side of the dike plane. This distribution provides an explanation for the formation of joints on either side of the plane of a dike. As dike propagation continues, joints formed become adjacent to the dike contact.

As a propagating dike nears the earth's surface, the tensile stress concentration above its tip spreads outward and upward, intersecting the surface at two points to form secondary stress maxima. Patterns of ground cracks and normal faults can be related to this stress distribution above dikes. In general, the secondary maxima will produce extensional structures in two clusters that align with the strike of the dike and straddle the ground through which a fissure eruption may occur. This middle ground is subject to smaller tensile stresses and may be dropped down along the flanking normal faults to form a graben. Preliminary mapping of cracks in the Inyo Domes area just north of Long Valley Caldera indicates the presence of a buried dike whose alignment parallels the trend of the domes. A "rule of thumb" for estimating the depth to a dike top has been derived which states that depth equals one-third to one-

half of the spacing between sets of parallel cracks. For the Inyo area depth estimates vary from several tens of meters to several hundreds of meters depending upon the precise location and our interpretation of the crack sets. Refinements of this method could allow one to make more precise estimates and thereby contribute to our understanding of recent igneous events.

Reports

Segall, P., P. Reasenberg, and R. F. Yerkes, Crustal stress changes and subsidence resulting from subsurface fluid withdrawal in the epicentral region of the 1983 Coalinga earthquake, *Trans. Am. Geophys. Union (EOS)*, vol. 64, p. 747.

Segall, P. and D. D. Pollard, 1983, Joint formation in granitic rock of the Sierra Nevada, *Geol. Soc. Am. Bull.*, v. 94, p. 563-575.

Segall, P., 1984, Formation and growth of extensional fracture sets, *Geol. Soc. Am. Bull.*, v. 95, p. 454-462.

Pollard, D. D., and A. Aydin, 1984, Propagation and linkage of oceanic ridge segments, *J.G.R.* in press.

Pollard, D. D., P. T. Delaney, and J. H. Fink, 1984, Igneous dikes at Long Valley, California: Emplacement mechanisms and associated geologic structures. *Napa Red Book Conference Proceedings, U.S.G.S. Open-File Report*, in press.

EXPERIMENTS OF ROCK FRICTION CONSTITUTIVE LAWS APPLIED TO EARTHQUAKE INSTABILITY ANALYSIS

USGS Contract 14-08-0001-G-821

Terry E. Tullis
John D. Weeks
Department of Geological Sciences
Brown University
Providence, Rhode Island 02912
(401) 863-3829

Investigations

1. We have investigated experimentally the dependence of friction of granite on velocity at a variety of normal stresses to 84 MPa. We have used numerical methods developed by Gu et. al (1984) to model our observations and estimate parameters of a state variable constitutive law for rock friction, which was developed by Ruina (1983) based on work by Dieterich (1979).
2. Using these constitutive parameters, we have investigated the question of what conditions will cause unstable sliding, using non-linear stability analysis by Gu et. al (1984).
3. We have used the same techniques to investigate sliding friction of calcite marble at 75 MPa normal stress.
4. We have continued our optical, SEM, and TEM examination of fault gouge generated in our experiments, in an effort to determine the physical processes responsible for the observed frictional characteristics.

Results

1. We find that the constitutive behavior of Westerly granite at normal stresses to 84 MPa is similar to that found by previous workers at normal stresses from 2 to 10 MPa. The steady state frictional resistance is proportional to the negative logarithm of the sliding velocity. Abrupt changes in sliding velocity result in initial changes in the frictional resistance which have the same sign as the change in velocity, followed by a decay to a new steady state value over a characteristic distance of sliding. Because of machine compliance, we cannot observe the constitutive parameters directly, but estimate them from trial and error modelling using a numerical solution of the interaction between the machine compliance and the friction law. An example of such modelling is shown in Figure 1, in which data for a jump in load point velocity from 0.05 to 0.1 microns per second (rough line) is compared with two simulations. Figure 1a shows the results of a friction law having one characteristic decay distance (one state variable) while Figure 1c shows the effect of including a second state variable having a very long decay distance. The second state variable is necessary to match the long-term downward trend shown by the data. We include both fits as the stability analysis is currently only available for the case of one state variable.

It is possible to measure directly the long-term steady state dependence of friction on sliding velocity even with a compliant machine. We have done this by running through a series of steps in load point velocity, allowing 200 to 300 microns of sliding displacement between steps to allow the system to come to steady state. The results of several such measurements are displayed in Figure 2. Some problems with this technique have become apparent, however. In Figure 2a, in which the results of increasing velocity steps are shown, it is clear that the data at 75 MPa and 6 mm displacement are quite different from the others. In Figure 2b in which the decreasing steps are shown for selected runs from Figure 2a, it is apparent that some of the runs are not

reversible. We find that long term trends such as that shown in Figure 1 are quite common and that if this trend is removed by a procedure similar to that shown in Figure 1b, the data become more consistent, as shown by the traces in Figure 2c. In addition, the value for the steady state dependence determined this way is consistent with the results of numerical modelling, and as in Figure 1c, this trend can be interpreted as a second decay distance in the friction law.

2. Using the values of the friction law parameters determined from numerical modelling, we are able to compare our experimental observations of stick slip sliding with the predictions of a non-linear stability analysis by Gu et. al (1984). Some qualitative observations that are predicted by this theory are: 1) Conditions that permit stable sliding following small load point velocity increases, may cause instability following large increases. We find this to be true even for small and large velocity steps applied consecutively during a single experiment. 2) We find that even under conditions leading to stick slip following increases in the driving velocity, decreases are stable. We also have quantitative agreement between the predictions and observations of the size of velocity jump necessary to cause instability. In Figure 3 on the left are plotted the results of two velocity increases in terms of coefficient of friction versus slip velocity. In addition, there is a curve marking the theoretical boundary between stable and unstable sliding, calculated using the friction parameters determined from the modelling shown in Figure 1a. On this phase plane plot, an increase in loading point velocity starts at the upper left and spirals toward a new steady state point, marked by the "x". In the top half of the figure, a velocity jump ratio of 2 is shown, which started in the stable portion of the plot and led to stable sliding. On the bottom, a velocity jump ratio of 3 in the same experiment started outside the boundary and resulted in a stick slip event. In addition, it is apparent that the 3 to 1 jump is just barely outside the boundary. In fact, a 3 to 1 jump was not always unstable, whereas a 2 to 1 jump was always stable. The fact that the data do not fall on top of the new steady state point reflects the fact that the stability analysis includes only one state variable and does not take into account the long term trends. The difference between the ordinate of the "x" and that of the center of the spiral is the amount by which the coefficient of friction changed due to evolution of the second state variable during sliding following the velocity change. Because the second state variable has a long decay distance (Figure 1b) it is apparently possible to neglect its presence and still obtain a good description of the instability behavior. These results are very encouraging for the eventual understanding of earthquakes through the use of constitutive laws and stability analysis of the type we have used.

3. In a preliminary investigation of friction of calcite marble, we have found that this rock displays steady state velocity strengthening, that is, for higher velocity the steady state response gives a higher frictional resistance, in contrast with granite and quartzite which show velocity weakening under the same conditions. In most other respects, we find that the friction laws developed for granite and quartzite can be used to describe the friction of calcite, with some interesting variations. Figure 4 shows a comparison of granite (4a) and calcite(4b) responses to a 10 to 1 load point velocity increase, illustrating the contrast in the steady state response. Figure 5 shows two cases of velocity decreases for calcite, along with simulations using the same form of constitutive law as used for granite. This modelling reveals that it necessary to use two state variables to describe these results and, in contrast to previous assumptions based on the behavior of granite and quartzite, the magnitude of the second decay is negative, causing a decay toward lower friction with increased displacement following a decrease in velocity. For granite and quartzite in which the decay magnitudes seem always to be positive, the steady state response must be velocity weakening to permit unstable sliding, whereas in the case of calcite it is possible to have unstable or oscillatory sliding even in the presence of velocity strengthening if the magnitude of the change in friction associated with the shorter decay is large enough. Another way in which calcite differs from granite is that the friction parameters vary strongly with velocity. A transition from unstable to stable sliding with increasing velocity has been observed previously (Logan, 1978) and our observed variation of the constitutive parameters for calcite can explain this behavior. There is some indication that the state variables evolve as a function of time for calcite rather than displacement as is the case for granite and quartzite. These results suggest that there

may be fundamental differences in the frictional response of different rock types to changes in velocity that could cause variations in regional styles of seismicity in the earth.

4. Our sample surfaces initially have no gouge on them, but develop a layer 100 to 250 microns thick. We have used optical, SEM and TEM microscopy to try to infer the micromechanical processes occurring in the gouge and the physical basis for the constitutive law parameters. Optical and scanning electron microscopy indicate that the layer is composed of discrete flakes bounded by slip surfaces with predominantly normal sense of offset and by layer-parallel slip surfaces. That these microscopic faults are slip surfaces is confirmed by their extreme smoothness and the presence of lineations resembling slickensides. It has been suggested that the decay distance might be related to the grain size of the fault gouge. However, TEM photos of fault gouge produced during sliding on granite revealed grain sizes from about 1 micron down to less than 100 Angstroms. As the observed decay distance is about 8 microns, a direct connection between grain size and decay distance seems unlikely. The extremely fine grain size is most likely responsible for changes that we have observed when gouge is exposed to air even for a few days. After some exposure to the air, grape-like masses of spheroidal particles about one half micron in diameter form which were not present during deformation. Their formation suggests that the gouge is very sensitive to small amounts of water present in the air. Measurements of the refractive index indicate that over the course of 6 months the gouge may increase its water content by 10 percent.

Reports

Bechtel, T. D., Weeks, J. D. and Tullis, T. E., 1983, Observations of experimentally produced fault gouge, *Eos Trans. AGU*, 64, p. 834.

Weeks, J. D., Tullis, T. E. and Bechtel, T. D., 1983, Nonlinear instability effects in experiments on rock friction, *Eos Trans. AGU*, 64, p. 850.

Tullis, T. E., Weeks, J. D. and Bechtel, T. D., 1983, Inverse dependence of frictional resistance on sliding velocity at elevated normal stress, *Eos Trans. AGU*, 64, p. 850.

Tullis, T. E., Weeks, J. D., Constitutive behavior and stability of frictional sliding of granite, to be submitted to *Jour. Geophys. Res.*

Weeks, J. D. and Tullis, T. E., Frictional sliding of calcite: an interesting variation in constitutive behavior, submitted to *J. Geophys. Res.*

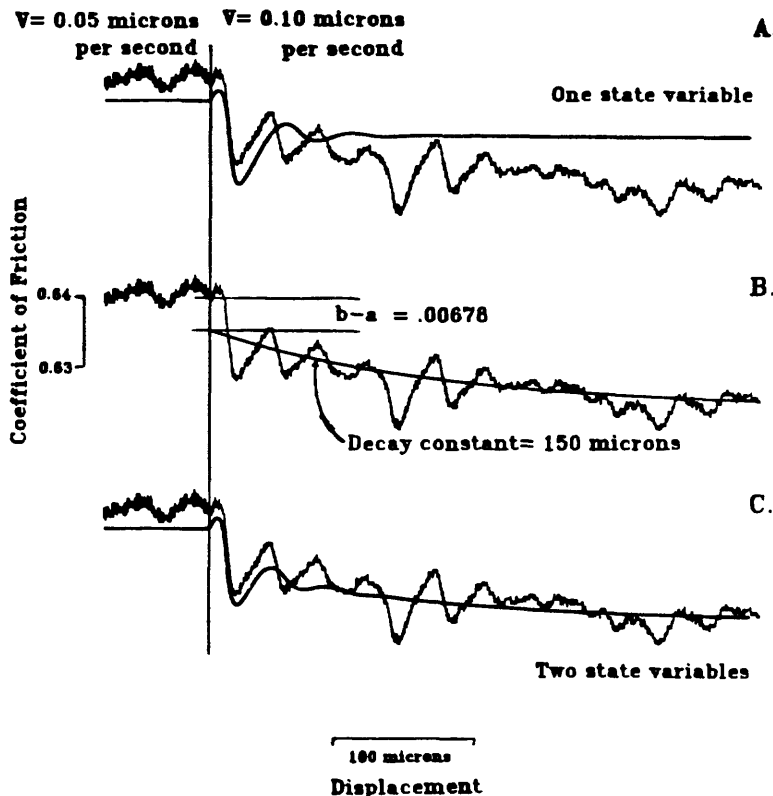
References Cited

Dieterich, J. H., Modelling of rock friction, 1, Experimental results and constitutive equations, *J. Geophys. Res.*, 84, 2161-2168, 1979a.

Gu, J. C., Rice, J. R., Ruina, A. L., and Tse, S., Stability of frictional slip for a single degree of freedom elastic system with non-linear rate and state dependent friction, manuscript in preparation, 1984.

Logan, J. M., Creep, stable sliding, and premonitory slip, *Pure Appl. Geophys.*, 116, 773-789, 1978.

Ruina, A. L., Slip instability and state variable friction laws, *J. Geophys. Res.*, 88, 10359-10370, 1983.



A. Figure 1. Examples of numerical simulations of friction data on Westerly granite at 75 MPa normal stress. Data is rough line, the simulations are the smooth lines. The simulations in parts A and C have been shifted downward for clarity. The data are for an increase in load point velocity from 0.05 to 0.1 microns per second at the vertical line. A. Simulation using one state variable (decay distance). The parameters used were $a=0.004$, $b=0.01078$, $L=11.5$ microns. B. Data trace with superimposed exponential to show how the long term decay was removed to determine an appropriate short term value for $b-a$ (the steady state velocity response) to be used in A. C. Simulation using two state variables. The parameters for this simulation are $a=0.004$, $b_1=0.0075$, $b_2=0.01454$, $L_1=8$ microns, $L_2=150$ microns. Note that whereas the value of L_2 matches the exponential used to correct the one state variable simulation, the value of b_1-a , which could be interpreted as the short term velocity response, does not match the value of $b-a$ in A. This is caused by interaction between the long term state variable and the high velocity caused by the short term variable. This is implicitly taken into account for the one state variable simulation by the different parameter values.

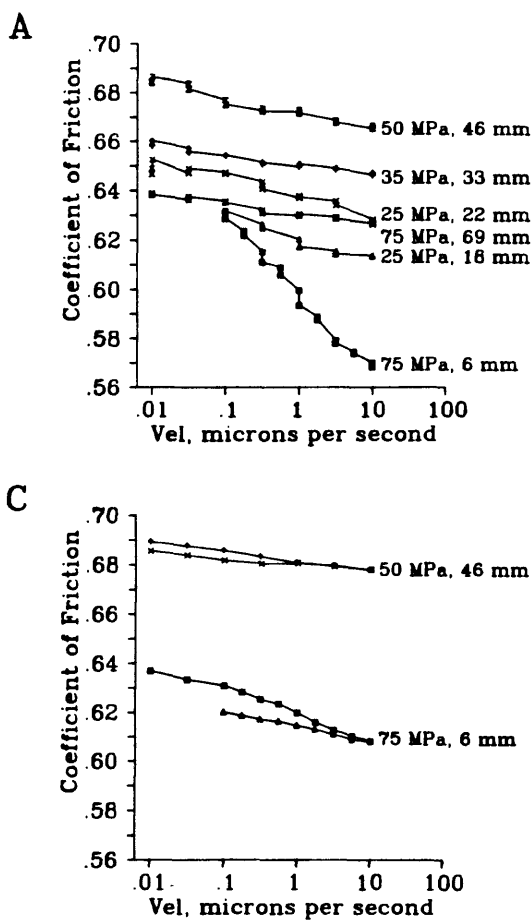


Figure 2. Results of several velocity stepping sequences at various values of normal stress. All this data was taken on one sample in one experiment, starting at 75 MPa normal stress at 6 mm displacement, then going to 25 MPa at 18 mm, and working back up to 75 MPa at 69 mm. The normal stresses shown indicate the nominal normal stress, uncorrected for the true sample area. A. Data for velocity increases. At all levels of normal stress the steady state response was velocity weakening, although the magnitude of the effect decreased markedly after the first series at 75 MPa. B. Same as in A, but with the decreasing velocity steps shown also. Note that at 75 MPa and low total displacement the velocity decreases do not retrace the increases. C. Two of the data sets shown in B have been corrected for long term trends by a process similar to the one shown in Figure 1b. Note that the 75 MPa data more nearly re-trace on the decreasing velocity part and the slopes for the two traces shown are more nearly equal.

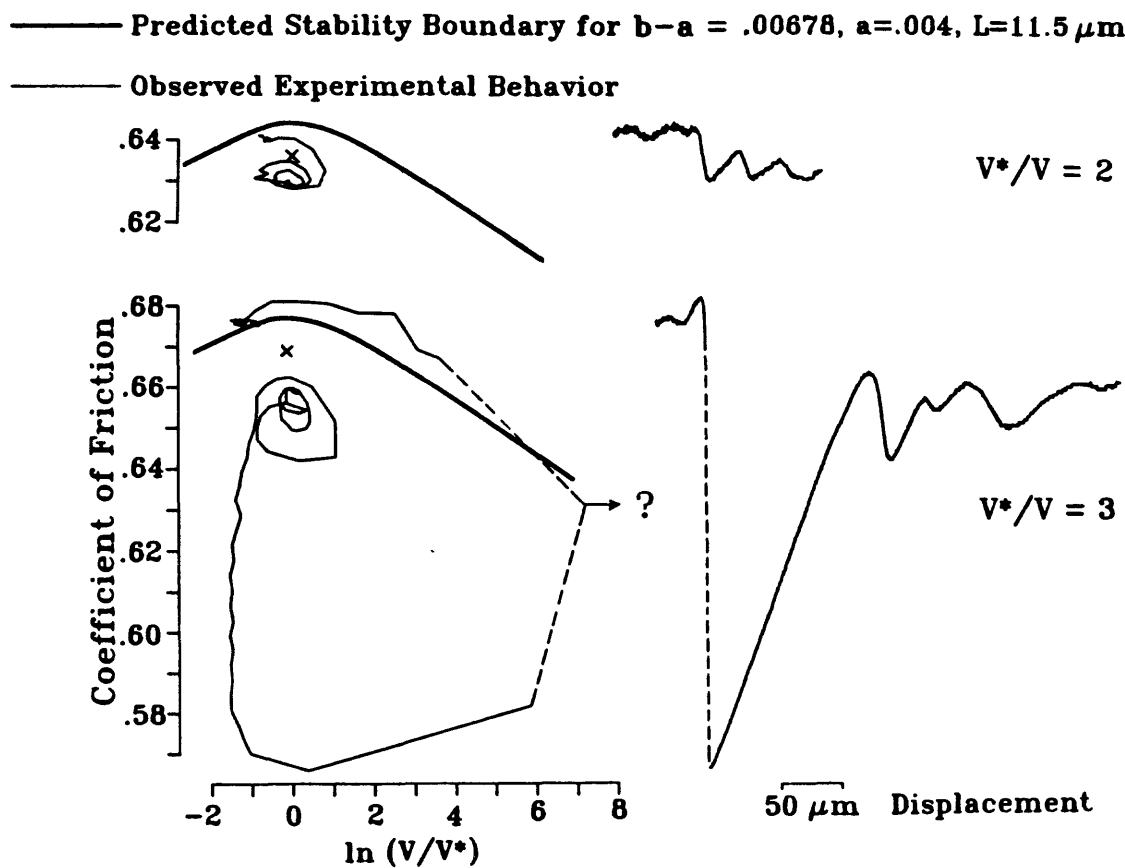


Figure 3. Comparison between predicted and observed stability behavior, on plots of friction versus slip velocity. On the left are plots of our data, together with stability boundaries calculated for the one state variable case in Figure 1a. On the right are the same data plotted versus displacement. On the top, for a velocity jump of 2 to 1, the theory predicts stable sliding while for a jump of 3 to 1 unstable behavior is predicted. The data point marked by the question mark could lie much farther to the right because our current sampling interval of one second cannot resolve high velocities. The crosses mark the steady state point for the friction parameters used to calculate the stability boundary. The fact that the data do not approach this point reflects the long term effects noted in Figure 1.

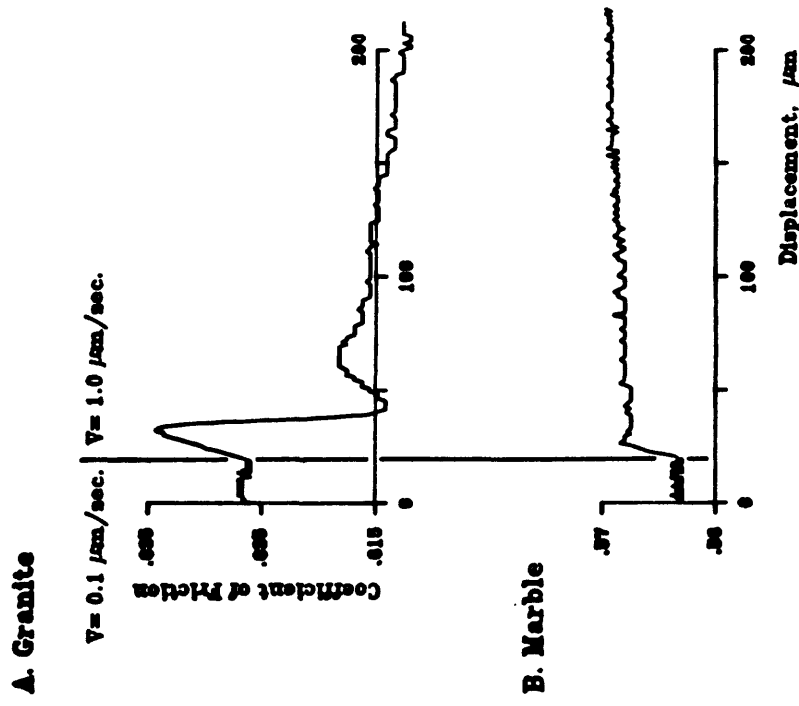


Figure 4. Comparison between granite and marble behavior for a velocity jump from 0.1 micron per second to 1 micron per second. **A.** Granite shows a transient increase in friction followed by a decay to a lower steady state frictional strength, response termed "velocity weakening". **B.** Marble shows the same increase in frictional stress, with a small peak, but followed by a decay to a higher frictional strength, or velocity strengthening.

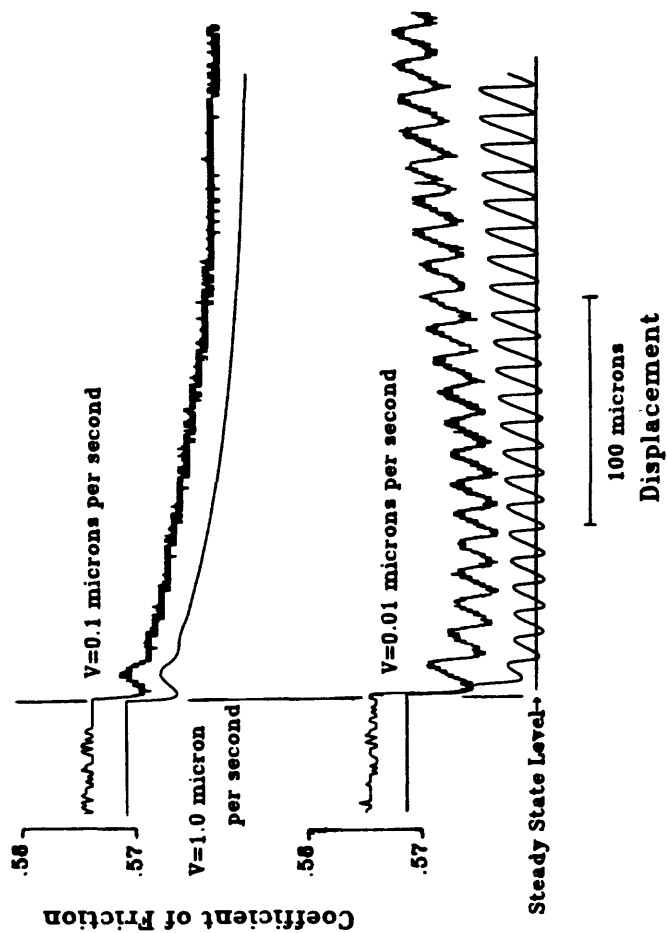


Figure 5. A comparison of experimental data for calcite marble at 0.1 and 0.01 microns per second with numerical simulations. The match at 0.1 microns per second is almost perfect; the parameters used are $a = 0.2$, $b_1 = 0.1988$, $b_2 = -0.0037$, $L_1 = 0.03$ microns and $L_2 = 100$ microns. The simulation at 0.01 microns per second is not exact, but captures two important aspects: it reproduces the oscillatory behavior and the fact that the centerline of the oscillations is gradually climbing. The parameters used to simulate this behavior are $a = 0.08$, $b_1 = 0.08045$, $b_2 = -0.00295$, $L_1 = 0.05$ microns and $L_2 = 5$ microns. Data and simulations are shifted vertically for clarity. The labeled steady state line is positioned relative to the simulation. Whereas the machine compliance and the number of parameters make the simulations non-unique, it is certain that the differences between b_1 and L_2 for the two velocities are necessary, violating one of the assumptions behind the constitutive descriptions.

New Model of Earthquake Faulting

Contract No. 14-08-0001-21803

Joseph B. Walsh
Dept. of Earth, Atmospheric and Planetary Sciences
Victor C. Li
Dept. of Civil Engineering

Massachusetts Institute of Technology
Cambridge, Massachusetts 02139
617-253-5731

Investigations

We have been studying a model for faulting in which an earthquake is triggered by aseismic slip on a 'detachment zone' at the interface between the lithosphere and the underlying viscous strata. The detachment zone is a consequence of spatially and temporally non-uniform viscous forces as the lithosphere is dragged over the aesthenosphere. Slip on the detachment zone loads a fault in the elastic lithosphere, and, if frictional resistance on the fault is sufficiently low, an earthquake ensues.

Our studies so far have been directed toward calculating surface displacements, strains, and gravity changes associated with slip on the detachment zone. A graduate student, Steven C. Ho, developed a computer program which allowed him to find these parameters quickly for arbitrary dislocation distributions over the detachment zone, and he applied his results to uplift and strain data for the Palmdale (Cal.) region during an episode (1959-1977) of aseismic tectonic deformation. Preliminary results of the analysis were presented at the Fall Meeting of the AGU and at an informal meeting with R. O. Castle, J. C. Savage, and William Stuart at the U.S.G.S. Office of Earthquake Studies in Menlo Park, Cal.

Results

Ho found acceptable correlation between observed and calculated values of uplift and strain for his model. One difficulty with this tentative model is that the average slip rate over the detachment zone is about an order of magnitude larger than the estimated relative tectonic movement for this region. We examined two modifications of the model in an exploratory way: in one, the detachment zone is tilted 5° rather than horizontal, and in the other, slip on a vertical

is allowed at depth, simulating aseismic creep on the San Andreas, the upper portion remaining fixed. Both modifications reduce the average slip required for agreement with observed values without changing the overall pattern.

Reports

Ho, S.C., V.C. Li, and J.B. Walsh, Surface deformation associated with aseismic slippages on detachment surfaces, EOS, Trans. Am. Geophys. Union, 64(45), 1983.

Ho, S.C., V.C. Li, and J.B. Walsh, Surface deformation associated with aseismic slippages on detachment surfaces, Research rept. R84-03, order no. 763, M.I.T. Department of Civil Eng., Feb. 1984.

Ho, S.C., Surface deformation associated with aseismic slippages on detachment surfaces, M. Sc. Thesis, M.I.T. Dept. Civil Eng., Cambridge, Mass., Feb. 1984.

Aftershock Investigations and Geotechnical Studies

9910-02089

Richard E. Warrick and Eugene D. Sembera
Branch of Engineering Seismology and Geology
U.S. Geological Survey
345 Middlefield Road, MS 977
Menlo Park, CA 94025
(415) 323-8111, Ext. 2757

Investigations:

1. The development of techniques for the improvement of field data acquisition, specifically in the application of triggered digital recording systems to aftershock studies.
2. Improvement in the methods used in generating, recording, and interpreting shear waves in downhole surveys.

Results:

1a. Earthquake aftershock studies:

The October 1983 Newcomb, New York earthquake aftershocks were recorded with GEOS instruments by E. Cranswick, R. McClearn, G. Mendoza, and G. Sembera.

The Mt. Borah, Idaho earthquake aftershocks were recorded with GEOS instruments by J. Boatwright, G. Sembera, and C. Criley.

A series of experiments of high-frequency energy propagation were conducted in January and February of 1984 at the Raymond, CA quarry by E. Cranswick, G. Sembera and C. Dietal.

- 1b. The GEOS instrument development proceeds with the involvement of E. Jensen, R. McClearn, C. Dietal, C. Criley, and G. Sembera. The process includes testing circuit boards, assembling and testing complete recorders and conducting post-mortems to determine the necessary corrections.
- 2a. The deep-hole logging equipment was reassembled and tested. Then the McGee Creek hole in the vicinity of Mammoth Lakes, CA was surveyed for P- and S-wave velocity by J. Gibbs, T. Fumal, E. Roth and B. Silverstein.
- 2b. A survey of alignment methods for downhole instrumentation packages revealed that the costs and complexity of magnetic or inertial techniques would, in many instances, override the incremental benefits such methods may have over the empirical, surface source to downhole sensor, orientation method.

Reports:

None

UPDATE ON THE OROVILLE VERTICAL SEISMIC PROFILING EXPERIMENT

CONTRACT NO. 14-08-0001-21238

P. E. Malin
 Marine Sciences Institute
 University of California
 Santa Barbara, CA. 93106
 ph. (805) 961-3520

Investigations

Between April and September 1984 eleven micro-earthquakes were recorded on a vertical array of downhole seismometers at Oroville, CA. (Malin and Waller, 1983, The Oroville VSP Experiment, USGS Open-File Report 83-918). The array was deployed in a 1500 foot deep well, drilled through the Cleveland Hill fault. Three-component seismometers in this "Vertical Seismic Profiling" array were positioned at ground level, immediately above the fault zone, and at the bottom of the well (depths= 0, 1000, and 1500 ft respectively).

The frequency content and particle motions produced by these events have been examined as a function of observation depth. Particle motions were rotated into radial and transverse components. The dissipation of high frequencies (>10 hz) across the fault and in the weathering zone was modeled as a first order, constant Q process. The particle motions were studied for polarization splitting effects due to local anisotropic material properties.

Results

An example of a 3-component VSP recording of an Oroville micro-earthquake is shown in Figure 1. Stations 4 and 6 correspond to the 3-component seismometers at 1000 and 1500 ft respectively. Note the change in waveform across the fault between stations 4 and 6. Figure 2 shows s wave spectral ratios between these stations and two vertical-component stations along the well. The s wave Q values calculated from least squares fits to these ratios are listed Table 1.

The particle motion study has revealed that two separate s wave arrivals are present for some of the micro-earthquakes. The two waves are characterized by different travel times and polarizations. Figure 3 illustrates these features, showing the two components of transverse displacement and the resulting particle motion diagram. The initial s wave particle motion was along the direction of component no.3. The subsequent motion was more along the direction of component no.2.

The results of the micro-earthquake/VSP study suggest that substantial attenuation of high-frequency earthquake waves occurs in the upper .5 km of the crust at Oroville. It is also possible that this region is anisotropic, producing s wave splitting, and thus accounting for the two s wave arrivals shown in Figure 3.

| TABLE 1 | |
|--------------|----------|
| Station Pair | s wave Q |
| 5/6 | 11 |
| 4/6 | 7 |
| 3/6 | 7 |
| surface/6 | 9 |

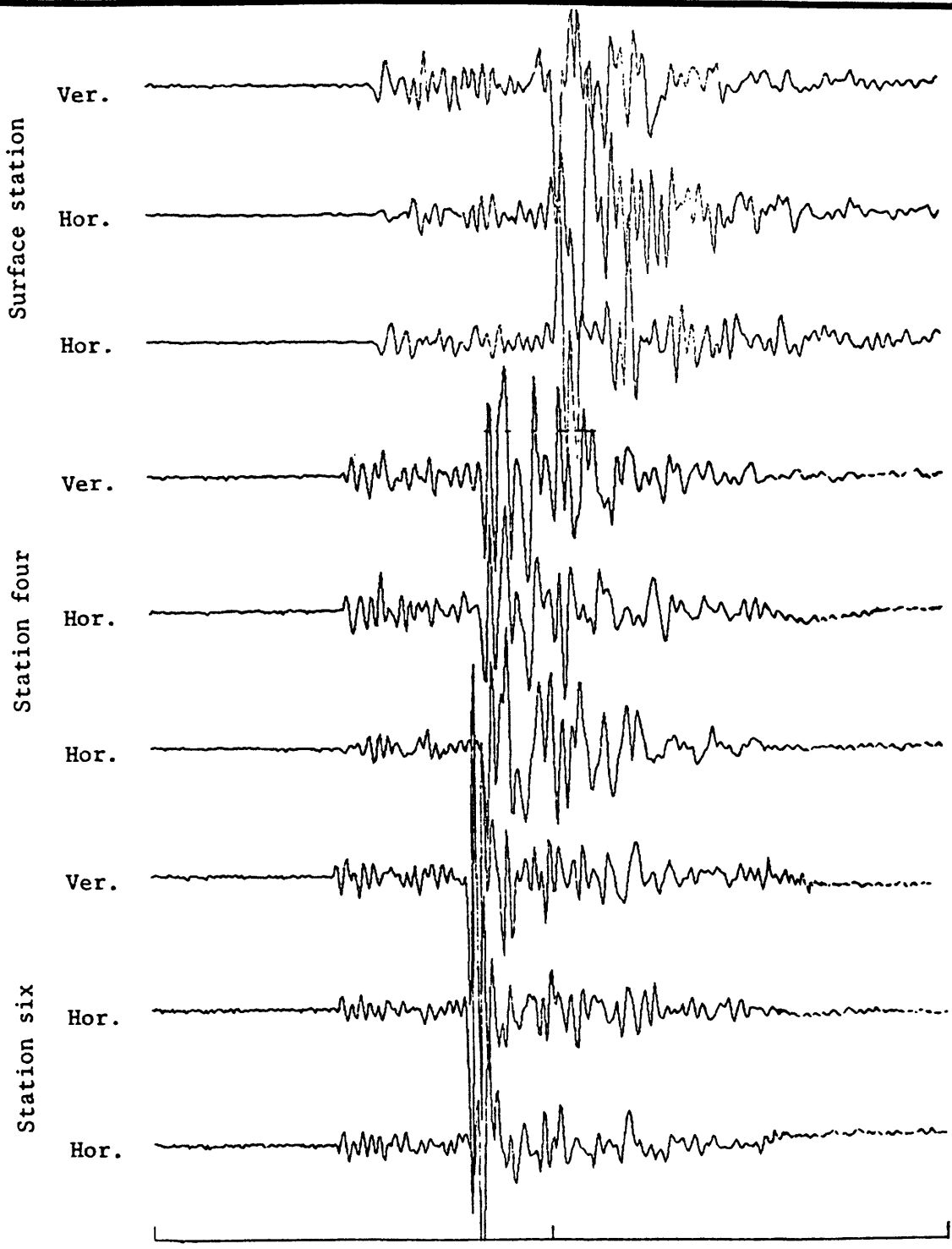


FIGURE 1. Three-component VSP seismograms of an Oroville micro-earthquake. Stations 4 and 6 are at 1000 and 1500 feet depth in the VSP well and straddle the Cleveland Hill fault zone. The time marks are 1 second apart.

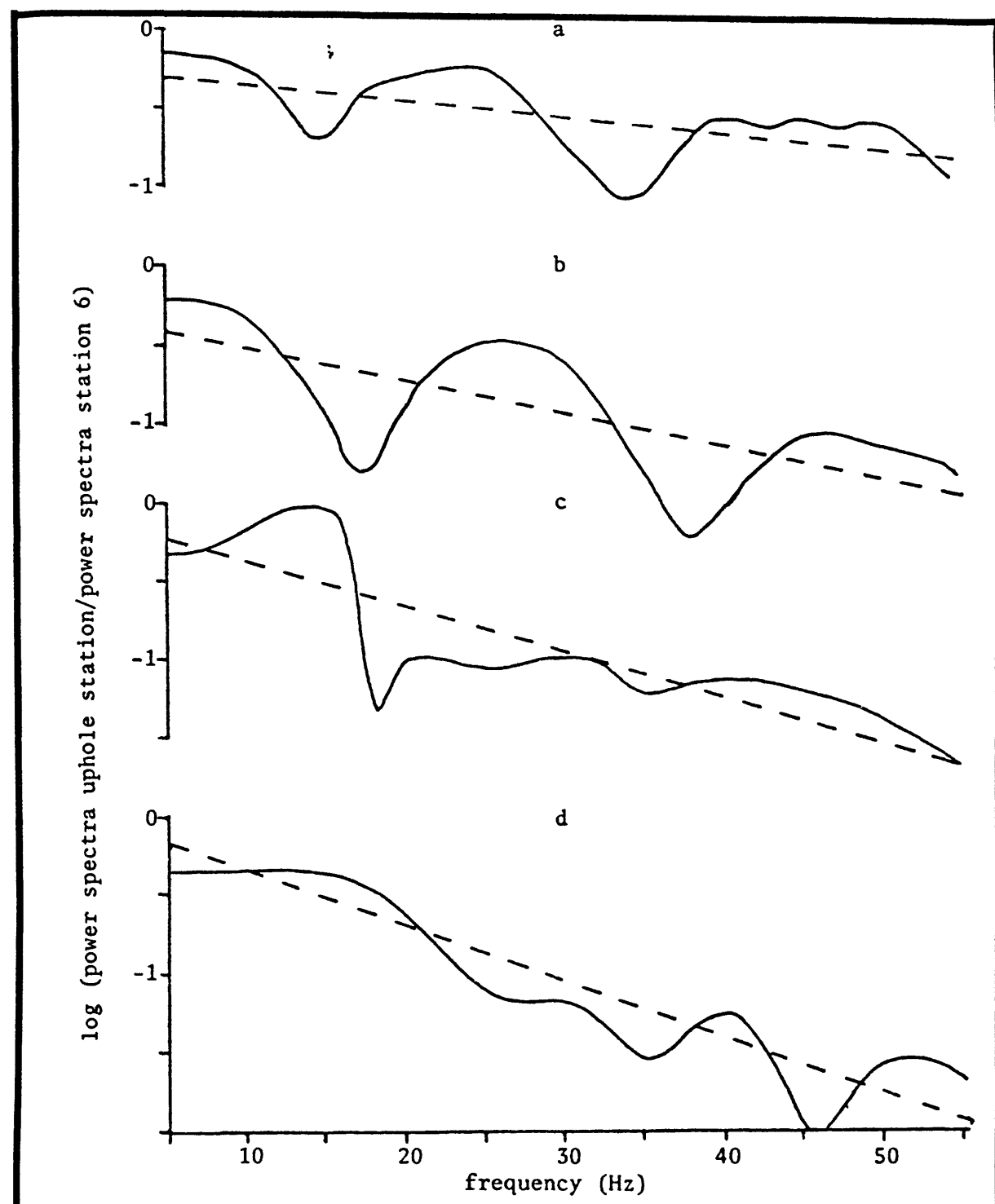


FIGURE 2. Spectral ratios of micro-earthquake s waves as a function of observation depth. The solid line is the ratio and the broken line is the least squares fit for use in determining the s wave Q value. The ratios shown are: a. st5/st6, b. st4/st6, c. st3/st6, d. surface/st6. Stations 5 and 3 contained vertical seismometers while 6, 4 and surface are 3-component stations.

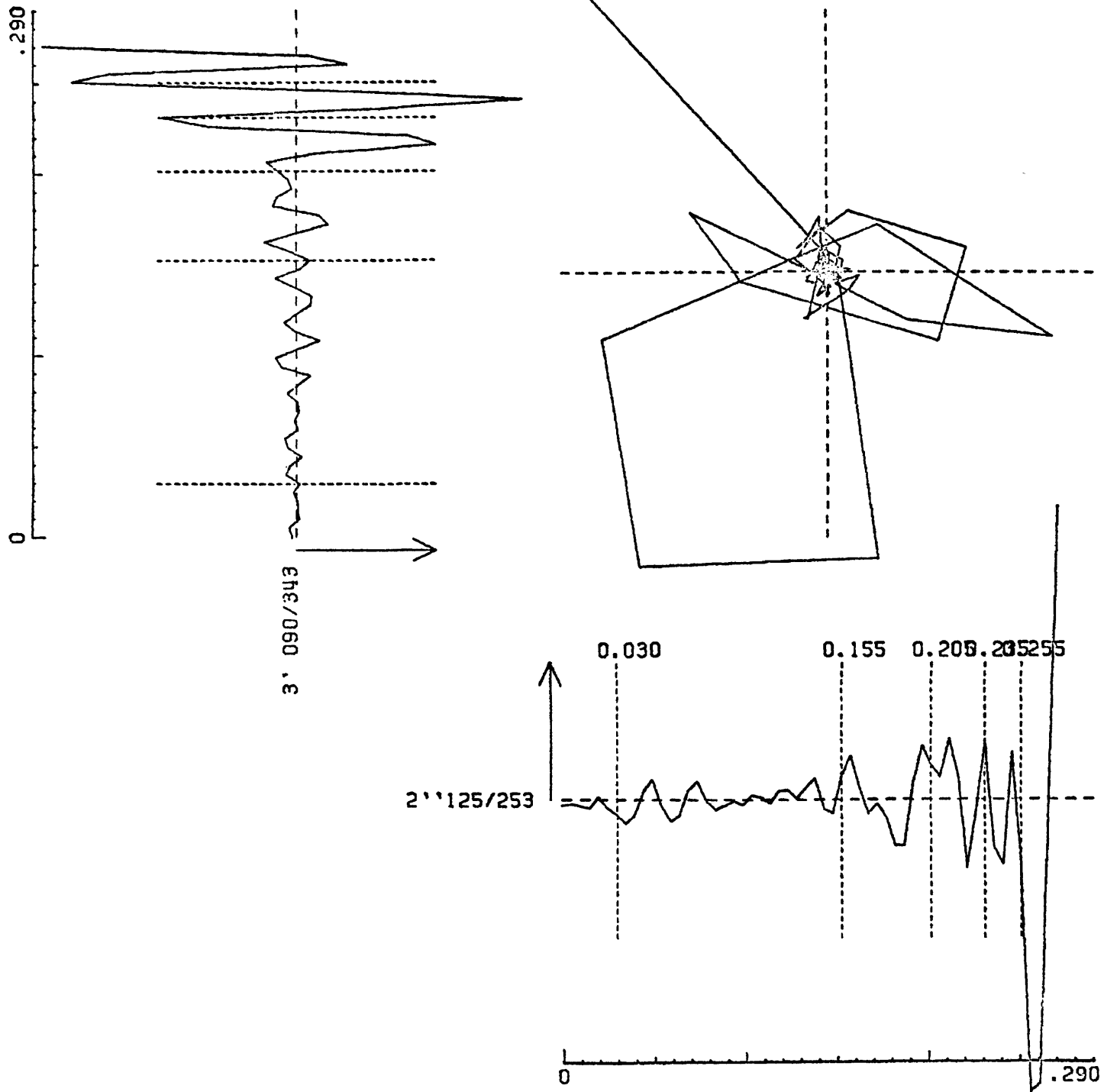


FIGURE 3. The transverse particle motion of an Oroville micro-earthquake as observed at station 6, 1500 ft underground. The two transverse displacements are plotted, along with time scales in seconds, below and to the left of the particle motion diagram. The high density of lines at the center of the latter diagram represents that portion of the p wave that was not successfully rotated into the radial direction. By comparing the timing lines, displacements, and particle motions, it can be seen that the initial s motion was in the no. 3 component direction. This arrival is followed by a second one that produces the elliptic motion seen on the particle motion diagram.

Earthquake Studies in The Geysers Area
9930-02106

David H. Oppenheimer
Branch of Seismology
U.S. Geological Survey
345 Middlefield Road - M/S 977
Menlo Park, California 94025

Investigations

1. Invert microearthquake traveltimes data collected at The Geysers geothermal field for 3-D velocity structure.
2. Relocate seismicity at The Geysers on weekly basis for new evidence of induced seismicity.
3. Analyze aftershock distribution of May 2, 1983 Coalinga earthquake.
4. Analyze teleseismic traveltimes data recorded by CALNET for 3-D structure of the mantle.
5. Investigate frequency-wavenumber spectra of near-field strong motion array data to detect position of rupture front.

Results

1. A combined set of microearthquake and refraction traveltimes data recorded on temporary and permanent seismic stations is used to model 3-D velocity variations in The Geysers-Clear Lake area. Preliminary analysis indicates low velocities along the Healdsburg-Rodgers Creek-Maacama fault system, and higher velocities between the Maacama and Bartlett Springs/Green Valley faults. A region of surficial low-velocity near Konocti Bay may be associated with either Clear Lake volcanics or Cache formation. No velocity anomaly is observed associated with The Geysers geothermal steam reservoir.
2. Microearthquake activity continues to be induced adjacent to steam production and fluid injection wells at The Geysers. Previous studies have shown that seismicity commences in previously aseismic regions within 1 year after nearby geothermal activity begins. As production activities continue to expand into new areas at The Geysers, we expect to observe a corresponding increase in seismicity.
3. Coalinga earthquake traveltimes obtained from the permanent seismic network are being augmented with data recorded by temporary 5-day analogue recorders during the May 2, 1983 aftershock sequence. An automated system has been developed to time the 5-day P arrivals and merge them with the permanent data. Station corrections have been calculated by a joint hypocenter-velocity inversion and correlate well with known geologic structure of Anticline Ridge.
4. Analysis has begun on 11,683 traveltimes from 60 teleseisms recorded by 296 stations of the central California seismic network. Obvious

data errors have been corrected, revealing large azimuthal traveltime variations at many stations. In particular, stations in the Sierra Nevada foothills show traveltime variations of as much as 1.7 s over azimuth ranges of 30 degrees. Stations near Parkfield also show azimuthal traveltime variations of 1.4 s, perhaps revealing structure associated with the plate boundary. In addition to the azimuthal traveltime variations, relative travelttime variations of 1.0 s over narrow azimuthal ranges are observed due to changes in ray slowness. Inversion programs are being modified to accomodate the large data set and to correct the data for the crustal travelttime based upon a model for crustal thickening derived from Pn data.

5. Large aftershocks of the Coalinga earthquake, and more recently the mainshock of the Morgan Hill earthquake, have been recorded in the near-field on small strong-ground-motion arrays. High resolution frequency-wavenumber spectra of the wavetrain at different time windows may resolve expansion of the rupture front. Current efforts are directed towards demonstrating the capability of the technique using synthetic data.

Reports

Oppenheimer, D. H., and J. P. Eaton, 1984, Moho orientation beneath central California from regional earthquake traveltimes, submitted to J. Geophys. Res., 28 pgs.

Oppenheimer, D. H., 1984, Crustal thickness in central California and its effect upon teleseismic traveltimes, Earthquake Notes, 1 pg. (in press).

Deep Hole Desalination of the Dolores River

9920-03464

William Spence
Branch of Global Seismology and Geomagnetism
U.S. Geological Survey
Denver Federal Center, MS 967
Denver, Colorado 80225
(303) 234-4041

Investigations

This project provides monitoring and interpretation of the seismicity in the region of the intersection of the Dolores River and Paradox Valley, southwest Colorado. This project is a part of the Paradox Valley Unit of the Colorado River Basin Salinity Control Project and is being performed for the U.S. Bureau of Reclamation with support from the Induced Seismicity program of the USGS. In this desalinization project it is proposed to pump approximately 30,000 barrels/day from brine-saturated rocks beneath the Dolores river through a borehole to the Madison-Leadville limestone formation of Mississippian age, some 15,000 feet below the surface. There is a possibility of seismicity being induced, especially in the long term, by this desalinization procedure. The project objectives are to establish a pre-pumping seismicity baseline and, during the pumping phase, to closely monitor the discharge zone for possible induced seismicity. If induced seismicity does occur it should be possible to relate it to formation characteristics and to the pumping pressure and discharge rates.

Results

A ten-station seismograph network has been installed, centered on the location of the proposed pumping station. This high-gain network has a diameter of about 60 kilometers. Seismic data are presently being brought to Golden, Colorado, via microwave and phone line transmission. These data are fed through an A/D converter and then through an event detection algorithm. Final installation of the network was complete in September, 1983 and detected seismic events, which include many blasts, are presently being studied.

Study of Reservoir Induced Seismicity and
Earthquake Prediction in South Carolina

Contract No. 14-08-0001-21229

Pradeep Talwani
Geology Department
University of South Carolina
Columbia, S.C. 29208
(803) 777-6449

Investigations

1. Continue to monitor seismic activity near Monticello Reservoir and Lake Jocassee.
2. Aftershock monitoring.
3. The seismicity near Richard Russell Dam appears to have increased following its impoundment. We propose to monitor it for a few weeks this summer.
4. A new dam is planned at Bad Creek about 16 km NW of Jocassee dam. We plan some preliminary studies.

Results

1. Induced seismicity at Monticello Reservoir, South Carolina.

A total of 190 events were located in the Monticello Reservoir area during 1983, two with magnitudes greater than 2.0 (Feb. 19, $M_L = 2.0$; June 11, $M_L = 2.2$) and 14 with magnitudes between 1.0 and 2.0. Most of the seismicity occurred between February and May with no significant peak in the level at any time. Spatially, the seismicity was concentrated near the center of the west side of the reservoir (Fig. 1). Depth analyses indicate most of the activity occurs in the 1.5 to 2.0 km increment and that a significant percentage is occurring at depths greater than 3.0 km.

2. Induced seismicity at Lake Jocassee, South Carolina.

Seismicity at Lake Jocassee has been monitored since 1975, first with portable instruments, and now through permanent stations. We have acquired the equipment and instrumentation to set up a solar powered permanent station near Union. All of the seismicity at Lake Jocassee for the last six months of 1983 was small ($M_L < 2.0$). The spatial extent has continued to be confined within the epicentral area defined in the first year of activity, with the exception of the events in the northwest area of the lake (Fig. 3) which are suspected blasts related to the construction of a new dam.

3. Aftershock monitoring

A magnitude 3.0 earthquake occurred in the Summerville area on November 6, 1983. Portable instruments set out for aftershock monitoring recorded two small events ($M_L < 1.0$).

Reports

Rawlins, J. and P. Talwani, Earthquake swarms near Newberry, S.C.: SE-NC Section Meeting of Geol. Soc. of America, Lexington, KY, April, 1984.

Talwani, P. and S. Acree, Pore pressure diffusion and the mechanism of reservoir induced seismicity, submitted to PAGEOPH, Dec. 1983.

MONTICELLO EARTHQUAKES
JANUARY - DECEMBER 1983

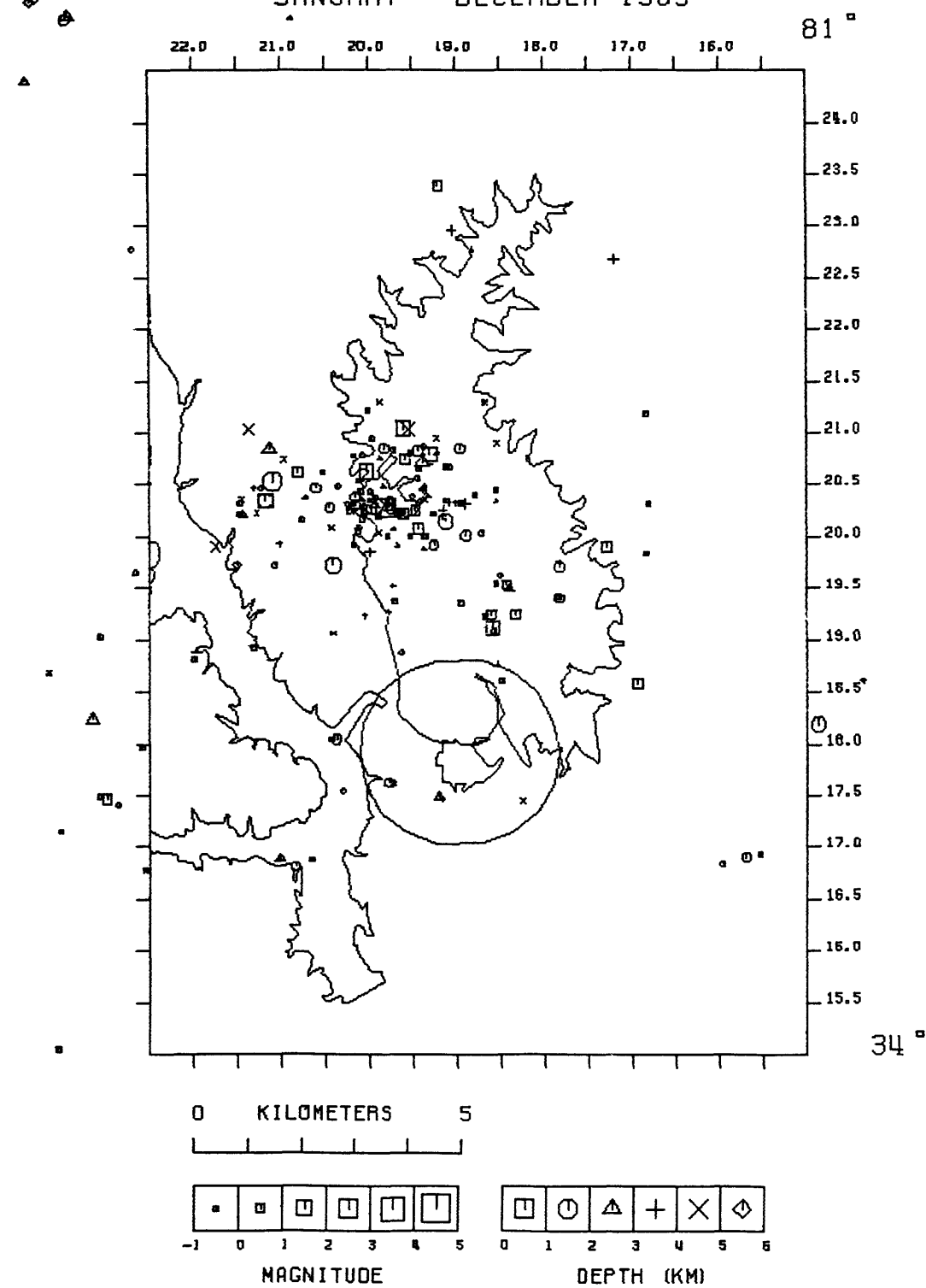


Figure 1

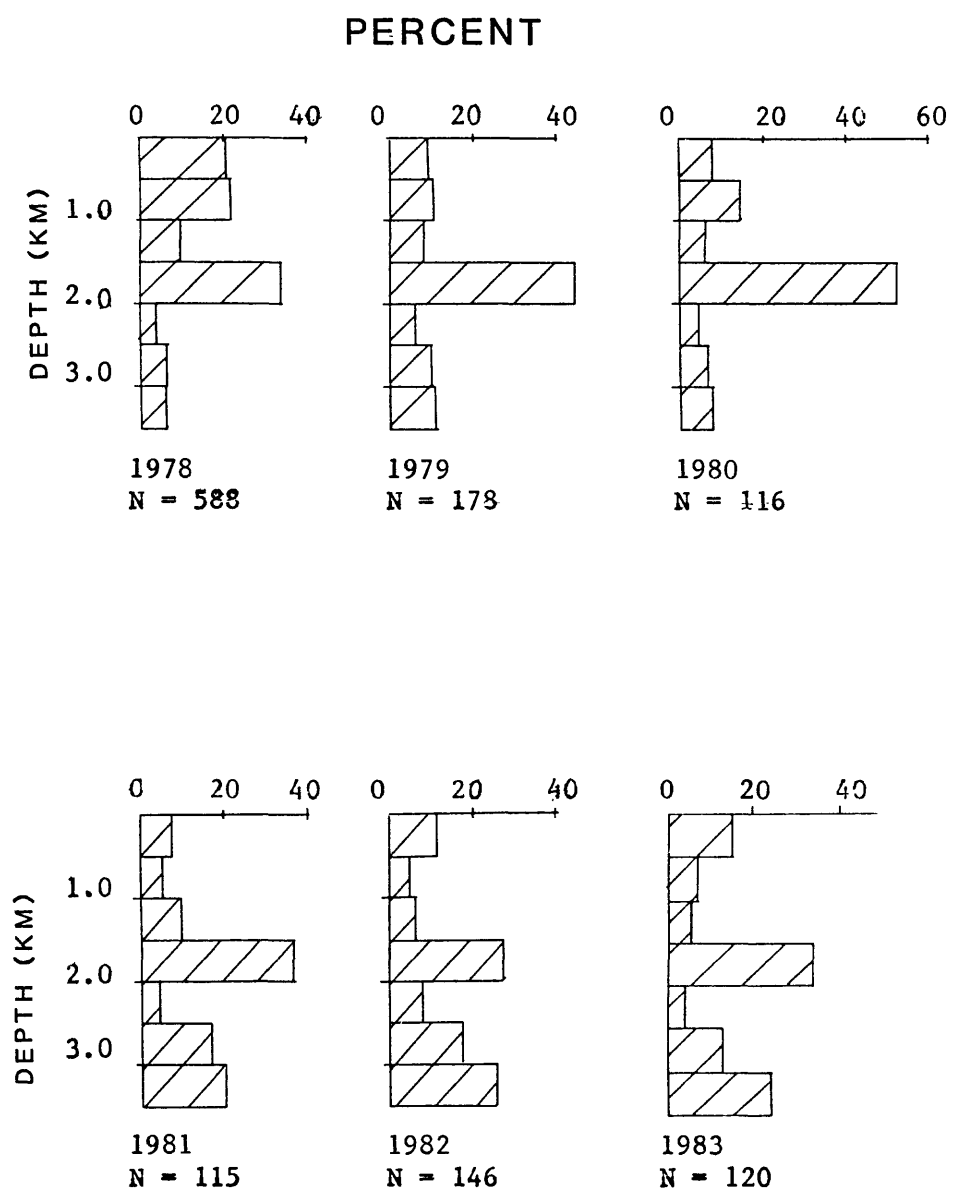


Figure 2

JOCASSEE EARTHQUAKES JULY - DECEMBER 1983

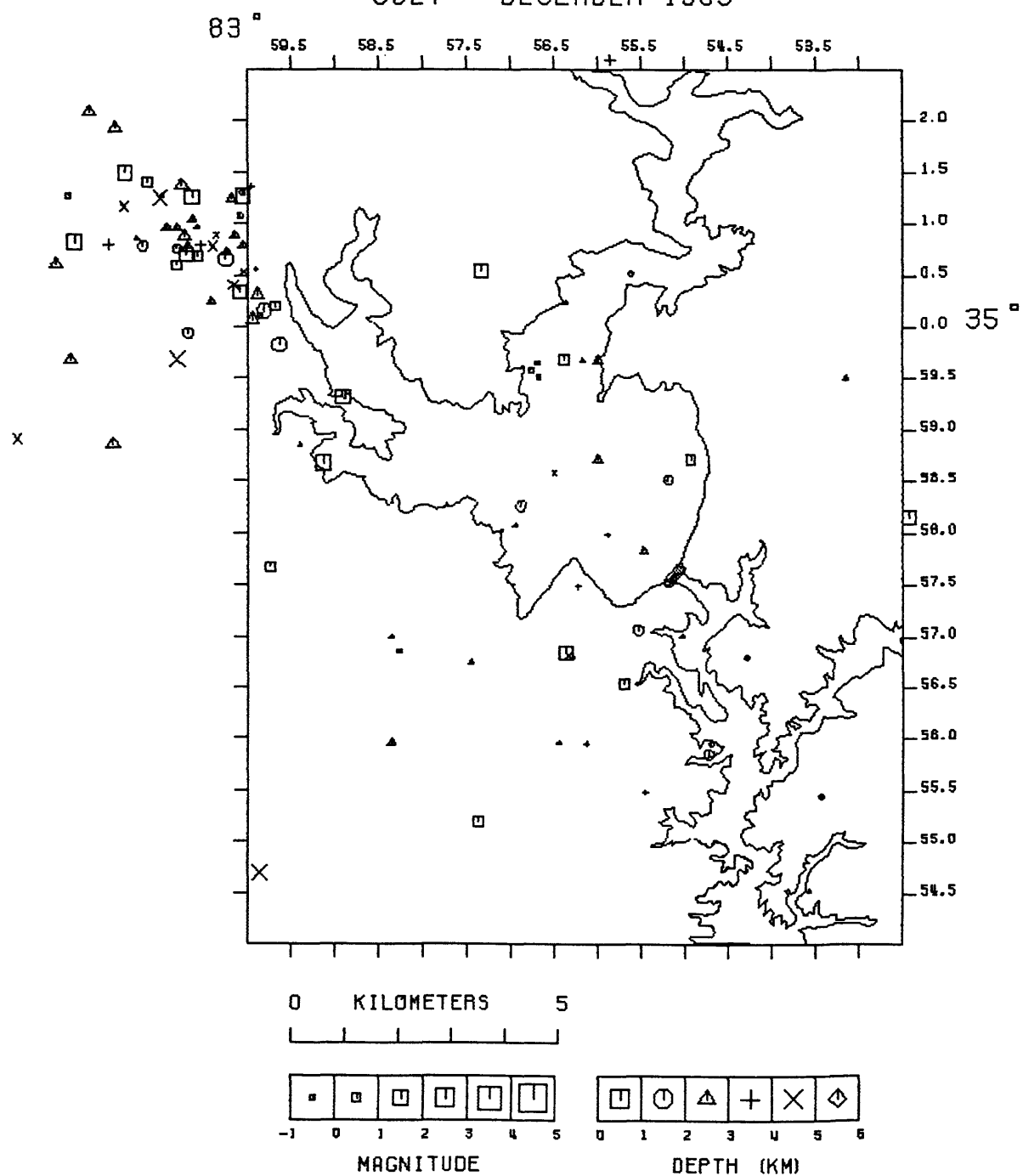


Figure 3

SEISMICITY NEAR ASWAN HIGH DAM, EGYPT,
WITH APPLICATION TO INDUCED SEISMICITY IN CALIFORNIA P-4

Contract No. 14-08-0001-21266

by

Tousson R. Toppozada and Chris Cramer,
California Division of Mines and Geology
2815 O Street
Sacramento, CA
(916) 322-9309

On 14 November 1981, a magnitude 5.5 earthquake occurred 60 km southwest of Aswan High Dam, under a large embayment of the lake. This embayment is a structural depression that has been submerged only since 1976. It marks the intersection of two major sets of faults, trending approximately east-west and north-south.

A month after the mainshock, the Egyptian Geological Survey (EGS) installed a network of 6 MEQ800 seismographs. This portable network was serviced daily in difficult field conditions for eight months until it was replaced by a telemetry network in July 1982.

CDMG cooperated with EGS to analyze the seismograms recorded on the MEQ800 network. More than 700 earthquakes of magnitude 1 or greater were located. More than 500 epicenters were of quality C or better. The seismicity was concentrated at Gebel Marawa, near the intersection of the easterly trending Kalabsha fault with a northerly trending fault. Seismicity also clustered some 15 km further to the east near the intersection of the Kalabsha fault with another northerly trending fault. The focal mechanisms in these two seismic zones suggest right-lateral strike slip on the Kalabsha trend, or left-lateral strike slip on the north-south trend. The 10 km span of the

Kalabsha fault separating these two seismic zones is remarkably nonseismic.

Seismicity also clustered in between these two zones, and some 10 km north of the Kalabsha fault. These three seismic zones are located under a major western branch of the lake. Finally, a few well-located epicenters fall in the mainstream of the Nile, to within 5 km of the High Dam.

The best determined hypocenters were located at Gebel Marawa. These indicate an easterly trending, vertically dipping seismic zone at depths of 15 to 25 km. This is consistent with the observed focal mechanisms suggesting right-lateral strike slip motion on the Kalabsha fault.

Aswan, like Oroville, California, overlies crystalline basement rocks in an area of extensional tectonics. The Aswan and Oroville mainshocks are of similar magnitude, and both occurred several years after reservoir filling. At Oroville, the 1975 earthquake followed the largest refilling of the lake since first filling. The Aswan earthquake followed a seasonal refilling, that was not the largest in amplitude, but was the most rapid in rate since the epicentral area was submerged in 1976. The occurrence of the Aswan and the Oroville earthquakes some time after first filling, following a refilling of the lake that was unprecedented either in amplitude or in rate, suggests that time must elapse for water to infiltrate the subsurface before earthquakes can be triggered.

Strong Motion Data Management

9910-02757

A.G. Brady

Branch of Engineering Seismology and Geology
U.S. Geological Survey
345 Middlefield Road, MS 977
Menlo Park, California 94025
(415) 323-8111, ext. 2881

Investigations

Research continues on the development of analytical test records for testing processing steps.

We continue to make adjustments to the processing procedures as new developments arise. The Mt. Hamilton earthquake (4/24/84) provided approximately equal numbers of analog film records (for example, Anderson Dam crest and downstream) and digital records (for example, the Hollister differential digital array, and the San Jose 101/280/680 overpass). Investigations continue into the high frequency limitations of the digital, and the long period limitations of the analog.

Results

Routine digitizing (D), and computer processing (P), of strong-motion earthquake recordings continues: 5 records (P), Idaho earthquake 10/28/83, for U.S. Corps of Engineers; 13 records (D), Coalinga aftershock 7/22/83, 0239; 8 records (D), Coalinga aftershock 7/22/83, 0343; 9 records (D), Coalinga Aftershock, 7/25/83; 4 records (D), Coalinga aftershock, 5/4/83; 9 records (P), Coalinga aftershock 7/9/83; 13 records (D), Coalinga aftershock, 5/24/83; 3 records (D), Fiji, 2/83; 5 records (P), Anchorage, 5/5/82, for USGS Denver, Col.; 5 records (D), Papua New Guinea, 1981 and 1983; 7 records (P), Mt. Hamilton earthquake 4/24/84.

Tapes containing processed data (Coalinga, 5/2/83 and 5/9/83), Anchorage, 5/5/82) are available from NGDC, NOAA, Boulder, Colorado. Descriptions of the Coalinga data can be found in the Coalinga Report (U.S. Geological Survey Open-File Report 83-511) published prior to this reporting period.

Reports

None.

Worldwide Standardized Seismograph Network (WWSSN)

4-9920-01201

O. J. Britton

Branch of Global Seismology and Geomagnetism
U. S. Geological Survey
Albuquerque Seismological Laboratory
Building 10002, Kirtland AFB-East
Albuquerque, New Mexico 87115
(505) 844-4637

Investigations

1. Technical and operational support was provided to each station in the Worldwide Standardized Seismograph Network (WWSSN) as needed and required.
2. One hundred fifty-nine (159) modules and components were repaired and three hundred twenty-one (321) separate items were shipped to support the network during this period. Several emergency shipments of photographic supplies were made to stations. The routine shipments from Kodak are still incomplete from the much delayed GSA order of 1983. This situation should soon be resolved.
3. The Kongsberg, Norway, (KON) station discontinued photographic recording on January 1, 1984. Helicorder records are made on the vertical components.
4. Dr. Gary Holcomb and Mr. Bob Hutt visited the South Pole (SPA) station from January 3-5, 1984. They conducted a major calibration including a frequency response. Some filtering was added to the long period components to reduce the background noise. Reinforcements were made to the seismometer pier to eliminate or reduce seismometer drift.
5. Training was provided to Mr. Gary Foltz and Mr. Chris Bauman. They are presently operating the South Pole station.

Results

A continuous flow of high quality seismic data from the cooperating stations within the network is provided to the users in the seismological community.

Digital Data Analysis

9920-01788

Ray Buland
Branch of Global Seismology and Geomagnetism
U.S. Geological Survey
Denver Federal Center, MS 967
Denver, Colorado 80225
(303) 234-4041

Investigations

1. Moment Tensor Inversion. Apply methods for inverting body phase waveforms for the best point source description to research problems.
2. Computation of Free Oscillations. Study the effects of anelasticity on free oscillation eigenfrequencies and eigenfunctions.
3. Near Source Structure. Study the effects of near source structure on telesismic body waves recorded on broadband instruments.
4. Earthquake Location Technology. Study techniques for improving the robustness, honesty, and portability of earthquake location algorithms, as well as locating events in real time using a regional network.
5. Detection Capabilities. Study the seismic event detection capability of each proposed station in the Southern Hemisphere Seismic Net (SHSN) now under development.
6. Network Day/Event Tapes. Support and enhance portable software for retrieving data from the Global Digital Seismograph "Network Day Tapes." Develop software for creating "Network Event Tapes."
7. NEIS Monthly Listing. Contribute both fault plane solutions (using first-motion direction) and moment tensors (using long-period body-phase waveforms) for all events of magnitude 5.8 or greater when sufficient data exist. Contribute waveform/focal sphere figures of selected events.

Results

1. Moment Tensor Inversion. Work on the Mammoth Lakes earthquake sequence has been completed and is being prepared for publication. A study of the Coalinga earthquake has been finished and submitted for publication. This study indicates that the event was a simple rupture, but was accompanied by a co-seismic rotation of the principal stress axes. Also moment tensors have been derived for all possible events in 1981-1983 in preparation for a comparative study of moment tensor techniques.

2. Computation of Free Oscillations. First order perturbation theory was tested by computing anelastic toroidal free oscillations directly using simple Earth models and simple model rheologies. For periods longer than 200s, first order perturbation theory was found to be adequate for both eigenfrequency and eigenfunction given a reasonable Earth model. For higher frequencies, it appears that the anelasticity may result in significant "source" phase shifts, though the effect is not yet completely understood.

3. Near Source Structure. Additional synthetic seismogram techniques are being developed to better model the effects of near source structure on broadband, teleseismic records.

4. Earthquake Location Technology. The travel-time algorithm of Buland and Chapman has been extended to compute Pg, Pb, Pn, P, Pdiff, PKP, pP, sP, PcP, SKP, ScP, PKKP, SKKP, PP, P'P', Sg, Sb, Sn, S, Sdiff, and SKS. Preliminary experiments indicate that phase reidentification should be practical given the proper balance between automation and analyst control. Further, the location of crustal events with close in control should be greatly enhanced as secondary phases seem to be well recorded and reported. Experiments on the use of a robust R-estimator in teleseismic location indicate that good resolution of the epicenter and rejection of outliers is possible even when azimuthal coverage is poor. In support of this work, probability distributions have been derived for travel-time residuals (as well as magnitudes) using historical NEIS data. Finally, work is progressing on combining the US Net signal detection system, either the Hunter or Murdock and Hutt trigger algorithm, and the robust location algorithm to produce real time earthquake locations.

5. Detection Capabilities. Each of the ten stations comprising the proposed SHSN network is to be studied in detail for ability to well record seismic events. The study of two more stations has been completed to bring the total to four.

6. Network Day/Event Tapes. The Event Tape software has been completed and the first event tape produced. The first three reels for 1984 (Jan.-Feb) will be shipped to five data centers within a week. Event tapes for the first five months of 1980 have also been produced for a historical series. Eventually, the tapes will cover 1980-present.

7. NEIS Monthly Listing. Since May 1981, fault plane solutions for large events have been contributed to the Monthly Listing. Beginning in November 1982, moment tensors and waveform/focal sphere plots are also being contributed. In the last six months the fault plane solutions and moment tensors of approximately 90 events were published. Catalogs of all fault plane solutions along with first motions data is being prepared for publication as a USGS circular.

Reports

Sipkin, S. A. and Needham, R. E., 1984, Kinematic source parameters of the 2 May 1983 Coalinga earthquake determined by time-dependent moment tensor inversion and an analysis of teleseismic first motions: in U.S. Geological Survey Professional Paper, in press.

Julian, B. R. and Sipkin, S. A., 1984, Earthquake processes in the Long Valley Caldera area, California: in U.S. Geological Survey Professional Paper, in preparation.

Needham, R. E., 1984, Preliminary report on the detection capabilities of the SHSN stations: ZOBO-Zongo Valley and LPB-La Paz, Bolivia; internal report.

Systems Engineering

4-9920-01262

Harold E. Clark, Jr.
Branch of Global Seismology and Geomagnetism
U. S. Geological Survey
Albuquerque Seismological Laboratory
Building 10002, Kirtland AFB-East
Albuquerque, New Mexico 87115
(505) 844-4637

Investigations

1. Design, develop, and test microprocessor based seismic instrumentation.
2. Design, develop, procure, and test special electronic systems required by seismic facilities.
3. Design, develop, and test microprocessor/computer software programs for seismic instrumentation and seismic recording systems.

Results

1. Procurement packages and contracts were prepared for the ordering of parts and components for eleven field systems and one depot repair facility for the China Digital Seismograph Network (CDSN). Initially parts and components for two systems and all of the depot repair equipments were ordered for the CDSN Prototype Field Digital Seismograph System, the Beijing Depot Repair Facility, and the CDSN system that will remain at the Albuquerque Seismological Laboratory. The remaining parts and components were ordered at a later date and will be delivered during the FY 84 and FY 85 time periods.
2. A 10-KVA electric motor-generator unit was installed at the Albuquerque Seismological Laboratory to provide the 230 VAC, 50 hertz power to simulate the China power system. All equipment purchased for the CDSN is designed for 230 VAC, 50 hertz frequency. This new power system will allow all 50 hertz frequency equipment to be tested and checked out at Albuquerque. Both 120 VAC and 240 VAC power options are available. Another feature of this motor-generator unit is to test under and over voltage conditions. The output of the motor-generator unit can be adjusted from 200 to 270 VAC with ease. The 10-KVA capacity will allow fairly large units to be tested.
3. The Depot Repair Facility will have extensive electronic test equipment such as oscilloscopes, counters, multimeters, and general laboratory test equipment. In addition, five automatic test equipment (ATE) units will test the complex systems such as: the HCD-75 controllers, recorders, and even the magnetic tape cassettes; the 8085 and 8086 CPU-based mini-computer boards; the complete digital system emulator and tester; and an Integrated Circuit (IC) tester for semiconductor devices. Most of the system repair can be accomplished at the Beijing CDSN Repair Facility. Only major damage and repair problems will require the various units to be shipped to the factory repair facilities.

Seismic Observatories

4-9920-01193

Leonard Kerry
Branch of Global Seismology and Geomagnetism
U. S. Geological Survey
Albuquerque Seismological Laboratory
Building 10002, Kirtland AFB-East
Albuquerque, New Mexico 87115
(505) 844-4637

Investigations

Recorded seismological data at Albuquerque ASL, New Mexico, on a continuing basis. Recorded and provisionally interpreted seismological and geomagnetic data at observatories operated at Newport, Washington; Cayey, Puerto Rico; Agana, Guam. Assisted in the operation of the Puerto Rican Seismic Telemetry Network from the main base located in Cayey, Puerto Rico. Operated advanced equipment for gathering research data for universities and other agencies at Cayey, Puerto Rico, and Agana, Guam. At Agana, Guam, a 24-hour standby duty was maintained to provide input to the Tsunami Warning Service operated at Honolulu Observatory by NOAA and to support the Early Earthquake Reporting function of the National Earthquake Information Service.

Results

Provided data on an immediate basis to the National Earthquake Information Service and the Tsunami Warning Service. Continued to send seismograms obtained from the WWSSN Systems to NEIS for use in the ongoing USGS programs. Analog seismic records and digital seismic tape records were obtained from the SRO system and forwarded to ASL for use in ongoing USGS and other users' programs. Data from advanced research equipment was forwarded to universities or other agencies working in conjunction with USGS. Seismic data from the Puerto Rican net was provided on a continuing basis to the University of Puerto Rico for their use in studying and research of the seismicity of the Puerto Rican area.

Responded to requests from the public, interested scientists, universities, state, and Federal agencies regarding geophysical data and phenomena.

During this period, a USGS geophysicist assumed duties at the San Juan Observatory, Cayey, Puerto Rico, and a geological field assistant began duty at the Newport Observatory, Newport, Washington.

Seismic Data Library

9930-01501

W. H. K. Lee
U. S. Geological Survey
Branch of Seismology
345 Middlefield Road, Mail Stop 977
Menlo Park, California 94025
(415) 323-8111, ext. 2630

This is a non-research project and its main objective is to provide access of seismic data to the seismological community. This Seismic Data Library was started by Jack Pfluke at the Earthquake Mechanism Laboratory before they joined the Geological Survey. Over the past ten years, we have built up one of the world's largest collections of seismograms (almost all on microfilm) and related materials. Our collection includes approximately 4.5 million WW NSS seismograms (1962 - present), 1 million USGS local earthquake seismograms (1966-1979), 0.5 million historical seismograms (1900-1962), and 20,000 earthquake bulletins, reports and reprints.

The Seismic Data Library was recently moved to 333 Middlefield Road, one block north of our office. It is housed in an adequate quarter and we are now in the painful stage of getting our materials systematically organized. Nevertheless, the seismograms have been organized and are open to users.

Seismic Review and Data Services

9920-01204

R. P. McCarthy

Branch of Global Seismology and Geomagnetism
U.S. Geological Survey
Denver Federal Center, MS 969
Denver, Colorado 80225
(303) 234-5080

Investigations and Results

Technical review and quality control were carried out on 469 station-months of seismograms from the World-Wide Standardized Seismograph Network (WWSSN). Seventy-two station-months of Seismic Research Observatory (SRO & ASRO) seismograms were provided to the National Earthquake Information Service (NEIS) for their PDE programs on a current basis. An average of forty-five WWSSN current station-months were supplied monthly for the NEIS fault plane solution program. Under the cooperative WDC-A International Data Exchange (IDE), seismograms from the WWSSN sent for this program outside normal schedules were forwarded to the WDC-A covering four separate events.

The special filming project was halted to correct an imagery problem in the camera which resulted in partial data losses. The problem has been corrected and most of the recordings affected have been reworked.

Fifty-two WWSSN Station Performance Reports were sent to directors during this period. The WWSSN high standards were maintained. The polarity difference noted on all components compared between the WWSSN Chiang Mai, Thailand (CHG), and the SRO station at Chiang Mai (CHTO) was checked by the Albuquerque Laboratory personnel. Weight lifts were performed and showed that the WWSSN CHG was correct, and the SRO (CHTO) components were reversed. Bulawayo, Zimbabwe (BUL) continued to operate its short periods in reversed polarity. The former Balboa Heights, Panama (BHP) has been relocated at the University of Panama (UPA) and has been operating since August 23, 1983. Recordings are sent on a fairly current basis (2-3 month lag). The magnifications are 25K and 1.5K for the SP's and LP's respectively. The station operations are excellent.

Consultations regarding station data and operations were provided to government officials, researchers and private parties as needed. Up-to-date monthly reports on the analog and digital data collected from the GSN were distributed to USGS, NOAA, DOD officials, and to researchers in the Branch of Global Seismology and Geomagnetism.

National Earthquake Information Center

9920-01194

Waverly J. Person
Branch of Global Seismology and Geomagnetism
U.S. Geological Survey
Denver Federal Center, MS 967
Denver, Colorado 80225
(303) 234-3994

Investigation and Results

The weekly publication, Preliminary Determination of Epicenters (PDE), continues to be published on a weekly basis, averaging about 65 earthquakes. The PDE, Monthly Listing, and Earthquake Data Report (EDR) are working very well on the VAX, with very little down time encountered. We have had some improvements on data flow from our foreign contributors.

The personal contacts with many of our foreign visitors, explaining the need for faster reporting of data, have been the most productive way for receiving data. We continue to receive telegraphic data from the U.S.S.R. in a very timely manner on magnitude 6.5 or greater earthquakes and some smaller damaging quakes in the U.S.S.R. and bordering countries. Data from the PR China via the American Embassy are being received presently after a few weeks delay because of poor readability of the telegrams. We are now receiving 4 stations on a weekly basis from the PR of China and about 22 from SSB by mail in time for the Monthly. We now have rapid data exchange (alarm quakes) with Centre Seismologique European-Mediterranean (CSEM), Strasbourg, France; Instituto Nazionale di Geofisica, Rome, Italy; data by telephone from Mundaring Geophysical Observatory, Mundaring, W.A.; and routine telegraphic data from Seismological Geophysical Institute of Montenegro, Titograd, Yugoslavia.

The Monthly Listing of earthquakes are up to date. To date the Monthly Listings and Earthquake Data Reports (EDR) have been completed through December, 1983, 4,758 earthquakes published. Fault Plane Solutions are being determined when possible and published in the Monthly Listing and EDR for any earthquake having mb magnitude \geq 5.8. Centroid Moment Tensor Solutions from Harvard University continue to be published in the Monthly Listing and EDR. Moment Tensor Solutions are being computed by the USGS and are also published in the Monthly Listing and EDR. Digital Waveform Plots continue to be published in the Monthly Listing which provides an opportunity for graphically displaying focal parameters presented within the text of the publication. Waveform plots are being published for selected events having mb magnitudes \geq 5.8. Within a few months these waveform plots will be published in the ISC bulletins.

The Earthquake Early Alerting Service continues to provide information on recent earthquakes on a 24-hour basis to scientists, news media, and the general public. Sixty-nine releases were made from October 1, 1983

through March 31, 1984. The largest earthquake released during this time period was a magnitude 7.6 in the Chagos Archipelago region on November 30. In the United States the largest was a magnitude 7.3 in eastern Idaho on October 28. Two others of interest were a magnitude 5.3 in New York on October 7 and a magnitude 5.8 in central California (Morgan Hill) on April 24.

Reports

Preliminary Determination of Epicenters (PDE) (25 weekly publications October 5, 1983 to March 29, 1984 - Numbers 37-83 through 10-84).
Compilers: Leroy Irby, Willis Jacobs, John Minsch, Waverly Person, Bruce Presgrave, William Schmieder.

Monthly Listing of Earthquakes and Earthquake Data Reports (EDR) (7 publications - June 1983 through December 1983). Compilers:
Leroy Irby, Willis Jacobs, John Minsch, Russell Needham, Waverly Person, Bruce Presgrave, William Schmieder.

Seismological Notes, BSSA: Waverly J. Person

January-February 1983

March-April 1983

May-June 1983

Earthquake Information Bulletin:

Vol. 15, No. 4, Earthquakes, Waverly J. Person, January-February 1983

Vol. 15, No. 5, Earthquakes, Waverly J. Person, March-April 1983

Vol. 15, No. 6, Earthquakes, Waverly J. Person, May-June 1983

Vol. 16, No. 1, Earthquakes, Waverly J. Person, July-August 1984

Source Properties of Great Basin Earthquakes

New Project

Arthur C. Tarr
Branch of Engineering Geology and Tectonics
U.S. Geological Survey
Box 25046, MS 966, Denver Federal Center
Denver, CO 80225
(303) 234-4268

Investigations

Three principal investigations were begun in the first two quarters of FY 1984 under this new project. Those investigations are as follows:

1. Update and review Great Basin focal mechanism catalog.
2. Development of software to analyze digital data recorded by portable seismic systems.
3. Analysis of digital data recorded by portable seismic systems at Nevada Test Site in 1981.

The focal mechanism catalog was compiled earlier (1977) as part of the circum-Pacific map project and the purpose of the first investigation of the current project was to review the older data and update the catalog with focal mechanisms and other source parameter determinations for earthquakes within and bordering the Great Basin. Another objective of this investigation was to revise the structure of the focal mechanism data base so that accessing and displaying source parameters for Great Basin earthquakes would be easier.

The ability to perform spectral analyses on digital data recorded by portable seismic systems did not exist at the Golden facility previously. Existing computer programs in Golden were appropriate for other types of digital data (for example, teleseismic records) or were written in computer languages for which no compiler existed on the VAX/VMS computer. Therefore, the objective of the second investigation was to locate existing software, written in FORTRAN, that would perform spectral analyses on digital data recorded in the field and implement the software on the Golden computer.

The objective of the third investigation was to analyze digital seismic data that had been recorded in 1981 at Jackass Flats on the Nevada Test Site. The microearthquakes recorded in that field exercise had been played back from the original cassettes but were never analyzed because of the lack of appropriate software on either of the computers in Golden.

Results

A review of the circum-Pacific focal mechanism catalog revealed several omissions in coverage of the Great Basin, probably because the area was marginal to the main areas of interest to the circum-Pacific maps. A literature search revealed significant lists of source parameters published since the earlier compilation; these lists are most complete for southern

Nevada and Utah. Entry of the new source parameter data awaits final testing of the revised data base structure and associated software. The revised data base design emphasizes the moment tensor description of the seismic source which permits representation of compensated linear vector dipole models as well as the conventional double-couple model.

FORTRAN software for the analysis of digital seismic data recorded by field systems had been written several years ago by Edward Cranswick (U.S. Geological Survey, Menlo Park, Calif.) and implemented on the DEC 11/70 RSX computer system in Menlo Park. This extensive set of programs seemed ideal for the present investigation because the programs were used to analyze GEOS and DR100 records recorded in New Brunswick, Idaho, and California (among other places). With the assistance of Cranswick, the software was made available and the computer code was installed on the Golden VAX/VMS computer. The conversion took a surprisingly short time (about 1 month) considering the differences between the two computer sites in the operating systems and plotting software. Additional programs have been written to convert digital data recorded by other field systems (for example, MCR-600 and DR-200) into the format used by the software. Documentation of the converted software and a user's guide are currently underway.

The Jackass Flats digital data have been examined and approximately 15 events with at least one on-scale trace were selected for further analysis. Several events were large enough to have been recorded on the southern Great Basin seismic network. Thus, the field recordings provided additional phase times and P-wave first motions to supplement the network location and focal mechanism determinations. Because the spectra have not been corrected for system response, modifications to the software to correct the spectra are currently being tested. A. M. Rogers (USGS, Golden, Colo.) expects to use the corrected spectra to assist him in calibrating a local magnitude--seismic moment relationship for the southern Great Basin.

Reports

None

National Strong Motion Data Center

9910-02085

Joanne Vinton
Branch of Engineering Seismology and Geology
U. S. Geological Survey
345 Middlefield Road, MS 977
Menlo Park, California 94025
(415) 323-8111, ext. 2982

Investigations

The goals of the National Strong Motion Data Center are to:

- 1) Maintain a strong capability for processing, analyzing, and disseminating all strong motion data collected on the National Strong Motion Network and portable arrays;
- 2) Support research projects in the Branch of Engineering Seismology and Geology by providing programming and computer support for computation of numerical models;
- 3) Provide digitizing and processing capabilities rapidly in the event of an earthquake as an aid to earthquake investigations.

Results

The National Strong Motion Data Center consists of a Digital Equipment Corporation PDP-11/70 computer running the VMS operating system, and a PDP-11/70 and two LSI-11/23 computers running the RSX operating system. The VAX has been installed since February 1984, and programs are being transferred to it from the PDP-11/70, to take advantage of the large address space. The LSI-11/23's are for use in the field, to locate and plot aftershocks on site.

All four computers are connected to the Office VAX-11/780 and to each other to allow file transfers and remote logons. In the near future, these computers will also be connected to ISD's VAX 11/780 and Marine Geology's VAX 11/780.

Data collected during this six month period were from the strong motion experiment in the Anza desert in southern California, and from the aftershock sequence in Idaho.

Reports

None.

Regional and National Seismic Hazard and Risk Assessment

9950-01207

S. T. Algermissen

Branch of Engineering Geology and Tectonics

U.S. Geological Survey

Denver Federal Center, MS 966

Denver, CO 80225

(303) 234-4014

Investigations

1. Refinement of statistical techniques for estimating earthquake recurrences among regional seismic source zones having low levels of historic seismicity.
2. Parameter Variability. The effect of incorporating attenuation variability by assuming a lognormal distribution of acceleration for magnitude and distance was investigated.
3. Seismic Source Zone Boundaries. Sharp contrasts in rates of seismic activity across source zone boundaries may or may not be warranted in certain regions, depending on how confidently active seismotectonic features can be identified. A technique of Gaussian smoothing of seismicity rates across source zone boundaries was devised and programmed for primary application in regions where specific seismotectonic features are poorly understood or presently unknown.
4. Pattern Recognition. Further investigations concerning a pattern-recognition algorithm previously developed and programmed.
5. Documentation of seismic source zones used in assessing long return-period earthquake ground motion for the eastern United States.
6. Liquefaction Studies. In a study of earthquake liquefaction hazard in the Los Angeles (CA) region, a probabilistic liquefaction opportunity map and supporting material has been readied for publication.

Results

1. Comparisons of six statistical techniques for allocating rates of seismic activity among weakly seismic zones against simulated data sets having known relative earthquake distributions were ranked according to 15 performance measures. Results indicate:
 - a. The maximum likelihood technique was superior in most efficiency measures for data in which temporal and magnitude independence of earthquakes is assumed.
 - b. Two techniques are superior to the maximum likelihood technique when the number of large events in a sample is anticorrelated with the number of small magnitude events. The minimum chi-squared technique and a composite technique of maximum likelihood allocations with average a-value allocations indicated superior performance under this condition.
2. Including acceleration variability may cause a considerable increase in the acceleration level calculated for a given return period.
3. The acceleration level calculated for a given return period may increase from 50-80% when a site is moved from 10 km outside a discrete source zone boundary to 10 km within the boundary. In regions where seismotectonic features are unknown, such large differences in ground motion values across short distances is an artificial requirement of discrete source zone boundaries. The Gaussian smoothing technique is one way of minimizing this effect.
4. Standard pattern recognition algorithms may lead to incorrect identification of "characteristic traits" due to dependencies between site characterization questions. An alternative maximum likelihood algorithm that takes into account dependencies among pattern recognition criteria and avoids some of the difficulties of standard pattern recognition procedures is being investigated. However, in a real example using eastern United States earthquakes, few inferences can be made because of the size of the sample and selection of the "safe" points. A journal paper is in preparation.
5. A manuscript describing the development of seismic source zones for long-term earthquake hazard analysis in the eastern United States is currently in revision following internal review for journal publication.
6. A text was prepared for one Los Angeles Professional Paper on earthquake hazard. The earthquake-induced liquefaction map shows an average return period of 33 years for liquefaction opportunity.

Reports

1. Bender, B., in press, A two state model for seismic hazard estimation: Seismological Society of America Bulletin.
2. Bender, B., in press, Seismic hazard estimation using a finite fault rupture model: Seismological Society of America Bulletin.
3. Bender, B., in press, Incorporating acceleration variability into seismic hazard analysis: Seismological Society of America Bulletin.
4. Thenhaus, P. C., 1983, Summary of workshops concerning regional seismic source zones of parts of the conterminous United States, convened by the U.S. Geological Survey 1979-1980, Golden, Colorado, U.S. Geological Survey Circular 898, 36 p.
 - A. Bucknam, R. C., and Thenhaus, P. C., Great Basin seismic source zones--Summary of workshop convened October 10-11, 1979, p. 4-9.
 - B. McKeown, F. A., Ross, D. C., and Thenhaus, P. C., Northern Rocky Mountains seismic source zones--Summary of workshop convened December 6-7, 1979, p. 9-14.
 - C. Anderson, R. E., Irwin, W. P., and Thenhaus, P. C., Southern Rocky Mountains seismic source zones--Summary of workshop convened January 23-24, 1980, p. 14-19.
 - D. McKeown, F. A., Russ, D. P., and Thenhaus, P. C., Central interior seismic source zones--summary of workshop convened September 10-11, 1980, p. 19-24.
 - E. Diment, W. H., McKeown, F. A., and Thenhaus, P. C., Northeastern United States seismic source zones--summary of workshop convened September 10-11, 1980, p. 24-31.

Seismic Hazards of the Hilo 7 1/2' Quadrangle

9950-02430

Jane M. Buchanan-Banks
Branch of Engineering Geology & Tectonics
U. S. Geological Survey
Hawaiian Volcano Observatory
Hawaii Volcanoes National Park
Hawaii, 96718
(808) 967-7328

Investigations

1. Began adaptation of field notes for computerization, and continued geologic mapping of the Hilo 7 1/2' quadrangle.
2. Conducted field investigations of the landslides and other earthquake-related damage resulting from the November 17, 1983, Kaoiki earthquake on the island of Hawaii.
3. Assisted with geologic observations during the March 25-April 15, 1984 eruption of Mauna Loa Volcano.

Results

1. Field notes from several seasons of geologic mapping have been adapted for computerization and will be entered into a data-base management system within the next few months. Key fields will enable sorting according to various geologic parameters.
2. The Kaoiki earthquake (M6.6) caused substantial damage in the southeastern part of the island generating intensities of VIII to IX. Field investigation of earthquake-induced ground failures and structural damage began immediately. Rock slides and falls were triggered on steep slopes as far away as Kealakekua Bay, South Kona (30 miles WNW of the epicenter) and Maulua Gulch along the Hamakua Coast (40 miles NNE). Most slides and rockfalls occurred on the steep caldera and crater walls within Hawaii Volcanoes National Park about 10 miles west of the epicenter, where the lava flows of Kilauea Volcano form cliffs as much as 120 m high. Volumes of the slides were from several hundred to a few thousand cubic meters. There were also numerous small soil slips (volumes generally only a few cubic meters) in the thick ash deposits near Hilo and Pahala. Vibrational settling of fill caused road collapse at several sites within the National Park. Evidence of slumping could also be seen in a few localities within the city of Hilo.

Many houses were thrown from their foundations some as much as 1.2 m, water tanks were toppled, some plate glass windows and underground water pipes were broken. Extensive damage occurred to loose objects within buildings. From reconnaissance studies indications are that severe structural damage occurred in areas that were underlain by thick ash deposits, or when structures were built near the edge of lava flows overlying thick ash deposits.

3. Mauna Loa Volcano began erupting in its summit caldera 01:30 (HST) on March 25, 1984. After several hours, the eruptive fissure broke both southwest and northeast from the caldera. The southwest vents extended down to about the 12,000-foot elevation and produced minor flows for a few hours. Activity continued along the northeast rift with the fissure system gradually moving downrift until about 17:00 when it had reached the 9,400 foot elevation. Mauna Loa continued to erupt from this 150-m-long fissure until April 15.

Four major lava flows that moved down the northeast slope of Mauna Loa toward sparsely populated areas produced during the early phases of the eruption. The three southernmost of these flows were relatively stagnant by March 28. The most northerly flow and its northern branch, however, continued to move with some vigor until about April 5 finally stagnating at about the 2,950-foot elevation, some 26 km downslope from their source and 8 km upslope from the outskirts of Hilo.

Continuous daytime geologic observations were made of the activity and lava production at the vents. Temperature were obtained with sample of lava collected at the same time. Flow advances were monitored from helicopters several times each day. Flow morphology, rates and densities were intensively studied.

Analytical Investigation of Soil Liquefaction

9910-03390

Albert T. F. Chen
Branch of Engineering Seismology and Geology
U.S. Geological Survey, MS-974
345 Middlefield Road
Menlo Park, CA 94025
(415) 323-8111, Ext. 2605

Investigations

- (1). Developed interactive computer programs to assess the liquefaction potential of a given site/region from standard penetration or cone penetration records.
- (2). Initiated a study on the liquefaction and slope failure hazards of the debris dams north of Mt. St. Helen, Washington.

Reports

Chen, A.T.F., 1983, A study of seismic response at Stations 6 and 7, El Centro Strong Motion Array, Imperial Valley, California: Report No. USGS-GD-83-010, NTIS-PB84-119924, National Technical Information Service, Springfield, VA 22161, 40p.

Chen, A.T.F., 1984, On transmitting boundaries: (accepted for publication in the Journal of the Geotechnical Engineering Division, ASCE).

Chen, A.T.F., 1984, PETAL - Penetration testing and liquefaction, an interactive computer program: U.S.G.S. Open-File Report 84-290, March, 23p.

Strong Ground Motion Studies
Application to Puget Sound

Contract No. 14-08-0001-21306

David M. Hadley and Steven M. Ihnen
Sierra Geophysics, Inc.
15446 Bell-Red Road, Suite 400
Redmond, WA 98052
(206) 881-8833

Investigations

The Puget Sound region is a metropolitan area with a potentially significant earthquake hazard. Earthquakes of magnitude 7.1 (1949) and 6.5 (1965) have occurred in the immediate vicinity at depths of 50-60 km. Given the tectonic setting and historical seismicity, it is quite likely that large events will affect this region in the future.

The ground response at a particular site is dependent upon the characteristics of the source, gross path propagational effects and near site response. Past modeling studies of strong ground motion records from the 1965 event (Langston, 1981, Langston and Lee, 1984) demonstrate that the three-dimensional geologic structure of this region profoundly affects the observed motions. A primary goal of this study is to assess the effect of three-dimensional velocity structure on the intensity of ground shaking in the Puget Sound region. In particular we are using 3-D ray-tracing to simulate the strong motion records and isoseismal distributions from the 1965 and 1949 earthquakes. Assuming that the geologic model can be refined to the point of adequately predicting past experience, a second goal is to estimate the expected ground motion from earthquakes spanning a range of hypocentral locations and magnitudes.

Results

We have constructed a seven-layer three-dimensional model for the velocity structure beneath Puget Sound. The model covers approximately 8300 square kilometers centered on 47.5 N, 122.5 W and extends to 120 km depth. Earthquakes in the Puget Sound region generally occur between 0-70 km depth. The principal elements of the model are: (1) a water layer for Lake Washington, Puget Sound and related structures, (2) a surface sediment layer with laterally varying velocities, (3) upper and lower crustal units, and (4) a layer representing the subducted Juan de Fuca plate.

The sediment layer is of particular interest. The depth to basement information was digitized from published maps which are in turn based on borehole and echo-sounding information. Laterally varying velocities were assigned based on the surface geology. Figure 1 shows an E-W trending horst structure flanked by two moderately deep (up to 1100 meters) sedimentary basins. The deep sediment lens north of the ridge is centered beneath downtown Seattle and may be partly

responsible for the high seismic intensities observed there during the 1965 event. We note that this structure is truly three-dimensional and cannot be adequately approximated in 2-D.

Figure 2 illustrates the lower portion of the model, including the subducted slab. The crustal velocities are based on work by Crosson (1976) and Langston and Blum (1977). The present model does not include a low-velocity zone, although one may be included at a later time. Densities and Q-values were estimated from the assigned velocities using standard relationships. The position and velocity of the subducted slab are based on the travel time inversion results described in Michaelson (1983). In this model, the fold axis strikes slightly west of north, and the slab dips more steeply in the southern part of the study area. Average dip of the subducted plate is about 45 degrees.

The seven layer model has been used to synthesize strong ground motion from the 1965 $M = 6.5$ earthquake. Twenty eight rays were propagated between the published (USCGS) hypocenter and each of 14 receivers extending from the epicenter north to Seattle. A point double couple source is assumed, using the focal mechanism derived by Langston and Blum (1977). It is apparent from Figure 3 that the 3-D model introduces considerable complexity into the raypaths. Rays with identical instructions may arrive at adjacent stations from opposite azimuths, and bounces out of the source-receiver plane are common.

Preliminary ray-trace results show a region of enhanced ground motion from the area east of Burien north to Seattle. This area approximately coincides with the center of the maximum intensity (VII) isoseismal in the 1965 event. Figure 4 shows the S-wave arrivals at the five stations nearest the epicenter. An order of magnitude increase in ground displacement is apparent between stations 3 and 5, only 6 km apart. A large variation in duration of S-waves is observed between the fourteen stations, suggesting that structure may have a pronounced effect on the duration of ground motion, as well as on peak acceleration.

References

- Crosson, R.S., 1976, Crustal structure modeling of earthquake data 2. Velocity structure of the Puget Sound Region, Washington, J. Geophys. Res., 81, pp 3047-3054.
- Langston, C.A., 1981, A study of Puget Sound ground motion, Bull. Seism. Soc. Amer., 71, pp. 883-903.
- Langston, C.A. and J. Lee, 1984, Effect of structure geometry on strong ground motions: The Duwamish River Valley, Seattle, Washington, in press
- Langston, C.A. and D.E. Blum, 1977, The April 19, 1965 Puget Sound earthquake and the crustal and upper mantle structure of western Washington, Bull. Seism. Soc. Amer., 67, pp. 693-711.
- Michaelson, C., 1983, Three-dimensional velocity structure beneath Puget Sound, Washington, University of Washington M.S. Thesis

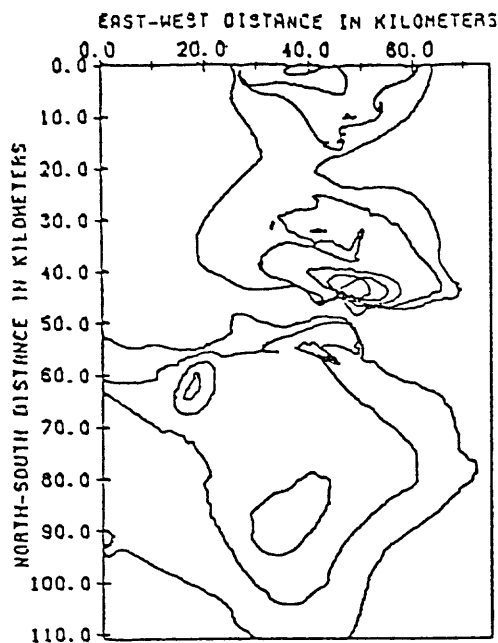


FIGURE 1. Contour plot of sediment thickness in study area. Contour interval is 200 meters. Maximum dimension of model is 111 km.

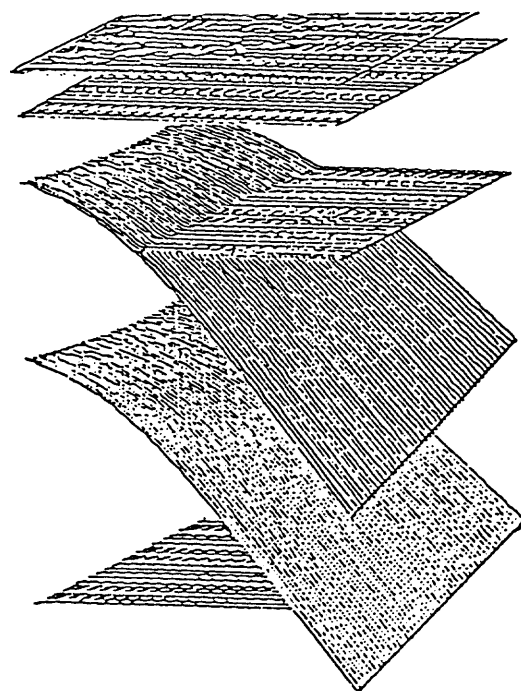


FIGURE 2. Perspective plot showing lower portion of model.

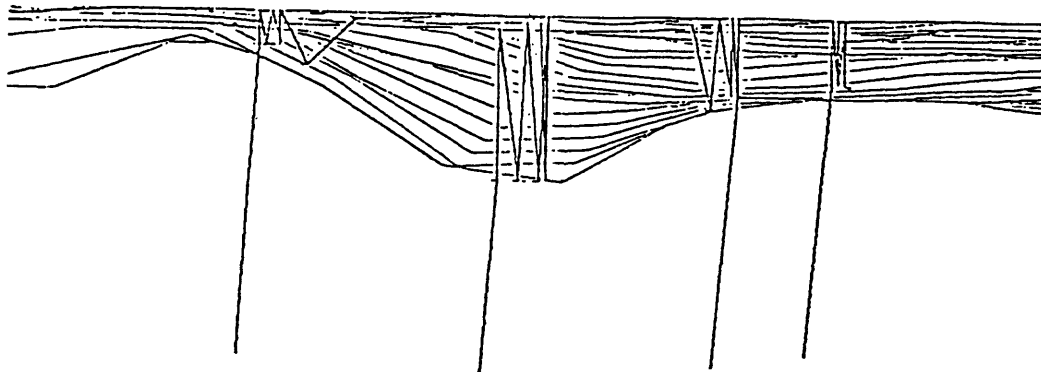


FIGURE 3. Side view of sediment-basement interface showing ray paths for arrivals with three bounces in the sediment layer. Adjacent stations are 6 km apart. The first ray on the left and the third ray arrive at their respective stations from opposite azimuths. The second rayset shows two bounces in the plane of the figure and one bounce parallel to the line of sight. 3X vertical exaggeration.

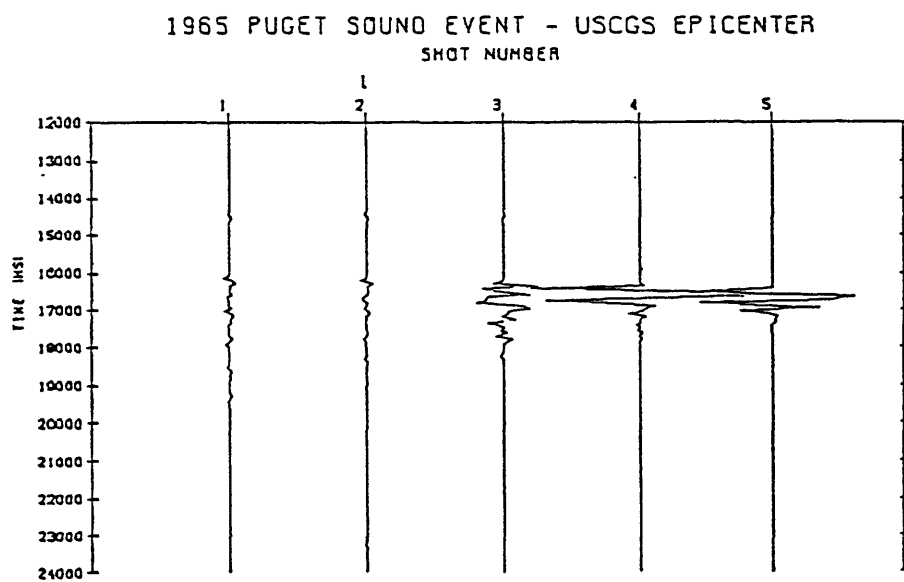


FIGURE 4. Synthetic S-waves at five stations, each 3 km apart. The spike seismograms have been convolved with a 4 Hz wavelet in order to integrate the effect of adjacent arrivals. The large increase in amplitude is due to the focusing effect of the sediment-basement interface.

Whole Waveform Inversion of Regional Digital Seismic Data
Estimation of Anelastic Attenuation in Surficial Layers

14-08-0001-20640

Robert B. Herrmann
Department of Earth and Atmospheric Sciences
Saint Louis University
P.O. Box 8099 Laclede Station
St. Louis, MO 63156
(314) 658-3131

Goals

1. Investigate the possibility of using high frequency regional network data for the direct inversion for focal mechanism and seismic moment by waveform inversion.
2. Use short period surface waves recorded as part of refraction surveys to determine shallow shear wave velocity and shear wave Q structure.

Investigations

1. For the waveform studies, we are working with the USGS acquired digital data for earthquakes in New Brunswick, Monticello, and Arkansas. The data are sieved to find traces suitable for simple modeling. The results of modeling are compared to regional Lg observations when such data are available. The biggest problem lies in finding data simple in appearance so that lack of knowledge of earth structure is not a major factor. Analysis of the New Brunswick data is not definitive, but yields focal mechanisms similar to those of the larger events determined by surface and teleseismic body wave studies.
2. The use of short period surface waves is just starting. An interactive analysis program is being extensively tested with actual data sets. The analysis package, developed by D. Russell, meshes surface wave theory, inversion and data analysis programs in a coherent manner.

The surface wave data sets assembled consist of USGS acquired data for Saudi Arabia, Mississippi Embayment and California Central Valley.

Publications

Herrmann, R. B. and C. Y. Wang. (1984). A comparison of synthetic seismograms, *Bull. Seism. Soc. Am.* (submitted).

Seismic Slope Stability

9950-03391

David K. Keefer

Branch of Engineering Geology and Tectonics
U.S. Geological Survey
345 Middlefield Road, MS 98
Menlo Park, CA 94025
(415) 856-7115

Investigations

1. Continued development of quantitative methods for predicting earthquake-induced landslides on a regional scale.
2. Began development of refined susceptibility criteria for predicting failure of rock slopes during earthquakes.
3. Conducted field studies following the Borah Peak, Idaho, earthquake of October 28, 1983.
4. Performed airphoto studies of landslides caused by the Coalinga, California, earthquake of May 2, 1983.
5. Conducted statistical analyses of landslide distribution along the Mississippi River bluffs to determine factors causing landslides and relation to the 1811-12 New Madrid, Missouri, earthquakes.
6. Completed analyses of pore-pressure records from the Mammoth Lakes, California, earthquakes of May 25-28, 1980.

Results

1. Using both theoretical and historic/empirical studies, we have delineated three zones surrounding a seismic event: (1) a zone within which there is a high probability of failure of susceptible slopes, (2) a zone with a less than even, but still finite, probability of failure of susceptible slopes, and (3) a zone, beyond the outer limit defined by data from worldwide historical events, which is so far from the seismic source that the probability of landslides is very small, even on susceptible slopes. Three maps have been prepared, showing these zones for each major category of landslides for a postulated M 6.5 event in the Los Angeles area.
2. The Borah Peak, Idaho, earthquake caused a few hundred rockfalls and rockslides; a large debris flow; a large mudflow; several slumps and cracks in manmade fill; several instances of soil liquefaction; and few ground failures of other types throughout an area of about 4,200 km². The earthquake caused rockfalls and rockslides as much as 48 km, slumps as much as 46 km, and mudflows as much as 29 km from the fault rupture. The number of landslides, area affected by landslides, and maximum distance of landslides from the fault rupture of the Borah Peak earthquake are small compared to other historical earthquakes of comparable magnitude.

The low number and restricted geographic distribution of landslides are probably due primarily to the ground-motion characteristics of the Borah Peak event and secondarily to the nature of the Paleozoic rocks in the Lost River Range, near the fault rupture. Observations of building damage and preliminary analysis of ground-motion records from the main shock and aftershocks suggest that shaking intensities and peak accelerations in the earthquake were relatively low for a M_s 7.3 event. The Paleozoic rocks that predominate in the Lost River Range are well cemented, massive, and contain few conspicuous, open joints.

The most significant landslide damage associated with the earthquake was in Challis, where several houses are located at or near the bases of steep, marginally stable hillsides. Damage from rockfalls in Challis was all within 70 m of the bases of these hillsides, which remain marginally stable, with steep cliffs composed of loose and shattered rock. These hillsides could produce future rockfalls both in seismic and nonseismic conditions.

3. From field and statistical evidence it appears probable that most coherent slides and earthflows along the Mississippi River bluffs are related to the 1811-12 earthquakes. From this we conclude that the bluffs in the study area are susceptible to large-scale landsliding in future major earthquakes. At present we cannot accurately evaluate the susceptibility of specific portions of the bluffs to earthquake-induced landsliding because we lack quantitative information about the effects of variation in geology, hydrology, and material properties. Our best indices of the potential for earthquake-induced landsliding along the bluffs are slope height and proximity to seismic sources. These factors can be used to predict the relative severity of landsliding along the bluffs in a future major earthquake.
4. Acceleration and wave-induced pore pressure were recorded in a saturated sand during the 1980 Mammoth Lakes, California, earthquake sequence. For the largest event recorded, the pore pressure was observed to be proportional to vertical surface acceleration during the P-wave arrivals and proportional to horizontal surface velocity during the S-wave arrivals. The results can be quantitatively explained with a linear elastic model of a porous saturated medium, such that pore pressure depends on dilatation and is independent of shear strain. A slight frequency dependence in the ratio of pore pressure to dilatation indicates local fluid flow on the scale of individual pores. The good agreement between observations and theory indicates that the deformation was primarily linear, even though the maximum shear strains were close to the typical thresholds for liquefaction.

Reports

Harp, E. L., Sarmiento, John, and Cranswick, Edward, 1984, Seismic-induced pore-water pressure records from the Mammoth Lakes, California, earthquake sequence of May 25-27, 1980: Seismological Society of America Bulletin, 13 p., 8 figs., 1 table [in press].

- Harp, E. L., Tanaka, Kohei, Sarmiento, John, and Keefer, D. K., 1984, Landslides from the May 25-27, 1980, Mammoth Lakes, California, earthquake sequence: U.S. Geological Survey Miscellaneous Investigations Series Map I-1612, scale 1:62,000 [in press].
- Jibson, R. W., 1984, Earthquake-induced landslides in the New Madrid seismic zone [abs.]: Seismological Society of America Annual Meeting, Anchorage [in press].
- Keefer, D. K., 1984, Rock avalanches caused by earthquakes--source characteristics: Science, v. 223, no. 4642, p. 1288-1290.
- Keefer, D. K., and Johnson, A. M., 1983, Earthflows--morphology, mobilization, and movement: U.S. Geological Survey Professional Paper 1264, 56 p., 3 pls.
- Keefer, D. K., Wilson, R. C., Harp, E. L., and Lips, E. W., 1984, Landslides in the Borah Peak, Idaho, earthquake of 1983, in Reaveley, L. D., ed., The Borah Peak, Idaho, earthquake of October 28, 1983: Earthquake Engineering Research Institute Reconnaissance Report, 32 p. [in press].
- Mavko, G. M., and Harp, E. L., 1984, Analysis of wave-induced pore-pressure changes: Seismological Society of America Bulletin, 21 p., 4 figs., 1 table [in press].
- Wieczorek, G. F., Wilson, R. C., and Harp, E. L., 1984, Map showing slope stability during earthquakes of San Mateo County, California: U.S. Geological Survey Miscellaneous Investigations Series Map I-1257-E, scale 1:62,500, with accompanying text [in press].
- Youd, T. L., Harp, E. L., Keefer, D. K., and Wilson, R. C., 1984, Liquefaction generated by the 1983 Borah Peak, Idaho, earthquake, in Reaveley, L. D., ed., The Borah Peak, Idaho, earthquake of October 28, 1983: Earthquake Engineering Research Institute Reconnaissance Report, 19 p. [in press].

Effect of Lateral Heterogenieties on
Strong Ground Motion

14-08-0001-21257

C.A. Langston
440 Deike Building
Department of Geosciences
The Pennsylvania State University
University Park, PA 16802
(814) 865-0083

Investigations

1. Simulation of high-frequency strong ground motions over plausible three-dimensional geologic structure. Synthetic seismograms are calculated for responses from arbitrary point sources in or near the structure of interest.
2. Calculation of strong ground motions over models of geologic structures in the Puget Sound area.
3. Study of anomalous site effects in the Pasadena, California area for strong ground shaking from the 1971 San Fernando earthquake.

Results

1. Existing ray codes for incident plane waves have been modified to include an arbitrary moment tensor point source located within or outside the structure of interest. Structural boundaries are specified by bicubic spline functions and separate regions of homogeneous velocity. The source may be located anywhere within the 3-D structure model. Receivers are confined to the free surface. The ray tracing algorithm and amplitude calculation has been successfully tested for plane layer models using generalized ray theory.
2. A study of anomalous site effects in the Pasadena, California area has been performed. The following is the abstract of a paper reporting on this study entitled "The influence of alluvium geometry on strong ground motions during the 1971 San Fernando earthquake":

Using short-period seismograms from small local and regional events, Gutenberg (1957) showed that high P and S wave amplitudes correlated well with alluvium thickness in the Pasadena area. However, Hudson (1972) demonstrated that these site amplification effects did not occur during the 1971 San Fernando earthquake. A study was made of the effect of alluvium geometry on the propagation of short-period body waves using standard propagator matrix methods and a ray tracing technique for 3-D structure under the assumption that differing wave incidence angles and azimuths between the San

Fernando earthquake and Gutenberg's events were the cause of the discrepancy. Amplification does not occur for plane layer responses of grazing S wave incidence. Synthetic seismograms constructed for S wave point sources at various depths and locations outside of a 3-D model of Pasadena alluvium structure indicate that particle motion can be quite complex from off-azimuth conversions and reverberations within the structure. The effective amplification can also be variable due to local shadow zones for the direct waves, particularly for shallow incidence angles. However, these effects tend to be homogenized if a finite source is assumed and that the principal effect of low velocity alluvium is to amplify amplitudes by factors of two or more. These results generally agree with Gutenberg's observations since he analyzed waves of lower incidence angle compared to the San Fernando event and found high amplifications with considerable amplitude scatter. 3D structures can be constructed to reconcile the San Fernando data with this result, but are clearly non-unique.

Reports

Lee, J.J. and C.A. Langston (1983). Wave propagation in a three-dimensional circular basin, Bull. Seism. Soc. Am., 73, 1637-1653.

Langston, C.A. and J.J. Lee (1983). Effect of structure geometry on strong ground motions: The Duwamish River Valley, Seattle, Washington, Bull. Seism. Soc. Am., 73, 1851-1863.

Lee, J.J. (1983). A three-dimensional ray method and its application to the study of wave propagation in crustal structure with curved layers, Ph.D. Thesis, Pennsylvania State University, University Park, PA 16802.

Langston, C.A. (1984). The influence of alluvium geometry on strong ground motions during the 1971 San Fernando earthquake (abstract), EOS, 65, 234.

ESTIMATION OF NEAR-SOURCE HIGH-FREQUENCY
GROUND MOTION FOR LARGE MAGNITUDE
EARTHQUAKES

14-08-0001-21349

Robin Keith McGuire

Dames & Moore
1626 Cole Blvd.
Golden, Colorado 80401
(303) 232-6262

Investigations

The estimation of near-source ground motion has been investigated using the Hanks-McGuire model of shear wave spectra. The source is represented as small segments of fault rupture, and distances from a site of interest to individual segments (as these distances influence the effects of geometric and anelastic attenuation) are taken into account. The method also accounts for the directivity of rupture propagation. Distributions of peak acceleration, as well as time series of ground motions (represented by time durations of motion and associated rms accelerations) result from the procedure.

The primary thrust of the investigation has been to overcome the mis-representation of source properties when a large rupture area is modeled as a series of small ruptures occurring sequentially. Specifically, the source corner frequency of the segments is higher than appropriate for a long rupture, and the average dynamic stress drop is not independent from segment to segment. Artificial reduction of the corner frequency, and modifying the rms- and peak-accelerations from each segment rupture, are methods being pursued to correct these problems.

Results

Distributions of peak acceleration at sites close to faults have been derived for faults segmented into small rupture zones. Under the assumption of independent rupture stress drops, the distribution of peak acceleration depends on the number of segments, which it should not, for large numbers of segments. Separate predictions of the distributions of rms acceleration (at the site during each rupture segment), and peak acceleration given rms, does not fully correct the dependence on number of segments. Additional methods which will be pursued are (1) artificial variation of corner frequency to obtain a value appropriate for a large earthquake, and (2) segment-to-segment correlation of site rms acceleration. Both of these will improve the peak acceleration distribution for large numbers of segments, to allow accurate estimation of ground motion close to the source for large ($M_L \approx 7-1/2$) earthquakes.

**Earthquake Hazard Maps for Selected Earthquake Scenarios
San Francisco Bay Area**

14-08-0001-21226

Jeanne B. Perkins
Association of Bay Area Governments
MetroCenter - 8th & Oak Streets
P.O. Box 2050
Oakland, CA 94604
(415) 464-7900

INTRODUCTION

A major earthquake in the San Francisco Bay Area will cause property damage, personal injury and death, and serious economic and social disruption. Earthquake hazard and risk maps play a key part in efforts to minimize these losses; organizations and people can use the maps (a) to develop ways to mitigate the mapped hazards through land use management and structural measures as well as (b) to develop loss estimates to enhance emergency response programs.

In February 1979, ABAG began a series of four projects to (1) use its computer-based geographic information system to produce maps of several types of earthquake hazards and (2) develop innovative methods of using these maps for hazard mitigation. The maps of maximum ground shaking intensity and cumulative damage potential from ground shaking produced by ABAG prior to this contract have three major inadequacies. First, the availability of detailed geologic mapping in digital form for only part of the Bay Area led to the maps being of uneven quality throughout the region. Second, the availability of more accurate fault location information in July 1983 rendered some parts of the ground shaking maps out of date. Last, and most significantly, these maps were a composite of the damage potential from ground shaking associated with many different earthquakes. Maps for selected individual earthquakes also are needed for certain applications.

RESULTS

ABAG expanded the area for which detailed mapping of geologic materials is available in digital form to cover all nine Bay Area counties. A map of these 277 material units, grouped into eight categories of similar seismic properties, was produced at 1:250,000. In addition, fault trace and fault study zone mapping available in June 1983 was incorporated into ABAG's existing computer files of these data. These fault maps also were produced at 1:250,000. The fault and geology files then were combined with seismologic data on ground shaking attenuation, the effects of local geology on intensity, and the recurrence intervals of major earthquakes to refine the maximum intensity maps and three

cumulative ground shaking maps produced in earlier contracts. The three cumulative damage potential maps for ground shaking were produced at 1:250,000 for three building types:

- o wood-frame dwellings;
- o concrete and steel-frame buildings; and
- o tilt-up concrete buildings.

A series of ground shaking intensity maps for ten selected earthquake events also was produced at 1:250,000:

- o San Andreas;
- o Northern San Andreas;
- o Southern San Andreas;
- o Hayward;
- o Calaveras;
- o Northern Calaveras;
- o San Gregorio;
- o Maacama;
- o Healdsburg-Rodger Creek; and
- o Concord-Green Valley.

Finally, maps showing hazards associated with liquefaction potential, liquefaction susceptibility, and dam failure inundation (based on work in previous contracts) were produced at 1:250,000 for ease in comparison with the maps described above. This scale (1:250,000) was chosen for this twenty map set as being appropriate for most users given the limitations of the analysis techniques.

ABAG has continued its successful program of extensive documentation and user interaction to ensure the continued and appropriate use of these maps by federal, state, and local government, other ABAG programs, transportation and utility groups, and the private sector. As an example of the usefulness of this mapped information, 38 cities and counties in the San Francisco region requested copies of over 350 of the hazard maps. ABAG, as the comprehensive regional planning agency for the Bay Area, is in a unique position to provide this service.

REPORTS

Earthquake Mapping Project Working Paper #17 - Using Earthquake Intensity and Related Damage to Estimate Maximum Earthquake Intensity and Cumulative Damage Potential from Earthquake Ground Shaking - San Francisco Bay Area, California (REVISED).

A Guide to ABAG's Earthquake Hazard Mapping Capability (REVISED).

Detailed Geologic Studies, Central San Andreas Fault Zone

9910-01294

John D. Sims
Branch of Engineering Seismology and Geology
U.S. Geological Survey
345 Middlefield Road, MS 977
Menlo Park, California 94025
(415) 323-8111, ext. 2252

Investigations

Detailed geologic field investigations of structure, and surficial and bedrock deposits in and adjacent to the central section of the San Andreas fault zone (San Juan Bautista to Wallace Creek, Carrizo Plain) were conducted to determine horizontal and vertical slip rates and the detailed tectonic environment of the zone. Investigations are conducted through detailed geologic mapping, trenching studies, and geomorphic study of offset terraces and stream courses.

Results

1. Trench studies of Holocene terrace deposits along Cholame Creek at Parkfield reveal features offset by the San Andreas fault. Age dates from sediment in these trenches yield preliminary minimum slip rate of 22-23 mm. yr⁻¹. Final slip rates await the analysis of additional ¹⁴C dates (submitted for analysis at the University of Arizona accelerator-mass spectrometry laboratory).
2. Holocene slip rate studies along the northern creeping section of the fault continue. Data reduction and interpretation of FY 83 trenching is nearly complete. Results thus far suggest the SAF at the Melendy Ranch site are nearing an average of ~800 years + 21 to 32 mm/yr during the last ~3000 years. These rates are on the base of 11 ¹⁴C dates and 2 measured affects. Additional charcoal have been submitted for ¹⁴C array. Additional trenching is scheduled for FY 84.
3. Mapping of the fault zone continues (fig. 1). Analysis of interpretation of the tectonic and stratigraphic data in the Parkfield area shows that the Gold Hill fault may be traced into the Stockdale Mountain quadrangle. Interpretation of drillers logs of boreholes for siting seismometers supports the interpretation that the Gold Hill fault NE of the San Andreas and an unnamed fault SW of the San Andreas are thrust faults resulting from N-S compression across the San Andreas zone. The geologic map data was used initially to suggest adequate sites for the dam hole seismometer.

The stratigraphic studies also reveal new correlations that are substantially at variance with existing open-file or published geologic maps for the Parkfield-Cholame area. Mapping in the Parkfield and Stockdale Mountain quadrangles will be complete in FY 84.

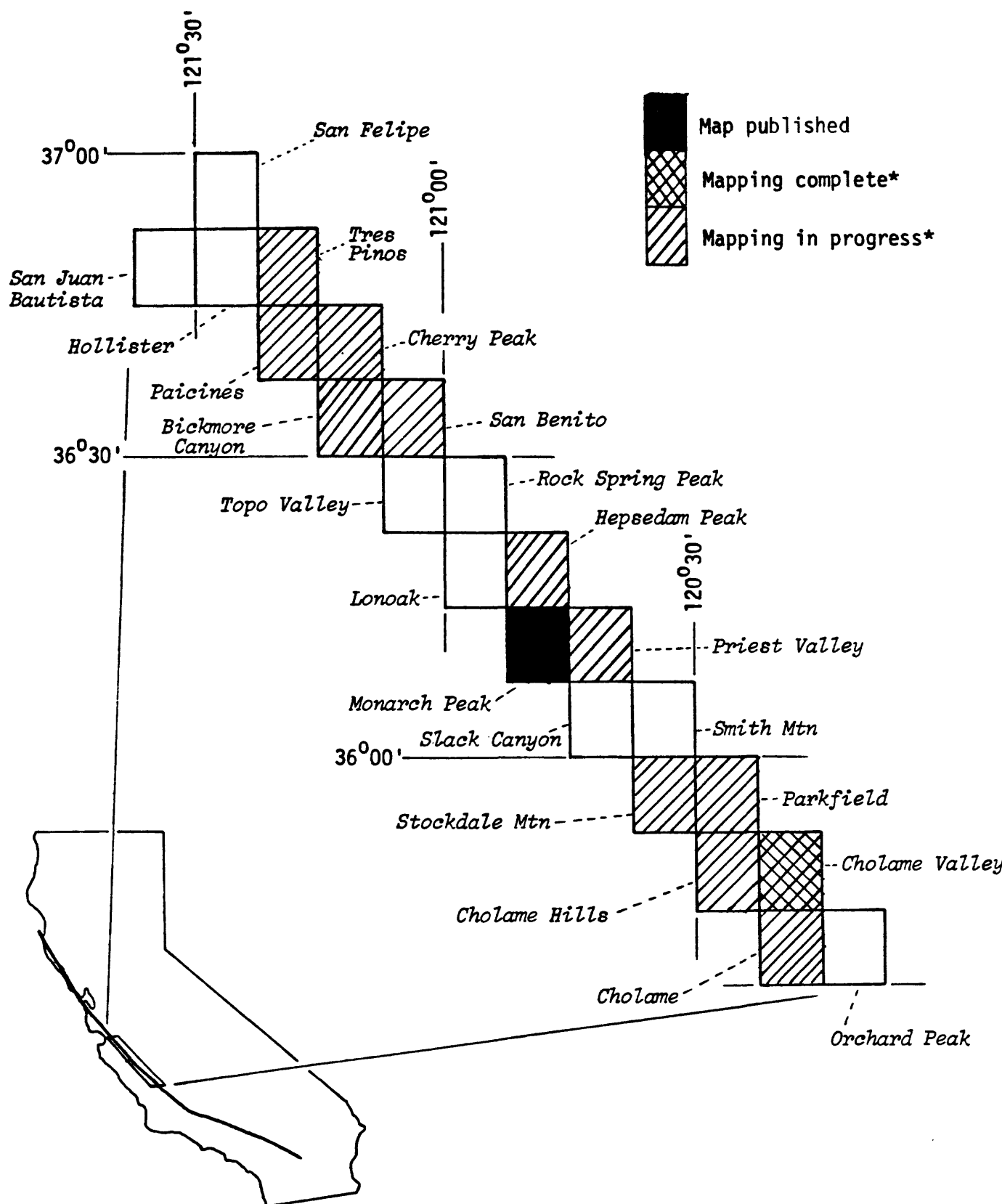


Figure 1 , Index map of 7 1/2-minute quadrangles to be studied in the detailed mapping part of the project. A part of each quadrangle is to be mapped in detail. The mapped part is a strip varying from 3 to 10 km wide that includes the San Andreas Fault Zone. The fault zone is approximately located in the middle of the mapped strip.

Reports

- Sims, J.D., 1984, Slip rates, recurrence intervals, and fault behavior--Are they related?: *Seismological Society of America, Earthquake Notes*, v. 56.
- Perkins, J.A., 1984, Problems associated with slip-rate determination from fluvial deposits: *Seismological Society of America, Earthquake Notes*, v. 56.
- Clark, M.M., Harms, K.K., Lienkaemper, J.J., Harwood, D.S., Lajoie, K.R., Matti, J.C., Perkins, J.A., Rymer, M.J., Sarna-Wojcicki, A.M., Sharp, R.V., Sims, J.D., Tinsley, J.C., III, and Zions, J.I., 1984, Preliminary slip-rate table and map of Late-Quaternary faults of California: U.S. Geological Survey Open-File Report 84-106.

Source Characteristics of Eastern and Central United States
Earthquakes from Broad-Band Digital Seismographs

14-08-0001-21261

G.H. Sutton, P.W. Pomeroy, and J.A. Carter
Rondout Associates, Incorporated
P.O. Box 224, Stone Ridge, New York 12484
(914) 687-9150

Investigations

Broad-band digital data, principally of the Catskill Seismic Array (CSA), from selected earthquakes in eastern and central United States and Canada are being analyzed and compared with "complete" synthetic seismograms in order to define the source characteristics as precisely as possible.

Results

The Long Island Sound earthquake of 10/21/81 ($m_b=3.5$, $\Delta=1.4^{\circ}$) recorded at CSA provides an example of the results of analyses conducted to date: seismic moments and corner frequencies are obtained from Lg, Figure 1; array processing and polarization filtering improves signal-to-noise ratio, sharpens signal onsets, and facilitates arrival identification, Figures 2A, 2B, and 3A; comparison with theoretical arrival times and with "full seismogram" synthetics provides information on focal depth and source mechanism, Figures 3A and 3B.

The match of synthetic to observation is good for the P arrivals but not for the S-Lg wavetrain. Other velocity models and focal mechanisms are being investigated to improve the fit and to establish an estimate of the uniqueness of the focal parameters determined. The following model is used for the arrival times and synthetics shown in the figures.

| DEPTH (km) | THICKNESS (km) | V _p (km/sec) | V _s (km/sec) | ρ (gm/cc) | Q |
|---------------|-------------------|----------------------------|----------------------------|-------------------|------|
| 7 | 7 | 6.1 | 3.3 | 2.85 | 250 |
| 17 | 10 | 6.6 | 3.59 | 3.05 | 250 |
| 34 | 17 | 6.6 | 3.59 | 3.05 | 2000 |
| 284 | 250 | 8.1 | 4.52 | 3.35 | 2000 |
| CAP | 10 | 20.0 | 15.0 | 10.00 | 10 |

Reports

Carter, J.A., G.H. Sutton, and P.W. Pomeroy, Analytical Procedures for 3-Component Digital Array Data, (Abs.), Seis. Soc. Am. Eastern Section Meeting Programs and Abstracts, 40, 1983.

Carter, J.A., G.H. Sutton, and P.W. Pomeroy, Depth and Focal Mechanisms of Shallow Eastern U.S. Earthquakes from Broad-Band Digital Array Data, (Abs.), EOS, 64, 767, 1983.

Sutton, G.H., J.A. Carter, and P.W. Pomeroy, Local and Regional Earthquakes Recorded at the Catskill Seismic Array, (Abs.), EOS, 64, 266, 1983.

Sutton, G.H., J.A. Carter, and P.W. Pomeroy, Source Characteristics of Eastern and Central North American Earthquakes from Broad-Band Digital Array, (Abs.), IASPEI Program and Abstracts, Hamburg, 86, 1983.

Sutton, G.H., J.A. Carter, and P.W. Pomeroy, Source Characteristics of Eastern and Central North American Earthquakes from a Broad-Band Digital Array, (Abs.), Seism. Soc. Amer. Eastern Section Meeting Program and Abstracts, 41, 1983.

Sutton, G.H., P.W. Pomeroy, and J.A. Carter, Source Characteristics of Eastern and Central United States Earthquakes from a Broad-Band Digital Array, Final Technical Report, Contract No. 14-08-0001-20522, U.S.G.S., 15 December 1981-14 December 1982, Rondout Associates, Inc., 1983.

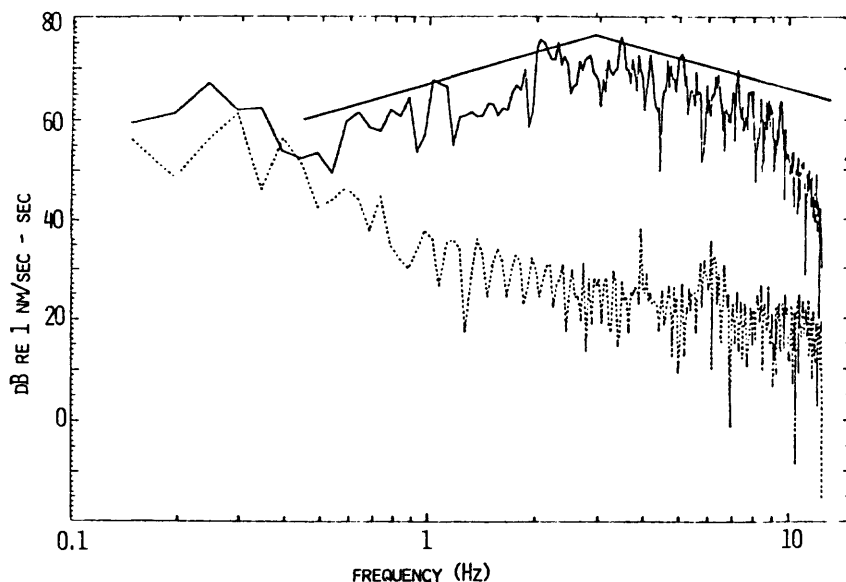


Figure 1

Figure 1. Velocity spectrum for Lg of Long Island Sound earthquake. Straight lines are ± 6 dB/oct (ω and ω^{-1}).

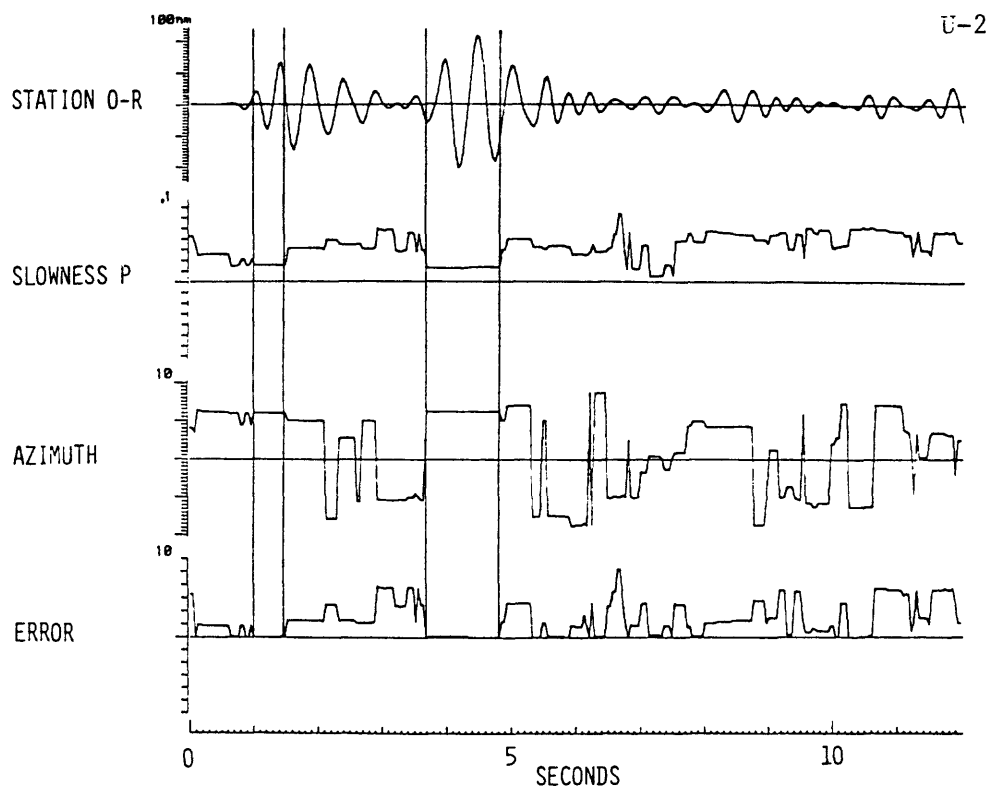


Figure 2A

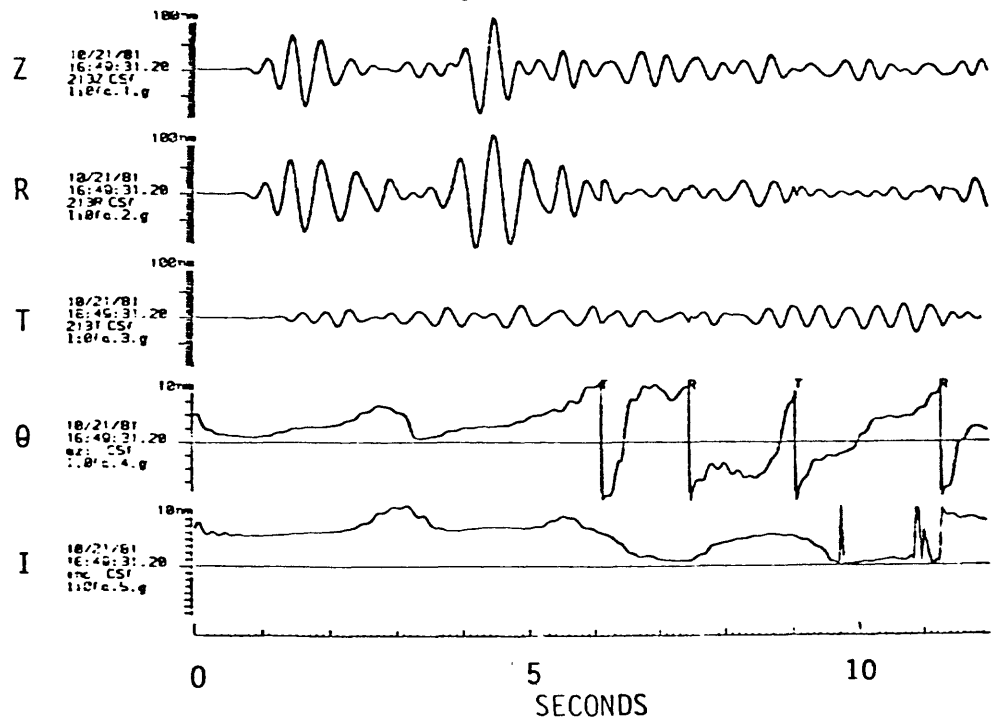


Figure 2B

Figure 2A. P-wave (1.5-3 Hz band-pass) beam forming using three radial (rotated) component elements of CSA; slowness in sec/km and azimuth in degrees; one element trace shown at top.

Figure 2B. Adaptive polarization analysis. T and R indicate times when relative azimuth, θ , exceeds 45° from great circle path reference direction and horizontal traces are interchanged. I is apparent angle of incidence.

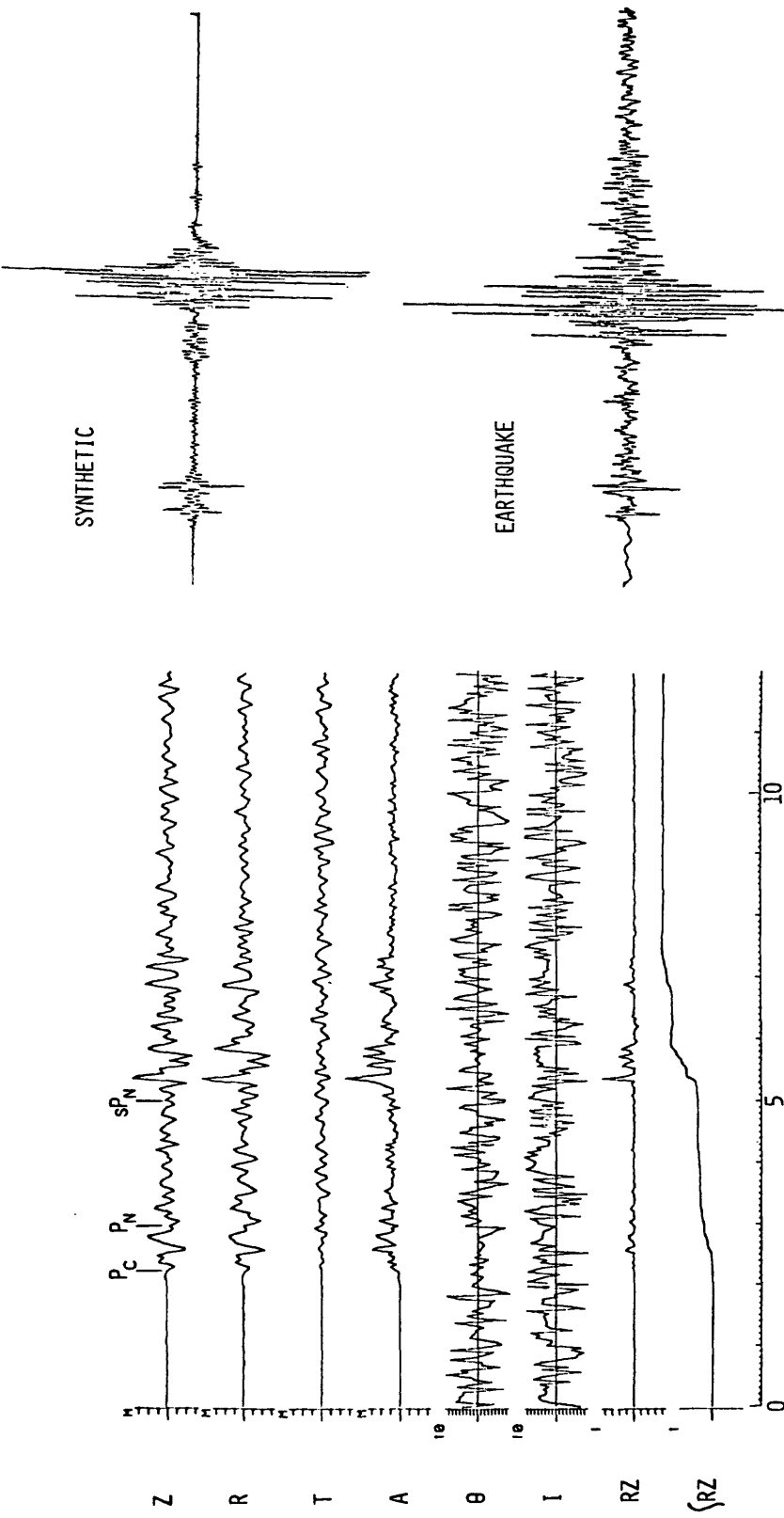


Figure 3A
Model arrival times for $h=5.25$ km compared with polarization filtered P-waves (1.5-6 Hz band-pass).



Figure 3B
Full seismogram synthetic

Figure 3A. Model arrival times for $h=5.25$ km compared with polarization filtered P-waves (1.5-6 Hz band-pass).
 SP_n if properly identified is a sensitive measure of focal depth.

Figure 3B. Full seismogram synthetic compared with observation: flat to velocity 0-3 Hz; $h=7$ km, strike 45° , dip 45° , normal dip slip, step function in time.

Source Characteristics of Recent Earthquakes in the Northeastern
United States - Implications for Earthquake Hazards

Contract No. 14-08-0001-21284

M. Nafi Toksöz and Jay J. Pulli
Earth Resources Laboratory
Massachusetts Institute of Technology
42 Carleton St.
Cambridge, MA 02142
(617) 253-6382

Investigations:

- 1) Determination of the source mechanism of the January 19, 1982 Gaza, NH earthquake using regional seismic data.
- 2) Development of routine computational procedures for the determination of microearthquake source spectra in New England.
- 3) Incorporation of the intensity data for the October 7, 1983 Adirondack, NY earthquake ($m_b=5.2$) into the ground motion attenuation models for the northeastern U.S.
- 4) Comparison of the strong motion records for the New Brunswick earthquakes and the central U.S. dataset with the ground motion attenuation models derived for the northeastern U.S.

Results:

- 1) The Gaza, NH earthquake of January 19, 1982 was of magnitude 4.6 (m_b) and produced intensity V (M.M.) effects in the epicentral area. The location we have obtained is: lat. 43.52, long. -71.61, depth 3 km¹. Twenty-four P-wave first motions were used to determine the focal mechanism of the main shock. The fault plane solution shows right-lateral strike-slip faulting. We have now begun to study this earthquake using regional seismic data from ECTN, DWWSSN, and RSTN stations. Much time has been spent reading and reformatting data tapes from the various networks. Instrument transfer functions were used to calculate ground motions, but in a number of cases, the published transfer functions were found to be in error. Figure 1 shows two examples of regional data for this earthquake. OTT is at a distance of 387 km and MNT is at 273 km. The spectra below each seismogram show the instrument deconvolved ground motion corrected for geometrical spreading and attenuation². The corner frequencies for these records are between 1 and 2 Hz. Results of the inversion of the teleseismic P-wave at the short

period station ANMO (also in Figure 1) indicate a seismic moment of $3E22$ dyne*cm and a focal depth of 3.4 km. The source time function is shorter or equal to the resolution limit of the data, which is about 0.2 sec¹.

2) The M.I.T. Seismic Network consists of 9 short period stations in New Hampshire and Massachusetts. The data are transmitted to the M.I.T. campus in Cambridge and recorded digitally on an HP/1000 computer at a sampling rate of 100 s/sec. We have now begun to routinely examine the source spectra for all new events, and are reviewing older records for processing. The goal is to be able to quickly measure the seismic moment and corner frequency for an event, and to compare the source spectrum versus moment relationship in New England with those of other parts of the country. Step function generators have been installed at some stations and we are examining the stability of the instrument responses with time. Preliminary results suggest that corner frequencies for a given seismic moment are higher in New England than in the central and southeastern U.S. However, we are closely examining possible sources of error (instrument effects, path effects, site effects) before this result can be deemed conclusive.

3) Because of the lack of an adequate strong motion database in the northeastern U.S., we have turned to the use of intensity data to develop ground motion attenuation models ³. The intensity attenuation model we have obtained to date is

$$I(r, m_b) = -1.43 + 1.79(m_b) - 0.0018(r) - 1.83[\log_{10}(r)]$$

where r is the epicentral distance in km. With the assistance of the Lamont-Doherty Geological Observatory, we have collected approximately 400 new intensity datapoints for the October 7, 1983 Adirondack earthquake. This earthquake was of magnitude 5.2 (m_b). This new data not only increases our database by 20%, but also provides better coverage for areas west of the Appalachians where the attenuation of seismic waves is lower ^{2,4}. Intensity attenuation models are now being recalculated by really separating the datasets. Isoseismals for the October 7, 1983 earthquake are in general larger than those predicted by the above equation, which is in agreement with the difference in seismic wave attenuation.

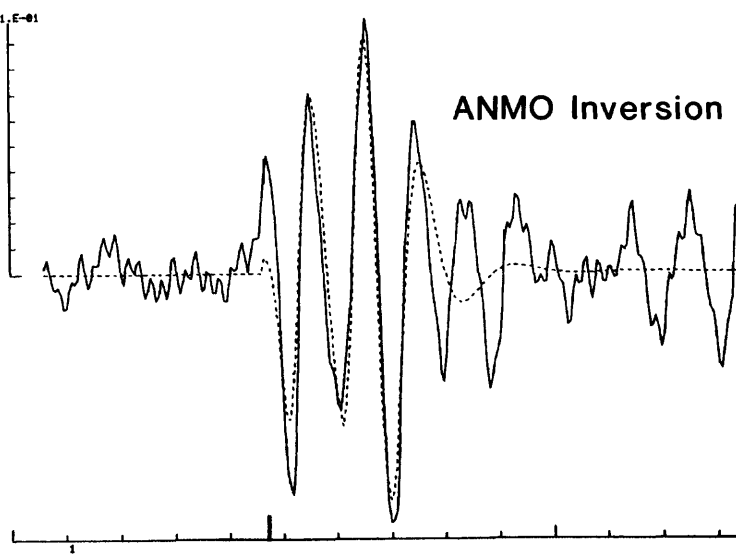
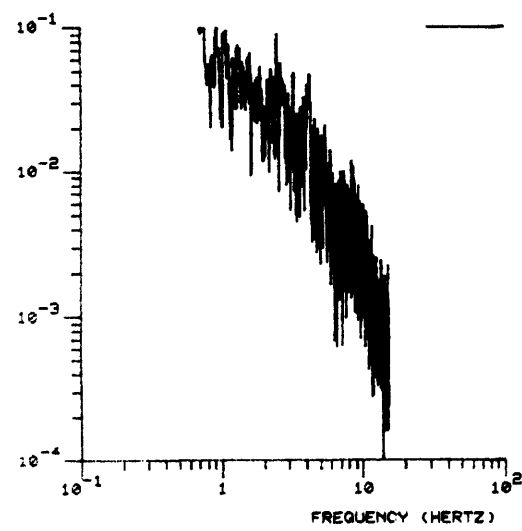
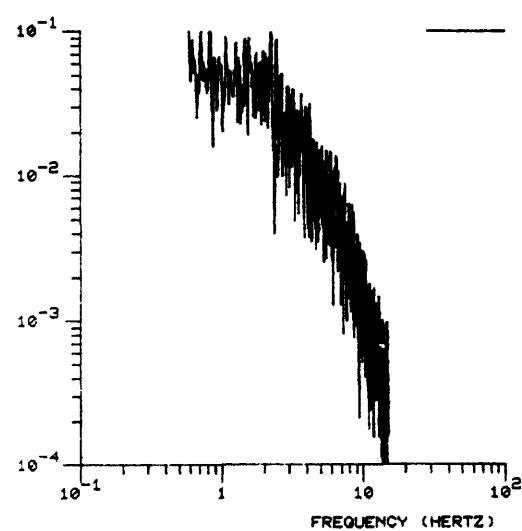
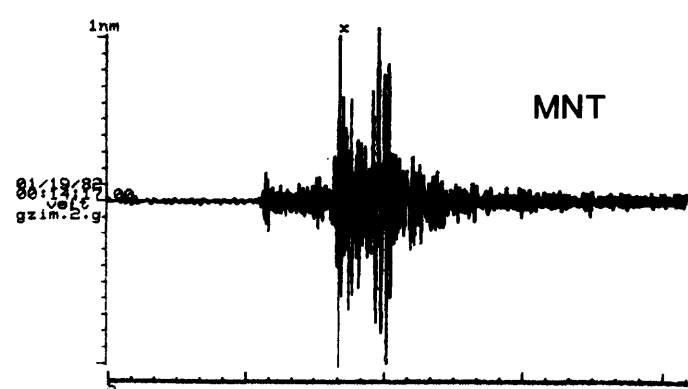
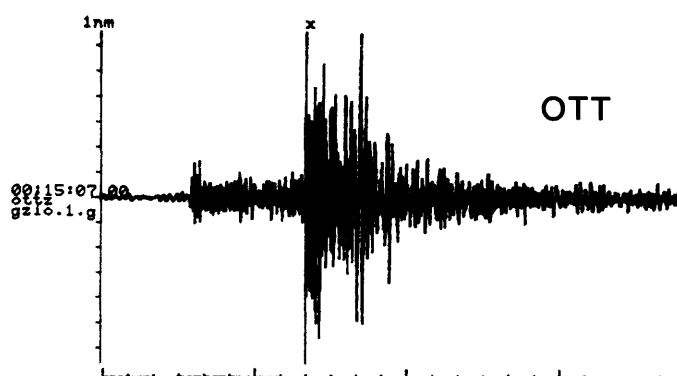
4) Recent publications of strong motion recordings in the northeastern U.S. ^{5,6} have allowed us to check the applicability of our intensity-derived ground motion attenuation relationships. Scatter in the acceleration data is in general greater than that in the velocity data. Using an interactive graphical statistical technique known as scatterplot matrices, we are examining the relationships of acceleration and velocity to earthquake magnitude, distance, intensity, site condition, and region (Appalachian versus Grenville). This has involves comparison with the strong motion dataset for the central U.S. ⁷.

Reports:

1. Pulli, J.J., Nabelek, J.L., and Sauber, J.M. (1983), Source parameters of the January 19, 1982 Gaza, NH earthquake, presented at the Eastern SSA Meeting, New Paltz, NY, September 19-21.
2. Pulli, J.J. (1984), Attenuation of coda waves in New England, *Bull. Seis. Soc. Amer.*, 74, in press (August issue).
3. Klimkiewicz, G.C. and Pulli, J.J. (1983), Ground motion attenuation models for New England, *abstract, Earthquake Notes*, 54, No. 1, 10-11.

References:

4. Singh, S. and Herrmann, R.B. (1983), Regionalization of crustal coda Q in the continental United States, *J. Geophys. Res.*, 88, 527-538.
5. Weichert, D.H., Pomeroy, P.W., Munro, P.S., and Mork, P.N. (1983), Strong motion records from Miramichi, New Brunswick, 1982 aftershocks, *Earth Physics Branch Open File Report 82-31*.
6. Chang, F.K. (1983), Analysis of strong motion data from the New Hampshire earthquake of 19 January 1982, NUREG/CR-3327, 17 pp. plus appendices.
7. Herrmann, R.B. (1977), Anaylsis of strong motion data from the New Madrid Seismic Zone: 1975-1976, Dept. of Earth and Atmospheric Sciences Report, St. Louis University.



Liquefaction Investigations

9910-01629

T. Leslie Youd
Branch of Engineering Seismology and Geology
U.S. Geological Survey
345 Middlefield Road, MS 977
(415) 323-8111, Ext. 2114

Investigations

1. With John Tinsley, Dave Perkins, and Albert Chen, continued compilation of liquefaction susceptibility and liquefaction opportunity maps for the Los Angeles basin area.
2. Made final revisions to a liquefaction susceptibility map for San Mateo County, California.
3. With Albert Chen, continued investigation of liquefaction potential of debris in the blockages impounding Spirit, Castle Creek, and Cold Water Lakes north of Mount St. Helens.
4. Continued studies of sites in the Imperial Valley, California where liquefaction occurred during earthquakes in 1979 and 1981.
5. Using observations from past earthquakes and engineering principles, analyzed the potential for recurrence of liquefaction at sites of past liquefaction.
6. Made a reconnaissance investigation of liquefaction effects generated by the October 28, 1983 Borah Peak, Idaho earthquake.

Results

1. Over the past few years this project has conducted subsurface investigations at several sites in the Imperial Valley where liquefaction developed during at least one of the earthquakes that occurred in 1957, 1979, and 1981. During the past 6 months a comprehensive set of data from those investigations were compiled into a report which lists results from cone penetration tests, standard penetration tests, and sediment property tests. Penetration data and sediment properties were used to classify sediment and develop sediment and geotechnical soil profiles at 68 sounding sites. These sounding sites are grouped into 11 study areas, of which five are described in detail. Some of these sites have been further probed, sampled, and tested in cooperative studies with researchers from Purdue University, Stanford University, Rensselaer Polytechnic Institute, the University of British Columbia, and the University of Texas. The studies show that in all instances liquefaction occurred in mixtures of loose fine sand and loose silt that were deposited in channel, flood plain, or deltaic environments during the late-Holocene.
2. A review of the literature from several past earthquakes revealed several localities in Japan and the United States where liquefaction has occurred

at the same site during two or more earthquakes. Using published data and geotechnical engineering principles to analyze recurrence of liquefaction, we found that earthquakes generally liquefy soil layers from the top downward and compact them from the bottom upward. This process usually creates a loose zone at the top of the layer which may persist through many earthquakes until compaction is complete and which may repeatedly liquefy. We also found that shear deformation produced by ground failure displacement, such as shear in the failure zone beneath a lateral spread, can dilate or loosen granular soils leaving them as susceptible or even more susceptible to liquefaction than they were before the initial episode of liquefaction. We concluded that sites of past liquefaction are likely to be hazardous sites during future earthquakes and maps and records of locations of past occurrences of liquefaction provide key information of earthquake hazard assessments.

3. On October 28, 1983, a magnitude 7.3 (M_s) earthquake struck the Borah Peak area of south-central Idaho causing considerable damage and generating liquefaction in susceptible sediment. A reconnaissance investigation of the affected area was made to locate, describe, document, and map liquefaction and associated ground failure effects. Liquefaction effects were found at many locations in the Big Lost River and Thousand Springs Valleys and at two localities in the Pahsimeroi Valley. The effects included sand boils, fissures, lateral spreads, and buoyant rise of a small buried tank. We found that most liquefaction developed in late Holocene sediment, but liquefaction also developed in late Pleistocene sediment where lateral spreads occurred at the distal end of alluvial fans along the north side of the Thousand Springs Valley. These findings are in agreement with experience in other parts of the world. On the other hand, we found that the distance from the fault rupture to the farthest localities of liquefaction was much less than generally would be expected for an earthquake of this magnitude.

Reports

Bennett, M.J., McLaughlin, P.V., Sarmiento, J.S., and Youd, T.L., 1984, Geotechnical investigation of liquefaction sites, Imperial Valley, California: U.S. Geological Survey Open-File Report 84-252, 103 p.

Youd, T.L., 1984, Recurrence of liquefaction at the same site: Eighth World Conference on Earthquake Engineering, San Francisco, California, Proceedings, v. 3, in press.

Youd, T.L., Harp, E.L., Keefer, D.K., and Wilson, R.C., 1984, Liquefaction generated by the 1983 Borah Peak, Idaho, earthquake: Earthquake Engineering Research Institute Reconnaissance Report, in press.

Physical Constraints on Source Ground Motion

9910-01915

D.J. Andrews
Branch of Engineering Seismology and Geology
U.S. Geological Survey
345 Middlefield Road, MS 977
Menlo Park, California 94025
(415) 323-8111, ext. 2752

Investigations

A numerical method for calculation of spontaneous rupture on a plane.

Results

A numerical boundary integral (Green function) method has been adapted for use with a generalized frictional sliding law on a fault plane.

Report

Andrews, D.J., 1984, Dynamic plane-strain rupture with a slip-weakening friction law calculated by a boundary integral method: to be submitted to *Bulletin, Seismological Society of America*.

Global Accelerograph Program (GAP)

9910-02689

R. D. Borcherdt
Branch of Engineering Seismology and Geology
U.S. Geological Survey
345 Middlefield Road, MS 977
Menlo Park, California 94025
(415) 323-8111, ext. 2755

Investigations

The objective of this program is to obtain critically needed records of damaging levels of ground motion close to the source of earthquakes of magnitude M 6.5 and greater.

During the second half of FY 83, the following activities were carried out:

- (1) Negotiation of formal GAP agreements with counterpart agencies in countries with significant earthquake potential was continued.
- (2) Field deployments of a General Earthquake Observation System (GEOS) were carried out near Morgan Hill, California.

Results

The prototype GAP agreement developed for the program identifies the following primary activity elements: (1) continued long-term strong-motion data and information exchange between the U.S. Geological Survey and the agency(ies) identified in the host country; 2) the rapid exchange (preferably as soon as possible--within 1-4 days following damaging events) of scientific teams to investigate engineering and scientific effects of large earthquakes in the U.S. and the host country; and 3) the rapid deployment of U.S. personnel and instruments to the host country after a large earthquake (M 7.5 and greater) has occurred to record large (M 6.5 and greater) aftershocks. In some cases, the installation and long-term operation of a permanent network of strong-motion instruments in the host country shall also be considered under the agreement.

- (1) Negotiation of agreements is proceeding, but not as quickly as desired. Changes in foreign government officials has in some cases required renegotiation of agreements. Negotiations for a GAP agreement were completed with the country of Turkey.
- (2) Final modifications of GEOS based on field deployment experience are being incorporated.
- (3) Wide dynamic range, broad frequency band-width data sets were collected near Morgan Hill, California using the General Earthquake Observation System (GEOS).

Reports

- Borcherdt, R.D., Jensen, E.G., Maxwell, G.L., Fletcher, J.P., McClearn, R., Van Schaack, J.R., and Warrick, R.E., 1983, A General Earthquake Observation System (GEOS) [abs.]: *Workshop on Portable Digital Seismograph Development*, Los Altos, California, October 1983.
- Borcherdt, R.D., 1982, Recent advances in the acquisition of strong-motion data [abs.]: *Eighth World Conference on Earthquake Engineering*, July 21-28, 1984, San Francisco, California.
- Borcherdt, R.D., 1983, On recent advances in strong-motion data acquisition capabilities: *Proceedings, 8th World Conference*, San Francisco, California, July 1984.
- Borcherdt, R.D., Anderson, J.G., Crouse, C.B., Donovan, N.C., McEvilly, T.V., and Shakal, T.F., 1984, National Planning considerations for the Acquisition of Strong Ground-Motion Data: *Earthquake Engineering Research Institute Special Publication*.
- Fletcher, J.B., Borcherdt, R.D., Mueller, C., and Cranswick, E., 1984, Data from the GEOS digital recorder: *Proceedings, Controlled Source Seismology Conference*.
- Maxwell, G.L., Jensen, E.G., Borcherdt, R.D., Fletcher, J.P., McClearn, R., Van Schaack, J.R., and Warrick, R.E., 1983, GEOS [abs.]: *American Geophysical Union Fall Meeting*, December 5-14, 1983, San Francisco, California.

Strong-Motion Interpretation for Structural Engineering

9910-02759

Joseph J. Fedock/ Hsi-Ping Liu
Branch of Engineering Seismology and Geology
U.S. Geological Survey
345 Middlefield Road, MS 977
Menlo Park, CA 94025

Investigations

Research efforts are directed towards improvements in our current understanding of the strong-motion response of engineering structures. For the first half of FY 84, these investigations have focused upon the following areas:

- 1) Development of a methodology for the dynamic testing of concrete dams,
- 2) Design of strong-motion instrumentation schemes for buildings, dams, and other structures, and
- 3) Analysis of strong-motion data obtained from well instrumented structures.

Results

A specific thin arch dam, Monticello Dam, California, has been identified as being suitable for testing of the methodology. A proposal to the U.S. Bureau of Reclamation, owners of the dam, outlining the testing procedures has been approved. Initial planning efforts, including modification of the air gun test equipment for this application, analysis of existing construction plans and maps, and coordination with Bureau of Reclamation personnel have been completed.

Strong-motion instrumentation has been implemented at the Hayward City Hall in which both free-field and structure accelerographs have been placed. The instrumentation design of the Transamerica Building is also being implemented and the designs of instrumentation schemes for several other buildings in the San Francisco Bay area have been completed. Several additional instrumentation designs are being planned.

An instrumentation scheme designed for Leroy Anderson Dam has yielded significant strong-motion records from the April 24, 1984 Mt. Hamilton Earthquake.

Analysis of the strong-motion records from Long Valley Dam during the May 1980 Mammoth Lakes Earthquakes shows that the dam response was characterized by complex behavior during the three largest events of the earthquake sequence. Several modes in both the transverse and longitudinal directions contributed significantly to the overall response of the embankment. Rocking behavior was also observed during all three events. More extensive analysis of these records is continuing.

Reports

None.

Estimating Strong Ground Motion
for Engineering Design and Seismic Zonation

9910-01168

W. B. Joyner
D. M. Boore

Branch of Engineering Seismology and Geology
U. S. Geological Survey
345 Middlefield Road, MS 977
Menlo Park, California 94025
(415) 323-8111, ext. 2754, 2698

Investigations

1. Analysis of strong-motion data leading to the development of predictive equations for strong-motion parameters and development of methodology for making predictive maps of strong ground motion.
2. Cooperation with professional groups in the development of code provisions for earthquake resistance.
3. Study of the scaling of earthquake spectra.

Results

See below.

Reports

Bakun, W.H., and Joyner, W.B., 1984, The M_L Scale in Central California: *Bulletin, Seismological Society of America*, submitted.

Boore, D.M., and Joyner, W.B., 1984, A note on the use of random vibration theory to predict peak amplitudes of transient signals: *Bulletin, Seismological Society of America*, in press.

Joyner, W.B., and Fumal, T.E., 1984, Predictive mapping of ground motion, in *Evaluating Earthquake Hazards in the Los Angeles Region: U.S. Geological Survey Professional Paper*, in press.

Joyner, W.B., and Boore, D.M., 1984, Ground motion prediction for design: progress and issues, *Proceedings ATC Seminar on Earthquake Ground Motion and Building Damage Potential*, March 1984, San Francisco, California.

Joyner, W.B., and Boore, D.M., 1984, Magnitude Saturation, *Proceedings EERI Workshop on Strong Ground Motion Simulation and Earthquake Engineering Applications*, April 30-May 3, 1984, Los Altos, California.

The Effects of Site Geology on Ground Shaking on the
Wasatch Front

9950-03788

A. M. Rogers
 Branch of Engineering Geology and Tectonics
 U.S. Geological Survey
 Box 25046, MS 966, Denver Federal Center
 Denver, CO 80225
 (303) 234-2869/5604

Investigations

During the reporting period we have examined ground motion data recorded in the Wasatch region (King and others, 1983) for correlations with the underlying geological conditions (Van Horn, 1972; Miller, 1982) at each recording site.

Results

We have constructed a matrix of site response data for the Ogden, Logan, Provo, and Salt Lake City areas based on recordings in these areas of Nevada Test Site nuclear tests and maps of site geology. This matrix contains the mean spectral ratios (alluvium-to-rock spectral ratio pairs) in three period bands, soil type, Quaternary formation, age of the surficial material, an approximation of Quaternary sediment thickness, and a description of the lithology at each site. More characteristics will be added to the data base as the study progresses.

Observed ground response for the Wasatch Front urban sites appears to increase with decreasing age:

Mean spectral ratios

| Age | 0.2-0.7 (s) | 0.7-1.0 (s) | Number of samples |
|----------------------------|----------------|----------------|----------------------|
| Post-Bonneville Lake----- | 6.4 | 9.1 | 12 |
| Late Bonneville Lake----- | 5.0 | 6.4 | 25 |
| Early Bonneville Lake----- | 4.2 | 3.7 | 5 |

Mean ground response is also a function of soil lithology:

Mean spectral ratios

| Soil | 0.2-0.7 (s) | 0.7-1.0 (s) | Number of samples |
|----------------------|----------------|----------------|----------------------|
| Silt and clay----- | 6.9 | 8.1 | 20 |
| Sand and gravel----- | 4.2 | 6.4 | 7 |
| Rubble | 3.3 | 3.6 | 5 |

Attempts to further sort the descriptions by lithology reduce the number of observations per category to the extent that meaningful averages are not possible.

In the future these results will be used to produce maps depicting the geographical variation in relative ground shaking expected in a large earthquake. These maps will cover a 10-county region including the Wasatch Front.

References

King, K. W., Hays, W. W., and McDermott, P. J., 1983 [1984], Wasatch Front urban area seismic response data report: U.S. Geological Survey Open-File Report 83-452, 70 p. (in press).

Miller, R. D., compiler, 1982, Surficial geologic map along part of the Wasatch Front, Great Salt Lake and Utah Lake valleys, Utah: U.S. Geological Survey Miscellaneous Field Studies Map MF-1477, scale 1:100,000, accompanied by a 14 p. text.

Van Horn, Richard, 1972, Surficial geologic map of the Sugar House quadrangle, Salt Lake County, Utah: U.S. Geological Survey Miscellaneous Geologic Investigations Map I-766-A, scale 1:24,000.

Strong Ground Motion Prediction in
Realistic Earth Structures

9910-03010

P. Spudich

Branch of Engineering Seismology and Geology
U.S. Geological Survey
345 Middlefield Road, MS 977
Menlo Park, California 94025
(415) 323-8111, ext. 2395
10/1/83 to 3/31/84

Investigations

1. Measurement of the transient soil strains observed at the El Centro differential array during the 1979 Imperial Valley earthquake.
2. Examination of the relative abilities of temporal changes in rupture velocity and spatial changes in slip velocity or stress drop on a fault to cause ground accelerations.
3. Preliminary design of a short-baseline two-dimensional accelerometer array for installation at Parkfield, California, for the observation of earthquake rupture dynamics.

Results

1. Strong ground motions caused by the 1979 Imperial Valley earthquake ($M_s = 6.9$) at the El Centro differential array, 5.6 km from the ground rupture, were caused primarily by direct P and S body waves originating from the fault at depth. Vertical and horizontal ground motions had propagation slownesses (1/velocity) of 0.11-0.19 s/km and 0.19-0.33 s/km, respectively, after near-surface perturbations were removed. Strains were deduced from the observed propagation slownesses and the measured ground velocities by assuming plane waves incident upon the array (a good approximation in this case). By far the largest strains were associated with derivatives of displacement with respect to depth. These strains went as high as 4.5×10^{-3} (5.5 inches/100 ft). However, strains in the horizontal direction were much smaller, reaching an upper bound of 2.2×10^{-4} (0.26 inches/100 ft). The reason why vertical derivatives overwhelm horizontal derivatives in this case is because the near-surface P and S waves travelled nearly vertically in the near-surface material. These strains are somewhat smaller than usually assumed by structural engineers because of the near-vertical incidence of the waves. These strains are of the type responsible for damaging large foundations, long structures like bridges, and underground pipes during earthquakes.
2. In collaboration with L. Neil Frazer of the Hawaii Institute of Geophysics, we analyzed the problem of calculating high-frequency ground motions (>1 Hz) caused by earthquakes having arbitrary spatial variations of rupture velocity and slip velocity (or stress drop) over the fault. Using geometric ray theory and assuming a simple parameterization of the slip function, the computational problem collapses to the evaluation of a

series of line integrals over the fault, with one line integral per each time t_i , in the observer seismogram. The path of integration corresponding to observation time t_i consists of only those points on the fault which radiate body waves arriving at the observer at exactly time t_i . This path is an isochron of the arrival time function. An isochron velocity may be defined that depends on rupture velocity and reduces to the usual directivity function in certain cases. Although ground motions are indirectly related to rupture velocity, they are directly dependent upon isochron velocity. Ground velocity is proportional to isochron velocity and ground acceleration is proportional to isochron acceleration in dislocation models of rupture. Ground acceleration may also be related to spatial variations of slip velocity on the fault, using isochron velocity as a constant of proportionality. We found two rupture models, one with variable rupture velocity and the other with variable stress drop, that caused the same ground acceleration at a single observer. In addition, the computer code we developed for these calculations runs 50 times faster than similar ground motion synthesis methods which use complete Green's functions.

3. In collaboration with David Oppenheimer, we have initiated design of a two-dimensional array of accelerometers to be installed at Parkfield, California. We hope to use this array to record the next Parkfield earthquake. The array will consist of about 25 digital, 3-component accelerometers, located within a 2 km^2 area. The array design is being optimized to observe the rupture front in two dimensions as it propagates down the fault, although it will also be of use for studies of transient soil strain during the earthquake. To design the array, we are synthesizing ground motions at each proposed array element site, using the method discussed in investigation 2, above. The motions are analyzed by a moving window frequency-wavenumber analysis method. We break the ground motion into short time slices (1-2 seconds), and do f-k analysis on each time slice. For each slice we thus determine the directions from which energy impinges on the array. We then raytrace this energy back to its source on the fault plane.

Reports

Spudich, P., and Ascher, U., 1983, Calculation of complete theoretical seismograms in vertically varying media using collocation methods, *Geophys. J. Roy. Astron. Soc.*, **75**, 101-124.

Spudich, P., and Cranswick, E., 1984, Soil strains and horizontal propagation velocities of strong ground motions observed during the 1979 Imperial Valley, California, earthquake [abs.]: *Eighth World Conference on Earthquake Engineering*, July 21-28, 1984, San Francisco, California.

Spudich, P., and Cranswick, E., 1984, Direct observation of rupture propagation during the 1979 Imperial Valley, California, earthquake using a short baseline accelerometer array, accepted, *Bull. Seism. Soc. Am.*

Spudich, P., and Frazer L.N., 1983, High frequency ray theory synthetic seismograms for earthquakes: theory and examples [abs.]: *EOS*, **64**, 773.

Spudich, P., and Frazer, L.N., 1984, The relationship between earthquake ground motions and spatial variations in rupture velocity and slip on a fault [abs.]: *EOS*, **65**, 234.

**INVESTIGATION OF AREAS OF RECURRING LIQUEFACTION
IN THE VICINITY OF THE NEW AND ALAMO RIVERS,
IMPERIAL VALLEY, CALIFORNIA**

Contract No. 14-08-0001-21232

Kenneth H. Stokoe, II
Civil Engineering Department
The University of Texas at Austin
Austin, Texas 78712 (512) 471-4929

INVESTIGATIONS

On April 26, 1981 an earthquake of magnitude 5.6 occurred in the northwestern part of the Imperial Valley. Damage due to this earthquake is estimated at 1 to 3 million dollars, mainly due to structural damage in the towns of Westmorland and Calipatria. In addition, liquefaction and other secondary ground effects occurred over a large area.

Field personnel were deployed in January, 1983 to investigate sand deposits in this area which have liquefied in past earthquakes. The locations of five study sites investigated are shown in Figure 1. The Wildlife site was of most interest because it has been instrumented to monitor ground motions and porewater pressure buildup in the soil in order to monitor soil behavior during future earthquakes. At each of the study sites investigated a sand or silt layer liquefied during the 1979 Imperial Valley earthquake and/or the 1981 Westmorland earthquake.

Field tests performed at the sites included: Standard Penetration Tests (SPT), Electrical Cone Penetration Tests (CPT), Crosshole Seismic Tests, and Spectral-Analysis-of-Surface-Waves Tests (SASW). The last two tests listed were used to determine the shear wave velocity versus depth profiles. A composite profile of the Wildlife site is shown in Figure 2.

Soil samples of the liquefiable sands and silts were taken at four of the sites. These samples were drained in the field to prevent excessive disturbance and transported to the laboratory. Resonant column tests were then performed on trimmed specimens. The resonant column tests were used to obtain the relationship between shear modulus and material damping ratio as a function of duration of confinement, magnitude of confining pressure, and shearing strain amplitude. The resonant column test results as well as the field test results were then used in the liquefaction analyses described below.

ANALYSES

In terms of the analytical study, the main objective is to evaluate the predictive capabilities of the methods which are in use at the present time (empirical correlations with SPT and CPT, Seed's simplified procedure, and the cyclic stress approach). In addition, a recently developed method (the cyclic strain approach) is also being evaluated. These predictive methods are being compared through the use of the study sites. The case histories derived from these sites are unusual in that there was much recorded seismic data from two recent earthquakes which

occurred in the Imperial Valley region (1979 and 1981 earthquakes). In addition, field observations of surface manifestations of liquefaction are very detailed and thorough.

The empirical correlations used in this study consist of relating the SPT resistance and CPT resistance with the cyclic stress ratio occurring at a site at the time of a given earthquake. This relationship is then compared to other case histories to give an estimate of the liquefaction susceptibility of the site. In the simplified procedure, the shear stresses occurring in the field are correlated with shear stresses causing liquefaction in the laboratory (usually determined by cyclic triaxial tests) to estimate whether or not liquefaction should have occurred during that earthquake.

In the cyclic stress approach, stresses occurring in the field are estimated by computer analyses (SHAKE and DESRA are being used) which take digitized earthquake records and propagate them numerically through a soil profile. In this study, the earthquake records are being scaled (multiplied by a certain factor to increase or decrease the peak horizontal ground surface acceleration (a_{max}) of the motion) and then the stresses correlated with these scaled motions are compared to the laboratory results to estimate the a_{max} at which a given site will liquefy (see Figure 3). The earthquake records used for the computer analyses were taken from the 1979 and 1981 earthquakes.

Finally, the newly developed cyclic strain approach is also being used to estimate site behavior. This method is employed in much the same way as the cyclic stress approach, except that strains occurring at a site during an earthquake (estimated by SHAKE and DESRA) are compared to strains causing liquefaction in laboratory tests. For the cyclic strain method, the laboratory tests are strain controlled, whereas the stress approach employs stress-controlled testing.

This study is in progress, and the results are preliminary. However, the cyclic strain approach is proving to be very promising towards estimating liquefaction, while the stress approach and the simplified procedure seem to be somewhat conservative. Predictions of liquefaction at the study sites for the 1981 Westmoreland Earthquake using the cyclic stress and cyclic strain methods are summarized in Table 1. The table shows that both methods predicted the liquefaction behavior of the study sites correctly, however, the cyclic stress approach tends to be more conservative.

REPORTS

Three reports in progress.

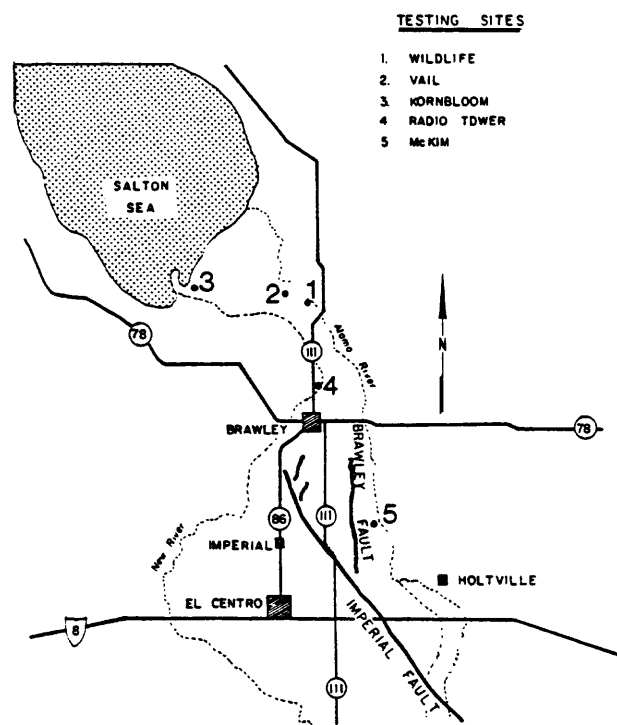


Figure 1 - Map showing locations of Imperial Valley study site.

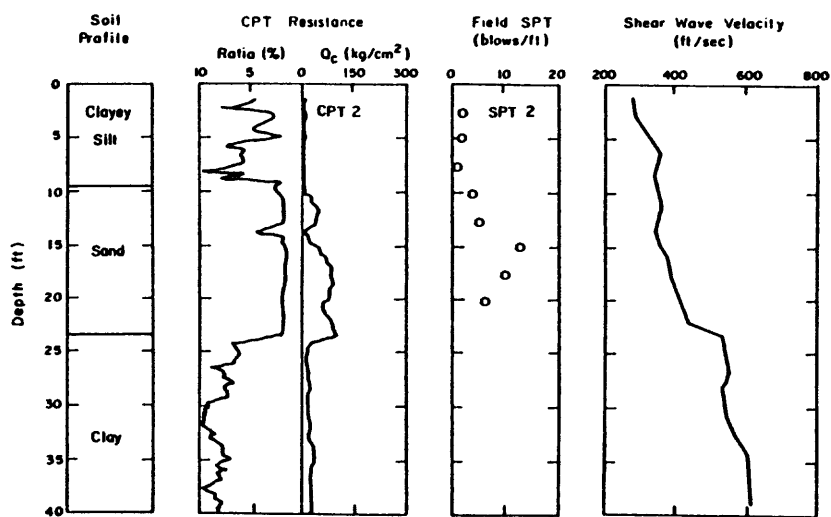


Figure 2 - Composite profile of Wildlife site.

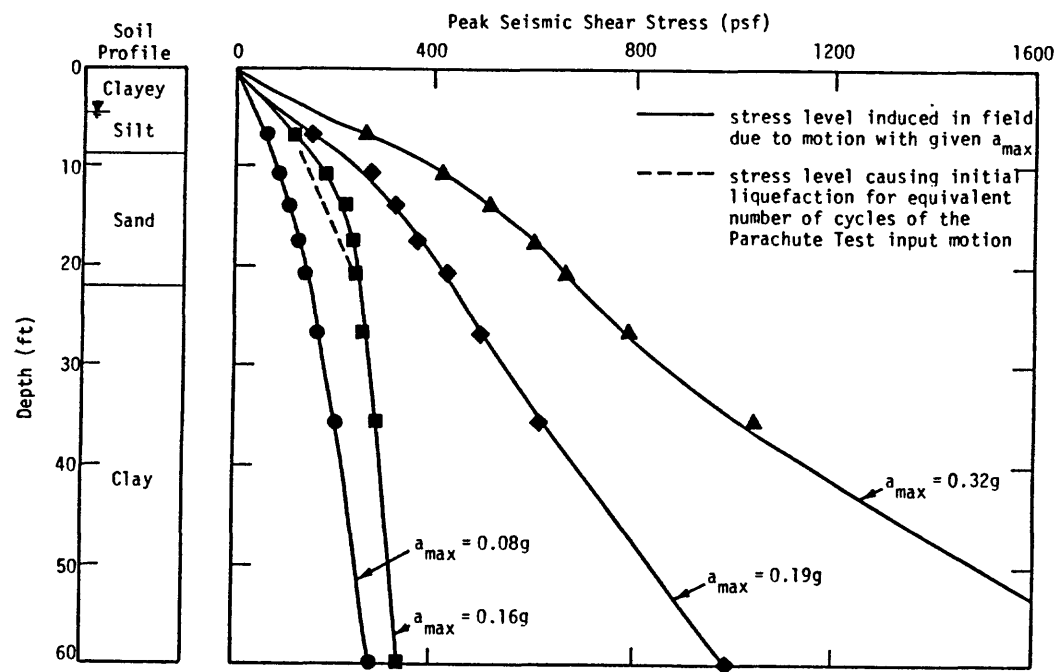


Figure 3 - Variation in cyclic shear stress with depth for Wildlife site using program SHAKE.

| Site | estimated a_{max} for 1981 earthquake | a_{max} causing liquefaction | | estimation of liquefaction | | Observed Liquefaction |
|-------------|--|--------------------------------|---------------------------|----------------------------|---------------------------|--------------------------|
| | | cyclic strain approach | cyclic stress approach | cyclic strain approach | cyclic stress approach | |
| Wildlife | 0.26g | 0.23g | 0.15g | yes | yes | yes |
| Radio Tower | 0.18 | 0.17 | 0.14 | yes | yes | yes |
| McKim | 0.12 | 0.35 | 0.15 | no | no | no |
| Vail Canal | 0.26 | 0.22 | 0.14 | yes | yes | yes |
| Kornbloom | 0.28 | 0.25 | 0.15 | yes | yes | yes |

Table 1 - Summary of predictions of liquefaction of study sites during the 1981 Westmorland earthquake using program SHAKE.

Earthquake Hazard Studies near Charleston, South Carolina

Contract No. 14-08-0001-21334

Pradeep Talwani
Geology Department
University of South Carolina
Columbia, S.C. 29208
(803) 777-6449

Investigations

1. Search for paleoliquefaction sites near Charleston, S.C., to try and establish recurrence rates of large earthquakes.
2. Evaluation of releveling data near Charleston, S.C.
3. Detailed gravity surveys in the South Carolina Coastal Plain.

Results

1. A sandblow which was associated with the 1886 Charleston earthquake was revealed by shallow trenching during the summer of 1983. Three trenches were dug by backhoe which transected the preserved sandblow nearly normal to the strike of the structure. Two shorter cross-trenches were subsequently hand-dug so as to afford both a sagittal cross-sectional series and a three-dimensional perspective of the subsurface geometric and stratigraphic relationships of this earthquake-induced feature. Approximately 400 ft of exposed trench walls were logged, five soil samples were taken for radiometric dating, and 35 samples for grain-size analysis. The results of the radiometric dating were inconclusive due to a lack of strategic position of recoverable organic materials, and due to the small amounts of organic material present at the site in general.

Grain size distributions were determined for 35 samples (both liquefied and nonliquefied sands). In general, both populations of sand had similar grain size characteristics, with the exception that those sands which did not liquefy all contained some silt and finer sediment fraction. The percentage of silt and finer fraction of the nonliquefied population was generally low (< 2%); however, this may be significant in that the possibility exists that subtle differences in sediment texture may have profound effects on the liquefaction susceptibility of various soils.

The configuration of this sandblow suggests that coseismic fissuring of the overburden (\approx 6' thick) controlled the emplacement of the liquefied sediment. An alternative explanation may be that liquefaction-induced lateral spreading of the subsurface material was responsible for the opening of the observed fissure. Although the ground surface at this site is nearly level, a slope of only a few degrees could be enough to cause a gravitational spreading effect when liquefaction is involved.

2. There have been at least three first order level lines run in the eastern U.S. since 1915. Of special interest to us are the data in the Summerville-Charleston area, the site of historical and current seismic activity (Fig. 2).

Earlier work on interpretation of releveling data is ambiguous. In the present study, we reexamined unadjusted first order leveling lines in the Charleston-Summerville area as shown in Figure 3. To check the accuracy of the data, misclosure analyses were performed along closed loops. The misclosure for the loop shown in Figure 3 is 3.56 cm for 1960 data over a length of ~ 700 km, which is well within the allowable misclosure of 9.21-11.5 cm, indicating that the data is reliable. Using the 1960 survey as reference, the misclosure was recalculated using certain segments of the loop leveled in 1974 and 1979 together with 1960 data for the remaining segments. The misclosure is -18.87 cm when the loop is closed with 1979 data along the Columbia-Lane-Charleston segment, and 65.99 cm when the loop is closed with 1974 data along the Charleston-Yemassee segment. These are considerably larger than the reference misclosure suggesting localized crustal movement since the 1960's (Figure 3).

In Figure 4 we have plotted the observed and projected annual rates of vertical movement along the two lines that run from Lane to Charleston and Charleston to Yemassee. Benchmark F67 is the tie point for the two lines. The line that runs from Charleston to Yemassee passes through the extension of the Ashley River Fault (ARF) and into the region between the Edisto and Ashley rivers. Velocities were used for comparison purposes, and were calculated with respect to the 1960/1961 surveys. Negative values indicate subsidence.

From Lane to Charleston (N-S) we note a gradual subsidence of about 2 mm/yr up with increased subsidence from about 25 km north of Charleston seaward to the Ashley River where the subsidence rate is over 4 mm/yr (this is similar to seaward tilt observed by earlier workers).

From F67 westward we see subsidence also. However, the block located roughly between the Ashley and Edisto rivers shows a lower rate of subsidence than the neighboring blocks. This anomalous decrease in subsidence rate can also be interpreted as relative uplift in a small portion of a subsiding block.

The data were projected on a line connecting Lane to Yemassee and perpendicular to the Ashley River fault (Fig. 4, bottom). Topography is also shown in Figure 4. Results of correlation tests between topography and velocity indicate that there is no significant correlation between the two. This further suggests that the data are reliable.

These results are compatible with the sense of motion inferred from fault plane solutions of microearthquakes on the ARF and geomorphic data, i.e. the area SW of ARF is undergoing uplift.

3. We are continuing to collect gravity data in the Coastal Plain of South Carolina.

Reports

Cox, J. and P. Talwani, Discovery of a paleoliquefaction site near Charleston, South Carolina: SE-NC Section Meeting of Geol. Soc. of America, Lexington, KY, April, 1984.

Cox, J. and P. Talwani, Three-dimensional description of an earthquake-induced sandblow near Charleston, S.C., Spring Am. Geophys. Union meeting: EOS Trans. Am. Geophys. Union, 65:16, p. 241, 1984.

Poley, C.M. and P. Talwani, Vertical tectonics in the Charleston, S.C. area: SE-NC Section Meeting of Geol. Soc. of America, Lexington, KY, April, 1984.

Poley, C.M. and P. Talwani, Vertical tectonics in the South Carolina Coastal Plain, Spring Am. Geophys. Union meeting: EOS Trans. Am. Geophys. Union, 65:16, p. 190, 1984.

Talwani, P., Earthquakes and crustal structure in southeastern U.S.: SE-NC Section Meeting of Geol. Soc. of America, Lexington, KY, April, 1984.



Figure 1. Photo of the sandblow at Ravenel, S.C. The grids are 1 foot squares. Note the clasts which sank into the central portion of the conduit. The sand unit which underwent liquefaction during the 1886 event lies about one foot below the bottom of the trench.

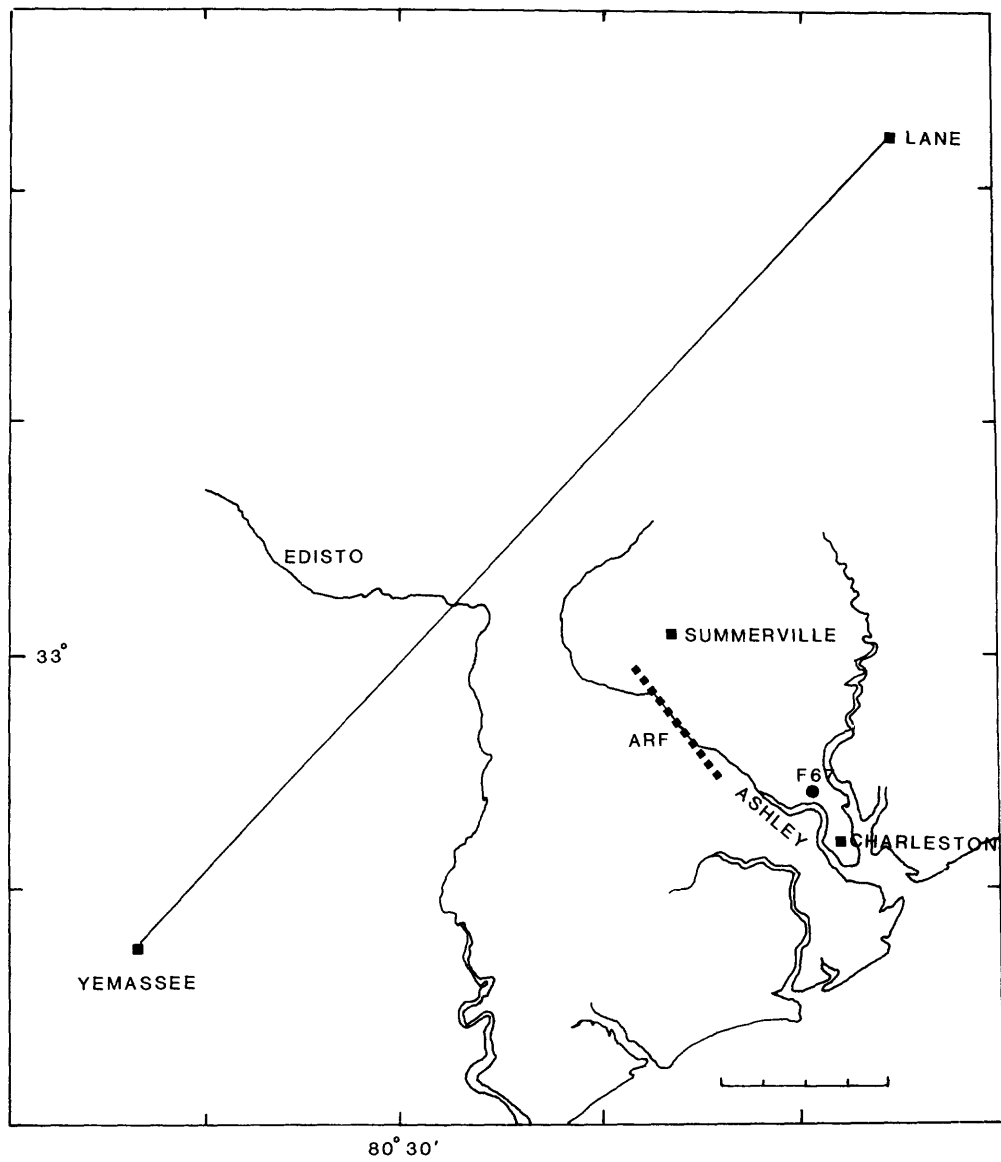


Figure 2

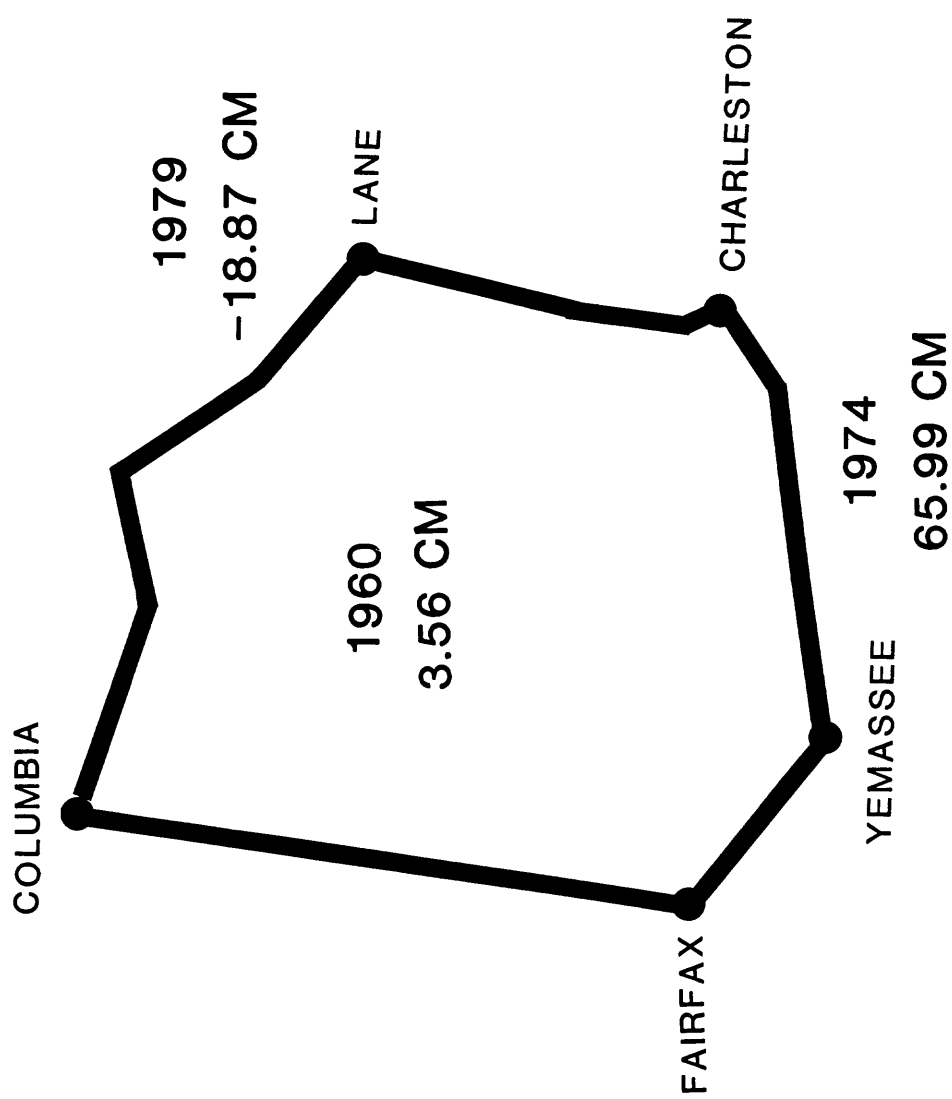
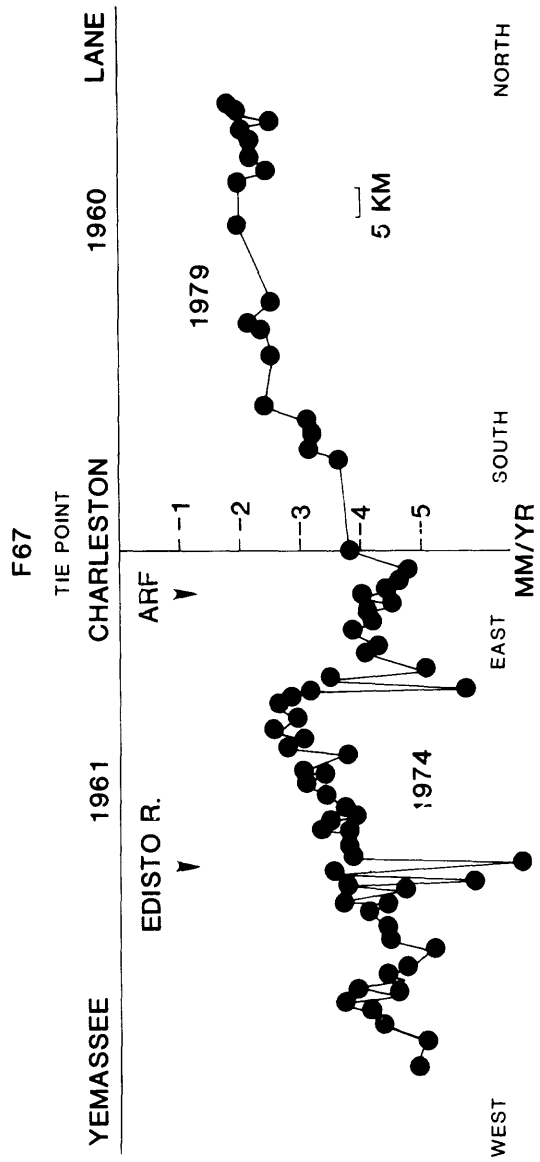


Figure 3

**PROFILE CHARLESTON
OBSERVED**



**PROFILE CHARLESTON
PROJECTED**

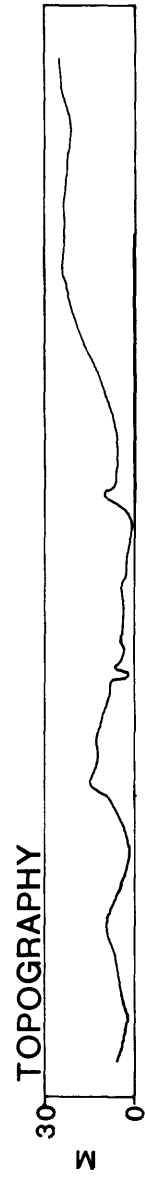
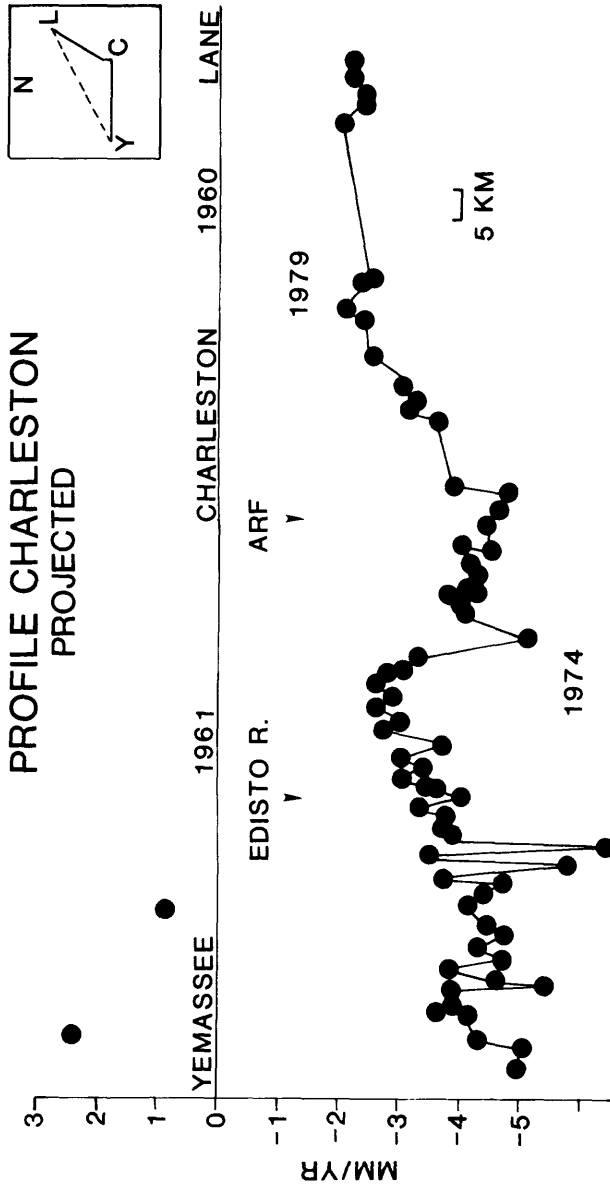


Figure 4

LATE PLEISTOCENE-HOLOCENE SOIL CHRONOLOGY
FOR EVALUATING TECTONIC FRAMEWORK AND EVENTS,
TRANSVERSE RANGES, CALIFORNIA

14-08-0001-21829

Edward A. Keller
Department of Geological Sciences
University of California, Santa Barbara
Santa Barbara, California 93106

Investigations

Analyze late Pleistocene-Holocene tectonic framework, history of deformation and chronology by developing a soil chronosequence (set of soils arranged in chronological order based on relative development of the soil profile) for relative and absolute dating of geologically young deposits in the "Big Bend" region of the San Andreas fault.

Results

Interpretation of imagery and maps suggest that there are several geomorphic surfaces (erosion surfaces, river terraces, and alluvial fans) of different geologic age in the study area. Reconnaissance field work suggests that soils representing several stages of profile development, are preserved on deformed geomorphic surfaces. Detailed field work during the summer of 1984 will provide the data base necessary to develop the soil chronosequence.

STUDY OF SEISMIC ACTIVITY BY
SELECTIVE TRENCHING ALONG THE
ELSI NORE FAULT ZONE, SOUTHERN CALIFORNIA

Contract No. 14-08-0001-21376

D. L. Lamar
Lamar-Merifield Geologists, Inc.
1318 Second Street, Suite 25
Santa Monica, California 90401
Telephone: (213) 395-4528

Investigations

A trench was dug and logged at a previously studied site across the Glen Ivy North fault, a strand of the Elsinore fault zone between Corona and Lake Elsinore (Lamar and Swanson, 1981, 1982).

Results

Evidence of two distinct earthquakes and five layers rich in organic material were observed in a three meter deep trench (Fig. 1). Ground water prevented deepening the trench. Two dewatering wells were drilled and are pumping. We estimate that the water table will be low enough to permit deepening the trench this fall.

References

Lamar, D. L. and S. C. Swanson, 1981, Study of seismic activity by Selective trenching along the Elsinore fault zone, southern California: Lamar-Merifield Technical Report 81-4, Final Report U.S.G.S. Contract 14-08-0001-19144, 50 p.

Lamar, D. L. and S. C. Swanson, 1982, Ages of displaced strata in trenches along Elsinore fault zone, southern California: Geol. Soc. Amer. Abstracts with Programs, v. 14, p. 179.

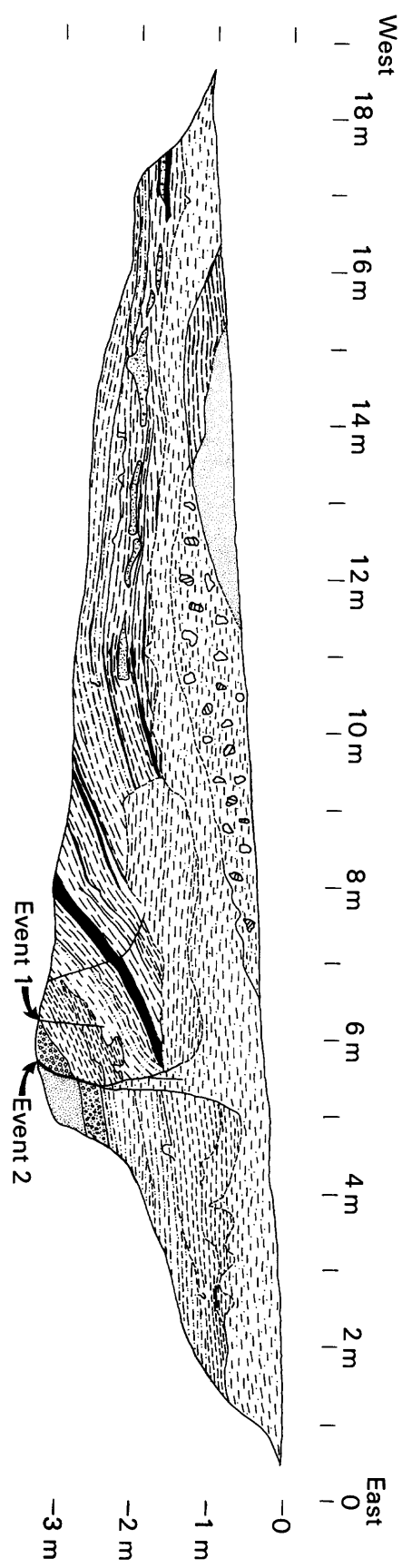


Fig. 1 - Log of test trench across Glen Ivy North fault showing two distinct displacement events and carbonaceous layers (black).

FAULT ACTIVITY AND RECURRENCE INTERVALS
OF THE WESTERN SEGMENT OF THE WHITTIER FAULT, CALIFORNIA

Contract #14-08-0001-21368

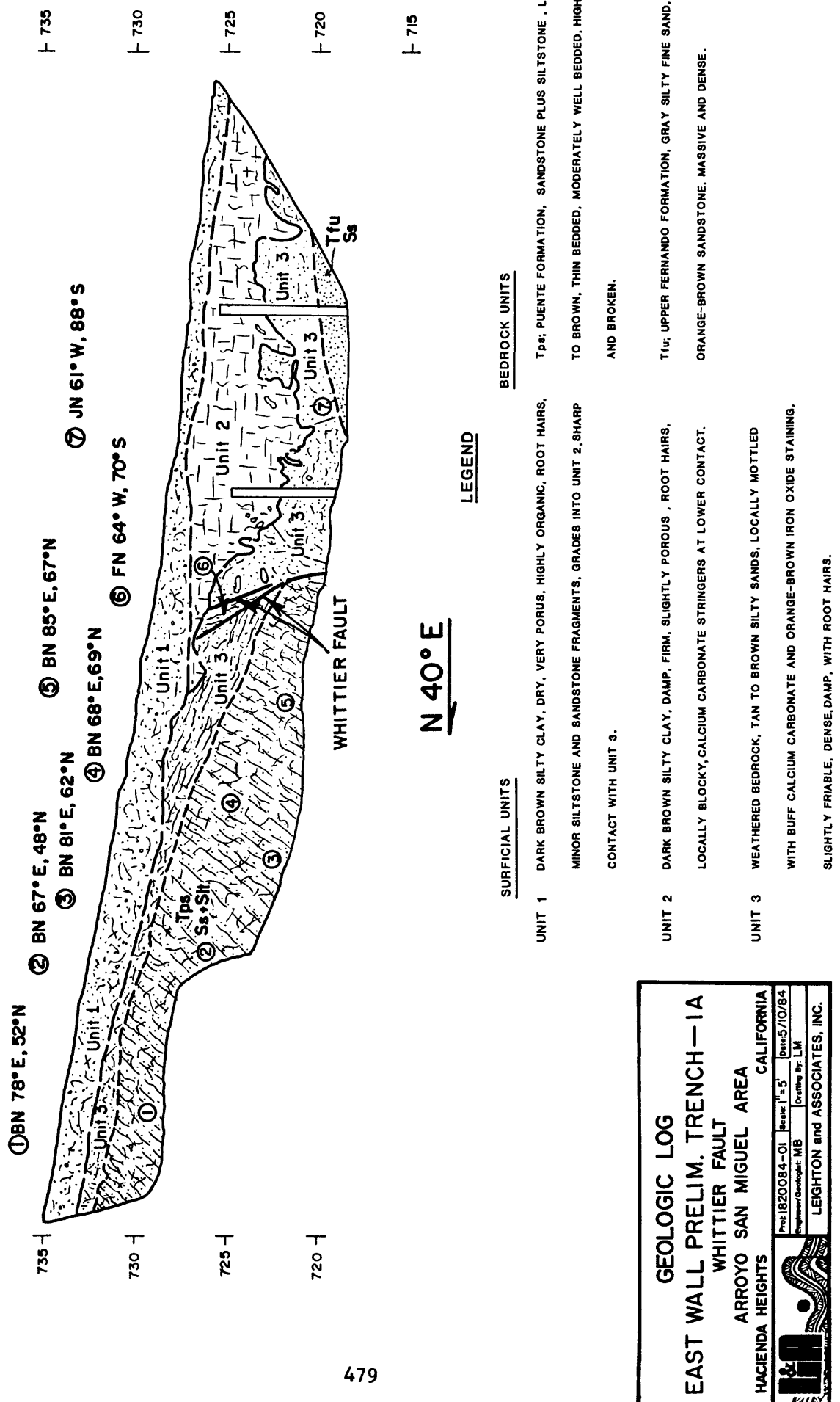
F. BEACH LEIGHTON, LAWRENCE R. CANN,
ERNEST R. ARTIM AND MARK C. BERGMANN
Leighton and Associates, Inc.
1151 Duryea Avenue
Irvine, California 92714
(714) 250-1421

Investigations

1. Select locations for trenching of the western portion of the Whittier fault for analysis of recency of faulting along this segment.
2. Trench the most likely traces of recent faulting and log, in detail, the relationships between faulted and unfaulted units. Obtain absolute ages of movement by radiometric age-dating techniques if appropriate materials are available.
3. Improve the technique and tools used for estimating future earthquake recurrence intervals on the Whittier fault, including data on past recurrence intervals.
4. Prepare guidelines on the type and extent of subsurface exploration that should precede building and development projects in the vicinity of the fault zone.

Results

1. Four sites for exploratory trenching were selected in the Hacienda Heights area where the suspected active trace of the Whittier fault is overlain by appropriate sequences of Recent colluvial and alluvial deposits. The sites were selected on the basis of our reviews of: (a) existing literature, including published and unpublished investigations and maps, (b) fourteen separate sets of stereoscopic aerial photographs from 1928 through 1977, and (c) field reconnaissance and mapping, including accessibility for trenching equipment and public protection. Permission was finally granted by the property owner to trench the proposed sites.
2. Approximately 500 lineal feet of preliminary exploratory trenches have been excavated at the four sites and logging at a scale of 1 inch to 5 feet is currently underway. At the first site, the fault was observed to offset bedrock, but not the overlying colluvial soils (Figure 1). Additional exploratory trenching at this location and at others is still being evaluated, but at least three of the four sites appear to be very promising.



SOIL-STRUCTURES INTERACTION EFFECTS ON STRONG MOTION
ACCELEROGrams RECORDED ON INSTRUMENT SHELTERS AND SMALL
STRUCTURES
USGS Contract No. 14-08-0001-21374

J.E. Luco

J.G. Anderson

Department of Applied Mechanics and Engineering Sciences
University of California, San Diego
La Jolla, California 92093
(619) 452-4338 (JEL)
(619) 452-2169 (JGA)

Investigations:

1. Conduct parametric soil-structure interaction analyses on instrument shelters and small shelters. The results will be presented in the form of comparisons of the assumed free-field motion with the resulting response within the instrument housing.
2. Guided by the results of the parametric study and by the typical use on various strong-motion arrays, select a small number (~6) of specific stations for detailed modeling and analysis.

Results:

1. An extensive parametric study for instrument shelters is completed. For this study, we have considered an instrument shelter with a circular base on a uniform half space. The effect of an instrument housing, with dimensions comparable to the "T-hut" commonly employed by both the US Geological Survey and the California Division of Mines and Geology has been included. The calculations incorporate the effect of rocking at the height of accelerograph sensors above the ground level. The parametric study covers a wide range of embedments, a wide range of soil rigidity, a reasonable range of heights of the accelerograph above the ground, and so far, two pier diameters.

Figures 1 and 2 show some results for a case in which the surface area of the circular foundation is similar to the area of the square free-field designs employed by USGS and CDMG. (Radius = 0.75 m). The sensor is 25 cm above the ground surface (The pier surface is 15 cm above the ground, and the sensor is 10 cm above the pier surface). The results are presented in the form of transfer functions for the Fourier amplitude spectrum of ground motion. The transfer function for "UZ" gives the ratio of the vertical component recorded on the pier to the vertical component in the free field, for a vertically incident P-wave. The transfer function for "ACCEL UY" gives the ratio of the

horizontal component recorded by the accelerograph, including effects of rocking, to the horizontal component in the free field, for a vertically incident S-wave.

In Figure 1, we consider the effect of the shear velocity of the soil on the response of a foundation. This foundation is not embedded. Five shear velocities are considered: = 0.1. 0.25 0.5- 1.0 and 3.0 km/sec. We see that as increases, the effects of soil-structure interaction occur at higher frequencies, and that for this model pier. when exceeds 1 km/sec, the effects are negligible. The five curves shown on Fig. 1 could be collapsed into one curve through the use of a normalized frequency . In Figure 2- the effects of embedment of the foundation are shown for a shear velocity of 100 m/sec. The case of zero embedment is the same as in Figure 1. other embedments are 37.5 cm and 75 cm. For these very slow shear velocities, one sees that an embedded foundation has a strong effect of filtering the high frequency ground motion. On the other hand. for frequencies less than 30 Hz. embedment to 37.5 cm actually causes the transfer function to be closer to unity than in the case where no embedment is present. For these particular calculations rocking of the foundation does not make an important contribution to the recorded values of UY. but for a pier surface extending 50 cm above the ground surface, rocking becomes very important in the presence of low shear velocity.

2 No results are available at this time.

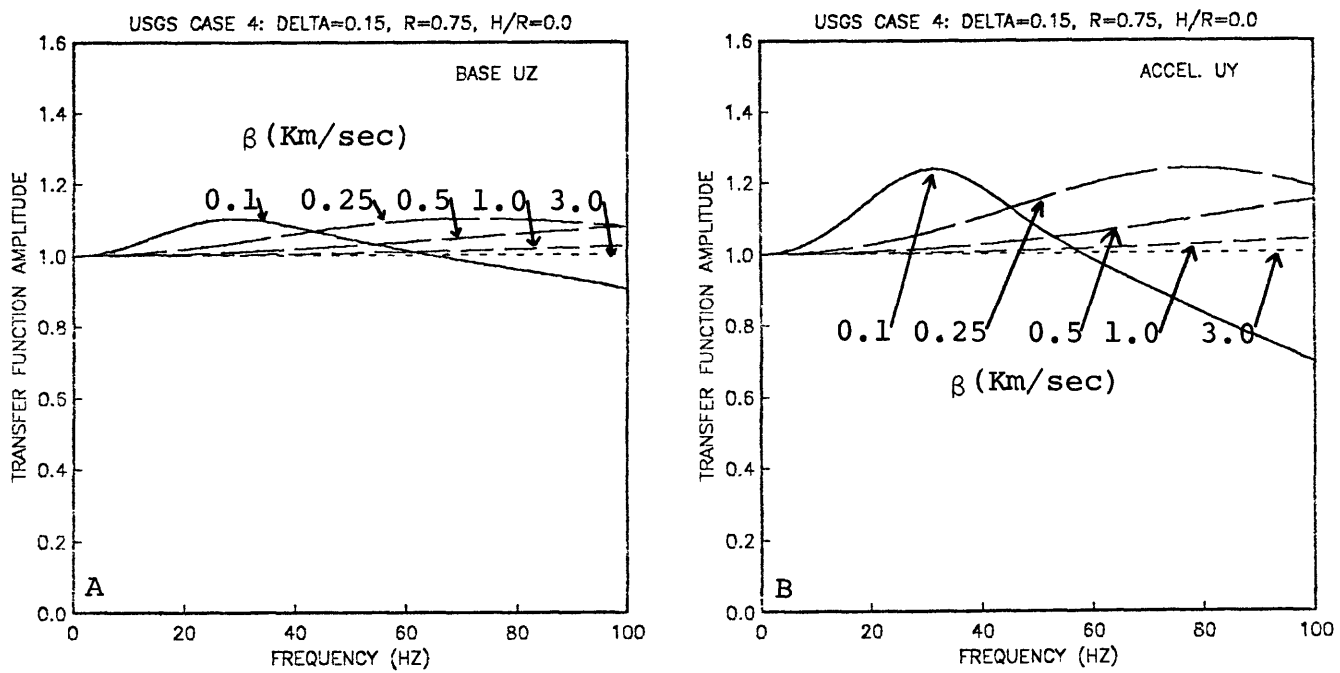


FIGURE 1

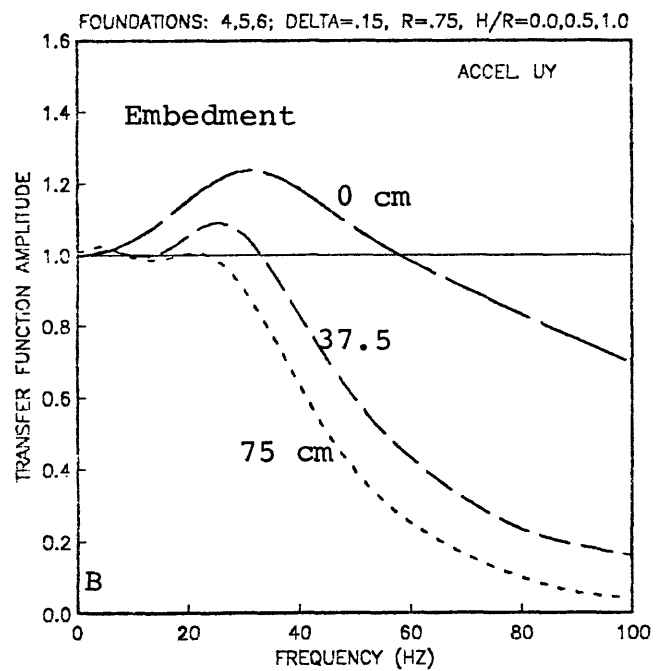
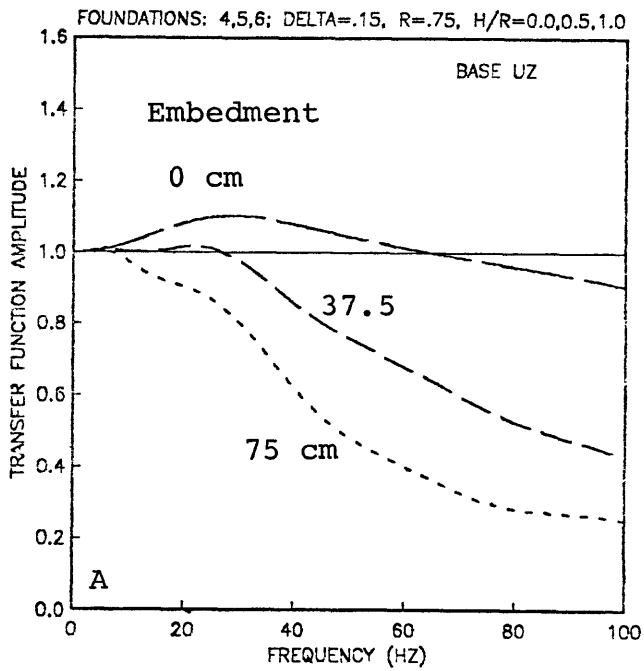


FIGURE 2

**Subsurface Velocity and Attenuation Measurements
at a Strong Motion Site**

Contract No. 14-08-0001-21823

Bruce Redpath, Reuben Hale and Richard Lee
URS/Blume Engineers
2855 Telegraph Avenue, Suite 303
Berkeley, California 94705
415-849-2700

Investigations:

- [1] Measure the **in situ** shear-wave velocity and **Q** at the strong motion recording site located at the Richmond Field Station of the University of California at Berkeley.
- [2] Compare the **in situ** value of **Q** with damping values obtained from resonant column laboratory tests.
- [3] Compare observed strong motion records with those predicted on the basis of the measured anelastic structure of the site.

Results:

A 190-ft deep test hole was drilled approximately 15 ft from the subsurface strong motion accelerometer array at the Richmond Field Station. Plastic Slope Indicator casing with internal grooves, which allows our downhole transducers to maintain a fixed azimuthal orientation, was grouted in place for the entire depth. Pitcher-tube soil samples were taken at depths of 25 and 100 ft during the drilling operation for resonant column laboratory tests to determine damping at various strain levels. In general, the soils are categorized as Bay muds, primarily silty clays and sands, to a depth of 115 ft, below which is the Franciscan formation consisting of shales and cherts.

Shear- and compression-wave arrival times were measured at 10-ft intervals. The shear source consisted of hammer blows on the ends of a wooden plank weighted down by a vehicle. Observed shear signals with an E-W polarization are shown in Fig.1. A velocity survey was also performed with the shear source oriented N-S to determine if any velocity anisotropy exists; from a depth of 20 to 65 ft the velocity of the E-W polarized shear waves is about 12% greater than the N-S polarized shear waves. A casing wave becomes quite pronounced on the records below a depth of 120 ft; there is a significant acoustic boundary at 115 ft that accounts for the marked increase in the amplitude of the casing wave, relative to that of the shear wave, below this depth. Shear- [E-W polarization] and compression-wave velocities are shown in Fig.2.

Two-channel measurements of shear-wave signals were made in order to determine the spectral ratio between the signal at depth and the same pulse detected by a reference transducer fixed at a depth of 20 ft. These data are used to compute the **in situ** value of **Q**.

A representative spectral ratio is shown in Fig.3 together with a least-squares best fit to the ratio over a specific frequency bandwidth. The meaningful portion of the spectral ratio, i.e. the segment from which the spectral slope is obtained, is established by the value of the coherence function for each pair of signals; the slope of the ratio was evaluated only over the bandwidth for which the coherence was >0.9 . The coherence function is the square of the magnitude of the cross spectrum divided by the product of the input [i.e. reference transducer] and output [i.e. deep transducer] spectra. Each measurement consisted of at least 4 blows to the shear-wave source and the coherence was measured with a Hewlett-Packard 5423A analyzer. Values of spectral slope are plotted against depth, as shown in Fig.4, and the rate of change of the slope with increasing depth is the value of the attenuation constant k as used in the exponential decay factor:

$$e^{-kfR}$$

where f is the frequency in Hz
and R is the reference-to-measurement point distance in ft.

The quality factor Q is directly related to k by:

$$Q = \frac{\pi}{kc}$$

where c is the propagation velocity in ft/sec.

A more complete explanation of this technique for measuring Q is given by Redpath et al [1982] and Hauge [1981].

The average shear-wave velocity for the material between depths of 15 and 110 ft is 965 ft/sec which, when combined with a k value of 0.00026 sec/ft, results in a value of 12.5 for the Q of these soils. A Q of 12.5 is equivalent to a damping factor of 4% of critical. The laboratory values at a strain level of 0.000008 were 2.44% at 25 ft and 2.56% at 100 ft. Our finding that the *in situ* damping is somewhat higher than the laboratory values is in accord with our prior experience.

The Q of the material below 115 ft is comparatively high and cannot be measured easily using our shear-wave source on the surface; not only is the bandwidth of the downward travelling signal too narrow to resolve meaningful changes in spectral slope below this depth, but the casing wave below 115 ft presents a significant noise problem. The relative amplitude of the casing wave can be decreased somewhat by increasing the source-to-hole offset, but it should be noted that a Q value below 115 ft is not necessary for this program.

We have transferred strong motion data at the Richmond Field Station from tapes at the U.C. Berkeley Seismograph Station to our H-P 5451 computer. The remainder of this program will be directed towards comparing actual surface motions with those computed on the basis of the measured soil properties.

References:

Hauge, Paul S., 1981, Measurements of Attenuation from Vertical Seismic Profiles, **Geophysics**, v.46, pp. 1548-1558.

Redpath, Bruce B., Edwards, Robert B., Hale, Reuben J. and Kintzer, Frederick C., 1982, Development of Field Techniques to Measure Damping Values for Near-Surface Rocks and Soils, URS/John A. Blume & Associates, NSF Grant No. PFR-7900192, San Francisco, California.

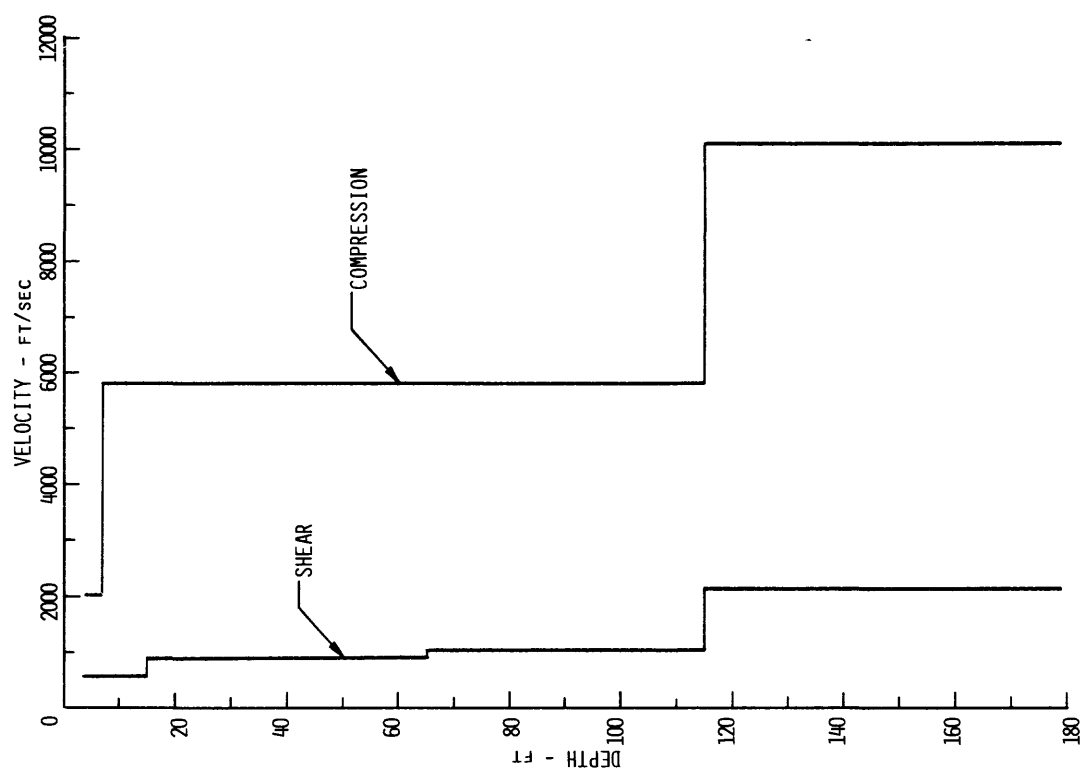


Fig.1 Observed downhole signals generated by reversed [E-W] blows to shear-wave source on the surface, Richmond Field Station.

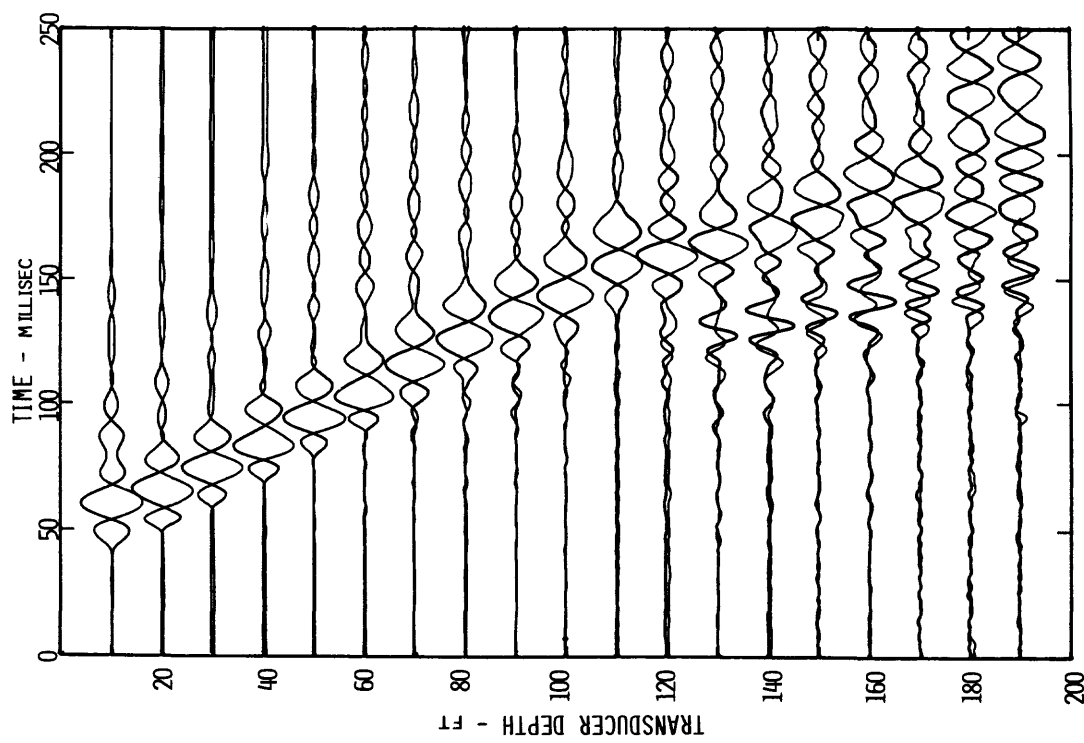


Fig.2 Vertical velocity profile at Richmond Field Station test site.

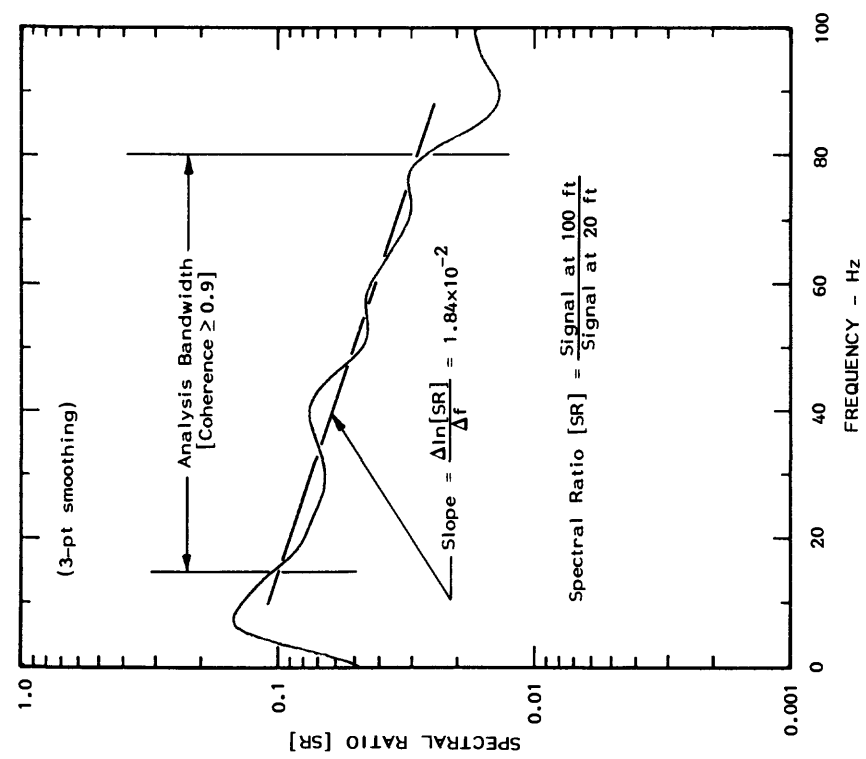


Fig.3 Example of spectral ratio and corresponding spectral slope obtained from shear-wave signals at 20 and 100 ft depths.

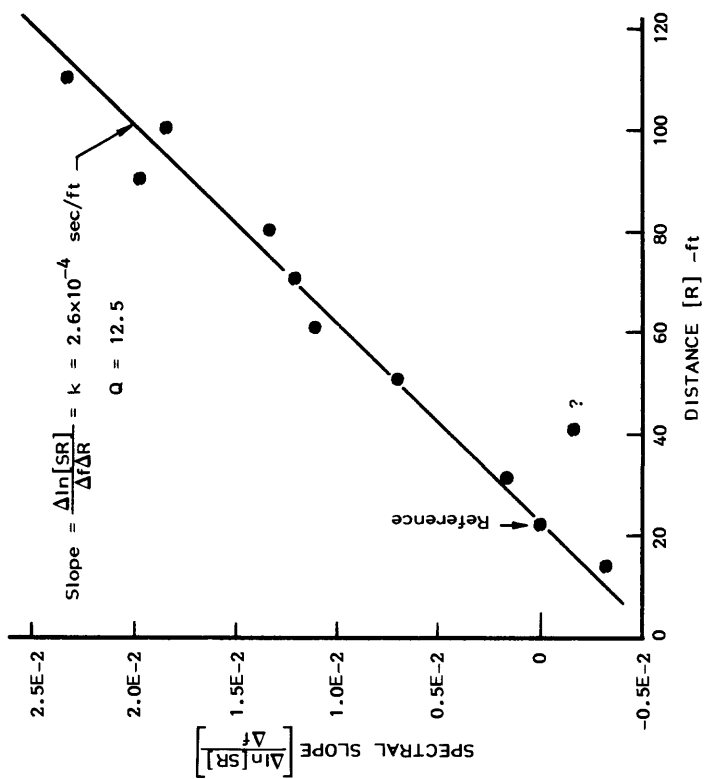


Fig.4 Slopes of spectral ratios plotted vs source-to-transducer distance to determine attenuation constant k .

**Fast Computation of Near Field Strong Motion
for Complex Source Earthquakes and Inversion
of Source Slip for Some Recent Events in Italy and California**

14-08-0001-19883

M. Nafi Toksöz, Vernon F. Cormier, Anas Abo-Zena
 Earth Resources Laboratory
 Department of Earth & Planetary Sciences
 Massachusetts Institute of Technology
 Cambridge, MA 02139
 (617)253-6382

Investigation

The research completed under this contract included (1) computation of the displacement history of a two-dimensional, frictionally controlled, dynamic source model, and (2) application of a ray-based method to body wave propagation in a low velocity wedge of fault gouge surrounding the San Andreas and Hayward-Calaveras faults. Computations with the dynamic source model can be used to investigate the importance of the contribution of near surface slip and surface waves to the ground motion observed near a fault. Development of ray-based methods to the two- and three-dimensional structure surrounding a fault offers the opportunity of investigating the effects of structural focusing and defocusing. These effects may be confused with features of the rupture process when accelerograms are interpreted using a propagation model based on plane-layered, laterally homogeneous crustal models.

The results of both investigations (1) and (2) are relevant to fast approximate methods of evaluating strong ground motion^{1,2}, which assume the strong ground motion within several source depths can primarily be explained by body rather than surface waves and which can incorporate the effects of three-dimensional structure surrounding the fault.

Results

The theoretical source model (1) can be used to explain why the slip associated with an earthquake is frequently smaller at the surface than the slip estimated below the ground surface. This observation can be shown to follow from the shape of the depth functions of pre-stress, dynamic friction stress, and static friction stress (Figs. 1a-b). An analytical solution for the slip history was obtained by parameterizing the stress functions as polynomials in depth and by evaluating the double integral for displacement on the fault by coordinate rotation and Abel's integral³. The solution for the time history of displacement is shown in Fig. 2 for a series of stress drops. Displacement increases with stress drop. Because of the shapes assumed for the stress functions, fault displacement tends towards zero at the free-surface.

In investigation (2) P wave seismograms at ranges less than 10 km. were synthesized by asymptotic ray theory and by summation of Gaussian beams⁴ for point sources located in a low-velocity wedge surrounding a fault. The computations were performed using models of the wedge inferred from the analysis of reflection and refraction experiments across the San Andreas and Hayward-Calaveras. Calculations in these models show that the 10-20 Hz. vertical displacements of earthquakes located at 3-10 km. depth are amplified by up to an order of magnitude in a 1-2 km. wide region centered on the fault trace compared to displacements predicted by laterally homogeneous models of the crust. This amplification is not canceled by high attenuation in the fault zone and compensates for the reduction in amplitudes directly above the source predicted from the radiation pattern of a strike slip earthquake. Depending on the source depth of the earthquake and the structure and velocity contrast of the wedge, multiple triplications in the travel time curve of direct P and S waves will occur at stations in the fault zone. A wedge model successfully predicts the triplications observed in the P waveforms of aftershocks of the Coyote Lake earthquake recorded in the fault zone (Fig. 3), showing that body waves from microearthquakes can be used to determine the three-dimensional velocity structure of the fault zone. The amplification, waveform complexity, and distortion of ray paths introduced by the low velocity wedge suggest that its effects should be included in the interpretation of strong ground motion and travel times observed in the fault zone. For realistic models of the wedge, asymptotically approximate methods of calculating the body waveforms are strictly valid for frequencies greater than 20 Hz. Numerical methods may be necessary to accurately calculate the wavefield at lower frequencies.

Reports

Abo-Zena, A.M., Dynamic analysis of strike-slip faulting for general friction and pre-stress variation (abs.); *EOS, Trans. Am. Geophys. Un.*, 64: 18, 262.

Cormier, V.F., and P. Spudich, Amplification of ground motion and waveform complexity in fault zones: examples from the San Andreas and Calaveras faults, *Geophys. J. R. Astr. Soc.*, (in press; to appear in special issue Oct., 1984 of papers presented at the Conference on Wave Propagation in Heterogeneous Media, Liblice, Czechoslovakia), 1984.

References

1. Bernard, P., and R. Madariaga, A new asymptotic method for the modeling of near field accelerograms, *Bull. Seism. Soc. Am.*, in press, 1984.
2. Spudich, P., and L.N. Frazer, Use of ray theory to calculate high- frequency radiation from earthquake sources having spatially variable rupture velocity and stress drop, *Bull. Seism. Soc. Am.*, in press, 1984.
3. Achenbach, J.D., and A.M. Abo-Zena, Analysis of the dynamics of strike slip faulting, *J. Geophys. Res.*, 78, 866-875, 1973.
4. Červený, V., and I. Pšenčík, Gaussian beams in elastic two-dimensional laterally varying structures, *Geophys. J. R. Astr. Soc.*, in press, 1984.

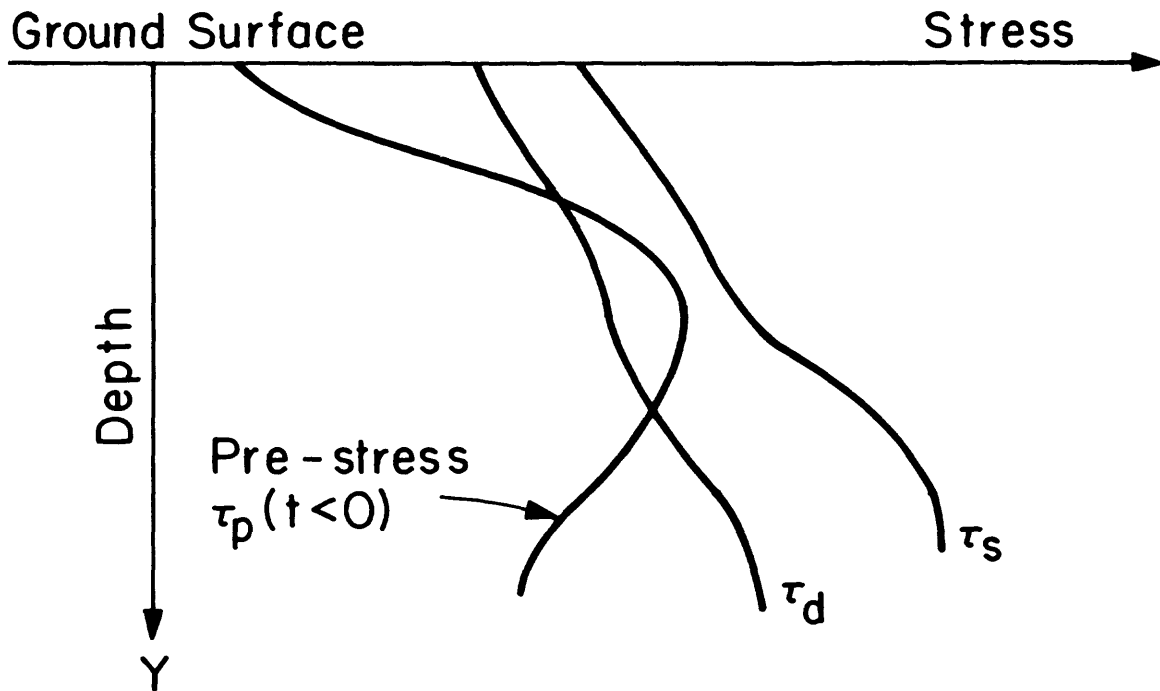


Figure 1a. The static friction stress τ_s , dynamic friction stress τ_d , and the pre-stress τ_p , on the surface of the fault as a function of the depth y before rupture starts.

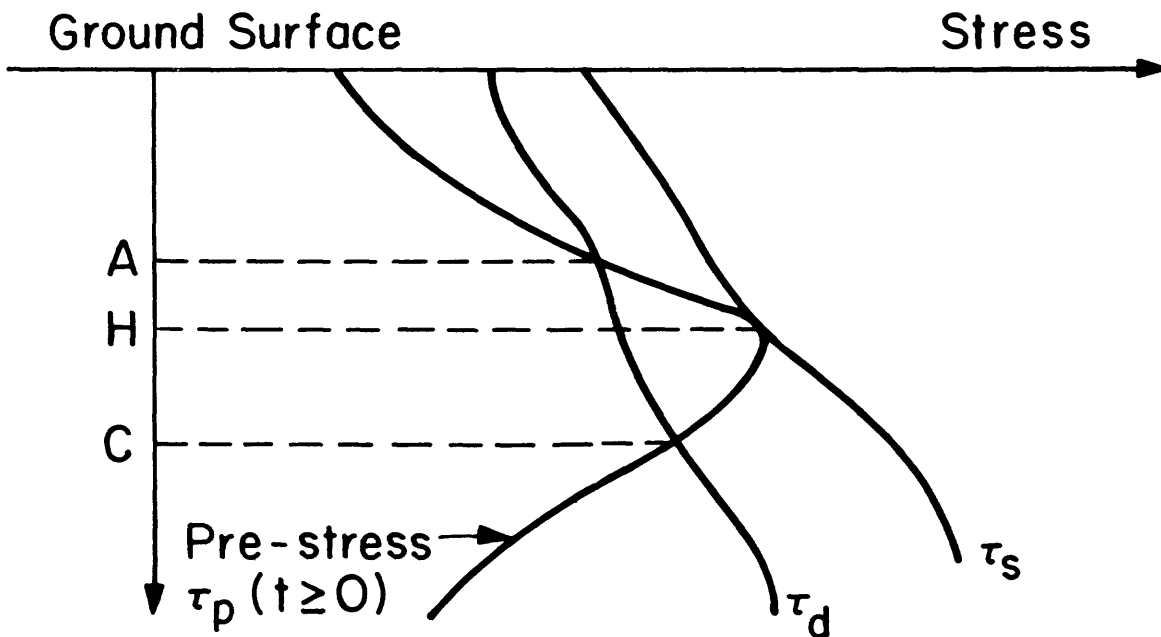


Figure 1b. Same as Figure 1a but showing the start of the rupture. At point H the pre-stress equals the static friction stress. The region between depth points A and C will start sliding first.

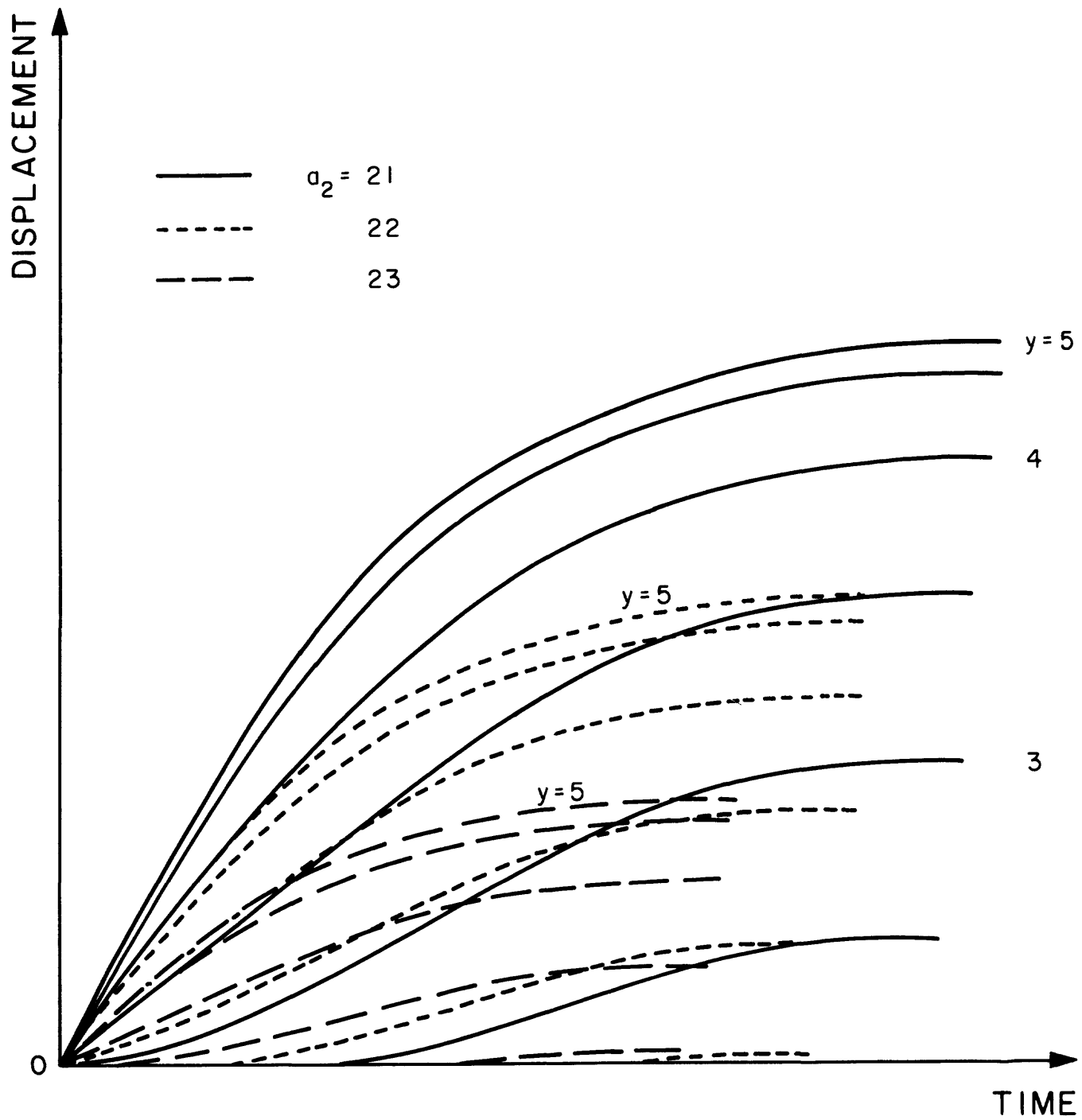


Figure 2. The time history of the displacement at different depths y (km). The difference between the dynamic friction and the pre-stress is $\alpha_0 - \alpha_1 y + \alpha_2 y^2$ in bars, with $\alpha_1 = 90$ and $\alpha_2 = 1$. Three cases are presented with, $\alpha_0 = 21, 22$, and 23 . These cases correspond to a maximum stress drop of 4, 3, and 2 bars, respectively.

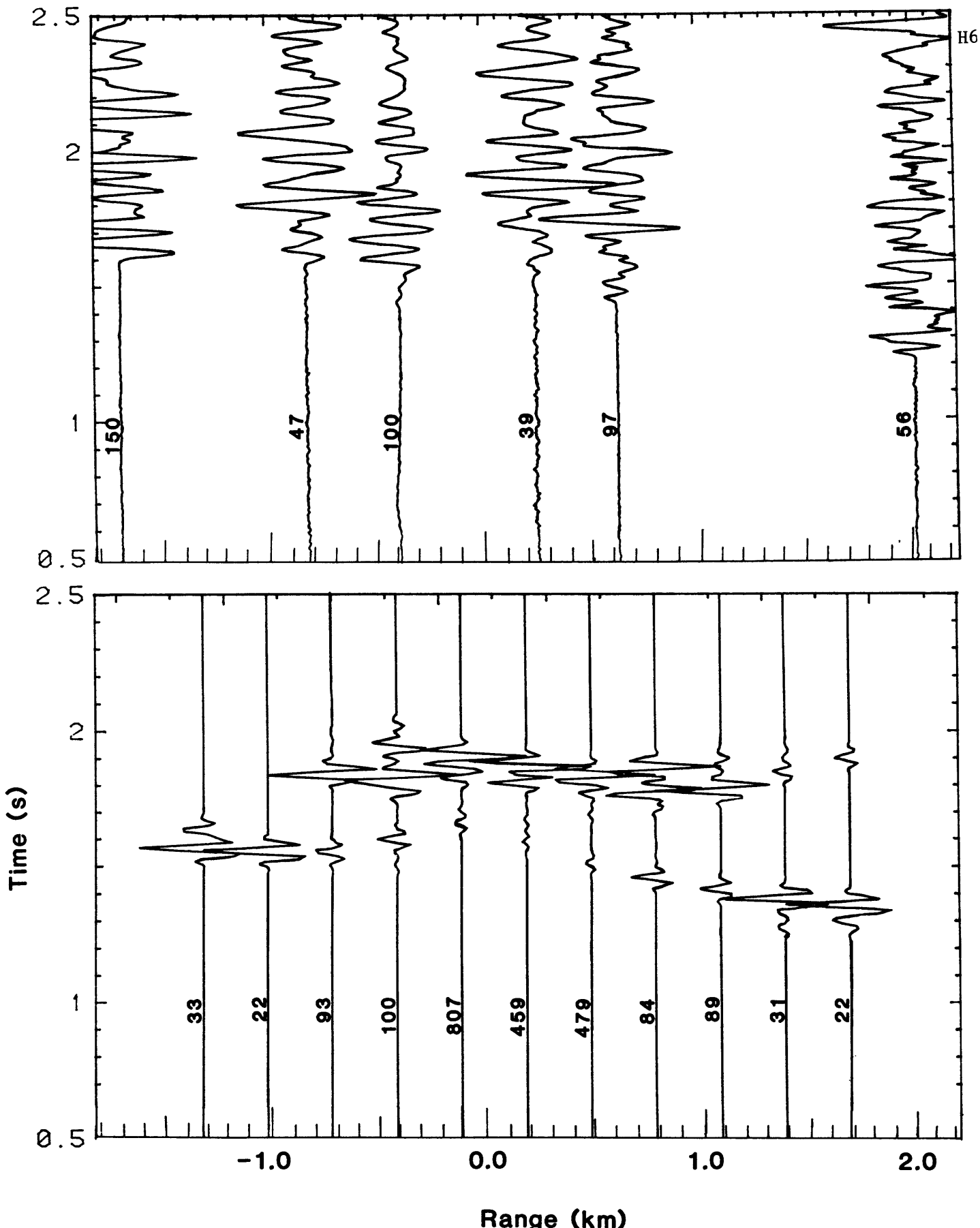


Figure 3. Comparison of Gaussian beam synthetics using a 20 Hz Gabor wavelet with data from Coyote Lake. Both data and synthetic amplitudes are scaled by normalizing to the distance with amplitude labeled 100. The synthetics do not include the effects of a radiation pattern, which may account for the scatter and lack of discernible amplification over the source in the data amplitudes. Note, however, that the data amplitudes show no diminution over the double node in the radiation pattern directly over the source.

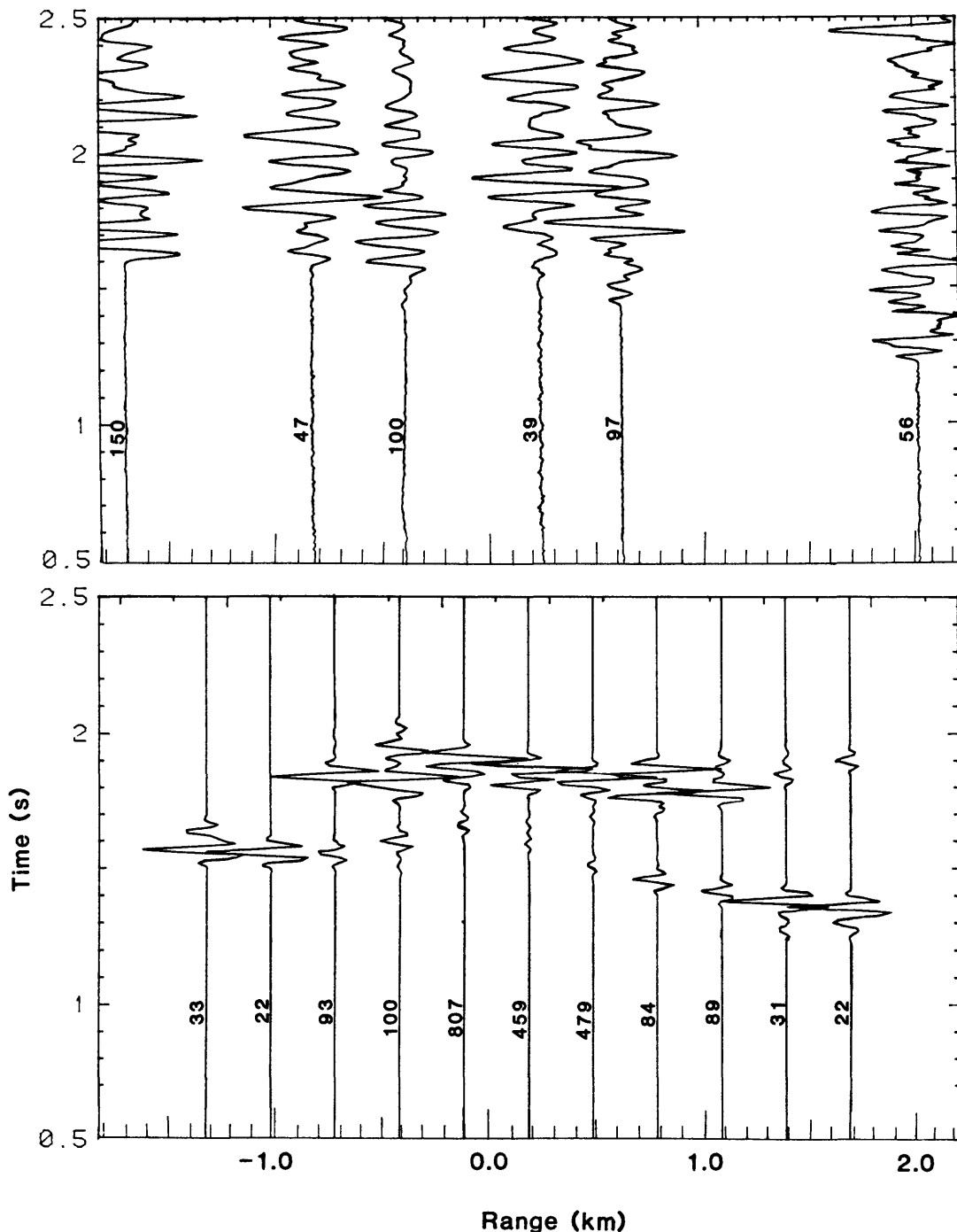


Figure 3. Comparison of Gaussian beam synthetics using a 20 Hz Gabor wavelet with data from Coyote Lake. Both data and synthetic amplitudes are scaled by normalizing to the distance with amplitude labeled 100. The synthetics do not include the effects of a radiation pattern, which may account for the scatter and lack of discernible amplification over the source in the data amplitudes. Note, however, that the data amplitudes show no diminution over the double node in the radiation pattern directly over the source.

Development of a
Liquefaction Potential Map
for Utah County, Utah

Contract No. 14-08-0001-21359

Loren R. Anderson
Department of Civil & Environmental Engineering
Utah State University
Logan, Utah 84322
(801) 753-5119

Jeffrey R. Keaton
Dames & Moore
250 East Broadway
Suite 200
Salt Lake City, UT 84111
(801) 521-9255

A liquefaction potential map is being compiled for Utah County, Utah. The map is being developed primarily from existing data that was obtained from the files of private consulting firms and government agencies. The existing data was supplemented by drilling test borings and making cone penetrometer soundings at selected locations throughout the County. During the period from March 26 through April 13, 1984, forty-three cone penetrometer soundings to depths up to 69 feet and seventeen conventional borings up to 42 feet deep were made. Samples were collected from the borings for laboratory testing.

Standard penetration test (SPT) results have been obtained from soil boring data. The blow count, N_1 , or the cone penetrometer resistance q_c , corrected to an overburden pressure of 1 Ton/ft², and the relationship proposed by Seed, Idriss and Arango (1983) were used to obtain the cyclic stress ratio, (τ/σ_o) , required to cause liquefaction. The critical acceleration (that required to cause liquefaction), was then computed by the method suggested by Seed, Idriss and Arango (1983).

$$a_{max} = \frac{(\tau_{ave})}{(\bar{\sigma}_o)} \frac{(\bar{\sigma}_o)}{(\sigma_o)} \frac{(g)}{(0.65r_d)}$$

where,

a_{max} = maximum acceleration at ground surface

$\frac{(\tau_{ave})}{(\bar{\sigma}_o)}$ = cyclic stress ratio required to cause liquefaction

$\bar{\sigma}_o$ = total overburden pressure on sand layer under consideration

$\bar{\sigma}_o$ = effective overburden pressure on sand layer under consideration

r_d = a stress reduction factor varying from a value of 1.0 at the ground surface to 0.9 at a depth of 30 feet

For silt and silty sand it was necessary to correct the SPT blow count and the cone penetrometer resistance to account for the influence of the fines on liquefaction susceptibility. This correction was applied by the method suggested by Seed, Idriss and Arango (1983).

The liquefaction potential will be classified as high, moderate, low and very low depending on the probability that the critical acceleration will be exceeded in 100 years (Anderson, et. al., 1982). The critical acceleration for a given location is defined as the lowest value of the maximum ground surface acceleration required to induce liquefaction. The categories of high, moderate, low and very low correspond to probabilities of exceeding the critical acceleration in the ranges of greater than 50 percent, 10 to 50 percent, 5 to 10 percent and less than 5 percent, respectively.

The critical accelerations have been computed and plotted on a map for all boring and penetrometer sounding locations. Boundaries will be drawn delineating zones of high, moderate, low and very low liquefaction potential. In establishing the boundaries consideration will be given to the geologic conditions throughout the area.

All boring locations have been digitized and stored on magnetic tape along with the boring log information. This information will be used to produce computer generated maps that summarize the data.

In assessing the Liquefaction Potential in Utah County, Utah, four maps will be developed: (1) Soil Data and Ground Water Map, (2) Critical Acceleration and Ground Slope Map, (3) Geologic Ground Failure Map and (4) Liquefaction Potential Map. The Liquefaction Potential Map will identify areas of high, moderate, low and very low liquefaction potential, and will be used in conjunction with the soil data and ground slope maps to suggest the most likely type of liquefaction induced ground failure.

REFERENCES

Anderson, Loren R., Keaton, Jeffrey R., Aubry, Kevin and Ellis, Stanley J. (1982); "Liquefaction Potential Map for Davis County, Utah; U.S. Geological Survey, Contract 14-08-0001-19127; Utah State University, Logan, Utah.

Seed, H.B., Idriss, I.M. and Arango, I., (1983), "Evaluation of Liquefaction Potential Using Field Performance Data," Journal of Geotechnical Engineering, ASCE, Vol 109, No. 3, March.

EVALUATION OF LIQUEFACTION OPPORTUNITY AND LIQUEFACTION
POTENTIAL IN THE SAN DIEGO, CALIFORNIA URBAN AREA

14-08-0001-20607

M.S. Power, A.W. Dawson, I.M. Idriss,
R.R. Youngs, and K.J. Coppersmith

Woodward-Clyde Consultants
One Walnut Creek Center 3467 Kurtz Street
100 Pringle Avenue San Diego, CA 92110
Walnut Creek, CA 94596 (714) 224-2911
(415) 945-3000

Investigations

1. Liquefaction potential of the San Diego, California urban area was assessed in this study. This assessment was based on the liquefaction susceptibility and liquefaction opportunity of the area. Liquefaction susceptibility is the relative likelihood that a geologic unit would undergo liquefaction and ground failure during intense seismic shaking; this was assessed for the San Diego area during a previous Woodward-Clyde Consultants study (Power and others, 1982a, 1982b). Liquefaction opportunity, which was evaluated in this study, is a function of the seismicity of the area and the frequency of occurrence of earthquake ground motions capable of causing liquefaction in susceptible materials. When liquefaction susceptibility and liquefaction opportunity are combined, the liquefaction potential of an area can be assessed.
2. Potentially significant sources of earthquakes in the San Diego region were identified and characterized with respect to the parameters necessary for probabilistic seismic hazard analyses (e.g. fault geometry, maximum earthquake magnitude, and earthquake recurrence). The uncertainty in each of these parameters was accounted for through the use of a probabilistic approach (Coppersmith and Youngs, 1982, 1983; Kulkarni and others, 1984) in which input parameters are assigned conditional probabilities that reflect the relative degree of confidence in each parameter.
3. A seismic hazard analysis was conducted to calculate the annual mean number of events that exceed certain acceleration levels as a result of the occurrence of earthquakes of specified magnitudes. This analysis was based on the information for each of the potentially significant seismic sources.

4. The probability of occurrence of liquefaction during a specified time period was assessed using two different methods. The first method is based on a correlation developed by H.B. Seed and I.M. Idriss. In this correlation, the liquefaction criterion is expressed as curves of peak ground acceleration required to cause liquefaction versus the standard penetration resistance of the soil deposit. The normalized standard penetration test data was obtained for the study area during the previous study of liquefaction susceptibility (Power and others, 1982a). In the second method, developed by T.L. Youd and D.M. Perkins, the occurrence of liquefaction in susceptible soils is related to distance from fault sources and the magnitudes of the earthquakes that originate on the individual faults.

Results

1. The tectonic setting and historic seismicity of the San Diego region were reviewed in this study. Based on this review, fourteen potentially significant fault sources were identified and characterized. Geologic and geophysical data are used to define fault length, fault dip and down-dip width. The maximum earthquake magnitude on each fault was assessed using fault dimensions. The frequency of occurrence of earthquakes of various magnitudes was estimated for each fault based on geologic slip rate. These rates were found to yield recurrence relationships compatible with the historical seismicity of the region.

2. Ground acceleration levels for three different return periods were estimated at locations throughout the study area. The ranges of acceleration values obtained are: 0.10-0.15 g for a 100-year return period; 0.20-0.30 g for a 500-year return period; and 0.35-0.55 for a 2500 year return period.

3. Return periods for liquefaction were estimated for the various geologic units identified in the previous study (Power and others, 1982a, 1982b). In Holocene deposits, the computed return periods for liquefaction range from 250 to over 500 years. In Pleistocene deposits, the computed return periods range from 2,000 to 10,000 years. Use of the Youd and Perkins approach yielded longer return periods for liquefaction than use of the correlations developed by Seed and Idriss.

References

Coppersmith, K.J. and Youngs, R.R. (1982), Probabilistic Earthquake Source Definition for Seismic Exposure Analyses (abstract): *Earthquake Notes* Vol. 53, No. 1, January-March, p. 67.

Coppersmith, K.J. and Youngs, R.R. (1983), Source Characterization for Seismic Hazard Analyses within Intraplate Tectonic Environments (abstract): Earthquake Notes Vol. 54, No. 1, January-March, p. 7.

Kulkarni, R.B., Youngs, R.R., and Coppersmith, K.J. (1984), Assessment of Confidence Intervals for Results of Seismic Hazard Analysis: Proceedings of 8th World Conference on Earthquake Engineering (in press).

Power, M.S., Dawson, A.W., Streiff, D.W., Perman, R.C., and Berger, V. (1982a), Evaluation of Liquefaction Susceptibility in the San Diego, California Urban Area: Final technical report prepared for the U.S. Geological Survey under Contract No. 14-08-0001-19110 by Woodward-Clyde Consultants, San Diego, California.

Power, M.S., Dawson, A.W., Streiff, D.W., Perman, R.C., and Haley, S.C. (1982b), Evaluation of Liquefaction Susceptibility in the San Diego, California Urban Area: Proceedings of the Third International Earthquake Microzonation Conference, Seattle, June 28-July 1, 1982.

CONSTRUCTION OF AN ELECTROMAGNETIC
DISTANCE-MEASURING SYSTEM

110121

Judah Levine

Time and Frequency Division
National Bureau of Standards
Boulder, Colorado 80303
(303) 497-3903

Investigations

We have continued our testing and evaluation of a three-wavelength system for measuring baselines up to 50 km long with fractional uncertainties of about 0.02 ppm. The instrument is designed to measure the refractivity of the atmosphere by measuring the path differences between three signals: two optical and one microwave. The optical wavelengths used are 632 nm (He-Ne red) and 441.6 nm (He-Cd blue); the microwave frequency is 8.1 GHz.

Results

During the last few months, we have been working on the evaluation of several systematic errors whose existence has not been previously reported. These errors involve a dependence of the measured red-blue dispersion on the angle between the optical beams and the axis of the microwave modulators. We do not understand exactly where this error comes from. The magnitude of the error depends on geometry; under unfavorable conditions, it can cause errors of almost 0.2 ppm in the measured distance. The error is systematic and cannot be removed by averaging. We are trying to find its cause in the laboratory; at the same time, we will minimize its effect in the field with a series of stops to more accurately limit the acceptance angle of the optical system. We do not know if this error exists in other geometries; it is not clear, for example, if the error is exactly cancelled in two-way systems. Since our two modulators operate at slightly different frequencies, we cannot easily investigate the magnitude of the error in a two-way configuration.

We have also been working on the averaging scheme for determining the index of refraction and the distance. If

the noise is a white process, there is no optimum averaging time. The average value obtained at any time is unbiased and only the standard deviation improves as the averaging time increases. If the noise is not stationary, however, an optimum averaging time usually exists. Loosely speaking, this averaging time is a trade-off between the improvement resulting from a decrease in the random-noise contribution and the degradation resulting from averaging together values which are "different." Our results indicate that the optimum averaging time for the determination of the refractivity is on the order of a few seconds, although longer averages might be useful during periods of unusually quiet conditions. Although the decrease in the standard deviation of the measurements is not a strong function of averaging time, we have found that times much longer than about ten seconds are almost always too long.

MEKOMETER MEASUREMENTS IN THE IMPERIAL VALLEY

Contract No. 14-08-0001-20557

Ronald G. Mason, Christopher N. Crook
and Andrew D. Pullen
Geology Department, Imperial College,
London SW7 2BP, England (011-441) 589 5111

This project, which was started in the early seventies, involves the repeated measurement of a network of about 300 geodetic stations about 800 m apart in the vicinity of El Centro, California, the most important part of which comprises a block of about 150 stations spanning the Imperial fault (figure 1). The purpose is twofold, (1) to obtain detailed information about movements on the fault itself, and strain adjustments around it, and (2) to look more generally for evidence of any previously unrecognized active faulting in the area. The measurements have been made with a mekometer, an edm, with which standard errors approaching 1mm (1 ppm) are routinely achieved.

During the period reported on, the entire network was remeasured. This was the third, and most complete, remeasurement since the 1979 earthquake, and it has provided a very detailed picture of coseismic and subsequent deformation up to more than 8 km from the fault. It was also the first remeasurement since 1975 of the E-W limbs of the network, whose purpose was to look for faulting sub-parallel to the Imperial fault.

The most unexpected feature of the deformation is the complexity of the strain pattern around the fault, and in particular the large components of linear strain, and consequent relative displacements, normal to it (figure 3.b). Thus, on its northeast side the fault is flanked by a 4 km wide zone of linear compression normal to it, averaging about 200 ppm, and this in turn is flanked by a zone of up to 100 ppm extension. On its southwest side the situation is reversed, a 4 km wide zone of linear extension normal to the fault, averaging 150 ppm, being followed by a zone of up to 100 ppm compression. The net result is that points 4 km from the fault on its northeast side have moved more than 65 cm towards it, while points a similar distance away on the southwest side have moved more than 25 cm away from it.

Another interesting fact concerns the right lateral displacement in the few km on either side of the fault. Coseismic right-lateral slip on the fault itself decreased generally from south to north, being about 60 cm at the southern end of the surface rupture, and less than 40 cm at the northern boundary of the network, beyond which it died away rapidly. Since the earthquake, the fault has continued to creep, at a rate decreasing approximately logarithmically with time, but in contrast to the coseismic slip, the post-earthquake creep is a maximum near the middle of the surface break, near Waterman's corner. There, the present rate of creep is about 22 mm/yr, and as of mid-October 1983, four years after the 1979 earthquake, the fault had crept another 29.5 cm, two thirds as much as the 43.6 cm of coseismic displacement.

The present position away from the fault is shown in figure 3(a). Up to about 4 km from the fault, right-lateral displacement (parallel to the fault) supplements movement on the fault itself, so that in the northern part of the area the total right-lateral displacement between points 4 km from the fault on opposite sides now exceeds 1.3 m. Whether or not the blocks as a whole are moving at the same rate as the fault is creeping has not yet been determined.

Remeasurement of the E-W limbs of the network has not revealed any evidence for strike-slip faulting sub-parallel to the Imperial fault. However, three of six zones identified in 1975 as being potentially interesting show large changes, predominantly of a dilatational nature. These have not yet been fully analyzed.

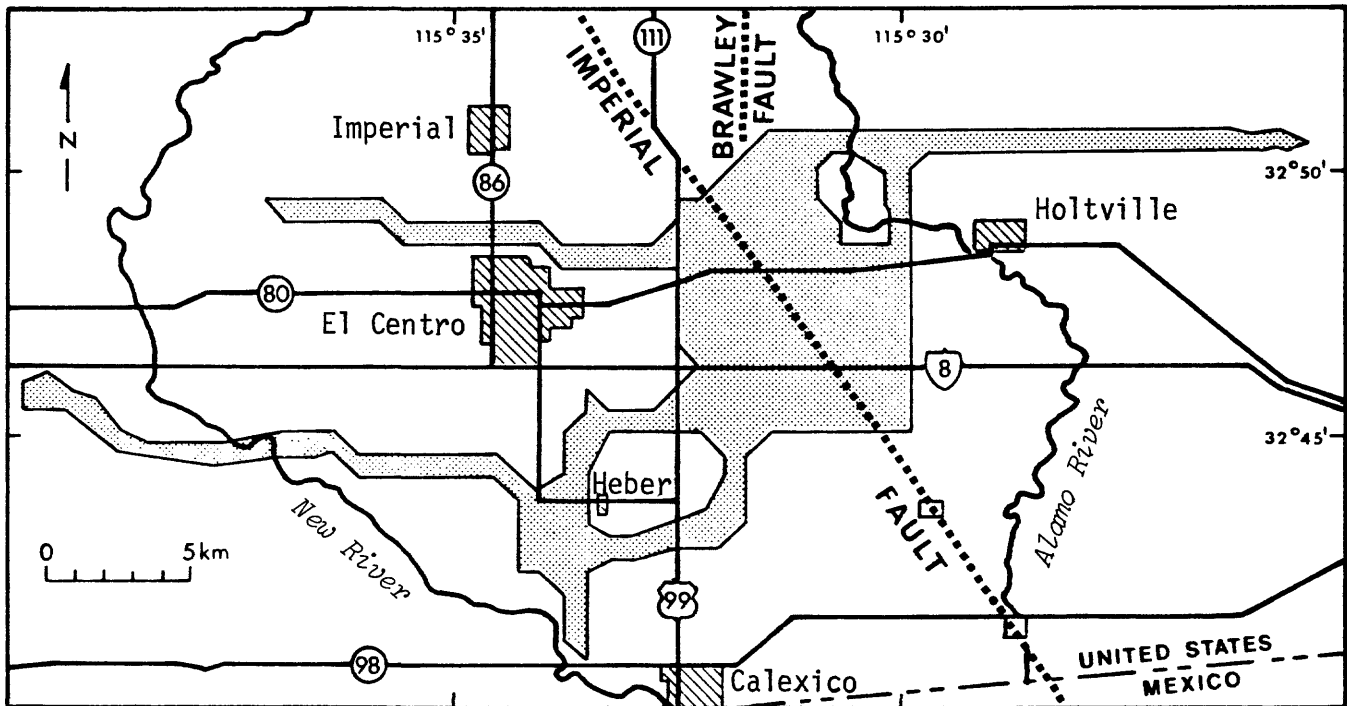


Figure 1. The Imperial Valley mekometer network.

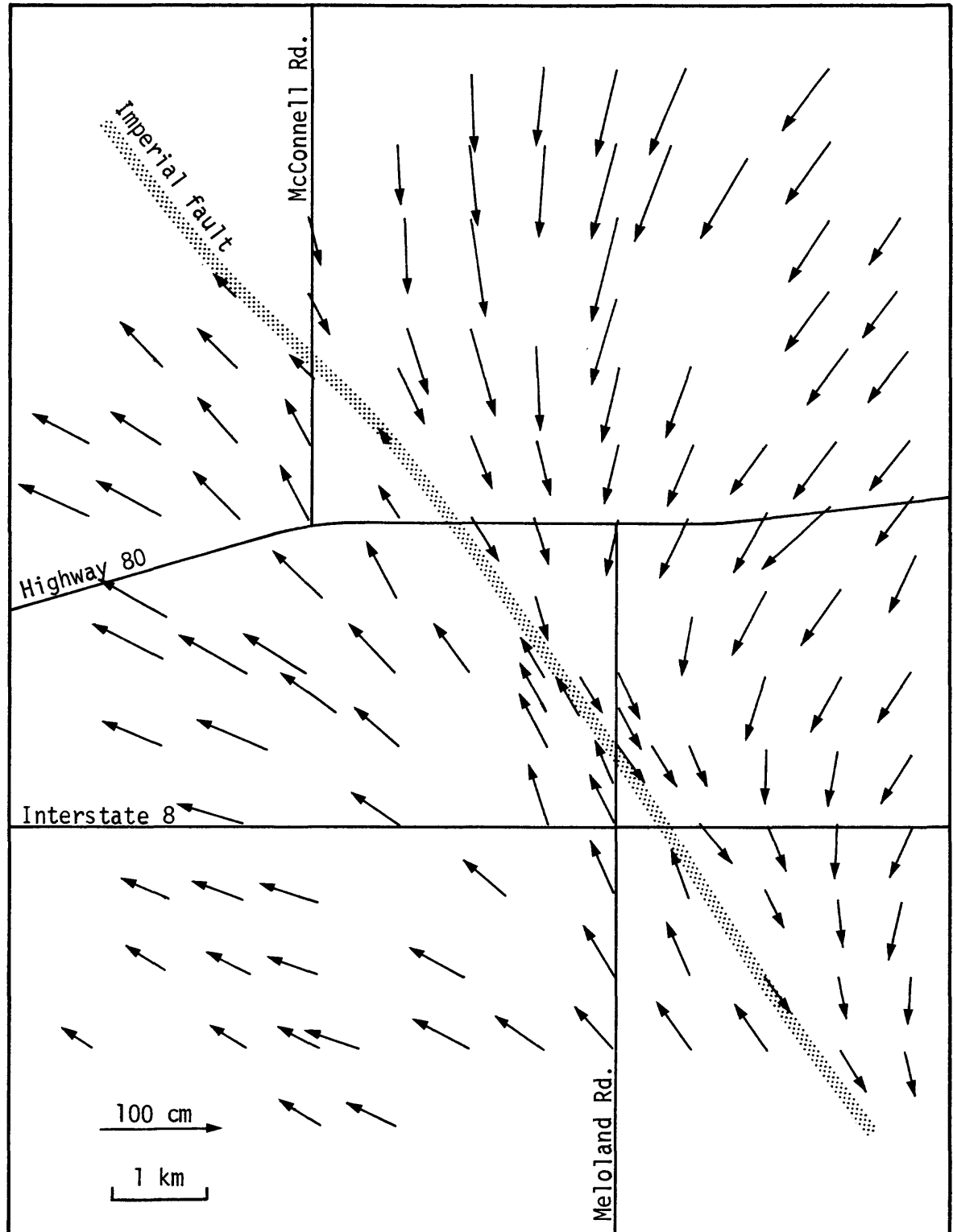


Figure 2. Station displacements between 1978 and 1983, "balanced" about the fault.

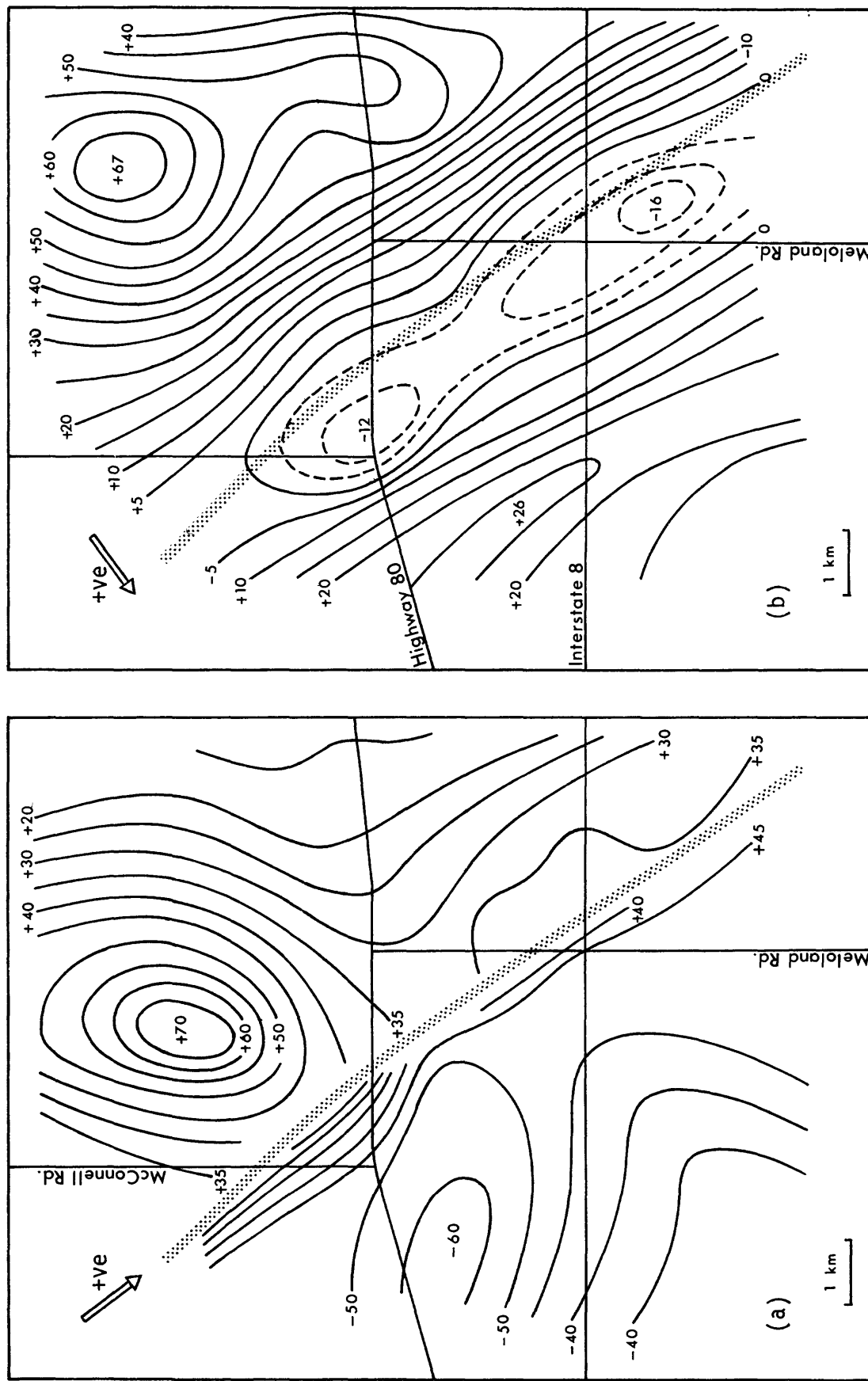


Figure 3. Components of displacement between 1978 and 1983 (a) parallel, and (b) normal, to the fault, in cm. Zero values are chosen arbitrarily, as in figure 2.

COOPERATIVE EARTHQUAKE PREDICTION RESEARCH WITH
INSTITUTE OF GEOPHYSICS, SSB, PRC

14-08-001-21341

Francis T. Wu
Department of Geological Sciences
Center for Study of Natural Hazards
State University of New York
Binghamton, New York 13901

Ta-liang Teng
Department of Geological Sciences
University of Southern California
Los Angeles, California 90008

Investigations

1. Augmentation of the Beijing-Tangshan-Tianjin (BTT) telemetered seismic network to lower event detection threshold and improve data acquisition system.
2. Research concerning seismicity and tectonics of the Beijing-Tangshan-Tianjin area and the use of seismicity toward earthquake prediction.
3. Fabrication and installation of water well level monitoring instrumentation in the vicinity of Beijing and the study of data gathered from these stations.
4. Study of other data pertaining to earthquake prediction work in China.

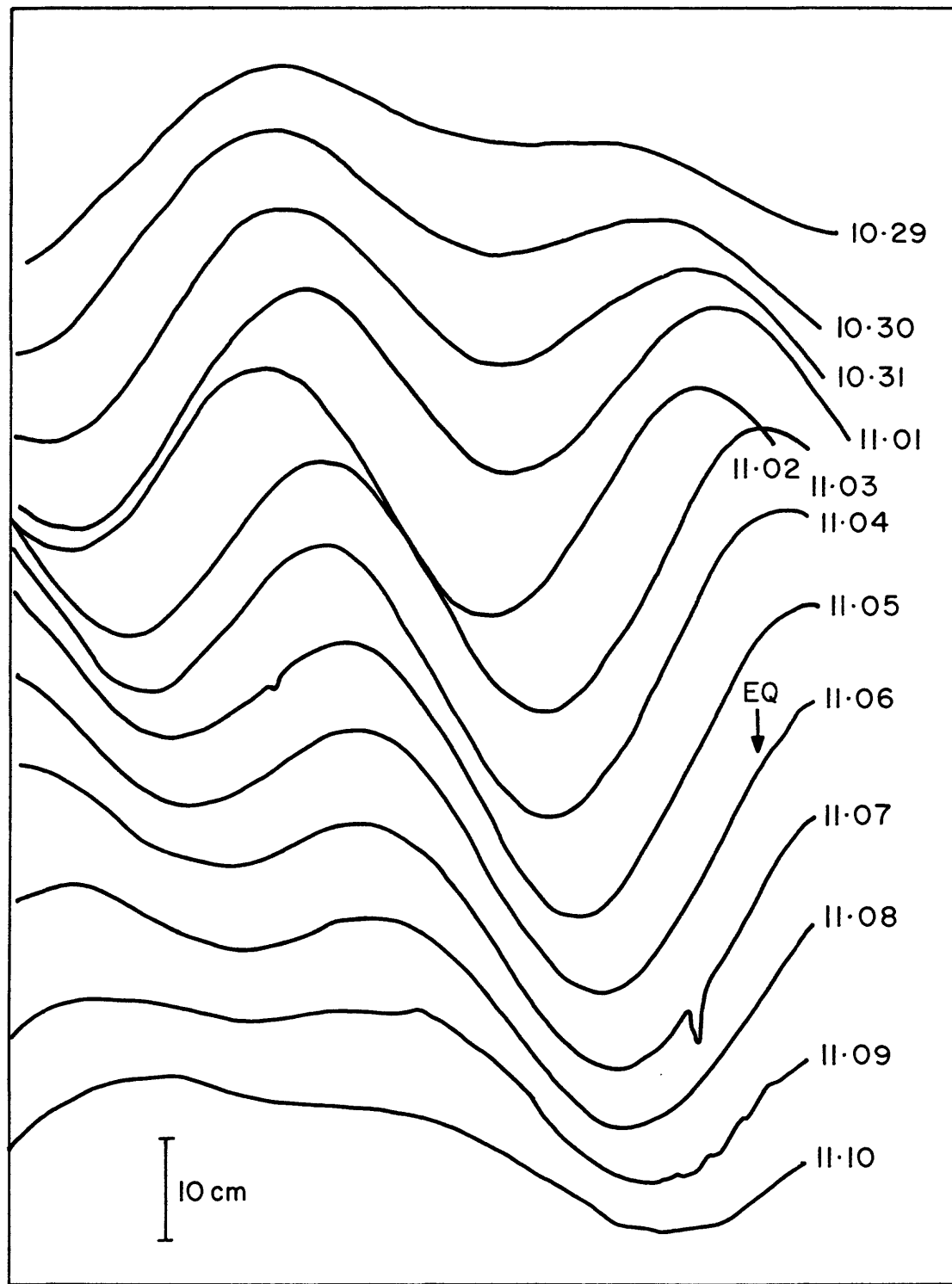
Results

1. The VHF transmission-receiving instruments procured under previous contracts under the same title continues to function well. They form critical links between stations that cannot be connected with existing Chinese equipment. A total of about 60 channels of seismic signals are now being transmitted back to Beijing recording center. The signals are to be fed into a PDP11/44 computer system that has been installed early last year (1983) through USGS efforts. However, due to hardware (Analog to digital converter in particular), the implementation of real-time data acquisition on the computer has not been able to be carried out even though the needed software has been installed last October.
2. Portable stations deployed in the region of a magnitude 5.5

earthquake in October, 1982 near the city of Lulong northeast of Tangshan has shown that nearly east-west normal faulting and northwest trending right-lateral faulting are the modes of deformation in the area. Interestingly, in eastern U.S. northeast trending right-lateral strike-slip faults coexist with northwest trending thrust faulting; the cause probably lies in the difference in the stress regimes of these two regions.

3. Water level recording systems, including USC designed sensors and SUNY Binghamton designed digital recorder/printer and clock, have functioned well. Two months after installation, an earthquake of magnitude 5.7 occurred about 500 km away, in Shandong Province, from Gaocun, a deep well site. No coseismic effects has been observed (Fig. 1). This 3404 m deep well (capped to about 2700 m) responds to earth tides and barometric pressure variations very clearly (Fig.2). A closer and/or larger event should produce clear coseismic if not precursory signals based on Chinese experience of the Tangshan earthquake.

4. New crystal clocks manufactured from commonly available modules has been installed in the water well monitoring systems to improve the timing. It is now possible to study the phase characteristics of the earth tides.



0800 GMT

Figure 1. Daily water level variations at Gaocun station.

OBSERVED WATER LEVEL, ATMOSPHERIC PRESSURE
AND THEORETICAL GRAVITY CURVES AT GAOCUN
(1983 · 10 · 25 -- 11 · 10)

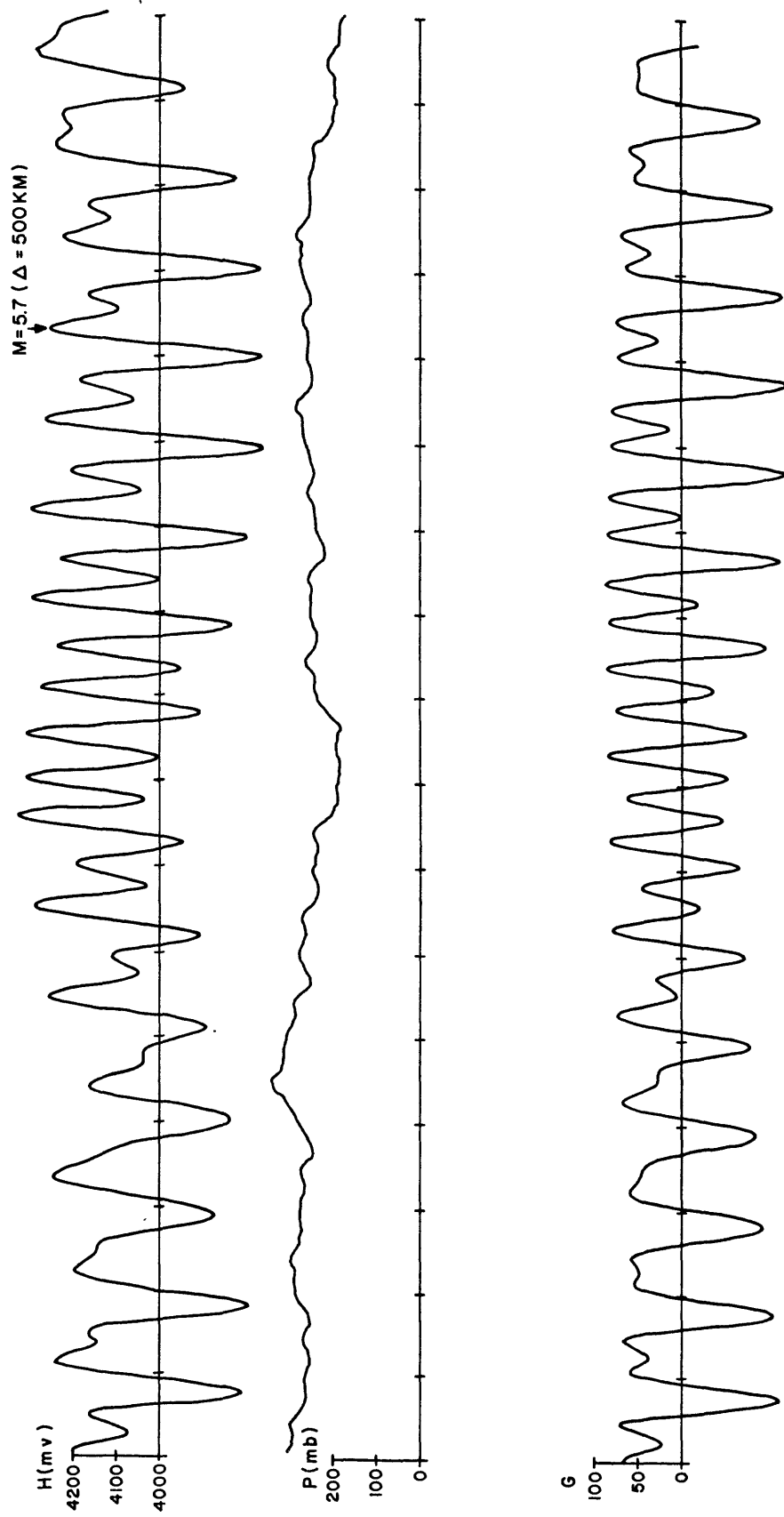


Figure 2. Water level ($1.8 \text{ mmv}=1\text{mm}$), atmospheric pressure and calculated gravity curves at Gaocun for a sixteen day period.

Earthquake Prediction Based on Seismicity Patterns

14-08-0001-21324

M. Wyss and R. E. Habermann
 CIRES, Box 449
 University of Colorado
 Boulder, Colorado 80309
 (303) 492-8028

Investigations:

We are presently working on three major tasks: the determination of levels of homogeneous reporting in subduction zones, seismicity of the Imperial Valley, and a summary paper on precursory quiescence.

Results:

Minimum Magnitudes of Consistent Reporting

The determination of the magnitude level above which events are consistently reported through time is a crucial first step in the study of seismicity rate changes. The vast majority of rate changes observed in teleseismic and local seismicity catalogs are due to changes in the detection and reporting systems. Such changes must be recognized and dealt with before real changes can be examined. The most straight-forward way to deal with detection changes is to use magnitude cutoffs. These are effective because smaller events are most sensitive to such changes.

We have continued our effort to determine the magnitudes above which events are consistently reported in the subduction zones of the world. A number of subduction zones have been examined. The results are listed in Table 1.

TABLE 1. MINIMUM MAGNITUDES OF HOMOGENEOUS REPORTING

| REGION | CUTOFF (m_b) | REGION | CUTOFF (m_b) |
|---------------|------------------|----------------|------------------|
| South America | | Kuriles | 4.7+ |
| 0-0°N | 5.1+ | New Hebrides | 4.8+ |
| 0-10°S | 5.0+ | Tonga Kermadec | 4.9+ |
| 10-18°S | 4.9+ | Marianas | 5.1+ |
| 18-26.5°S | 4.9+ | Izu-Bonin | 4.9+ |
| 26.5-35.5°S | 4.8+ | Indonesia | 5.5+ |
| 35.5-46°S | 4.8+ | Aleutians | 4.7+ |

Seismicity of the Imperial Valley

We have finished an analysis of the seismicity rates in the Imperial Valley region of California. The first step of this investigation was the determination of a background seismicity rate for the region. Figure 1 illustrates the steps in this process.

Figure 1A shows the cumulative number of events as a function of time in the original data set. Note the numerous vertical jumps in the curve and the general upward curvature. These reflect swarms and increasing detection respectively. The other curve in this Figure gives the z value resulting from the comparison of the rate during every 15 week period in the data with the long term rate. Positive values indicate that the rate surrounding the point is lower than the long term rate. The lack of values of this function near zero indicates that few 15 week periods exist with rates which are near the long-term rate. Figure 1B shows the data set after swarms were removed using the algorithm designed by McNally. The vertical jumps are gone but the upward curvature (increasing detection) still makes it impossible to determine a meaningful background rate.

We found that events with $M_L > 2.4$ have been consistently reported in this region since 1973. When these events are considered, the cumulative number curve becomes remarkably linear throughout the time period examined. Most 15 week periods have a rate similar to the long-term rate as indicated by the fact that the statistical function is well centered on $z=0$. Thus, we believe a meaningful background rate can be determined for this region if dependent events and events which are not consistently reported are removed from consideration.

A quiet period occurred during the 15 weeks prior to the Imperial Valley earthquake of 1979. Unfortunately, this quiet period begins very close to the time of a change in the seismic instrumentation in the Imperial Valley. At present, therefore, we cannot unambiguously determine whether this quiescence is related to this change or if it is a real precursor. The solution to this problem lies in a detailed determination of the spatial distribution of the change.

During the course of our work in Imperial Valley we recognized several changes which affected the larger events and not the smaller (Figure 2). These changes are interpreted as being due to changes in the reporting system, not the detection system. The low rates of events with $M_L > 1.4$ during 1977 and 1979 reflect the preliminary nature of the Cal Tech catalog for those years. The low rates of events with $M_L > 2.5$ between Sept. 1975 and Sept. 1977 are related to operation of the network there by the USGS. These reporting changes, in contrast to simple detection changes, can not be eliminated using simple magnitude cutoffs. In fact, they are accentuated by such cutoffs (Figure 2).

Summary Paper on Seismic Quiescence:

We are presently involved in compiling a summary of work on precursory seismic quiescence. This paper is an attempt to define the state of understanding of this phenomena at this time. In connection with this project, we would appreciate it if people who have studied quiescence would send reprints of their work to Dr. R. E. Habermann, Geophysical Sciences, Georgia Institute of Technology, Atlanta, GA 30332. This will help insure the broadest possible outlook in our paper.

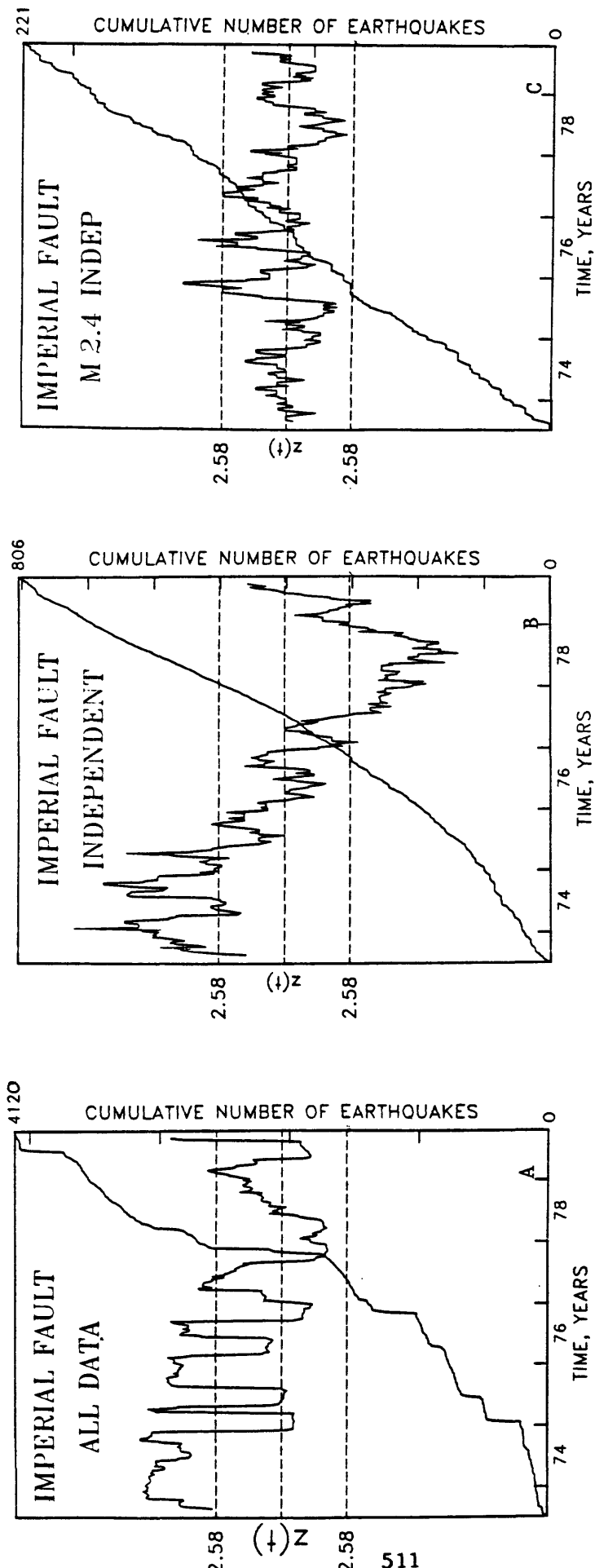


Figure 1. Cumulative number of events curves for all events (A), independent events (B), and independent events with $m > 2.4$ (C) in the area used by Johnson and Hutton (1982) for examining possible precursors to the Imperial Valley, $\text{earthquake of October 15, 1979}$. This region includes the most active section of the Imperial Valley. The jumps in the curve in A reflect the frequent swarms in this region. The upward curvature of the curves in A and B reflect increased detection. This Figure demonstrates the steps necessary in determining a background seismicity rate. First, the step from A to B shows the effect of removing dependent events. The step from B to C shows the effect of removing events which are not consistently reported. The necessity of this step is clear, for it would be impossible to define a background rate on the basis of the data in B.

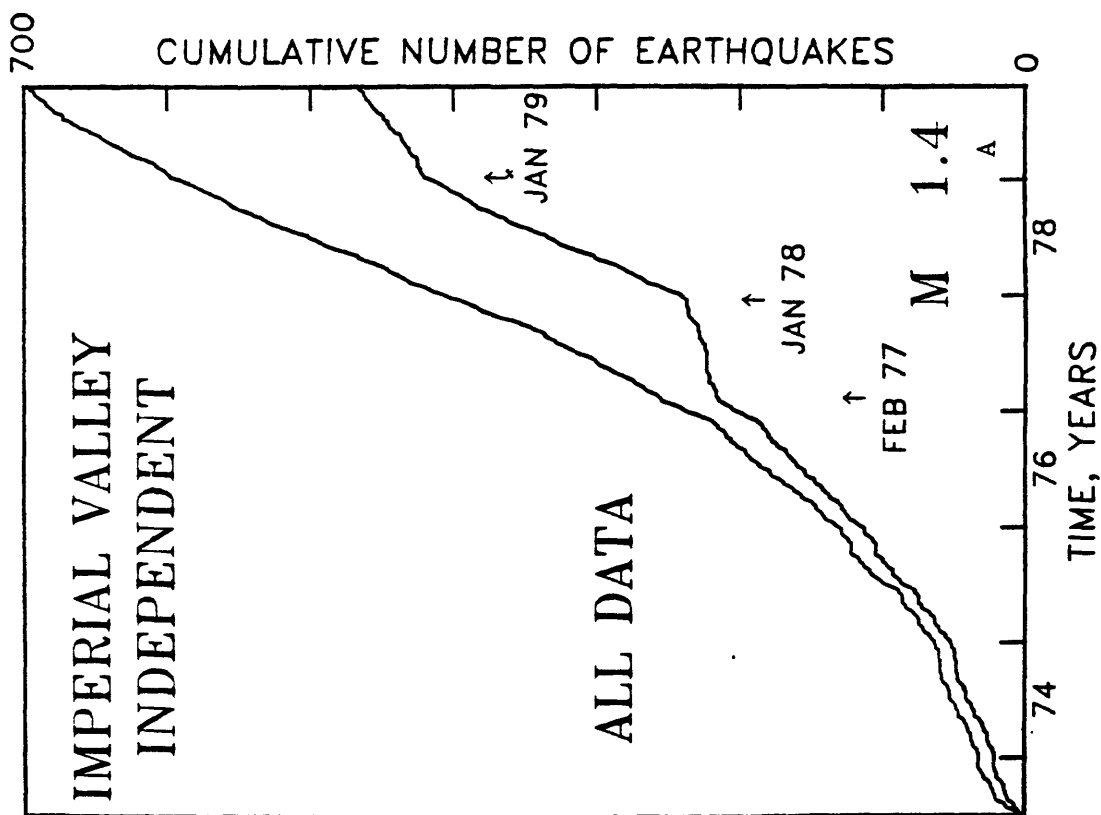
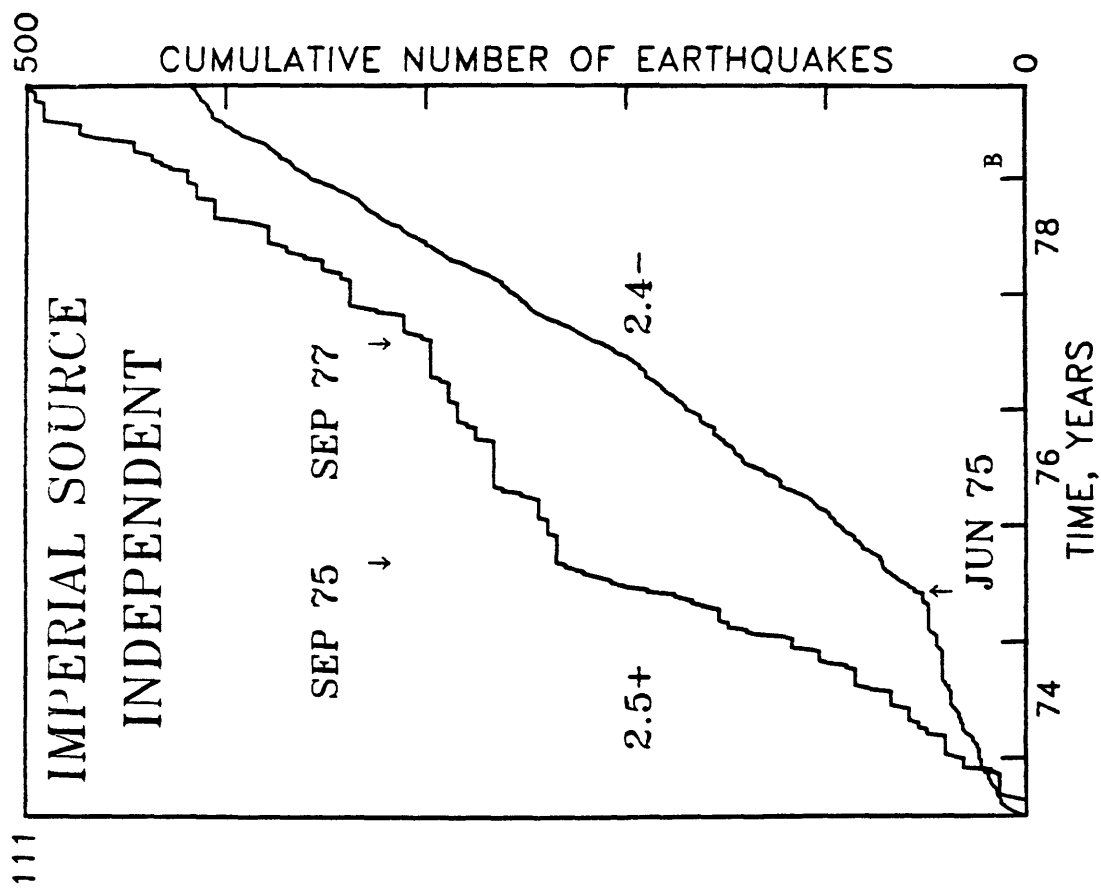


Figure 2. (A) Cumulative number of events curves for the Imperial Valley excluding the Imperial Fault area. Both data sets show independent events only. The upper curve includes events of all sizes; the lower curve includes events with $m > 1.4$. The same scale applies to both curves. Note the contrast between the smooth increase in all events with the clear quiet periods observed when a magnitude cutoff is applied. (B) CNET curves for the 1979 source volume showing independent events with $m > 2.5$ (scale on the right) and $m < 2.4$ (scale on the left). Note the period of low rate between 1975 and 1979 in the larger events and the coincidence of the beginning of this period with an increase in the rate of smaller events. This suggests that this change in the rate is related to reporting, not to detection.

In-Situ Seismic Wave Velocity Monitoring

14-08-0001-19251

T.V. McEvilly
R. ClymerSeismographic Station
Department of Geology and Geophysics
University of California
Berkeley, California 94720
(415) 642-3977

On-going monitoring of first-arrival travel times on 8 paths and down-hole times at 7 boreholes at sites adjacent to the San Andreas fault in central California continued smoothly through this report period. Measurements are made with a Vibroseis® system. We experienced intermittent malfunctions of the vibrator control electronics in the late fall of 1982 which slowed data collection but had no effect on data quality. Repairs were made in the winter and spring of 1983 but have not yet been field tested. To cut costs, the field crew was put on lay-off status for the period January-April, 1983 (the local rainy season). The start of the 1983 field season has been delayed by the unexpected need to transfer the recording system to a new vehicle. We expect to resume measurements in July.

Software to manipulate and archive the present data base has been developed on a small computer system. At some point in the future, we will move the data base to a VAX computer at the Lawrence Berkeley Laboratory. A new field recording system has been developed which records the 512-point correlated seismograms on a digital cassette deck and allows for phone-line data transmission to the LBL VAX computer. VAX software will be developed to automatically update the data archive with new field data.

Repeated measurements indicate a travel-time precision below 1 msec for first arrivals. Travel-times on monitoring paths have followed smooth trajectories that primarily represent seasonal variations of several msec of very near-surface origin. Borehole data sets, collected at most sites, have been used to develop preliminary corrections to remove the near-surface effects. We see a stability of about 1 msec in the corrected travel-time data.

Monitoring of deep crustal reflections in the Bear Valley area has continued to proceed slowly and with difficulty, due to severe cultural noise and the destruction of the permanent long geophone array by rodents. By recording in the late-night and early morning hours and adequately filtering the geophone signal before correlation, data precision appears to be acceptable, though not as good as we had hoped.

A 24-hour series of repeated measurements of the travel time of a deep crustal reflection was conducted in Bickmore Canyon west of Bear Valley. A random scattering of travel-times of about 1 msec was observed. There was no indication of a dependence of travel time on tidal stress.

A number of short experiments were carried out to test the feasibility of replacing surface arrays with various types of borehole receiver, with mixed results. A geophone package cemented in competent rock at 100-m depth proved to be an excellent receiver, producing a high signal-to-noise ratio (S/N). A geophone package clamped in the Stone Canyon deep well at 100-m depth produced a distinctly lower but still adequate S/N, and will replace the surface array used to date at that site. A hydrophone at the bottom of the deep well (600-m depth) produced poor S/N and was unreliable. A single geophone at 42-m depth in the San Andreas fault zone likewise proved to be a poor receiver.

**Continuation of Gravimetric Monitoring
in Southern California**

USGS Contract No. 14-08-0001-20556

James H. Whitcomb

**Cooperative Institute for Research in Environmental Sciences
Campus Box 449
Boulder, CO 80309
(303)492-8028**

During the February 1983 to January 1984 period, five field observation sessions were conducted over the gravity network during the months of February, May, June, July and October. In all sessions, three LaCoste-Romberg gravity meters, G395, G465, and G541 were used. These meters are calibrated by means of the absolute gravity calibration range established in Southern California in April 1982. This absolute gravity range is monitored on a regular basis in the normal gravity network operations.

Within the network, as reported last year, only two stations have gravity changes that cannot be attributed to groundwater or other causes. They are at LUCAS and CIT2. LUCAS is a crystalline rock site in the middle of the Transverse Range San Gabriel mountains. A decrease of 30-40 microgals is seen from 1977 to 1983. However, the gravity data from LUCAS appear to be quite stable aside from this monotonic long-term change.

CIT2 is located on the Malibu coast. This was one of the data sets singled out last year as showing the largest unexplained gravity change, and gravity has continued to show rapid changes. Gravity in the first half of 1983 decreased by 50 microgals from the unusual highs seen in latter 1982. The 1983 decrease was not enough to bring gravity back to 1974-1977 levels, however. As a check of the sudden gravity drop, a second summer survey was made within one month of the first and the two surveys compare well. No cause of the gravity variations at CIT2 has been determined as yet. It is clear that gravity drop cannot be attributed to groundwater levels which generally increased over Southern California in early 1982 as evidenced by the gravity increase at our "groundwater monitoring" stations. As noted previously, other gravity stations along the Malibu coast do not show the variations seen in CIT2 by January 1984. However, some indication of similar behavior has been seen for adjacent stations in later data.

Several stations in the network have exhibited a high level of stability over their lifetime, some with a baseline as long as ten years. Here stability is defined as no significant variation from constant gravity of the plus/minus two-standard-error smoothing band (with the possible exception of LUCAS).

CIT1/1a (#4) is on the coast at Santa Monica and shows only minor deviations from constant gravity.

CIT4 (#8) is on the western Malibu coast and has some $\pm 10\text{-}15$ microgal oscillations but the trend is zero.

ECHO/GSC (#23) became an absolute gravity reference for the network in 1982 and is at the NASA Goldstone radio antenna complex in the northeast Mojave desert. Oscillations of $\pm 15\text{-}20$ microgals occur but the trend over nine years is zero.

TUJUNGA (#25) overlies crystalline rock and is on the central upthrown block of the 1971 San Fernando earthquake. Oscillations are minimal and the trend is zero.

RITTER (#30) overlies a pediment of low porosity metamorphic rocks in the San Gabriel mountains a few kilometers southwest of Palmdale and the San Andreas fault. There are small $\pm 10\text{-}15$ microgal excursions from a zero trend.

Lucas (#38) is on a crystalline rock site in the San Gabriel mountains. As discussed earlier, a long term decreasing trend of gravity is seen but oscillations are minimal.

CLYDE R. (#43) is on the trace valley of the San Andreas fault just northwest of San Bernardino. It is one of the most stable stations with minimal oscillations and zero trend.

OAK FLAT (#49) is in the San Gabriel mountains overlying crystalline rock. Oscillations are minimal and the trend is zero.

ARIES1 (#50) and **ARIES3 (#51)** are adjacent stations on the coast of the Palos Verdes Peninsula. They are intended to correlate with measurements of the tide gauge in the Los Angeles harbour and a NASA VLBI site. No significant change is seen in the gravity data. This is confirmed by the Los Angeles tide gauge data that show elevation relative to La Jolla as being within $\pm 2\text{-}3$ cm from 1974 to 1983.

Time and Environment Dependent Failure in Rock
14-08-0001-21354

P.L. Swanson, H.A. Spetzler and I.C. Getting
Cooperative Institute for Research in Environmental Sciences
University of Colorado
Boulder, CO 80309
(303) 492-8028

Investigations

Our overall objective is to understand the mechanisms responsible for time-dependent phenomena that are precursory to or concomitant with the rock failure process. Laboratory studies of mode-I (tensile) subcritical fracture were undertaken to understand this particular element of time and environment dependent deformation of upper crustal rocks. By probing subcritically-propagating fractures in Westerly granite with ultrasonic waves (P,S, and surface waves), the evolution of the micro-mechanical fracture structure has been characterized in terms of wave-amplitude attenuation and travel-time delay.

Introduction

In order to assess the effect of time and environment on rock fracture it is necessary to first characterize the fracture process under constant environmental conditions. In an earlier laboratory investigation (Swanson, 1984) experimental techniques that were originally developed for use with glass and ceramics were used to study subcritical fracture of a variety of macroscopically homogeneous rock types. Due to large deviations between the actual material's behavior and that usually assumed in the analyses, consistently repeatable measurements were not possible. The nature of the results hinted at the complexity of time-dependent rock fracture and the possible existence of several competing mechanisms which limit crack propagation rates. The most widely accepted model of fracture propagation incorporates a cloud of microcracks which surrounds the ends of macroscopic fractures. Macrocrack extension is thought to occur by microcrack coalescence. The process-zone microcracks are susceptible to time- and environment- dependent growth and so the size and shape of the process zone is predicted to be dependent on macrocrack velocity and environment. In this study, subcritically-propagating fractures in Westerly granite were acoustically interrogated in order to delineate the micro-mechanical structure. The experiments provide data to test microcrack process zone models and further our understanding of the mechanisms responsible for subcritical fracture.

Results

A series of wedge-loaded double-cantilever beam specimens (16x76x200mm) were split longitudinally at room temperature and 50% relative humidity. Both compressional and surface waves were made to propagate perpendicular to the fractures. Waveforms were digitally recorded at 1-5mm intervals along a traverse parallel to the crack. On a different propagation path, a compressional source was concentrated to a 1.5mm diameter to measure the width of the fracture zone. Waveforms from this source contained many phases and were recorded at 1mm intervals along a perpendicular traverse. Measurements were taken at various positions along the load versus crack-opening displacement curve. Such force-displacement relations have frequently been characterized in terms of linear, non-linear, and post-peak regions (Hoagland

et al., 1973). The non-linearity has been attributed to the creation of micro-cracks surrounding the starter-notch tip. Propagation of the macrocrack by the coalescence of microcracks has been interpreted as starting at the peak of the force-displacement curve.

Summary of Experimental Observations:

- (1) Variation of approximately 15% was found in the amplitude of both P and surface waves in Westerly granite under zero-load conditions (Figure 1). Such amplitude variation was not found in identical experiments on glass. Travel-time variation over the 78mm path dimension in the granite showed less than 1% variation at zero load.
- (2) Upon loading to the middle of the non-linear region of the force-displacement curve, P and surface-wave amplitudes begin to decrease as far as 14-40mm ahead of the 0.6mm radius starter-notch tip. The variability in attenuation-zone lengths suggests that the force and displacement measurements do not consistently correspond to identical states of damage.
- (3) With further loading to the peak of the force-displacement curve, the position, at which amplitudes began to decrease following the first load excursion, does not significantly penetrate further into the specimen. The length of the partial-transmission zone remains the same but the amplitudes decrease considerably.
- (4) Unlike the granite experiments, the form of the amplitude roll-off curve for glass remains unchanged as cracks propagate. The roll-off curve translates with the crack tip in glass.
- (5) The width of the zone of partial transmission in granite was found to be very narrow compared to its length, ranging from one to at most four millimeters.
- (6) With further application of load, the amplitude roll-off curve becomes steeper and more closely resembles the roll-off slope associated with the unfractured sawn slot. Continued post-peak loading of the samples sometimes resulted in a rapid surge of crack extension that frequently diverged from the original fractures at angles between ~20-45°. The fracture would leave the mid-plane at the position, referred to as the "pinning point", where the amplitudes were found to begin to decrease during the previous acoustic scans. As loading continues, the acoustic scans undergo another cycle very similar to that observed over the first increment of crack-surface separation.
- (7) The location of maximum travel time increase was always found toward the starter-notch and was at most 8% over the 78mm path length.
- (8) Upon unloading the samples, the partial acoustic transmission was sometimes found to increase, implying crack closure. Reloading resulted in a progression of the amplitude roll-off curves that was very similar to that found for the initially unfractured sample.

The standard interpretation of force-displacement measurements, yielding the popular picture of a discrete macrofracture propagating in minute increments, appears incorrect for these wedge-loaded double-cantilever beam experiments on Westerly granite. Instead, fractures appear to form as gradually separating surfaces having a lateral extent of several tens of millimeters and ending at a "pinning point" or barrier to further gradual separation. The scale of the separation process does not approach "small-scale yielding" and consequently the stresses responsible for the fracture processes are not adequately described by the asymptotic solution represented by K_I , the stress-intensity factor of linear elastic fracture mechanics.

The gradual decrease in acoustic transmission coefficients with distance and load suggests that there is probably frictional contact between the surfaces even during the macroscopically mode-I extension. Restraining forces, provided by crack surface interference, reduce the severity of the crack-tip singular field thus reducing the size of the critically stressed microcrack volume (Figure 2). Both of these mechanisms, frictional resistance and microcracking, are time and environment dependent. Without frictional constraints, the calculated extent of microcracking would be greater. In total, the combined effects of microcracking and friction produce a process zone that is much more elongated and narrower than predicted by microcracking alone and is closer to the observed shape of the zone of partial transmission.

References

- Hoagland, R.G., Hahn, G.T., and Rosenfield, A.R., 1973, "Influence of microstructure on fracture propagation in rock", *Rock Mechanics* 5, pp. 77-106.
 Swanson, P.L., 1984, "Subcritical crack growth and other time- and environment-dependent behavior in crustal rocks", *J. Geophys. Res.*, (in press).

Reports

Swanson, P.L., Subcritical Crack Growth and Other Time and Environment Dependent Behavior in Crustal Rocks, *J. Geophys. Res.*, (in press) 1984.

Swanson, P.L. and H. Spetzler, Ultrasonic probing of the fracture process zone in rock using surface waves, in *Proc. 25th U.S. Symp. Rock Mech.*, Northwestern Univ., June 25-27, 1984 (in press).

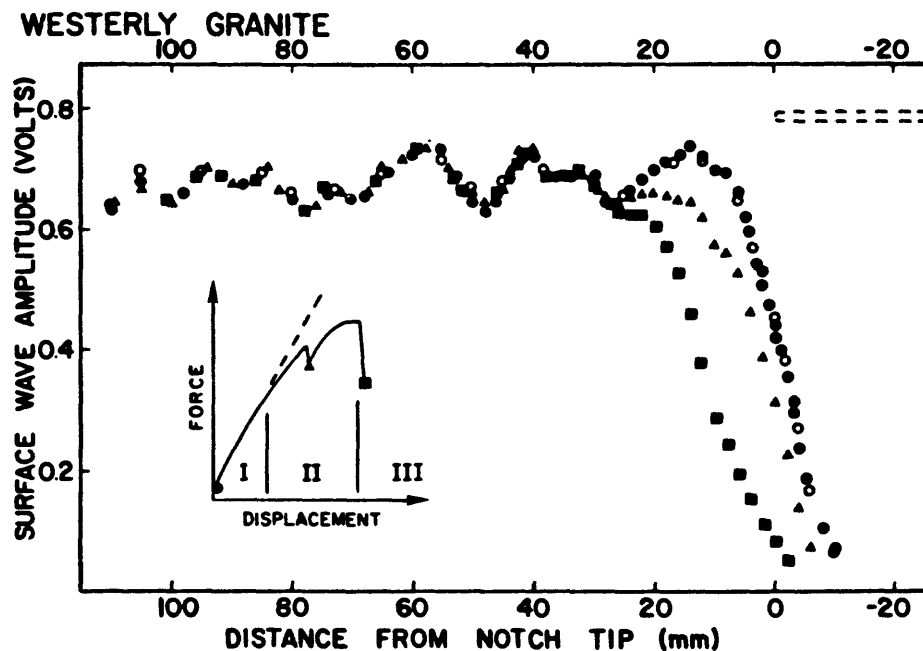
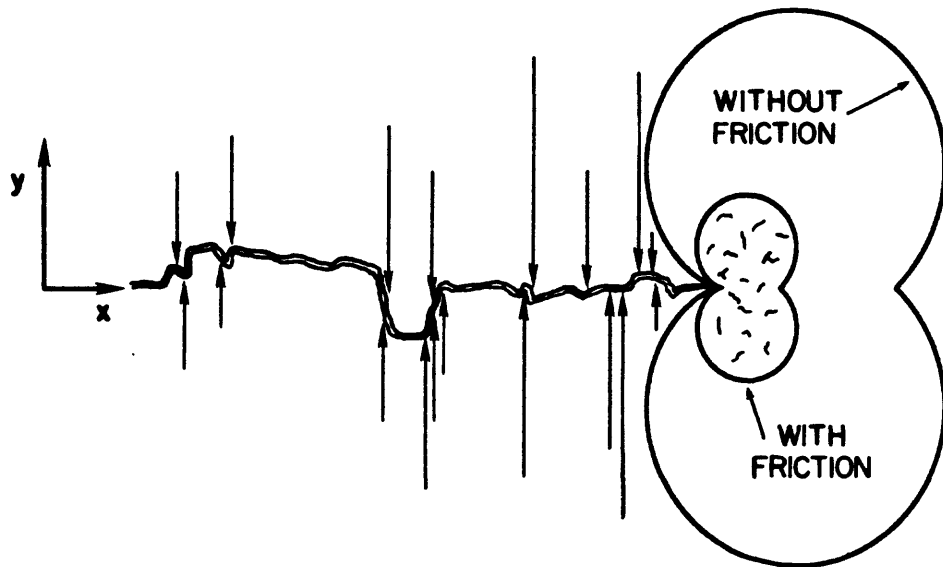


Figure 1. Surface wave amplitudes - parallel traverse: Circles represent data from two separate scans near zero load. Data represented by triangles and squares were obtained after time-dependent deformation which began in the middle of the non-linear region and the peak of the force-displacement curve, respectively.

PREDICTED MICROCRACK VOLUME WITH AND WITHOUT
FRICTION BETWEEN FRACTURE SURFACES



$$K_I = K_{\text{NO FRICTION}} + 2(a/\pi)^{1/2} \int_0^a [\sigma_y(x)/(a^2 - x^2)^{1/2}] dx$$

$a = \text{effective crack length}$

Figure 2. Effect of point restraining forces (friction) on the predicted micro-crack volume. Friction elongates the zone of energy dissipation.

Time-dependent Constitutive Relation for the San Andreas and
Hayward Fault Gouges

USDI 14-08-0001-21352

C.Y. Wang
Department of Geology and Geophysics
University of California, Berkeley 94720

Investigation

We have investigated the relationship between friction coefficient and the textures of sheared chlorite gouge samples sheared under high confining pressure. The purpose is to seek a physical explanation of the observed workhardening of fault gouge during frictional sliding and to determine the dominant mechanism.

Results

We studied the fabrics of chlorite samples using high-magnification (x400) microscopy. These samples include (1) oven-dried powder (<200 mesh) of the original sample, (2) samples consolidated at 20-400 Mpa confining pressures, and (3) sheared samples at confining pressures of 50 to 200 Mpa at slip rates from 10^{-3} to 10^{-5} mm/sec. The results of these fabric studies can be used, together with void ratio, slip rate and displacement to model the friction coefficients in the sliding experiments. These results are illustrated as follows:

(A) Fabric Analysis:

- 1) Under confining pressure, a preferred orientation of chlorite particles is generated, i.e., the long axes of chlorite grains aligned in the direction perpendicular to the direction of consolidation. This may have to do with the drainage pattern of pore fluid during the consolidation process, or it may be a stable configuration under the confinement of rigid boundaries. The average grain size, on the other hand, is not affected.

2) After deviatoric stress is applied to the sample, two deformation regimes are recognized: a) Before yielding, the shear stress enhances the alignment of chlorite particles; no effect on grain size is evident. b) After yielding, the particle size of chlorite is reduced, with the magnitude of reduction being inversely proportional to the magnitude of applied deviatoric stress.

(B) The Results of Grain Size Analysis

After the measurement of grain size, several distribution functions have been used to fit the results. It is found that the grain size distribution of chlorite samples, deformed or undeformed, follows Gamma Distribution function, with the following observations.

- 1) Before yielding, deviatoric stress only enhances the alignment of chlorite particles; no effect on grain size.
- 2) After yielding, empirical relationships between the mean grain size $\langle d \rangle$ (in μm), standard deviation $\langle sd \rangle$ (in μm) and the deviatoric stress $\Delta\sigma$ (in MPa) are as follows (referring to Figure 1):

(i) Along the sliding direction

$$\langle d \rangle = 0.6048(\ln(\Delta\sigma))^2 + 0.9450\ln(\Delta\sigma) + 35.0722\mu\text{m} \quad (1)$$

$$\langle sd \rangle = 1.3119(\ln(\Delta\sigma))^2 + 8.9232\ln(\Delta\sigma) - 1.2883\mu\text{m} \quad (2)$$

(ii) Perpendicular to the sliding direction

$$\langle d \rangle = 10.1 \pm 1.0 \mu\text{m} \text{ and}$$

$$\langle sd \rangle = 4.5 \pm 1.0 \mu\text{m}$$

The values of $\langle d \rangle$ and $\langle sd \rangle$ are reduced to half of those in the original samples.

It is suggested that the greatest deviatoric stress experienced by the chlorite sample can be estimated from studying the grain size distribution of the sample and vice versa.

C) Friction Coefficient

Since the sample of smaller void ratio and smaller grains is generally stronger, a phenomenological representation of the friction coefficient of chlorite sample may be suggested as follows:

$$\begin{aligned}\text{Friction Coefficient} &= \frac{\tau}{\sigma_N P_w} \\ &= F_1 v + F_2 D + \frac{F_3 e_Y}{1+e} + \frac{F_4}{\langle d \rangle^n} + F_5 \\ &= v(F_1 + F_2 t) + \frac{F_3 e_Y}{1+e} + \frac{F_4}{\langle d \rangle^n} + F_5\end{aligned}$$

in which e_Y is the void ratio at yield, $\langle d \rangle$ is the average grain size along the sliding direction (Equation (1)), τ is the shear stress, σ_N is the normal stress, P_w is the pore pressure and $F_i (i=1-5)$ are empirical constants.

Here we use $1+e$ instead of e in the equation to avoid the situation when the coefficient goes to infinity as e approaches 0. The agreement between the model and experimental results is best when $n=1$ (Figure 2). It is obvious that the frictional behavior between soft and hard mediums (like chlorite and granite respectively) is greatly influenced by the physical properties of soft medium. The ratios between the terms in equation (3), i.e.,

$$\frac{F_1 v}{F_3 e_Y / (1+e)}, \quad \frac{F_1 v}{F_4 / \langle d \rangle}, \quad \frac{F_2 D}{F_3 e_Y / (1+e)}, \quad \text{and} \quad \frac{F_2 D}{F_4 / \langle d \rangle} \quad \text{are less than 0.0002.}$$

It is suggested that void ratio and grain size are the dominant parameters for friction coefficient; the coefficient becomes greater at smaller void ratio and smaller grain size. On the other hand, slip rate or displacement has little influence on the coefficient. Equation (3) can, therefore, be simplified as follows:

$$\text{Friction coefficient} = \frac{F_3 e_Y}{1+e} + \frac{F_4}{\langle d \rangle} + F_5 .$$

Samples of chlorite of different thicknesses, i.e. 0.5 mm and 0.25 mm, were experimentally studied. The friction coefficient of these experiments is found to be independent of the thickness of the sample, further suggesting that the effect of shear strain on friction coefficient may be insignificant in the sliding experiment.

Report

Chu, C.L. and C.Y. Wang, "A Constitutive Relation of Saturated Clayey Gouges at High Pressures", EOS, 64, No. 45, 835, Nov. 1983.

Figure 1. Mean grain size and standard deviation in grain-size distribution in sheared chlorite gouge as functions of the deviatoric stress.

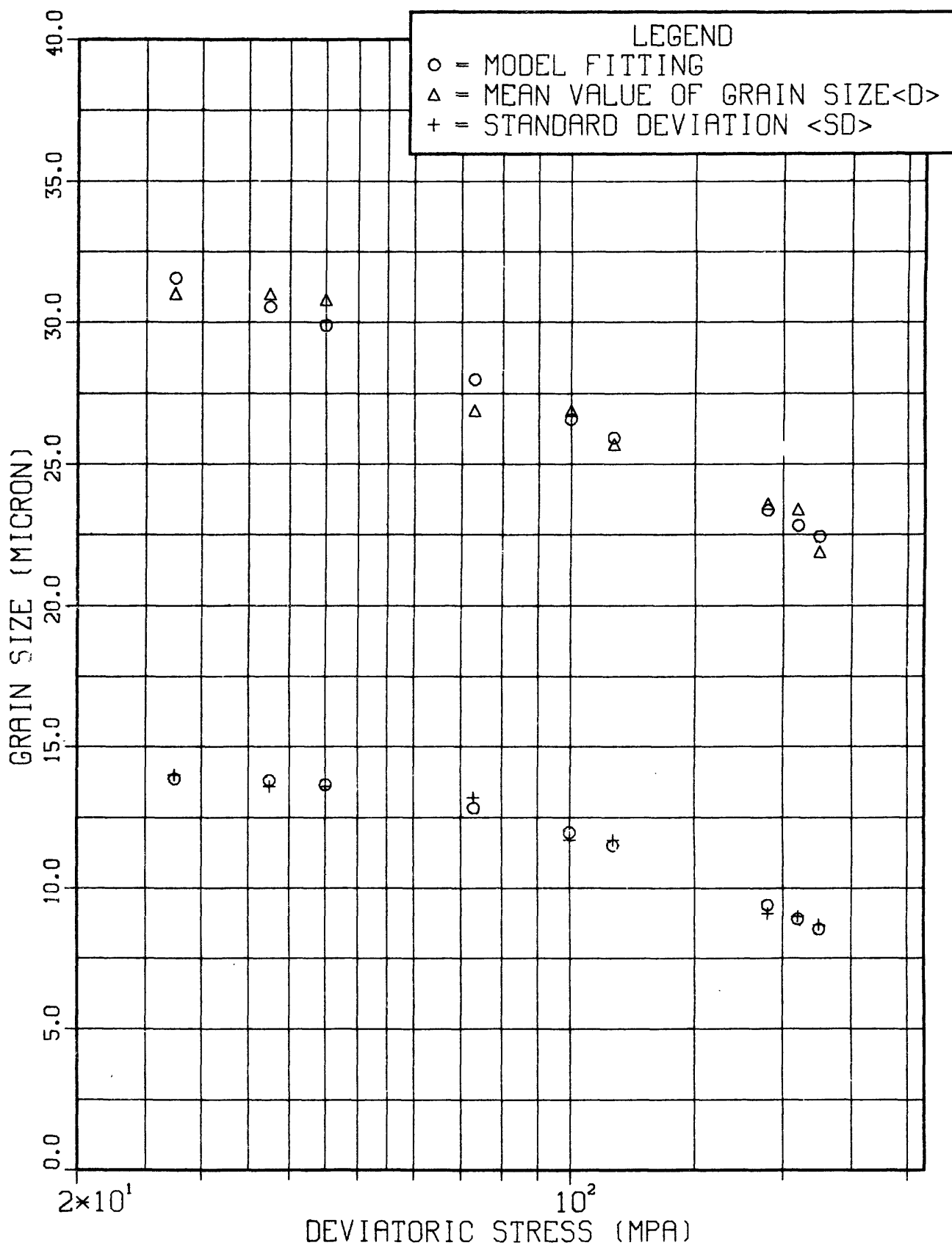
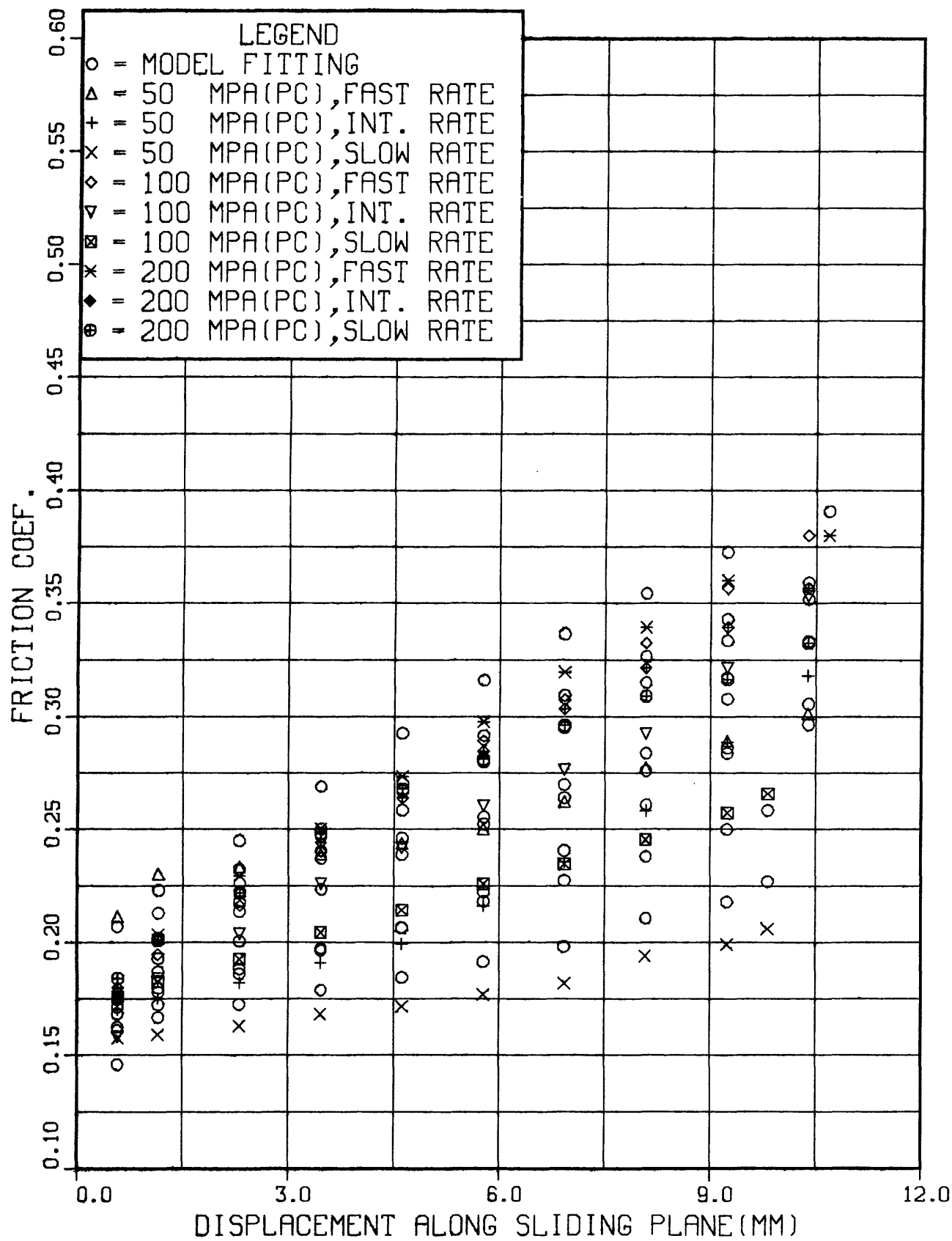


Figure 2. Friction coefficient of chlorite gouge as a function of shear displacement, at various confining pressures and displacement rates.



INDUCED SEISMICITY IN THE SLEEPY HOLLOW OIL FIELD,
RED WILLOW COUNTY, NEBRASKA

14-08-0001-20544

Don W. Steeples
Kansas Geological Survey
The University of Kansas
Lawrence, Kansas 66044
(913) 864-4991

Investigations

1. Continue to monitor earthquake activity in and near the Sleepy Hollow oil field, southwestern Nebraska.
2. Correlate earthquake occurrences with injection data.
3. Determine fault plane solutions and source parameters for earthquakes in the vicinity of the oil field.
4. Acquire and analyse digital seismograms for events in the vicinity of the oil field.

Results

1. Seismicity of the Sleepy Hollow Oil Field

In two years of network operation (1 April 1982 - 1 April 1984), 330 microearthquakes have been detected in the vicinity of the Sleepy Hollow oil field. Over one-third of these events occurred in three earthquake swarms: 1) a swarm of 9 events over three days beginning 24 May 1983; 2) a swarm of 40 events over 9 days beginning 29 September 1983; and 3) a swarm of 69 events occurring over 4 days beginning 26 October 1983. The overall level of activity has increased slightly following this last swarm.

Two-thirds of the earthquakes have been recorded well enough to locate. Earthquakes are located using a velocity model derived from a combination of well data (giving the depth to basement), a refraction experiment (giving basement velocity), and a joint hypocenter determination (giving layer velocity). Analysis of network geometry indicates that most events occur in an area where resolution of hypocentral parameters is better than 1 km horizontally and 2 km vertically.

The epicenters trend southwest-northeast in a broad linear band approximately 10 km long and 3 km wide. Much of the activity, however, is limited to a cluster of events on the western lease limits of the oil field. The earthquakes show little or no trend in depth. Most events (66%) have been located in the basement rocks (i.e., deeper than 1.1 km). Standard errors in locations, however, indicate that the depth of some of these events is questionable.

2. Correlation of Earthquakes with Injection

We have not yet received injection data for 1983. Through discussions with AMOCO engineers, we know that between May and June, 1983, 12 new injection wells were added to the complex of wells injecting the Reagan sandstone unit. This could explain the increase in activity during the subsequent months.

3. Fault Plane Solutions

No single event produced a well-constrained fault plane solution. Consequently, a number of composite first-motion plots were compiled. The first-motion data were divided into a number of data sets representing spatial and temporal clusters. None of these composite data sets yields a first-motion plot that can be interpreted as a double-couple focal mechanism. Furthermore, the direction of the first motion at at least two stations is of opposite polarity within each composite data set. Polarity reversals are not temporally related. This indicates one of three things: that the earthquake sources are not double-couple mechanisms, that the stations for which polarity reverses are near a nodal plane, or that more than one faulting mechanism is active in each data set. The latter of these possibilities is the preferred interpretation since stations with polarity changes record large amplitude impulsive first arrivals, and since in each data set all polarity conflicts cannot be accommodated by nearby nodal planes.

4. Acquisition of Digital Seismograms

In mid-October, 1983, we began recording the Sleepy Hollow earthquakes on digital magnetic tape. Since then 64 events have been recorded digitally. We are currently developing analysis software. Playbacks of digital records indicate that some of the earthquake activity occurs in groups of events with nearly identical waveforms. In addition to allowing us to determine common source parameters, these events will allow us to select events with similar sources for meaningful composite fault plane solutions.

Reports

Evans, D.G., Rothe, G.H., and Steeples, D.W., 1984, Seismicity of the Sleepy Hollow oil field, Red Willow County, Nebraska (abstract): Earthquake Notes (in press).

INDEX 1

INDEX ALPHABETIZED BY PRINCIPAL INVESTIGATOR

| | | Page |
|-----------------------|---------------------------------------|------|
| Aki, K. | Massachusetts Institute of Technology | 157 |
| Aki, K. | Massachusetts Institute of Technology | 283 |
| Algermissen, S. T. | U.S. Geological Survey | 423 |
| Allen, C. R. | California Institute of Technology | 1 |
| Allen, C. R. | California Institute of Technology | 287 |
| Allen, R. V. | U.S. Geological Survey | 159 |
| Anderson, L. B. | Utah State University | 494 |
| Anderson, R. E. | U.S. Geological Survey | 160 |
| Andrews, D. J. | U.S. Geological Survey | 455 |
| Arabasz, W. J. | Utah, University of | 3 |
| Arabasz, W. J. | Utah, University of | 35 |
| Bakun, W. H. | U.S. Geological Survey | 351 |
| Bekins, B. | U.S. Geological Survey | 162 |
| Berger, J. | California, University of, San Diego | 7 |
| Bilham, R. | Lamont-Doherty Geological Observatory | 164 |
| Bonilla, M. G. | U.S. Geological Survey | 86 |
| Borcherdt, R. D. | U.S. Geological Survey | 456 |
| Brady, A. G. | U.S. Geological Survey | 88 |
| Brady, A. G. | U.S. Geological Survey | 409 |
| Britton, O. J. | U.S. Geological Survey | 410 |
| Buchanan-Banks, J. M. | U.S. Geological Survey | 426 |
| Buland, R. | U.S. Geological Survey | 411 |
| Bull, W. B. | Arizona, University of | 41 |
| Byerlee, J. D. | U.S. Geological Survey | 353 |
| Byerlee, J. D. | U.S. Geological Survey | 354 |
| Carlson, M. A. | U.S. Geological Survey | 8 |
| Carlson, M. A. | U.S. Geological Survey | 9 |
| Castle, R. O. | U.S. Geological Survey | 90 |
| Chen, A. T. F. | U.S. Geological Survey | 428 |
| Choy, G. L. | U.S. Geological Survey | 168 |
| Choy, G. L. | U.S. Geological Survey | 169 |
| Chung, Y. | California, University of, San Diego | 355 |
| Clark, B. R. | Leighton and Associates, Inc. | 289 |
| Clark, H. E., Jr. | U.S. Geological Survey | 414 |
| Clark, M. M. | U.S. Geological Survey | 91 |
| Cotton, W. R. | Foothill-De Anza Community College | 94 |
| Crosson, R. S. | Washington, University of | 95 |
| Darrow, A. C. | Dames & Moore | 98 |
| Dewey, J. W. | U.S. Geological Survey | 10 |
| Dieterich, J. H. | U.S. Geological Survey | 358 |
| Doering, W. P. | U.S. Geological Survey | 46 |

| | | |
|--------------------|--|-----|
| Engdahl, E. R. | U.S. Geological Survey | 54 |
| Espinosa, A. F. | U.S. Geological Survey | 56 |
| Fedock, J. J. | U.S. Geological Survey | 458 |
| Galehouse, J. S. | San Francisco State University | 294 |
| Hadley, D. M. | Sierra Geophysics, Inc. | 429 |
| Hall, N. T. | Foothill-De Anza Community College | 58 |
| Hall, W. | U.S. Geological Survey | 170 |
| Harding, S. T. | U.S. Geological Survey | 59 |
| Harkrider, D. G. | California Institute of Technology | 298 |
| Healy, J. H. | U.S. Geological Survey | 361 |
| Heaton, T. H. | U.S. Geological Survey | 171 |
| Henyey, T. L. | Southern California, University of | 300 |
| Herriot, J. | U.S. Geological Survey | 174 |
| Herrmann, R. B. | Saint Louis, University of | 433 |
| Hoffman, J. P. | U.S. Geological Survey | 177 |
| Irwin, W. P. | U.S. Geological Survey | 100 |
| Isacks, B. L. | Cornell University | 179 |
| Jacob, K. H. | Lamont-Doherty Geological Observatory | 181 |
| Jachens, R. C. | U.S. Geological Survey | 304 |
| Jaksha, L. H. | U.S. Geological Survey | 187 |
| Jensen, E. G. | U.S. Geological Survey | 189 |
| Johnson, C. | U.S. Geological Survey | 191 |
| Johnston, A. C. | Memphis State University | 193 |
| Johnston, M. J. S. | U.S. Geological Survey | 196 |
| Joyner, W. B. | U.S. Geological Survey | 459 |
| Julian, B. R. | U.S. Geological Survey | 200 |
| Kanamori, H. | California Institute of Technology | 204 |
| Kanamori, H. | California Institute of Technology | 306 |
| Keefer, D. K. | U.S. Geological Survey | 434 |
| Keller, E. A. | California, University of, Santa Barbara | 475 |
| Kelleher, J. | Redwood Research, Inc. | 208 |
| Kerry, L. | U.S. Geological Survey | 415 |
| King, C. -Y | U.S. Geological Survey | 209 |
| King, K. W. | U.S. Geological Survey | 103 |
| Kirby, S. | U.S. Geological Survey | 364 |
| Kisslinger, C. | Colorado, University of | 211 |
| Koteff, C. | U.S. Geological Survey | 61 |
| Lachenbruch, A. H. | U.S. Geological Survey | 378 |
| Lahr, J. C. | U.S. Geological Survey | 214 |
| Lajoie, K. R. | U.S. Geological Survey | 105 |
| Lamar, D. L. | Lamar-Merifield, Geologists | 309 |
| Lamar, D. L. | Lamar-Merifield, Geologists | 476 |
| Langbein, J. | U.S. Geological Survey | 220 |
| Langer, C. J. | U.S. Geological Survey | 219 |
| Langston, C. A. | Pennsylvania State University | 437 |

| | | |
|--------------------|--|-----|
| Leary, P. C. | Southern California, University of | 312 |
| Lee, W. H. K. | U.S. Geological Survey | 227 |
| Lee, W. H. K. | U.S. Geological Survey | 416 |
| Leighton, F. B. | Leighton and Associates, Inc. | 478 |
| Lester, F. W. | U.S. Geological Survey | 228 |
| Levi, S. | Oregon State University | 109 |
| Levine, J. | U.S. National Bureau of Standards | 499 |
| Lindh, A. G. | U.S. Geological Survey | 317 |
| Liu, H. -P | U.S. Geological Survey | 366 |
| Luco, J. E. | California, University of, San Diego | 480 |
| | | |
| Madole, R. F. | U.S. Geological Survey | 62 |
| Malin, P. E. | California, University of, Santa Barbara | 395 |
| Mason, R. G. | Imperial College | 501 |
| Matti, J. C. | U.S. Geological Survey | 118 |
| Mavko, G. M. | U.S. Geological Survey | 232 |
| McCarthy, R. P. | U.S. Geological Survey | 417 |
| McEvilly, T. V. | California, University of, Berkeley | 318 |
| McEvilly, T. V. | California, University of, Berkeley | 513 |
| McGuire, R. K. | Dames & Moore | 439 |
| McKeown, F. | U.S. Geological Survey | 120 |
| Miller, R. D. | U.S. Geological Survey | 63 |
| Mooney, W. D. | U.S. Geological Survey | 368 |
| Morrissey, S-T. | Saint Louis, University of | 322 |
| Mortensen, C. E. | U.S. Geological Survey | 239 |
| Mueller, R. J. | U.S. Geological Survey | 242 |
| Myren, G. D. | U.S. Geological Survey | 246 |
| | | |
| Nason, R. | U.S. Geological Survey | 248 |
| | | |
| O'Neil, J. R. | U.S. Geological Survey | 64 |
| Oppenheimer, D. H. | U.S. Geological Survey | 399 |
| | | |
| Park, R. B. | U.S. Geological Survey | 67 |
| Perkins, J. B. | Association of Bay Area Governments | 440 |
| Person, W. J. | U.S. Geological Survey | 418 |
| Peterson, J. | U.S. Geological Survey | 249 |
| Power, M. S. | Woodward-Clyde Consultants | 496 |
| Prescott, W. H. | U.S. Geological Survey | 250 |
| | | |
| Ratcliffe, N. M. | U.S. Geological Survey | 69 |
| Reasenberg, P. A. | U.S. Geological Survey | 255 |
| Redpath, B. | URS/John A. Blume & Associates | 483 |
| Reimer, G. M. | U.S. Geological Survey | 71 |
| Reynolds, R. D. | U.S. Geological Survey | 257 |
| Robertson, E. C. | U.S. Geological Survey | 74 |
| Rogers, A. M. | U.S. Geological Survey | 460 |
| Ross, D. C. | U.S. Geological Survey | 77 |
| Rudnicki, J. W. | Northwestern University | 374 |
| Ryall, A. S. | Nevada, University of | 12 |
| Ryall, A.S. | Nevada, University of | 122 |
| | | |
| Seeber, L. | Lamont-Doherty Geological Observatory | 16 |

| | | |
|-------------------|--|-----|
| Segall, P. | U.S. Geological Survey | 383 |
| Shapiro, M. H. | California Institute of Technology | 328 |
| Sharp, R. V. | U.S. Geological Survey | 125 |
| Shaw, H. R. | U.S. Geological Survey | 259 |
| Sieh, K. | California Institute of Technology | 79 |
| Sieh, K. | California Institute of Technology | 126 |
| Sims, J. D. | U.S. Geological Survey | 442 |
| Slater, L. A. | Colorado, University of | 334 |
| Spence, W. | U.S. Geological Survey | 80 |
| Spence, W. | U.S. Geological Survey | 401 |
| Spudich, P. | U.S. Geological Survey | 462 |
| Stauder, W. | Saint Louis University | 21 |
| Steeple, D. W. | Kansas, University of | 526 |
| Stokoe, K. H., II | Texas, University at Austin | 464 |
| Stewart, S. W. | U.S. Geological Survey | 260 |
| Stover, C. W. | U.S. Geological Survey | 24 |
| Street, R. L. | Kentucky, University of | 26 |
| Sutton, G. H. | Rondout, Associates, Incorporated | 445 |
| Sylvester, A. G. | California, University of, Santa Barbara | 338 |
| Sylvester, A. G. | California, University of, Santa Barbara | 339 |
| Swanson, P. L. | Colorado, University of | 516 |
| Taggart, J. N. | U.S. Geological Survey | 263 |
| Talwani, P. | South Carolina, University of | 402 |
| Talwani, P. | South Carolina University of | 468 |
| Tarr, A. C. | U.S. Geological Survey | 420 |
| Teng, T. | Southern California, University of | 30 |
| Teng, T. | Southern California, University of | 340 |
| Thatcher, W. | U.S. Geological Survey | 265 |
| Tinsley, J. C. | U.S. Geological Survey | 129 |
| Toppozada, T. R. | California Division of Mines and Geology | 407 |
| Toksoz, M. N. | Massachusetts Institute of Technology | 449 |
| Toksoz, M. N. | Massachusetts Institute of Technology | 488 |
| Tullis, T. E. | Brown University | 386 |
| Van Schaack, J. | U.S. Geological Survey | 268 |
| Van Schaack, J. | U.S. Geological Survey | 269 |
| Van Schaack, J. | U.S. Geological Survey | 270 |
| Vincent, K. R. | U.S. Geological Survey | 130 |
| Vinton, J. | U.S. Geological Survey | 422 |
| Wallace, R. E. | U.S. Geological Survey | 82 |
| Walsh, J. B. | Massachusetts Institute of Technology | 392 |
| Wang, C. Y. | California, University of, Berkeley | 520 |
| Ware, R. H. | Colorado, University of | 271 |
| Warren, D. H. | U.S. Geological Survey | 278 |
| Warrick, R. E. | U.S. Geological Survey | 394 |
| Weaver, C. S. | U.S. Geological Survey | 134 |
| Wentworth, C. M. | U.S. Geological Survey | 139 |
| Wesson, R. L. | U.S. Geological Survey | 279 |
| Whitcomb, J. H. | Colorado, University of | 514 |
| White, R. A. | U.S. Geological Survey | 280 |
| Wood, S. H. | U.S. Geological Survey | 142 |

| | | |
|---------------|---|-----|
| Wu, F. T. | New York, State University of, Binghamton | 505 |
| Wyatt, F. | California, University of, San Diego | 344 |
| Wyatt, F. | California, University of, San Diego | 347 |
| Wyss, M. | Colorado, University of | 509 |
| Yeats, R. S. | Oregon State University | 147 |
| Yeats, R. S. | Oregon State University | 281 |
| Yerkes, R. F. | U.S. Geological Survey | 148 |
| Youd, T. L. | U.S. Geological Survey | 453 |
| Ziony, J. I. | U.S. Geological Survey | 151 |
| Zoback, M. L. | U.S. Geological Survey | 84 |

INDEX 2
INDEX ALPHABETIZED BY INSTITUTION

| | Page |
|--|----------------------|
| Arizona, University of | Bull, W. B. 41 |
| Association of Bay Area Governments | Perkins, J. B. 440 |
| Brown University | Tullis, T. E. 386 |
| California Division of Mines and Geology | Toppozada, T. R. 407 |
| California Institute of Technology | Allen, C. R. 1 |
| California Institute of Technology | Allen, C. R. 287 |
| California Institute of Technology | Harkrider, D. G. 298 |
| California Institute of Technology | Kanamori, H. 204 |
| California Institute of Technology | Kanamori, H. 306 |
| California Institute of Technology | Shapiro, M. H. 328 |
| California Institute of Technology | Sieh, K. 79 |
| California Institute of Technology | Sieh, K. 126 |
| California, University of, Berkeley | McEvilly, T. V. 318 |
| California, University of, Berkeley | McEvilly, T. V. 513 |
| California, University of, Berleley | Wang, C. Y. 520 |
| California, University of, San Diego | Berger, J. 7 |
| California, University of, San Diego | Chung, Y. 355 |
| California, University of, San Diego | Luco, J. E. 480 |
| California, University of, San Diego | Wyatt, F. 344 |
| California, University of, San Diego | Wyatt, F. 347 |
| California, University of, Santa Barbara | Keller, E. A. 475 |
| California, University of, Santa Barbara | Malin, P. E. 395 |
| California, University of, Santa Barbara | Sylvester, A. G. 338 |
| California, University of, Santa Barbara | Sylvester, A. G. 339 |
| Colorado, University of | Kisslinger, C. 211 |
| Colorado, University of | Slater, L. E. 334 |
| Colorado, University of | Swanson, P. L. 516 |
| Colorado, University of | Ware, R. H. 271 |
| Colorado, University of | Whitcomb, J. H. 514 |
| Colorado, University of | Wyss, M. 509 |
| Cornell University | Isacks, B. L. 179 |
| Dames & Moore | Darrow, A. C. 98 |
| Dames & Moore | McGuire, R. K. 439 |
| Foothill-De Anza Community College | Cotton, W. R. 94 |
| Foothill-De Anza Community College | Hall, N. T. 58 |

| | | |
|---|------------------|-----|
| Imperial College | Mason, R. G. | 501 |
| Kansas, University of | Steeple, D. W. | 526 |
| Kentucky, University of | Street, R. L. | 26 |
| Lamar-Merifield Geologists, Inc. | Lamar, D. L. | 309 |
| Lamar-Merifield Geologists, Inc. | Lamar, D. L. | 476 |
| Lamont-Doherty Geological Observatory | Bilham, R. | 164 |
| Lamont-Doherty Geological Observatory | Jacob, K. H. | 181 |
| Lamont-Doherty Geological Observatory | Seeber, L. | 16 |
| Leighton and Associates, Inc. | Clark, B. R. | 289 |
| Leighton and Associates, Inc. | Leighton, F. B. | 478 |
| Massachusetts Institute of Technology | Aki, K. | 157 |
| Massachusetts Institute of Technology | Aki, K. | 283 |
| Massachusetts Institute of Technology | Toksoz, M. N. | 449 |
| Massachusetts Institute of Technology | Toksoz, M. N. | 488 |
| Massachusetts Institute of Technology | Walsh, J. B. | 392 |
| Memphis State University | Johnston, A. C. | 193 |
| Nevada, University of | Ryall, A. S. | 12 |
| Nevada, University of | Ryall, A. S. | 122 |
| New York, State University of, Binghamton | Wu, F. T. | 505 |
| Northwestern University | Rudnicki, J. W. | 374 |
| Oregon State University | Levi, S. | 109 |
| Oregon State University | Yeats, R. S. | 147 |
| Oregon State University | Yeats, R. S. | 281 |
| Pennsylvania State University | Langston, C. A. | 437 |
| Redwood Research, Inc. | Kelleher, J. | 208 |
| Rondout Associates, Incorporated | Sutton, G. H. | 445 |
| Saint Louis University | Herrmann, R. B. | 433 |
| Saint Louis University | Morrissey, S-T. | 322 |
| Saint Louis University | Stauder, W. | 21 |
| San Francisco State University | Galehouse, J. S. | 294 |
| Sierra Geophysics, Inc. | Hadley, D. M. | 429 |
| South Carolina, University of | Talwani, P. | 402 |
| South Carolina, University of | Talwani, P. | 468 |

| | | |
|------------------------------------|-----------------------|-----|
| Southern California, University of | Henyey, T. L. | 300 |
| Southern California, University of | Leary, P. C. | 312 |
| Southern California, University of | Teng, T. | 30 |
| Southern California, University of | Teng, T. | 340 |
| Texas, University at Austin | | |
| U.S. Geological Survey | Stokoe, K. H., II | 464 |
| U.S. Geological Survey | Algermissen, S. T. | 423 |
| U.S. Geological Survey | Allen, R. V. | 159 |
| U.S. Geological Survey | Anderson, R. E. | 160 |
| U.S. Geological Survey | Andrews, D. J. | 455 |
| U.S. Geological Survey | Bakun, W. H. | 351 |
| U.S. Geological Survey | Bekins, B. | 162 |
| U.S. Geological Survey | Bonilla, M. G. | 86 |
| U.S. Geological Survey | Borcherdt, R. D. | 456 |
| U.S. Geological Survey | Brady, A. G. | 88 |
| U.S. Geological Survey | Brady, A. G. | 409 |
| U.S. Geological Survey | Britton, O. J. | 410 |
| U.S. Geological Survey | Buchanan-Banks, J. M. | 426 |
| U.S. Geological Survey | Buland, R. | 411 |
| U.S. Geological Survey | Byerlee, J. D. | 353 |
| U.S. Geological Survey | Byerlee, J. D. | 354 |
| U.S. Geological Survey | Carlson, M. A. | 8 |
| U.S. Geological Survey | Carlson, M. A. | 9 |
| U.S. Geological Survey | Castle, R. O. | 90 |
| U.S. Geological Survey | Chen, A. T. F. | 428 |
| U.S. Geological Survey | Choy, G. L. | 168 |
| U.S. Geological Survey | Choy, G. L. | 169 |
| U.S. Geological Survey | Clark, H. E., Jr. | 414 |
| U.S. Geological Survey | Clark, M. M. | 91 |
| U.S. Geological Survey | Dewey, J. W. | 10 |
| U.S. Geological Survey | Dieterich, J. H. | 358 |
| U.S. Geological Survey | Doering, W. P. | 46 |
| U.S. Geological Survey | Engdahl, E. R. | 54 |
| U.S. Geological Survey | Espinosa, A. F. | 56 |
| U.S. Geological Survey | Fedock, J. J. | 458 |
| U.S. Geological Survey | Hall, W. | 170 |
| U.S. Geological Survey | Harding, S. T. | 59 |
| U.S. Geological Survey | Healy, J. H. | 361 |
| U.S. Geological Survey | Heaton, T. H. | 171 |
| U.S. Geological Survey | Herriot, J. | 174 |
| U.S. Geological Survey | Hoffman, J. P. | 177 |
| U.S. Geological Survey | Irwin, W. P. | 100 |
| U.S. Geological Survey | Jachens, R. C. | 304 |
| U.S. Geological Survey | Jaksha, L. H. | 187 |
| U.S. Geological Survey | Jensen, E. G. | 189 |
| U.S. Geological Survey | Johnson, C. | 191 |
| U.S. Geological Survey | Johnston, M. J. S. | 196 |
| U.S. Geological Survey | Joyner, W. B. | 459 |
| U.S. Geological Survey | Julian, B. R. | 200 |
| U.S. Geological Survey | Keefer, D. K. | 434 |
| U.S. Geological Survey | Kerry, L. | 415 |

| | | |
|------------------------|--------------------|-----|
| U.S. Geological Survey | King, C. -Y. | 209 |
| U.S. Geological Survey | King, K. W. | 103 |
| U.S. Geological Survey | Kirby, S. | 364 |
| U.S. Geological Survey | Koteff, C. | 61 |
| U.S. Geological Survey | Lachenbruch, A. H. | 378 |
| U.S. Geological Survey | Lahr, J. C. | 214 |
| U.S. Geological Survey | Lajoie, K. R. | 105 |
| U.S. Geological Survey | Langbein, J. | 220 |
| U.S. Geological Survey | Langer, C. J. | 219 |
| U.S. Geological Survey | Lee, W. H. K. | 227 |
| U.S. Geological Survey | Lee, W. H. K. | 416 |
| U.S. Geological Survey | Lester, F. W. | 228 |
| U.S. Geological Survey | Lindh, A. G. | 317 |
| U.S. Geological Survey | Liu, H. -P | 366 |
| U.S. Geological Survey | Madole, R. F. | 62 |
| U.S. Geological Survey | Matti, J. C. | 118 |
| U.S. Geological Survey | Mavko, G. M. | 232 |
| U.S. Geological Survey | McCarthy, R. P. | 417 |
| U.S. Geological Survey | McKeown, F. A. | 120 |
| U.S. Geological Survey | Miller, R. D. | 63 |
| U.S. Geological Survey | Mooney, W. D. | 368 |
| U.S. Geological Survey | Mortensen, C. E. | 239 |
| U.S. Geological Survey | Mueller, R. J. | 242 |
| U.S. Geological Survey | Myren, G. D. | 246 |
| U.S. Geological Survey | Nason, R. | 248 |
| U.S. Geological Survey | O'Neil, J. R. | 64 |
| U.S. Geological Survey | Oppenheimer, D. H. | 399 |
| U.S. Geological Survey | Park, R. B. | 67 |
| U.S. Geological Survey | Person, W. J. | 418 |
| U.S. Geological Survey | Peterson, J. | 249 |
| U.S. Geological Survey | Prescott, W. H. | 250 |
| U.S. Geological Survey | Ratcliffe, N. M. | 69 |
| U.S. Geological Survey | Reasenberg, P. A. | 255 |
| U.S. Geological Survey | Reimer, G. M. | 71 |
| U.S. Geological Survey | Reynolds, R. D. | 257 |
| U.S. Geological Survey | Robertson, E. C. | 74 |
| U.S. Geological Survey | Rogers, A. M. | 460 |
| U.S. Geological Survey | Ross, D. C. | 77 |
| U.S. Geological Survey | Segall, P. | 383 |
| U.S. Geological Survey | Sharp, R. V. | 125 |
| U.S. Geological Survey | Shaw, H. R. | 259 |
| U.S. Geological Survey | Sims, J. D. | 442 |
| U.S. Geological Survey | Spence, W. | 80 |
| U.S. Geological Survey | Spence, W. | 401 |
| U.S. Geological Survey | Spudich, P. | 462 |
| U.S. Geological Survey | Stewart, S. W. | 260 |
| U.S. Geological Survey | Stover, C. W. | 24 |
| U.S. Geological Survey | Taggart, J. N. | 263 |
| U.S. Geological Survey | Tarr, A. C. | 420 |
| U.S. Geological Survey | Thatcher, W. | 265 |
| U.S. Geological Survey | Tinsley, J. C. | 129 |
| U.S. Geological Survey | Van Schaack, J. | 268 |
| U.S. Geological Survey | Van Schaack, J. | 269 |

| | | |
|---------------------------------------|---------------------|---------|
| U.S. Geological Survey | Van Schaack, J. | 270 |
| U.S. Geological Survey | Vincent, K. R. | 130 |
| U.S. Geological Survey | Vinton, J. | 422 |
| U.S. Geological Survey | Wallace, R. E. | 82 |
| U.S. Geological Survey | Warren, D. H. | 278 |
| U.S. Geological Survey | Warrick, R. E. | 394 |
| U.S. Geological Survey | Weaver, C. S. | 134 |
| U.S. Geological Survey | Wentworth, C. M. | 139 |
| U.S. Geological Survey | Wesson, R. L. | 279 |
| U.S. Geological Survey | White, R. A. | 280 |
| U.S. Geological Survey | Wood, S. H. | 142 |
| U.S. Geological Survey | Yerkes, R. F. | 148 |
| U.S. Geological Survey | Youd, T. L. | 453 |
| U.S. Geological Survey | Ziony, J. I. | 151 |
| U.S. Geological Survey | Zoback, M. L. | 84 |
| U.S. National Bureau of Standards | Levine, J. | 499 |
| URS/John A. Blume & Associates | Redpath, B. | 483 |
| Utah State University | Anderson, L. R. | 494 |
| Utah, University of | Arabasz, W. J. | 3 |
| Utah, University of | Arabasz, W. J. | 35 |
| Washington, University of | Crosson, R. S. | 95 |
| Woodward-Clyde Consultants | Power, M. S. | 496 |